frontiers | Research Topics

T cell specificity and cross-reactivity – implications in physiology and pathology

Edited by
Samuele Notarbartolo, Daniela Latorre, Tomasz Piotr Wypych, Silvia Monticelli and Dominik Aschenbrenner

Published in
Frontiers in Immunology

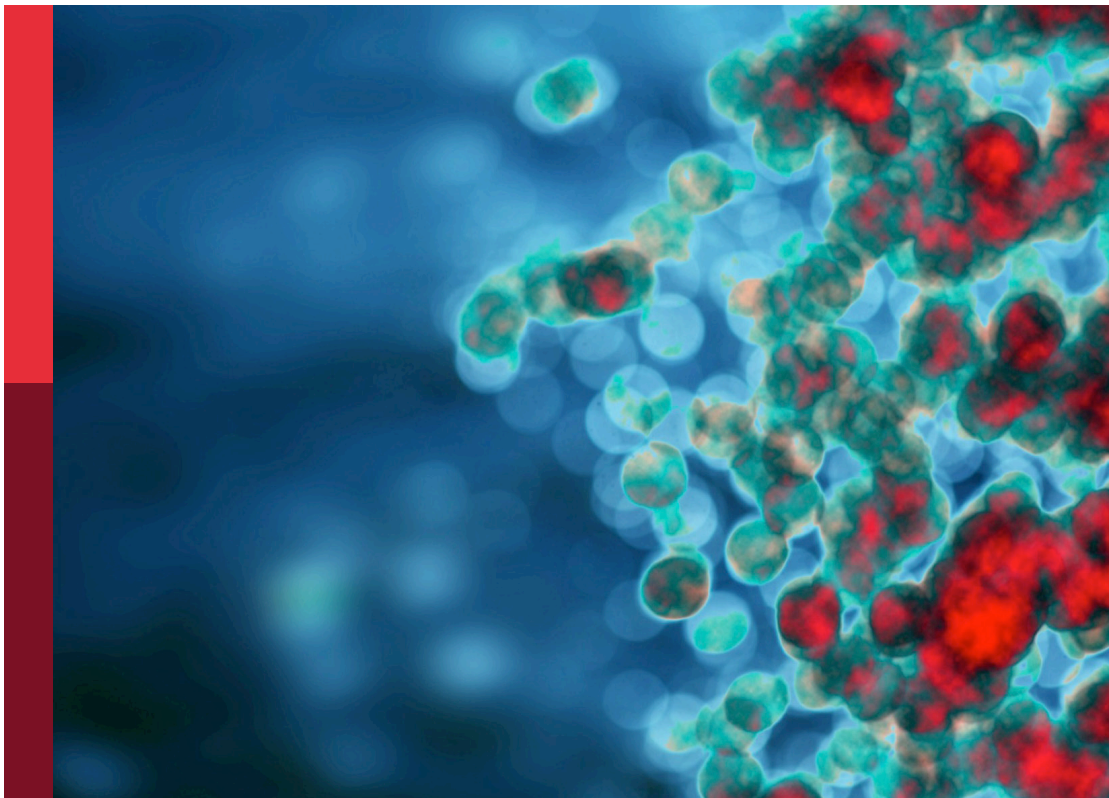

ISSN 1664-8714
ISBN 978-2-8325-4573-7
DOI 10.3389/978-2-8325-4573-7

About Frontiers

Frontiers is more than just an open access publisher of scholarly articles: it is a pioneering approach to the world of academia, radically improving the way scholarly research is managed. The grand vision of Frontiers is a world where all people have an equal opportunity to seek, share and generate knowledge. Frontiers provides immediate and permanent online open access to all its publications, but this alone is not enough to realize our grand goals.

Frontiers journal series

The Frontiers journal series is a multi-tier and interdisciplinary set of open-access, online journals, promising a paradigm shift from the current review, selection and dissemination processes in academic publishing. All Frontiers journals are driven by researchers for researchers; therefore, they constitute a service to the scholarly community. At the same time, the *Frontiers journal series* operates on a revolutionary invention, the tiered publishing system, initially addressing specific communities of scholars, and gradually climbing up to broader public understanding, thus serving the interests of the lay society, too.

Dedication to quality

Each Frontiers article is a landmark of the highest quality, thanks to genuinely collaborative interactions between authors and review editors, who include some of the world's best academicians. Research must be certified by peers before entering a stream of knowledge that may eventually reach the public - and shape society; therefore, Frontiers only applies the most rigorous and unbiased reviews. Frontiers revolutionizes research publishing by freely delivering the most outstanding research, evaluated with no bias from both the academic and social point of view. By applying the most advanced information technologies, Frontiers is catapulting scholarly publishing into a new generation.

What are Frontiers Research Topics?

Frontiers Research Topics are very popular trademarks of the *Frontiers journals series*: they are collections of at least ten articles, all centered on a particular subject. With their unique mix of varied contributions from Original Research to Review Articles, Frontiers Research Topics unify the most influential researchers, the latest key findings and historical advances in a hot research area.

Find out more on how to host your own Frontiers Research Topic or contribute to one as an author by contacting the Frontiers editorial office: frontiersin.org/about/contact

T cell specificity and cross-reactivity – implications in physiology and pathology

Topic editors

Samuele Notarbartolo — IRCCS Ca 'Granda Foundation Maggiore Policlinico Hospital, Italy

Daniela Latorre — ETH Zürich, Switzerland

Tomasz Piotr Wypych — Nencki Institute of Experimental Biology, Polish Academy of Sciences, Poland

Silvia Monticelli — Institute for Research in Biomedicine (IRB), Switzerland

Dominik Aschenbrenner — Novartis, Switzerland

Citation

Notarbartolo, S., Latorre, D., Wypych, T. P., Monticelli, S., Aschenbrenner, D., eds. (2024). *T cell specificity and cross-reactivity – implications in physiology and pathology*. Lausanne: Frontiers Media SA. doi: 10.3389/978-2-8325-4573-7

Table of contents

frontiers | Frontiers in Immunology

TYPE Editorial
PUBLISHED 28 February 2024
DOI 10.3389/fimmu.2024.1385415

OPEN ACCESS

EDITED AND REVIEWED BY
Mariolina Salio,
Immunocore, United Kingdom

*CORRESPONDENCE
Samuele Notarbartolo
samuele.notarbartolo@policlinico.mi.it

†These authors have contributed equally to this work

RECEIVED 12 February 2024
ACCEPTED 19 February 2024
PUBLISHED 28 February 2024

CITATION
Latorre D, Monticelli S, Wypych TP, Aschenbrenner D and Notarbartolo S (2024) Editorial: T cell specificity and cross-reactivity – implications in physiology and pathology. *Front. Immunol.* 15:1385415. doi: 10.3389/fimmu.2024.1385415

Editorial: T cell specificity and cross-reactivity – implications in physiology and pathology

Daniela Latorre[1†], Silvia Monticelli[2†], Tomasz P. Wypych[3†], Dominik Aschenbrenner[4†] and Samuele Notarbartolo[5*†]

[1]Institute of Microbiology, ETH Zurich, Zurich, Switzerland, [2]Institute for Research in Biomedicine, Università della Svizzera italiana (USI), Bellinzona, Switzerland, [3]Nencki Institute of Experimental Biology, Polish Academy of Sciences, Warsaw, Poland, [4]Immunology Disease Area, Novartis BioMedical Research, Basel, Switzerland, [5]Infectious Diseases Unit, Fondazione IRCCS Ca' Granda Ospedale Maggiore Policlinico, Milan, Italy

KEYWORDS

cross-reactive T cells, T cell cross-reactivity, T cell receptor (TCR), molecular mimicry, T cell repertoire, autoimmune diseases, heterologous immunity and protection, evolution of T cell immunity

Editorial on the Research Topic
T cell specificity and cross-reactivity – implications in physiology and pathology

T cells are pivotal in orchestrating adaptive immune responses against a myriad of threats. Their ability to recognize antigens presented by specialized antigen-presenting cells (APCs), discern between self and non-self, and regulate and execute tailored immune responses lies at the heart of our immunological defenses. At the forefront of T cell function is the T cell receptor (TCR), a complex molecular machinery tasked with the daunting challenge of discriminating between an extensive array of antigens. Conventional $CD8^+$ and $CD4^+$ T cells recognize antigens exposed by APCs in the form of short peptides loaded onto major histocompatibility complex (MHC) class I and class II molecules, through their TCR (1). This interaction is key for T cell immune function as it triggers a signaling cascade that results in T cell activation, differentiation, and effector response.

The specificity of T cell-mediated immune responses is driven by the diversification of TCRs. TCRs are heterodimers of alpha and beta chains (αβTCR), which are encoded by genes on human chromosome 14 and chromosome 7, respectively. Both loci contain variable (V), joining (J), and constant (C) gene fragments, while only the TCR β locus includes two diversity (D) gene fragments between V and J. TCR diversity is determined at three different levels: the recombination of the V(D)J gene fragments, the generation of random junctional sequences by the terminal deoxynucleotidyl transferase enzyme, and the pairing of the productive alpha and beta chains. The theoretical repertoire of human T cells is enormous [possibly 10^{19}-10^{20} (2, 3)], with the sole V(D)J recombination contributing with more than 5×10^6 possible combinations of TCR gene fragments, assuming these are all equally possible (Table 1). However, 10^8-10^{10} is the estimated number of unique TCRs surviving clonal (positive and negative) selection in the thymus and forming the mature T cell repertoire (5–7). These numbers are several orders of magnitude lower than the possible array of peptides that can be generated and accommodated into an MHC molecule

TABLE 1 TCR diversity based on V(D)J recombination and αβ chains pairing.

Gene name	Number of functional gene segments
TRAV	45
TRAJ	50
TRAC	1
Possible TCRα *VJC* triplets	2,250
TRBV	47
TRBD	2
TRBJ	13
TRBC	2
Possible TCRβ *VDJC* quadruplets	2,444
Total possible TCRαβ pairs	5,499,000

Number of unique human TCRs that can be generated by the process of V(D)J recombination, without considering the junctional-derived diversity, and assuming that all the combinations of gene segments are equally possible. The indicated number of functional gene segments, based on data from the International Immunogenetics Information System (IMGT, https://www.imgt.org/IMGTrepertoire/), does not include pseudogenes and open-reading frames (ORFs). Recently published data indicate that inter-individual allelic variation in TCR genes may further broaden the TCR diversity reported here (4).

(8). Considering the disparity between the number of possible foreign antigens and TCRs, the "one-clonotype–one-specificity" paradigm would result in a breach of the adaptive immune barrier.

This deficit in TCR diversity is resolved by T cell cross-reactivity, that is the ability of a single TCR to bind multiple peptide-MHC complexes, albeit with different affinities. In addition to the theoretical need, numerous independent studies have experimentally demonstrated the existence of cross-reactive T cells [reviewed in (9, 10)].

In this Research Topic, we aim to offer an overview of established knowledge and recent advances in the field of T cell cross-reactivity, providing novel insights into the processes governing this phenomenon.

First, Acuto comprehensively analyzes the mechanisms regulating TCR activation and signaling portraying the context of T cell reactivity and cross-reactivity. He reviews the role of MHC-I and MHC-II, TCR αβ, and the uncertainties in understanding how peptide-MHC binding induces TCR signals. Next, he discusses various models of TCR activation, such as oligomerization, mechanotransduction, and allosteric activation, including recent evidence suggesting that TCR-CD3 activation may be controlled by an allosteric mechanism requiring only monomeric peptide-MHC binding. Finally, he proposes a unifying model for TCR activation.

TCR signaling is key for T cell activation in the periphery and governs T cell clonal selection in the thymus. Thymic selection shapes the mature T cell repertoire by eliminating non-reactive or strongly self-reactive T cell clones and directing the differentiation of conventional naïve and regulatory T (Treg) cells. Welsh et al. show that H2-O, an MHC-II peptide editing molecular chaperon, limits Treg cell differentiation in the thymus and $CD4^+$ T cell hyperactivity in the periphery, possibly by modulating the range of peptides with different affinities presented on MHC-II during the thymic selection.

Still in the context of modulating TCR responses, Balasubramanian and Sundrud review the role of ATP-binding cassette (ABC) transporters in immune regulation, specifically focusing on MDR1. ABC transporters are increasingly recognized for their involvement in T cell development and function. MDR1, in particular, contributes to T cell antioxidant function, influencing TCR signaling, metabolic pathways, and oxidative stress responses. The authors discuss how MDR1 may be central to shaping the magnitude, type, and even the repertoire of T cells during antigen-specific responses and highlight the potential of ABC transporters as targets to improve therapeutic immune responses.

Cross-reactivity has evolved to cope with the enormous diversity of mutating pathogens. T cell cross-reactivity facilitates polyclonal immune responses to a single antigen and increases resistance to escape mutants. It can also induce heterologous immunity, that is the generation of memory to a pathogen different from the one against which the immune response has been originally raised. These concepts have become evident in the recent SARS-CoV-2 infection pandemics (11). Westphal et al. bring new evidence to this topic, demonstrating that $CD4^+$ T cells responding to the nonstructural protein 12 (NSP12) of SARS-CoV-2 can be found both in COVID-19 patients and seronegative individuals and cross-react with the homologous protein of common-cold coronaviruses. Interestingly, they observed that NSP12 immunodominant epitopes are recognized by $CD4^+$ T cells with different frequencies in COVID-19 patients and seronegative individuals and that the frequency of the response does not necessarily correlate with the NSP12 sequence conservation in different coronavirus species. These data suggest that epitope similarity is only one of the drivers of T cell cross-reactivity.

A deeper understanding of the principles underlying T cell cross-reactivity may also have implications for therapeutic applications. For instance, Bodas-Pinedo et al. explore the cross-reactivity between bacteria and viruses as a tool for designing better vaccines. Using an *in-silico* approach, they analyzed shared peptidome spaces and cross-reactive T cells between a selected bacterial consortium and the Influenza A virus and identified cross-reactivity patterns between bacterial and viral epitopes that might be harnessed to design better vaccines against flu.

Besides, using data from peptide:MHC-I and pMHC:TCR structures, Papadaki et al. identified residues important for MHC-I binding to peptides and TCR. Then, they developed a computational platform to design synthetic HLA molecules that could be used as screening tools to evaluate peptide-centric interactions with TCRs, such as for the development of improved chimeric antigen receptors (CARs).

Nonetheless, T cell cross-reactivity is a double-edged sword and can have both positive and negative consequences. Gouttefangeas et al. describe the dilemma faced by T cells that need to achieve both optimal target specificity and complete coverage of the complex spectrum of foreign antigens while avoiding reactivity to self-derived

peptides. They provide an overview of the basic mechanisms underlying T cell cross-reactivity and comprehensively review its main detrimental consequence, namely the recognition of self-antigens causing autoimmunity. They also highlight a less frequently appreciated positive aspect of cross-reactivity, namely enabling T cells to recognize tumor-associated antigens.

On the same line, Thomas and Olsson focus on the role of molecular mimicry and cross-reactive T cells in the pathogenesis of multiple sclerosis (MS). They delve into the current knowledge of the intricate autoantigen repertoire targeted by autoreactive T cells in MS, detailing the evidence of cross-reactivity between antigens derived from Epstein-Barr virus (but also other microbes) and autoantigens in the host's central nervous system (CNS). These data highlight the urgent need for further research to fully understand the role of foreign antigens in the development and progression of CNS demyelinating diseases.

Finally, Carbone et al. investigate immune-related adverse events (irAEs) in oncologic patients undergoing immunotherapy, focusing on cases of vitiligo onset in melanoma patients receiving therapeutic anti-PD-1. They show that T cells in patients with spontaneous and immunotherapy-associated vitiligo had a different immune profile, suggesting a different etiopathology of the two autoimmune clinical manifestations. Moreover, using TCR-sequencing, they find shared T cell clones in vitiligo skin lesions and metastatic (but not primary) melanoma biopsies, suggesting that an immune response against metastatic cells may trigger vitiligo development. Considering that irAEs are the main cause of immunotherapy discontinuation, increasing our understanding of the cross-reactivity of T cells to tumor-associated and self-antigens will be instrumental in developing innovative immunotherapies with limited irAEs.

In conclusion, despite all the acquired knowledge, a lot remains to be learned about cross-reactive T cells, such as phenotype and function in health and disease, TCR repertoires, and target antigens. A deeper understanding of the processes and principles associated with T cell activation, specificity, and cross-reactivity will have relevant implications in the prevention and treatment of autoimmune diseases, the development of vaccines, the optimization of engineered TCRs targeting tumor antigens, and the advancement of innovative approaches for precision medicine.

Author contributions

SN: Conceptualization, Writing – original draft, Writing – review & editing. DL: Writing – review & editing. SM: Writing – review & editing. TW: Writing – review & editing. DA: Writing – review & editing.

Funding

The author(s) declare financial support was received for the research, authorship, and/or publication of this article. SN is supported by a Ricerca Finalizzata Giovani Ricercatori grant from the Italian Ministry of Health (RF GR-2021-12374097). DL work on this topic is supported by the Swiss National Science Foundation PRIMA grant (PR00P3_185742), the Elevation Research Grant from the GBS/CIDP Foundation International and the Novartis Foundation for medical-biological Research. Work in the SM lab on this topic is funded by the Swiss National Science Foundation Excellence grant number 310030_205197. TW is supported by the National Science Centre, grants number 2020/39/D/NZ6/02146 and 2021/41/B/NZ6/02219.

Conflict of interest

Author DA is employed by Novartis Pharma AG and a shareholder of Novartis Pharma AG.

The remaining authors declare that the research was conducted in the absence of any commercial or financial relationships that could be construed as a potential conflict of interest.

Publisher's note

References

1. Davis MM, Boniface JJ, Reich Z, Lyons D, Hampl J, Arden B, et al. Ligand recognition by alpha beta T cell receptors. *Annu Rev Immunol.* (1998) 16:523–44. doi: 10.1146/annurev.immunol.16.1.523

2. Zarnitsyna VI, Evavold BD, Schoettle LN, Blattman JN, Antia R. Estimating the diversity, completeness, and cross-reactivity of the T cell repertoire. *Front Immunol.* (2013) 4:485. doi: 10.3389/fimmu.2013.00485

3. Dupic T, Marcou Q, Walczak AM, Mora T. Genesis of the alphabeta T-cell receptor. *PloS Comput Biol.* (2019) 15:e1006874. doi: 10.1371/journal.pcbi.1006874

4. Corcoran M, Chernyshev M, Mandolesi M, Narang S, Kaduk M, Ye K, et al. Archaic humans have contributed to large-scale variation in modern human T cell receptor genes. *Immunity.* (2023) 56:635–652.e6. doi: 10.1016/j.immuni.2023.01.026

5. Britanova OV, Putintseva EV, Shugay M, Merzlyak EM, Turchaninova MA, Staroverov DB, et al. Age-related decrease in TCR repertoire diversity measured with deep and normalized sequence profiling. *J Immunol.* (2014) 192:2689–98. doi: 10.4049/jimmunol.1302064

6. Qi Q, Liu Y, Cheng Y, Glanville J, Zhang D, Lee JY, et al. Diversity and clonal selection in the human T-cell repertoire. *Proc Natl Acad Sci USA.* (2014) 111:13139–44. doi: 10.1073/pnas.1409155111

7. Sun X, Nguyen T, Achour A, Ko A, Cifello J, Ling C, et al. Longitudinal analysis reveals age-related changes in the T cell receptor repertoire of human T cell subsets. *J Clin Invest.* (2022). 1;132(17):e158122 doi: 10.1172/JCI158122

8. Sewell AK. Why must T cells be cross-reactive? *Nat Rev Immunol.* (2012) 12:669–77. doi: 10.1038/nri3279

9. Petrova G, Ferrante A, Gorski J. Cross-reactivity of T cells and its role in the immune system. *Crit Rev Immunol.* (2012) 32:349–72. doi: 10.1615/CritRevImmunol.v32.i4.50

10. Jiang N, Malone M, Chizari S. Antigen-specific and cross-reactive T cells in protection and disease. *Immunol Rev.* (2023) 316:120–35. doi: 10.1111/imr.13217

11. Sette A, Sidney J, Crotty S. T cell responses to SARS-cov-2. *Annu Rev Immunol.* (2023) 41:343–73. doi: 10.1146/annurev-immunol-101721-061120

frontiers | Frontiers in Immunology

TYPE Original Research
PUBLISHED 25 January 2023
DOI 10.3389/fimmu.2023.1116906

OPEN ACCESS

EDITED BY
Samuele Notarbartolo,
National Institute of Molecular Genetics (INGM), Italy

REVIEWED BY
Gabriele Giachin,
University of Padua, Italy
Michael Birnbaum,
Massachusetts Institute of Technology, United States

*CORRESPONDENCE
Nikolaos G. Sgourakis
Nikolaos.Sgourakis@Pennmedicine.upenn.edu

†These authors have contributed equally to this work and share first authorship

SPECIALTY SECTION
This article was submitted to T Cell Biology, a section of the journal Frontiers in Immunology

RECEIVED 05 December 2022
ACCEPTED 10 January 2023
PUBLISHED 25 January 2023

CITATION
Papadaki GF, Ani O, Florio TJ, Young MC, Danon JN, Sun Y, Dersh D and Sgourakis NG (2023) Decoupling peptide binding from T cell receptor recognition with engineered chimeric MHC-I molecules.
Front. Immunol. 14:1116906.
doi: 10.3389/fimmu.2023.1116906

Decoupling peptide binding from T cell receptor recognition with engineered chimeric MHC-I molecules

Georgia F. Papadaki[1,2†], Omar Ani[1†], Tyler J. Florio[1,2†], Michael C. Young[1,2], Julia N. Danon[1,2], Yi Sun[1,2], Devin Dersh[3] and Nikolaos G. Sgourakis[1,2*]

[1]Center for Computational and Genomic Medicine, Department of Pathology and Laboratory Medicine, The Children's Hospital of Philadelphia, Philadelphia, PA, United States, [2]Department of Biochemistry and Biophysics, Perelman School of Medicine, University of Pennsylvania, Philadelphia, PA, United States, [3]Department of Radiation Oncology, Perelman School of Medicine, University of Pennsylvania, Philadelphia, PA, United States

Major Histocompatibility Complex class I (MHC-I) molecules display self, viral or aberrant epitopic peptides to T cell receptors (TCRs), which employ interactions between complementarity-determining regions with both peptide and MHC-I heavy chain 'framework' residues to recognize specific Human Leucocyte Antigens (HLAs). The highly polymorphic nature of the HLA peptide-binding groove suggests a malleability of interactions within a common structural scaffold. Here, using structural data from peptide:MHC-I and pMHC:TCR structures, we first identify residues important for peptide and/or TCR binding. We then outline a fixed-backbone computational design approach for engineering synthetic molecules that combine peptide binding and TCR recognition surfaces from existing HLA allotypes. X-ray crystallography demonstrates that chimeric molecules bridging divergent HLA alleles can bind selected peptide antigens in a specified backbone conformation. Finally, *in vitro* tetramer staining and biophysical binding experiments using chimeric pMHC-I molecules presenting established antigens further demonstrate the requirement of TCR recognition on interactions with HLA framework residues, as opposed to interactions with peptide-centric Chimeric Antigen Receptors (CARs). Our results underscore a novel, structure-guided platform for developing synthetic HLA molecules with desired properties as screening probes for peptide-centric interactions with TCRs and other therapeutic modalities.

KEYWORDS

major histocompatibility complex (MHC), antigen presentation, chimeric molecules, T cell receptors, structural immunology, cancer immunotherapy

Introduction

The class I proteins of the Major Histocompatibility Complex (MHC-I) present epitopic peptide antigens on the cell surface, thereby enabling immune surveillance of the intracellular proteome by CD8+ T cells and Natural Killer cells (1–5). Under physiological conditions, peptide:MHC (pMHC-I) molecules are assembled in the endoplasmic reticulum (ER) and are trafficked to the cell surface to present a pool of millions of different peptides derived from either host (self-peptides) or aberrant proteins, including viral factors and dysregulated oncoproteins (non-self-peptides) (2). The human MHC-I molecules, referred to as Human Leukocyte Antigens (HLAs), are among the most polymorphic genes with over 35,000 different allotypes reported in the human genome and are classified into the *HLA-A*, *-B*, and *-C* subfamilies (6–10). Several studies have proposed that the vast HLA diversity and extended peptide binding repertoire was driven by evolutionary pressures to adapt in pathogen-rich environments (11–14). Nonetheless, HLAs are structurally conserved with a variable heavy chain, an invariant light chain (β_2-microglobulin, β_2m), and a bound peptide typically ranging between 8-15 amino acids in length (15–18). The heavy chain is comprised of three domains, the α_1 and α_2 helices define the peptide binding groove in the MHC-I structure, while α_3 stabilizes the molecule by creating an extensive binding interface with β_2m. The peptide-binding groove consists of several adjacent 'pockets' referred to as A-F, and polymorphisms within the groove govern the respective antigen repertoire of different HLA allotypes, and induce specific peptide conformations (17, 19). While in most HLA allotypes, such as the common HLA-A*02:01 allele, the B- and F-pockets are the primary sites of stabilizing interactions with two specific peptide anchor residues at positions 2 (P2) and 9 (P9), respectively, several allotypes exhibit different anchor residues (20, 21). These variations across different HLA allotypes enable immune surveillance of diverse peptide repertoires at the population level, thus ensuring species adaptability to emerging pathogens (22).

The ability of T cells to recognize epitopic peptides in the context of specific MHC molecules is known as MHC restriction, and two hypotheses have been proposed to explain this phenomenon. The clonal selection theory poses that only TCRs binding specific MHCs will survive thymic selection (23), whereas the germline hypothesis supports that TCRs co-evolved for inherent reactivity to their MHC counterparts (24). However, experimental data for and against both models suggest that they are not mutually exclusive, and can be interpreted by a combined hypothesis (25). Cell-mediated adaptive immune responses depend upon recognition of specific pMHC-I proteins by T cell receptors present in a polyclonal repertoire encompassing $1x10^8$ distinct antigen specificities, leading to stimulation and clonal expansion (26, 27). The association between pMHC-I molecules and TCRs is highly dependent upon interactions with polymorphic residues on the α_1 and α_2 helices, as well as with exposed peptide residues. These interactions are mediated by six complementarity-determining regions (CDRs) within the variable domains of the TCR-α and -β chains, which adopt a classical diagonal orientation (25, 28–31). T cells are required to respond to a large number of different epitopic peptides, therefore TCR interactions with their pHLA antigens are characterized by a high degree of cross-reactivity, and inherently low affinity interactions to mitigate the risk of autoimmune responses. A recent study has employed targeted mutagenesis of conserved residues on the α_1 and α_2 helices which mediate key germline interactions with TCRs, to enhance recognition by alloreactive T cells while preserving the presentation of peptide antigens in a conserved conformation (32), as a means to break tolerance for specific self-antigens with possible applications in cancer therapy (33). This work provides a rationale for the design of synthetic molecules bridging TCR recognition surfaces with peptide-binding specificities from multiple HLA allotypes as a potential platform for eliciting CD8+ responses against specific tumor-associated antigens. More recently, the advent of peptide-centric, antibody based pMHC engagers as targeting modalities for Chimeric Antigen Receptor (CAR) T cell therapy highlight one additional application of synthetic HLA molecules as probes to screen for and verify allotype-independent recognition of specific antigens with the potential to treat a broader cohort of patients (34). The wide range of peptide-binding specificities covered by the known HLA allotypes is attained through specific combinations of the 33 polymorphic residues which mediate peptide binding (6, 35), suggesting that the peptide-binding groove provides a highly malleable structural scaffold for protein engineering applications aiming to expand naturally occurring T cell repertoires, or to design novel HLA-targeted therapeutics.

Here, we perform an extensive analysis of existing pMHC-I and pMHC-TCR structures to identify key residues that form contacts with peptides and TCRs, respectively. We then outline a systematic, fixed-backbone approach for engineering synthetic MHC-I molecules with desired peptide binding and TCR interface properties. Using the HLA-A*02:01, B*08:01 and B*35:01 alleles as structural scaffolds we generate stable, properly conformed molecules encompassing the peptide-binding specificities of divergent allotypes, including HLA-A*11:01, A*24:02, B*08:01, A*02:01 and C*07:02. We demonstrate that the designed molecules form stable complexes with peptides specific for the desired HLA groove, and adopt an identical conformation compared to their parental, wild-type pMHC-I complexes. Finally, we provide direct evidence that engineered chimeric HLAs presenting disease-related epitopes disrupt interactions with known TCRs but not with peptide-centric CARs, highlighting the importance of HLA framework residues in TCR recognition. Our results underscore a use of chimeric HLAs as screening probes to identify and expand TCR or CAR specificities for distinct peptide antigens, with a minimal reliance on interactions with HLA framework residues. Conversely, in analogy to altered peptide ligands (36, 37), chimeric HLAs provide a rational approach to manipulate interactions between established peptide:HLA antigens and their TCR repertoires in applications aiming to overcome central and peripheral tolerance for eliciting cross-reactive T cell responses against specific self-antigens that are overexpressed in tumor cells, as supported by previous studies (33).

Materials and methods

Chimeric MHC-I generation

Chimeric MHC-I molecules were designed using 'CHaMeleon', a fixed-backbone approach developed herein. The method requires the structure of an MHC-I allele that binds a desired peptide (groove or

template allele), and the sequence of an MHC-I allele with different peptide repertoire and TCR contact surfaces of interest (base allele). The structure of the groove allele was preprocessed to optimize its compatibility with the *Rosetta* software (38). Only the α_1 and α_2 helices of the MHC-I heavy chain and the bound peptide were retained, while the conserved α_3 domain of the heavy chain, the light chain, and all cofactors were removed to reduce the computing time in the subsequent relax protocol. The residues in the structure were renumbered such that the first residue in the structure had residue ID one (Appendix Script 1). The peptide binding groove of the template allele was defined as the set of residues within 5 Å of a peptide heavy atom on the processed structure using PyMOL (Appendix Script 2). A sequence alignment between the groove MHC-I allele and the base MHC-I allele was performed using EMBOSS Needle pairwise sequence alignment (EMBL-EBI). Starting with the base allele sequence, the chimeric MHC-I sequence was created by substituting every residue in the peptide-binding groove of the base with the corresponding residue of the template allele. To assess the stability and binding affinities of the generated chimeric HLAs, we created and evaluated the structures by threading the chimeric sequence through the preprocessed base allele structure using RosettaCM (Appendix Script 3). The threaded structures were then relaxed using the score function 'REF2015' in *Rosetta* (Appendix Scripts 4, 5). Since we were only interested in the structures that bound the target peptide in the same conformation as the groove allele, the peptide residues were fixed in place using 'PreventRepackingRLT'. The 'Fast_Relax Mover' was used with 3 repeats of the relax protocol allowing both the side chains and backbone of the heavy chain to relax during the simulation. 'InterfaceAnalyzerMover' was then used to calculate the binding energy of the peptide to the chimeric MHC-I, after repacking them separately using the 'pack_seperated' option. The standard options were used to optimize computational cost while creating realistic relaxed structures (Appendix Script 4). The options used in the command line were: '-nstruct 3' to generate three relaxed structures and calculate total and binding energies in each of the triplicates, '-no_optH' to prevent hydrogen placement optimization, 'flip_HNQ' to prevent flipping Histidine, Asparagine, and Glutamine, and '-use_input_sc'to use the input rotamers as part of the rotamer set explored by the relax algorithm.

Combinatorial sampling of polymorphic groove residues

An exhaustive assessment of every possible chimeric molecule that could be generated was performed using *Rosetta* software (38). The sequence of the base allele was threaded through the preprocessed structure of the groove allele as described above (Appendix Script 3). The threaded structure was then idealized and relaxed using *Rosetta*'s applications with the default options. From three decoy output structures, we used the most stable to introduce each set of mutations on the threaded structure of the base allele using *Rosetta* remodel. A blueprint file was generated for every possible combination of mutations in the polymorphic groove residues between the template and base alleles. For instance, for 9 polymorphic residues between two alleles within 5 Å of the peptide, $2^9 = 512$ blueprint files would be generated and used in conjunction with *Rosetta* remodel to build 512 chimeric-MHC structures. The generated models were refined with a final relax step with a single decoy for each structure and were ranked based on the calculated peptide:MHC binding energy. For the top 2.5% of structures with the lowest energies, we calculated the enrichment score for each polymorphic peptide binding groove position as the ratio of structures among the defined pool, in which a substitution from base to template allele residue was introduced.

Peptide sequence logo generation

The peptide binding profile of the designed chimeric HLAs was predicted using an in-house method based on NetMHCpan4.0 (39). Briefly, a list of all the experimentally measured peptide epitopes for the MHC class I alleles were extracted from IEDB (7) and were used to predict binding by the chimeric sequences using NetMHCpan4.0. The final sequence logos were generated using Seq2logo (40).

Recombinant protein expression, refolding, and purification

Plasmid DNA encoding the luminal domain of HLA-A*02:01 and A*24:02 heavy chains, and human β_2m (β_2m, light chain) were provided by Dale Long of the NIH Tetramer Core Facility. DNA encoding the HLA-A*11:01-A*02:01, A*11:01-A*02:01^{6M}, B*08:01-A*02:01, C*07:02-A*02:01, A*02:01-B*08:01, and A*24:02-B*35:01 chimeric constructs (Table 1) was cloned into pET-22b(+) vector using NdeI/BamHI restriction sites (Genscript). For tetramer staining and binding assays, proteins were tagged with the BirA substrate peptide (BSP, LHHILDAQKMVWNHR). The NYE-S1 TCR-α and -β chains were cloned into pET-22b(+) vector with NdeI/BamHI restriction sites (Genscript). DNA plasmids were transformed into *Escherichia coli* BL21(DE3) (New England Biolabs). Proteins were expressed in Luria Broth and inclusion bodies were solubilized using guanidine hydrochloride as previously described (41). pMHC-I complexes were generated by *in vitro* refolding as 200 mg mixtures of heavy chain:light chain at a 1:3 molar ratio and 10 mg of peptide in 1 L of refolding buffer (0.4 M L-Arginine-HCl, 2 mM EDTA, 4.9 mM reduced L-Glutathione, 0.57 mM oxidized L-Glutathione, 100 mM Tris pH 8.0) at 4°C. MHC-I molecules refolded with photolabile peptides were protected from light with aluminum foil. Refolding proceeded for 4 days and the pMHC-I complexes were purified by size-exclusion chromatography (SEC) using a HiLoad 16/600 Superdex 75 pg column at 1 mL/min with 150 mM NaCl, 25 mM Tris buffer, pH 8.0. The luminal domain of the TCR NYE-S1 α/β complex was expressed and purified as previously described (30). The 10LH scFv protein was provided by Myrio Therapeutics (Australia). Protein concentrations were determined using A_{280} measurements on Nanodrop with extinction coefficients estimated by ExPASy ProtParam tool (42).

10.3389/fimmu.2023.1116906

TABLE 1 Summary of amino acid substitutions introduced in the sequence of a base allele to derive chimeric HLAs.

Template (Groove) Allele	Base Allele	Mutations on Base Allele	Resulting Chimeric HLA
A*11:01 (9/18)	**A*02:01**	G62Q, K66N, H70Q, H74D, V95I, R97I, H114R, Y116D, V152E	**HLA-A*11:01-A*02:01**
A*11:01 (6/18)		H70Q, H74D, V95I, R97I, H114R, Y116D	**HLA-A*11:01^{6M}-A*02:01**
C*07:02 (14/35)		F9D, A24S, G62R, V67Y, H70Q, T73A, D77S, T80N, V95L, Y99S, H114D, Y116S, W147L, V152A	**HLA-C*07:02-A*02:01**
B*08:01 (18/35)		F9D, A24S, G62R, E63N, K66I, V67F, A69T, H70N, H74D, V76E, D77S, T80N, V95L, R97S, H114N, Y116N, T142I, L156D	**HLA-B*08:01-A*02:01**
A*02:01 (11/35)	**B*08:01**	D9F, E45M, N63E, I66K, F67V, N70H, D74H, S77D, S97R, N114H, D156L	**HLA-A*02:01-B*08:01**
A*24:02 (16/38)	**B*35:01**	Y9S, T45M, N63E, I66K, F67V, N70H, Y74D, S77N, L81A, I95L, R97M, Y99F, D114H, S116Y, L156Q, W167G	**HLA-A*24:02-B*35:01**

The number of amino acid substitutions introduced in the sequence of the base allele, versus the total number of polymorphic residues between the template (groove) and base alleles, are shown in brackets.

Peptides

A full list of the peptides used in this study and their abbreviations is shown in Supplementary Table 1. All peptide sequences are given as standard single-letter codes and were purchased from Genscript, NJ, USA, at >90% purity. The photolabile peptide used was purchased from Biopeptek Inc, PA, USA, using J as 3-amino-3-(2-nitrophenyl)-propionic acid (43). For the peptide solutions, lyophilized peptides were solubilized in distilled water and centrifuged at 14,000 rpm for 15 min. Concentrations were calculated using the respective absorbance and extinction coefficient at 205 nm wavelength.

Differential scanning fluorimetry

For DSF experiments, samples were prepared at a final concentration of 7 µM in PBS buffer (50 mM NaCl, 20 mM sodium phosphate pH 7.2) and mixed with 10X SYPRO Orange dye (ThermoFisher) to a final volume of 20 µL. Samples were then loaded into a MicroAmp Fast 384-well plate and ran in triplicates (n=3) on a QuantStudio™ 5 Real-Time PCR machine with excitation and emission wavelengths set to 470 nm and 569 nm, respectively. Temperature was incrementally increased at a rate of 1°C/min between 25°C and 95°C to measure the thermal stability of the proteins. Data analysis and fitting were performed in GraphPad Prism v9.

Peptide exchange

Peptide exchange mediated by UV-irradiation was performed by incubating 7 µM of HLA-B*08:01-A*02:01/FLRGRAJGL with 70 µM of the desired peptide in PBS buffer (50 mM NaCl, 20 mM sodium phosphate pH 7.2) for 1 hour at room temperature (RT), followed by UV-irradiation for 1 hour at 365 nm. Samples were centrifuged at 10,000 rpm for 10 minutes at 4°C to remove aggregates. Peptide exchange was determined by performing DSF analysis in triplicates (n=3), as previously described (44).

X-ray crystallography and structure determination

Purified HLA-A*11:01-A*02:01/HIV-1 RT and HLA-B*08:01-A*02:01/CMV complexes were concentrated to 12.5-15 mg/ml in SEC Buffer (150 mM NaCl, 25 mM Tris buffer, pH 8.0) and used for crystallization in 1:1 ratio of protein-crystallization buffer at 21 °C by sitting drops. Large plate crystals for HLA-A*11:01-A*02:01/HIV-1 RT were obtained in 0.02 M Sodium/Potassium phosphate, 0.1 M BIS-TRIS propane pH 8.5, 18-22% w/v PEG 3350 after 3 days. Small cubic crystals for HLA-B*08:01-A*02:01/CMV were obtained in 0.2 M Sodium fluoride, 0.1 M BIS-TRIS propane pH 8.5, 20-24% w/v PEG 3350 after 2 weeks. All crystals were harvested in crystallization buffer with 27% ethylene glycol using nylon cryo-loops (Hampton Research) and flash frozen in liquid nitrogen. Complete data collection was performed from single crystals under cryogenic conditions at Advanced Proton Source beamlines 19-ID-D and 24-ID-E for HLA-A*11:01-A*02:01/HIV-1 RT and B*08:01-A*02:01/CMV complexes, respectively. Diffraction images were indexed, integrated, and scaled using MOSFLM and HKL3000 in CCP4 Package. Structures were determined by molecular replacement method using Phaser and the previously published structure of HLA-A*02:01 (PDB ID: 5HHN) as a search model. Model building and refinement was performed using COOT and Phenix, respectively. Full data collection and refinement statistics are given in Table 2. Crystallographic figures were created using PyMOL.

Phylogenetic analysis

Multiple sequence alignments of the TCR-contact residues from approximately 10 most common allotypes from each subfamily *HLA-A*, *-B*, and *-C*, and of the α_1 and α_2 domains between the most similar wild-type alleles with the designed HLA-A*11:01-A*02:01^{6M} chimera were performed using ClustalOmega (46). Alignment files were further processed in ESPript (47). Phylogenetic trees were generated using best-fit models as calculated by MEGA7 (48) and processed in iTOL (49).

Biotinylation and tetramer formation

Biotinylation of the pMHC-I and soluble 10LH molecules was performed as previously described (50). In brief, BSP-tagged proteins were biotinylated using the BirA biotin-ligase bulk reaction kit (Avidity), according to the manufacturer's instructions. For the pMHC-I tetramer formation, Streptavidin-PE (Agilent Technologies, Inc.) at 4:1 monomer:streptavidin molar ratio was added to the biotinylated pMHC-I in the dark, every 10 min at room temperature over 10-time intervals.

Surface plasmon resonance

SPR experiments were conducted in duplicates or triplicates (n=2 or 3) using a BiaCore T200 instrument (Cytiva) in SPR buffer (50 mM NaCl, 20 mM sodium phosphate pH 7.2, 0.1% Tween-20). Approximately 650 resonance units (RU) of biotinylated-A*02:01/NY-ESO-1, A*02:01-B*08:01/NY-ESO-1, or the scFV 10LH were immobilized at 10 µL/min on a streptavidin-coated chip (GE Healthcare). TCR NYE-S1 or A*24:02/PHOX2B, and A*24:02-B*35:01/PHOX2B were captured on the coated surface followed

TABLE 2 Crystallography data collection and refinement statistics for the HLA-A*11:01-A*02:01/HIV-1 RT and B*08:01-A*02:01/CMV chimeras.

Data Collection	A*11:01-A*02:01/HIV-1 RT	B*08:01-A*02:01/CMV
PDB ID	8ERX	8ESH
Beamline	APS 19-ID-D	APS 24-ID-E
Space Group	$P_1 2_1 1$	I 2 3
Unit Cell (Å)	56.35 79.32 57.64 90.00 116.10 90.00	147.37 147.37 147.37 90.00 90.00 90.00
Wavelength (Å)	0.979	0.979
Resolution (Å)[1]	2.0 (2.03-2.00)	2.72 (9.01-2.72)
Rsym[2]	0.119 (0.416)	–
$\langle I/\sigma I \rangle$[3]	18.6 (3.5)	24.9 (2.2)
CC(1/2)	0.982 (0.859)	0.99 (0.834)
Completeness (%)[4]	99.6 (99.7)	99.9 (99.4)
Redundancy	3.6 (3.5)	17.4 (7.9)
Refinement		
Resolution (Å)	2.07	2.72
R-Factor [5]	0.192	0.214
Rfree [6]	0.231	0.259
Protein atoms	3171	3167
Ligands	1	1
Water Molecules	361	35
Unique Reflections	27641	14510
RMSD[7]		
Bonds	0.002	0.109
Angles	0.534	11.57
MolProbity Score (45)	0.79	1.59
Clash Score (45)	0.97	8.49
Percent Ramachandran plot		
Favored, allowed, outlier (%)	(98, 2, 0)	(97, 2, 0)

[1]Statistics for highest resolution bin of reflections in parentheses.
[2]$R_{sym} = \Sigma_h \Sigma_j \mid I_{hj} - \langle I_h \rangle \mid / \Sigma_h \Sigma_j I_{hj}$, where I_{hj} is the intensity of observation j of reflection h and $\langle I_h \rangle$ is the mean intensity for multiply recorded reflections.
[3]Intensity signal-to-noise ratio.
[4]Completeness of the unique diffraction data.
[5]R-factor = $\Sigma_h \mid IF_oI - IF_cI \mid / \Sigma_h |F_o|$, where F_o and F_c are the observed and calculated structure factor amplitudes for reflection h.
[6]R_{free} is calculated against a 5% random sampling of the reflections that were removed before structure refinement.
[7]Root mean square deviation of bond lengths and bond angles.

by a wash-out step with buffer at desired concentrations. Samples were injected over the chip at 25°C at a flow rate of 20 μL/min for 60 sec followed by a buffer wash with 180 sec dissociation time and equilibrium data were collected. The SPR sensorgrams, association/dissociation rate constants (k_a, k_d) and equilibrium dissociation constant K_D values were analyzed in BiaCore T200 evaluation software (Cytiva) using kinetic analysis settings or fitted using one-site specific binding by GraphPad Prism v9. SPR sensorgrams and saturation curves were prepared in GraphPad Prism v9.

1G4 TCR lentivirus production

Lenti-X 293T cells (Takara) were cultured in DMEM (Gibco), 10% FBS (Gibco), and Glutamax (Gibco) and were plated one day before transfection. Cells were transfected at a confluency of 80-90% with TransIT-293 (Mirus) using pMD2.G (Addgene #12259, gift from Didier Trono), psPAX2 (Addgene #12260, gift from Didier Trono), and pSFFV-1G4. Virus-containing media was collected 24- and 48-hours post-transfection, clarified by centrifugation at 500 g for 10 min, and incubated with Lenti-X concentrator (Takara) for at least 24 hours. Virus was pooled and concentrated 50-100x, resuspended in PBS, aliquoted, and stored at -80°C for subsequent T cell infections.

Primary human T cell tetramer staining

The studies involving human participants were reviewed and approved by the University of Pennsylvania review board. Written informed consent to participate in this study was provided by the participants. Healthy donor T cells were processed by the Human Immunology Core by magnetic separation of CD8+ T cells. Cells were cultured in Advanced RPMI (Gibco), 10% heat inactivated FBS (Gibco), Glutamax (Gibco), penicillin/streptomycin (Gibco), and 10mM HEPES (Quality Biological), supplemented with 300 U/mL recombinant IL-2 (NCI Biological Resources Branch). T cells were maintained at ~1 million cells/mL and were activated with a 1:1 ratio of Dynabeads Human T-Activator CD3/CD28 beads (Gibco) for 48 hours. 24 hours after initial activation, cells were either left untransduced or were transduced with lentivirus expressing the 1G4 TCR. Cells were debeaded by magnetic separation and expanded in the presence of IL-2. Transduction efficiency was determined by staining with an anti-Vβ13.1-APC antibody (Miltenyi Biotec.), typically greater than 50%. Cells were cryopreserved with CryoStor CS10 (StemCell Technologies). Thawed T cells were recovered and regrown in IL-2-containing complete medium for ~3 days prior to staining. Cells were harvested and washed with PBS, 1% BSA, 2 mM EDTA with 5 μg/mL PE-conjugated tetramers and incubated for 25 min at room temperature with mild agitation. After two washes with an RPMI-based buffer containing 1% FBS, cells were resuspended in 1:1000 Sytox Blue diluted in wash buffer to distinguish dead cells. Samples were processed on an LSR Fortessa (BD) and data analyzed by FlowJo v10.8.1.

Results

Structural analysis reveals discrete HLA surfaces for peptide binding and TCR recognition

We first sought to evaluate the degree of overlap between the residues which mediate interactions with the peptide and T cell receptor complementarity-determining regions, respectively. To do this, we analyzed 384 pMHC-I structures from a curated, in-house database derived from the Protein Data Bank (HLA3DB; https://hla3db.research.chop.edu/) and 36 pMHC-TCR structures from the ATLAS database (51). For each pMHC-I structure, we calculated a peptide-contact frequency as the percent of structures in which each position P of the first 180 amino acids comprising the peptide binding groove was within 4 Å from any peptide heavy atom (Figure 1A). Likewise, we calculated a TCR-contact frequency for each P using the available pMHC-TCR structures from the ATLAS database (Figure 1B). Based on this analysis, we classified MHC-I positions into three groups: *i)* peptide-only binding (PB) positions that primarily affect peptide binding with a non-zero peptide-contact frequency and a TCR-contact frequency less than 10%, *ii)* TCR-only binding (TB) positions which primarily affect TCR binding with a non-zero TCR-contact frequency and a peptide-contact frequency less than 10%, and *iii)* peptide-TCR binding (PTB) positions that affect both the peptide and TCR binding specificity with peptide- and TCR-contact frequencies greater than 10% (Figure 1C and Supplementary Table 2). In cases where both frequencies were below 10%, we selected the highest frequency to classify a given residue position as PB or TB. This analysis confirms that the HLA regions that mediate peptide binding show minimal overlap with TCR interaction surfaces.

We next aimed to evaluate the degree of sequence variance among residues belonging to the three identified structural groups, towards understanding whether these positions could be modified to create synthetic molecules with specific binding properties. Therefore, we aligned 2,896 sequences curated from the IMGT/HLA sequence database (53) using as reference the most common allotype HLA-A*02:01, and calculated a consensus score as the frequency of the most common amino acid at each position P. High consensus score implied highly conserved residues whereas low score suggested positions amendable to substitutions without compromising the stability of the pMHC-I complex (Figure 1D). For instance, position 80 with a TCR-contact frequency of 5% and a peptide-contact frequency of 74% belongs in the PB category, whereas position 69 with frequencies of 89% and 13%, respectively, is implicated in the formation of more significant contacts with TCRs. Both positions are good targets for designing MHCs with novel peptide or TCR binding profiles, since they have low consensus scores (45% and 42%) and thus are highly polymorphic. On the other hand, nearly all the residues involved in the formation of hydrogen bond networks with the peptide main chain have a consensus score above 90%, implying strictly conserved interactions (52) (Figure 1C and Supplementary Table 2). Notably, TB residues were overall more conserved, with the lowest consensus score at 67.3% (Supplementary Table 2), suggesting that the peptide- and

10.3389/fimmu.2023.1116906

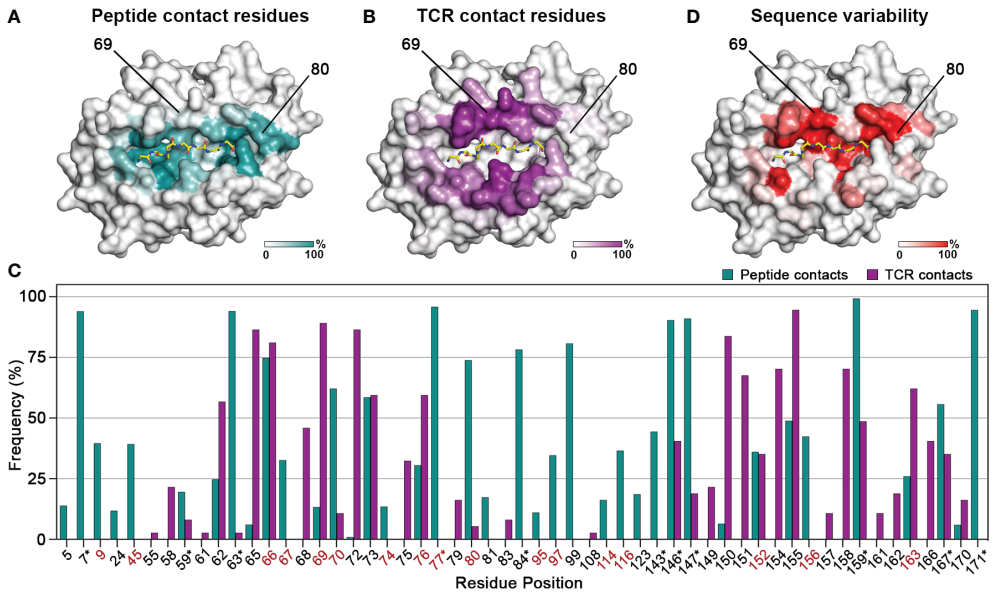

FIGURE 1
Contiguous molecular surfaces defined by polymorphic HLA residues mediate interactions with peptides, and TCRs. The calculated **(A)** peptide-contact, and **(B)** TCR-contact frequencies of the first 180 amino acids are highlighted in a white (low) and teal or purple (high) gradient, respectively. The structure of HLA A*02:01 (PDB ID: 1S9W) was used as template. **(C)** Bar graph of the peptide- and TCR-contact frequencies for positions with at least one value higher than 2%. Polymorphic positions with a consensus score below 60% are highlighted in red, while residues that form conserved hydrogen bond networks with the peptide main chain are marked with an asterisk (*) (52). **(D)** Sequence variability for each position P plotted as (100 - Consensus score) on the HLA-A*02:01 structure, from a white (low) to red (high) gradient.

TCR- contact residues followed distinct evolutionary paths to confer adaptability of interactions in the peptide binding groove. Taken together, we demonstrate that results from both structural and sequence analysis can be used to define a set of MHC-I residues that could be altered to modify peptide binding while maintaining the MHC-TCR binding surface intact and *vice versa*.

Engineering chimeric MHC-I molecules using a structure-guided approach

Driven by our sequence and structural analysis, we sought to explore the plasticity of existing HLA structures to accommodate novel peptides using a fixed-backbone design approach. We developed a method called 'CHaMeleon', to generate synthetic molecules that combine the peptide binding specificity of one allele (template or groove allele) with the TCR binding surface of another (base allele). Our approach takes as input an existing pHLA template structure and introduces a novel TCR binding surface in three steps: *i)* Generating a threaded model of a base allele sequence using a groove pHLA structural template, *ii)* Model optimization and binding energy analysis to identify the minimal set of mutations necessary to achieve an altered peptide binding specificity, and *iii)* experimental validation of the chimeric MHC-I refolded with the peptide that was observed in the original template structure of the groove allele (Figure 2A).

First, we used a 5 Å heavy atom distance threshold to define peptide contacting residues in the structure of a groove HLA with a known antigen, which would be used as a modeling template (Figure 2B). Next, we identified polymorphic residues which differ between the sequences of the groove and base alleles, and for all possible combinations of substitutions introduced on the base allele, we threaded the corresponding protein sequences on the template structure. We then performed energy optimization and assessed the stability of the resulting models by calculating the peptide:HLA interface energies using the *Rosetta* software (38) (Appendix Scripts 1-5) and (Figures 2C, D). This allowed us to evaluate the effect of specific residues on the overall stability for each chimeric molecule and, subsequently, narrow down the selection of groove residues to a minimal set of substitutions that would confer binding to the provided peptide. As expected, for all cases the chimeric models were more stable than models of the threaded base sequence on the groove template, but less stable than the corresponding native groove structures (Supplementary Table 3). For the top 2.5% structures with the lowest energies, we calculated enrichment scores for each polymorphic position, which represent the fraction of top chimeric HLAs carrying a specific substitution for a groove allele residue. More specifically, positions with an enrichment score of 1.0 indicate substitutions that are present in all structures, whereas substitutions with very low or 0 enrichment scores most likely affect the overall stability of the pHLA complex and thus are not favorable (Figure 2D). Additionally, mutations conferring different chemical properties at a certain position, such as a charged in the place of a neutral residue and *vice versa*, were always included in the minimal set whereas mutations replacing similar residues were excluded. To limit the number of substitutions impacting the TCR surface of the base allele, mutations in PTB positions were considered only if they contained a heavy atom within a more stringent threshold of 3.5 Å from the peptide. For the experimental validation of the designed chimeric HLAs, we performed previously established protein refolding (54) using groove-specific peptides, stability measurements by differential

10.3389/fimmu.2023.1116906

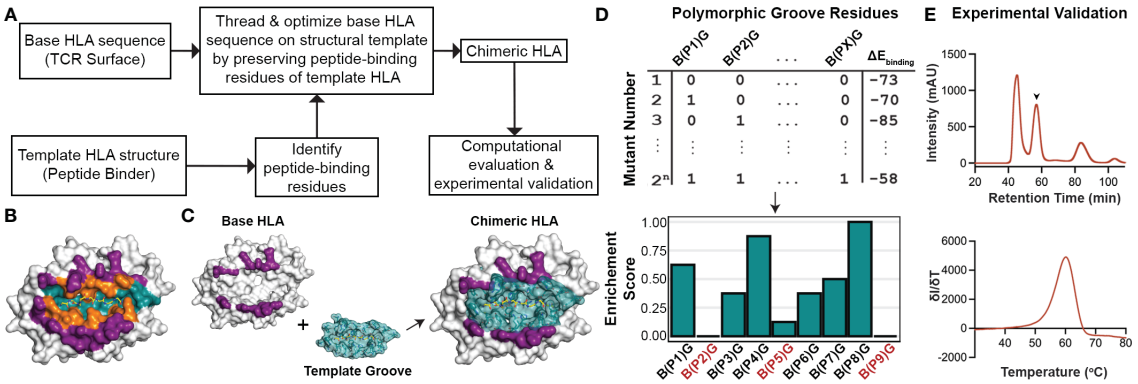

FIGURE 2
General workflow for generating chimeric HLA molecules using a fixed-backbone, structure-guided approach. **(A)** The general workflow of the CHaMeleon approach to generate chimeric MHC-I molecules. **(B)** The structure of HLA-A*02:01 bound to the peptide SLLMWITQC (PDB ID:1S9W) where the peptide-only (teal), TCR-only (purple) and peptide-TCR-binding (orange) residues are highlighted. **(C)** Grafting the peptide-biding groove of a template onto a base allele to create chimeric molecules. TCR-only positions are highlighted in purple and peptide-only or peptide-TCR-binding residues are highlighted in teal. The structure of HLA-A*02:01 (PDB ID:1S9W) was used as an example. **(D)** Exhaustive combinatorial sampling of groove allele substitutions on the base allele and binding energy calculations was performed to evaluate the chimeric HLA models. The top 2.5% of structures with lowest binding energies were used to calculate Enrichment Scores at each polymorphic position (PX) in the groove, which represents the fraction of chimeric HLAs with a specific mutation from base (B) to groove (G) allele residue. Positions with 0 or very low enrichment scores are highlighted in red. **(E)** Experimental validation of the chimeric pMHC-I by size exclusion chromatography (SEC; top). The protein peak is indicated by the arrow (57.5 min), while the additional peaks correspond to protein aggregates (47 min) and free β_2m (84 min). Thermal stability of the purified molecules was assessed using differential scanning fluorimetry (DSF; bottom) experiments.

scanning fluorimetry (DSF) analysis (55), and peptide binding assays *in vitro* (56) (Figure 2E). Our proposed rational approach for exploring combinations of groove specificities and TCR contact surfaces from naturally occurring MHC-I alleles provides the means to study the principles of pMHC-I/TCR recognition and assess TCR cross-reactivity, with important biomedical ramifications in the design of peptide-centric therapeutics.

Altering B- and F-Pocket specificities on HLA-A*02:01

Considering that the primary anchor positions for peptide binding onto MHC-I molecules are the P2 and P9 (20), we employed the CHaMeleon approach to design synthetic pMHC-I molecules with altered peptide specificities by changing the B- and F-pockets of a base allele. For this purpose, we used the common human HLA-A*02:01 allotype as base with a preference for hydrophobic residues at positions P2 and P9 (Figure 3A and Supplementary Figure 1A). As structural templates, we used the previously defined X-ray structures of HLA-A*11:01 (PDB ID: 1Q94) and C*07:02 (PDB ID: 5VGE) together with the high affinity, immunodominant peptide antigens HIV-1 RT (AIFQSSMTK) and RYR (RYRPGTVAL), respectively. These alleles show distinct peptide specificities with a preference for the charged Lys/Arg residues in the P9 anchor for HLA-A*11:01, and aromatic or charged residues in the P2 anchor for C*07:02 (Supplementary Figure 1B). We identified and substituted 9 and 14 residues from HLA-A*11:01 and C*07:02 within the A*02:01 groove to generate the HLA-A*11:01-A*02:01 and C*07:02-A*02:01 chimeras, respectively (Table 1). We next predicted the peptide specificities of the chimeric molecules (see Methods) and confirmed that the introduced amino acid substitutions resulted in altered peptide-binding specificities in positions P2 and P9, to resemble the sequence of the groove alleles (Figure 3A). Comparison of the calculated energy values of the threaded structures showed that in both cases the chimeric molecules were more stable than the base but not the groove alleles (Supplementary Table 3). Electrostatic surface potential analysis using the *Rosetta* models of each designed chimeric MHC-I, revealed altered surface charges of the HLA-A*02:01 groove, which are known to play a crucial role in selective peptide binding (35). As expected, the groove of HLA-A*11:01-A*02:01 was negatively charged, while HLA-C*07:02-A*02:01 changed to negatively charged A- and B-pockets but maintained a positively charged F-pocket (Figure 3B).

To experimentally validate the designed chimeric HLAs, we refolded HLA-A*11:01-A*02:01 and C*07:02-A02:01 with the HLA-A*11:01-specific HIV-1 RT and HLA-C*07:02-specific RYR peptides, respectively. In both cases we were able to purify recombinant pMHC-I complexes by SEC (Supplementary Figure 1C) and further DSF analysis revealed melting temperatures characteristic of properly conformed peptide-bound molecules (T_m=51.8°C for A*11:01-A*02:01/HIV-1 RT and 49.8°C for C*07:02-A*02:01/RYR, Figure 3C) (55). Taken together, our SEC and DSF results revealed that HLA groove-specific mutations can form properly folded and stable chimeric pMHC-I molecules after introducing target groove-specific peptides. We then sought to determine whether these peptides adopted a similar conformation compared to their parental template HLA, considering that the conformation and mobility of the bound peptide could affect the affinity for TCR recognition (32, 57). While we attempted to solve the crystal structures for both complexes, diffraction-quality crystals were obtained solely for the HLA-A*11:01-A*02:01/HIV-1 RT chimera. The best crystal diffracted to a 2.02 Å resolution and had clear electron density for the HIV-1 RT peptide, which we modeled in the F_0-F_c electron density map (Table 2 and Supplementary Figure 2). Overlay of the HIV-1 RT peptide from the wild-type HLA-A*11:01 versus the chimeric pMHC-I complex,

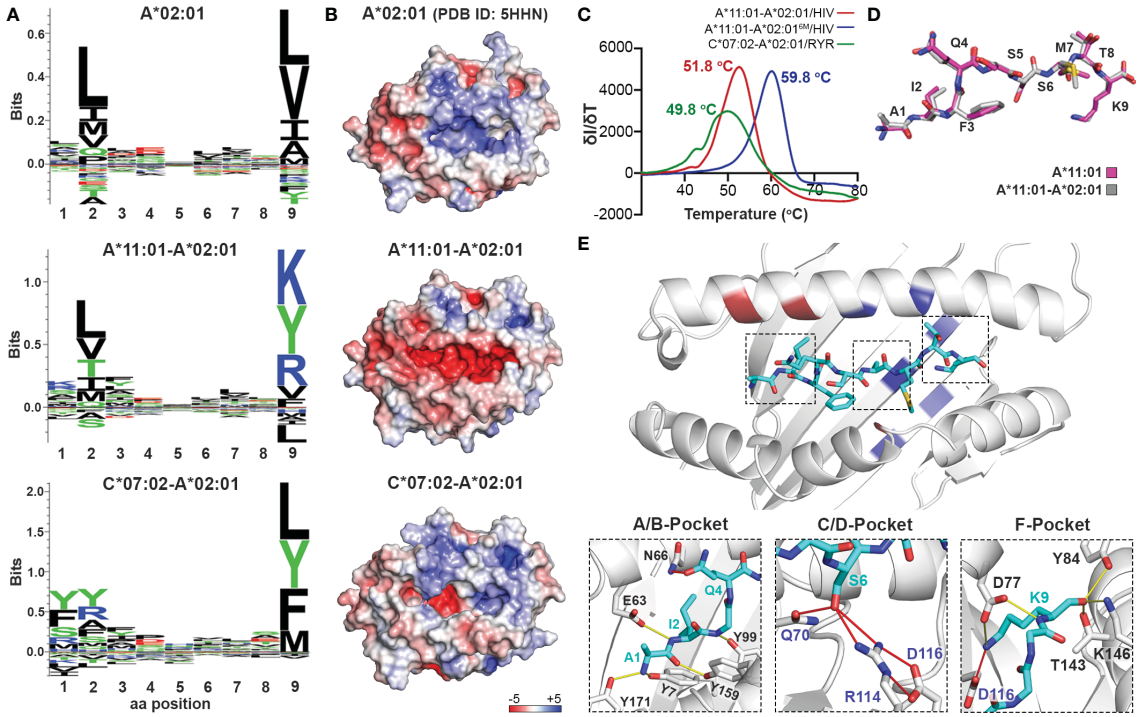

FIGURE 3
Production of chimeric HLA-A*02:01 peptide complexes with altered B- or F-pocket specificities according to A*11:01 or C*07:02 structural templates. **(A)** Sequence logos of HLA- A*02:01, A*11:01-A*02:01, and C*07:02-A*02:01 molecules rendered using an in-house protocol and visualized in Seq2Logo from the NetMHCpan4.0 (40). **(B)** Electrostatic surface potential analysis for HLA-A*02:01 (PDB ID: 5HHN), A*11:01-A*02:01, and C*07:02-A*02:01 calculated using the APBS solver in PyMOL. In all panels, the electrostatic surface potential is shown as a range between +5 kT/e (in blue) to -5 kT/e (in red) representing positive and negative charges, respectively. k_B, Boltzmann constant; T, temperature; e, unit charge. **(C)** Thermal stabilities of HLA-A*11:01-A*02:01/HIV-1 RT (red), A*11:01-A*02:01^{6M}/HIV-1 RT (blue), and C*07:02-A*02:01/RYR (green). Data are mean ± SD obtained for n = 3 technical replicates. **(D)** Overlay of the HIV-1 RT peptide bound to the chimeric HLA-A*11:01-A*02:01 (grey) and wild-type A*11:01 (magenta) molecules. **(E)** Crystal structure of the HLA-A*11:01-A*02:01/HIV-1 RT complex. Substitutions of the HLA-A*11:01-A*02:01 (red and blue) and A*11:01-A*02:01^{6M} (blue) chimeras are highlighted. Hydrogen bonds and salt bridges between the peptide and the base or groove allele residues are represented by yellow or red lines, respectively. Peptide, A*02:01-specific, and A*11:01-specific residues are labeled in cyan, black, and blue font, respectively.

revealed that both peptides adopted an identical backbone conformation with a deviation of 0.543 Å in RMSD values (Figure 3D and Supplementary Table 4). Additionally, we observed that while the B-pocket was occupied by Ile2 which was principally stabilized through hydrogen bonds with the peptide main chain, the F-pocket was occupied by Lys9 projecting directly into the HLA groove (Figure 3E). The observed accommodation of Lys9 into the F-pocket was the result of two salt bridge interactions between the Lys side chain and the introduced HLA-A*11:01 groove-specific residues Asp74 and Asp116 (Figure 3E). These residues appeared to orient and stabilize the Lys9 side chain within the groove, while the main chain was further stabilized by hydrogen bonds with the HLA-A*11:01-specific Asp74 and A*02:01-specific Tyr84, Thr143, Lys146, and Trp147 (Figure 3E). Interestingly, the introduced mutations Gln70 and Arg114 were responsible for forming multiple hydrogen bonds with Ser6 of the peptide within the C/D-pocket (Figure 3E). While we identified distinct HLA-A*11:01 groove-specific mutations crucial for peptide binding, several residues did not appear to be necessary for peptide association. We, thus, hypothesized we could optimize and refine the HLA-A*11:01-A*02:01 chimera, by re-engineering the HLA-A*02:01 base to introduce only six groove-specific mutations as opposed to the previous nine. This new six mutant HLA-A*11:01-A*02:01 (A*11:01-A*02:01^{6M}) chimera was not only capable of refolding with the HIV-1 RT peptide (Supplementary Figure 1C) but was also significantly more stable (T_m=59.8 °C) compared to the initial construct (T_m=51.8 °C) (Figure 3C). Taken together, our HLA-A*11:01-A*02:01 structure revealed that the newly introduced peptide antigen adopted an identical conformation to that seen in the wild-type, parental HLA-A*11:01 structure (Supplementary Table 4) (58), further validating our fixed-backbone design approach. Finally, based on the observed interactions with the peptide backbone, our design could be further optimized to improve pMHC-I complex stability.

Introducing a new P5 anchor within the C-Pocket of HLA-A*02:01

Naturally occurring HLA molecules can bind and display a wide distribution of peptide sequences (termed peptide repertoires), that consist of polar, hydrophobic, or charged amino acids at defined anchor positions. However, the peptide pools presented by known alleles do not cover the entire range of amino acid combinations on a peptide sequence, implying that the displayed repertoire at the population level contains blind spots of 'forbidden' peptides (22). Thus, we explored further the applications of the CHaMeleon workflow to modify the set of binder peptides of an HLA molecule of interest, by introducing novel anchor positions within the HLA-A*02:01 groove. For this purpose, we selected HLA-B*08:01 with a

distinct preference for peptides with charged residues (Arg/Lys) at position P5 (Figure 4A). To generate the HLA-B*08:01-A*02:01 chimera, a minimal set of 18 B*08:01-specific residues was identified and substituted within the A*02:01 groove based upon *Rosetta* threading and binding energy analysis, using the crystal structure of wild-type HLA-B*08:01 refolded with the CMV (ELNRKMIYM) peptide as a modeling template (PDB ID: 4QRT; Table 1). We experimentally validated the ability of the designed chimeric HLA to form stable protein complexes with the desired CMV peptide, using *in vitro* refolding, purification and DSF analysis which revealed a T_m of 49.8°C (Supplementary Figure 1D and Figure 4B).

We next examined whether the HLA-B*08:01-A*02:01 chimera could recapitulate the peptide-binding specificity of the groove allele we used as a structural template, namely HLA-B*08:01. We selected the HLA*B:08:01 specific CMV and EBV (FLRGRAYGL), the A*02:01 specific TAX9 (LLFGYPVYV) and p90 (RLRGVYAAL), and the B*40:01 specific B40 (TEADVQQWL) peptides, as well as the H2-L^d specific p29 (YPNVNIHNF) epitope from the HIV gp120 protein, based on established epitopic sequences that were further validated by NetMHCPan4.0 predicted binding affinities (Supplementary Table 5). We then refolded the chimeric HLA with a B*08:01-specific photolabile peptide (EBV* = FLRGRAJGL, where J is the 3-amino-3-(2-nitrophenyl)-propionic acid) (43) with a T_m=48.2°C, to perform UV-mediated peptide exchange experiments (Supplementary Figure 1D and Figure 4B) (44). Incubation with 10-fold molar excess of peptide followed by UV-irradiation led to an up-shift in the T_m peak for EBV (T_m=52.9°C) (Figure 4B), indicating the formation of stable pMHC-I molecules. Contrariwise, the p29 weak-binder peptide was unable to exchange (T_m=40.4°C), demonstrating that the chimeric HLA groove is selective for HLA-B*08:01-specific peptides (Figure 4B). Based on the sequence logo for HLA-B*08:01 peptide specificity profile (Figure 4A), we hypothesized that introduction of a charged residue in P5 of the weak-binder p29 peptide would enhance binding, and therefore designed the mutant peptide N5R p29 ($p29^{N5R}$, YPNVRIHNF). Notably, peptide exchange experiments with HLA-B*08:01-A*02:01/FLRGRAJGL and excess of the mutant peptide resulted in a thermal shift of 23°C compared to p29 (T_m=63.6°C vs. 40.4°C, Figure 4B), suggesting the formation of stable complexes. The p90 peptide showed very little exchange with a T_m of 37.9°C, while the A*02:01- and B*40:01-specific peptides TAX9 and B40 were unable to exchange (Supplementary Table 6). Altogether, our peptide exchange data further support that the HLA-B*08:01-A*02:01 chimera can preferably bind epitopes with high affinity for the binding groove of the template allele, namely B*08:01.

While we were able to demonstrate that a synthetic MHC-I molecule with an additional P5 anchor could be designed and refolded, whether the B*08:01-specific peptide adopted an identical conformation compared to the wild-type template allele remained to be evaluated. Hence, we attempted to solve the structure of HLA-B*08:01-A*02:01/CMV complex in an I23 space group and obtainedcrystals which diffracted to a 2.72 Å resolution (Table 2). As in the HLA-A*11:01-A*02:01 crystal structure, we observed unambiguous electron densities for the CMV peptide that we modeled within the F_0-F_C electron density map (Supplementary Figure 3). Overlay of the CMV peptide bound to the wild-type HLA-B*08:01 and the B*08:01-A*02:01 chimera revealed an identical backbone conformation with a deviation of 0.495 Å in RMSD values between the two structures (Figure 4C and Supplementary Table 4), in agreement with our previous results for the HLA-A*11:01-A*02:01 chimera. While the F-pocket was occupied by Met9 and stabilized by hydrogen bonds along the main chain, the A-pocket was occupied by Glu1 which side chain interacted with the

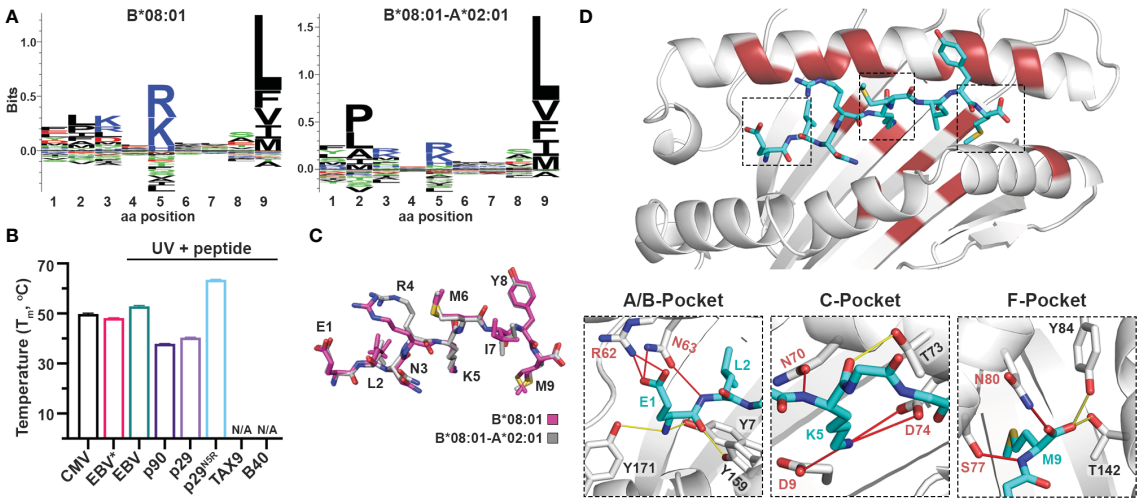

FIGURE 4
Introduction of a P5 anchoring specificity into the C-pocket of HLA-A*02:01 using a B*08:01 structural template. **(A)** The sequence logos of the HLA-B*08:01 (left), and B*08:01-A*02:01 (right) rendered using an in-house method and visualized in Seq2Logo from the NetMHCpan4.0 (40). **(B)** Thermal stabilities of HLA-B*08:01-A*02:01 refolded with CMV (ELNRKMIYM) or EBV* (FLRGRAJGL, where J is the 3-amino-3-(2-nitrophenyl)-propionic acid) and after UV-irradiation in the presence of 10-fold molar excess of EBV, p90, p29, $p29^{N5R}$, TAX9, and B40 peptides. Data are mean ± SD obtained from n = 3 technical replicates. N/A, no exchange. **(C)** Overlay of the CMV peptide bound to the chimeric B*08:01-A*02:01 (grey) and wild-type B*08:01 (magenta) molecules. **(D)** Crystal structure of HLA-B*08:01-A*02:01/CMV complex where substitutions of the groove residues are highlighted in red. Hydrogen bonds and salt bridges between the peptide and the base or groove allele residues are shown as yellow or red lines, respectively. Peptide, A*02:01-specific, and B*08:01-specific residues are labeled in cyan, black, and red font, respectively.

B*08:01-specific residues Arg62 and Asn63 (Figure 4D). A strong electron density was observed for Lys5 within the C-pocket which formed three salt bridge interactions and one hydrogen bond with the B*08:01-specific residues Asp9, Asn70 and Asp74 (Figure 4D), suggesting that these residues are crucial for stabilizing the peptide within the HLA groove. Altogether, these findings support the introduction of a novel P5 anchor within the HLA-A*02:01 groove to generate a chimeric molecule with a distinct peptide repertoire, without affecting the adopted conformation of the bound peptide.

Use of chimeric HLAs as molecular probes for identifying peptide-centric receptors

We next sought to address whether we can use chimeric HLAs to evaluate the extent to which interactions with specific TCRs or therapeutic antibodies are dependent upon interactions with HLA framework residues. Towards this goal, we tested the wild-type TCRs 1G4 (31) and NYE-S1 (30) which recognize the tumor epitope NY-ESO-1 (SLLMWITQV) on HLA-A*02:01, as well as the peptide-centric engineered CAR 10LH that targets the neuroblastoma peptide PHOX2B (QYNPIRTTF) presented by A*24:02 (34). To design chimeric HLAs able to bind these epitopes on their non-physiological base we, first, performed a phylogenetic analysis of the TCR contacting residues of selected *HLA-A*, *-B*, and *-C* allotypes to identify alleles with the most dissimilar TCR interacting surfaces compared to HLA-A*02:01 and A*24:02 (Figure 5A). Based on our analysis, we selected HLA-B*08:01 and B*35:01 to generate the HLA-A*02:01-B*08:01 and HLA-A*24:02-B*35:01 chimeras presenting the NY-ESO-1 and PHOX2B peptide antigens, respectively. Using the CHaMeleon approach, we identified and introduced 11 HLA-A*02:01 and 16 A*24:02 residues in the peptide-binding grooves of B*08:01 and B*35:01, respectively (Table 1). Both chimeric molecules were successfully refolded with their respective target peptides (Figure 5B) and, notably, the HLA-A*02:01-B*08:01 chimera was able to form a more stable complex with NY-ESO-1 compared to the wild-type A*02:01 (T_m=65.2°C vs. T_m=62.0°C), as revealed by DSF experiments (Figure 5C). Contrariwise, the HLA-A*24:02-B*35:01 chimera was destabilized by almost 15 °C compared to the wild-type A*24:02 (T_m=48.3°C vs. T_m=65.9°C), although was still able to form loaded pMHC-I complexes (Figure 5C).

To test our hypothesis, we stained primary CD8+ T cells transduced with the wild-type TCR 1G4 that recognizes the NY-ESO-1 peptide presented by A*02:01 (31) (Supplementary Figure 4), and generated phycoerythrin (PE) tetramers of HLA-A*02:01/NY-ESO-1 and A*02:01-B*08:01/NY-ESO-1, as previously described (59). As a negative control, we used HLA-A*02:01 refolded with the NY-ESO-1 peptide carrying an Ala substitution in position 5, namely NY-ESO-1^{W5A} (SLLMAITQV), which has been shown to be essential for TCR recognition (60). Analysis by flow cytometry revealed lack of staining with HLA-A*02:01/NY-ESO-1^{W5A} and A*02:01-B*08:01/NY-ESO-1 compared to the wild-type A*02:01/NY-ESO-1 tetramers (Figure 5D). These results confirm that TCR 1G4 recognizes specific peptide:HLA antigens in a highly restricted manner (61), as interactions were disrupted both in the case of the wild-type MHC-I presenting a peptide with a single amino acid substitution and the chimeric pMHC-I presenting the target peptide. We, next, used the newly characterized NYE-S1 TCR selective for HLA-A*02:01/NY-ESO-1 (30) to quantitively assess pMHC-I/TCR interactions using surface plasmon resonance (SPR) experiments. Soluble NYE-S1 bound weakly to immobilized HLA-A*02:01/NY-ESO-1 with a dissociation equilibrium constant K_D = 4.9 μM, in agreement with previous studies (30), but was unable to interact with both HLA-A*02:01/NY-ESO-1^{W5A} and A*02:01-B*08:01/NY-ESO-1 chimeric molecules (Figure 5E and Supplementary Figures 5A, B). Additionally, we tested the scFv-based CAR 10LH, which is selective for A*24:02/PHOX2B and has been shown to interact with this specific epitope even when presented by different HLAs, i.e. HLA-A*23:01 and B*14:02 (34). As a negative control, we used HLA-A*24:02 refolded with PHOX2B peptide carrying an Ala substitution in P6, namely PHOX2B^{R6A}, which completely disrupts interactions with 10LH (34). As expected, 10LH bound to HLA-A*24:02 presenting the wild-type PHOX2B peptide with a K_D of 11.1 nM but not the mutated PHOX2B^{R6A} (Figure 5E and Supplementary Figures 5C, D). Notably, the chimeric HLA-A*24:02-B*35:01/PHOX2B and 10LH interactions were 20-fold weaker with an estimated nanomolar range K_D compared to the wild-type (Figure 5E and Supplementary Figures 5E, F). However, the observed 200 nanomolar binding still falls within the affinity range (up to micromolar) for TCRs/CARs and their pHLA targets which has been demonstrated to sufficiently trigger T cell killing (62, 63).

To explore the structural basis of the loss of TCR recognition for the chimeric pMHC-I molecules, we compared the TCR-interacting surfaces of the generated chimeric models. We observed that 6 out of 8 polymorphic TCR residues for HLA-A*02:01-B*08:01 and 7 out of 10 for A*24:02-B*35:01 chimeras were residues of the base allele and could, thus, affect TCR/CAR recognition (Figure 5F). To further determine which HLA-B*08:01 base residues were responsible for the loss of NYE-S1 recognition, we compared them to the A*02:01 residues responsible for TCR binding based on the solved crystal structures of HLA-A*02:01/NY-ESO-1 with the TCRs 1G4 and NYE-S1 (30, 31). We identified the HLA-A*02:01 residue Arg65 to be important for 1G4 and NYE-S1 binding along the α_1 helix, forming interactions with Asp55 and Asp67 of the CDR2β loops, respectively (Figure 5G). In HLA-A*02:01-B*08:01 chimera, this residue was replaced by Gln65 of the wild-type B*08:01, suggesting that disruption of these interactions is crucial for TCR binding. Interestingly, the same position differs between HLA-A*24:02 and B*35:01 (Figure 5F), however had no effect on 10LH recognition, as expected for the peptide-centric CARs which are not constrained by the germline-encoded CDR1-2/MHC interactions. Taken together, our cell-based and biophysical data confirm that the peptide antigen alone is not sufficient to maintain known pMHC-I/TCR interactions when presented in the context of a divergent HLA framework surface and suggest that loss of binding can occur even with a single amino acid substitution on the MHC-I/TCR interacting surface. In contrast, recognition by the peptide-centric CAR 10LH was not disrupted, highlighting the potential of scFV-based immunotherapies to target a broad range of allotypes.

Discussion

The highly polymorphic nature of the MHC-I peptide binding groove highlights a stable structural scaffold which can be adapted to accommodate a diverse panel of ligands (6). While human MHC-I

10.3389/fimmu.2023.1116906

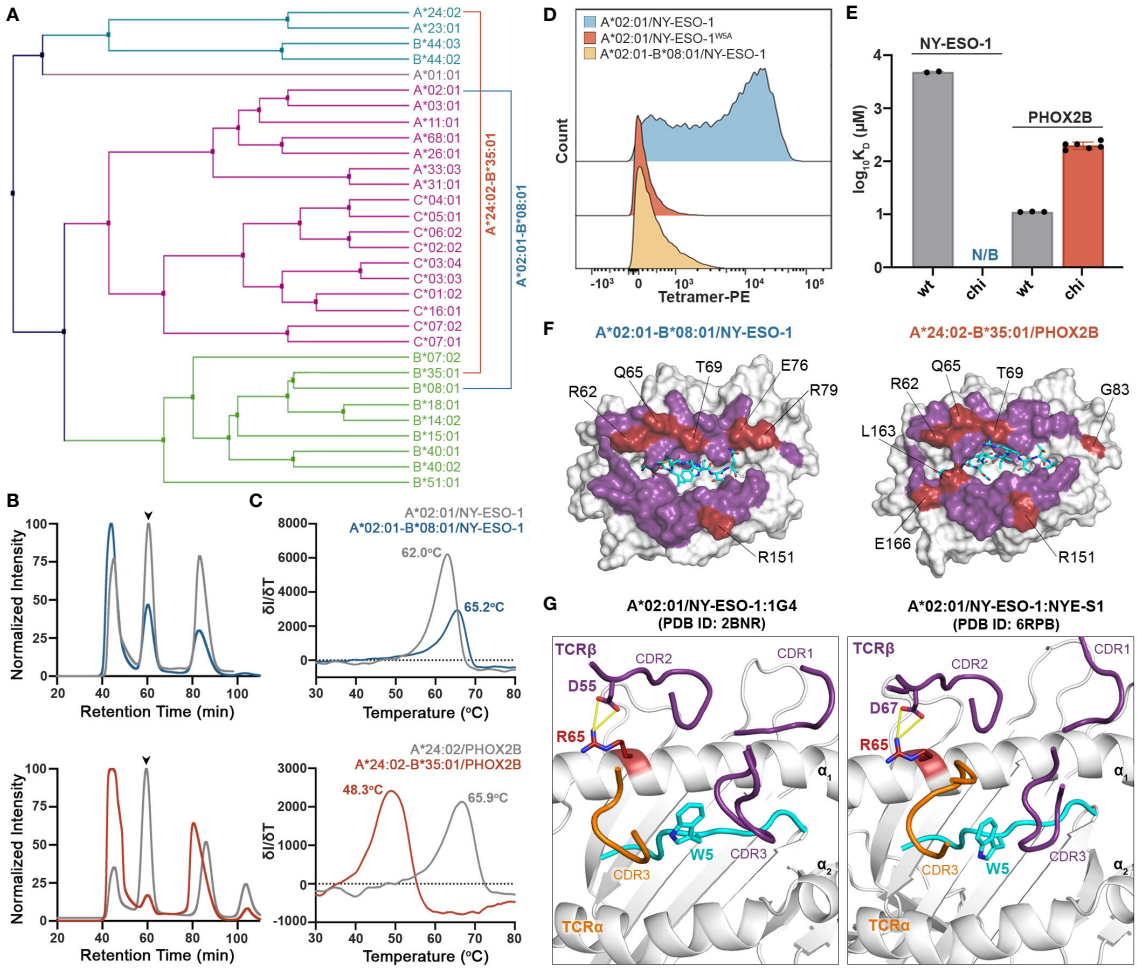

FIGURE 5
Application of chimeric HLAs as probes for assessing peptide-centric interactions with immune receptors for targeted therapy. **(A)** Phylogenetic analysis of a divergent set of common HLA allotypes using the TCR contacting residues to define sequence similarity. **(B)** SEC traces of recombinant HLA-A*02:01/NY-ESO-1, A*02:01-B*08:01/NY-ESO-1, A*24:02/PHOX2B, and A*24:02-B*35:01/PHOX2B molecules. The protein peaks are indicated by the arrows. **(C)** Melting temperatures (T_m, °C) of the pMHC alleles in **(B)** determined by DSF experiments. Data are mean ± SD obtained for n = 3 technical replicates. **(D)** Staining of 1G4-transduced primary CD8+ T cells with PE-conjugated tetramers of A*02:01 presenting the wild-type NY-ESO-1 or the mutated NY-ESO-1^{W5A} peptides, and the chimeric A*02:01-B*08:01/NY-ESO-1 complex. Staining was observed only in the case of A*02:01/NY-ESO-1, suggesting positive recognition by the TCR, whereas in the case of the negative control and the chimeric pMHC the interactions are disrupted. **(E)** Comparison of the SPR determined K_D values for NYE-S1 and 10LH interacting with HLA-A*02:01 and A*24:02 wild-type and chimeric molecules presenting NY-ESO-1 and PHOX2B peptides, respectively. Data are mean ± SD for n = 2 (NYE-S1) or n = 3 (10LH) technical replicates. K_D, equilibrium constant; N/B, no binding. **(F)** Surface structure of the *Rosetta* model of HLA-A*02:01-B*08:01/NY-ESO-1 and A*24:02-B*35:03/PHOX2B chimeras, where all TCR-contact residues are highlighted (purple and red). The wild-type B*08:01 or B*35:01 residues are shown in red. **(G)** Structural comparison of the HLA-A*02:01/NY-ESO-1 complex bound by the TCRs 1G4 (PDB ID: 2BNR) and NYE-S1 (PDB ID: 6RPB). The HLA-A*02:01, the NY-ESO-1 peptide, and the TCR-α and -β chains are colored in white, cyan, orange, and purple, respectively. The identified Arg65 is represented as a single stick (in red) and its interactions with TCR-β chain are in yellow.

allotypes encompass a plethora of peptide binding specificities, there remain gaps in the repertoire of antigens which can be recognized and displayed by the existing HLA proteins (20, 22). On the other hand, TCRs can recognize different peptide:MHC-I complexes through a combination of peptide-centric and germline contacts with MHC-I framework residues and are limited to a restricted range of interactions with HLAs. Here, we outline a systematic approach to generate synthetic MHC-I molecules blending desired peptide and TCR interaction properties. Our analysis shows that we can use existing structural information to discern MHC-I residues responsible for peptide binding and TCR recognition, enabling us to design chimeric molecules according to a fixed-backbone protocol that is guided by a structural template. We provide biochemical evidence that the HLA pockets within the groove can be altered to accommodate new peptides while maintaining the TCR surface features of a specific HLA allotype. Our approach is further validated by the solved crystal structures for two chimeric MHC-I molecules, which reveal that the peptide is presented in the specified conformation. Notably, all-atom RMSD values between the crystal structure and the *Rosetta* model were below 2 Å both for the peptide and MHC-I α_1/α_2 domains (Supplementary Table 4). Finally, functional characterization using *in vitro* tetramer staining and biophysical binding experiments demonstrates the practical utility of our chimeric molecules as screening tools to evaluate peptide-centric interactions with T cell receptors and therapeutic antibodies, respectively.

Our work offers insights into principles underpinning the molecular evolution of MHC-I allotypes, and the emergence of distinct supertypes (7). Owning to the stability and malleability of the MHC-I scaffold, a minimal set of amino acid substitutions can lead to drastic changes in peptide binding preference, and thereby supertype divergence (64). It is worth noting that for some of the chimeric molecules designed in our study, we can identify known HLA allotypes with similar peptide-binding groove sequences and assumed peptide binding preferences. In particular, the HLA-A*11:01-A*02:01 chimera, designed to accommodate peptides with positively charged P9 residues, is similar in sequence (4 amino acid differences among peptide-binding residues) to the known allotypes HLA-A*03:05 and A*03:17 (A03 supertype) (64) that have acidic F-pockets, and therefore are predicted to bind positively charged peptides (Supplementary Figure 6). Likewise, the designed HLA-A*11:01-A*02:01^{6M} chimera possessing the groove of A*11:01 (A03 supertype), differs in 4 peptide-binding residues with each of the HLA-A*02:35 and A*02:246 allotypes (A02 supertype) (64) (Supplementary Figure 6). Interestingly, a combination of all substitutions from the wild-type alleles, where two of them are shared, results in our computationally designed chimeric sequence (Supplementary Figure 6). This in turn suggests that our synthetic molecules incorporate features from distinct supertypes that could naturally occur over time and represents an example of convergent evolution between A03 and A02 supertypes. However, there is no structural evidence that these allotypes bind the peptides in a similar backbone conformation compared to the wild-type template allele. Our study also describes a chimeric HLA, namely HLA-B*08:01-A*02:01, with no direct equivalent amongst naturally occurring HLAs (15 amino acid differences with the closest allotype). This could be either due to lack of sequence data on already existing allotypes in the population, or because this specific peptide binding motif has not yet been sampled by the ongoing evolutionary process for A02 alleles. In summary our designed molecules provide evidence that barriers between different supertypes are low and provide an avenue for creating novel allotypes which are not represented in the existing HLA repertoires.

Chimeric MHC molecules designed with desired peptide-binding grooves and TCR-interacting surfaces have potential immune system engineering applications towards the development of targeted therapies for breaking tolerance for weak disease- or cancer-associated antigens. Current approaches to break self-tolerance include the use of altered peptide ligands for personalized cancer vaccines (65, 66), and the introduction of checkpoint inhibitors to overcome peripheral tolerance (67). A recent study has shown that introduction of point mutations at the TCR binding interface of native MHCs presenting tumor-associated antigens can be used to activate T cells through allorecognition (33). Using the CHaMeleon approach outlined in this work, we can introduce novel anchor positions to the peptide-binding groove of selected MHCs and generate chimeric molecules presenting established tumor-associated antigens with modified TCR interaction surfaces, relative to a specific HLA allotype. These chimeric HLAs can be then used as immunogens, to elicit alloreactive T cell responses for self-antigens that are upregulated in cancer (68). In a similar manner, epitope-focused vaccination strategies are based on eliciting antibodies towards non-immunogenic antigens with multiple applications against diseases and cancer therapy (69, 70). More importantly, with the advent of CAR-T cell therapies (71), there has been an increasing interest in designing peptide-centric receptors that are highly specific for a certain peptide sequence and are relatively tolerant to amino acid substitutions of HLA framework residues within the peptide:MHC complex (34). As implied by our proof of concept *in vitro* binding studies, chimeric MHC-I molecules can serve as screening tools to identify peptide-centric CARs for specific antigens. When prepared in tetramerized form and used as selection markers in existing directed evolution and antibody panning approaches (72), chimeric peptide:MHC complexes can enable the development of therapies which can cover larger cohorts of patients.

Collectively, our results suggest that we are capable of re-capitulating and potentially expanding the antigen presentation profile of target alleles through a structure-guided, systematic redesign of the MHC-I peptide binding groove. Our approach serves as a toehold for understanding the molecular evolution and functional divergence of HLA allotypes, while also providing useful screening tools to facilitate the development of tolerance-breaking vaccines and targeted CAR-T therapies.

Data availability statement

The datasets presented in this study can be found in online repositories. The names of the repository/repositories and accession number(s) can be found below: http://www.wwpdb.org/, 8ERX; http://www.wwpdb.org/, 8ESH.

Author contributions

OA and NS conceived and designed the CHaMeleon workflow. OA performed phylogenic analysis of HLA sequences and analysis of existing database structures. TF, GP, and MY prepared and purified all recombinant MHC-I and TCRs. TF, GP, and MY performed DSF analysis of MHC-I complexes. TF and JD performed UV-irradiation photo-exchange and DSF analysis of MHC-I complexes. TF performed X-ray crystallography and structural analysis. TF and YS performed SPR analysis. JD and DD performed MHC-I tetramerization and flow cytometry analysis. NS acquired funding and supervised the project. GP, TF, and NS wrote the manuscript, with feedback from all the authors. All authors contributed to the article and approved the submitted version.

Funding

This research was supported through grants by NIAID (5R01AI143997), NIGMS (5R35GM125034), and NIDDK (5U01DK112217) to NS. DD is supported by The Mark Foundation for Cancer Research.

Acknowledgments

We acknowledge Dr. Andy Minn (University of Pennsylvania) for providing the primary CD8+ cells for tetramer staining and flow-cytometry, and Myrio Therapeutics (Australia) for providing us with the 10LH scFv protein sample for SPR studies. We are grateful to Drs. Ronen Marmorstein and Leena Mallik (University of Pennsylvania) for assistance with data collection scheduling, structure validation and final PDB deposition. We thank Sagar Gupta for assistance with computational analysis. We further acknowledge the staff at APS beamlines 19-ID-D and 24-ID-E for beamtime and data collection assistance.

Conflict of interest

Authors NS, TF, and OA are co-inventors in provisional patent applications related to this work.

The remaining authors declare that the research was conducted in the absence of any commercial or financial relationships that could be construed as a potential conflict of interest.

Publisher's note

All claims expressed in this article are solely those of the authors and do not necessarily represent those of their affiliated organizations, or those of the publisher, the editors and the reviewers. Any product that may be evaluated in this article, or claim that may be made by its manufacturer, is not guaranteed or endorsed by the publisher.

Supplementary material

The Supplementary Material for this article can be found online at: https://www.frontiersin.org/articles/10.3389/fimmu.2023.1116906/full#supplementary-material

References

1. Zimmer J, Andrès E, Donato L, Hanau D, Hentges F, de la Salle H. Clinical and immunological aspects of HLA class I deficiency. *QJM: Int J Med* (2005) 98:719–27. doi: 10.1093/qjmed/hci112

2. Blum JS, Wearsch PA, Cresswell P. Pathways of antigen processing. *Annu Rev Immunol* (2013) 31:443–73. doi: 10.1146/annurev-immunol-032712-095910

3. Riedhammer C, Weissert R. Antigen presentation, autoantigens, and immune regulation in multiple sclerosis and other autoimmune diseases. *Front Immunol* (2015) 6:322. doi: 10.3389/fimmu.2015.00322

4. Koutsakos M, Illing PT, Nguyen THO, Mifsud NA, Crawford JC, Rizzetto S, et al. Human CD8+ T cell cross-reactivity across influenza a, b and c viruses. *Nat Immunol* (2019) 20:613–25. doi: 10.1038/s41590-019-0320-6

5. Dhatchinamoorthy K, Colbert JD, Rock KL. Cancer immune evasion through loss of MHC class I antigen presentation. *Front Immunol* (2021) 12:636568. doi: 10.3389/fimmu.2021.636568

6. Robinson J, Guethlein LA, Cereb N, Yang SY, Norman PJ, Marsh SGE, et al. Distinguishing functional polymorphism from random variation in the sequences of >10,000 HLA-a, -b and -c alleles. *PloS Genet* (2017) 13:e1006862. doi: 10.1371/journal.pgen.1006862

7. Vita R, Mahajan S, Overton JA, Dhanda SK, Martini S, Cantrell JR, et al. The immune epitope database (IEDB): 2018 update. *Nucleic Acids Res* (2019) 47:D339–43. doi: 10.1093/nar/gky1006

8. Norman PJ, Norberg SJ, Guethlein LA, Nemat-Gorgani N, Royce T, Wroblewski EE, et al. Sequences of 95 human *MHC* haplotypes reveal extreme coding variation in genes other than highly polymorphic *HLA class i* and *II*. *Genome Res* (2017) 27:813–23. doi: 10.1101/gr.213538.116

9. Serçinoğlu O, Ozbek P. Sequence-structure-function relationships in class I MHC: A local frustration perspective. *PloS One* (2020) 15:e0232849. doi: 10.1371/journal.pone.0232849

10. Barker DJ, Maccari G, Georgiou X, Cooper MA, Flicek P, Robinson J, et al. The IPD-IMGT/HLA database. *Nucleic Acids Res* (2022), 51:D1053–D1060. doi: 10.1093/nar/gkac1011

11. Penn DJ, Damjanovich K, Potts WK. MHC heterozygosity confers a selective advantage against multiple-strain infections. *Proc Natl Acad Sci USA* (2002) 99:11260–4. doi: 10.1073/pnas.162006499

12. Zernich D, Purcell AW, Macdonald WA, Kjer-Nielsen L, Ely LK, Laham N, et al. Natural HLA class I polymorphism controls the pathway of antigen presentation and susceptibility to viral evasion. *J Exp Med* (2004) 200:13–24. doi: 10.1084/jem.20031680

13. Prugnolle F, Manica A, Charpentier M, Guégan JF, Guernier V, Balloux F. Pathogen-driven selection and worldwide HLA class I diversity. *Curr Biol* (2005) 15:1022–7. doi: 10.1016/j.cub.2005.04.050

14. Cagliani R, Sironi M. Pathogen-driven selection in the human genome. *Int J Evol. Biol* (2013) 2013:1–6. doi: 10.1155/2013/204240

15. Falk K, Rötzschke O, Stevanović S, Jung G, Rammensee H-G. Allele-specific motifs revealed by sequencing of self-peptides eluted from MHC molecules. *Nature* (1991) 351:290–6. doi: 10.1038/351290a0

16. Yewdell JW, Bennink JR. Immunodominance in major histocompatibility complex class I-restricted T lymphocyte responses. *Annu Rev Immunol* (1999) 17:51–88. doi: 10.1146/annurev.immunol.17.1.51

17. Adams EJ, Luoma AM. The adaptable major histocompatibility complex (MHC) fold: Structure and function of nonclassical and MHC class I–like molecules. *Annu Rev Immunol* (2013) 31:529–61. doi: 10.1146/annurev-immunol-032712-095912

18. Bjorkman PJ, Saper MA, Samraoui B, Bennett WS, Strominger JL, Wiley DC. Structure of the human class I histocompatibility antigen, HLA-A2. *Nature* (1987) 329:506–12. doi: 10.1038/329506a0

19. van Deutekom HWM, Keşmir C. Zooming into the binding groove of HLA molecules: which positions and which substitutions change peptide binding most? *Immunogenetics* (2015) 67:425–36. doi: 10.1007/s00251-015-0849-y

20. Rasmussen M, Harndahl M, Stryhn A, Boucherma R, Nielsen LL, Lemonnier FA, et al. Uncovering the peptide-binding specificities of HLA-c: A general strategy to determine the specificity of any MHC class I molecule. *JI* (2014) 193:4790–802. doi: 10.4049/jimmunol.1401689

21. Smith AR, Alonso JA, Ayres CM, Singh NK, Hellman LM, Baker BM. Structurally silent peptide anchor modifications allosterically modulate T cell recognition in a receptor-dependent manner. *Proc Natl Acad Sci USA* (2021) 118:e2018125118. doi: 10.1073/pnas.2018125118

22. Lee K-H, Chang Y-C, Chen T-F, Juan H-F, Tsai H-K, Chen C-Y. Connecting MHC-i-binding motifs with HLA alleles *via* deep learning. *Commun Biol* (2021) 4:1194. doi: 10.1038/s42003-021-02716-8

23. Van Laethem F, Tikhonova AN, Singer A. MHC restriction is imposed on a diverse T cell receptor repertoire by CD4 and CD8 co-receptors during thymic selection. *Trends Immunol* (2012) 33:437–41. doi: 10.1016/j.it.2012.05.006

24. Marrack P, Scott-Browne JP, Dai S, Gapin L, Kappler JW. Evolutionarily conserved amino acids that control TCR-MHC interaction. *Annu Rev Immunol* (2008) 26:171–203. doi: 10.1146/annurev.immunol.26.021607.090421

25. Christopher Garcia K, Adams JJ, Feng D, Ely LK. The molecular basis of TCR germline bias for MHC is surprisingly simple. *Nat Immunol* (2009) 10:143–7. doi: 10.1038/ni.f.219

26. Arstila TP, Casrouge A, Baron V, Even J, Kanellopoulos J, Kourilsky P. A direct estimate of the human alphabeta T cell receptor diversity. *Science* (1999) 286:958–61. doi: 10.1126/science.286.5441.958

27. Wooldridge L, Ekeruche-Makinde J, van den Berg HA, Skowera A, Miles JJ, Tan MP, et al. A single autoimmune T cell receptor recognizes more than a million different peptides. *J Biol Chem* (2012) 287:1168–77. doi: 10.1074/jbc.M111.289488

28. Blevins SJ, Pierce BG, Singh NK, Riley TP, Wang Y, Spear TT, et al. How structural adaptability exists alongside HLA-A2 bias in the human αβ TCR repertoire. *Proc Natl Acad Sci USA* (2016) 113(9):E1276-85. doi: 10.1073/pnas.1522069113

29. Rudolph MG, Stanfield RL, Wilson IA. HOW TCRS BIND MHCS, PEPTIDES, AND CORECEPTORS. *Annu Rev Immunol* (2006) 24:419–66. doi: 10.1146/annurev.immunol.23.021704.115658

30. Coles CH, Mulvaney RM, Malla S, Walker A, Smith KJ, Lloyd A, et al. TCRs with distinct specificity profiles use different binding modes to engage an identical peptide–HLA complex. *JI* (2020) 204:1943–53. doi: 10.4049/jimmunol.1900915

31. Chen J-L, Stewart-Jones G, Bossi G, Lissin NM, Wooldridge L, Choi EML, et al. Structural and kinetic basis for heightened immunogenicity of T cell vaccines. *J Exp Med* (2005) 201:1243–55. doi: 10.1084/jem.20042323

32. Saito NG, Chang HC, Paterson Y. Recognition of an MHC class I-restricted antigenic peptide can be modulated by para-substitution of its buried tyrosine residues in a TCR-specific manner. *J Immunol* (1999) 162:5998–6008. doi: 10.4049/jimmunol.162.10.5998

33. Parks CA, Henning KR, Pavelko KD, Hansen MJ, Van Keulen VP, Reed BK, et al. Breaking tolerance with engineered class I antigen-presenting molecules. *Proc Natl Acad Sci USA* (2019) 116:3136–45. doi: 10.1073/pnas.1807465116

34. Yarmarkovich M, Marshall QF, Warrington JM, Premaratne R, Farrel A, Groff D, et al. Cross-HLA targeting of intracellular oncoproteins with peptide-centric CARs. *Nature* (2021) 599:477–84. doi: 10.1038/s41586-021-04061-6

35. Nguyen AT, Szeto C, Gras S. The pockets guide to HLA class I molecules. *Biochem Soc Trans* (2021) 49:2319–31. doi: 10.1042/BST20210410

36. Candia M, Kratzer B, Pickl WF. On peptides and altered peptide ligands: From origin, mode of action and design to clinical application (Immunotherapy). *Int Arch Allergy Immunol* (2016) 170:211–33. doi: 10.1159/000448756

37. Hoppes R, Oostvogels R, Luimstra JJ, Wals K, Toebes M, Bies L, et al. Altered peptide ligands revisited: Vaccine design through chemically modified HLA-A2–restricted T cell epitopes. *JI* (2014) 193:4803–13. doi: 10.4049/jimmunol.1400800

38. Leman JK, Weitzner BD, Lewis SM, Adolf-Bryfogle J, Alam N, Alford RF, et al. Macromolecular modeling and design in Rosetta: recent methods and frameworks. *Nat Methods* (2020) 17:665–80. doi: 10.1038/s41592-020-0848-2

39. Reynisson B, Alvarez B, Paul S, Peters B, Nielsen M. NetMHCpan-4.1 and NetMHCIIpan-4.0: improved predictions of MHC antigen presentation by concurrent motif deconvolution and integration of MS MHC eluted ligand data. *Nucleic Acids Res* (2020) 48:W449–54. doi: 10.1093/nar/gkaa379

40. Thomsen MCF, Nielsen M. Seq2Logo: a method for construction and visualization of amino acid binding motifs and sequence profiles including sequence weighting, pseudo counts and two-sided representation of amino acid enrichment and depletion. *Nucleic Acids Res* (2012) 40:W281–287. doi: 10.1093/nar/gks469

41. Li H, Natarajan K, Malchiodi EL, Margulies DH, Mariuzza RA. Three-dimensional structure of h-2Dd complexed with an immunodominant peptide from human immunodeficiency virus envelope glycoprotein 120. *J Mol Biol* (1998) 283:179–91. doi: 10.1006/jmbi.1998.2091

42. Gasteiger E, Gattiker A, Hoogland C, Ivanyi I, Appel RD, Bairoch A. ExPASy: The proteomics server for in-depth protein knowledge and analysis. *Nucleic Acids Res* (2003) 31:3784–8. doi: 10.1093/nar/gkg563

43. Toebes M, Coccoris M, Bins A, Rodenko B, Gomez R, Nieuwkoop NJ, et al. Design and use of conditional MHC class I ligands. *Nat Med* (2006) 12:246–51. doi: 10.1038/nm1360

44. Rodenko B, Toebes M, Hadrup SR, van Esch WJE, Molenaar AM, Schumacher TNM, et al. Generation of peptide–MHC class I complexes through UV-mediated ligand exchange. *Nat Protoc* (2006) 1:1120–32. doi: 10.1038/nprot.2006.121

45. Chen VB, Arendall WB, Headd JJ, Keedy DA, Immormino RM, Kapral GJ, et al. *MolProbity*: All-atom structure validation for macromolecular crystallography. *Acta Crystallogr D Biol Crystallogr* (2010) 66:12–21. doi: 10.1107/S0907444909042073

46. Sievers F, Wilm A, Dineen D, Gibson TJ, Karplus K, Li W, et al. Fast, scalable generation of high-quality protein multiple sequence alignments using clustal omega. *Mol Syst Biol* (2011) 7:539. doi: 10.1038/msb.2011.75

47. Robert X, Gouet P. Deciphering key features in protein structures with the new ENDscript server. *Nucleic Acids Res* (2014) 42:W320–324. doi: 10.1093/nar/gku316

48. Kumar S, Stecher G, Tamura K. MEGA7: Molecular evolutionary genetics analysis version 7.0 for bigger datasets. *Mol Biol Evol* (2016) 33:1870–4. doi: 10.1093/molbev/msw054

49. Letunic I, Bork P. Interactive tree of life (iTOL) v5: An online tool for phylogenetic tree display and annotation. *Nucleic Acids Res* (2021) 49:W293–6. doi: 10.1093/nar/gkab301

50. Overall SA, Toor JS, Hao S, Yarmarkovich M, Sara M, O'Rourke, et al. High throughput pMHC-I tetramer library production using chaperone-mediated peptide exchange. *Nat Commun* (2020) 11:1909. doi: 10.1038/s41467-020-15710-1

51. Borrman T, Cimons J, Cosiano M, Purcaro M, Pierce BG, Baker BM, et al. ATLAS: A database linking binding affinities with structures for wild-type and mutant TCR-pMHC complexes: Linking TCR-pMHC affinities with structure. *Proteins* (2017) 85:908–16. doi: 10.1002/prot.25260

52. Wu Y, Zhang N, Wei X, Lu S, Li S, Hashimoto K, et al. The structure of a peptide-loaded shark MHC class I molecule reveals features of the binding between β_2-microglobulin and h chain conserved in evolution. *JI* (2021) 207:308–21. doi: 10.4049/jimmunol.2001165

53. Robinson J. IMGT/HLA and IMGT/MHC: Sequence databases for the study of the major histocompatibility complex. *Nucleic Acids Res* (2003) 31:311–4. doi: 10.1093/nar/gkg070

54. Garboczi DN, Hung DT, Wiley DC. HLA-A2-peptide complexes: Refolding and crystallization of molecules expressed in escherichlia coli and complexed with single antigenic peptides. *Proc Natl Acad Sci USA* (1992) 89(8):3429–33. doi: 10.1073/pnas.89.8.3429

55. Hellman LM, Yin L, Wang Y, Blevins SJ, Riley TP, Belden OS, et al. Differential scanning fluorimetry based assessments of the thermal and kinetic stability of peptide–MHC complexes. *J Immunol Methods* (2016) 432:95–101. doi: 10.1016/j.jim.2016.02.016

56. Bakker AH, Hoppes R, Linnemann C, Toebes M, Rodenko B, Berkers CR, et al. Conditional MHC class I ligands and peptide exchange technology for the human MHC gene products HLA-A1, -A3, -A11, and -B7. *Proc Natl Acad Sci* (2008) 105:3825–30. doi: 10.1073/pnas.0709717105

57. Rossjohn J, Gras S, Miles JJ, Turner SJ, Godfrey DI, McCluskey J. T Cell antigen receptor recognition of antigen-presenting molecules. *Annu Rev Immunol* (2015) 33:169–200. doi: 10.1146/annurev-immunol-032414-112334

58. Li L, Bouvier M. Structures of HLA-A*1101 complexed with immunodominant nonamer and decamer HIV-1 epitopes clearly reveal the presence of a middle, secondary anchor residue. *J Immunol* (2004) 172:6175–84. doi: 10.4049/jimmunol.172.10.6175

59. Altman JD, Moss PAH, Goulder PJR, Barouch DH, McHeyzer-Williams MG, Bell JI, et al. Phenotypic analysis of antigen-specific T lymphocytes. *Science* (1996) 274:94–6. doi: 10.1126/science.274.5284.94

60. Ishihara M, Kitano S, Kageyama S, Miyahara Y, Yamamoto N, Kato H, et al. NY-ESO-1-specific redirected T cells with endogenous TCR knockdown mediate tumor response and cytokine release syndrome. *J Immunother Cancer* (2022) 10:e003811. doi: 10.1136/jitc-2021-003811

61. Archbold JK, Ely LK, Kjer-Nielsen L, Burrows SR, Rossjohn J, McCluskey J, et al. T Cell allorecognition and MHC restriction–a case of Jekyll and Hyde? *Mol Immunol* (2008) 45:583–98. doi: 10.1016/j.molimm.2006.05.018

62. Natarajan K, McShan AC, Jiang J, Kumirov VK, Wang R, Zhao H, et al. An allosteric site in the T-cell receptor cβ domain plays a critical signalling role. *Nat Commun* (2017) 8:15260. doi: 10.1038/ncomms15260

63. Laugel B, van den Berg HA, Gostick E, Cole DK, Wooldridge L, Boulter J, et al. Different T cell receptor affinity thresholds and CD8 coreceptor dependence govern cytotoxic T lymphocyte activation and tetramer binding properties. *J Biol Chem* (2007) 282:23799–810. doi: 10.1074/jbc.M700976200

64. Sidney J, Peters B, Frahm N, Brander C, Sette A. HLA class I supertypes: a revised and updated classification. *BMC Immunol* (2008) 9:1. doi: 10.1186/1471-2172-9-1

65. Ott PA, Hu Z, Keskin DB, Shukla SA, Sun J, Bozym DJ, et al. An immunogenic personal neoantigen vaccine for patients with melanoma. *Nature* (2017) 547:217–21. doi: 10.1038/nature22991

66. Sahin U, Derhovanessian E, Miller M, Kloke B-P, Simon P, Löwer M, et al. Personalized RNA mutanome vaccines mobilize poly-specific therapeutic immunity against cancer. *Nature* (2017) 547:222–6. doi: 10.1038/nature23003

67. Ribas A, Wolchok JD. Cancer immunotherapy using checkpoint blockade. *Science* (2018) 359:1350–5. doi: 10.1126/science.aar4060

68. Bright RK, Bright JD, Byrne JA. Overexpressed oncogenic tumor-self antigens. *Hum Vaccin Immunother* (2014) 10:3297–305. doi: 10.4161/hv.29475

69. Oscherwitz J. The promise and challenge of epitope-focused vaccines. *Hum Vaccines Immunother.* (2016) 12:2113–6. doi: 10.1080/21645515.2016.1160977

70. Correia BE, Bates JT, Loomis RJ, Baneyx G, Carrico C, Jardine JG, et al. Proof of principle for epitope-focused vaccine design. *Nature* (2014) 507:201–6. doi: 10.1038/nature12966

71. June CH, Riddell SR, Schumacher TN. Adoptive cellular therapy: a race to the finish line. *Sci Transl Med* (2015) 7:280ps7. doi: 10.1126/scitranslmed.aaa3643

72. Beasley MD, Niven KP, Winnall WR, Kiefel BR. Bacterial cytoplasmic display platform retained display (ReD) identifies stable human germline antibody frameworks. *Biotechnol J* (2015) 10:783–9. doi: 10.1002/biot.201400560

frontiers | Frontiers in Immunology

TYPE Original Research
PUBLISHED 05 May 2023
DOI 10.3389/fimmu.2023.1182504

OPEN ACCESS

EDITED BY
Samuele Notarbartolo,
National Institute of Molecular Genetics (INGM), Italy

REVIEWED BY
Anthony Tanoto Tan,
Duke-NUS Medical School, Singapore
Julie Boucau,
Ragon Institute, United States

*CORRESPONDENCE
Julian Schulze zur Wiesch
julianszw@gmail.com

RECEIVED 08 March 2023
ACCEPTED 06 April 2023
PUBLISHED 05 May 2023

CITATION
Westphal T, Mader M, Karsten H, Cords L, Knapp M, Schulte S, Hermanussen L, Peine S, Ditt V, Grifoni A, Addo MM, Huber S, Sette A, Lütgehetmann M, Pischke S, Kwok WW, Sidney J and Schulze zur Wiesch J (2023) Evidence for broad cross-reactivity of the SARS-CoV-2 NSP12-directed CD4$^+$ T-cell response with pre-primed responses directed against common cold coronaviruses.
Front. Immunol. 14:1182504.
doi: 10.3389/fimmu.2023.1182504

Evidence for broad cross-reactivity of the SARS-CoV-2 NSP12-directed CD4$^+$ T-cell response with pre-primed responses directed against common cold coronaviruses

Tim Westphal[1,2], Maria Mader[1], Hendrik Karsten[1], Leon Cords[1], Maximilian Knapp[1], Sophia Schulte[1], Lennart Hermanussen[1], Sven Peine[3], Vanessa Ditt[3], Alba Grifoni[4], Marylyn Martina Addo[1,2,5,6], Samuel Huber[1], Alessandro Sette[4], Marc Lütgehetmann[2,7], Sven Pischke[1,2], William W. Kwok[8], John Sidney[4] and Julian Schulze zur Wiesch[1,2]*

[1]Infectious Diseases Unit I, Department of Medicine, University Medical Center Hamburg-Eppendorf, Hamburg, Germany, [2]German Center for Infection Research Deutsches Zentrum für Infektionsforschung (DZIF), Partner Site Hamburg-Lübeck-Borstel-Riems, Hamburg, Germany, [3]Institute of Transfusion Medicine, University Medical Center Hamburg-Eppendorf, Hamburg, Germany, [4]Center for Infectious Disease and Vaccine Research, La Jolla Institute for Immunology (LJI), La Jolla, CA, United States, [5]Department for Clinical Immunology of Infectious Diseases, Bernhard Nocht Institute for Tropical Medicine, Hamburg, Germany, [6]Institute of Infection Research and Vaccine Development, University Medical Center Hamburg-Eppendorf, Hamburg, Germany, [7]Institute of Medical Microbiology, Virology and Hygiene, University Medical Center Hamburg-Eppendorf, Hamburg, Germany, [8]Benaroya Research Institute at Virginia Mason, Seattle, WA, United States

Introduction: The nonstructural protein 12 (NSP12) of the severe acute respiratory syndrome coronavirus type 2 (SARS-CoV-2) has a high sequence identity with common cold coronaviruses (CCC).

Methods: Here, we comprehensively assessed the breadth and specificity of the NSP12-specific T-cell response after *in vitro* T-cell expansion with 185 overlapping 15-mer peptides covering the entire SARS-CoV-2 NSP12 at single-peptide resolution in a cohort of 27 coronavirus disease 2019 (COVID-19) patients. Samples of nine uninfected seronegative individuals, as well as five pre-pandemic controls, were also examined to assess potential cross-reactivity with CCCs.

Results: Surprisingly, there was a comparable breadth of individual NSP12 peptide-specific CD4$^+$ T-cell responses between COVID-19 patients (mean: 12.82 responses; range: 0–25) and seronegative controls including pre-pandemic samples (mean: 12.71 responses; range: 0–21). However, the NSP12-specific T-cell responses detected in acute COVID-19 patients were on average of a higher magnitude. The most frequently detected CD4$^+$ T-cell

peptide specificities in COVID-19 patients were aa236–250 (37%) and aa246–260 (44%), whereas the peptide specificities aa686–700 (50%) and aa741–755 (36%), were the most frequently detected in seronegative controls. In CCC-specific peptide-expanded T-cell cultures of seronegative individuals, the corresponding SARS-CoV-2 NSP12 peptide specificities also elicited responses *in vitro*. However, the NSP12 peptide-specific $CD4^+$ T-cell response repertoire only partially overlapped in patients analyzed longitudinally before and after a SARS-CoV-2 infection.

Discussion: The results of the current study indicate the presence of pre-primed, cross-reactive CCC-specific T-cell responses targeting conserved regions of SARS-CoV-2, but they also underline the complexity of the analysis and the limited understanding of the role of the SARS-CoV-2 specific T-cell response and cross-reactivity with the CCCs.

KEYWORDS

SARS-CoV-2, NSP12, CD4+ T-cells, RNA-dependant RNA polymerase, Cross-reactivities, epitope analysis, sequence identities, common cold coronaviruses

1 Introduction

The severe acute respiratory syndrome coronavirus type 2 (SARS-CoV-2) is the virus responsible for the ongoing pandemic with extensive global implications, and infection leads to the coronavirus disease 2019 (COVID-19), which presents as a flu-like illness and is divided into different severity levels by the WHO, ranging from asymptomatic through clinical progression levels up to death due to the disease (1).

SARS-CoV-2 is a large single-strand positive RNA virus that encodes four structural proteins (spike glycoprotein, envelope, mebrane, and nucleoprotein), nine accessory proteins, and 16 nonstructural proteins (NSPs), resulting in a total number of at least 29 proteins. It has been shown that exposure to structural proteins can elicit a virus-specific $CD4^+$ T-cell response that varies in magnitude and breadth (2, 3).

The RNA-dependent RNA polymerase (RdRp), which is encoded by the *NSP12* gene, consists of 932 amino acids and is crucial for the replication of the virus. This genomic region is highly conserved, as evidenced by the sequence similarity with other Coronaviridae (4, 5). The NSP12 of SARS-CoV-2 has a higher sequence identity with common cold coronaviruses (CCCs) than, for example, the spike glycoprotein (6, 7). After the assembly with the co-factors NSP7 and NSP8, the functional polymerase fulfills its task of replicating the SARS-CoV-2 genome (8). The NSP12 "without has protein" has an essential role in the life cycle of the virus, and NSP12 is the target of the antiviral nucleoside analog inhibitor remdesivir (9).

Recently, it has been shown that there might be complex immunological interactions between CCCs (HKU1, NL63, 229E, OC43) and the SARS-CoV-2-specific immune response, potentially altering the clinical course of COVID-19 (10–16).

We and others have previously mapped the breadth and specificity of the spike-specific $CD4^+$ T-cell response (3, 17), as well as N-, E-, and M-specific $CD4^+$ T-cell responses (2, 18). In the current study, we characterized the NSP12-specific T-cell response in COVID-19 patients with an overlapping 15-mer peptide set. Furthermore, we examined the potential SARS-CoV-2 NSP12-specific cross-reactivity with other corresponding CCC proteins with pronounced sequence identities to gain further insight into SARS-CoV-2-specific T-cell responses.

2 Materials and methods

2.1 Ethics statement

All study participants gave written informed consent. The study was conducted in accordance with the Declaration of Helsinki and approved by the local ethics board of the Ärztekammer Hamburg (PV4780, PV7298).

2.2 Patient cohort

Study participants were recruited at the University Medical Center Hamburg-Eppendorf between May and December 2021. The “acutely infected” group comprised patients hospitalized with COVID-19 infection who were admitted to the infectious diseases ward. An infection with SARS-CoV-2 was confirmed by polymerase chain reaction (PCR) from oropharyngeal and/or nasopharyngeal swabs, as previously described (19). “Acute COVID-19 patients” were defined as being hospitalized due to a SARS-CoV-2 infection with a maximum of 2 months between the date of diagnosis and

blood sampling. HH-N12-8, who was acutely ill with COVID-19 and had blood drawn after 2 months, was still viremic at the time of collection.

The "resolved COVID-19 patients" group, defined as patients who tested positive for COVID-19 but have since recovered and were moved out of isolation, included medical and nonmedical staff of the University Medical Center Hamburg-Eppendorf and associated institutions. A resolved SARS-CoV-2 infection was confirmed by a previous positive PCR result and/or positive SARS-CoV-2 nucleocapsid (NP) antibodies and a history of acute flu-like illness. The time since infection in this group ranged between 11 and 448 days (average: 102 days).

2.3 Seronegative and pre-pandemic controls

Seronegative controls were individuals who were recruited when fewer than 5% of the general population had been infected with COVID-19 and were defined as (A) NP seronegative, (B) neither believably having a history of flu-like symptoms since the beginning of the pandemic, nor (C) having ever been tested SARS-CoV-2 PCR positive. Pre-pandemic samples were defined as peripheral blood mononuclear cells (PBMCs) that were frozen and stored before 01 January 2020.

2.4 Nonstructural protein 12 peptides

In total, 15-mer peptides overlapping by 10 amino acids and corresponding to the complete NSP12 amino acid sequence were synthesized (peptides and elephants, Hennigsdorf, Germany). The complete amino acid sequence is depicted in Supplementary Table S1. All peptides were divided into four pools of either 46 or 47 peptides. For *in vitro* culture, peptide pools were used at a concentration of 10 µg/ml per single peptide. For the enzyme-linked immunospot assay (ELISpot), the final concentration of every single peptide was 10 µg/ml.

2.5 CCC peptides

A total of 18 15-mer peptides corresponding to the CCC (HKU1, NL63, 229E) NSP12 amino acid sequences were synthesized (peptides and elephants, Hennigsdorf, Germany). Because none of the seronegative controls included in the CCC cross-reactivity experiment tested positive for OC43, we did not order 15-mer peptides corresponding to the OC43 sequence. Canonical protein amino acid sequences of CCCs were extracted from the reviewed UniProtKB database (20). Six different peptide specificities were produced, and each specificity was generated in variants matching the amino acids specific to each of the three CCCs (Supplementary Table S1).

2.6 Sample processing and T-cell expansion

Venous whole blood samples from the study participants were collected in a BD Vacutainer® CPT™ (Becton Dickinson GmbH, Heidelberg, Germany). PBMCs were isolated by centrifugation and used fresh. Frozen PBMCs of pre-pandemic samples, acquired before 01 January 2020, were thawed. In 24-well culture plates, 30–50 × 10^6 PBMCs were cultured per patient in Roswell Park Memorial Institute medium (RPMI) supplemented with 10% fetal calf serum, penicillin, and streptomycin (R10).

The T-cell expansion was induced in duplicates by stimulation with one of the four peptide pools consisting of overlapping 15-mer peptides covering the whole SARS-CoV-2 NSP12 at 10 µg/ml, anti-CD28/anti-CD49d co-stimulation, and 50 U/ml recombinant interleukin 2 (rIL-2) at 37°C and 5% CO_2. When necessary, 50 U/ml rIL-2 and R10 were used for exchanges of medium. After 11–13 days, the cells were harvested and used for the T-cell assays described below.

2.7 IFN-γ EliSpot assay

IFN-γ-ELISpot assays were performed as described before (2). In short, approximately 100,000 pre-cultured cells were distributed into each well of 96-well plates pre-coated with IFN-γ antibodies (clone 1-D1K, Mabtech AB, Nacka Strand, Sweden). The cells were then separately stimulated with each of the 46 or 47 peptides from the corresponding peptide pool at a concentration of 10 µg/ml for 18–20 h at 37°C and 5% CO_2. Anti-CD3-stimulated cells served as a positive control, and unstimulated cells in R10 medium served as a negative control.

After a washing step, IFN-γ was detected with a biotinylated anti-IFN-γ antibody (clone 7-B6-1; Mabtech AB, Nacka Strand, Sweden), alkaline phosphatase-conjugated streptavidin, and a 5-bromo-4-chloro-3-indolyl phosphate (BCIP)/nitroblue tetrazolium (NBT) substrate solution. Results were considered positive if a single peptide well showed at least three times the number of IFN-γ spots compared to the corresponding control well.

2.8 Intracellular cytokine staining

Positive results in the ELISpot assay were validated by intracellular cytokine staining (ICS) for IFN-γ, as described previously (2). The pre-cultured cells were re-stimulated with the peptides showing a positive result at a concentration of 10 µg/ml for 16 h at 37°C and 5% CO_2. One negative control per pool consisting of cells and R10 medium only and a positive control per patient stimulated with phorbol-12-myristate-13-acetate and ionomycin (10 µg/ml) were also set up. After 1 h, 5 µl/ml of Brefeldin A (Sigma-Aldrich, St. Louis, MO, USA) solution was added to inhibit cytokine secretion.

The cells were stained with Zombie NIR fixable viability dye (BioLegend, San Diego, CA, USA) per the manufacturer's instructions and the following fluorochrome-conjugated monoclonal antibodies on the cell surface: anti-CD3 (clone UCHT1, AlexaFluor700), anti-CD4 (clone SK3, BV510), anti-CD8 (clone RPA-T8, PerCP-Cy5.5), anti-CD14 (clone 63D3, APC-Cy7), and anti-CD19 (clone HIB19, APC-Cy7). After fixation and permeabilization of the cells using the FoxP3 transcription factor staining buffer set (eBioscience, Thermo Fisher Scientific), the cells were stained for intracellular IFN-γ using a monoclonal anti-IFN-γ antibody (clone 4S.B3, PE-Dazzle594). All monoclonal antibodies were purchased from BioLegend.

We defined a T-cell response as positive under three conditions: a percentage of $CD4^+$ or $CD8^+$ T cells positive for the secretion of IFN-γ three times higher than the negative control, at least 0.02% IFN-γ-positive cells, and if the population could be visibly separated from the negative control. The cells were acquired on an LSRFortessa II cytometer (BD Biosciences) using FACSDiva version 8 for Windows (BD Biosciences). The gating strategy is shown in Supplementary Figure 1.

2.9 HLA typing

High-definition molecular HLA class I and II typing from whole blood samples was performed for 17 individuals at the Institute of Transfusion Medicine at the University Medical Center Hamburg-Eppendorf by PCR sequence-specific oligonucleotide (PCR-SSO) technique using the commercial kit SSO LabType (One Lambda, Canoga Park, CA, USA), as previously described (21). The gating strategy is shown in Supplementary Figure 1.

2.10 SARS-CoV-2 and CCC serologies

Antibody levels were determined by the Roche Elecsys SARS-CoV-2 S assay in arbitrary units (AU) per milliliter as described previously (22) with a linear range from 0.4 to 25,000 AU/ml. A negative test result was defined as a result <0.8 AU/ml, a low positive response between 0.8 and 103 AU/ml, and a positive response >103 AU/ml. SARS-CoV-2 nucleocapsid antibodies were assessed by the Elecsys anti-NC-SARS-CoV-2 Ig assay (Roche, Mannheim, Germany; cutoff: ≥ 1 COI/ml). Serologies for the CCCs HKU1, NL63, 229E, and OC43 were available for 14 individuals by a line blot assay using the recomLine SARS-CoV-2 IgG kit (MIKROGEN GmbH, Neuried, Bavaria, Germany) as previously described (23).

2.11 *Ex vivo* ICS

Ex vivo ICS was performed as previously described (3). In short, cryopreserved PBMCs from COVID-19 patients were stimulated with an NSP12 Best-Of peptide pool consisting of 11 peptides that elicited responses in most of the previously studied patients. The cells were then washed and stained with Zombie NIR fixable viability dye (BioLegend) and fluorochrome-labeled monoclonal antibodies targeting CD3 (clone UCHT1, AlexaFluor700), CD4 (clone RPA-T4, BV785), CD8 (clone RPA-T8, BV650), CD14 (clone 63D3, APC-Cy7), and CD19 (clone HIB19, APC-Cy7).

After fixation and permeabilization of the cells using the FoxP3 transcription factor staining buffer set (eBioscience, Thermo Fischer Scientific), the cells were stained for intracellular IFN-γ using a monoclonal anti-IFN-γ antibody (clone 4S.B3, PE-Dazzle594).

2.12 HLA (MHC class II) binding capacity

In vitro HLA binding assays with 14 peptides that frequently elicit NSP12-specific $CD4^+$ T-cell responses were performed using purified HLA-class II molecules, as previously described (24). Worldwide population coverage at the DRB1 locus afforded by each epitope was predicted using the population coverage tool hosted by the IEDB (25, 26). These data are based on allele frequency data provided by The Allele Frequency Net Database (27). Coverage of an allele was considered based on a corresponding binding affinity of 1,000 nM or lower, a binding threshold associated with >80% of known $CD4^+$ epitopes for their reported HLA-restricting molecule (28). For this purpose, coverage estimates imply, but cannot confirm T-cell recognition, and thus may be overestimated. Conversely, because coverage estimates only consider alleles for which binding has been examined experimentally, they may also underestimate coverage.

2.13 Data analysis and statistics

The analysis of all flow cytometric data was performed in FlowJo version 10 for Windows (Treestar, Ashland, OR, USA). All graphs and statistical analyses were conducted in GraphPad Prism version 7.0 for Windows (GraphPad Software Inc., San Diego, CA, USA). Data are visualized as the mean with a standard deviation. The following tests for statistical significance were used: the Mann–Whitney *U* test (for testing of two groups) and Kruskal–Wallis and ANOVA with Dunn's correction for multiple analyses (for testing of three or more groups). For all tests, two-tailed *p*-values were generated. Results with a *p*-value less or equal to 0.05 were considered statistically significant. (levels of significance: $^*p < 0.05$; $^{**}p < 0.01$; $^{***}p < 0.001$; and $^{****}p < 0.0001$).

3 Results

3.1 Clinical features of the study cohort

The demographic and clinical characteristics of the patients are outlined in Table 1. The study cohort consisted of 27 patients with a SARS-CoV-2 infection, of whom we were able to collect (A) PBMCs early during SARS-CoV-2 infection ($n = 15$) or patients or (B) at the stage of resolved infection in 12 individuals (1–15 months after the infection). The study included 19 male and eight female patients, with a mean age of 49.2 years (range: 19–95).

According to the WHO severity classification, 11 (41%) of the patients had ambulatory mild disease. Six (22%) patients were hospitalized with a moderate disease and nine (33%) patients

10.3389/fimmu.2023.1182504

TABLE 1 Study cohort characteristics including demographical and clinical data.

	Acute COVID-19 infection	Resolved COVID-19 infection	Seronegative controls	Pre-pandemic controls
	n = 15	*n* = 12	*n* = 9	*n* = 5
Age in years (range)	61 (19–95)	37.4 (21–63)	25.3 (21–34)	–
Sex at birth				
Female (%)	4 (26.7%)	4 (33.3%)	3 (33.3%)	–
Male (%)	11 (73.3%)	8 (66.7%)	6 (66.7%)	–
Unknown (%)	–	–	–	5 (100%)
Disease severity				
Uninfected—WHO 0 (%)	–	–	9 (100%)	5 (100%)
Ambulatory mild disease—WHO 1–3 (%)	3 (20%)	8 (66.7%)	–	–
Hospitalized: moderate disease—WHO 4–5 (%)	5 (33.3%)	1 (8.3%)	–	–
Hospitalized: severe disease—WHO 6–9 (%)	7 (46.7%)	2 (16.7%)	–	–
Unknown	–	1 (8.3%)	–	–

with a severe disease. The detailed clinical characteristics can be found in Supplementary Table S2.

Furthermore, PBMC samples from 14 individuals without a history of SARS-CoV-2 infection were included. They were substratified into seronegatives (n = 9) (without a history of COVID-19) and pre-pandemic controls (n = 5). There were no characteristics available on the pre-pandemic controls because they were anonymous buffy coats from healthy blood donors.

3.2 Similar breadth of the NSP12-specific CD4$^+$ T-cell response regardless of the infection status, but a higher magnitude of the T-cell response in acute COVID-19 patients

In the current study, we assessed the breadth of the virus-specific T-cell response and its specificities within the SARS-CoV-2 NSP12 on a single-peptide level in patients with acute and resolved COVID-19. As described earlier, *ex vivo* ELISpot assays after stimulation with single peptides and NSP12 peptide pools showed a low overall IFN-γ response with a magnitude barely above the limit of detection of this assay (data not shown).

Next, we investigated the T-cell responses, after *in vitro* NSP12 peptide-specific cell culture using four pools of 46 to 47 peptides and re-stimulating with single 15-mer peptides of the SARS-CoV-2 NSP12 using IFN-g ELISpot after 11–13 days (Figure 1). Each positive ELISpot response was confirmed and classified as a CD4$^+$ or CD8$^+$ T-cell response by intracellular cytokine staining (ICS) for IFN-γ after re-stimulation with the respective single peptide (Figure 2). Representative flow-cytometric plots for NSP12-specific CD4$^+$ T-cell responses are shown in Figure 2, and representative plots for CD8$^+$ T-cell responses are shown in Supplementary Figure S2.

The majority of the elicited IFN-γ responses proved to be CD4$^+$ T-cell responses in the flow-cytometric analysis. Of the COVID-19 patients, 81% (22 out of 27) and 92% (13 out of 14) of the seronegative controls showed peptide-specific CD4$^+$ T-cell responses to at least one NSP12 peptide specificity. Five COVID-19 patients, four of them acutely ill and one recovered after a SARS-CoV-2 infection, did not show any responses, three of whom were receiving immunosuppressive medication at the time of blood sampling.

Altogether, there were 348 CD4$^+$ T-cell responses detected in 27 COVID-19 patients and 178 responses in 14 seronegative controls. The detailed response pattern can be found in Supplementary Table S3. Somewhat unexpectedly, the number of NSP12-specific CD4$^+$ T-cell responses directed against individual peptides in an individual did not significantly differ between COVID-19 patients (mean: 12.82 responses; range: 0–25; $p > 0.05$) and seronegative or pre-pandemic controls (mean: 12.71 responses; range: 0–21) (Figure 2).

However, the average magnitude of the individual peptide-specific responses was significantly higher in acute COVID-19 patients (mean: 0.2%; range: 0.02–0.53) compared to individuals after a recovered SARS-CoV-2 infection (mean: 0.05%; range: 0.02–0.15) or individuals without previous exposure to SARS-CoV-2 (mean: 0.06%; range: 0.04–0.1; $^*p < 0.05$). We found no statistically significant difference in the number of detected peptides between patients with a resolved COVID-19 infection and seronegative controls (Figure 2).

In either disease status, 160 out of 185 (86%) 15-mer overlapping peptides elicited a CD4$^+$ T-cell response in at least one individual.

The peptide specificities NSP12_48 (aa236–250) and NSP12_50 (aa246–260) were each recognized by more than 35% of patients with an ongoing or a resolved SARS-CoV-2 infection (Table 2).

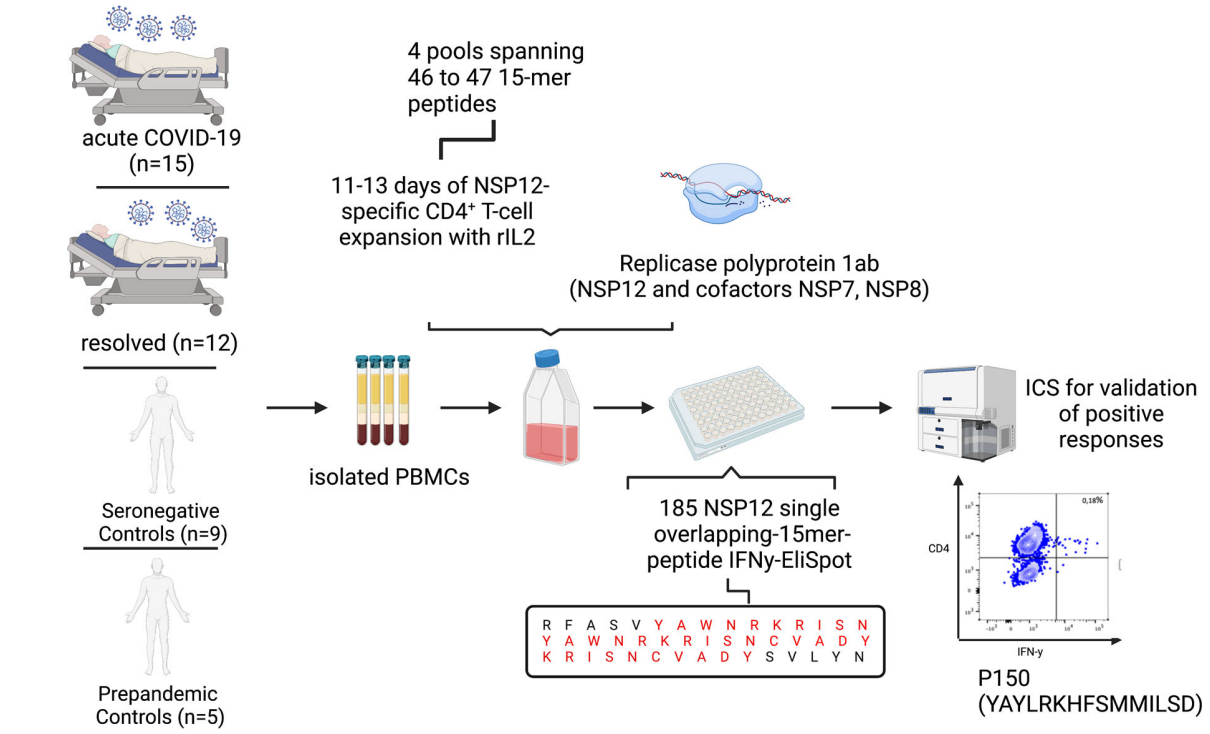

FIGURE 1
Experimental setup of the 15-mer single-peptide IFN-γ-ELISpot after 11–13 days of *in vitro* peptide-specific culture with different peptide pools, each spanning 46 to 47 peptides, and ICS after single-peptide re-stimulation for validation of positive peptide-specific T-cell responses.

Furthermore, we were able to define nine peptides that each elicited a $CD4^+$ T-cell response in more than 25% of individuals (Table 2) in our SARS-CoV-2 seronegative cohort. Of interest, the peptide specificity aa686–700 was recognized by 50% of the seronegative controls and by 22% of the COVID-19 patients. It showed sequence identity with the corresponding sequences of the CCCs of up to 90% (Table 3).

Overall, we found a broadly directed, low-level NSP12-specific $CD4^+$ T-cell response in COVID-19 patients, with a higher magnitude in the acutely infected patients. Surprisingly, in pre-pandemic and seronegative samples, we detected a similar range of NSP12-specific $CD4^+$ T-cell responses.

3.3 HLA binding and prediction of HLA restriction

In vitro HLA class II binding assays were performed with a subset of frequently detected SARS-CoV-2 NSP12 peptides (Supplementary Table S1). These studies indicated that the peptide specificities aa236–250 and aa246–260 that were most frequently recognized in this study (response frequency: 37% and 44%, respectively) could bind seven or more of the 11 DRB1-HLA molecules tested with an affinity of 1,000 nM or better (Table 4). This could imply a broad presentation by multiple HLA specificities and might explain the broad recognition in our cohort.

3.4 The breadth and specificity of the NSP12-specific $CD8^+$ T-cell response in COVID-19 patients and seronegative controls

The *in vitro* culture assay using 15-mer peptides favors the detection of $CD4^+$ T-cell responses; however, we did not want to exclude analysis of NSP12-specific $CD8^+$ responses from this study *a priori*. The flow-cytometric analyses identified most of the peptide-specific IFN-γ responses as $CD4^+$ T-cell responses.

Generally, there was a less broad NSP12-specific $CD8^+$ T-cell response with a low magnitude in the majority of individuals (Supplementary Figure S2). We detected a median of nine (range: 0–25) NSP12-specific $CD8^+$ T-cell responses in every participant. The average magnitude of $CD8^+$ T-cell responses per patient showed no statistically significant differences between the three groups of acute and resolved COVID-19 patients and seronegative controls. There were fewer NSP12-specific $CD8^+$ T-cell responses with a lower magnitude compared to the $CD4^+$ T-cell responses. The overall response pattern closely resembled that of the NSP12 $CD4^+$ T-cell responses (Supplementary Figure S2). The location and patient-specific distribution of all individual NSP12-specific $CD8^+$ T-cell responses are shown in Supplementary Table S5.

10.3389/fimmu.2023.1182504

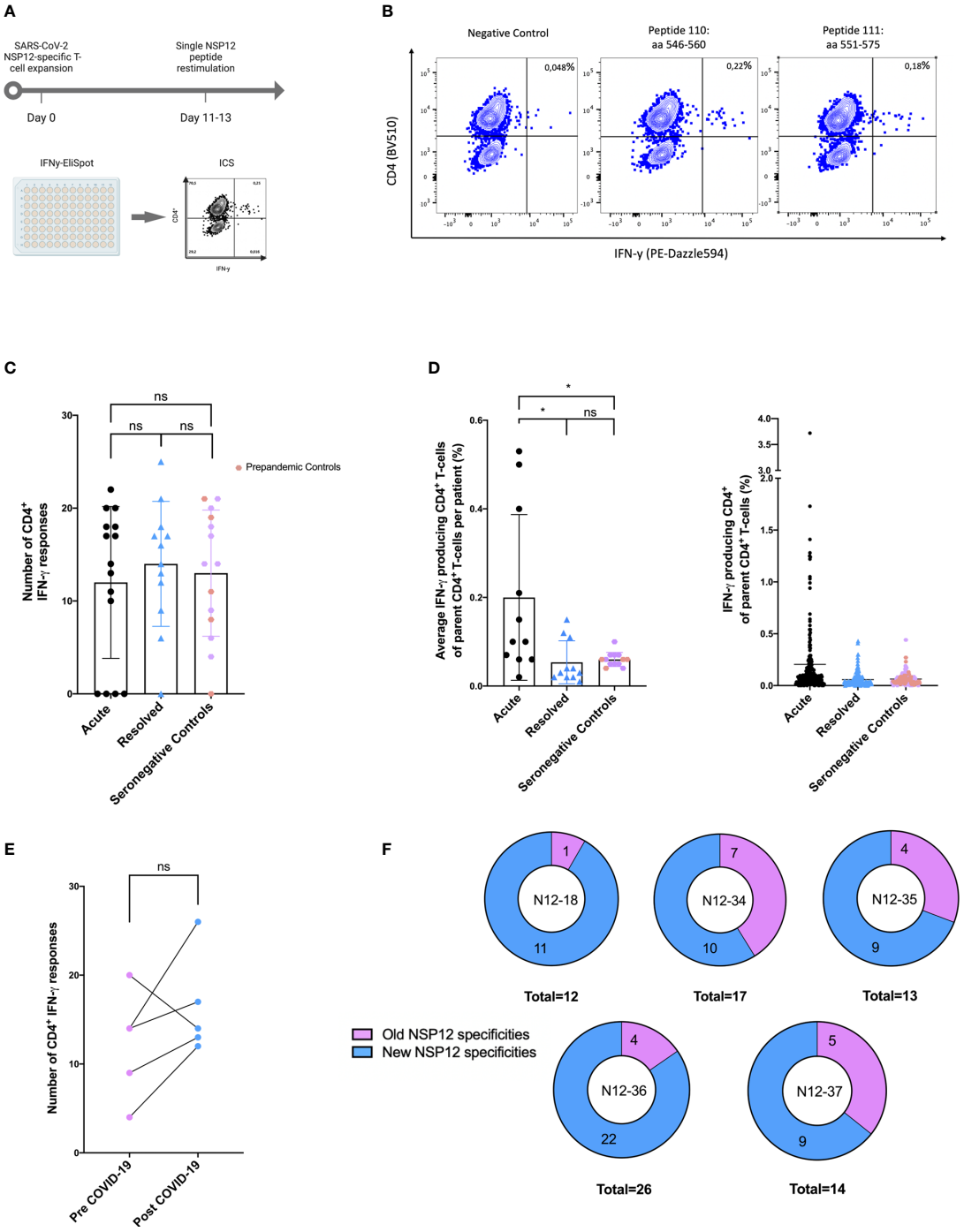

FIGURE 2
(A–F) SARS-CoV-2 seronegative individuals demonstrated highly cross-reactive NSP12-specific $CD4^+$ T-cell responses with low IFN-γ magnitude comparable to post-acute SARS-CoV-2 infection. **(A)** NSP12-specific T-cells were expanded *in vitro* with pools of overlapping NSP12 peptides in the presence of anti-CD28/anti-CD49d antibodies and IL-2. After 11–13 days, the cells were analyzed for IFN-γ production by ELISpot and validated by intracellular cytokine staining after restimulation with single peptides. **(B)** $CD4^+$ T-cells predominated NSP12-specific IFN-γ responses in all groups. Representative flow cytometry plots of HH-N12-7 with acute SARS-CoV-2 infection. **(C)** Comparable numbers of recognized NSP12 peptides between individuals with acute or resolved SARS-CoV-2 infection and seronegative controls indicated relevant cross-reactivity of previously primed $CD4^+$ T-cells. **(D)** The magnitude of IFN-γ production of NSP12-specific $CD4^+$ T-cells in individuals with resolved SARS-CoV-2 infection and seronegative individuals compared to individuals with acute infection. **(E)** The breadth of cross-reactive NSP12-specific $CD4^+$ T-cell responses in seronegative individuals is boosted by SARS-CoV-2 infection. **(F)** Increased breadth derives mostly from newly recognized specificities. Data are expressed as mean with a standard deviation. Mann–Whitney *U* test was performed to assess statistical significance. ns < 0.05; *p < 0.05.

TABLE 2 Most frequently detected peptides in COVID-19 patients and seronegative individuals.

Peptide	aa position	Sequence															RF
COVID-19 patients: most frequently detected peptides of the NSP12																	
NSP12_48	236–250	S	Y	Y	S	L	L	M	P	I	L	T	L	T	R	A	37%
NSP12_49	241–255	L	M	P	I	L	T	L	T	R	A	L	T	A	E	S	30%
NSP12_50	246–260	T	L	T	R	A	L	T	A	E	S	H	V	D	T	D	44%
NSP12_106	526–540	A	L	F	A	Y	T	K	R	N	V	I	P	T	I	T	22%
NSP12_129	641–655	K	H	T	T	C	C	S	L	S	H	R	F	Y	R	L	26%
NSP12_130	646–660	C	S	L	S	H	R	F	Y	R	L	A	N	E	C	A	26%
NSP12_131	651–665	R	F	Y	R	L	A	N	E	C	A	Q	V	L	S	E	26%
NSP12_138	686–700	T	T	A	Y	A	N	S	V	F	N	I	C	Q	A	V	22%
NSP12_139	691–705	N	S	V	F	N	I	C	Q	A	V	T	A	N	V	N	22%
NSP12_149	741–755	F	V	N	E	F	Y	A	Y	L	R	K	H	F	S	M	30%
NSP12_170	846–860	D	I	V	K	T	D	G	T	L	M	I	E	R	F	V	26%
Seronegative controls: most frequently detected peptides of the NSP12																	
NSP12_48	236–250	S	Y	Y	S	L	L	M	P	I	L	T	L	T	R	A	29%
NSP12_125	621–635	K	C	D	R	A	M	P	N	M	L	R	I	M	A	S	29%
NSP12_131	651–665	R	F	Y	R	L	A	N	E	C	A	Q	V	L	S	E	29%
NSP12_135	671–685	G	S	L	Y	V	K	P	G	G	T	S	S	G	D	A	29%
NSP12_138	686–700	T	T	A	Y	A	N	S	V	F	N	I	C	Q	A	V	50%
NSP12_139	691–705	N	S	V	F	N	I	C	Q	A	V	T	A	N	V	N	29%
NSP12_149	741–755	F	V	N	E	F	Y	A	Y	L	R	K	H	F	S	M	36%
NSP12_154	766–780	F	N	S	T	Y	A	S	Q	G	L	V	A	S	I	K	29%
NSP12_170	846–860	D	I	V	K	T	D	G	T	L	M	I	E	R	F	V	36%

3.5 Longitudinal assessment of the NSP12-specific T-cell response before and after SARS-CoV-2 infection

The NSP12-specific peptide set elicited a similar breadth of responses in SARS-CoV-2-naive and SARS-CoV-2-exposed individuals—most likely because of the high preservation of this protein among Coronaviridae and therefore due to pre-primed CCC-specific T-cell responses. Therefore, in the next step, we also assessed the NSP12 peptide-specific response repertoire longitudinally, before and after a SARS-CoV-2 infection. For five patients, longitudinal samples (before and after contracting COVID-19) were available for further analysis.

The mean number of individual peptide-specific $CD4^+$ T-cell responses detected before infection was 12.2 (range: 4–20) in these patients. This number increased only marginally and not significantly to 16.4 (range: 12–26) after SARS-CoV-2 infection (Figure 2). Patient HH-N12-37 even showed a decrease in responses after the COVID-19 infection (before: 20; afterward: 14).

Of note, each of the five individuals showed novel NSP12 peptide-specific $CD4^+$ T-cell responses after COVID-19 infection (Figure 2). In Supplementary Figure S3 and Supplementary Table S4, the detailed response repertoire and the distribution of NSP12-specific $CD4^+$ T-cell responses are listed for each patient.

Patient HH-N12-34 recognized the highest number of peptide specificities ($n = 7$), which primed an NSP12 peptide-specific $CD4^+$ T-cell response before and after SARS-CoV-2 infection. Overall, the NSP12 peptide-specific response repertoire only partially overlapped for the five individuals analyzed longitudinally at two time points, with the detection of new responses and loss of others —most likely CCC-specific T-cell responses—at the two different time points (31).

3.6 *In silico* analysis of the sequence similarity of SARS-CoV-2 NSP12 with CCC-specific peptides and serological evidence of previous exposure to CCCs

In a first step, to investigate the degree of T-cell response cross-reactivity with the four circulating CCCs, we started by analyzing the sequence identity of the most frequently detected SARS-CoV-2 epitopes in this study with the most widely circulating CCCs: 229E, HKU1, OC43, and NL63 (Figure 3). The amino acid sequences of these CCCs corresponding to the NSP12 of SARS-CoV-2 showed a sequence identity genome homology of up to 67.1% (range: 58.8%–67.1%) (Figure 3).

To put this in context with the degree of sequence identity of the structural proteins between different Coronaviridae, we also aligned

10.3389/fimmu.2023.1182504

TABLE 3 SARS-CoV-2 NSP12 peptide sequence identity with CCCs of the three most frequently detected peptides in seronegative and pre-pandemic controls.

Virus	Sequence														
NSP12_138 (aa686–700)															
SARS-CoV-2	T	T	A	Y	A	N	S	V	F	N	I	C	Q	A	V
229 E	•	•	•	•	•	•	•	•	•	•	•	F	•	•	•
NL63	S	•	•	•	•	•	•	I	•	•	•	F	•	•	•
OC43	•	•	•	F	•	•	•	•	•	•	•	•	•	•	•
HKU1	•	•	•	F	•	•	•	•	•	•	•	•	•	•	•
NSP12_149 (aa741–755)															
SARS-CoV-2	F	V	N	E	F	Y	A	Y	L	R	K	H	F	S	M
229 E	•	•	D	D	•	•	G	•	•	Q	•	•	•	•	•
NL63	•	I	D	D	Y	•	G	•	•	•	•	•	•	•	•
OC43	•	•	T	•	Y	•	E	F	•	•	•	•	•	•	•
HKU1	•	•	•	•	Y	•	E	F	•	C	•	•	•	•	•
NSP12_170 (aa846–860)															
SARS-CoV-2	D	I	V	K	T	D	G	T	L	M	I	E	R	F	V
229 E	•	•	T	•	•	•	A	V	I	L	L	•	•	Y	•
NL63	•	V	•	•	•	•	A	V	V	L	L	•	•	Y	•
OC43	•	L	L	•	•	•	S	V	•	L	•	•	•	•	•
HKU1	•	L	L	•	•	•	S	V	•	L	•	•	•	•	•

the SARS-CoV-2 amino acid sequences of the spike glycoprotein and the nucleoprotein with the corresponding CCC sequences. The SARS-CoV-2 spike glycoprotein and nucleoprotein showed a sequence similarity of up to 40.8% (range: 29.5%–40.8%) with the corresponding CCC sequences (Figure 3).

Next, we also determined CCC IgG serologies for ten COVID-19 patients and four seronegative individuals by performing the recomLine SARS-CoV-2 IgG as described earlier. Positive results above the cutoff value indicated a prior CCC infection (32). Each of the four SARS-CoV-2 seronegative patients with available CCC serology showed IgG antibodies against NL63.

The absence of nucleocapsid and spike antibodies indicated the SARS-CoV-2 seronegative status of all four included seronegative individuals. One of the seronegative patients showed IgG antibodies against each of the four CCCs (median: 2; range: 1–4). The 10 COVID-19 patients with available CCC serology data had at least IgG antibodies against two CCCs (median: 3.5; range: 0–4). The most often positively tested CCC in our cohort was NL63 (11 out of 14). Overall, the CCC with the fewest positive IgG antibody responses was OC43 (seven out of 14 patients) (Figure 3; Table 5).

In addition, we identified the three SARS-CoV-2 NSP12 peptide specificities with the highest response frequency in our seronegative cohort and their amino acid sequence identity between different human coronaviruses. (Table 3) The peptide specificity NSP12_138 (aa686–700) with the highest response frequency of 50% differed from corresponding sequences in the four CCCs by a mean of 1.5 amino acids (range: 1–3). The peptide specificities NSP12_149 (aa741–755) and NSP12_170 (aa846–860), both showing a response frequency of 36% in the seronegative cluster, differed by a mean of 5.13 amino acids (range: 4–7).

We compared the distribution response pattern of the peptide-specific $CD4^+$ T-cell responses with respect to the location within the NSP12 in protein in COVID-19 patients and seronegative individuals. We also aligned the 15-mer amino acid sequences of the SARS-COV-2 peptides and corresponding CCC peptides to determine the sequence identity with NSP12 on a single-peptide level (Figure 3).

Two regions of the NSP12 with especially high response frequencies in COVID-19 patients were the peptide specificities NSP12_48–50 (aa236–260) and the peptide specificities NSP12_137–139 (aa681–705) in the seronegative controls. All study groups showed only low response rates for peptide specificities NSP12_1–35 (aa1–185).

Furthermore, the peptide specificities NSP12_60–80 (aa296–410) elicited only a low response rate in COVID-19 patients, and the peptide specificities NSP12_89–102 (aa441–520) elicited no response at all in individuals without exposure to SARS-CoV-2 (Figure 3). The single-peptide sequence identity for the four different CCCs is also shown in parallel to the depicted distribution of NSP12 $CD4^+$ T-cell responses (Figure 3). The sequence analysis further revealed that the sequence identity did not exceed 60% for the peptide specificties NSP12 1-20 (aa1-110), which is a possible explanation for the low response frequency of seronegative controls in this area.

However, there were also areas such as the peptide specificities NSP12_140–148 (aa696–750) where, despite low sequence identity for

TABLE 4 *In vitro* and *in silico* HLA binding and HLA predictions.

Peptide	aa sequence	aa position		DRB1*01:01	DRB1*03:01	DRB1*04:01	DRB1*04:05	DRB1*07:01	DRB1*08:02	DRB1*09:01	DRB1*11:01	DRB1*12:01	DRB1*13:02	DRB1*15:01	Alleles bound
48	SYYSLLMPILTLTRA	236–250	*In vitro* (IC_{50} nM)	7.7	9,119	224	147	115	498	1,551	73	1,353	–	23	7
			In silico (rank)	0.16	38	1.9	5.6	13	33	2.8	4.2	12.65	61	21	
49	LMPILTLTRALTAES	241–255	*In vitro* (IC_{50} nM)	136	12,112	20	367	15	283	123	37	131	409	37	10
			In silico (rank)	5.6	13	6.3	9.7	5	0.37	18	2.2	10.2	26	13	
50	TLTRALTAESHVDTD	246–260	*In vitro* (IC_{50} nM)	2,099	1,644	4.1	99	14	501	59	301	4,486	–	1,293	6
			In silico (rank)	33	42	23	23	39	18	29	55	51	84	68	
91	SDYDYYRYNLPTMCD	451–465	*In vitro* (IC_{50} nM)	6,666	–	830	3,278	549	3,511	1,431	18,219	29,644	13,645	1,479	2
			In silico (rank)	26	48	6.4	9.9	38	47	11	23	68.5	23	30	
92	YRYNLPTMCDIRQLL	456–470	*In vitro* (IC_{50} nM)	12,010	–	5,315	4,645	1,845	–	1,488	8,942	5,124	–	2,915	0
			In silico (rank)	46	26	44	23	56	75	49	29	49.5	59	61	
105	YEDQDALFAYTKRNV	521–535	*In vitro* (IC_{50} nM)	15,983	39,384	3,086	–	35	495	8,573	21	–	–	480	4
			In silico (rank)	43	67	41	62	55	47	50	19	38.5	53	22	
106	ALFAYTKRNVIPTIT	526–540	*In vitro* (IC_{50} nM)	7,355	709	3,659	12,985	1.6	190	52	6.6	756	32	770	8
			In silico (rank)	28	35	33	48	2.7	9.1	31	3.1	38	7.4	20	
129	KHTTCCSLSHRFYRL	641–655	*In vitro* (IC_{50} nM)	279	916	613	644	56	1,009	286	235	59	1,175	447	9
			In silico (rank)	37	33	86	86	15	98	45	51	47.5	80	73	
130	CSLSHRFYRLANECA	646–660	*In vitro* (IC_{50} nM)	233	36,524	108	161	792	3,115	345	504	513	–	950	8
			In silico (rank)	3.7	63	4.4	9.8	26	47	32	14	25.5	73	23	
131	RFYRLANECAQVLSE	651–665	*In vitro* (IC_{50} nM)	53	8,410	27	270	279	2,347	48	367	6,324	23,820	611	7
			In silico (rank)	8	60	1.7	15	45	26	12	16	34.5	23	48	
137	SSGDATTAYANSVFN	681–695	*In vitro* (IC_{50} nM)	1,799	–	5,182	27,195	3,965	–	197	15,925	22,725	–	567	2
			In silico (rank)	63	93	84	74	36	93	59	94	81.5	28	59	
148	DVDTDFVNEFYAYLR	736–750	*In vitro* (IC_{50} nM)	856	28,451	16,886	–	–	2,198	6,954	949	–	–	1,181	2
			In silico (rank)	37	18	36	30	48	49	50	65	20.5	35	15	
149	FVNEFYAYLRKHFSM	741–755	*In vitro* (IC_{50} nM)	36,126	–	8,366	–	3,835	828	2,515	70	2,537	–	1,252	2
			In silico (rank)	12	43	26	19	31	4.8	20	0.11	16.5	64	4.5	
150	YAYLRKHFSMMILSD	746–760	*In vitro* (IC_{50} nM)	495	5,015	102	318	0.73	138	4.8	7.9	96	755	0.23	10
			In silico (rank)	11	21	7.6	9.7	0.88	8	4.4	1.8	9.05	3.1	3	

*_In silico_ predictions: the MHCII binding predictions were made on 8 August 2022 using the IEDB analysis resource Consensus tool. REFs: (29, 30).

10.3389/fimmu.2023.1182504

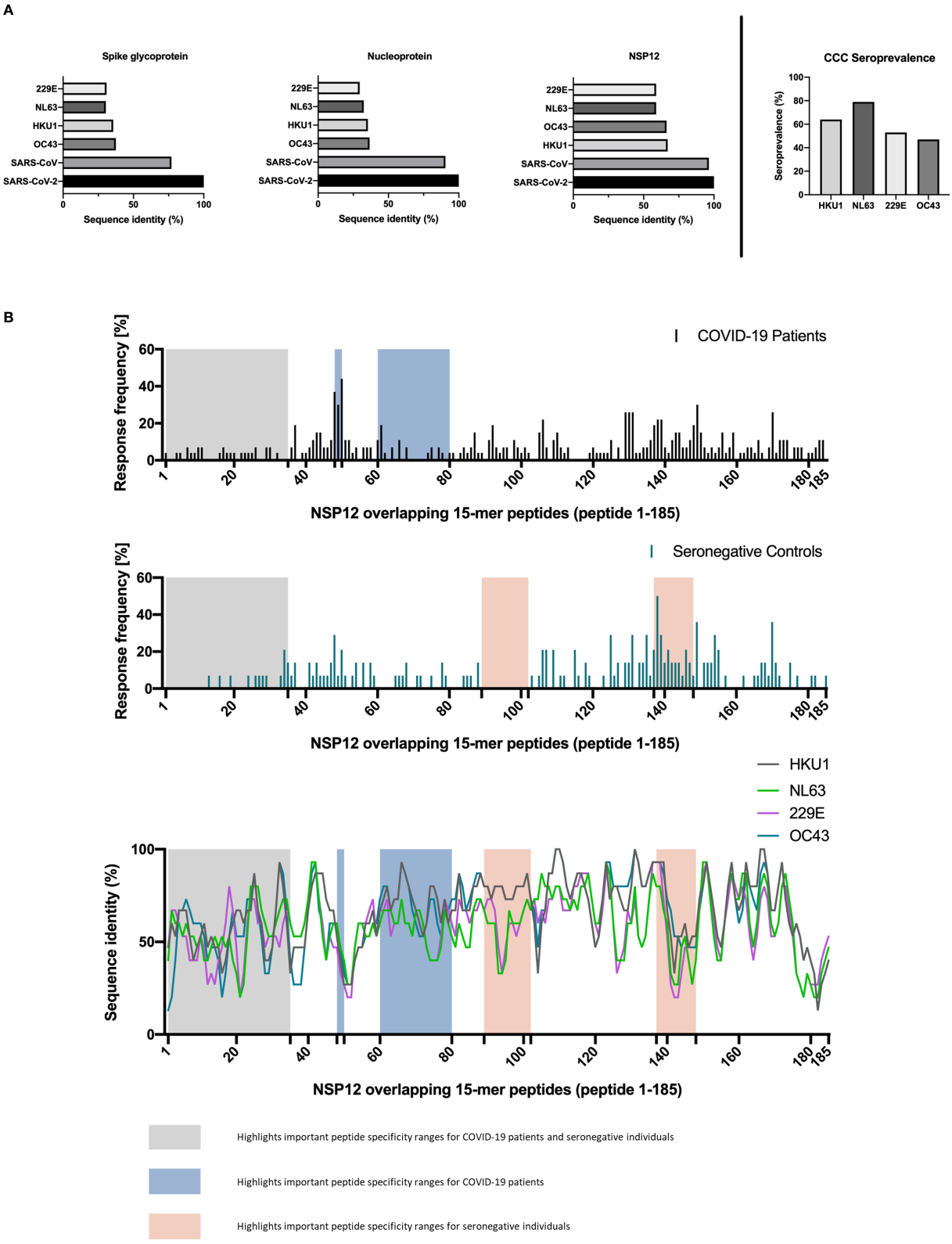

FIGURE 3
(A, B) Regions of SARS-CoV-2 NSP12 frequently targeted by seronegative individuals show different degrees of sequence identity with common cold coronaviruses. Canonical protein amino acid sequences of SARS-CoV-2 and common cold coronaviruses were extracted from the UniProtKB database and aligned using the UniProt blast tool. **(A)** The SARS-CoV-2 NSP12 protein has a higher sequence identity with the corresponding proteins of the 229E, NL63, OC43, and HKU1 common cold coronaviruses than the structural spike glycoprotein and nucleocapsid protein. Serologic positivity for common cold coronaviruses was highly prevalent in the study cohort. **(B)** High response rates to SARS-CoV-2 NSP12 peptides in SARS-CoV-2-infected individuals and seronegative individuals are not restricted to regions with higher than overall sequence identity.

TABLE 5 Available CCC and SARS-CoV-2 IgG serologies (LineBlot Assay) for COVID-19 patients and seronegative controls.

Patient ID	Human coronavirus 229E	Human coronavirus NL63	Human coronavirus OC43	Human coronavirus HKU1	SARS-CoV-2
HH-N12-8	☒	✓	✓	✓	✓
HH-N12-10	✓	✓	✓	✓	✓
HH-N12-11	☒	☒	☒	☒	✓
HH-N12-23	☒	✓	☒	☒	☒
HH-N12-27	☒	✓	☒	☒	☒
HH-N12-25	✓	✓	☒	✓	☒
HH-N12-12	☒	☒	☒	☒	✓
HH-N12-6	☒	☒	☒	✓	✓
HH-N12-1	✓	✓	✓	✓	✓
HH-N12-15	✓	✓	☒	☒	✓
HH-N12-26	✓	✓	✓	✓	☒
HH-N12-3	✓	✓	✓	✓	✓
HH-N12-17	✓	✓	✓	✓	✓
HH-N12-24	✓	✓	✓	✓	✓

all CCCs, a response rate of over 20% was observed for the seronegative controls. Peptide specificities NSP12_137–139 (aa681–705), which had the highest response rate for seronegative controls, showed a median amino acid sequence match of 93% (range: 67%–93%).

A detailed analysis of the distribution of NSP12-specific $CD4^+$ T-cell responses in COVID-19 patients and seronegative individuals and the sequence similarity with CCCs over the different NSP12 regions revealed a broad overall distribution of the individual peptide-specific $CD4^+$ T-cell responses across the entire protein. Peptides with high detection frequencies seemed to be located in areas with high genetic conservation of SARS-CoV-2 and high sequence identity with other CCCs.

3.7 Assessment of the *in vitro* cross-reactivity of CCC-specific peptide specificities in pre-pandemic samples with corresponding SARS-CoV-2 NSP12 peptide specificities

PBMCs of three seronegative controls (HH-N12-23, HH-N12-25, and HH-N12-27) who had detectable NSP12-specific T-cell responses were subsequently stimulated *in vitro* with the different, individual corresponding CCC 15-mer peptide specificities. We then re-stimulated these antigen T-cell cultures after 12 days with either the CCC peptide or the respective SARS-CoV-2 peptide and performed IFN-γ-ELISpot and ICS for testing for the subsequent analysis of potential cross-reactivity (Figure 4).

In detail, the cross-reactivity was assessed for peptide-specific T cells of pre-pandemic samples directed against CCC-specific peptides compared to their SARS-CoV-2 peptide analogs. Cells were cultured with NL63, 229E, and HKU1 15-mer peptides in separate wells and restimulated after 11–13 days with the corresponding SARS-CoV-2 NSP12 15-mer peptides and the CCC 15-mer peptide in a different IFN-γ-ELISpot well. In the case of a positive IFN-γ-ELISpot response, an ICS was performed for the validation of the $CD4^+$/$CD8^+$ T-cell response (Figure 5).

Eight different NSP12-specific peptide specificities that had previously elicited $CD4^+$ T-cell responses in at least two of the three seronegative samples were synthesized for the CCCs HKU1, NL63, and 229E. Each of the three individuals had serological evidence for exposure, defined as testing positive for IgG antibodies, against at least one of the three CCCs. Only the second individual (HH-N12-23) displayed antibodies against all three CCCs. In each of the three seronegative individuals, we detected specific $CD4^+$ T-cell responses against the CCC peptide and the corresponding NSP12 SARS-CoV-2 peptide at a similar breadth (mean: 4; range, 3–5).

The amino acid sequences for both viruses are shown below each graph, but some peptide specificities did not show any response in the IFN-γ-ELISpot. They are labeled with an asterisk "*" (Figure 5). This experimental setup clearly demonstrates $CD4^+$ T-cell cross-reactivity of several NSP12-specific 15-mer peptides with the corresponding CCC amino acid sequence-derived peptides and vice versa.

4 Discussion

Recently, we and others published in-depth characterizations of the breadth of the single-peptide-specific response directed against the spike glycoprotein and other structural SARS-CoV-2 proteins

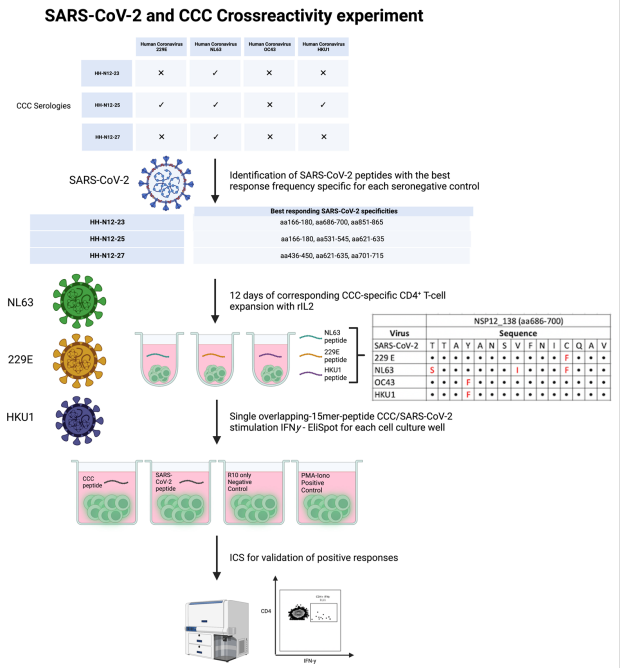

FIGURE 4
Experimental setup for CCC and SARS-CoV-2 T-cell cross-reactivity assessment.

(N, M, E) using highly sensitive techniques (2, 3). In analogy to these studies, the current study provides a detailed dataset on the range and specificity of the T-cell response directed against the SARS-CoV-2 NSP12 (RdRp).

We detected a high response rate and a rather broad, low-level (33) NSP12-specific T-cell response. The majority of these NSP12 peptide-specific T-cell responses were $CD4^+$ T-cell responses, as has been described for the T-cell response directed human COVID-19 T-cell response directed against other SARS-CoV-2 proteins (2, 3). We identified 160 out of 185 individual peptide specificities within this comprehensive overlapping peptide set that elicited an antigen-specific $CD4^+$ T-cell response in at least one of the 41 patients. We also found low-magnitude $CD8^+$ T-cell responses to a lesser extent in COVID-19 patients as well as in seronegative controls (34).

Previous investigations showed evidence for some degree of cross-reactivity between pre-primed CCC-specific T-cell responses and the SARS-CoV-2 response directed against the spike glycoprotein or the N, M, or E proteins (2, 3, 35–37). Furthermore, there are clinical observations that CCC seropositivity or the presence of cross-reactive T cells might affect the outcome of a subsequent SARS-CoV-2 infection (38). However, these results were not consistently found in all cohorts and are sometimes difficult to assess since the clinical outcome depends on a multitude of variables (39–42).

Importantly, the NSP12 is highly conserved between the different CCCs and SARS-CoV-2 (up to 67.1% sequence identity). SARS-CoV-1 even shows an NSP12 sequence identity of 96.4% with SARS-CoV-2 (43). Also, the NSP12 is highly conserved between the different variants of concern (VoC) and lineages under monitoring (LuM) of SARS-CoV-2 (44, 45). In our current study, 12 out of 14 patients had positive IgG antibody titers for at least one CCC.

Remarkably, the number of NSP12-specific $CD4^+$ T-cell responses was only slightly lower in the samples of individuals without a history of SARS-CoV-2 or pre-pandemic samples compared to COVID-19 patients, indicating an extremely high degree of cross-reactivity of CCC- and SARS-CoV-2 NSP12-specific T-cell responses.

Detailed sequence analysis and further *in vitro* experiments confirmed that some of the CCC and SARS-CoV-2 NSP12 epitopes had identical sequences, and other peptide sequences only differed by one or two amino acids and showed a high cross-reactivity *in vitro*. These results are in agreement with the recent findings of other studies (46, 47) that identified specific and cross-reactive $CD4^+$ T-cell epitopes in the CCC OC43 genome. The impact of evolving SARS-CoV-2 variants on the antigen-specific T-cell response is subject to extensive further research (48–50).

Previously, we and others showed that the magnitude but not the number of spike-specific peptide responses increased after repeated vaccination with mRNA spike glycoprotein vaccines (3, 51). This result is not unexpected, as a pre-primed spike- or CCC-specific T cells will expand upon re-encounter with the variant spike or NSP12 antigen according to the theory of antigenic imprinting (31, 52).

However, the interferences between SARS-CoV-2 and the other four CCCs, each having different epidemiology, tropism, and antigenicity, seem to be more complex (34, 53). Lately, it has also been reported that exposure to SARS-CoV-2 might interfere with CCC responses, either directly or indirectly. $CD4^+$ T-cell responses against CCCs are both increased and decreased in COVID-19 patients.

Of note, a number of other viruses also seem to exhibit some structural similarities with SARS-CoV-2 (54–56). The relevance of these potential cross-reactivities for the clinical course of infection and immunological parameters is yet to be investigated in detail. Similarly, while we saw a high level of cross-virus reactivity between CCC and the corresponding SARS-CoV-2-NSP12 epitopes, the picture was much more heterogeneous in the longitudinal analysis of five CCC seropositive individuals.

While we detected slightly more NSP12-specific responses after SARS-CoV-2 infection, this difference was not statistically significant. Also, the response repertoire changed over time—some responses decreased in magnitude or could not be detected again. It has to be taken into account that, methodically, (A) we analyzed T cells, not *ex vivo* but after short-term expansion; (B) the patient's histories differed in terms of past infections as well as the SARS-CoV-2 course of infection; and (C) the timing of sampling after infection differed.

The individual HLA haplotype and even the timing and kinetics of the NSP12 antigen processing should be considered being highly heterogeneous. No broader conclusions can be drawn from this small patient cohort about the clinical implications of the detected cross-reactivities. However, there is a clear interdependence that is highly complex, might differ from patient to patient depending on the exact previous exposure to different antigens, and is—judged on its own—of yet unclear clinical significance (40).

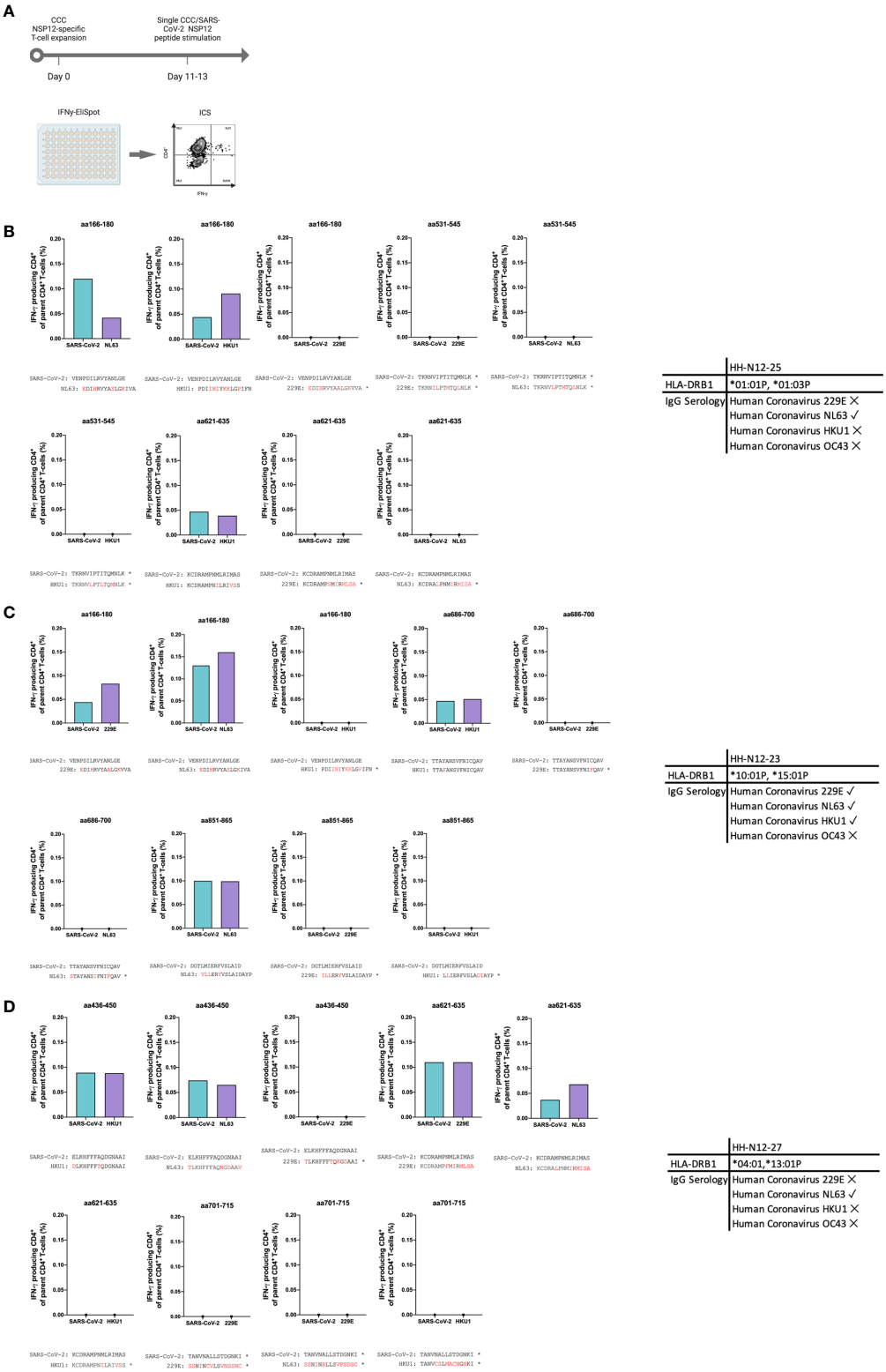

FIGURE 5
(A–D) *In vitro*-expanded common cold coronavirus NSP12-specific CD4$^+$ T-cells of seronegative controls cross-recognize corresponding SARS-CoV-2 NSP12 peptides. **(A)** PBMC of n = 3 seronegative controls were expanded *in vitro* with common cold coronavirus NSP12 peptides (according to their serologic positivity) as described before. After 11-13 days, the cells were analyzed for IFN-γ after individual restimulation with single peptides with the sequence of common cold coronaviruses and the corresponding SARS-CoV-2 peptides. **(B–D)** In all three individuals, considerable cross-recognition to corresponding SARS-CoV-2 peptides could be detected despite amino acid differences at certain positions (the asterisk shows sequences from 15-mer peptides used for stimulation that did not elicit a CD4$^+$ T-cell response in the IFN-γ-ELISpot).

The current study has several limitations: firstly, our seronegative controls could have theoretically been exposed to SARS-CoV-2 despite a negative history of acute viral illness and negative serology for nucleocapsid antibodies (NC-Abs) (57, 58), since it has been described that NC-Abs are sometimes not primed after infection or decline below the limit of detection in some cases (59, 60). However, the seronegative controls in the current study were recruited early during the pandemic, and nine out of nine seronegative controls later exhibited a COVID-19 infection with a positive SARS-CoV-2 PCR result and NC seroconversion in the highly sensitive and specific routine immunoassay [see the **Materials and methods** section (61)]. Of note, the profile of the NSP12-specific T-cell responses did not differ between the pre-pandemic and seronegative individuals. Secondly, the NSP12-specific responses were assessed only after NSP12-specific *in vitro* expansion in polyclonal cell cultures, which to some extent limits the comparability with *ex vivo* or *in vivo* settings. It might be influenced by stochastic effects due to the preferential expansion of certain peptide-specific clones when expanding with peptide mixes. Potentially, our results are biased by the study design, in which we used overlapping 15-mer peptides and one epitope might be located in between two adjacent peptides. Also, our methodology might bias toward the detection of NSP12 $CD4^+$ T-cell responses.

Also, the exact CCC infection history of the study participants (some of whom were also immunosuppressed) is not known, and we were also only able to obtain the CCC serologies of a subset of individuals. Additionally, the CCC-serological response can wane over time (62, 63), and a previous exposure might have been missed by just relying on the current serological test applied (64, 65). Furthermore, the autologous sequences of any of the respective infecting viruses are not known. Lastly, the assessment of the samples was not standardized in terms of sample acquisition and time after the SARS-CoV-2 infection.

Larger prospective studies need to assess (A) the impact of the T-cell response directed against structural proteins versus nonstructural proteins on the clinical course of a SARS-CoV-2 infection and as potential vaccination antigens; (B) the overall influence of positive CCC serology (and previous CCC infection) on disease outcome and certain T-cell responses; as well as (C) the influence of pre-pandemic imprinting on T-cell responses after a COVID-19 infection on the clinical course of other subsequent CCC infections and vice versa (66, 67).

Also, the *ex vivo* phenotype and *ex vivo* functionality of the NSP12-specific T-cell response in different tissues and after vaccination with inactivated whole virus vaccines (that include NSP12 as antigen) will be of interest.

Further research with newly developed methods (68, 69) could help to extend the results of this current study. The validation of our results in the context of complex antigens is needed (70). Also, the analysis of other NSPs of SARS-CoV-2 could prove useful for assessing the validity and relevance of these findings (71). The current study will be a useful resource for the development of novel NSP12 MHC class II tetramers (72) and provide further insight into the possibility of NSP12-based vaccines (73, 74).

This comparative high-resolution analysis of immunodominant NSP12 single-peptide T-cell specificities in COVID-19 patients with different infections and HLA backgrounds is evidence of the complexity and interdependence between pre-primed CCC T-cell responses and those directed against SARS-CoV-2 (7, 10).

In summary, we present a detailed investigation into the breadth of the single-peptide NSP12 $CD4^+$ T-cell response in a cohort of COVID-19 patients with known HLA backgrounds. We find a uniformly low-level, broadly directed T-cell response with several frequently detected NSP12 peptide specificities both in COVID-19 patients and SARS-CoV-2-naive individuals.

Simultaneously, we find evidence using sequence comparison, pre-pandemic samples, and *in vitro* experiments for a high degree of cross-reactivity of these responses with pre-primed CCC-specific responses. Only acutely infected SARS-CoV-2 patients show a significantly higher magnitude of the NSP12-specific T-cell response compared to SARS-CoV-2 seronegative individuals.

Data availability statement

The raw data supporting the conclusions of this article will be made available by the authors, without undue reservation.

Ethics statement

The studies involving human participants were reviewed and approved by Ärztekammer Hamburg (PV4780, PV7298). The patients/participants provided their written informed consent to participate in this study.

Author contributions

TW: Conceptualization; data curation; formal analysis; investigation; methodology; visualization; writing – original draft; writing – review and editing. MM: Conceptualization, investigation; methodology, project administration, supervision. HK: Conceptualization; data curation; investigation; methodology; writing – review and editing. LC: Data curation; investigation; methodology; visualization; writing – original draft. MK: Data curation; investigation; visualization. SS: formal analysis; investigation; methodology. LH: Data curation; resources. SPe: Resources. VD: Resources. AG: Resources, Validation. MA: Resources. SH: Resources, Validation. AS: Resources, Validation. ML: Resources. SPi: Resources. WK: Resources; validation. JS: Resources; validation. JSzW: Conceptualization; funding acquisition; methodology; project administration; resources; supervision; writing – original draft; writing – review and editing. All authors contributed to the article and approved the submitted version.

Funding

This project was funded (all to JSzW) by Deutsches Zentrum für Infektionsforschung (DZIF; TTU 04.816; TI07.003), the DFG (SFB

841 A6 and SFB1328 A12), the Damp Stiftung, and the ERC (European HIV Vaccine Alliance 681032). Figures 1, 2A, 4, and 5A were created with BioRender.com. We thank the NIH/NIAID for supporting AF (P01 AI168347) and AS (Contract No. 75N93019C00065).

Acknowledgments

We express our sincerest gratitude to all patients, co-workers, and healthy volunteers who participated in this study. We thank the staff of the I. Department of Medicine and Sophia Cichutek for their assistance with the recruitment of the patients and the collection and analysis of clinical data. We thank Silke Kummer, Robin Woost, and the staff of the Department of Transfusion Medicine and Institute of Medical Microbiology, Virology, and Hygiene for their continuous excellent technical assistance. We thank all former members of the working group Schulze zur Wiesch who provided us with their experiences, their help, and their support.

Conflict of interest

The authors declare that the research was conducted in the absence of any commercial or financial relationships that could be construed as a potential conflict of interest.

Publisher's note

Supplementary material

The Supplementary Material for this article can be found online at: https://www.frontiersin.org/articles/10.3389/fimmu.2023.1182504/full#supplementary-material

SUPPLEMENTARY FIGURE 1
Representative gating strategy.

SUPPLEMENTARY FIGURE 2
(A–C) NSP12-specific $CD8^+$ T-cells responses. **(A)** Number of individual NSP12-peptide-specific $CD8^+$ T-cell responses and average magnitude per individual of IFN-γ producing $CD8^+$ T-cells. **(B)** Representative flow cytometry plots of HH-N12-38. **(C)** Distribution of SARS-CoV-2 NSP12 $CD8^+$ T-cell responses in COVID-19 patients and seronegative individuals on a single 15-mer peptide level.

SUPPLEMENTARY FIGURE 3
Longitudinal characterization of the distribution and magnitude of NSP12-specific $CD4^+$ T-cell responses of each individual (n=5) before and after COVID-19 infection.

References

1. Marshall JC, Murthy S, Diaz J, Adhikari NK, Angus DC, Arabi YM, et al. A minimal common outcome measure set for COVID-19 clinical research. *Lancet Infect Dis* (2020) 20(8):e192–e7. doi: 10.1016/S1473-3099(20)30483-7

2. Heide J, Schulte S, Kohsar M, Brehm TT, Herrmann M, Karsten H, et al. Broadly directed SARS-CoV-2-specific CD4+ T cell response includes frequently detected peptide specificities within the membrane and nucleoprotein in patients with acute and resolved COVID-19. *PLoS Pathog* (2021) 17(9):e1009842. doi: 10.1371/journal.ppat.1009842

3. Karsten H, Cords L, Westphal T, Knapsp M, Brehm TT, Hermanussen L, et al. High-resolution analysis of individual spike peptide-specific CD4(+) T-cell responses in vaccine recipients and COVID-19 patients. *Clin Transl Immunol* (2022) 11(8):e1410. doi: 10.1002/cti2.1410

4. Shannon A, Le NT, Selisko B, Eydoux C, Alvarez K, Guillemot JC, et al. Remdesivir and SARS-CoV-2: Structural requirements at both nsp12 RdRp and nsp14 exonuclease active-sites. *Antiviral Res* (2020) 178:104793. doi: 10.1016/j.antiviral.2020.104793

5. Zhang WF, Stephen P, Thériault JF, Wang R, Lin SX. Novel coronavirus polymerase and nucleotidyl-transferase structures: potential to target new outbreaks. *J Phys Chem Lett* (2020) 11(11):4430–5. doi: 10.1021/acs.jpclett.0c00571

6. Pushpakumara PD, Madhusanka D, Dhanasekara S, Jeewandara C, Ogg GS, Malavige GN. Identification of novel candidate CD8(+) T cell epitopes of the SARS-CoV2 with homology to other seasonal coronaviruses. *Viruses.* (2021) 13(6). doi: 10.3390/v13060972

7. Milighetti M, Peng Y, Tan C, Mark M, Nageswaran G, Byrne S, et al. Large Clones of pre-existing T cells drive early immunity against SARS-COV-2 and LCMV infection. *bioRxiv.* (2022) 2022:11.08.515436. doi: 10.1101/2022.11.08.515436

8. Wang Q, Wu J, Wang H, Gao Y, Liu Q, Mu A, et al. Structural basis for RNA replication by the SARS-CoV-2 polymerase. *Cell.* (2020) 182(2):417–28.e13. doi: 10.1016/j.cell.2020.05.034

9. Heyer A, Günther T, Robitaille A, Lütgehetmann M, Addo MM, Jarczak D, et al. Remdesivir-induced emergence of SARS-CoV2 variants in patients with prolonged infection. *Cell Rep Med* (2022) 3(9):100735. doi: 10.1016/j.xcrm.2022.100735

10. Murray SM, Ansari AM, Frater J, Klenerman P, Dunachie S, Barnes E, et al. The impact of pre-existing cross-reactive immunity on SARS-CoV-2 infection and vaccine responses. *Nat Rev Immunol* (2022), 1–13. doi: 10.1038/s41577-022-00809-x

11. Lin CY, Wolf J, Brice DC, Sun Y, Locke M, Cherry S, et al. Pre-existing humoral immunity to human common cold coronaviruses negatively impacts the protective SARS-CoV-2 antibody response. *Cell Host Microbe* (2022) 30(1):83–96.e4. doi: 10.1016/j.chom.2021.12.005

12. Meyerholz DK, Perlman S. Does common cold coronavirus infection protect against severe SARS-CoV-2 disease? *J Clin Invest.* (2021) 131(1):e144807. doi: 10.1172/JCI144807

13. García-Jiménez ÁF, Cáceres-Martell Y, Fernández-Soto D, Martínez Fleta P, Casasnovas JM, Sánchez-Madrid F, et al. Cross-reactive cellular, but not humoral, immunity is detected between OC43 and SARS-CoV-2 NPs in people not infected with SARS-CoV-2: possible role of cTFH cells. *J Leukocyte Biol* (2022) 112(2):339–46. doi: 10.1002/JLB.4COVCRA0721-356RRR

14. Grifoni A, Weiskopf D, Ramirez SI, Mateus J, Dan JM, Moderbacher CR, et al. Targets of T cell responses to SARS-CoV-2 coronavirus in humans with COVID-19 disease and unexposed individuals. *Cell.* (2020) 181(7):1489–501.e15. doi: 10.1016/j.cell.2020.05.015

15. Wang R, Simoneau CR, Kulsuptrakul J, Bouhaddou M, Travisano KA, Hayashi JM, et al. Genetic screens identify host factors for SARS-CoV-2 and common cold coronaviruses. *Cell.* (2021) 184(1):106–19.e14. doi: 10.1016/j.cell.2020.12.004

16. Mateus J, Grifoni A, Tarke A, Sidney J, Ramirez SI, Dan JM, et al. Selective and cross-reactive SARS-CoV-2 T cell epitopes in unexposed humans. *Science.* (2020) 370 (6512):89–94. doi: 10.1126/science.abd3871

17. Parker R, Partridge T, Wormald C, Kawahara R, Stalls V, Aggelakopoulou M, et al. Mapping the SARS-CoV-2 spike glycoprotein-derived peptidome presented by HLA class II on dendritic cells. *bioRxiv* (2020) 35(8):109179. doi: 10.1101/2020.08.19.255901

18. Le Bert N, Tan AT, Kunasegaran K, Tham CYL, Hafezi M, Chia A, et al. SARS-CoV-2-specific T cell immunity in cases of COVID-19 and SARS, and uninfected controls. *Nature.* (2020) 584(7821):457–62. doi: 10.1038/s41586-020-2550-z

19. Nörz D, Fischer N, Schultze A, Kluge S, Mayer-Runge U, Aepfelbacher M, et al. Clinical evaluation of a SARS-CoV-2 RT-PCR assay on a fully automated system for rapid on-demand testing in the hospital setting. *J Clin Virol* (2020) 128:104390. doi: 10.1016/j.jcv.2020.104390

20. Consortium TU. UniProt: the universal protein knowledgebase in 2023. *Nucleic Acids Res* (2022) 51(D1):D523–D31. doi: 10.1093/nar/gkac1052

21. da Costa Lima Caniatti MC, Borelli SD, Guilherme AL, Tsuneto LT. Association between HLA genes and dust mite sensitivity in a Brazilian population. *Hum Immunol* (2017) 78(2):88–94. doi: 10.1016/j.humimm.2016.10.014

22. Brehm TT, Ullrich F, Thompson M, Küchen J, Schwinge D, Spier A, et al. Three separate spike antigen exposures by COVID-19 vaccination or SARS-CoV-2 infection elicit strong humoral immune responses in healthcare workers. *Vaccines.* (2022) 10 (7):1086. doi: 10.3390/vaccines10071086

23. Medrano S, Martínez-Rodríguez M, Vallejo L, Culebras E, Delgado-Iribarren A. [Evaluation of two immunocromatographic tests for the detection of antibodies against SARS-CoV-2]. *Rev Esp Quimioter.* (2022) 35(6):538–43. doi: 10.37201/req/019.2022

24. Sidney J, Southwood S, Moore C, Oseroff C, Pinilla C, Grey HM, et al. Measurement of MHC/peptide interactions by gel filtration or monoclonal antibody capture. *Curr Protoc Immunol* (2013) Chapter 18:Unit 18.3. doi: 10.1002/0471142735.im1803s100

25. Bui HH, Sidney J, Dinh K, Southwood S, Newman MJ, Sette A. Predicting population coverage of T-cell epitope-based diagnostics and vaccines. *BMC Bioinf* (2006) 7:153. doi: 10.1186/1471-2105-7-153

26. *Immune epitope database and analysis resource 2005* (2023). Available at: http://www.iedb.org.

27. Gonzalez-Galarza FF, McCabe A, Santos E, Jones J, Takeshita L, Ortega-Rivera ND, et al. Allele frequency net database (AFND) 2020 update: Gold-standard data classification, open access genotype data and new query tools. *Nucleic Acids Res* (2020) 48(D1):D783–d8. doi: 10.1093/nar/gkz1029

28. Greenbaum J, Sidney J, Chung J, Brander C, Peters B, Sette A. Functional classification of class II human leukocyte antigen (HLA) molecules reveals seven different supertypes and a surprising degree of repertoire sharing across supertypes. *Immunogenetics.* (2011) 63(6):325–35. doi: 10.1007/s00251-011-0513-0

29. Wang P, Sidney J, Dow C, Mothé B, Sette A, Peters B.. A systematic assessment of MHC class II peptide binding predictions and evaluation of a consensus approach. *PLoS Comput Biol* (2008) 4:e1000048.

30. Wang P, Sidney J, Kim Y. Peptide binding predictions for HLA DR, DP and DQ molecules. *BMC Bioinform* (2010) 11:568.

31. Aguilar-Bretones M, Fouchier RA, Koopmans MP, van Nierop GP. Impact of antigenic evolution and original antigenic sin on SARS-CoV-2 immunity. *J Clin Invest.* (2023) 133(1):e162192. doi: 10.1172/JCI162192

32. Steiner A, Pletz M, Löffler B, Baier M. A novel SARS-CoV-2 IgG line-blot for evaluating discrepant IgG test results - observations in pre-pandemic and follow-up samples of five patients. *J Microbiol Immunol Infect* (2021) 54(5):979–82. doi: 10.1016/j.jmii.2021.03.004

33. Landahl J, Bockmann JH, Scheurich C, Ackermann C, Matzat V, Heide J, et al. Detection of a broad range of low-level major histocompatibility complex class II-restricted, hepatitis delta virus (HDV)-specific T-cell responses regardless of clinical status. *J Infect Dis* (2019) 219(4):568–77. doi: 10.1093/infdis/jiy549

34. Nesterenko PA, McLaughlin J, Tsai BL, Burton Sojo G, Cheng D, Zhao D, et al. HLA-A(*)02:01 restricted T cell receptors against the highly conserved SARS-CoV-2 polymerase cross-react with human coronaviruses. *Cell Rep* (2021) 37(13):110167. doi: 10.1016/j.celrep.2021.110167

35. Bertoletti A, Le Bert N, Tan AT. SARS-CoV-2-specific T cells in the changing landscape of the COVID-19 pandemic. *Immunity.* (2022) 55(10):1764–78. doi: 10.1016/j.immuni.2022.08.008

36. Dykema AG, Zhang B, Woldemeskel BA, Garliss CC, Cheung LS, Choudhury D, et al. Functional characterization of CD4+ T cell receptors crossreactive for SARS-CoV-2 and endemic coronaviruses. *J Clin Invest* (2021) 131(10):e146922. doi: 10.1172/JCI146922

37. Johansson AM, Malhotra U, Kim YG, Gomez R, Krist MP, Wald A, et al. Cross-reactive and mono-reactive SARS-CoV-2 CD4+ T cells in prepandemic and COVID-19 convalescent individuals. *PLoS Pathog* (2021) 17(12):e1010203. doi: 10.1371/journal.ppat.1010203

38. Moss P. The T cell immune response against SARS-CoV-2. *Nat Immunol* (2022) 23(2):186–93. doi: 10.1038/s41590-021-01122-w

39. Swadling L, Diniz MO, Schmidt NM, Amin OE, Chandran A, Shaw E, et al. Pre-existing polymerase-specific T cells expand in abortive seronegative SARS-CoV-2. *Nature.* (2022) 601(7891):110–7. doi: 10.1038/s41586-021-04186-8

40. Sette A, Crotty S. Adaptive immunity to SARS-CoV-2 and COVID-19. *Cell.* (2021) 184(4):861–80. doi: 10.1016/j.cell.2021.01.007

41. Loyal L, Braun J, Henze L, Kruse B, Dingeldey M, Reimer U, et al. Cross-reactive CD4+ T cells enhance SARS-CoV-2 immune responses upon infection and vaccination. *Science* (2021) 374(6564):eabh1823. doi: 10.1126/science.abh1823

42. Gupta AM, Mandal S, Mandal S, Chakrabarti J. Immune escape facilitation by mutations of epitope residues in RdRp of SARS-CoV-2. *bioRxiv.* (2021) 2021:11.18.469065. doi: 10.1101/2021.11.18.469065

43. Abdelrahman Z, Li M, Wang X. Comparative review of SARS-CoV-2, SARS-CoV, MERS-CoV, and influenza a respiratory viruses. *Front Immunol* (2020) 11:552909. doi: 10.3389/fimmu.2020.552909

44. Pitts J, Li J, Perry JK, Du Pont V, Riola N, Rodriguez L, et al. Remdesivir and GS-441524 retain antiviral activity against delta, omicron, and other emergent SARS-CoV-2 variants. *Antimicrob Agents Chemother* (2022) 66(6):e0022222. doi: 10.1128/aac.00222-22

45. Sahin E, Bozdayi G, Yigit S, Muftah H, Dizbay M, Tunccan OG, et al. Genomic characterization of SARS-CoV-2 isolates from patients in Turkey reveals the presence of novel mutations in spike and nsp12 proteins. *J Med Virol* (2021) 93(10):6016–26. doi: 10.1002/jmv.27188

46. Muik A, Lui BG, Diao H, Fu Y, Bacher M, Toker A, et al. Progressive loss of conserved spike protein neutralizing antibody sites in omicron sublineages is balanced by preserved T-cell recognition epitopes. *bioRxiv.* (2022) 2022:12.15.520569. doi: 10.1101/2022.12.15.520569

47. Becerra-Artiles A, Nanaware PP, Muneeruddin K, Weaver GC, Shaffer SA, Calvo-Calle JM, et al. Immunopeptidome profiling of human coronavirus OC43-infected cells identifies CD4 T cell epitopes specific to seasonal coronaviruses or cross-reactive with SARS-CoV-2. *bioRxiv.* (2022) 2022:12.01.518643. doi: 10.1101/2022.12.01.518643

48. Emmelot ME, Vos M, Boer MC, Rots NY, van Els CACM, Kaaijk P. SARS-CoV-2 omicron BA.4/BA.5 mutations in spike leading to T cell escape in recently vaccinated individuals. *Viruses* (2023) 15(1):101. doi: 10.3390/v15010101

49. Tarke A, Sidney J, Methot N, Yu ED, Zhang Y, Dan JM, et al. Impact of SARS-CoV-2 variants on the total CD4(+) and CD8(+) T cell reactivity in infected or vaccinated individuals. *Cell Rep Med* (2021) 2(7):100355. doi: 10.1016/j.xcrm.2021.100355

50. Tarke A, Coelho CH, Zhang Z, Dan JM, Yu ED, Methot N, et al. SARS-CoV-2 vaccination induces immunological T cell memory able to cross-recognize variants from alpha to omicron. *Cell.* (2022) 185(5):847–59.e11. doi: 10.1016/j.cell.2022.01.015

51. Koerber N, Priller A, Yazici S, Bauer T, Cheng CC, Mijočević H, et al. Dynamics of spike-and nucleocapsid specific immunity during long-term follow-up and vaccination of SARS-CoV-2 convalescents. *Nat Commun* (2022) 13(1):153. doi: 10.1038/s41467-021-27649-y

52. Lim JME, Tan AT, Le Bert N, Hang SK, Low JGH, Bertoletti A. SARS-CoV-2 breakthrough infection in vaccinees induces virus-specific nasal-resident CD8+ and CD4+ T cells of broad specificity. *J Exp Med* (2022) 219(10):e20220780. doi: 10.1084/jem.20220780

53. Lehmann AA, Kirchenbaum GA, Zhang T, Reche PA, Lehmann PV. Deconvoluting the T cell response to SARS-CoV-2: specificity versus chance and cognate cross-reactivity. *Front Immunol* (2021) 12:635942. doi: 10.3389/fimmu.2021.635942

54. Lustig Y, Keler S, Kolodny R, Ben-Tal N, Atias-Varon D, Shlush E, et al. Potential antigenic cross-reactivity between severe acute respiratory syndrome coronavirus 2 (SARS-CoV-2) and dengue viruses. *Clin Infect Diseases.* (2020) 73(7): e2444–e9. doi: 10.1093/cid/ciaa1207

55. Hunsawong T, Buddhari D, Rungrojcharoenkit K, Suthangkornkul R, Mongkolsirichaikul D, Lohachanakul J, et al. Anti-arbovirus antibodies cross-react with severe acute respiratory syndrome coronavirus 2. *Microbiol Spectrum.* (2022) 10 (6):e02639–22. doi: 10.1128/spectrum.02639-22

56. Aljuaid A, Salam A, Almehmadi M, Baammi S, Alshabrmi FM, Allahyani M, et al. Structural homology-based drug repurposing approach for targeting NSP12 SARS-CoV-2. *Molecules* (2022) 27(22):7732. doi: 10.3390/molecules27227732

57. Ripperger TJ, Uhrlaub JL, Watanabe M, Wong R, Castaneda Y, Pizzato HA, et al. Orthogonal SARS-CoV-2 serological assays enable surveillance of low-prevalence communities and reveal durable humoral immunity. *Immunity.* (2020) 53(5):925–33.e4. doi: 10.1016/j.immuni.2020.10.004

58. Tan CW, Chia WN, Qin X, Liu P, Chen MI, Tiu C, et al. A SARS-CoV-2 surrogate virus neutralization test based on antibody-mediated blockage of ACE2-spike protein-protein interaction. *Nat Biotechnol* (2020) 38(9):1073–8. doi: 10.1038/s41587-020-0631-z

59. Krutikov M, Palmer T, Tut G, Fuller C, Azmi B, Giddings R, et al. Prevalence and duration of detectable SARS-CoV-2 nucleocapsid antibodies in staff and residents of long-term care facilities over the first year of the pandemic (VIVALDI study): prospective cohort study in England. *Lancet Healthy Longev* (2022) 3(1):e13–21. doi: 10.1016/S2666-7568(21)00282-8

60. Van Elslande J, Oyaert M, Lorent N, Vande Weygaerde Y, Van Pottelbergh G, Godderis L, et al. Lower persistence of anti-nucleocapsid compared to anti-spike antibodies up to one year after SARS-CoV-2 infection. *Diagn Microbiol Infect Dis* (2022) 103(1):115659. doi: 10.1016/j.diagmicrobio.2022.115659

61. Riester E, Findeisen P, Hegel JK, Kabesch M, Ambrosch A, Rank CM, et al. Performance evaluation of the Roche elecsys anti-SARS-CoV-2 s immunoassay. *J Virol Methods* (2021) 297:114271. doi: 10.1016/j.jviromet.2021.114271

62. Lynch SA, Subbarao K, Mahanty S, Barber BE, Roulis EV, van der Hoek L, et al. Prevalence of neutralising antibodies to HCoV-NL63 in healthy adults in Australia. *Viruses.* (2021) 13(8):1618. doi: 10.3390/v13081618

63. Edridge AWD, Kaczorowska J, Hoste ACR, Bakker M, Klein M, Loens K, et al. Seasonal coronavirus protective immunity is short-lasting. *Nat Med* (2020) 26 (11):1691–3. doi: 10.1038/s41591-020-1083-1

64. Hamady A, Lee J, Loboda ZA. Waning antibody responses in COVID-19: what can we learn from the analysis of other coronaviruses? *Infection* (2022) 50(1):11–25. doi: 10.1007/s15010-021-01664-z

65. Ortega N, Ribes M, Vidal M, Rubio R, Aguilar R, Williams S, et al. Seven-month kinetics of SARS-CoV-2 antibodies and role of pre-existing antibodies to human coronaviruses. *Nat Commun* (2021) 12(1):4740. doi: 10.1038/s41467-021-24979-9

66. Yu ED, Narowski TM, Wang E, Garrigan E, Mateus J, Frazier A, et al. Immunological memory to common cold coronaviruses assessed longitudinally over a three-year period pre-COVID19 pandemic. *Cell Host Microbe* (2022) 30(9):1269–78.e4. doi: 10.1016/j.chom.2022.07.012

67. da Silva Antunes R, Pallikkuth S, Williams E, Dawen Yu E, Mateus J, Quiambao L, et al. Differential T-cell reactivity to endemic coronaviruses and SARS-CoV-2 in community and health care workers. *J Infect Dis* (2021) 224(1):70–80. doi: 10.1093/infdis/jiab176

68. Feng Y, Zhao X, White AK, Garcia KC, Fordyce PM. A bead-based method for high-throughput mapping of the sequence- and force-dependence of T cell activation. *Nat Methods* (2022) 19(10):1295–305. doi: 10.1038/s41592-022-01592-2

69. Vazquez-Lombardi R, Jung JS, Schlatter FS, Mei A, Mantuano NR, Bieberich F, et al. High-throughput T cell receptor engineering by functional screening identifies candidates with enhanced potency and specificity. *Immunity*. (2022) 55(10):1953–66.e10. doi: 10.1016/j.immuni.2022.09.004

70. Jing L, Wu X, Krist MP, Hsiang TY, Campbell VL, McClurkan CL, et al. T Cell response to intact SARS-CoV-2 includes coronavirus cross-reactive and variant-specific components. *JCI Insight* (2022) 7(6):e158126. doi: 10.1172/jci.insight.158126

71. Braun J, Loyal L, Frentsch M, Wendisch D, Georg P, Kurth F, et al. SARS-CoV-2-reactive T cells in healthy donors and patients with COVID-19. *Nature*. (2020) 587 (7833):270–4. doi: 10.1038/s41586-020-2598-9

72. Cords L, Knapp M, Woost R, Schulte S, Kummer S, Ackermann C, et al. High and sustained *ex vivo* frequency but altered phenotype of SARS-CoV-2-Specific CD4 (+) T-cells in an anti-CD20-Treated patient with prolonged COVID-19. *Viruses* (2022) 14(6). doi: 10.3390/v14061265

73. Safavi A, Kefayat A, Mahdevar E, Abiri A, Ghahremani F. Exploring the out of sight antigens of SARS-CoV-2 to design a candidate multi-epitope vaccine by utilizing immunoinformatics approaches. *Vaccine*. (2020) 38(48):7612–28. doi: 10.1016/j.vaccine.2020.10.016

74. Ali Z, Cardoza JV, Basak S, Narsaria U, Singh VP, Isaac SP, et al. Computational design of candidate multi-epitope vaccine against SARS-CoV-2 targeting structural (S and n) and non-structural (NSP3 and NSP12) proteins. *J Biomolecular Structure Dynamics* (2023), 1–20. doi: 10.1080/07391102.2023.2173297

frontiers | Frontiers in Immunology

TYPE Review
PUBLISHED 19 June 2023
DOI 10.3389/fimmu.2023.1212546

OPEN ACCESS

EDITED BY
Tomasz Piotr Wypych,
Polish Academy of Sciences, Poland

REVIEWED BY
Kenichi Hanada,
National Institutes of Health (NIH), United States
Olivier Gasser,
Malaghan Institute or Medical Research, New Zealand

*CORRESPONDENCE
Cécile Gouttefangeas
cecile.gouttefangeas@uni-tuebingen.de

RECEIVED 26 April 2023
ACCEPTED 24 May 2023
PUBLISHED 19 June 2023

CITATION
Gouttefangeas C, Klein R and Maia A (2023) The good and the bad of T cell cross-reactivity: challenges and opportunities for novel therapeutics in autoimmunity and cancer. *Front. Immunol.* 14:1212546. doi: 10.3389/fimmu.2023.1212546

The good and the bad of T cell cross-reactivity: challenges and opportunities for novel therapeutics in autoimmunity and cancer

Cécile Gouttefangeas[1,2,3]*, Reinhild Klein[4] and Ana Maia[1,2]

[1]Department of Immunology, Institute for Cell Biology, University of Tübingen, Tübingen, Germany, [2]Cluster of Excellence iFIT (EXC2180) "Image-Guided and Functionally Instructed Tumor Therapies", University of Tübingen, Tübingen, Germany, [3]German Cancer Consortium (DKTK) and German Cancer Research Center (DKFZ) partner site Tübingen, Tübingen, Germany, [4]Department of Hematology, Oncology, Clinical Immunology and Rheumatology, University Hospital Tübingen, Tübingen, Germany

T cells are main actors of the immune system with an essential role in protection against pathogens and cancer. The molecular key event involved in this absolutely central task is the interaction of membrane-bound specific T cell receptors with peptide-MHC complexes which initiates T cell priming, activation and recall, and thus controls a range of downstream functions. While textbooks teach us that the repertoire of mature T cells is highly diverse, it is clear that this diversity cannot possibly cover all potential foreign peptides that might be encountered during life. TCR cross-reactivity, i.e. the ability of a single TCR to recognise different peptides, offers the best solution to this biological challenge. Reports have shown that indeed, TCR cross-reactivity is surprisingly high. Hence, the T cell dilemma is the following: be as specific as possible to target foreign danger and spare self, while being able to react to a large spectrum of body-threatening situations. This has major consequences for both autoimmune diseases and cancer, and significant implications for the development of T cell-based therapies. In this review, we will present essential experimental evidence of T cell cross-reactivity, implications for two opposite immune conditions, i.e. autoimmunity vs cancer, and how this can be differently exploited for immunotherapy approaches. Finally, we will discuss the tools available for predicting cross-reactivity and how improvements in this field might boost translational approaches.

KEYWORDS

T cell receptor, cross-reactivity, autoimmunity, cancer, immunotherapy

1 Introduction: basics on TCR cross-reactivity

T cells are essential players of the adaptive immunity that are not only responsible for long-term immune memory, but also orchestrate innate and adaptive immune responses. Immature T cells undergo a strict selection in the thymus which leads to the release of mature, largely self-tolerant, T cells. Each of these cells bears several 10.000 copies of a unique kind of T cell receptor (TCR) that results from the assembly of two recombined TCR chains (in most cases α and β) (1, 2). The TCRαβ interacts with antigens presented as peptides by cell membrane-bound molecules of the major histocompatibility complex (pMHC) on the antigen presenting cell (APC) or on the target cell, for example, after pathogen infection (Figure 1A). Importantly, the binding of peptides to the various MHC allelic products is subject to specific rules (anchor or preferred residues) (4, 5). The diversity of the TCRαβ T cell repertoire is high, but not unlimited. Based on the V, D and J fragments´ recombination at the two chain loci, the theoretical number of single TCRs is estimated to reach at least 10^{15}. In fact, the sum of all different TCRs present in the human blood has been estimated to be much less, in the range of 2.5 x 10^7 for naïve T cells and approximately 100-fold lower for memory T cells (6–8). The number of potential pathogen- (and tumour-) derived epitopes presented as pMHC throughout life might well exceed this number of T cell clones. It became therefore progressively clear that the clonal selection theory, which proposed that one lymphocyte/receptor is available for each single antigen, needed to be revised, and that cross-reactivity, i.e. the ability of single TCRs to recognise multiple peptide sequences, is a frequent event (9–11).

Cross-reactivity is commonly observed when testing nearly identical peptides which differ only in 1 or 2 amino acids (aa) (for a total length of 8-10 aa for a $CD8^+$ T cell epitope presented by MHC-class I). This is physiologically highly relevant for fighting rapidly mutating viruses like HIV, SARS-Cov-2 or dengue viruses (9, 12–14). An interesting example is that of HIV elite controllers who are often HLA-B*5701$^+$, an allelic product which, according to *in silico* models, is recognised by T cells with high cross-reactive potential (15). Heterologous immunity, whereby T cells cross-react with different viruses, is also frequently reported and has been reviewed elsewhere (16). In addition, many examples of T cells reacting to very different aa sequences are known (17, 18). Kersh and colleagues claimed that a peptide is recognised as long as it contains a motif for binding to the MHC and one key residue for the TCR (18). This concept was refined by the observation that no single residue was strictly required for recognition, if the available residues allow for a sufficient affinity between the MHC and TCR molecules (19). Thus, peptides not sharing a single residue may productively interact with the same TCR. A similar flexibility was also observed for the length of the MHC-class II peptide, with some $CD4^+$ T cells requiring as little as four aa for recognition as long as these optimally fit to the MHC and TCR (20). In contrast, in a more recent study based on a unique experimental approach, Birnbaum et al. tested a set of murine and human $CD4^+$ T cell clones and observed that the diversity of the peptide sequences recognised by single TCRs could be smaller than previously thought (21). Still, pluriallelic restriction, as well as alloreactivity have also been experimentally observed (22–24), increasing the number of cross-reactivity scenarios. The structural features that rule cross-recognition have been described in detail (3, 14, 17, 23, 25). They include several mechanisms of conformational adaptation of the TCR and pMHC units (e.g. changes in the TCR docking, displacement of the CDR loop), as summarised in Figure 1B. Hence, TCR-pMHC interactions are not rigidly conserved, but rather allow for considerable flexibility within the confines of some general orientation and binding rules. It is also important to note that *in vivo*, T cell cross-reactivity is very likely fine-tuned by the set of co-receptors (inhibitory or activating) and adhesion molecules that the T cell expresses at a given time (26).

A very convincing hint that our T cell immunity is shaped by cross-reactivity was provided in the elegant study of Su et al. (27): a search for HLA-DRB1*0401 restricted $CD4^+$ T cells specific for HIV-, CMV- and HSV-derived epitopes in the blood of virus-unexposed healthy donors revealed that although the frequency of such cells was very low (< 10 cells per million), a large fraction (variable between individuals but in average > 50%) were found in the $CD45RO^+$ subset. Looking at HIV-specific cells more precisely, the authors confirmed that these $CD45RO^+$ cells represent a memory cell pool by assessing IFN-γ production, sequencing the TCR, and analysing further memory markers by gene expression. In addition, such cells were not found in umbilical cord blood. Finally, cross-reactivity of HIV-specific T cell clones with a range of bacterial- or algae-derived peptides suggested that such cells had been primed by unrelated antigens. Also relevant for vaccination, the authors further showed that Influenza-specific clones derived after Flu vaccination were able to recognise related peptidic sequences derived from other microbes. Similar observations were done by the group of F. Sallusto that demonstrated that HIV-specific $CD4^+$ T cells could be detected in both the naive and memory T cell subsets (defined with the two markers CD45RA and CCR7) of HIV-unexposed healthy donors (28). The large majority (>80%) of the HIV-epitopes activating memory T cells matched strongly with human microbiome aa sequences. A further notable observation in this report was that both the specificity and the frequency of these HIV-specific T cells were different across donors. This highlights the inter-individual variability of T cell responses, likely to be shaped by both MHC-polymorphism and the environment.

Despite clear evidences about the cross-reactive nature of the TCR, it remains unclear how many single peptides can a unique TCR recognise in "real life". According to early estimates, it should be approx. 10^6 (29). Meanwhile, there is evidence from several studies that individual T cell clones can indeed sense over a million different peptides in the context of a single MHC molecule (30–32). Studying the cross-reactive repertoire of an autoimmune HLA-A*0201 $CD8^+$ T cell clone which recognises a 10 aa-long preproinsulin-derived peptide, Sewell and co-workers showed that many of the "cross-reactive" peptides were better agonists than the original one, despite some sequences differing in up to 7 out of the 10 aa positions (31). Based on the assumption that only 1% of all peptides will end up being presented on MHC, they also estimated the "true" frequency of cross-reactivity to be approximately 1 in 10^4 peptides (11, 31). This is in the same range as the frequency of 1 in $3x10^4$ found by Ishizuka et al. when using a peptide library derived from pathogen sequences (33).

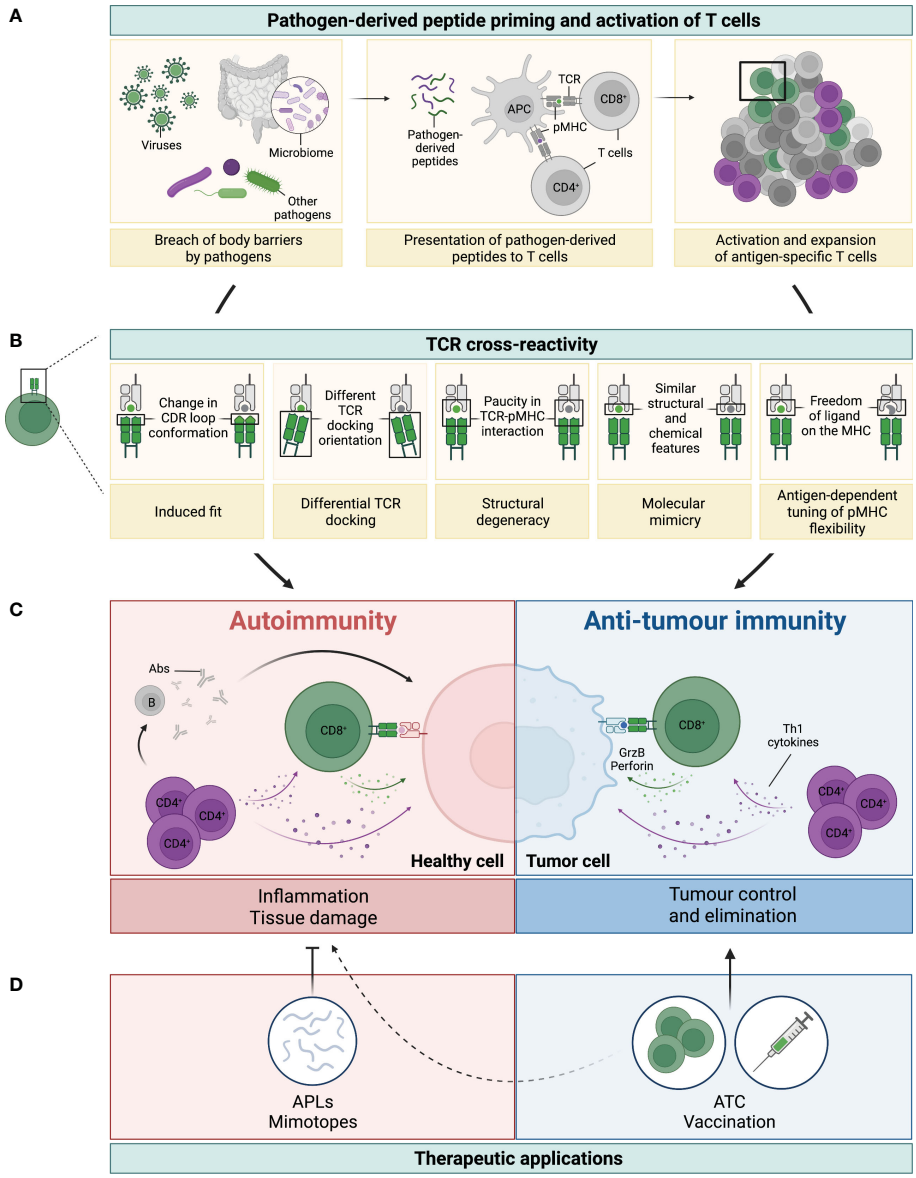

FIGURE 1
Legend: TCR cross-reactivity: a double-edged sword. **(A)** Microorganisms, such as viruses, microbiota or other pathogens, can penetrate body barriers and get into contact with our immune system (left panel). Processing and presentation of pathogen (foreign)-derived peptides by antigen-presenting cells (APCs) on MHC-class I (represented by the green dot) and MHC-class II (represented by the purple dot) primes and drives the activation of $CD8^+$ and $CD4^+$ T cells, respectively (middle panel). A polyclonal population of activated T cells then proliferates and expands to fight the invading microorganism (right panel). **(B)** Several mechanisms have been reported to be involved in TCR cross-reactivity. This figure has been adapted from reference (3). A representative $CD8^+$ T cell and its TCR is shown in green interacting with the pathogen-derived peptide (in green) presented by an MHC-class I molecule (grey). Due to cross-reactivity, the same TCR can interact with another peptide (shown in grey). **(C)** If this peptide is presented by healthy cells (depicted in pink) or by cancer cells (depicted in blue) this can ultimately result in either autoimmunity or anti-tumour immunity, respectively. On the one hand, recognition of healthy tissues by cross-reactive TCRs (mainly from $CD4^+$, but also from $CD8^+$ T cells), leads to inflammation and tissue damage with deleterious consequences. Secretion of Th1 cytokines by $CD4^+$ T cells (colored in purple) can directly affect healthy cells, but also support the activation of auto-reactive B (grey) and $CD8^+$ T (green) cells, which then secrete Abs and cytotoxic molecules (i.e. granzyme B and perforin, illustrated with the green arrow and dots), respectively (left panel in **C**). On the other hand, recognition of tumour antigens by cross-reactive T cells can prompt cell killing and tumour elimination, highlighting the contrasting impact of TCR cross-reactivity in this setting (right panel in **C**). **(D)** TCR cross-reactivity can be exploited for therapeutic applications. Usage of mimotopes or APLs to drive a Th1 to Th2 or regulatory switch in autoimmunity is an attractive strategy to reduce tissue inflammation and its damage. In cancer, usage of cross-reactive TCRs in adoptive T cell therapy (ATC), or of pathogen-derived peptides for vaccination are promising nascent strategies. Potential side effects against healthy tissues of this novel anti-cancer therapies (represented by the dotted line) need to be carefully considered to prevent damage and severe toxicities.

2 T cell cross-reactivity and autoimmunity

The most obvious and detrimental consequence of T cell cross-reactivity to vast numbers of individual peptides is the risk of developing autoimmunity (Figure 1C, left panel). Although self-reactive T cells are deleted in the thymus, weakly cross-reactive T cells may survive and become activated in the periphery through the recognition of epitopes from infectious agents (microorganism antigens, MoAs), a phenomenon known as "molecular mimicry". Memory T cells can be stimulated by peptide concentrations more than 50-fold lower than those required to stimulate naïve T cells (34, 35). It is, therefore, likely that a memory T cell could be stimulated by a cross-reactive self-peptide with an affinity for the TCR that is far lower than that of the original pathogen-derived peptide. This goes in line with the quite frequent observation that infections can precipitate autoimmune diseases (36), and is of particular interest for novel therapies (37, 38). In autoimmunity, preferentially TCR cross-reactivity of $CD4^+$ T cells has been analysed as a consequence of their central role in the development of autoimmune disorders. This is in contrast to cancer where analysis of cytotoxic anti-tumour response, i.e. $CD8^+$ T cells is more important.

Here, we mainly present three examples for the involvement of TCR cross-reactivity in the induction of autoimmune diseases: one resulting from a bacterial infection, i.e. rheumatic fever; another induced by a food component, i.e. celiac disease; and a third example representative for the many autoimmune disorders for which no clear connection to an environmental agent has been found, as for instance multiple sclerosis.

2.1 Rheumatic fever (RF)

Acute rheumatic fever is a typical example of systemic autoimmunity which occurs subsequently to an infection, namely with group A β-haemolytic streptococci (39, 40). It can affect synovial joints, cardiac valves and the brain, resulting in clinical features as arthritis, carditis, chorea, erythema marginatum and subcutaneous nodules. Molecular mimicry between group A streptococci and heart tissue was first described by Kaplan in 1960 (41). In the early 1980s, the role of both humoral and cellular autoimmune responses was reported in several studies (42). The cross-reactive antibody (Ab) response against *S. pyogenes* has been well described (43, 44). Meanwhile, it is clear that also T cell-mediated immune reactions play an important role in RF (40, 44, 45). Three types of protein antigens present on the *S. pyogenes* surface are M, T, and R proteins. M protein is the most virulent one and shares structural similarities with various host proteins, including cardiac myosin, laminin, vimentin, and tropomyosin (43, 46, 47). During this cellular response, streptococcal antigens are presented via MHC-class II molecules and activate autoreactive T cells (40). Indeed, T cells from patients with RF recognise different alpha (α)-helical coiled-coil proteins such as streptococcal M protein, myosin, laminin, and tropomyosin, and identical epitopes on the N-terminal portions of both streptococcal M protein and cardiac myosin were identified (45). In addition, in the valvular tissue and myocardium of patients with RF, T cells with three patterns of cross-reactivity were found: 1) cardiac myosin and valve-derived proteins, 2) cardiac myosin and streptococcal M peptides, and 3) cardiac myosin, streptococcal M peptides and valve-derived proteins (48). Potential sites of mimicry were revealed in the S2- and light meromyosin (LMM)-region of human cardiac myosin peptides and distinct peptides in the B repeat region of streptococcal M protein (peptides B2 and B3A) (45). Other mechanisms which are involved in the pathogenesis of RF are epitope spreading and TCR degeneracy. Ellis et al. investigated the degeneracy of the cross-reactive T cell responses towards different α-helical proteins such as human cardiac myosin, laminin, tropomyosin, and streptococcal M protein, and observed a mosaic of different T cell clones reacting with at least six distinct α-helical proteins demonstrating different degrees of cross-reactivity (45). Moreover, T cells are activated in RF when auto-Abs interact with the endothelium cells, leading to upregulation of vascular cell adhesion molecule 1 (VCAM-1) and facilitating increased T cell infiltration into the heart valve (49). These activated auto-reactive T cells produce inflammatory cytokines and lead to valve damage but also promote activation of B cells which produce cross-reactive Abs. Due to the destruction of valvular tissue, epitope spreading may occur, thus enhancing the humoral and cellular autoimmune reaction.

Another crucial streptococcal antigen is N-acetyl ß D-glucosamine (GlcNac), a carbohydrate moiety of the bacteria cell wall (43). In a neurologic manifestation of RF, the Sydenham chorea, T cells as well as Abs that recognise this bacterial antigen have been shown to cross-react with the brain cell antigens lysogangliosides and tubulin (39, 50, 51). The humoral responses correlate with clinical symptoms and mediate neuronal cell signalling (52).

2.2 Celiac disease (CeD)

Celiac disease is highly interesting in view of the fact that autoimmune reactions are induced by a food component, i.e. dietary gluten (gliadin in wheat, hordein in barley, and secalin in rye are the most prominent examples). Antibodies against gliadin-peptides and the enzyme transglutaminase-2 (TG2) are highly-specific diagnostic markers of CeD, and a $CD4^+$ T cell response towards post-translationally modified gluten peptides has been described. The disease shows a clear genetic association to the MHC-class II allelic products HLA-DQ2 (DQ2.5: DQA1*05:01-DQB1*02:01 or DQ2.2: DQA1*02:01-DQB1*02:02, approx. 95% of the patients) and HLA-DQ8 (DQA1*03:01-DQB1*03:02, approx. 5% of the patients) (53).

Interestingly, gliadin is a substrate for the TG2 enzyme which catalyses deamination at glutamine residues. The conversion of Q to E aa leads to increased binding affinity of peptides to the HLA-DQ2.5/2.2/8 molecules and enhanced recognition by gluten-specific $CD4^+$ T cells (54–56). Hence, CeD-associated T cells preferably react with "self-produced mimotopes" that result from the deamidation of gliadin-derived peptides. Another level of cross-

reactivity that has been documented in CeD is the recognition by a single DQ2.5-restricted TCR of peptides of similar, but not identical, aa sequences derived from various gliadins (i.e. α1a and ω1) (57). To which extend this cross-reactivity participates in the immune response against various gliadins and/or hordein or secalin is still not fully investigated, but is starting to be explored at large-scale (57–59). Altogether, the strong anti-gluten $CD4^+$ T cell response present in CeD is providing help to B cells that bind TG2-gliadin complexes and deaminated gluten peptides to mature into plasma cells in the gut that in turn produce deaminated gluten-specific, as well as autoreactive, TG2-specific, Abs (60–62). In addition, gluten-specific $CD4^+$ T cells are consistently found in the small intestine of celiac disease patients, where they activate intraepithelial $CD8^+$ T cells (IELs) via the production of IFN-γ, IL-21 and IL-2 (62). Although these IELs are thought to largely contribute to disease pathogenesis, the link between the gliadin-specific $CD4^+$ T cell response and the recruitment and activation of IELs in the gut remains obscure, especially because these IELs have not been shown to recognise gluten.

Even if there is ample evidence that HLA-DQ2.5, HLA-DQ2.2, or HLA-DQ8 molecules present gluten-derived peptides, expression of these allelic products alone is insufficient to cause disease. Other risk factors which may induce increased expression and activity of TG2 may also be involved. For instance, *in vivo* and *in vitro* studies support an association between gut microbiota alterations and celiac disease (63). First, the microbiota composition differs between individuals with active celiac disease, patients on a gluten-free diet, and normal controls in both oral, duodenal and faecal samples, with an increase in virulent strains noted in patients with active CeD (64). Bacteria can modify immunogenic food antigens resulting in an increase or decrease in antigenicity, and also utilise undigested particles as substrates, producing metabolites such as short-chain fatty acids that affect intestinal homeostasis. For instance, *Pseudomonas aeruginosa*, an opportunistic pathogen isolated from CeD patients, processes gluten to T cell reactive epitopes whereas bacterial species from healthy controls inactivate these reactive epitopes by further proteolytic breakdown (65). Second, and more relevant in the context of T cell cross-reactivity, peptides from common commensal and pathogenic bacteria, especially from several *Pseudomonas* and *Bordetella* species can mimic gliadin-derived peptides and activate gliadin-specific, HLA-DQ2.5-restricted T cells from CeD patients (66). It has been, therefore, hypothesised that celiac disease may be induced not only by gluten ingestion but also by infectious processes inducing pathogen-specific T cells that cross-react with gluten epitopes (66).

2.3 Multiple sclerosis (MS)

Multiple sclerosis is one of the most prevalent autoimmune disorders of the central nervous system (CNS), and is characterised by the loss of the protective myelin sheath that surrounds the axons of neurons (67, 68). Its pathophysiology has been extensively studied, especially in experimental allergic encephalomyelitis (EAE) which is a generally accepted animal model for the human disease. Nevertheless, the aetiology of MS is still unclear. Its association with an infection has been postulated already in the late 1800s, after it was first described (67). Nowadays, several factors such as genetic susceptibility, environment including infectious agents, obesity, lack of sun exposure and vitamin, have been suggested to be involved (69).

Autoantibodies specific for a variety of CNS proteins, as for instance myelin basic protein (MBP) or myelin oligodendrocyte glycoprotein (MOG), are present in the serum, cerebrospinal fluid (CSF), and brain of MS patients (70). Similarly, $CD4^+$ T cells specific for myelin antigens are found in the blood. Studies on antigen recognition demonstrated that $CD4^+$ autoreactive, MBP-specific, T cells from MS patients cross-react with peptides derived from bacterial or viral proteins (71, 72). As shown by structural analyses performed by Lang et al., the same TCR binds a MBP peptide presented by HLA-DRB1*1501 and an unrelated Epstein Barr virus (EBV)-derived peptide bound to HLA-DRB5*0101, a typical example of molecular mimicry (73, 74). A link between EBV infection and MS had already been suggested by the observation that the infection may precede MS pathology and the identification of cross-reactive Abs in MS patients (67). EBV is a well-investigated candidate for antigenic mimicry, from mimotope peptides recognised by T cells to cross-reactive Abs (75). Also, an altered anti-EBV T cell reaction was suggested in MS (76, 77).

These findings led to the concept that an immune response initially activated and expanded by an infectious agent may, in general, cross-react with autoantigens mediating CNS inflammation and induce destruction of the brain. To date, numerous infectious agents have been described to induce cross-reactive T cells against brain-specific epitopes. As an example, peptides from HSV and *Pseudomonas aeruginosa* bound to MHC molecules are recognised by cross reactive myelin-specific T cells (78). Furthermore, peptides from *M. tuberculosis*, *S. typhimurium* and *E. coli* lead to strong *in vitro* proliferation of MBP-specific T cells and induced EAE in mice with the same severity and incidence as the autoantigen peptide of MBP (79).

T cell clones isolated from the blood of patients with MS show high specificity for the immunodominant MBP epitope $MBP_{85–99}$ (80). However, this specificity is not absolute. Indeed, changing the TCR contact residue lysine at position 93 to an arginine, or even just removing a hydroxyl group by changing a phenylalanine to a tyrosine at position 91, can totally abrogate T cell reactivity. This lysine-to-arginine substitution can also result in a more degenerate pattern of TCR recognition, in that a tyrosine or other aa residues can now be tolerated at positions 91 or even 90 (81). Hence, while a TCR appears to be highly specific in one situation, altering the peptide ligand can change the TCR conformation to yield a higher degree of T cell cross-reactivity. Analysis of a further series of $MBP_{85–99}$ reactive T cell clones led to a similar conclusion, showing that a number of virus-derived epitopes can trigger autoreactive T cell clones in a manner that would not be predicted by simple algorithms (71). One of the studied MBP-reactive T cell clones recognised an epitope of MOG, an entirely different self-protein. Thus, a significant degree of functional degeneracy exists in the recognition of self-antigens by T cells.

2.4 Evidence for TCR cross-reactivity in other autoimmune diseases

The link between infection and autoimmunity *via* molecular mimicry has also been investigated in other inflammatory CNS diseases, particularly in chronic Lyme disease. Following acute infection with *Borrelia burgdorferi* (Bb), a chronic inflammatory disease can emerge which targets joints or the CNS in the absence of residual bacterial infection. In this condition, an autoimmune response to self-antigens (similarly as described above for RF) may arise from bacterial-specific T cells (82). Indeed, in Lyme arthritis, $CD4^+$ T cells isolated from the synovial fluid of patients were shown to recognise a 9mer peptide from an outer surface antigen from Bb ($OspA_{165–173}$) and an analogous, but not identical, sequence from the human LFA-1 molecule ($CD11a_{332–340}$) (83). Similarly, Bb-specific T cells from the CSF of a patient with CNS manifestation of borreliosis cross-reacted with several self-antigens, one of them being a myelin antigen (84).

In uveitis, it has also been shown that peptides with similar structure rather than similar aa sequences can induce cross-reactive T cell responses. For instance, similarities of 6 to 7 aa with the 14mer autoantigen peptide from retinal S-antigen (PDSAg) with peptides of 11 or 12 aa in length from different environmental proteins is sufficient to induce autoreactive $CD4^+$ T cell recognition and experimental anterior uveitis in rats (85). Although the pathogenic cells in uveitis are MHC-class II restricted $CD4^+$ T lymphocytes, statistical associations with HLA-class I molecules (B*27, B*51) are well known. Interestingly, the HLA-class I molecule seems to serve as an autoantigen itself, being presented as a peptide ($B27_{125–138,}$ termed B27PD) on HLA-class II and mimicking the retinal PDSAg peptide (86). Oral administration of B27BP peptide to patients was also shown to improve uveitis symptoms, suggesting that cross-reactivity could be even exploited for inducing oral tolerance to autoimmune antigens (87). In a recent study including patients with acute anterior uveitis and ankylosing spondylitis, an HLA-B27-linked rheumatic disease frequently associated with uveitis, TCRs responding to HLA-B*27-bound peptides derived from microbial antigens or from self-antigens were identified. These peptides shared common TCR binding motifs, supporting the idea that HLA-B*27-presented microbial peptides could act as trigger for autoimmunity by activating anti-self $CD8^+$ T cells (88). Interestingly, the ankylosing spondylitis-associated TCRs showed weaker affinity for the human peptide ligands than for a peptide from a conserved bacterial inner membrane protein. Evaluating the structures of seven of the HLA-B*27:05 peptide-TCR complexes, the authors showed that in all of these structures, the TCRs used a similar solution to interact with the conserved motifs in the self and bacterial peptides (89).

In type I diabetes, a T cell-mediated, HLA-DQ2 (DQA1*05:01-DQB1*02:01) and -DQ8 (DQA1*03:01-DQB1*03:02)-associated autoimmune disease directed at pancreatic β cells, insulin B-$chain_{9-23}$ (B:9-23) is a key epitope presented by MHC-class II to $CD4^+$ T cells targeting pancreatic β-cells. Lack of an acidic aa residue (i.e. aspartic acid and glutamic acid) at position 57 of the DQ8 β chain of the MHC molecule favours binding of the insulin-B peptide and is associated with increased risk of developing the disease (90). Without this acidic residue, the presented peptide repertoire is typically negatively charged (91, 92). Mimotopes with acidic aa substitutions at P9 have been shown to detect self-reactive, IFNγ-producing T cells much stronger than the wild-type peptide (93, 94). Interestingly, an immune response to this mimotope was also observed in control subjects without diabetes, but in these individuals, rather IL-10 producing, hence, anti-inflammatory $CD4^+$ T cells were activated (93).

2.5 Therapeutic implications in autoimmune diseases

Distinct cytokine patterns of T cell subsets make them unique and define their role in host defence or their contribution in disease pathogenesis. In autoimmune diseases, the role of Th1 and Th2 cells along with their cytokine profiles is well documented. In particular, the priming signal (specificity, affinity and avidity of the pMHC/TCR, APC/T cell interaction) controls the maturation, differentiation and function (i.e. cytokine profile) of the T cell (37). Alteration of peptides and of their binding to MHC may, therefore, influence the strength of the immune response. For the development of therapeutic agents in autoimmune diseases, silencing the armful anti-self T cell activity by either shifting the inflammatory Th1 response towards a Th2 profile, inducing regulatory T cells (Tregs), or even completely inhibiting T cells using strong antagonists are all strategies of interest (Figure 1D, left panel). Many of such "mimotopes" have been meanwhile designed based on *in vitro* testing of the responsiveness of T cells isolated from patients or *in vivo* using animal models (38). Especially those reducing pathogenic responses have been tested for therapeutic purposes in clinical trials.

The ability of altered peptide ligands (modified peptide sequences derived from an original antigenic peptide, i.e APLs) to shift an unfavourable Th1- in a more favourable Th2-response in the murine EAE model of MS has first been shown by Nicholson and colleagues (95). The authors used an analogue of the encephalitogenic myelin proteolipid $PLP_{139-151}$ (the common T cell antigen in EAE) with substitutions at the two main TCR contact residues (L144/R147) which had been shown to be a powerful TCR antagonist for the encephalitogenic PLP-specific T cell clones *in vitro* (96). Injection of this analogue protected the animals from developing EAE. Kuchroo et al. showed that this APL can activate IL-4 secretion by both encephalitogenic T cells and naive T cell clones that cross-react with self-antigens and inhibit autoimmunity by the induction of Tregs leading to bystander suppression of EAE (96). In further animal models of EAE, APLs have been proven to have a significant therapeutic value (97). Meanwhile, autoreactive human T cell clones have been shown to secrete the anti-inflammatory cytokines IL-4 and TGF-β after TCR engagement by APLs (98). However, application of APLs in MS

may be a double-edged sword. On the one hand, it was shown that an altered $MBP_{85–99}$ peptide induces Th2 cytokine secretion by MBP-reactive T cells isolated from the peripheral blood of MS patients while on the other hand, it can induce disease in some patients by activating these MBP-reactive T cells against the patient's own tissues (99). Moreover, in a phase II clinical trial with this peptide, two out of seven MS patients developed high frequencies of MBP-reactive T cells, and these responses were associated with significant increases in MRI-detectable lesions (100). In contrast, patients treated with lower doses of the same APL experienced some degree of immune deviation towards increases in IL-4 secretion by MBP-reactive T cells (101, 102).

A mimotope was also developed for patients with diabetes mellitus type 1 in order to preserve pancreatic β cell function. It was modified from the human insulin peptide B:9-23 which binds to HLA-DQ8 and is recognised by $CD4^+$ T cells present in the islets of organ donors with type 1 diabetes ((103) and section 2.4). The substitutions in this modified peptide are known to be important in the diabetes-prone NOD mouse model (104, 105). However, a four-arm phase II clinical study conducted by Walter et al. could not show any clinical improvement (as measured by C-peptide concentrations, a measure of pancreatic β cell function), after subcutaneous administration of the mimotopes over two years compared to the placebo (103).

For celiac disease, and as mentioned in section 2.2, disease-associated T cells preferably react with "naturally produced mimotopes" that result from deamidation of gliadin-derived peptides. Epitope-specific immunotherapies are, therefore, a logical translational step. In HLA-DQ2.5-positive celiac disease patients, clinical trials using a combination of three gluten-derived peptides, which contain at least five gliadin-specific T cell epitopes presented by HLA-DQ2.5 (Nexvax2) were conducted. While the phase I studies showed preferable outcomes in terms of safety and tolerability, the recent Nexvax2 phase II trial had to be discontinued due to lack of protection to gluten challenge.

An alternative approach to the use of a single APL is the administration of peptide mixtures that contain many different antigen specificities. Random copolymers that contain aa commonly used as MHC anchors and TCR contact residues have been proposed as possible "universal APLs." The synthetic immuno-active copolymer glatiramer acetate (GA) is comprised of four aa in random order with an average length of 40-100 residues which resemble MBP (106). It was first synthesised in 1967 to induce EAE in murine models, but was then unexpectedly found to reduce signs and progression of the disease (107). Rather than inducing an autoimmune disease, GA was found to induce regulatory and protective neuroimmune responses. In most patients, daily injection with GA causes a striking loss of responsiveness to this polymer antigen, accompanied by greater secretion of IL-5 and IL-13 by $CD4^+$ T cells, indicating a shift towards a Th2 response (108, 109). In addition, the GA-reactive T cells exhibit a high degree of degeneracy, as measured by their ability to cross-react with a large variety of peptides represented in a combinatorial library (108). GA-induced migration of those highly cross-reactive Th2 (and perhaps regulatory $FoxP3^-$ Th3) cells to the sites of inflammation may allow their highly degenerate TCRs to contact self-antigens, which they recognise as weak agonists. These T cells then apparently secrete suppressive, Th2/Th3 cytokines, thus restricting local inflammation (108). Due to these beneficial effects, GA was approved for therapeutic use in 1996 and is since then a first-line treatment of relapsing remitting MS (110, 111).

3 TCR cross-reactivity in the context of cancer

With the notable exception of rare antigenic aberrant sequences, e.g. mutated antigens, tumours generally present self-antigens on their MHC molecules and are poorly immunogenic (112). This can be globally seen as the result of the thymic negative selection where highly self-reactive T cells are eliminated to prevent the development of autoimmune diseases, leaving us with a TCR repertoire with only low to moderate affinity to self-antigens (113). Although this is beneficial in a healthy state, it makes tumour targeting by T cells a hard task, as it impairs the mounting of an effective and strong immune response. Hence, in contrast to the situation in autoimmune diseases, cross-reactivity of potential pathogen-specific T cells against self-antigens specifically presented by tumour cells is not only desirable, but would likely result in favourable anti-tumour immunity (114).

An early and staggering example of TCR cross-reactivity was described by the group of P. Romero for the tumour-associated antigen (TAA) Melan-A. While the frequency of any antigen-reactive T cell in the peripheral immune naïve repertoire is generally extremely low (< 1 in 100.000 T cells), up to 1 out of 1000 $CD8^+$ T cells bind the immunodominant peptide from Melan-A_{26-35} (the modified A27L ligand), when presented by HLA-A*0201, both in healthy donors as in melanoma patients (115). Although numerous T cells were able to bind the pMHC, as assessed by MHC-tetramer staining, a subgroup failed to be significantly activated by the Melan-A peptide in a cytotoxicity assay. In contrast, several other tested peptides, which included proteins of self- or pathogen- origin, generated a strong response in the same assay, hinting at the highly cross-reactive nature of this repertoire of T cells (116). Further supporting this, a following study of the same group showed that a tumour-reactive $CD8^+$ T cell clone, also specific to the same immunodominant peptide mentioned above, was able to cross-recognise numerous peptides and that stimulation of this clone with these peptides drove the expansion of a heterogeneous $CD8^+$ T cell population, with only a fraction actually reacting to the Melan-A peptide (117). Importantly, immunisation with Melan-A peptide through vaccination leads to a reduction on the population of cross-reactive T cells and an enrichment of antigen-restricted T cells that can react with the tumour (118). These early works on TCR cross-reactivity demonstrated its relevance not only in tumour biology but also in the design of effective anti-cancer immunotherapies.

3.1 Evidence for tumour antigen recognition by pathogen-specific T cells

3.1.1 T cell cross-reactivity between virus-derived sequences and tumour antigens

Studies have described viral-specific T cells within the microenvironment of several tumour entities with no prior known viral aetiology (119). Although there is experimental evidence for the presence of intracellular bacteria or viruses in tumour cells (120–122), this local pathogen load might not be the only reason for the presence of pathogen-specific T cells within tumours. After sequencing the TCRs of tumour-infiltrating lymphocytes (TILs) in non-small cell lung carcinoma (NSCLC), Chiou et al. identified a novel TAA derived from the epithelial protein TMEM161A. A TCR recognising this peptide was shown to readily cross-react with epitopes from EBV (and *E. coli*). Specific T cells were not only found in NSCLC patients, but also in healthy donors, an observation which the authors offer as an explanation to the presence of virus-specific T cells within NSCLCs, but possibly also in other tumours (123). In another *in silico*-based approach, Ragone et al. examined the cancer peptide database and identified numerous TAAs with shared homology with viral sequences. The viruses whose sequences were most commonly shared with the tumour antigens were HIV type 1 (HIV-1), HSV, and human papillomaviruses (HPV). In addition to sequence homology, the authors also report that these peptides share structural similarities with comparable patterns of contact between the HLA molecule and the TCR (114). A recent case report has also described tumour reduction in three metastatic colorectal cancer patients upon SARS-CoV-2 infection (124). Altogether, these studies point out to the fact that pathogen- and tumour antigen- cross-reactive T cell responses might play an important role in anti-cancer immunity, and that the immune repertoire of each patient, shaped by previous infections, might be a crucial factor in disease control.

In murine melanoma models, Chiaro et al. showed that similarities between tumour- and viral- derived antigens can influence the clearance of tumours upon peptide cancer vaccination as a consequence of cross-reactive T cell activity. Upon immunisation with viral peptide pools previously selected based on their homology to tyrosinase related protein ($TRP2_{180–188}$) or glycoprotein 100 ($gp100_{25–33}$), a strong reduction in tumour growth was seen. Interestingly, the authors further argue that viral molecular mimicry is an important factor that dictates immune response also in metastatic human melanoma by showing a direct correlation between pre-existing Abs against CMV, and response to the immune checkpoint inhibitor (ICI) anti-PD-1 (125). TCRβ sequencing experiments further suggested that the same T cell clone recognised similar peptide sequences of MAGE-A10 and CMV. Further studies using pre-clinical murine models suggest the relevance of activating virus-specific T cells for tumour growth control (119, 126). The authors describe the formation of an immune-permissive microenvironment upon *in vivo* virus-peptide vaccination, whereby cross-reactivity of these viral-specific T cells with tumour antigens, although not tested, could be responsible for the effect observed. Interestingly, another study simulating immunisation of mice with the TAA and homologous viral peptides predicted a similar clearance of tumour cells in both scenarios, suggesting equivalent anti-tumour efficacy of the effector T cell response (114).

3.1.2 T cell cross-reactivity between bacterial-derived sequences and tumour antigens

Cross-reactivity of tumour-specific T cells with bacterial epitopes has also been described. In melanoma, a MAGE-A6-derived peptide ($MAGE\text{-}A6_{172\text{-}187}$) was shown to be cross-reactive with its highly immunogenic homolog $HF\text{-}2_{216\text{-}229}$. This mycoplasma-derived peptide and MAGE-A6 can drive the formation of memory $CD8^+$ T cells. Interestingly, *in vitro* priming with dendritic cells loaded with the bacterial-derived peptide resulted in $CD8^+$ T cells with 100-fold higher avidity to the MAGE-A6 peptide compared to that of cells primed with the MAGE-A6 peptide itself (127).

The main *in vivo* source of bacteria-derived antigens is the microbiota. The human gut is colonised by approximately 10^{14} microbes (128). The sheer number of colonising microorganisms means that exposure of immune cells to these bacteria throughout life is unavoidable, which results in the generation of an immune response against commensal-derived peptides. In a similar analysis to the one performed earlier, Ragone et al. compared all TAAs from the cancer peptide database against the microbiota species *Firmicutes* (taxid:1239) and *Bacteroidetes* (taxid:976) sequences. The authors demonstrated a high level of homology of tumour antigens and peptides derived from these species, which account for 90% of all gut microbiota (129). Flückiger et al. showed that T cell clones that recognise the cancer antigen protein glycerol-3-phosphate dehydrogenase 1-like (GPD1-L) and cross-react with epitopes derived from the tail tape measure protein (TMP) of an *Enterococcus hirae* (*E. hirae*) bacteriophage, could be detected in melanoma patients. Importantly, the authors further observed an association between the presence of this prophage in the stools of patients with renal and lung cancer, expression of GPD1-L by tumour cells, and a long-term benefit to PD-1 checkpoint blockade (130). Interestingly, in the same study, cyclophosphamide treatment of tumour-bearing mice, which induces the translocation of *E. hirae* from the gut lumen to the mesenteric and splenic immune tissues, resulted in improved anti-cancer $CD8^+$ T cell responses. This anti-tumour effect was abrogated once the mice were given antibiotics and rescued by administration of *E. hirae* isolates. Moreover, lack of expression of the TAA by the tumour cells also abolished any anti-tumour immunity previously observed.

Other studies have also shown a favourable clinical outcome in cancer patients presenting $CD4^+$ and $CD8^+$ T cells specific for *E. hirae*, *Bacteroides fragilis*, *Ruminococcaceae* (131), and *Akkermansia muciniphila* (131–134). The immune repertoire, namely the frequency of precursor T cells prior to antigen exposure, is a critical factor in determining the magnitude of an immune response. Based on the aforementioned observations of cross-reactivity between numerous pathogen-derived epitopes and tumour antigens, it is plausible that the gut microbiome is an

important modulator and dictator of how individuals will mount an immune response to tumours but also how they will respond to immunotherapies.

3.2 Neoantigens and T cell cross-reactivity

In contrast to the demonstrated potential of T cells to be cross-reactive (11), neoantigens generally activate specific T cells that react only very weakly against the wild-type (wt) peptide which often differs only in 1 aa (135–138). This apparent contradiction may be explained when considering the position of the mutated aa in the peptide sequence (e.g. if a novel anchor residue for binding to the MHC molecule is created by the new aa) or its structural properties (e.g. changes in peptide charge which renders the peptide "visible" to the TCR). Still, the large majority of predicted neoantigens probably activate similar TCRs to that specific for the self-peptide and are, therefore, not of interest. If this is the case, these neoantigens do not trigger a strong anti-tumour response as a result of central tolerance. On the other hand, neoantigens can share homology to pathogen-derived antigens. In this case, these neoantigens could elicit an efficient response against tumours by activating cross-reactive pre-existing memory T cells that have been previously generated against such pathogens, as discussed above for wt tumour antigens (139). Bessel et al. identified an epitope (SVYRYYGL (SVY)) derived from the genome of the commensal *Bifidobacterium breve* (*B. breve*), homologous to the neoepitope expressed by the murine model B16-SIY (SIYRYYGL (SIY)) (140). They further demonstrate that *B. breve* promotes the expansion of SVY-specific $CD8^+$ T cells and that these are able of effective tumour control in SIY-expressing tumours, although comparison with SIY-specific T cells was not performed. In pancreatic cancer patients, Balachandran et al. demonstrate that the quality of the tumour neoantigens, namely the similarity to pathogen-derived epitopes, rather than the quantity, greatly associates with long-term survival (141).

Importantly, cross-reactive neoantigens seem to be a critical predictive factor for checkpoint inhibitor therapy efficacy. In the seminal study by Snyder et al. which first identified mutated antigens as T cell targets during checkpoint blockade, the authors observed that patients with long-term benefit to anti-CTLA-4 therapy share neoepitopes homologous to more viral and bacterial antigens, in contrast to patients with minimal or no benefit (142). These intriguing findings strongly suggest that cross-reactive T cells specific for pathogens can get activated upon checkpoint inhibition and participate in a clinically significant anti-tumour response. This is in line with the different studies presented above where the importance of the gut microbiome in checkpoint therapy responsiveness has been highlighted (143).

3.3 The two faces of TCR cross-reactivity in tumour immunotherapy

In addition to being able to dictate the outcome of immunotherapies such as checkpoint inhibition and therapeutic cancer vaccination with tumour-derived antigens, TCR cross-reactivity is currently being exploited for the development of novel and more potent cancer therapies, which we will discuss in more detail below.

3.3.1 Overcoming self-tolerance

3.3.1.1 Improving affinity

If numerous T cell clones recognise the same epitope, affinity and avidity for this epitope will be inevitable highly variable. Using checkpoint inhibitors will unleash the inhibition in all lymphocytes present in the tumour microenvironment (TME), high or low functional ones. Differently, the goal of therapeutic vaccination is to selectively drive the recruitment of high-avidity T cells and promote strong and long-lasting anti-tumour responses. As mentioned above, high-affinity T cells against TAAs are usually lacking as a consequence of negative selection in the thymus, which leaves us only with a low-affinity repertoire. This tolerance is observed when A2xneu mice (Her2/neu mice crossed with A2.1/K^b mice) are injected with the immunodominant $Her2_{773\text{-}782}$ peptide, which results in little to no tumour control (144). A similar tolerance was observed when mice were injected with p53-derived peptides. In this case, the authors demonstrated that using the $p53_{261\text{-}269}$ self-epitope led to the expansion of cytotoxic T lymphocytes (CTLs) in p53 wt mice with an avidity more than 10-fold lower than the ones obtained from p53 null mice (145). This nicely shows the importance of circumventing tolerance to achieve an effective cancer vaccination.

One way to improve the immunogenicity of TAAs would be to exploit the cross-reactive nature of TCRs. Identification of peptides that are not naturally processed and presented but that can be used to elicit strong cross-reactive T cell responses against the original TAAs is already an old idea. The design of such heteroclitic peptides, where the stability of interaction between the peptide and MHC molecule is improved by replacement of certain aa was shown to be a powerful strategy for both improving CTL reactivity *in vitro* and controlling tumor growth in mice (144, 146–150). Importantly, these heteroclitic peptides need to be recognised by T cells that cross-react with the native sequence and can, therefore, drive the killing of tumour cells naturally presenting the original peptide. Despite the encouraging results seen in pre-clinical models, this concept has failed yet to lead to the development of an effective cancer therapeutic vaccine (151, 152). A famous example was the observation by Speiser et al. that immunisation of melanoma patients with the wt Melan-$A_{26\text{-}35}$ (together with CpG as adjuvant) was superior in generating high avidity, tumour-reactive T cells, compared to the Melan-$A_{26\text{-}35}$ modified peptide (152). Since the only difference between the two peptides is one aa substitution at an anchoring position (A27L), it suggests that increasing pMHC binding properties is not the ultimate key for improving T cell reactivity to TAAs.

3.3.1.2 Microorganism antigens (MoAs) molecular mimicry

Recently, a novel concept exploiting TCR cross-reactivity for therapeutic purposes has emerged. It is based on the identification of natural analogue peptides capable of inducing strong T cell responses against the tumour antigen. The shared homology

between pathogen-derived peptides and tumour antigens and the aforementioned correlations between cross-reactive T cells and clinical outcome makes this an attractive and promising strategy that is currently being further investigated.

We have introduced in sections 3.1 and 3.2 that tumour antigens share homology with numerous pathogen-derived epitopes which, as a consequence, can drive the activation of T cells that share the same TCR. In other words, T cells that have been activated upon exposure to a certain pathogen can cross-react with tumour antigens (Figures 1A–C). The reasons for exploiting this cross-reactivity in the context of therapeutic cancer vaccination are manifold: first, it allows to overcome the low immunogenicity and affinity of natural TAAs, since TCRs that recognise MoAs have not been depleted from the T cell repertoire. Second, memory T cells can be activated by much lower peptide concentrations as compared to their naïve counterparts (see section 2). Third, recalling T cell responses upon immunisation is obviously easier to achieve than priming new effectors, especially when considering the current lack of gold-standard strong adjuvants. Fourth, exploiting "natural" T cells that were already expanded in the body after infection should present less risk of autoimmunity, although, as exemplified in section 2, autoimmunity cannot be fully excluded.

In summary, activation of viral- or commensal- specific T cells that cross-react to the tumour cells have shown promising results in a couple of pre-clinical models. Furthermore, correlations between the presence of these T cells and clinical outcome in patients have also been drawn. All this is opening a new field of research, to identify tumour antigens and MoAs that share high homology for the developing of novel T cell-based immunotherapies for cancer (Figure 1D). Since the presence of MoAs-specific memory T cells depends on prior infections, the composition of the microbiota, and the MHC-allotype, one could speculate that the development of such strategies should be done in an individualised manner to guarantee a high success rate and decrease the risk of side effects. Combination of such therapeutic vaccinations with ICIs could unleash the expansion of potent effector memory cells that readily target the tumour antigen and are able to control tumour growth.

3.3.2 The dark side of TCR cross-reactivity

TCR cross-reactivity undoubtedly opens large avenues for developing more potent cancer therapies. However, there are important bottlenecks to consider. The possible side effects in immunotherapy, especially in adoptive T cell therapies, where optimised TCRs with high affinity against a certain peptide are administered to patients is a serious issue. Side effects with these engineered TCRs are not rare, due to the strong interaction between the TCR and its target. Very low expression levels of the antigen in healthy tissue, which was initially dismissed as potentially dangerous led to severe consequences (153, 154). This on-target toxicity is not that unexpected (Figure 1D). However, overlooking off-target effects due to TCR cross-reactivity can have similarly severe and fatal adverse effects as it was observed in the case of anti-MAGE-A3 TCR engineered T cells. Due to its restrictive expression to immune privileged sites such as placenta and testis which lack the expression of HLA molecules, MAGE-A3 was considered a genuinely tumour-specific target, since it is found to be overexpressed in multiple tumours. This *bona fide* target attracted the attention and promptly immunotherapies that target this molecule were developed. Contrary to the expectations, severe cases of toxicity were observed, despite the lack of antigen expression in any of the tissues affected. In the first of two well-known incidents, engineered anti-MAGE-A3$_{112–120}$ (KVAELVHFL) T cells were adoptively transferred to cancer patients after nonmyeloablative lymphodepletion, who then received high doses of IL-2. This led to severe neurological damages, and even to a patient death. This fatal toxicity was attributed to a cross-reactivity of the effector TCRs with a MAGE-A12 sequence (KMAELVHFL) which has a superior binding affinity for HLA-A*0201 than MAGE-A3$_{112–120}$. MAGE-A12 was found *a posteriori* to be expressed in the brain (153). In the second, even less predictable case, engineered lymphocytes with affinity-enhanced TCRs against the HLA-A*01-restricted MAGE-A3$_{168-176}$ peptide (EVDPIGHLY) drove cardiotoxicity and patient death due to recognition of an unrelated peptide derived from the muscle protein titin (ESDPIVAQY) which is presented by cardiomyocytes (155, 156) (Figure 1D). Experimental and computational tools for prediction of potential toxicities have been improved since then and will be presented in section 4.

In general, therapeutic cancer vaccines are safe and no severe side effects have been observed to date. This may arise from the relatively low affinity of the induced T cells. The potential of MoAs to be used in immunisation approaches against tumour antigens, renders caution to what kind of side effects can arise. In a recent study, Gil-Cruz et al. showed that microbiota-derived peptide mimicry can induce lethal cardiomyopathy through the activation of heart-specific (MYH6-specific TCR) Th17 CD4$^+$ T cells (157). In their mouse model, cross-reactive CD4$^+$ T cells are primed in the intestine and later circulate and infiltrate the myocardium where they can damage myosin-expressing cells. In the context of checkpoint inhibition, it is tempting to speculate that not only self-, but also cross-reactive pathogen-specific T cells could be responsible for driving lethal cases of myocarditis that were observed in some patients (158, 159). The large number of auto-immune diseases that are associated with pathogen infection itself (section 2) demonstrate the delicate balance in the selection of these MoAs for therapeutic intervention.

4 Assessing TCR cross-reactivity: experimental evidence, *in silico* predictions and the need for high through-put testing platforms

A number of the examples of TCR cross-reactivity discussed so far have been brought to light using *in vitro* systems based on the testing of T cell activity against synthetic peptides. In early works, epitopic peptides of interest were modified by introducing aa substitutions at various positions. Later advances, supported by increased automatization of peptide synthesis, led to the development of synthetic peptide libraries. One common approach is to generate combinatorial (sub)libraries of peptides with each of the 20 aa fixed at one position while all other positions can be occupied by all other aa (160). Such approach can

theoretically generate all possible aa sequences for a given peptide length and allows screening of up to 10^{12} peptides. *In vitro* testing of agonists or antagonists´ effects on T cell activity can be performed either by measuring cytokine secretion, killing of loaded target cells (for $CD8^+$ T cells), or proliferation (for $CD4^+$ and $CD8^+$ T cells) (32, 161). Once a library has been shown to activate the T cell of interest, sub-libraries can be consecutively tested until the sequence(s) responsible for cross-reactivity is (are) identified. Subsequent database search can finally reveal whether the random peptide is indeed part of a known protein.

Together with the development of TCR engineering and adoptive transfer therapies, currently most advanced in the oncology clinical setting, high through-put and comprehensive approaches for testing TCR cross-reactivity have become mandatory for pre-clinical development. The main interest here is to assess TCR-mediated toxicity, i.e. the potential of transferred T cells to exert deleterious effects *in vivo* via recognition of non-related pMHC expressed on healthy tissues (Figure 1D). This is particularly relevant when the TCR has been manipulated for increasing its affinity to the cognate pMHC or has been obtained from HLA-unmatched donors (allorestricted). Challenges for the safe use of engineered TCRs in solid tumours have been very recently reviewed (162), and we have presented examples of fatal toxicities in section 3.3. In the context of clinical development, *in vitro* testing of T cell reactivity against random peptide sequences, as mentioned above, is the most straight-forward approach to assess cross-reactivity. DNA-tagged pMHC multimers, which allow to address TCR-pMHC affinity more easily is an elegant alternative method (163, 164). From the point of view of experimental feasibility, all these assays require high amount of material (e.g. T cell clones), which might be circumvented by modern methods. TCR cloning and subsequent transfer in reporter cells or MHC-matched PBMCs, and possibly the use of soluble TCRs and yeast pMHC libraries can overcome the aforementioned limitations (21). By titrating the peptide concentrations, TCR affinities can be more precisely assessed.

Which threshold of reactivity will lead to *in vivo* toxicity is likely impossible to predict with high accuracy and might even vary between individuals. One weakness of synthetic peptide testing is that recognition of a particular sequence by a certain TCR as measured *in vitro* cannot ultimately predict *in vivo* reactivity, since it is unknown whether this aa sequence is indeed processed and to which extent it is presented on body tissues. More sophisticated platforms try to overcome these limitations. First, testing primary normal cells from a range of organs representing essential human tissues (e.g. cardiovascular, gastrointestinal, brain, liver, among other systems) and/or a panel of tumour cell lines will assess potential off-target recognition (22, 165). Second, alloreactivity against MHC-mismatched cell lines can also be assessed (22, 166). As an example, reactivity of a TCR specific for a MAGEA4-derived epitope presented by HLA-A*0201 was found to recognise HLA-A*0205 (in the absence of MAGEA4), indicating alloreactivity; hence, patients bearing the HLA-A*0205 allelic product should be excluded from the clinical study using this TCR (22). Third, recognition of similar, but not identical synthetic peptides (containing aa substitutions), can also be tested *in vitro*, and the occurrence of potentially recognised sequences in the human proteome predicted. This combined approach could advantageously replace combinatorial peptide libraries (167).

Lastly, a comprehensive view of all peptides presented by MHC molecules in normal cells is needed and of utmost importance. The typical experimental setting for assessing the MHC ligand "landscape", is to perform peptide immunoprecipitation followed by mass spectrometry analysis. First milestones steps have been engaged, with the Human Immunopeptidome Project (HIPP) and the HLA ligand atlas which both aim at deciphering the entire MHC-ligandome landscape of human healthy tissues (168, 169). In addition, quantitative analysis of peptide presentation by mass spectrometry has become possible. Using this method, it was recently shown that a peptide derived from collagen type VI A3 is present in 41% of the tumour samples analysed at an average of 228 (max 1928) copies per cell, but only in 6% of the normal tissues with an average of 28 copies (max of 49) per cell (165).

All these approaches are so far imperfect, since it cannot be excluded that an organ subpart, or specialised cells at a certain stage of differentiation or activation, may be targeted by cross-reactive T cells. As discussed earlier, the recognition by MAGE-A3 specific T cells of a titin-derived peptide expressed only in beating cardiomyocytes showed to be fatal for treated patients (155, 156). However, combining and refining them will decrease the chance of unexpected *in vivo* TCR cross-reactivity and toxicity. Possibly, tissue engineering and the development of 3D *in vitro* culture systems which better recapitulate the complexity of human organs and can be used in T cell assays might become a relevant addition to the testing pipelines.

In complement to experimental approaches, many efforts are ongoing for developing reliable *in silico* pipelines for predicting T cell cross-reactivity. It should be noted that many of such tools are not developed specifically for addressing cross-reactivity, but more generally to predict peptide immunogenicity (170). In principle, two aspects can be investigated: on the one hand, the probability for a peptidic sequence to be presented by various MHC allelic products, and on the other hand, the interaction of a specific TCR with a pMHC complex.

Regarding peptide MHC binding, the simplest strategy would be to start from the original peptide and deduce which altered sequence could or not bind to the presenting MHC allelic product. NetMHC and syfpeithi, which are essential publicly available tools, can deliver robust MHC-binding predictions, but they cannot directly interrogate TCR cross-reactivity. In addition, immunogenicity prediction tools based on aa properties (size, charge, aromaticity, gravy score) are also being developed (171, 172). In the tool available at the Immune Epitope Database (IEDB) (173), TCR preferences were deduced from the study of 600 immunogenic and 181 non-immunogenic 9mer peptides: the authors found out that peptides containing aromatic and large side chains aa (in particular phenylalanine) were preferentially recognised by T cells, and that positions 4-6 were the most critical, confirming previous findings. The task is much more complex when addressing the direct binding of a specific TCR to pMHC (see also section 1). Current approaches aiming at modelling such interactions in 3D are based on x-ray crystallography data (174–176). In addition, pMTnet, NetTCR and

ERGO are neural networks that predict pMHC-TCR (CDR3 regions of the TCR β, and more recently, α chains) and are in continuous refinement (177–179).

In silico tools rely on the exploitation of experimental data. Hence, *in vitro* testing of e.g. peptide library scanning is not only useful for current assessment of T cell cross-reactivity, it is also needed for training and improving prediction tools. In this respect, repository of TCR-pMHC interactions and affinities, as well as 3D information, such as those available at the IEDB, Altered TCR Ligand Affinities and Structures (Atlas) (180), Structural T-cell Receptor Database (STCRDab) (181) or TCR associated with pathology conditions (McPAS-TCR) (182) and PMID databases are essential. Implementation of more information, in particular for rare MHC allelic products, is still necessary and will help improving the robustness of these approaches in the next years.

5 Concluding remarks

Cross-reactivity is a very smart property of our adaptive immune system to cope with the large pathogen universe. It also plays a significant role in pathological conditions as different as autoimmunity and cancer. While it has been longer discussed that virus- or bacteria-specific T cells are associated with some autoimmune diseases, more recent research is uncovering their role in cancer. This knowledge can be exploited for therapy in both diseases. Application of mimotopes in the treatment of autoimmune diseases will depend to a large extent upon their ability to suppress immunoreactivity, for instance by stimulating regulatory anti-inflammatory $CD4^+$ T cells, or by directly inhibiting pathogenic cytotoxic $CD8^+$ T cells. This is obviously a complex task, and identification and prediction of self-epitopes and mimotopes recognised by particular TCRs is, therefore, important to make such antigen-specific approaches successful in autoimmune diseases. In cancer immunotherapy, TCR cross-reactivity is becoming an essential consideration, not only for designing more efficient T cell-based treatments, but also for preventing severe side effects. Considering the ongoing personalisation of therapeutic approaches, the upstream TCR selection process needs to be speed up. The development of novel and refined prediction methods is of utmost importance, but is a challenging process due to the numerous aspects that can impact cross-reactivity.

Author contributions

CG, AM, and RK conceived the review and jointly wrote the manuscript. AM prepared the figure which was reviewed by all authors. All authors contributed to the article and approved the submitted version.

Funding

CG and AM are supported by the Deutsche Forschungsgemeinschaft (DFG, German Research Foundation) under Germany's Excellence Strategy EXC 2180, 390900677.

Acknowledgments

We acknowledge support from the Open Access Publishing Fund of the University of Tübingen.

Conflict of interest

The authors declare that the research was conducted in the absence of any commercial or financial relationships that could be construed as a potential conflict of interest.

Publisher's note

References

1. Schodin BA, Tsomides TJ, Kranz DM. Correlation between the number of T cell receptors required for T cell activation and TCR-ligand affinity. *Immunity* (1996) 5 (2):137–46. doi: 10.1016/s1074-7613(00)80490-2

2. Labrecque N, Whitfield LS, Obst R, Waltzinger C, Benoist C, Mathis D. How much TCR does a T cell need? *Immunity* (2001) 15(1):71–82. doi: 10.1016/s1074-7613(01)00170-4

3. Yin Y, Mariuzza RA. The multiple mechanisms of T cell receptor cross-reactivity. *Immunity* (2009) 31(6):849–51. doi: 10.1016/j.immuni.2009.12.002

4. Falk K, Rötzschke O, Stevanović S, Jung G, Rammensee HG. Allele-specific motifs revealed by sequencing of self-peptides eluted from MHC molecules. *Nature* (1991) 351 (6324):290–6. doi: 10.1038/351290a0

5. Rammensee H, Bachmann J, Emmerich NP, Bachor OA, Stevanović S. SYFPEITHI: database for MHC ligands and peptide motifs. *Immunogenetics* (1999) 50(3-4):213–9. doi: 10.1007/s002510050595

6. Arstila TP, Casrouge A, Baron V, Even J, Kanellopoulos J, Kourilsky P. A direct estimate of the human alphabeta T cell receptor diversity. *Science* (1999) 286 (5441):958–61. doi: 10.1126/science.286.5441.958

7. Nikolich-Zugich J, Slifka MK, Messaoudi I. The many important facets of T-cell repertoire diversity. *Nat Rev Immunol* (2004) 4(2):123–32. doi: 10.1038/nri1292

8. Zarnitsyna VI, Evavold BD, Schoettle LN, Blattman JN, Antia R. Estimating the diversity, completeness, and cross-reactivity of the T cell repertoire. *Front Immunol* (2013) 4:485. doi: 10.3389/fimmu.2013.00485

9. Hu C, Shen M, Han X, Chen Q, Li L, Chen S, et al. Identification of cross-reactive CD8(+) T cell receptors with high functional avidity to a SARS-CoV-2 immunodominant epitope and its natural mutant variants. *Genes Dis* (2022) 9 (1):216–29. doi: 10.1016/j.gendis.2021.05.006

10. Jerne NK. The natural-selection theory of antibody formation. *Proc Natl Acad Sci USA* (1955) 41(11):849–57. doi: 10.1073/pnas.41.11.849

11. Sewell AK. Why must T cells be cross-reactive? *Nat Rev Immunol* (2012) 12 (9):669–77. doi: 10.1038/nri3279

12. Lineburg KE, Grant EJ, Swaminathan S, Chatzileontiadou DSM, Szeto C, Sloane H, et al. CD8(+) T cells specific for an immunodominant SARS-CoV-2 nucleocapsid epitope cross-react with selective seasonal coronaviruses. *Immunity* (2021) 54(5):1055–65.e5. doi: 10.1016/j.immuni.2021.04.006

13. Imrie A, Meeks J, Gurary A, Sukhbataar M, Kitsutani P, Effler P, et al. Differential functional avidity of dengue virus-specific T-cell clones for variant peptides representing heterologous and previously encountered serotypes. *J Virol* (2007) 81(18):10081–91. doi: 10.1128/JVI.00330-07

14. Su LF, Davis MM. Antiviral memory phenotype T cells in unexposed adults. *Immunol Rev* (2013) 255(1):95–109. doi: 10.1111/imr.12095

15. Kosmrlj A, Read EL, Qi Y, Allen TM, Altfeld M, Deeks SG, et al. Effects of thymic selection of the T-cell repertoire on HLA class I-associated control of HIV infection. *Nature* (2010) 465(7296):350–4. doi: 10.1038/nature08997

16. Welsh RM, Che JW, Brehm MA, Selin LK. Heterologous immunity between viruses. *Immunol Rev* (2010) 235(1):244–66. doi: 10.1111/j.0105-2896.2010.00897.x

17. Borbulevych OY, Piepenbrink KH, Gloor BE, Scott DR, Sommese RF, Cole DK, et al. T Cell receptor cross-reactivity directed by antigen-dependent tuning of peptide-MHC molecular flexibility. *Immunity* (2009) 31(6):885–96. doi: 10.1016/j.immuni.2009.11.003

18. Kersh GJ, Allen PM. Structural basis for T cell recognition of altered peptide ligands: a single T cell receptor can productively recognize a large continuum of related ligands. *J Exp Med* (1996) 184(4):1259–68. doi: 10.1084/jem.184.4.1259

19. Hemmer B, Vergelli M, Gran B, Ling N, Conlon P, Pinilla C, et al. Predictable TCR antigen recognition based on peptide scans leads to the identification of agonist ligands with no sequence homology. *J Immunol* (1998) 160(8):3631–6. doi: 10.4049/jimmunol.160.8.3631

20. Hemmer B, Kondo T, Gran B, Pinilla C, Cortese I, Pascal J, et al. Minimal peptide length requirements for CD4(+) T cell clones–implications for molecular mimicry and T cell survival. *Int Immunol* (2000) 12(3):375–83. doi: 10.1093/intimm/12.3.375

21. Birnbaum ME, Mendoza JL, Sethi DK, Dong S, Glanville J, Dobbins J, et al. Deconstructing the peptide-MHC specificity of T cell recognition. *Cell* (2014) 157 (5):1073–87. doi: 10.1016/j.cell.2014.03.047

22. Sanderson JP, Crowley DJ, Wiedermann GE, Quinn LL, Crossland KL, Tunbridge HM, et al. Preclinical evaluation of an affinity-enhanced MAGE-A4-specific T-cell receptor for adoptive T-cell therapy. *Oncoimmunology* (2020) 9 (1):1682381. doi: 10.1080/2162402X.2019.1682381

23. Macdonald WA, Chen Z, Gras S, Archbold JK, Tynan FE, Clements CS, et al. T Cell allorecognition via molecular mimicry. *Immunity* (2009) 31(6):897–908. doi: 10.1016/j.immuni.2009.09.025

24. Doherty DG, Penzotti JE, Koelle DM, Kwok WW, Lybrand TP, Masewicz S, et al. Structural basis of specificity and degeneracy of T cell recognition: pluriallelic restriction of T cell responses to a peptide antigen involves both specific and promiscuous interactions between the T cell receptor, peptide, and HLA-DR. *J Immunol* (1998) 161(7):3527–35. doi: 10.4049/jimmunol.161.7.3527

25. Dai S, Huseby ES, Rubtsova K, Scott-Browne J, Crawford F, Macdonald WA, et al. Crossreactive T cells spotlight the germline rules for alphabeta T cell-receptor interactions with MHC molecules. *Immunity* (2008) 28(3):324–34. doi: 10.1016/j.immuni.2008.01.008

26. Attaf M, Legut M, Cole DK, Sewell AK. The T cell antigen receptor: the Swiss army knife of the immune system. *Clin Exp Immunol* (2015) 181(1):1–18. doi: 10.1111/cei.12622

27. Su LF, Kidd BA, Han A, Kotzin JJ, Davis MM. Virus-specific CD4(+) memory-phenotype T cells are abundant in unexposed adults. *Immunity* (2013) 38(2):373–83. doi: 10.1016/j.immuni.2012.10.021

28. Campion SL, Brodie TM, Fischer W, Korber BT, Rossetti A, Goonetilleke N, et al. Proteome-wide analysis of HIV-specific naive and memory CD4(+) T cells in unexposed blood donors. *J Exp Med* (2014) 211(7):1273–80. doi: 10.1084/jem.20130555

29. Mason D. A very high level of crossreactivity is an essential feature of the T-cell receptor. *Immunol Today* (1998) 19(9):395–404. doi: 10.1016/s0167-5699(98)01299-7

30. Maynard J, Petersson K, Wilson DH, Adams EJ, Blondelle SE, Boulanger MJ, et al. Structure of an autoimmune T cell receptor complexed with class II peptide-MHC: insights into MHC bias and antigen specificity. *Immunity* (2005) 22(1):81–92. doi: 10.1016/j.immuni.2004.11.015

31. Wooldridge L, Ekeruche-Makinde J, van den Berg HA, Skowera A, Miles JJ, Tan MP, et al. A single autoimmune T cell receptor recognizes more than a million different peptides. *J Biol Chem* (2012) 287(2):1168–77. doi: 10.1074/jbc.M111.289488

32. Hiemstra HS, van Veelen PA, Willemen SJ, Benckhuijsen WE, Geluk A, de Vries RR, et al. Quantitative determination of TCR cross-reactivity using peptide libraries and protein databases. *Eur J Immunol* (1999) 29(8):2385–91. doi: 10.1002/(SICI)1521-4141(199908)29:08<2385::AID-IMMU2385>3.0.CO;2-B

33. Ishizuka J, Grebe K, Shenderov E, Peters B, Chen Q, Peng Y, et al. Quantitating T cell cross-reactivity for unrelated peptide antigens. *J Immunol* (2009) 183(7):4337–45. doi: 10.4049/jimmunol.0901607

34. Curtsinger JM, Lins DC, Mescher MF. CD8+ memory T cells (CD44high, ly-6C +) are more sensitive than naive cells to (CD44low, ly-6C-) to TCR/CD8 signaling in response to antigen. *J Immunol* (1998) 160(7):3236–43. doi: 10.4049/jimmunol.160.7.3236

35. Veiga-Fernandes H, Walter U, Bourgeois C, McLean A, Rocha B. Response of naive and memory CD8+ T cells to antigen stimulation. *in vivo. Nat Immunol* (2000) 1 (1):47–53. doi: 10.1038/76907

36. Rose NR. Infection, mimics, and autoimmune disease. *J Clin Invest* (2001) 107 (8):943–4. doi: 10.1172/JCI12673

37. Hafler DA. Degeneracy, as opposed to specificity, in immunotherapy. *J Clin Invest* (2002) 109(5):581–4. doi: 10.1172/JCI15198

38. Slansky JE, Nakayama M. Peptide mimotopes alter T cell function in cancer and autoimmunity. *Semin Immunol* (2020) 47:101395. doi: 10.1016/j.smim.2020.101395

39. Cunningham MW. Rheumatic fever, autoimmunity, and molecular mimicry: the streptococcal connection. *Int Rev Immunol* (2014) 33(4):314–29. doi: 10.3109/08830185.2014.917411

40. Toor D, Sharma N. T Cell subsets: an integral component in pathogenesis of rheumatic heart disease. *Immunol Res* (2018) 66(1):18–30. doi: 10.1007/s12026-017-8978-z

41. Kaplan MH. The concept of autoantibodies in rheumatic fever and in the postcommissurotomy state. *Ann N Y Acad Sci* (1960) 86:974–91. doi: 10.1111/j.1749-6632.1960.tb42854.x

42. Kaplan MH. Rheumatic fever, rheumatic heart disease, and the streptococcal connection: the role of streptococcal antigens cross-reactive with heart tissue. *Rev Infect Dis* (1979) 1(6):988–86. doi: 10.1093/clinids/1.6.988

43. Cunningham MW. Pathogenesis of group a streptococcal infections. *Clin Microbiol Rev* (2000) 13(3):470–511. doi: 10.1128/CMR.13.3.470

44. Guilherme L, Kalil J. Rheumatic fever and rheumatic heart disease: cellular mechanisms leading autoimmune reactivity and disease. *J Clin Immunol* (2010) 30 (1):17–23. doi: 10.1007/s10875-009-9332-6

45. Ellis NM, Li Y, Hildebrand W, Fischetti VA, Cunningham MW. T Cell mimicry and epitope specificity of cross-reactive T cell clones from rheumatic heart disease. *J Immunol* (2005) 175(8):5448–56. doi: 10.4049/jimmunol.175.8.5448

46. Guilherme L, Ramasawmy R, Kalil J. Rheumatic fever and rheumatic heart disease: genetics and pathogenesis. *Scand J Immunol* (2007) 66(2-3):199–207. doi: 10.1111/j.1365-3083.2007.01974.x

47. Krisher K, Cunningham MW. Myosin: a link between streptococci and heart. *Science* (1985) 227(4685):413–5. doi: 10.1126/science.2578225

48. Fae KC, da Silva DD, Oshiro SE, Tanaka AC, Pomerantzeff PM, Douay C, et al. Mimicry in recognition of cardiac myosin peptides by heart-intralesional T cell clones from rheumatic heart disease. *J Immunol* (2006) 176(9):5662–70. doi: 10.4049/jimmunol.176.9.5662

49. Roberts S, Kosanke S, Terrence Dunn S, Jankelow D, Duran CM, Cunningham MW. Pathogenic mechanisms in rheumatic carditis: focus on valvular endothelium. *J Infect Dis* (2001) 183(3):507–11. doi: 10.1086/318076

50. Taranta A, Stollerman GH. The relationship of sydenham's chorea to infection with group a streptococci. *Am J Med* (1956) 20(2):170–5. doi: 10.1016/0002-9343(56)90186-3

51. Kirvan CA, Swedo SE, Heuser JS, Cunningham MW. Mimicry and autoantibody-mediated neuronal cell signaling in sydenham chorea. *Nat Med* (2003) 9(7):914–20. doi: 10.1038/nm892

52. Ben-Pazi H, Stoner JA, Cunningham MW. Dopamine receptor autoantibodies correlate with symptoms in sydenham's chorea. *PloS One* (2013) 8(9):e73516. doi: 10.1371/journal.pone.0073516

53. Ciacchi L, Reid HH, Rossjohn J. Structural bases of T cell antigen receptor recognition in celiac disease. *Curr Opin Struct Biol* (2022) 74:102349. doi: 10.1016/j.sbi.2022.102349

54. Jabri B, Sollid LM. Tissue-mediated control of immunopathology in coeliac disease. *Nat Rev Immunol* (2009) 9(12):858–70. doi: 10.1038/nri2670

55. Molberg O, McAdam SN, Korner R, Quarsten H, Kristiansen C, Madsen L, et al. Tissue transglutaminase selectively modifies gliadin peptides that are recognized by gut-derived T cells in celiac disease. *Nat Med* (1998) 4(6):713–7. doi: 10.1038/nm0698-713

56. van de Wal Y, Kooy Y, van Veelen P, Peña S, Mearin L, Papadopoulos G, et al. Selective deamidation by tissue transglutaminase strongly enhances gliadin-specific T cell reactivity. *J Immunol* (1998) 161(4):1585–8. doi: 10.4049/jimmunol.161.4.1585

57. Ciacchi L, Farenc C, Dahal-Koirala S, Petersen J, Sollid LM, Reid HH, et al. Structural basis of T cell receptor specificity and cross-reactivity of two HLA-DQ2.5-restricted gluten epitopes in celiac disease. *J Biol Chem* (2022) 298(3):101619. doi: 10.1016/j.jbc.2022.101619

58. Dahal-Koirala S, Ciacchi L, Petersen J, Risnes LF, Neumann RS, Christophersen A, et al. Discriminative T-cell receptor recognition of highly homologous HLA-DQ2-bound gluten epitopes. *J Biol Chem* (2019) 294(3):941–52. doi: 10.1074/jbc.RA118.005736

59. Chlubnová M, Christophersen AO, Sandve GKF, Lundin KEA, Jahnsen J, Dahal-Koirala S, et al. Identification of gluten T cell epitopes driving celiac disease. *Sci Adv* (2023) 9(4):eade5800. doi: 10.1126/sciadv.ade5800

60. Hoydahl LS, Richter L, Frick R, Snir O, Gunnarsen KS, Landsverk OJB, et al. Plasma cells are the most abundant gluten peptide MHC-expressing cells in inflamed intestinal tissues from patients with celiac disease. *Gastroenterology* (2019) 156 (5):1428–39 e10. doi: 10.1053/j.gastro.2018.12.013

61. Ting YT, Dahal-Koirala S, Kim HSK, Qiao SW, Neumann RS, Lundin KEA, et al. A molecular basis for the T cell response in HLA-DQ2.2 mediated celiac disease. *Proc Natl Acad Sci USA* (2020) 117(6):3063–73. doi: 10.1073/pnas.1914308117

62. Abadie V, Sollid LM, Barreiro LB, Jabri B. Integration of genetic and immunological insights into a model of celiac disease pathogenesis. *Annu Rev Immunol* (2011) 29:493–525. doi: 10.1146/annurev-immunol-040210-092915

63. Caminero A, Meisel M, Jabri B, Verdu EF. Mechanisms by which gut microorganisms influence food sensitivities. *Nat Rev Gastroenterol Hepatol* (2019) 16 (1):7–18. doi: 10.1038/s41575-018-0064-z

64. Sacchetti L, Nardelli C. Gut microbiome investigation in celiac disease: from methods to its pathogenetic role. *Clin Chem Lab Med* (2020) 58(3):340–9. doi: 10.1515/cclm-2019-0657

65. Caminero A, Galipeau HJ, McCarville JL, Johnston CW, Bernier SP, Russell AK, et al. Duodenal bacteria from patients with celiac disease and healthy subjects distinctly affect gluten breakdown and immunogenicity. *Gastroenterology* (2016) 151(4):670–83. doi: 10.1053/j.gastro.2016.06.041

66. Petersen J, Ciacchi L, Tran MT, Loh KL, Kooy-Winkelaar Y, Croft NP, et al. T Cell receptor cross-reactivity between gliadin and bacterial peptides in celiac disease. *Nat Struct Mol Biol* (2020) 27(1):49–61. doi: 10.1038/s41594-019-0353-4

67. Soldan SS, Lieberman PM. Epstein-Barr Virus and multiple sclerosis. *Nat Rev Microbiol* (2023) 21(1):51–64. doi: 10.1038/s41579-022-00770-5

68. Steinman L. Antigen-specific therapy of multiple sclerosis: the long-sought magic bullet. *Neurotherapeutics* (2007) 4(4):661–5. doi: 10.1016/j.nurt.2007.07.007

69. Zarghami A, Li Y, Claflin SB, van der Mei I, Taylor BV. Role of environmental factors in multiple sclerosis. *Expert Rev Neurother* (2021) 21(12):1389–408. doi: 10.1080/14737175.2021.1978843

70. Genain CP, Cannella B, Hauser SL, Raine CS. Identification of autoantibodies associated with myelin damage in multiple sclerosis. *Nat Med* (1999) 5(2):170–5. doi: 10.1038/5532

71. Hemmer B, Fleckenstein BT, Vergelli M, Jung G, McFarland H, Martin R, et al. Identification of high potency microbial and self ligands for a human autoreactive class II-restricted T cell clone. *J Exp Med* (1997) 185(9):1651–9. doi: 10.1084/jem.185.9.1651

72. Wucherpfennig KW, Strominger JL. Molecular mimicry in T cell-mediated autoimmunity: viral peptides activate human T cell clones specific for myelin basic protein. *Cell* (1995) 80(5):695–705. doi: 10.1016/0092-8674(95)90348-8

73. Lang HL, Jacobsen H, Ikemizu S, Andersson C, Harlos K, Madsen L, et al. A functional and structural basis for TCR cross-reactivity in multiple sclerosis. *Nat Immunol* (2002) 3(10):940–3. doi: 10.1038/ni835

74. Vergelli M, Hemmer B, Kalbus M, Vogt AB, Ling N, Conlon P, et al. Modifications of peptide ligands enhancing T cell responsiveness imply large numbers of stimulatory ligands for autoreactive T cells. *J Immunol* (1997) 158 (8):3746–52. doi: 10.4049/jimmunol.158.8.3746

75. Robinson WH, Steinman L. Epstein-Barr Virus and multiple sclerosis. *Science* (2022) 375(6578):264–5. doi: 10.1126/science.abm7930

76. Bjornevik K, Cortese M, Healy BC, Kuhle J, Mina MJ, Leng Y, et al. Longitudinal analysis reveals high prevalence of Epstein-Barr virus associated with multiple sclerosis. *Science* (2022) 375(6578):296–301. doi: 10.1126/science.abj8222

77. Schneider-Hohendorf T, Gerdes LA, Pignolet B, Gittelman R, Ostkamp P, Rubelt F, et al. Broader Epstein-Barr virus-specific T cell receptor repertoire in patients with multiple sclerosis. *J Exp Med* (2022) 219(11). doi: 10.1084/jem.20220650

78. Sethi DK, Gordo S, Schubert DA, Wucherpfennig KW. Crossreactivity of a human autoimmune TCR is dominated by a single TCR loop. *Nat Commun* (2013) 4:2623. doi: 10.1038/ncomms3623

79. Grogan JL, Kramer A, Nogai A, Dong L, Ohde M, Schneider-Mergener J, et al. Cross-reactivity of myelin basic protein-specific T cells with multiple microbial peptides: experimental autoimmune encephalomyelitis induction in TCR transgenic mice. *J Immunol* (1999) 163(7):3764–70. doi: 10.4049/jimmunol.163.7.3764

80. Ota K, Matsui M, Milford EL, Mackin GA, Weiner HL, Hafler DA. T-Cell recognition of an immunodominant myelin basic protein epitope in multiple sclerosis. *Nature* (1990) 346(6280):183–7. doi: 10.1038/346183a0

81. Ausubel LJ, Kwan CK, Sette A, Kuchroo V, Hafler DA. Complementary mutations in an antigenic peptide allow for crossreactivity of autoreactive T-cell clones. *Proc Natl Acad Sci USA* (1996) 93(26):15317–22. doi: 10.1073/pnas.93.26.15317

82. Martin R, Gran B, Zhao Y, Markovic-Plese S, Bielekova B, Marques A, et al. Molecular mimicry and antigen-specific T cell responses in multiple sclerosis and chronic CNS Lyme disease. *J Autoimmun* (2001) 16(3):187–92. doi: 10.1006/jaut.2000.0501

83. Gross DM, Forsthuber T, Tary-Lehmann M, Etling C, Ito K, Nagy ZA, et al. Identification of LFA-1 as a candidate autoantigen in treatment-resistant Lyme arthritis. *Science* (1998) 281(5377):703–6. doi: 10.1126/science.281.5377.703

84. Hemmer B, Gran B, Zhao Y, Marques A, Pascal J, Tzou A, et al. Identification of candidate T-cell epitopes and molecular mimics in chronic Lyme disease. *Nat Med* (1999) 5(12):1375–82. doi: 10.1038/70946

85. Wildner G, Diedrichs-Mohring M. Autoimmune uveitis induced by molecular mimicry of peptides from rotavirus, bovine casein and retinal s-antigen. *Eur J Immunol* (2003) 33(9):2577–87. doi: 10.1002/eji.200324058

86. Wildner G. Antigenic mimicry - the key to autoimmunity in immune privileged organs. *J Autoimmun* (2022), 102942. doi: 10.1016/j.jaut.2022.102942

87. Thurau SR, Diedrichs-Mohring M, Fricke H, Burchardi C, Wildner G. Oral tolerance with an HLA-peptide mimicking retinal autoantigen as a treatment of autoimmune uveitis. *Immunol Lett* (1999) 68(2-3):205–12. doi: 10.1016/s0165-2478(99)00071-1

88. Yang X, Garner LI, Zvyagin IV, Paley MA, Komech EA, Jude KM, et al. Autoimmunity-associated T cell receptors recognize HLA-B*27-bound peptides. *Nature* (2022) 612(7941):771–7. doi: 10.1038/s41586-022-05501-7

89. Bordon Y. Autoimmune TCRs cross-react with microbial and self-antigens. *Nat Rev Immunol* (2023) 23(2):72. doi: 10.1038/s41577-022-00831-z

90. Hu X, Deutsch AJ, Lenz TL, Onengut-Gumuscu S, Han B, Chen WM, et al. Additive and interaction effects at three amino acid positions in HLA-DQ and HLA-DR molecules drive type 1 diabetes risk. *Nat Genet* (2015) 47(8):898–905. doi: 10.1038/ng.3353

91. Suri A, Walters JJ, Gross ML, Unanue ER. Natural peptides selected by diabetogenic DQ8 and murine I-A(g7) molecules show common sequence specificity. *J Clin Invest* (2005) 115(8):2268–76. doi: 10.1172/JCI25350

92. van Lummel M, van Veelen PA, Zaldumbide A, de Ru A, Janssen GM, Moustakas AK, et al. Type 1 diabetes-associated HLA-DQ8 transdimer accommodates a unique peptide repertoire. *J Biol Chem* (2012) 287(12):9514–24. doi: 10.1074/jbc.M111.313940

93. Nakayama M, McDaniel K, Fitzgerald-Miller L, Kiekhaefer C, Snell-Bergeon JK, Davidson HW, et al. Regulatory vs. inflammatory cytokine T-cell responses to mutated insulin peptides in healthy and type 1 diabetic subjects. *Proc Natl Acad Sci USA* (2015) 112(14):4429–34. doi: 10.1073/pnas.1502967112

94. Spanier JA, Sahli NL, Wilson JC, Martinov T, Dileepan T, Burrack AL, et al. Increased effector memory insulin-specific CD4(+) T cells correlate with insulin autoantibodies in patients with recent-onset type 1 diabetes. *Diabetes* (2017) 66 (12):3051–60. doi: 10.2337/db17-0666

95. Nicholson LB, Murtaza A, Hafler BP, Sette A, Kuchroo VK. A T cell receptor antagonist peptide induces T cells that mediate bystander suppression and prevent autoimmune encephalomyelitis induced with multiple myelin antigens. *Proc Natl Acad Sci USA* (1997) 94(17):9279–84. doi: 10.1073/pnas.94.17.9279

96. Kuchroo VK, Greer JM, Kaul D, Ishioka G, Franco A, Sette A, et al. A single TCR antagonist peptide inhibits experimental allergic encephalomyelitis mediated by a diverse T cell repertoire. *J Immunol* (1994) 153(7):3326–36. doi: 10.4049/jimmunol.153.7.3326

97. Brocke S, Gijbels K, Allegretta M, Ferber I, Piercy C, Blankenstein T, et al. Treatment of experimental encephalomyelitis with a peptide analogue of myelin basic protein. *Nature* (1996) 379(6563):343–6. doi: 10.1038/379343a0

98. Ausubel LJ, Krieger JI, Hafler DA. Changes in cytokine secretion induced by altered peptide ligands of myelin basic protein peptide 85-99. *J Immunol* (1997) 159 (5):2502–12. doi: 10.4049/jimmunol.159.5.2502

99. Ausubel LJ, Bieganowska KD, Hafler DA. Cross-reactivity of T-cell clones specific for altered peptide ligands of myelin basic protein. *Cell Immunol* (1999) 193 (1):99–107. doi: 10.1006/cimm.1998.1447

100. Bielekova B, Goodwin B, Richert N, Cortese I, Kondo T, Afshar G, et al. Encephalitogenic potential of the myelin basic protein peptide (amino acids 83-99) in multiple sclerosis: results of a phase II clinical trial with an altered peptide ligand. *Nat Med* (2000) 6(10):1167–75. doi: 10.1038/80516

101. Crowe PD, Qin Y, Conlon PJ, Antel JP. NBI-5788, an altered MBP83-99 peptide, induces a T-helper 2-like immune response in multiple sclerosis patients. *Ann Neurol* (2000) 48(5):758–65. doi: 10.1002/1531-8249(200011)48:5<758::AID-ANA9>3.0.CO;2-2

102. Kappos L, Comi G, Panitch H, Oger J, Antel J, Conlon P, et al. Induction of a non-encephalitogenic type 2 T helper-cell autoimmune response in multiple sclerosis after administration of an altered peptide ligand in a placebo-controlled, randomized phase II trial. the altered peptide ligand in relapsing MS study group. *Nat Med* (2000) 6 (10):1176–82. doi: 10.1038/80525

103. Walter M, Philotheou A, Bonnici F, Ziegler AG, Jimenez R, Group NBIS. No effect of the altered peptide ligand NBI-6024 on beta-cell residual function and insulin needs in new-onset type 1 diabetes. *Diabetes Care* (2009) 32(11):2036–40. doi: 10.2337/dc09-0449

104. Crawford F, Stadinski B, Jin N, Michels A, Nakayama M, Pratt P, et al. Specificity and detection of insulin-reactive CD4+ T cells in type 1 diabetes in the nonobese diabetic (NOD) mouse. *Proc Natl Acad Sci USA* (2011) 108(40):16729–34. doi: 10.1073/pnas.1113954108

105. Nakayama M, Beilke JN, Jasinski JM, Kobayashi M, Miao D, Li M, et al. Priming and effector dependence on insulin B:9-23 peptide in NOD islet autoimmunity. *J Clin Invest* (2007) 117(7):1835–43. doi: 10.1172/JCI31368

106. Kasindi A, Fuchs DT, Koronyo Y, Rentsendorj A, Black KL, Koronyo-Hamaoui M. Glatiramer acetate immunomodulation: evidence of neuroprotection and cognitive preservation. *Cells* (2022) 11(9). doi: 10.3390/cells11091578

107. Keith AB, Arnon R, Teitelbaum D, Caspary EA, Wisniewski HM. The effect of cop 1, a synthetic polypeptide, on chronic relapsing experimental allergic encephalomyelitis in guinea pigs. *J Neurol Sci* (1979) 42(2):267–74. doi: 10.1016/0022-510x(79)90058-3

108. Duda PW, Krieger JI, Schmied MC, Balentine C, Hafler DA. Human and murine CD4 T cell reactivity to a complex antigen: recognition of the synthetic random polypeptide glatiramer acetate. *J Immunol* (2000) 165(12):7300–7. doi: 10.4049/jimmunol.165.12.7300

109. Neuhaus O, Farina C, Yassouridis A, Wiendl H, Then Bergh F, Dose T, et al. Multiple sclerosis: comparison of copolymer-1- reactive T cell lines from treated and untreated subjects reveals cytokine shift from T helper 1 to T helper 2 cells. *Proc Natl Acad Sci USA* (2000) 97(13):7452–7. doi: 10.1073/pnas.97.13.7452

110. Bell C, Anderson J, Ganguly T, Prescott J, Capila I, Lansing JC, et al. Development of Glatopa(R) (Glatiramer acetate): the first FDA-approved generic disease-modifying therapy for relapsing forms of multiple sclerosis. *J Pharm Pract* (2018) 31(5):481–8. doi: 10.1177/0897190017725984

111. Rommer PS, Milo R, Han MH, Satyanarayan S, Sellner J, Hauer L, et al. Immunological aspects of approved MS therapeutics. *Front Immunol* (2019) 10:1564. doi: 10.3389/fimmu.2019.01564

112. Schumacher TN, Schreiber RD. Neoantigens in cancer immunotherapy. *Science* (2015) 348(6230):69–74. doi: 10.1126/science.aaa4971

113. Rose NR. Negative selection, epitope mimicry and autoimmunity. *Curr Opin Immunol* (2017) 49:51–5. doi: 10.1016/j.coi.2017.08.014

114. Ragone C, Manolio C, Cavalluzzo B, Mauriello A, Tornesello ML, Buonaguro FM, et al. Identification and validation of viral antigens sharing sequence and structural homology with tumor-associated antigens (TAAs). *J Immunother Cancer* (2021) 9(5). doi: 10.1136/jitc-2021-002694

115. Pittet MJ, Valmori D, Dunbar PR, Speiser DE, Liénard D, Lejeune F, et al. High frequencies of naive melan-A/MART-1-specific CD8(+) T cells in a large proportion of human histocompatibility leukocyte antigen (HLA)-A2 individuals. *J Exp Med* (1999) 190(5):705–15. doi: 10.1084/jem.190.5.705

116. Dutoit V, Rubio-Godoy V, Pittet MJ, Zippelius A, Dietrich PY, Legal FA, et al. Degeneracy of antigen recognition as the molecular basis for the high frequency of naive A2/Melan-a peptide multimer(+) CD8(+) T cells in humans. *J Exp Med* (2002) 196(2):207–16. doi: 10.1084/jem.20020242

117. Rubio-Godoy V, Dutoit V, Zhao Y, Simon R, Guillaume P, Houghten R, et al. Positional scanning-synthetic peptide library-based analysis of self- and pathogen-derived peptide cross-reactivity with tumor-reactive melan-a-specific CTL. *J Immunol* (2002) 169(10):5696–707. doi: 10.4049/jimmunol.169.10.5696

118. Appay V, Speiser DE, Rufer N, Reynard S, Barbey C, Cerottini JC, et al. Decreased specific CD8+ T cell cross-reactivity of antigen recognition following vaccination with melan-a peptide. *Eur J Immunol* (2006) 36(7):1805–14. doi: 10.1002/eji.200535805

119. Rosato PC, Wijeyesinghe S, Stolley JM, Nelson CE, Davis RL, Manlove LS, et al. Virus-specific memory T cells populate tumors and can be repurposed for tumor immunotherapy. *Nat Commun* (2019) 10(1):567. doi: 10.1038/s41467-019-08534-1

120. Kalaora S, Nagler A, Nejman D, Alon M, Barbolin C, Barnea E, et al. Identification of bacteria-derived HLA-bound peptides in melanoma. *Nature* (2021) 592(7852):138–43. doi: 10.1038/s41586-021-03368-8

121. Bullman S, Pedamallu CS, Sicinska E, Clancy TE, Zhang X, Cai D, et al. Analysis of fusobacterium persistence and antibiotic response in colorectal cancer. *Science* (2017) 358(6369):1443–8. doi: 10.1126/science.aal5240

122. Nejman D, Livyatan I, Fuks G, Gavert N, Zwang Y, Geller LT, et al. The human tumor microbiome is composed of tumor type-specific intracellular bacteria. *Science* (2020) 368(6494):973–80. doi: 10.1126/science.aay9189

123. Chiou SH, Tseng D, Reuben A, Mallajosyula V, Molina IS, Conley S, et al. Global analysis of shared T cell specificities in human non-small cell lung cancer enables HLA inference and antigen discovery. *Immunity* (2021) 54(3):586–602.e8. doi: 10.1016/j.immuni.2021.02.014

124. Ottaiano A, Scala S, D'Alterio C, Trotta A, Bello A, Rea G, et al. Unexpected tumor reduction in metastatic colorectal cancer patients during SARS-Cov-2 infection. *Ther Adv Med Oncol* (2021) 13:17588359211011455. doi: 10.1177/17588359211011455

125. Chiaro J, Kasanen HHE, Whalley T, Capasso C, Grönholm M, Feola S, et al. Viral molecular mimicry influences the antitumor immune response in murine and human melanoma. *Cancer Immunol Res* (2021) 9(8):981–93. doi: 10.1158/2326-6066.Cir-20-0814

126. Ning J, Gavil NV, Wu S, Wijeyesinghe S, Weyu E, Ma J, et al. Functional virus-specific memory T cells survey glioblastoma. *Cancer Immunol Immunother* (2022) 71 (8):1863–75. doi: 10.1007/s00262-021-03125-w

127. Vujanovic L, Shi J, Kirkwood JM, Storkus WJ, Butterfield LH. Molecular mimicry of MAGE-A6 and mycoplasma penetrans HF-2 epitopes in the induction of antitumor CD8(+) T-cell responses. *Oncoimmunology* (2014) 3(8):e954501. doi: 10.4161/21624011.2014.954501

128. Thursby E, Juge N. Introduction to the human gut microbiota. *Biochem J* (2017) 474(11):1823–36. doi: 10.1042/bcj20160510

129. Ragone C, Manolio C, Mauriello A, Cavalluzzo B, Buonaguro FM, Tornesello ML, et al. Molecular mimicry between tumor associated antigens and microbiota-derived epitopes. *J Transl Med* (2022) 20(1):316. doi: 10.1186/s12967-022-03512-6

130. Fluckiger A, Daillère R, Sassi M, Sixt BS, Liu P, Loos F, et al. Cross-reactivity between tumor MHC class I-restricted antigens and an enterococcal bacteriophage. *Science* (2020) 369(6506):936–42. doi: 10.1126/science.aax0701

131. Andrews MC, Duong CPM, Gopalakrishnan V, Iebba V, Chen WS, Derosa L, et al. Gut microbiota signatures are associated with toxicity to combined CTLA-4 and PD-1 blockade. *Nat Med* (2021) 27(8):1432–41. doi: 10.1038/s41591-021-01406-6

132. Vétizou M, Pitt JM, Daillère R, Lepage P, Waldschmitt N, Flament C, et al. Anticancer immunotherapy by CTLA-4 blockade relies on the gut microbiota. *Science* (2015) 350(6264):1079–84. doi: 10.1126/science.aad1329

133. Daillère R, Vétizou M, Waldschmitt N, Yamazaki T, Isnard C, Poirier-Colame V, et al. Enterococcus hirae and barnesiella intestinihominis facilitate cyclophosphamide-induced therapeutic immunomodulatory effects. *Immunity* (2016) 45(4):931–43. doi: 10.1016/j.immuni.2016.09.009

134. Rong Y, Dong Z, Hong Z, Jin Y, Zhang W, Zhang B, et al. Reactivity toward bifidobacterium longum and enterococcus hirae demonstrate robust CD8(+) T cell response and better prognosis in HBV-related hepatocellular carcinoma. *Exp Cell Res* (2017) 358(2):352–9. doi: 10.1016/j.yexcr.2017.07.009

135. Bräunlein E, Lupoli G, Füchsl F, Abualrous ET, de Andrade Krätzig N, Gosmann D, et al. Functional analysis of peripheral and intratumoral neoantigen-specific TCRs identified in a patient with melanoma. *J Immunother Cancer* (2021) 9(9). doi: 10.1136/jitc-2021-002754

136. Li F, Deng L, Jackson KR, Talukder AH, Katailiha AS, Bradley SD, et al. Neoantigen vaccination induces clinical and immunologic responses in non-small cell lung cancer patients harboring EGFR mutations. *J Immunother Cancer* (2021) 9(7). doi: 10.1136/jitc-2021-002531

137. Linnemann C, van Buuren MM, Bies L, Verdegaal EM, Schotte R, Calis JJ, et al. High-throughput epitope discovery reveals frequent recognition of neo-antigens by CD4+ T cells in human melanoma. *Nat Med* (2015) 21(1):81–5. doi: 10.1038/nm.3773

138. Keskin DB, Anandappa AJ, Sun J, Tirosh I, Mathewson ND, Li S, et al. Neoantigen vaccine generates intratumoral T cell responses in phase ib glioblastoma trial. *Nature* (2019) 565(7738):234–9. doi: 10.1038/s41586-018-0792-9

139. Petrizzo A, Tagliamonte M, Mauriello A, Costa V, Aprile M, Esposito R, et al. Unique true predicted neoantigens (TPNAs) correlates with anti-tumor immune control in HCC patients. *J Transl Med* (2018) 16(1):286. doi: 10.1186/s12967-018-1662-9

140. Bessell CA, Isser A, Havel JJ, Lee S, Bell DR, Hickey JW, et al. Commensal bacteria stimulate antitumor responses via T cell cross-reactivity. *JCI Insight* (2020) 5 (8). doi: 10.1172/jci.insight.135597

141. Balachandran VP, Łuksza M, Zhao JN, Makarov V, Moral JA, Remark R, et al. Identification of unique neoantigen qualities in long-term survivors of pancreatic cancer. *Nature* (2017) 551(7681):512–6. doi: 10.1038/nature24462

142. Snyder A, Makarov V, Merghoub T, Yuan J, Zaretsky JM, Desrichard A, et al. Genetic basis for clinical response to CTLA-4 blockade in melanoma. *N Engl J Med* (2014) 371(23):2189–99. doi: 10.1056/NEJMoa1406498

143. Boesch M, Baty F, Rothschild SI, Tamm M, Joerger M, Früh M, et al. Tumour neoantigen mimicry by microbial species in cancer immunotherapy. *Br J Cancer* (2021) 125(3):313–23. doi: 10.1038/s41416-021-01365-2

144. Lustgarten J, Dominguez AL, Pinilla C. Identification of cross-reactive peptides using combinatorial libraries circumvents tolerance against her-2/neu-immunodominant epitope. *J Immunol* (2006) 176(3):1796–805. doi: 10.4049/jimmunol.176.3.1796

145. Theobald M, Biggs J, Hernández J, Lustgarten J, Labadie C, Sherman LA. Tolerance to p53 by A2.1-restricted cytotoxic T lymphocytes. *J Exp Med* (1997) 185 (5):833–41. doi: 10.1084/jem.185.5.833

146. Carrabba MG, Castelli C, Maeurer MJ, Squarcina P, Cova A, Pilla L, et al. Suboptimal activation of CD8(+) T cells by melanoma-derived altered peptide ligands: role of melan-A/MART-1 optimized analogues. *Cancer Res* (2003) 63(7):1560–7.

147. Parkhurst MR, Salgaller ML, Southwood S, Robbins PF, Sette A, Rosenberg SA, et al. Improved induction of melanoma-reactive CTL with peptides from the melanoma antigen gp100 modified at HLA-A*0201-binding residues. *J Immunol* (1996) 157 (6):2539–48. doi: 10.4049/jimmunol.157.6.2539

148. Chen JL, Dunbar PR, Gileadi U, Jäger E, Gnjatic S, Nagata Y, et al. Identification of NY-ESO-1 peptide analogues capable of improved stimulation of tumor-reactive CTL. *J Immunol* (2000) 165(2):948–55. doi: 10.4049/jimmunol.165.2.948

149. Bae J, Samur M, Munshi A, Hideshima T, Keskin D, Kimmelman A, et al. Heteroclitic XBP1 peptides evoke tumor-specific memory cytotoxic T lymphocytes against breast cancer, colon cancer, and pancreatic cancer cells. *Oncoimmunology* (2014) 3(12):e970914. doi: 10.4161/21624011.2014.970914

150. Dao T, Korontsvit T, Zakhaleva V, Jarvis C, Mondello P, Oh C, et al. An immunogenic WT1-derived peptide that induces T cell response in the context of HLA-A*02:01 and HLA-A*24:02 molecules. *Oncoimmunology* (2017) 6(2):e1252895. doi: 10.1080/2162402x.2016.1252895

151. Filipazzi P, Pilla L, Mariani L, Patuzzo R, Castelli C, Camisaschi C, et al. Limited induction of tumor cross-reactive T cells without a measurable clinical benefit in early melanoma patients vaccinated with human leukocyte antigen class I-modified peptides. *Clin Cancer Res* (2012) 18(23):6485–96. doi: 10.1158/1078-0432.Ccr-12-1516

152. Speiser DE, Baumgaertner P, Voelter V, Devevre E, Barbey C, Rufer N, et al. Unmodified self antigen triggers human CD8 T cells with stronger tumor reactivity

than altered antigen. *Proc Natl Acad Sci USA* (2008) 105(10):3849–54. doi: 10.1073/pnas.0800080105

153. Morgan RA, Chinnasamy N, Abate-Daga D, Gros A, Robbins PF, Zheng Z, et al. Cancer regression and neurological toxicity following anti-MAGE-A3 TCR gene therapy. *J Immunother* (2013) 36(2):133–51. doi: 10.1097/CJI.0b013e3182829903

154. Jones HF, Molvi Z, Klatt MG, Dao T, Scheinberg DA. Empirical and rational design of T cell receptor-based immunotherapies. *Front Immunol* (2020) 11:585385. doi: 10.3389/fimmu.2020.585385

155. Linette GP, Stadtmauer EA, Maus MV, Rapoport AP, Levine BL, Emery L, et al. Cardiovascular toxicity and titin cross-reactivity of affinity-enhanced T cells in myeloma and melanoma. *Blood* (2013) 122(6):863–71. doi: 10.1182/blood-2013-03-490565

156. Cameron BJ, Gerry AB, Dukes J, Harper JV, Kannan V, Bianchi FC, et al. Identification of a titin-derived HLA-A1-presented peptide as a cross-reactive target for engineered MAGE A3-directed T cells. *Sci Transl Med* (2013) 5(197):197ra03. doi: 10.1126/scitranslmed.3006034

157. Gil-Cruz C, Perez-Shibayama C, De Martin A, Ronchi F, van der Borght K, Niederer R, et al. Microbiota-derived peptide mimics drive lethal inflammatory cardiomyopathy. *Science* (2019) 366(6467):881–6. doi: 10.1126/science.aav3487

158. Johnson DB, Balko JM, Compton ML, Chalkias S, Gorham J, Xu Y, et al. Fulminant myocarditis with combination immune checkpoint blockade. *N Engl J Med* (2016) 375(18):1749–55. doi: 10.1056/NEJMoa1609214

159. Zhang L, Jones-O'Connor M, Awadalla M, Zlotoff DA, Thavendiranathan P, Groarke JD, et al. Cardiotoxicity of immune checkpoint inhibitors. *Curr Treat Options Cardiovasc Med* (2019) 21(7):32. doi: 10.1007/s11936-019-0731-6

160. Nino-Vasquez JJ, Allicotti G, Borras E, Wilson DB, Valmori D, Simon R, et al. A powerful combination: the use of positional scanning libraries and biometrical analysis to identify cross-reactive T cell epitopes. *Mol Immunol* (2004) 40(14-15):1063–74. doi: 10.1016/j.molimm.2003.11.005

161. Szomolay B, Liu J, Brown PE, Miles JJ, Clement M, Llewellyn-Lacey S, et al. Identification of human viral protein-derived ligands recognized by individual MHCI-restricted T-cell receptors. *Immunol Cell Biol* (2016) 94(6):573–82. doi: 10.1038/icb.2016.12

162. Baulu E, Gardet C, Chuvin N, Depil S. TCR-engineered T cell therapy in solid tumors: state of the art and perspectives. *Sci Adv* (2023) 9(7):eadf3700. doi: 10.1126/sciadv.adf3700

163. Bentzen AK, Hadrup SR. T-Cell-receptor cross-recognition and strategies to select safe T-cell receptors for clinical translation. *Immunooncol Technol* (2019) 2:1–10. doi: 10.1016/j.iotech.2019.06.003

164. Bentzen AK, Such L, Jensen KK, Marquard AM, Jessen LE, Miller NJ, et al. T Cell receptor fingerprinting enables in-depth characterization of the interactions governing recognition of peptide-MHC complexes. *Nat Biotechnol* (2018). doi: 10.1038/nbt.4303

165. Kim GB, Fritsche J, Bunk S, Mahr A, Unverdorben F, Tosh K, et al. Quantitative immunopeptidomics reveals a tumor stroma-specific target for T cell therapy. *Sci Transl Med* (2022) 14(660):eabo6135. doi: 10.1126/scitranslmed.abo6135

166. de Rooij MAJ, Remst DFG, van der Steen DM, Wouters AK, Hagedoorn RS, Kester MGD, et al. A library of cancer testis specific T cell receptors for T cell receptor gene therapy. *Mol Ther Oncolytics* (2023) 28:1–14. doi: 10.1016/j.omto.2022.11.007

167. Bijen HM, van der Steen DM, Hagedoorn RS, Wouters AK, Wooldridge L, Falkenburg JHF, et al. Preclinical strategies to identify off-target toxicity of high-affinity TCRs. *Mol Ther* (2018) 26(5):1206–14. doi: 10.1016/j.ymthe.2018.02.017

168. Vizcaíno JA, Kubiniok P, Kovalchik KA, Ma Q, Duquette JD, Mongrain I, et al. The human immunopeptidome project: a roadmap to predict and treat immune diseases. *Mol Cell Proteomics* (2020) 19(1):31–49. doi: 10.1074/mcp.R119.001743

169. Marcu A, Bichmann L, Kuchenbecker L, Kowalewski DJ, Freudenmann LK, Backert L, et al. HLA ligand atlas: a benign reference of HLA-presented peptides to improve T-cell-based cancer immunotherapy. *J Immunother Cancer* (2021) 9(4). doi: 10.1136/jitc-2020-002071

170. Wells DK, van Buuren MM, Dang KK, Hubbard-Lucey VM, Sheehan KCF, Campbell KM, et al. Key parameters of tumor epitope immunogenicity revealed through a consortium approach improve neoantigen prediction. *Cell* (2020) 183 (3):818–34.e13. doi: 10.1016/j.cell.2020.09.015

171. Calis JJ, Maybeno M, Greenbaum JA, Weiskopf D, De Silva AD, Sette A, et al. Properties of MHC class I presented peptides that enhance immunogenicity. *PloS Comput Biol* (2013) 9(10):e1003266. doi: 10.1371/journal.pcbi.1003266

172. Klatt MG, Mack KN, Bai Y, Aretz ZEH, Nathan LI, Mun SS, et al. Solving an MHC allele-specific bias in the reported immunopeptidome. *JCI Insight* (2020) 5(19). doi: 10.1172/jci.insight.141264

173. Mendes M, Mahita J, Blazeska N, Greenbaum J, Ha B, Wheeler K, et al. IEDB-3D 2.0: structural data analysis within the immune epitope database. *Protein Sci* (2023) 32(4):e4605. doi: 10.1002/pro.4605

174. Hellman LM, Foley KC, Singh NK, Alonso JA, Riley TP, Devlin JR, et al. Improving T cell receptor on-target specificity via structure-guided design. *Mol Ther* (2019) 27(2):300–13. doi: 10.1016/j.ymthe.2018.12.010

175. Antunes DA, Rigo MM, Freitas MV, Mendes MFA, Sinigaglia M, Lizée G, et al. Interpreting T-cell cross-reactivity through structure: implications for TCR-based cancer immunotherapy. *Front Immunol* (2017) 8:1210. doi: 10.3389/fimmu.2017.01210

176. Riley TP, Hellman LM, Gee MH, Mendoza JL, Alonso JA, Foley KC, et al. T Cell receptor cross-reactivity expanded by dramatic peptide-MHC adaptability. *Nat Chem Biol* (2018) 14(10):934–42. doi: 10.1038/s41589-018-0130-4

177. Springer I, Tickotsky N, Louzoun Y. Contribution of T cell receptor alpha and beta CDR3, MHC typing, V and J genes to peptide binding prediction. *Front Immunol* (2021) 12:664514. doi: 10.3389/fimmu.2021.664514

178. Montemurro A, Schuster V, Povlsen HR, Bentzen AK, Jurtz V, Chronister WD, et al. NetTCR-2.0 enables accurate prediction of TCR-peptide binding by using paired TCRα and β sequence data. *Commun Biol* (2021) 4(1):1060. doi: 10.1038/s42003-021-02610-3

179. Lu T, Zhang Z, Zhu J, Wang Y, Jiang P, Xiao X, et al. Deep learning-based prediction of the T cell receptor-antigen binding specificity. *Nat Mach Intell* (2021) 3 (10):864–75. doi: 10.1038/s42256-021-00383-2

180. Borrman T, Cimons J, Cosiano M, Purcaro M, Pierce BG, Baker BM, et al. ATLAS: a database linking binding affinities with structures for wild-type and mutant TCR-pMHC complexes. *Proteins* (2017) 85(5):908–16. doi: 10.1002/prot.25260

181. Leem J, de Oliveira SHP, Krawczyk K, Deane CM. STCRDab: the structural T-cell receptor database. *Nucleic Acids Res* (2018) 46(D1):D406–d12. doi: 10.1093/nar/gkx971

182. Tickotsky N, Sagiv T, Prilusky J, Shifrut E, Friedman N. McPAS-TCR: a manually curated catalogue of pathology-associated T cell receptor sequences. *Bioinformatics* (2017) 33(18):2924–9. doi: 10.1093/bioinformatics/btx286

frontiers | Frontiers in Immunology

TYPE Original Research
PUBLISHED 22 August 2023
DOI 10.3389/fimmu.2023.1235053

OPEN ACCESS

EDITED BY
Tomasz Piotr Wypych,
Polish Academy of Sciences, Poland

REVIEWED BY
Wendy W. J. Unger,
Erasmus Medical Center, Netherlands
Carmen Fernández,
Stockholm University, Sweden

*CORRESPONDENCE
Pedro A. Reche
parecheg@med.ucm.es
Jose L. Subiza
jlsubiza@inmunotek.com

†These authors have contributed equally to this work

RECEIVED 05 June 2023
ACCEPTED 02 August 2023
PUBLISHED 22 August 2023

CITATION
Bodas-Pinedo A, Lafuente EM, Pelaez-Prestel HF, Ras-Carmona A, Subiza JL and Reche PA (2023) Combining different bacteria in vaccine formulations enhances the chance for antiviral cross-reactive immunity: a detailed *in silico* analysis for influenza A virus. *Front. Immunol.* 14:1235053. doi: 10.3389/fimmu.2023.1235053

Combining different bacteria in vaccine formulations enhances the chance for antiviral cross-reactive immunity: a detailed *in silico* analysis for influenza A virus

Andrés Bodas-Pinedo[1†], Esther M. Lafuente[2†], Hector F. Pelaez-Prestel[2], Alvaro Ras-Carmona[2], Jose L. Subiza[3*] and Pedro A. Reche[2*]

[1]Children's Digestive Unit, Institute for Children and Adolescents, Hospital Clinico San Carlos, Madrid, Spain, [2]Department of Immunology & O2, Faculty of Medicine, University Complutense of Madrid, Ciudad Universitaria, Pza. Ramón y Cajal, Madrid, Spain, [3]Inmunotek, Alcalá de Henares, Spain

Bacteria are well known to provide heterologous immunity against viral infections through various mechanisms including the induction of innate trained immunity and adaptive cross-reactive immunity. Cross-reactive immunity from bacteria to viruses is responsible for long-term protection and yet its role has been downplayed due the difficulty of determining antigen-specific responses. Here, we carried out a systematic evaluation of the potential cross-reactive immunity from selected bacteria known to induce heterologous immunity against various viruses causing recurrent respiratory infections. The bacteria selected in this work were Bacillus Calmette Guerin and those included in the poly-bacterial preparation MV130: *Streptococcus pneumoniae*, *Staphylococcus aureus*, *Staphylococcus epidermidis*, *Klebsiella pneumoniae*, *Branhamella catarrhalis* and *Haemophilus influenzae*. The virus included influenza A and B viruses, human rhinovirus A, B and C, respiratory syncytial virus A and B and severe acute respiratory syndrome coronavirus 2 (SARS-CoV-2). Through BLAST searches, we first identified the shared peptidome space (identity ≥ 80%, in at least 8 residues) between bacteria and viruses, and subsequently predicted T and B cell epitopes within shared peptides. Interestingly, the potential epitope spaces shared between bacteria in MV130 and viruses are non-overlapping. Hence, combining diverse bacteria can enhance cross-reactive immunity. We next analyzed in detail the cross-reactive T and B cell epitopes between MV130 and influenza A virus. We found that MV130 contains numerous cross-reactive T cell epitopes with high population protection coverage and potentially neutralizing B cell epitopes recognizing hemagglutinin and matrix protein 2. These results contribute to explain the immune enhancing properties of MV130 observed in the clinic against respiratory viral infections.

KEYWORDS

MV130, bacteria, respiratory viruses, cross-reactivity, epitope, influenza A virus

1 Introduction

Recurrent respiratory tract infections (RRTIs) are a leading cause of morbidity and mortality in children and adults (1, 2). The most common cause of RRTIs are seasonal respiratory viruses like human rhinovirus (HRV), respiratory syncytial virus (RSV) and influenza A and B viruses (IAV and IBV), among others (3). Management of these infections is challenging and the search for new preventive and therapeutic interventions is a subject of intense research (2, 4). In the absence of effective specific vaccines, an interesting strategy is the use of poly-bacterial preparations that can stimulate mucosal immunity and increase the host resistance to respiratory viral infections (5–7). A relevant example is MV130 that contains different species of inactivated whole-cell Gram-positive and negative bacteria (8). MV130 has been shown effective in reducing the number of RRTIs in both children and adults, including those of viral etiology (5, 9–11). Moreover, it has been shown that MV130 immunization protects mice from respiratory infections caused by influenza A (12) and severe acute respiratory syndrome coronavirus 2 (SARS-CoV-2) (13). Overall, these data indicate that MV130 can induce heterologous immunity against common respiratory viruses. The mechanism by which MV130 mediates protective heterologous immunity has been linked to the induction of trained immunity, much like with other bacteria-based formulations like Bacille Calmette-Guérin (BCG) vaccine (14–18). Trained immunity was originally defined as a kind of non-specific immunological memory acquired by innate immune cells, involving epigenetic and metabolic cell reprogramming. Trained immunity memory is short-lived, usually lasting less than 1 year, and is independent of T and B cells (19, 20). Although unexplored, MV130 could also be providing protection against respiratory viruses by inducing cross-reactive adaptive immunity.

Cross-reactive immunity occurs when preexisting memory T and B cells elicited by a particular antigen/infectious agent recognize and respond against different antigens/infections (21, 22). The occurrence of cross-reactive immunity between unrelated pathogens, including between bacteria and viruses, is well documented (21, 23–26) and it is facilitated by the poly-specificity of B and T cell receptors (27–30) and also by the recognition on small portions within the antigens (epitopes) (31). Cross-reactive immunity between MV130 and respiratory viruses remain yet to be verified, as it requires of precision immune monitoring, testing responses to all potential cross-reactive antigens and epitopes (32). However, the chance for cross-reactive immunity can be assessed *in silico*. To that end, in this work, we followed an approach consisting on identifying highly similar peptide sequences between antigen sources (identity ≥ 80%, over at least 8 residues) and subsequently predicting T or B cell reactivity (33, 34).

In this way, we obtained the shared peptidome between common respiratory viruses (IAV, IBV, HRV A, B and C, RSV A and B and SARS-CoV-2) and BCG and bacteria included in the MV130 formulation: *S. pneumoniae, S. aureus, S. epidermidis, K. pneumoniae, B. catarrhalis* and *H. influenzae*. Interestingly, the peptidome space that is shared between the specific bacteria in MV130 and viruses is non-overlapping, highlighting that combining bacteria in vaccine formulations enhance the chance for cross-reactive immunity. Given that MV130 heterologous immunity to influenza A virus (IAV) has been confirmed in mice models, we also determined the potential cross-reactive T and B cell epitopes with this virus. We found that MV130 contain numerous potentially cross-reactive T cell epitopes with high population protection coverage and accessible B cell epitopes in the virion membrane. Overall, these results support the hypothesis that MV130 could induce protective cross-reactive immunity against respiratory viruses, particularly to IAV.

2 Methods

2.1 Microbial proteomes

The entire proteomes of 7 bacteria species and 8 respiratory viruses were obtained from NCBI after the entries indicated in Table 1 and assembled into individual files in FASTA format.

2.2 Identification of shared peptides between microbial proteomes

To identify shared peptides between virus and bacteria proteomes, the entire viral proteomes were first fragmented into overlapping 17-mer peptides with a 10-residue overlap.

TABLE 1 Amino acid sequences from pathogens and vaccines considered in this study.

Pathogen	NCBI Accession	Proteins/ CDS
Influenza A virus (IAV)	GCF_000865725	12
Influenza B virus (IBV)	GCF_000820495	10
Human rhinovirus A (HRVA)	NC_038311	1
Human rhinovirus B (HRVB)	NC_038312	1
Human rhinovirus C (HRVC)	NC_009996	1
Respiratory syncytial virus A (RSVA)	NC_038235	11
Respiratory syncytial virus A (RSVB)	NC_001781	11
Severe acute respiratory syndrome coronavirus 2 (SARS-CoV-2)	NC_045512	12
Bacille Calmette-Guérin (BCG)	GCF_000009445	4034
Branhamella catarrhalis (BCA)	GCF_000092265	1607
Haemophilus influenzae (HIN)	GCF_000027305	1597
Klebsiella pneumoniae (KPN)	GCF_000240185	5779
Staphylococcus aureus (SAU)	GCF_000013425	2767
Staphylococcus epidermidis (SEP)	GCF_000007645	2282
Streptococcus pneumoniae (SPN)	GCF_000007045	1861
*MV130**		15893

* MV130 includes all bacteria but BCG.

Subsequently, the peptides were used as queries in sequence similarity searches using BLASTP (35) against the target bacteria proteomes, previously formatted as BLAST databases. BLAST searches were performed with default parameters and the *e*-value set to 10,000. BLAST results were processed and shared peptides were identified from ungapped hit alignments including 8 or more residues with ≥ 80% identity. BLAST searches and processing of BLAST results were performed using an *ad-hoc* PERL script that will be provided by Dr. Reche upon writing request.

2.3 Prediction of T and B cell epitopes

Peptides were assessed as potential T cell epitopes by predicting their binding to major histocompatibility complex (MHC) molecules. Peptide binding to MHC class I (MHC I) molecules was predicted using standalone versions of RANKPEP (36, 37) and NetMHCpan (38, 39). RANKPEP and NetMHCpan prediction models were selected to match the size of the peptides if they include 8 or 9 residues. The binding of peptides with more than 9 residues to MHC I molecules was assessed by evaluating that of all nested 9mer peptides. Binding of a peptide to a given MHC I molecule was considered to occur at a 2% Rank cutoff given by both RANKPEP and NetMHCpan, which allows selecting weak and strong binders % Ranks of test peptides are obtained by ranking their predicted binding affinity or binding scores compared to a large set of random peptides. The use of binding thresholds based on % Rank removes bias of certain molecules towards higher or lower predicted affinities and facilitates comparing and combining predictions by distinct methods. Binding of peptides to MHC class II (MHC II) was predicted using NetMHCIIpan (40) using a 10% Rank cutoff, which allows detecting strong and weak binding peptides. Human MHC II molecules targeted for predictions included HLA-DR, HLA-DQ, and HLA-DP molecules.

B cell epitopes were predicted using an standalone version of BepiPred1.0 (41). BepiPred reports antigenicity values per residue (a_i), and a global B cell epitope score (B) was computed as indicated elsewhere (34, 42) consisting of the average a_i value. Peptides with B value ≥ 0.4 were considered as antigenic or potential B cell epitopes.

2.4 Statistical analyses

χ^2 tests were used as reported previously (43) to assess whether the distribution of the cross-reactive epitope sequences in proteins is proportional to the size of the proteins. The χ^2-statistics value was computed using equation 1.

$$\chi^2 = \sum_{i=1}^{k} \frac{(O_i - E_i)^2}{E_i} \qquad \text{Eq. 1}$$

In this equation, k is the number of protein antigens, O_i the number of observed epitopes in antigen i, and E_i the number of expected epitopes in antigen i if they were distributed proportionally to the size of the proteins. The null, H_0, hypothesis considers that epitopes are distributed proportionally to the size of proteins and it is rejected when the computed χ^2-statistic value is above the χ^2–distribution value at $k - 1$ degrees of freedom and a given α value.

2.5 Other procedures

The percentage of the world population that could respond to CD8 and CD4 T cell epitopes (population coverage) was computed after their MHC binding profiles using a command line version of EPISOPT (44) and the IEDB PPC tool at http://tools.iedb.org/tools/population/iedb_input (45), respectively, considering the relevant allele expression for the entire world population. The presence of a C-terminus in potential CD8 T cell epitopes compatible with cleavage by the proteasome was predicted from the relevant antigens using PCPS at http://imed.med.ucm.es/Tools/pcps/ with default settings (46, 47). Ectodomains of hemagglutinin (HA), neuraminidase (NA) and matrix protein 2 (M2) from IAV (A/Puerto Rico/8) were identified from UNIPROT accession H2KIW3_9INFA, H2KIW6_9INFA and H2KIW4_9INFA, respectively. PyMOL Molecular Graphics System Version 2.4.1 Schrödinger, LLC was used to map peptide sequences in tertiary structure of influenza A virus hemagglutinin (HA) (PDB: 1RU7) and to generate molecular renderings. Relative solvent accessibility (RSA) of peptide residues mapping in HA and M2 protein was calculated using NACCESS (48) and average solvent accessibility (ASA) of peptides was computed upon them as reported elsewhere (42, 49). Venn diagrams were generated using the nVennR package version 0.2.3 (50).

3 Results and discussion

3.1 Shared peptidome space between selected bacteria and respiratory viruses

Cross-reactive immunity is much more likely to happen between antigens with high sequence similarity. However, because B and T cells recognize small regions in protein antigens (epitopes), cross-reactivity is better predicted by the volume of peptides (peptidome) that are shared between antigens (34). Thereby, we determined the shared peptidomes between 8 common respiratory viruses (IAV, IBV, HRV A, B and C, RSV A and B, and SARS-CoV-2) and 7 bacteria species, including BCG and those in MV130. To that end, we obtained the relevant proteomes and through a BLAST based approach (details in Methods) identified all unique peptides with identity ≥ 80% and length ≥ 8 in common between viruses and bacteria. The results of this analysis are summarized in Table 2. As noted by previous works, the volume of shared peptides increases with the size of the proteomes (34, 51). Thus, of all the studied bacteria and viruses, *K. pneumoniae* (KPN) followed by Bacille Calmette-Guérin (BCG) share with SARS-CoV-2 (SARS) the largest number of peptides, 138 and 102, respectively.

Interestingly, the peptides that are shared between the selected respiratory viruses and each bacterium in MV130 are largely

TABLE 2 Size of the shared peptidome between bacteria in MV130 and respiratory viruses.

	ORF	IAV	IBV	HRVA	HRVB	HRVC	RSVA	RSVB	SARS
Streptococcus pneumoniae (SPN)	1861	12	17	8	13	17	25	31	52
Staphylococcus aureus (SAU)	2767	23	36	8	12	10	39	46	68
Staphylococcus epidermidis (SEP)	2282	27	30	11	14	10	27	30	53
Klebsiella pneumoniae (KPN)	5770	48	57	19	32	21	53	53	138
Branhamella catarrhalis (BCA)	1607	15	18	11	10	9	27	20	38
Haemophilus influenzae (HIN)	1597	25	18	4	9	8	31	20	50
Bacille Calmette-Guérin (BCG)	4045	46	41	13	27	25	32	32	102
MV130	15884	139	163	54	79	72	185	183	360

ORF, Open Reading Frame; IAV, Influenza A virus; IBV, Influenza B virus; HRVA, human rhinovirus A; HRVB, human rhinovirus B; HRVC, human rhinovirus C, RSVA, Respiratory Syncytial virus A, RSVB, Respiratory Syncytial virus B; SARS, SARS-CoV-2. Whole dataset available in Supplementary Dataset 1.

distinct, as highlighted by the Venn diagrams depicted in Figure 1. Within the set of peptides shared by any of the viruses and a particular MV130 bacterium, only a handful coincides with those shared with another bacterium. An exception occurs in the case of *S. aureus* (SAU) and *S. epidermidis* (SEP), whose shared peptidomes with viruses are highly overlapping, as one could expect for they are closely related bacteria. As a result, the number of peptides that are shared between MV130, as a whole, and the different viruses is close to the sum of peptides that are shared by each bacterium in MV130 (Table 2). This effect is far from trivial as indicates that combining different bacteria, as those in MV130, increases the chance for cross-reactive immunity. Moreover, it supports the noted view (34) that a diverse microbiota helps to fight viral infections (26) by enhancing cross-reactive immunity.

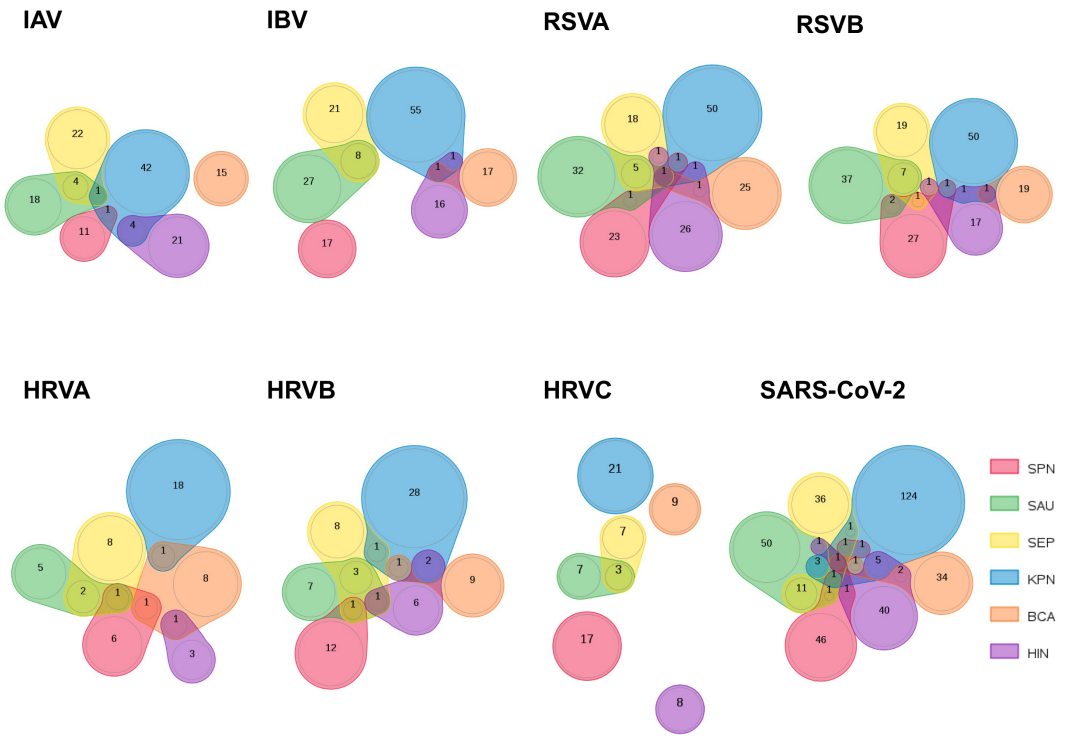

FIGURE 1
Comparison of peptidomes shared by respiratory viruses and bacteria in MV130. The sets of peptides that are shared between 8 respiratory viruses and each bacterium included in the MV130 formulation were compared and represented using Venn diagrams to visualize the overlaps. The number of peptides in overlapping and non-overlapping regions is indicated. The represented viruses are (from left to right and up to down): IAV: Influenza A virus; IBV: Influenza B virus; HRVA: human rhinovirus A; HRVB: human rhinovirus B; HRVC: human rhinovirus C, RSVA: Respiratory Syncytial virus A, RSVB: Respiratory Syncytial virus B; SARS: SARS-CoV-2. The six bacteria species included in MV130 are indicated and colored as follows: *S. pneumoniae* (SPN, red); *S. aureus* (SAU, green); *S. epidermidis* (SEP, yellow); *K. pneumoniae* (KPN, blue); *B. catarrhalis* (BCA, orange); *H. influenzae* (HIN, purple).

3.2 Potential cross-reactive immunity from MV130 to IAV

The large size of the peptidome shared between MV130 and the studied respiratory viruses is indicative that MV130 could be a major source of cross-reactive immunity against these viruses. However, for the realization of cross-reactive immunity these peptides must be recognized by the adaptive immune system. Here, we explored such realization for IAV, since it causes respiratory infections prevented by MV130 (10, 11) and MV130 confers resistance to lethal IAV challenges in mice (12). To that end, we predicted the potential of the peptides shared between MV130 and IAV to represent B and T cell epitopes. Briefly, peptides predicted to bind class I and/or class II MHC molecules (in human HLA molecules) were considered CD8 and CD4 T cell epitopes, respectively (details in Methods). Moreover, for fulfillment of T cell cross-reactivity we required that both, the IAV peptide and the equivalent MV130 peptide, bind to the same MHC/HLA molecule. Because B cell reactivity is somewhat less predictable than T cell reactivity, B cell cross-reactivity was considered when either the IAV peptide or the equivalent MV130 peptide had a B cell epitope score ≥ 0.4 (details in Methods). In Table 3, we summarize the results of this analysis. Many more cross-reactive CD8 than CD4 T cell epitopes were predicted. This is the expected result, as CD4 T cell epitopes are longer than CD8 T cell epitopes and there are few peptides in the shared peptidome with the size required to be CD4 T cell epitopes. Nonetheless, we realize that we identified fewer cross-reactive T cell epitopes than in a previous work (33, 34) using Immune Epitope Database (IEDB) MHC-binding models through the RESTful interface (52).

As expected, the number of distinct cross-reactive B and T cell epitope peptides correlated with the number of shared peptides and hence with the size of the proteomes of the bacteria in MV130 (Table 2 and Supplementary Dataset 1). These cross-reactive peptide epitopes were private, differ between bacteria, and so the potential cross-reactive immunity of the MV130 formulation is the sum of each individual bacterium. Hence, MV130 appears to be a truly enhanced source of cross-reactive immunity. We next examined in detail the predicted cross-reactive epitopes to evaluate to what extent they could provide protective immunity against IAV.

3.3 Cross-reactive T cell epitopes between MV130 and IAV target numerous HLA molecules

MHC molecules restricting T cells are highly polymorphic in humans (HLA), bind/present distinct sets of peptides that can nonetheless be overlapping, and are expressed at different frequency in the population depending on ethnicity and geography (53, 54). Subsequently, the immunogenicity of any given T cell epitope varies between individuals, as it is contingent on the expression/presence of the specific MHC molecule restricting the epitopes. In Table 4, we show all the potential cross-reactive T cell peptide epitopes along with their predicted HLA binding/presentation profiles (details in Methods). We also show the MHC molecules expressed by C57BL/6 and BALB/c mice strains that can present these same peptide epitopes (peptides that were only predicted to bind to mouse MHC molecules are not shown). Given the key role of CD8 T cells in clearing and containing viral infections we will pay particular attention to cross-reactive CD8 T cell epitopes.

MV130 encompasses 37 unique peptide sequences consisting of cross-reactive CD8 T cell epitopes with IAV that are distributed through all IAV antigens but M2 (Tables 3, 4). These epitopes are not distributed proportionally to the size of the IAV antigens as revealed by χ^2 statistics ($p< 0.005$). The largest contributions to χ^2 statistics are found in non-structural protein 2 (NS2), polymerase PA and M1 (Figure 2A). In particular, while NS2 and M1 bear more cross-reactive T cell epitopes than the expected, PA includes fewer than the expected (Figure 2B). The uneven distribution of cross-reactive CD8 T cell epitopes throughout the IAV proteome supports the specificity of T cell cross-reactivity. In fact, it is worth noting that 24 of the 37 cross-reactive peptides coincide with IAV-specific CD8 T cell epitopes deposited in the IEDB (Table 4).

The majority of potential MV130-IAV cross-reactive CD8 T cell epitopes can also be presented by more than one HLA I molecule and 5 of them can also be presented by HLA II molecules (Table 4). The combined phenotypic frequency in the population of all HLA I molecules restricting these cross-reactive CD8 T cell epitopes would imply that MV130 could elicit cross-reactive CD8 T cell immunity to IAV will in ≥ 95% of the population the regardless of their genetic background (details in Methods). Bacteria eliciting

TABLE 3 Potential cross-reactive epitopes between MV130 and IAV.

	IAV [1]	B [2]	CD8 T [H]	CD4 T [H]	CD8 T [M]	CD4 T [M]
Streptococcus pneumoniae (SPN)	12	2	4	1	1	0
Staphylococcus aureus (SAU)	25	5	2	0	3	0
Staphylococcus epidermidis (SEP)	27	6	7	1	7	1
Klebsiella pneumoniae (KPN)	48	10	13	1	4	1
Branhamella catarrhalis (BCA)	15	7	4	1	1	0
Haemophilus influenzae (HIN)	25	4	7	1	5	1
MV130	139	34	37	5	21	3

[1]Number of shared peptides between IAV (Puerto Rico 8 Strain) and bacteria, [2] number of cross-reactive B cell epitopes, [H] number of T cell epitopes restricted by human MHC molecules; [M] number of T cell epitopes restricted by mouse MHC molecules.

10.3389/fimmu.2023.1235053

TABLE 4 Potential cross-reactive T cell epitopes between MV130 and IAV.

IAV (1) ACN| ANTIGEN	MV130 (2) ACN|BACTE-RIA	IAV SEQ (3)	HIT SEQ (4)	ID (%) (5)	HLA I (6)	HLA II (7)	H-2I (8)	H-2II (9)	IEDB (10)
YP_418248| PB1-F2	WP_003657597.1| BCA|	GQQTPKLEHRN	GQLTGKLEHRN	81.81	HLA-A*31:01, HLA-A*33:01, HLA-B*15:01	–	–	–	
NP_040983| NS2	WP_041786745.1| BCA|	WLIEEVRHKLK*	WLIELLRHKLK*	81.81	HLA-A*02:01, HLA-A*02:03, HLA-A*02:06, HLA-A*03:01, HLA-A*11:01, HLA-B*07:02, HLA-B*08:01, HLA-B*40:01, HLA-B*44:02, HLA-B*44:03	–	H-2-Kk, H-2-Kq	–	148643
NP_040982| NP	WP_164927877.1| HIN|	SGYDFEREGY*	KGYQFEREGY*	80	HLA-A*30:02	–	–	–	21577
NP_040985| PB1	WP_001831697.1| SEP|	LNPFVSHKEI*	LNGFVPHKEI*	80	HLA-B*51:01	–	–	H-2-IEd	–
NP_040978| M1	YP_005224566.1| KPN|	PLKAEIAQRL*	PTRAEIAQRL*	80	HLA-A*31:01, HLA-A*33:01	–	H-2-Kk	–	48376
NP_040981| NA	YP_005229006.1| KPN|	TFFLTQGALL*	TFFLTFGSLL*	80	HLA-A*23:01, HLA-A*24:02, HLA-B*08:01	–	H-2-Kb, H-2-Kd	–	127810
NP_040987| PB2	YP_005226190.1| KPN|	LRISSSFSFG	LRIISSFGFG	80	HLA-A*32:01	–	–	–	2133253
NP_040985| PB1	WP_003658761.1| BCA|	EKIRPLLIEG	EKIRFLLLEG	80	HLA-A*30:01	–	–	–	212044
NP_040985| PB1	WP_002484992.1| SEP|	MDVNPTLLFL*	MDVMPTLLHL*	80	HLA-A*02:06, HLA-A*26:01, HLA-A*68:02, HLA-B*35:01, HLA-B*51:01, HLA-B*53:01	–	H-2-Db, H-2-Dd, H-2-Dq, H-2-Kb, H-2-Kk, H-2-Kq, H-2-Lq	–	41282
NP_040978| M1	WP_002440602.1| SEP|	DKAVKLYRK*	DKLVKHYRKL*	80	HLA-A*30:01, HLA-A*32:01, HLA-A*33:01, HLA-B*08:01	HLA-DRB1*13:02	H-2-Db, H-2-Dd, H-2-Kb	–	231836
NP_040984| NS1	YP_005225903.1| KPN|	LGDAPFLDRL*	LGIAPLLDRL*	80	HLA-B*51:01	–	H-2-Dd, H-2-Kb	–	–
NP_040983| NS2	YP_005226633.1| KPN|	RDSLGEAVMR*	RDSLLEAVLR*	80	HLA-A*31:01, HLA-A*33:01, HLA-A*68:01, HLA-B*40:01	–	–	–	1846494
NP_040981| NA	WP_010869183.1| HIN|	SVRQDVVAMT	SVAQDVDAMT	80	HLA-A*02:06, HLA-A*26:01, HLA-A*68:02, HLA-B*35:01	–	H-2-Db	–	–
NP_040983 NS2	YP_005226684.1| KPN|	EIRWLIEEVR	EIRWMIEELR	80	HLA-A*26:01, HLA-A*33:01, HLA-A*68:01, HLA-A*68:02	–	–	–	–
NP_040987| PB2	WP_013107773.1| BCA|	QSLIIAARNI*	QSLIGAVRNI*	80	HLA-A*02:03	HLA-DRB1*11:01	–	–	128453
NP_040987| PB2	YP_005225299.1| KPN|	LRVRDQRGNV*	VRVRLQRGNV*	80	HLA-A*30:01, HLA-B*07:02	–	–	–	129735
NP_040980| HA	WP_005693451.1| HIN|	QNAINGITNK*	QNAIAGLTNK*	80	HLA-A*03:01, HLA-A*11:01, HLA-A*68:01	HLA-DRB1*15:01	–	H-2-IAs	128451
NP_040980| HA	YP_005226466.1| KPN|	LGAINSSLPF*	LGVINSGLPF*	80	HLA-A*32:01, HLA-B*15:01, HLA-B*35:01	–	–	–	–

(Continued)

TABLE 4 Continued

IAV [1] ACN| ANTIGEN	MV130 [2] ACN|BACTE-RIA	IAV SEQ [3]	HIT SEQ [4]	ID (%) [5]	HLA I [6]	HLA II [7]	H-2I [8]	H-2II [9]	IEDB [10]
NP_040978| M1	WP_010869065.1| HIN|	LTEVETYVLS	LLEVETPVLS	80	HLA-B*40:01	–	H-2-Kk, H-2-Kq	–	128060
NP_040985| PB1	YP_005228858.1| KPN|	KLRTQIPAE	KLREQIPAE	88.89	HLA-A*30:01	HLA-DPA1*02:01/ DPB1*14:01	–	–	–
NP_040980| HA	WP_000260666.1| SPN|	TVLEKNVTV*	AVLEKNVTV*	88.9	HLA-A*02:01, HLA-A*02:03, HLA-A*02:06, HLA-A*32:01, HLA-A*68:02, HLA-B*08:01	HLA-DRB3*02:02	H-2-Db, H-2-Kb	–	238314
NP_040982| NP	WP_164927877.1| HIN|	GYDFEREGY*	GYQFEREGY*	88.9	HLA-A*30:02	–	–	–	128838
NP_040987| PB2	WP_001830401.1| SEP|	FVNRANQRL*	FVNRKNQRL*	88.9	HLA-A*02:03, HLA-A*02:06, HLA-A*33:01, HLA-A*68:02	–	H-2-Kb	–	97519
NP_040987| PB2	YP_005227236.1| KPN|	QSLIIAAR	QSLIIAAR	100	HLA-A*33:01	–	–	–	128453
NP_040980| HA	WP_000260666.1| SPN|	VLEKNVTV*	VLEKNVTV*	100	HLA-A*02:01, HLA-A*02:03	–	–	–	69459
NP_040983| NS2	WP_002468856.1| SEP|	FEEIRWLI*	FESIRWLI*	87.5	HLA-B*40:01	–	H-2-Kk, H-2-Kq	–	–
NP_040985| PB1	WP_005688698.1| HIN|	ALANTIEV*	ALANTIVV*	87.5	HLA-A*02:01, HLA-A*02:03	–	–	–	62904
NP_040985| PB1	WP_005693559.1| HIN|	RSKAGLLV*	RSKKGLLV*	87.5	HLA-A*30:01	–	–	–	–
NP_040985| PB1	YP_499926.1| SAU|	SMKLRTQI*	SPKLRTQI*	87.5	HLA-B*08:01	–	–	–	128581
NP_040987| PB2	WP_001832661.1| SEP|	PNEVGARI*	PNEVGRRI*	87.5	HLA-B*51:01	–	–	–	68545
NP_040984| NS1	YP_005228222.1| KPN|	ESDEALKM*	ESDELLKM*	87.5	HLA-A*01:01	–	–	–	97398
YP_006495785| PA-X	YP_005229545.1| KPN|	PREEKRQL*	PREEWRQL*	87.5	HLA-B*07:02	–	–	–	–
NP_040987| PB2	YP_500587.1| SAU|	FVNRANQR*	FVNRKNQR*	87.5	HLA-A*33:01	–	–	–	97519
NP_040978| M1	WP_000597995.1| SPN|	WLKTRPIL*	WLSTRPIL*	87.5	HLA-B*08:01	–	–	–	69642
NP_040981| NA	YP_005229237.1| KPN|	ITETIKSW*	IGETIKSW*	87.5	HLA-B*57:01, HLA-B*58:01	–	–	–	–
NP_040986| PA	WP_001830509.1| SEP|	VELAEKTM*	VELNEKTM*	87.5	HLA-B*40:01	–	H-2-Kk, H-2-Kq	–	–
NP_040983| NS2	WP_010976535.1| SPN|	LESSSEDL*	LESDSEDL*	87.5	HLA-B*40:01	–	–	–	–

[1] Accession and antigen of IAV peptide, [2] Accession of bacteria peptide, [3] Sequence of IAV peptide, [4] Sequence of bacteria peptide, [5] Percentage of identity between IAV and bacteria peptides, [6] HLA I and [7] HLA II molecules, and [8] Mouse H2-I and [9] H2-II molecules predicted to bind both the IAV and bacteria peptides, [10] Accession of IAV T cell epitope in IEDB coinciding with IAV cross-reactive peptide (≥ 90% identity and ≥ 8 residues). * Peptides have a C-terminus compatible with cleavage by the proteasome.

memory CD8 T cells capable of recognizing antigens displayed by virally infected cells can occur through antigen cross-presentation (55). This mechanism enables professional antigen presenting cells to redirect antigens taken from the extracellular milieu for presentation in the context of HLA I molecules and prime CD8 T cells against extracellular antigens (55). There are distinct cross-presentation pathways, including some that are proteasome dependent, just like the classical class I antigen presentation pathway (56). In this regard, 29 out of 37 shared peptides defining potential cross-reactive T cell epitopes have a C-terminus that is compatible with cleavage by the

10.3389/fimmu.2023.1235053

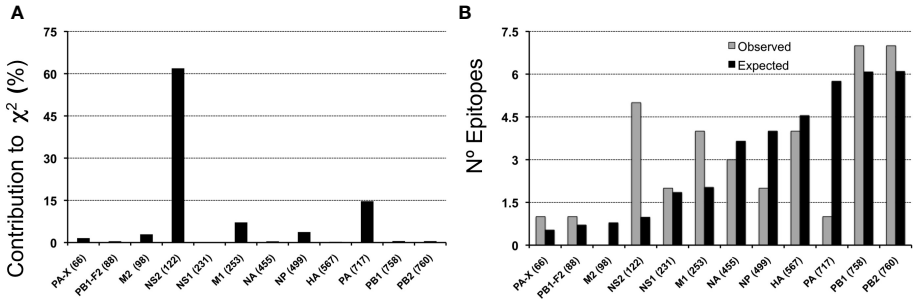

FIGURE 2
Antigen-size distribution of MV130 cross-reactive CD8 T cell epitopes in IAV. **(A)** Contribution to χ^2 -statics of each IAV antigen for the distribution of cross-reactive epitopes according to the size of antigens **(B)** Representation of the number of observed (grey bars) and expected (black bars) cross-reactive CD8 T cell epitopes in each IAV antigen. The number of residues of each antigen is shown in parenthesis adjacent to the antigen name.

proteasome (Table 4, details in Supplementary Dataset 1). Vaccines consisting of inactivated virus or viral antigens can likely induce protective anti-viral CD8 T cell memory thanks to this same mechanism.

Since only 5 potential cross-reactive CD4 T cell epitopes were detected (Tables 3, 4), it could be argued that MV130 may not induce enough T helper (Th) cells to support the whole antiviral potential of cross-reactive CD8 T cells. However, the percentage of the world population that could respond to any of these 5 cross-reactive CD4 T cell epitopes is actually about 33.7% as computed using the frequency of the relevant HLA II molecules (see Methods). Moreover, it is likely that there are many more cross-reactive CD4 T cell epitopes than those detected through our methodology. In fact, CD4 T cells are in general more cross-reactive than CD8 T cells and can recognize many distinct peptides despite sharing little sequence similarity (57, 58). In this context, our findings explain the increase (~ 30-fold) in the influenza virus-specific CD8 T cell response, following MV130 treatment in patients with RRTI (5).

In this study, we trusted the detected T cell cross-reactivity between MV130 and IAV on the predicted binding of shared peptides to the same HLA alleles. However, binding of peptides to MHC molecules is not enough to guarantee T cell reactivity *in vivo*. Thus, it has been shown that peptides with high binding affinity for MHC molecules *in vitro* can nonetheless be excluded from T cell recognition *in vivo*, very likely due to a lack of appropriate antigen processing (59). Hence, the actual realization of the predicted T cell cross-reactivity from MV130 to IAV is contingent on the appropriate processing of antigens. This processing will involve, on the one hand, the uptake of bacteria by antigen-presenting cells, processing of bacteria antigens and presentation of peptide antigens by HLA molecules to prime T cells. On the other hand, it will require that IAV infected cells and/or antigen-presenting cells that have captured IAV antigens do also process the antigens and present the counterpart peptides by the same HLA molecules. These antigen processing events were not taken in consideration in this study because of their complexity and because they are less predictable than binding to MHC molecules. Thereby, *in vivo* studies are required to confirm the predicted T cell cross-reactivity of MV130 to IAV. Given that there are cross-reactive CD8 T cell epitopes restricted by both human and mouse MHC molecules (Table 4), mouse infectious disease models could be used to identify cross-reactive immunity relevant to humans and contribution to IAV protection.

3.4 Cross-reactive B cell epitopes between MV130 and IAV could be neutralizing

Preexisting protective cross-reactive immunity to virus is more often linked to T cells (21, 60). However, cross-reactive antibodies between viruses and bacteria have been reported (61, 62) and we have previously shown that the spike protein of SARS-CoV-2 includes potentially neutralizing B cell epitopes that are shared with bacteria targeted by diphtheria-tetanus vaccines (33, 34). Thereby, we investigated MV130 cross-reactive B cell epitopes mapping on the ectodomains of IAV proteins that are known be targeted by antibodies hampering viral entry. These proteins are HA, NA and M2. We found 8 of such cross-reactive B cell epitopes in HA, one in M2 and none in NA (Table 5). The average solvent accessibility (ASA) of these cross-reactive B cell epitopes (details in Methods) is greater than 25% (Table 4), indicating that they are readily accessible to antibodies. Moreover, we verified that 5 of these cross-reactive B cell epitopes coincide with experimentally determined B cell epitopes deposited at IEDB, including LLTEVETP, which matches a known B cell epitope in M2 annotated as neutralizing in IEDB (targeted by neutralizing antibodies). M2 is a proton-selective transmembrane ion channel located in the viral envelope required for the efficient release of the IAV genome into host cells (63, 64). Interestingly, only the N-terminal region of M2 (residues 1-22) surfaces the virion membrane and it is in this precise region that lays LLTEVETP (residues 3-10). This region is extremely conserved across all reported influenza A viruses and hence cognate antibodies could provide heterotypic influenza immunity. Although our approach did not yield any cross-reactive T cell epitope in M2, CD4 and CD8 T cell epitopes in M2 ectodomain have been reported that can mediate protective immunity to IAV (65, 66). Whether these T cell epitopes could have been predicted as cross-reactive using less stringent criteria of

TABLE 5 Potential MV130-IAV cross-reactive B cell epitopes on ectodomains of HA and M2.

IAV [1] ACN/ANTIGEN	MV130 [2] ACN|BACTERIA|	ID [3] (%)	IAV PEP	MV130 PEP	B [4]	ASA [5] (%)	IEDB (6)
NP_040980 HA	WP_005693451.1|HIN|	80.0	QNAINGITNK	QNAIAGLTNK	0.4	44.50	1180011
NP_040980 HA	YP_005224881.1|KPN|	87.5	AIAGFIEG	AIAGQIEG	0.6	27.43	163243*
NP_040980 HA	YP_005229187.1|KPN|	87.5	LSRGFGSG	LSRGFASG	0.4	25.80	538658
NP_040980 HA	WP_161375000.1|SEP|	87.5	GIITSNAS	GAITSNAS	0.7	31.03	–
NP_040980 HA	YP_005220833.1|KPN|	87.5	LCRLKGIA	LCRLFGIA	0.5	30.05	–
NP_040980 HA	WP_003659222.1|BCA|	87.5	REKVDGVK	RQKVDGVK	0.7	50.02	–
NP_040980 HA	YP_005227766.1|KPN|	87.5	PKESSWPN	PDESSWPN	2.0	59.89	–
NP_040980 HA	WP_002440219.1|SEP|	87.5	KKGKEVLV	KKGKVVLV	0.4	32.76	151030
NP_040979 M2	YP_499789.1|SAU|	87.5	LLTEVETP	LLTMVETP	0.4	82.20	59316*

[1] Accession and antigen source of IAV peptide, [2] Accession of bacteria antigen from BLAST hit, [3] Percentage of identity between MV130 peptide hit to equivalent IAV peptide, [4] B cell reactivity as predicted by Bepipred1.0, [5] Average solvent accessibility of IAV peptides computed after RSA values of peptides residues obtained from the relevant 3D-structures (HA: PDB 1RU7; & M2: PDB 5DLM). [5] Accession of B cell epitope in IEDB coinciding with cross-reactive epitope (≥ 90% identity and ≥ 8 residues). * Epitopes annotated in IEDB as neutralizing (targeted by neutralizing antibodies).

similarity is something to consider. The main target of neutralizing antibodies against IAV is however HA, as this protein dominates the surface of IAV and facilitates viral entry into host cells (57). Hence, we investigated the neutralizing potential of HA cross-reactive B cell epitopes by mapping them on the 3D-structure of HA and examining relevant structural information.

The mature HA includes 3 HA1 and 3 HA2 subunits –derived from the same polypeptide chain – that fold into a trimeric structure depicting a globular head domain and a stem domain (Figure 3A) The globular domain is made of HA1 subunits and includes the receptor binding domain (RBD), which attach sialic acid in various membrane proteins, facilitating viral entry (67). This globular domain, particularly the vicinity of the RBD, is hence the subject of recognition by many neutralizing antibodies (68). Most of the selected cross-reactive B cell epitopes map in the surface of the globular domain, relatively close to the RBD (Figure 3A). Thus, one could speculate that antibodies recognizing these B cell epitopes could impede IAV attachment to host cells and block viral entry. This effect can be readily visualized for the cross-reactive B cell epitope PKESSWPN (HA residues 120-127) (Figures 3A, B), since this epitope is adjacent to the 130-loop (residues number 134-142) which takes part of RBD (67). To a lesser extent, the stem domain can also be the target of neutralizing antibodies, which generally interfere with conformational changes required for IAV membrane fusion (67, 68). Interestingly, one of the cross-reactive B cell epitopes in the stem domain of HA is AIAGFIEG (Figures 3A, C), which coincides with a known B cell epitope recognized by neutralizing antibodies (Table 5) (69). Thereby, we can foresee that the neighboring cross-reactive B cell epitope QNAINGITNK could also be neutralizing (Table 5 and Figure 3A).

4 Conclusion and limitations

Our findings indicate that MV130 is an enhanced source of cross-reactive immunity to common respiratory viruses and in particular to IAV, which result of combining distinct bacteria in the same formulation. MV130 indeed present many potential cross-reactive T cell epitopes with IAV that are restricted by a broad spectrum of HLA molecules. Hence, MV130 could induce anti-IAV T cell responses in individual regardless of their genetic background. Likewise, MV130 encompasses many potential cross-reactive B cell epitopes mapping in critical regions of IAV membrane proteins, so that neutralizing antibodies may also be induced. In sum, cross-reactive adaptive immunity surely contributes, together with trained innate immunity, to the heterologous antiviral immunity associated with MV130.

It is worth noting some limitations that could affect our results. First, we relied heavily on sequence similarity to anticipate potential cross-reactive epitopes. However, antigen receptors can recognize diverse antigens and the structural bases for their promiscuity are ill defined. Antigen recognition by T cell receptors can be particularly subtle (70). Thus, while an individual T cell clone can cross-reactively recognize many diverse peptides (71), a single amino acid change in a TCR contact of a cognate peptide can greatly alter T cell recognition (72). Secondly, we did not take in consideration

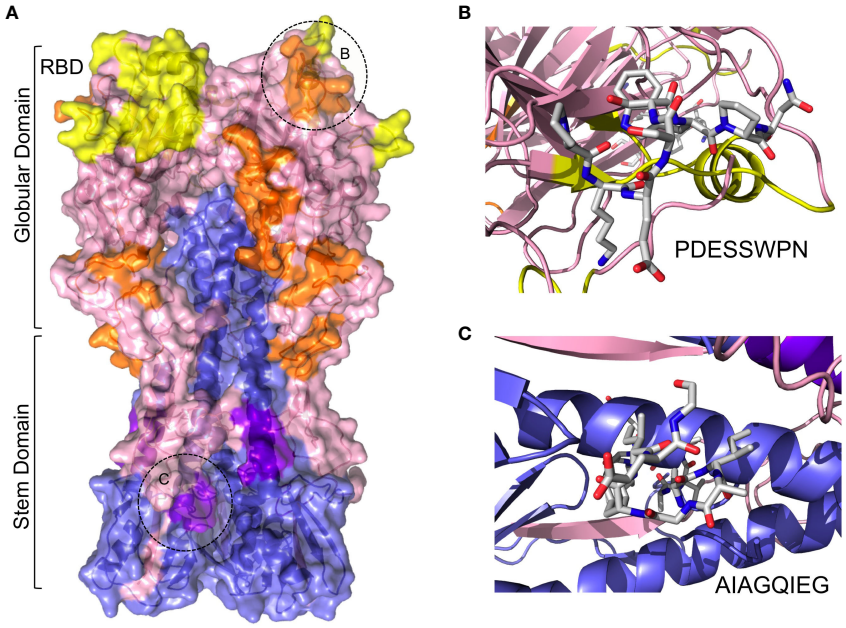

FIGURE 3
Cross-reactive B cell epitopes between MV130 and HA. **(A)** Molecular surface of HA with ribbon structure underneath showing cross-reactive B cell epitopes. HA1 and HA2 chains have been colored in blue and pink, respectively, and the RBD in yellow. Cross-reactive epitopes mapping in HA1 and HA2 are colored in orange and deep purple, respectively. Globular and stem domains are labeled as well as the RBD. The regions circled and labeled as B and C points to cross-reactive B cell epitopes PDESSWPN and AIAGQIEG, which are zoomed in the corresponding right panels. **(B)** Stick rendering of cross-reactive B cell epitope PDESSWPN. **(C)** Detail of cross-reactive B cell epitope AIAGQIEG in stick rendering.

antigen processing to predict potential cross-reactive T cell epitopes, nor evaluated the solvent accessibility of linear B cell epitopes in bacteria. These considerations along with the fact that epitope prediction is not a precise science could limit the realization of the predicted cross-reactivity between MV130 and IAV. Therefore, it is important to stress the need for experimental validation of the cross-reactive epitopes predicted in this work.

Data availability statement

The original contributions presented in the study are included in the article/Supplementary Material. Further inquiries can be directed to the corresponding authors.

Author contributions

Conceptualization: PAR & JLS. Methodology: EML, AR-C & PAR. Data Analysis: AB-P, EML & HFP-P. Investigation: AB-P, EML, PAR & JLS. Writing-Original Draft: AB-P, HFP-P & PAR. Final Writing & Editing: PAR & JLS.

Funding

This work was funded by a collaboration agreement between Inmunotek and UCM secured by PAR. HFP-P and AR-C are funded by scholarships from AEI and UCM, respectively.

Acknowledgments

We wish to thank to PAR lab members for comments and critical reading.

Conflict of interest

JLS was an employee of Inmunotek S.L. at the time of the work. PAR lab receives funds from a collaboration agreement between UCM and Inmunotek.

The remaining authors declare that the research was conducted in the absence of any commercial or financial relationships that could be constructed as a potential conflict of interest.

Publisher's note

Supplementary material

The Supplementary Material for this article can be found online at: https://www.frontiersin.org/articles/10.3389/fimmu.2023.1235053/full#supplementary-material

SUPPLEMENTARY DATA SHEET 1
Excel file with the amino acid sequences of shared peptides between MV130 and IAV and predicted cross-reactivity.

References

1. Marengo R, Ortega Martell JA, Esposito S. Paediatric recurrent ear, nose and throat infections and complications: can we do more? *Infect Dis Ther* (2020) 9:275–90. doi: 10.1007/s40121-020-00289-3

2. Guthrie R. Community-acquired lower respiratory tract infections: etiology and treatment. *Chest* (2001) 120:2021–34. doi: 10.1378/chest.120.6.2021

3. Boncristiani HFC, Arruda E. Respiratory viruses. *Encyclopedia Microbiol* (2009), 500–18. M. F. doi: 10.1016/B978-012373944-5.00314-X

4. Godman B, Haque M, McKimm J, Abu Bakar M, Sneddon J, Wale J, et al. Ongoing strategies to improve the management of upper respiratory tract infections and reduce inappropriate antibiotic use particularly among lower and middle-income countries: findings and implications for the future. *Curr Med Res Opin* (2020) 36:301–27. doi: 10.1080/03007995.2019.1700947

5. Alecsandru D, Valor L, Sanchez-Ramon S, Gil J, Carbone J, Navarro J, et al. Sublingual therapeutic immunization with a polyvalent bacterial preparation in patients with recurrent respiratory infections: immunomodulatory effect on antigen-specific memory CD4+ T cells and impact on clinical outcome. *Clin Exp Immunol* (2011) 164:100–7. doi: 10.1111/j.1365-2249.2011.04320.x

6. Pasquali C, Salami O, Taneja M, Gollwitzer ES, Trompette A, Pattaroni C, et al. Enhanced mucosal antibody production and protection against respiratory infections following an orally administered bacterial extract. *Front Med (Lausanne)* (2014) 1:41. doi: 10.3389/fmed.2014.00041

7. Tejera-Alhambra M, Palomares O, Perez de Diego R, Diaz-Lezcano I, Sanchez-Ramon S. New biological insights in the immunomodulatory effects of mucosal polybacterial vaccines in clinical practice. *Curr Pharm Des* (2016) 22:6283–93. doi: 10.2174/1381612822666160829143129

8. Cirauqui C, Benito-Villalvilla C, Sanchez-Ramon S, Sirvent S, Diez-Rivero CM, Conejero L, et al. Human dendritic cells activated with MV130 induce Th1, Th17 and IL-10 responses via RIPK2 and MyD88 signalling pathways. *Eur J Immunol* (2018) 48:180–93. doi: 10.1002/eji.201747024

9. Garcia Gonzalez LA, Arrutia Diez F. Mucosal bacterial immunotherapy with MV130 highly reduces the need of tonsillectomy in adults with recurrent tonsillitis. *Hum Vaccin Immunother* (2019) 15:2150–3. doi: 10.1080/21645515.2019.1581537

10. Nieto A, Mazon A, Nieto M, Calderon R, Calaforra S, Selva B, et al. Bacterial mucosal immunotherapy with MV130 prevents recurrent wheezing in children: A randomized, double-blind, placebo-controlled clinical trial. *Am J Respir Crit Care Med* (2021) 204:462–72. doi: 10.1164/rccm.202003-200520OC

11. Sanchez-Ramon S, Fernandez-Paredes L, Saz-Leal P, Diez-Rivero CM, Ochoa-Grullon J, Morado C, et al. Sublingual bacterial vaccination reduces recurrent infections in patients with autoimmune diseases under immunosuppressant treatment. *Front Immunol* (2021) 12:675735. doi: 10.3389/fimmu.2021.675735

12. Brandi P, Conejero L, Cueto FJ, Martinez-Cano S, Dunphy G, Gomez MJ, et al. Trained immunity induction by the inactivated mucosal vaccine MV130 protects against experimental viral respiratory infections. *Cell Rep* (2022) 38:110184. doi: 10.1016/j.celrep.2021.110184

13. Del Fresno C, Garcia-Arriaza J, Martinez-Cano S, Heras-Murillo I, Jarit-Cabanillas A, Amores-Iniesta J, et al. The bacterial mucosal immunotherapy MV130 protects against SARS-coV-2 infection and improves COVID-19 vaccines immunogenicity. *Front Immunol* (2021) 12:748103. doi: 10.3389/fimmu.2021.748103

14. Freyne B, Marchant A, Curtis N. BCG-associated heterologous immunity, a historical perspective: intervention studies in animal models of infectious diseases. *Trans R Soc Trop Med Hyg* (2015) 109:52–61. doi: 10.1093/trstmh/tru197

15. Rusek P, Wala M, Druszczynska M, Fol M. Infectious agents as stimuli of trained innate immunity. *Int J Mol Sci* (2018) 19:1–13. doi: 10.3390/ijms19020456

16. Sanchez-Ramon S, Conejero L, Netea MG, Sancho D, Palomares O, Subiza JL. Trained immunity-based vaccines: A new paradigm for the development of broad-spectrum anti-infectious formulations. *Front Immunol* (2018) 9:2936. doi: 10.3389/fimmu.2018.02936

17. Covian C, Fernandez-Fierro A, Retamal-Diaz A, Diaz FE, Vasquez AE, Lay MK, et al. BCG-induced cross-protection and development of trained immunity: implication for vaccine design. *Front Immunol* (2019) 10:2806. doi: 10.3389/fimmu.2019.02806

18. Kleinnijenhuis J, van Crevel R, Netea MG. Trained immunity: consequences for the heterologous effects of BCG vaccination. *Trans R Soc Trop Med Hyg* (2015) 109:29–35. doi: 10.1093/trstmh/tru168

19. Mourits VP, Wijkmans JC, Joosten LA, Netea MG. Trained immunity as a novel therapeutic strategy. *Curr Opin Pharmacol* (2018) 41:52–8. doi: 10.1016/j.coph.2018.04.007

20. Netea MG, Quintin J, van der Meer JW. Trained immunity: a memory for innate host defense. *Cell Host Microbe* (2011) 9:355–61. doi: 10.1016/j.chom.2011.04.006

21. Agrawal B. Heterologous immunity: role in natural and vaccine-induced resistance to infections. *Front Immunol* (2019) 10:2631. doi: 10.3389/fimmu.2019.02631

22. Welsh RM, Selin LK. No one is naive: the significance of heterologous T-cell immunity. *Nat Rev Immunol* (2002) 2:417–26. doi: 10.1038/nri820

23. Bartolo L, Afroz S, Pan YG, Xu R, Williams L, Lin CF, et al. SARS-CoV-2-specific T cells in unexposed adults display broad trafficking potential and cross-react with commensal antigens. *Sci Immunol* (2022) 7:eabn3127. doi: 10.1126/sciimmunol.abn3127

24. Hegazy AN, West NR, Stubbington MJT, Wendt E, Suijker KIM, Datsi A, et al. Circulating and tissue-resident CD4(+) T cells with reactivity to intestinal microbiota are abundant in healthy individuals and function is altered during inflammation. *Gastroenterology* (2017) 153:1320–1337.e1316. doi: 10.1053/j.gastro.2017.1307.1047

25. Mathurin KS, Martens GW, Kornfeld H, Welsh RM. CD4 T-cell-mediated heterologous immunity between mycobacteria and poxviruses. *J Virol* (2009) 83:3528–39. doi: 10.1128/JVI.02393-02308

26. Vojdani A, Vojdani E, Melgar AL, Redd J. Reaction of SARS-CoV-2 antibodies with other pathogens, vaccines, and food antigens. *Front Immunol* (2002) 13:1003094. doi: 10.3389/fimmu.2022.1003094

27. Kaur H, Salunke DM. Antibody promiscuity: Understanding the paradigm shift in antigen recognition. *IUBMB Life* (2015) 67:498–505. doi: 10.1002/iub.1397

28. Petrova G, Ferrante A, Gorski J. Cross-reactivity of T cells and its role in the immune system. *Crit Rev Immunol* (2012) 32:349–72. doi: 10.1615/CritRevImmunol.v32.i4.50

29. Sewell AK. Why must T cells be cross-reactive? *Nat Rev Immunol* (2012) 12:669–77. doi: 10.1038/nri3279

30. Van Regenmortel MH. Specificity, polyspecificity, and heterospecificity of antibody-antigen recognition. *J Mol Recognit* (2014) 27:627–39. doi: 10.1002/jmr.2394

31. Sanchez-Trincado JL, Gomez-Perosanz M, Reche PA. Fundamentals and methods for T- and B-cell epitope prediction. *J Immunol Res* (2017) 2017:2680160. doi: 10.1155/2017/2680160

32. Lehmann AA, Kirchenbaum GA, Zhang T, Reche PA, Lehmann PV. Deconvoluting the T cell response to SARS-coV-2: specificity versus chance and cognate cross-reactivity. *Front Immunol* (2021) 12:635942. doi: 10.3389/fimmu.2021.635942

33. Reche P. *Cross-reactive immunity from combination DTP vaccines could protect against COVID-19*. Osf Preprints (Charlottesville, Virginia, USA) (2020).

34. Reche PA. Potential cross-reactive immunity to SARS-coV-2 from common human pathogens and vaccines. *Front Immunol* (2020) 11:586984. doi: 10.3389/fimmu.2020.586984

35. Altschul SF, Madden TL, Schaffer AA, Zhang J, Zhang Z, Miller W, et al. Gapped BLAST and PSI-BLAST: a new generation of protein database search programs. *Nucleic Acids Res* (1997) 25:3389–402. doi: 10.1093/nar/25.17.3389

36. Reche PA, Glutting JP, Reinherz EL. Prediction of MHC class I binding peptides using profile motifs. *Hum Immunol* (2002) 63:701–9. doi: 10.1016/S0198-8859(02)00432-9

37. Reche PA, Glutting JP, Zhang H, Reinherz EL. Enhancement to the RANKPEP resource for the prediction of peptide binding to MHC molecules using profiles. *Immunogenetics* (2004) 56:405–19. doi: 10.1007/s00251-004-0709-7

38. Hoof I, Peters B, Sidney J, Pedersen LE, Sette A, Lund O, et al. NetMHCpan, a method for MHC class I binding prediction beyond humans. *Immunogenetics* (2009) 61:1–13. doi: 10.1007/s00251-008-0341-z

39. Reynisson B, Alvarez B, Paul S, Peters B, Nielsen M. NetMHCpan-4.1 and NetMHCIIpan-4.0: improved predictions of MHC antigen presentation by concurrent motif deconvolution and integration of MS MHC eluted ligand data. *Nucleic Acids Res* (2020) 48:W449–54. doi: 10.1093/nar/gkaa379

40. Jensen KK, Andreatta M, Marcatili P, Buus S, Greenbaum JA, Yan Z, et al. Improved methods for predicting peptide binding affinity to MHC class II molecules. *Immunology* (2018) 154:394–406. doi: 10.1111/imm.12889

41. Larsen JE, Lund O, Nielsen M. Improved method for predicting linear B-cell epitopes. *Immunome Res* (2006) 2:1–7. doi: 10.1186/1745-7580-2-2

42. Ballesteros-Sanabria L, Pelaez-Prestel HF, Ras-Carmona A, Reche PA. Resilience of spike-specific immunity induced by COVID-19 vaccines against SARS-coV-2 variants. *Biomedicines* (2022) 10:1–16. doi: 10.3390/biomedicines10050996

43. Diez-Rivero CM, Reche PA. CD8 T cell epitope distribution in viruses reveals patterns of protein biosynthesis. *PloS One* (2012) 7:e43674. doi: 10.1371/journal.pone.0043674

44. Molero-Abraham M, Lafuente EM, Flower DR, Reche PA. Selection of conserved epitopes from hepatitis C virus for pan-populational stimulation of T-cell responses. *Clin Dev Immunol* (2013) 2013:601943. doi: 10.1155/2013/601943

45. Vita R, Overton JA, Greenbaum JA, Ponomarenko J, Clark JD, Cantrell JR, et al. The immune epitope database (IEDB) 3.0. *Nucleic Acids Res* (2015) 43:D405–412. doi: 10.1093/nar/gku938

46. Diez-Rivero CM, Lafuente EM, Reche PA. Computational analysis and modeling of cleavage by the immunoproteasome and the constitutive proteasome. *BMC Bioinf* (2010) 11:479. doi: 10.1186/1471-2105-1111-1479

47. Gomez-Perosanz M, Ras-Carmona A, Lafuente EM, Reche PA. Identification of CD8(+) T cell epitopes through proteasome cleavage site predictions. *BMC Bioinf* (2020) 21:484. doi: 10.1186/s12859-12020-03782-12851

48. Hubbard SJ, Thornton JM. *NACCESS, computer program*. London, UK: Department of Biochemistry and Molecular Biology, University College London (1993).

49. Alonso-Padilla J, Lafuente EM, Reche PA. Computer-aided design of an epitope-based vaccine against epstein-barr virus. *J Immunol Res* (2017) 2017:9363750. doi: 10.1155/2017/9363750

50. Perez-Silva JG, Araujo-Voces M, Quesada V. nVenn: generalized, quasi-proportional Venn and Euler diagrams. *Bioinformatics* (2018) 34:2322–4. doi: 10.1093/bioinformatics/bty109

51. Urban S, Paragi G, Burian K, McLean GR, Virok DP. Identification of similar epitopes between severe acute respiratory syndrome coronavirus-2 and Bacillus Calmette-Guerin: potential for cross-reactive adaptive immunity. *Clin Transl Immunol* (2020) 9:e1227. doi: 10.1002/cti2.1227

52. Zhang Q, Wang P, Kim Y, Haste-Andersen P, Beaver J, Bourne PE, et al. Immune epitope database analysis resource (IEDB-AR). *Nucleic Acids Res* (2008) 36: W513–518. doi: 10.1093/nar/gkn1254

53. Reche PA, Reinherz EL. Sequence variability analysis of human class I and class II MHC molecules: functional and structural correlates of amino acid polymorphisms. *J Mol Biol* (2003) 331:623–41. doi: 10.1016/S0022-2836(03)00750-2

54. Reche PA, Reinherz EL. Definition of MHC supertypes through clustering of MHC peptide-binding repertoires. *Methods Mol Biol* (2007) 409:163–73. doi: 10.1007/978-1-60327-118-9_11

55. Embgenbroich M, Burgdorf S. Current concepts of antigen cross-presentation. *Front Immunol* (2018) 9:1643. doi: 10.3389/fimmu.2018.01643

56. Amigorena S, Savina A. Intracellular mechanisms of antigen cross presentation in dendritic cells. *Curr Opin Immunol* (2010) 22:109–17. doi: 10.1016/j.coi.2010.1001.1022

57. Su LF, Davis MM. Antiviral memory phenotype T cells in unexposed adults. *Immunol Rev* (2013) 255:95–109. doi: 10.1111/imr.12095

58. Carvalho T. Cross-reactive T cells. *Nat Med* (2020) 26:1807. doi: 10.1038/s41591-41020-01161-41590

59. Zhong W, Reche PA, Lai CC, Reinhold B, Reinherz EL. Genome-wide characterization of a viral cytotoxic T lymphocyte epitope repertoire. *J Biol Chem* (2003) 278:45135–44. doi: 10.41074/jbc.M307417200

60. Murray SM, Ansari AM, Frater J, Klenerman P, Dunachie S, Barnes E, et al. The impact of pre-existing cross-reactive immunity on SARS-CoV-2 infection and vaccine responses. *Nat Rev Immunol* (2023) 23:304–16. doi: 10.1038/s41577-41022-00809-x

61. Trama AM, Moody MA, Alam SM, Jaeger FH, Lockwood B, Parks R, et al. HIV-1 envelope gp41 antibodies can originate from terminal ileum B cells that share cross-reactivity with commensal bacteria. *Cell Host Microbe* (2014) 16:215–26. doi: 10.1016/j.chom.2014.1007.1003

62. Geanes ES, LeMaster C, Fraley ER, Khanal S, McLennan R, Grundberg E, et al. Cross-reactive antibodies elicited to conserved epitopes on SARS-CoV-2 spike protein after infection and vaccination. *Sci Rep* (2022) 12:6496. doi: 10.1038/s41598-41022-10230-y

63. Liu W, Li H. and Chen, YH. N-terminus of M2 protein could induce antibodies with inhibitory activity against influenza virus replication. *FEMS Immunol Med Microbiol* (2003) 35:141–6. doi: 10.1016/S0928-8244(1003)00009-00009

64. Cho KJ, Schepens B, Moonens K, Deng L, Fiers W, Remaut H, et al. Crystal structure of the conserved amino terminus of the extracellular domain of matrix protein 2 of influenza A virus gripped by an antibody. *J Virol* (2016) 90:611–5. doi: 10.1128/JVI.02105-15

65. Faner R, James E, Huston L, Pujol-Borrel R, Kwok WW, Juan M. Reassessing the role of HLA-DRB3 T-cell responses: evidence for significant expression and complementary antigen presentation. *Eur J Immunol* (2010) 40:91–102. doi: 10.1002/eji.200939225

66. Eickhoff CS, Terry FE, Peng L, Meza KA, Sakala IG, Van Aartsen D, et al. Highly conserved influenza T cell epitopes induce broadly protective immunity. *Vaccine* (2019) 37:5371–81. doi: 10.1016/j.vaccine.2019.5307.5033

67. Skehel JJ, Wiley DC. Receptor binding and membrane fusion in virus entry: the influenza hemagglutinin. *Annu Rev Biochem* (2000) 69:531–69. doi: 10.1146/annurev.biochem.1169.1141.1531

68. Wu NC, Wilson IA. Influenza hemagglutinin structures and antibody recognition. *Cold Spring Harb Perspect Med* (2020) 10:a038778. doi: 10.031101/cshperspect.a038778

69. Corti D, Voss J, Gamblin SJ, Codoni G, Macagno A, Jarrossay D, et al. A neutralizing antibody selected from plasma cells that binds to group 1 and group 2 influenza A hemagglutinins. *Science* (2011) 333:850–6. doi: 10.1126/science.1205669

70. Brazin KN, Mallis RJ, Das DK, Feng Y, Hwang W, Wang JH, et al. Structural features of the Œ±Œ≤TCR mechanotransduction apparatus that promote pMHC discrimination. *Front Immunol* (2015) 6:441. doi: 10.3389/fimmu.2015.00441

71. Wooldridge L, Ekeruche-Makinde J, van den Berg HA, Skowera A, Miles JJ, Tan MP, et al. A single autoimmune T cell receptor recognizes more than a million different peptides. *J Biol Chem* (2012) 287:1168–77. doi: 10.1074/jbc.M111.289488

72. Fridkis-Hareli M, Reche PA, Reinherz EL. Peptide variants of viral CTL epitopes mediate positive selection and emigration of Ag-specific thymocytes in *vivo*. *J Immunol* (2004) 173:1140–50. doi: 10.4049/jimmunol.1173.1142.1140

frontiers | Frontiers in Immunology

TYPE Correction
PUBLISHED 08 September 2023
DOI 10.3389/fimmu.2023.1284628

OPEN ACCESS

EDITED AND REVIEWED BY
Tomasz Piotr Wypych,
Polish Academy of Sciences, Poland

*CORRESPONDENCE
Jose L. Subiza
jlsubiza@inmunotek.com
Pedro A. Reche
parecheg@med.ucm.es

†These authors have contributed equally to this work

RECEIVED 28 August 2023
ACCEPTED 30 August 2023
PUBLISHED 08 September 2023

CITATION
Bodas-Pinedo A, Lafuente EM, Pelaez-Prestel HF, Ras-Carmona A, Subiza JL and Reche PA (2023) Corrigendum: Combining different bacteria in vaccine formulations enhances the chance for antiviral cross-reactive immunity: a detailed *in silico* analysis for influenza A virus.
Front. Immunol. 14:1284628.
doi: 10.3389/fimmu.2023.1284628

Corrigendum: Combining different bacteria in vaccine formulations enhances the chance for antiviral cross-reactive immunity: a detailed *in silico* analysis for influenza A virus

Andrés Bodas-Pinedo[1†], Esther M. Lafuente[2†], Hector F. Pelaez-Prestel[2], Alvaro Ras-Carmona[2], Jose L. Subiza[3*] and Pedro A. Reche[2*]

[1]Children's Digestive Unit, Institute for Children and Adolescents, Hospital Clinico San Carlos, Madrid, Spain, [2]Department of Immunology & O2, Faculty of Medicine, University Complutense of Madrid, Ciudad Universitaria, Pza. Ramón y Cajal, Madrid, Spain, [3]Inmunotek, Alcalá de Henares, Spain

KEYWORDS

MV130, bacteria, respiratory viruses, cross-reactivity, epitope, influenza A virus

A corrigendum on

Combining different bacteria in vaccine formulations enhances the chance for antiviral cross-reactive immunity: a detailed in silico analysis for influenza A virus

by Bodas-Pinedo A, Lafuente EM, Pelaez-Prestel HF, Ras-Carmona A, Subiza JL and Reche PA (2023) *Front. Immunol*. 14:1235053. doi: 10.3389/fimmu.2023.1235053

In the published article, there was an error in Table 1 as published. In row 1, column 2, ¨Accesion" was misspelled. It should be "Accession". In row 13, column 1, "Klebisella" was misspelled. It should be "Klebsiella". In addition, in row 9 for SARS-CoV2, column 2 was incorrect (the accession number listed was GCF_000009445, but should have been NC_045512) and column 2 was empty but should have been 12. The corrected Table 1 and its caption appear below.

In the published article, there was an error in Table 2 as published. "Klebisella" was misspelled. It should be "Klebsiella". The corrected Table 2 and its caption appear below.

In the published article, there was an error in Table 3 as published. "Klebisella" was misspelled. It should be "Klebsiella". In addition, the scientific names of bacteria were not in italic. The corrected Table 3 and its caption appear below.

In the published article, there was an error in the legend for Figure 1 as published. HRVA and HRVB, standing for human rhinovirus A and B, respectively, missed the relevant "A" and "B". The corrected legend appears below.

10.3389/fimmu.2023.1284628

TABLE 1 Amino acid sequences from pathogens and vaccines considered in this study.

Pathogen	NCBI Accession	Proteins/CDS
Influenza A virus (IAV)	GCF_000865725	12
Influenza B virus (IBV)	GCF_000820495	10
Human rhinovirus A (HRVA)	NC_038311	1
Human rhinovirus B (HRVB)	NC_038312	1
Human rhinovirus C (HRVC)	NC_009996	1
Respiratory syncytial virus A (RSVA)	NC_038235	11
Respiratory syncytial virus A (RSVB)	NC_001781	11
Severe acute respiratory syndrome coronavirus 2 (SARS-CoV-2)	NC_045512	12
Bacille Calmette-Guérin (BCG)	GCF_000009445	4034
Branhamella catarrhalis (BCA)	GCF_000092265	1607
Haemophilus influenzae (HIN)	GCF_000027305	1597
Klebsiella pneumoniae (KPN)	GCF_000240185	5779
Staphylococcus aureus (SAU)	GCF_000013425	2767
Staphylococcus epidermidis (SEP)	GCF_000007645	2282
Streptococcus pneumoniae (SPN)	GCF_000007045	1861
*MV130**		15893

* MV130 includes all bacteria but BCG.

In the published article, there was an error in the **Abstract**. "Klebisella" was misspelled. It should be "Klebsiella"

A correction has been made to the **Abstract**. The corrected sentence appears below.

"The bacteria selected in this work were Bacillus Calmette Guerin and those included in the poly-bacterial preparation MV130: *Streptococcus pneumoniae*, *Staphylococcus aureus*, *Staphylococcus epidermidis*, *Klebsiella pneumoniae*, *Branhamella catarrhalis* and *Haemophilus influenzae*."

In the published article, there was an error in the **Methods** section. HLA, standing for human leukocyte antigen, was used twice in Methods instead of MHC (major histocompatibility complex). MHCs are known as HLAs in humans, as indicated later in the Results section.

A correction has been made to the **Methods** section, subsection *2.3 Prediction of T and B cell epitopes*. This sentence previously stated:

"Binding of a peptide to a given HLA I molecule was considered to occur at a 2% Rank cutoff given by both RANKPEP and NetMHCpan, which allows selecting weak and strong binders."

The corrected sentence appears below.

"Binding of a peptide to a given MHC I molecule was considered to occur at a 2% Rank cutoff given by both RANKPEP and NetMHCpan, which allows selecting weak and strong binders."

Likewise, a correction has also been made to the **Methods** section, subsection *2.5 Other procedures*. This sentence previously stated:

"The percentage of the world population that could respond to CD8 and CD4 T cell epitopes (population coverage) was computed after their HLA binding profiles using a command line version of EPISOPT (44) and the IEDB PPC tool at http://tools.iedb.org/tools/population/iedb_input (45), respectively, considering HLA allele expression for the entire world population."

The corrected sentence appears below.

"The percentage of the world population that could respond to CD8 and CD4 T cell epitopes (population coverage) was computed after their MHC binding profiles using a command line version of EPISOPT (44) and the IEDB PPC tool at http://tools.iedb.org/tools/population/iedb_input (45), respectively, considering the relevant allele expression for the entire world population."

The authors apologize for these errors and state that this does not change the scientific conclusions of the article in any way. The original article has been updated.

10.3389/fimmu.2023.1284628

TABLE 2 Size of the shared peptidome between bacteria in MV130 and respiratory viruses.

	ORF	IAV	IBV	HRVA	HRVB	HRVC	RSVA	RSVB	SARS
Streptococcus pneumoniae (SPN)	1861	12	17	8	13	17	25	31	52
Staphylococcus aureus (SAU)	2767	23	36	8	12	10	39	46	68
Staphylococcus epidermidis (SEP)	2282	27	30	11	14	10	27	30	53
Klebsiella pneumoniae (KPN)	5770	48	57	19	32	21	53	53	138
Branhamella catarrhalis (BCA)	1607	15	18	11	10	9	27	20	38
Haemophilus influenzae (HIN)	1597	25	18	4	9	8	31	20	50
Bacille Calmette-Guérin (BCG)	4045	46	41	13	27	25	32	32	102
MV130	15884	139	163	54	79	72	185	183	360

ORF, Open Reading Frame; IAV, Influenza A virus; IBV, Influenza B virus; HRVA, human rhinovirus A; HRVB, human rhinovirus B; HRVC, human rhinovirus C; RSVA, Respiratory Syncytial virus A, RSVB: Respiratory Syncytial virus B; SARS, SARS-CoV-2. Whole dataset available in Supplementary Dataset 1.

TABLE 3 Potential cross-reactive epitopes between MV130 and IAV.

	IAV (1)	B (2)	CD8 T (H)	CD4 T (H)	CD8 T (M)	CD4 T (M)
Streptococcus pneumoniae (SPN)	12	2	4	1	1	0
Staphylococcus aureus (SAU)	25	5	2	0	3	0
Staphylococcus epidermidis (SEP)	27	6	7	1	7	1
Klebsiella pneumoniae (KPN)	48	10	13	1	4	1
Branhamella catarrhalis (BCA)	15	7	4	1	1	0
Haemophilus influenzae (HIN)	25	4	7	1	5	1
MV130	139	34	37	5	21	3

[1] Number of shared peptides between IAV (Puerto Rico 8 Strain) and bacteria, [2] number of cross-reactive b cell epitopes, [H] number of T cell epitopes restricted by human MHC molecules, [M] number of T cell epitopes restricted by mouse MHC molecules.

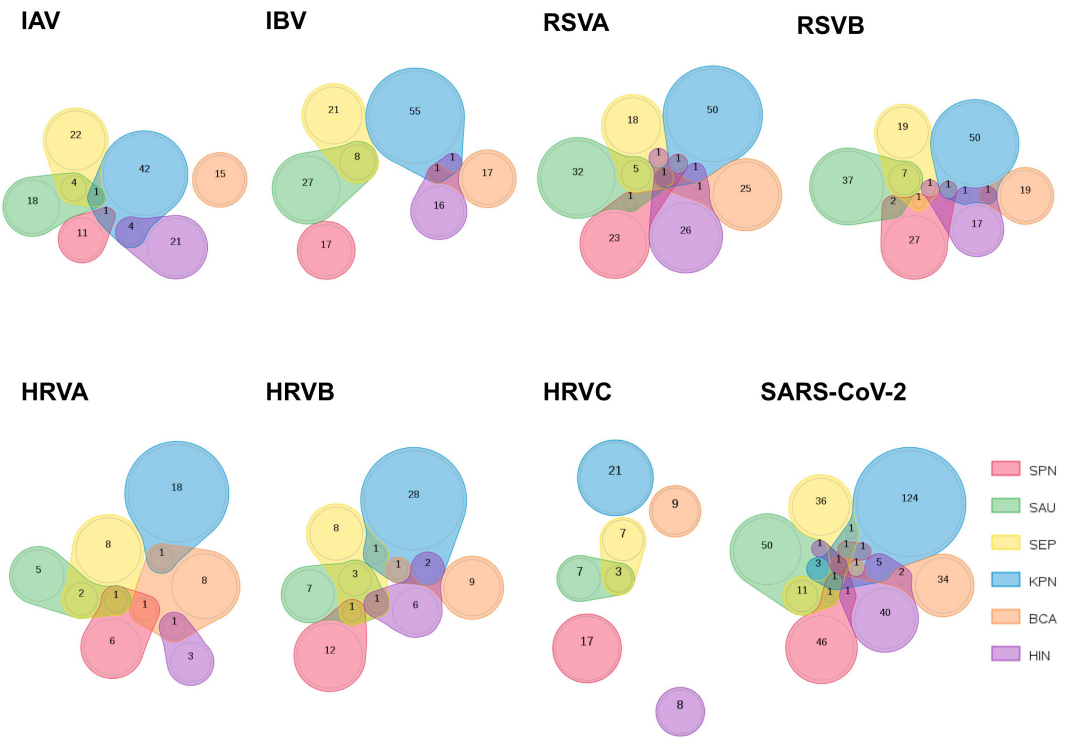

FIGURE 1
Comparison of peptidomes shared by respiratory viruses and bacteria in MV130. The sets of peptides that are shared between 8 respiratory viruses and each bacterium included in the MV130 formulation were compared and represented using Venn diagrams to visualize the overlaps. The number of peptides in overlapping and non-overlapping regions is indicated. The represented viruses are (from left to right and up to down): IAV: Influenza A virus; IBV: Influenza B virus; HRVA: human rhinovirus A; HRVB: human rhinovirus B; HRVC: human rhinovirus C; RSVA: Respiratory Syncytial virus A; RSVB: Respiratory Syncytial virus B; SARS: SARS-CoV-2. The six bacteria species included in MV130 are indicated and colored as follows: *S. pneumoniae* (SPN, red); *S. aureus* (SAU, green); *S. epidermidis* (SEP, yellow); *K. pneumoniae* (KPN, blue); *B. catarrhalis* (BCA, orange); *H. influenzae* (HIN, purple).

Publisher's note

frontiers | Frontiers in Immunology

TYPE Original Research
PUBLISHED 23 August 2023
DOI 10.3389/fimmu.2023.1197630

OPEN ACCESS

EDITED BY
Daniela Latorre,
ETH Zürich, Switzerland

REVIEWED BY
Jared Klarquist,
University of Colorado Anschutz Medical Campus, United States
Weiyi Peng,
University of Houston, United States

*CORRESPONDENCE
Elisabetta Volpe
e.volpe@hsantalucia.it

RECEIVED 31 March 2023
ACCEPTED 04 August 2023
PUBLISHED 23 August 2023

CITATION
Carbone ML, Capone A, Guercio M, Reddel S, Silvestris DA, Lulli D, Ramondino C, Peluso D, Quintarelli C, Volpe E and Failla CM (2023) Insight into immune profile associated with vitiligo onset and anti-tumoral response in melanoma patients receiving anti-PD-1 immunotherapy. *Front. Immunol.* 14:1197630. doi: 10.3389/fimmu.2023.1197630

Insight into immune profile associated with vitiligo onset and anti-tumoral response in melanoma patients receiving anti-PD-1 immunotherapy

Maria Luigia Carbone[1], Alessia Capone[2], Marika Guercio[3], Sofia Reddel[3], Domenico Alessandro Silvestris[3], Daniela Lulli[1], Carmela Ramondino[1], Daniele Peluso[4], Concetta Quintarelli[3,5], Elisabetta Volpe[2*] and Cristina Maria Failla[1]

[1]Laboratory of Experimental Immunology, Istituto Dermopatico dell'Immacolata (IDI)-IRCCS, Rome, Italy, [2]Laboratory of Molecular Neuroimmunology, Santa Lucia Foundation-IRCCS, Rome, Italy, [3]Department of Oncology-Hematology, and Cell and Gene Therapy, Bambino Gesù Children Hospital, IRCCS, Rome, Italy, [4]Department of Biology, University "Tor Vergata", Rome, Italy, [5]Department of Clinical Medicine and Surgery, University of Naples Federico II, Naples, Italy

Introduction: Immunotherapy with checkpoint inhibitors is an efficient treatment for metastatic melanoma. Development of vitiligo upon immunotherapy represents a specific immune-related adverse event (irAE) diagnosed in 15% of patients and associated with a positive clinical response. Therefore, a detailed characterization of immune cells during vitiligo onset in melanoma patients would give insight into the immune mechanisms mediating both the irAE and the anti-tumor response.

Methods: To better understand these aspects, we analyzed T cell subsets from peripheral blood of metastatic melanoma patients undergoing treatment with anti-programmed cell death protein (PD)-1 antibodies. To deeply characterize the antitumoral T cell response concomitant to vitiligo onset, we analyzed T cell content in skin biopsies collected from melanoma patients who developed vitiligo. Moreover, to further characterize T cells in vitiligo skin lesion of melanoma patients, we sequenced T cell receptor (TCR) of cells derived from biopsies of vitiligo and primary melanoma of the same patient.

Results and discussion: Stratification of patients for developing or not developing vitiligo during anti-PD-1 therapy revealed an association between blood reduction of CD8-mucosal associated invariant T (MAIT), T helper (h) 17, natural killer (NK) $CD56^{bright}$, and T regulatory (T-reg) cells and vitiligo onset. Consistently with the observed blood reduction of Th17 cells in melanoma patients developing vitiligo during immunotherapy, we found high amount of IL-17A expressing cells in the vitiligo skin biopsy, suggesting a possible migration of Th17 cells from the blood into the autoimmune lesion. Interestingly, except for a few cases, we found different TCR sequences between vitiligo and primary melanoma lesions. In contrast, shared TCR sequences were identified between vitiligo and metastatic tissues of the same patient. These data indicate that T cell response against normal

melanocytes, which is involved in vitiligo onset, is not typically mediated by reactivation of specific T cell clones infiltrating primary melanoma but may be elicited by T cell clones targeting metastatic tissues. Altogether, our data indicate that anti-PD-1 therapy induces a de novo immune response, stimulated by the presence of metastatic cells, and composed of different T cell subtypes, which may trigger the development of vitiligo and the response against metastatic tumor.

KEYWORDS

melanoma, immunotherapy, vitiligo, biomarkers, T-cell receptor

1 Introduction

Melanoma is an aggressive skin cancer, whose incidence rates have increased over the past few decades not only in adults, but also in children and adolescents. Cutaneous melanoma is characterized by a high mutational burden, providing a consistent number of antigens that could constitute targets of the immune response (1). Indeed, melanoma-specific cytotoxic T lymphocytes have been observed in patient's blood and melanoma tissues (2). However, this immune response rarely succeeds in effective tumor clearance. It is evident that tumor progression must be accompanied by impairment of immune responses and to overcome such an impairment, therapeutic treatments based on immune checkpoint inhibitors have been developed and proved highly effective in cutaneous melanoma (3). Nevertheless, the overall response rate observed in unresectable/metastatic stage III-IV melanoma patients treated with anti-programmed death (PD)-1 antibodies as monotherapy, is still low, around 40% (4). Thus, availability of early markers of response to treatment would permit to interrupt the therapy for not-responsive patients, promptly switching them towards alternative therapeutic approaches, and reducing the risk of developing immune-related adverse events (irAE). Among the possible irAE emerging during anti-PD-1 treatment, melanoma patients develop leukoderma lesions, also called vitiligo lesions due to their high similarity to those of the spontaneous autoimmune skin disease vitiligo. In fact, histopathological aspects of immunotherapy-induced vitiligo were almost indistinguishable from spontaneous vitiligo (5). Of note, development of vitiligo seems to be specific of cutaneous melanoma, as it is rarely reported as an irAE during other tumor type treatments (5); antibodies and $CD8^+$ T lymphocytes directed against melanocyte-specific antigens have been identified in both cases, suggesting that, in cutaneous melanoma, vitiligo appearance could reflect a broad immune cell activation, also effective against cancer cells (6). Actually, we and others have demonstrated that the onset of vitiligo during treatment with checkpoint inhibitors correlates with a better outcome in metastatic melanoma patients (6–9). Nevertheless, the mechanism underlying the association between vitiligo development and tumor regression is still unclear. Previously, it has been shown that the same T lymphocyte clone was present in a primary melanoma and in a vitiligo lesion spontaneously developed in the same patient (10). This result suggested that vitiligo appearance was exerted by T cells directed against antigens shared by primary melanoma and normal melanocytes. More recently, a patient affected by widespread uveal melanoma and treated with anti-cytotoxic T-lymphocyte antigen (CTLA)-4/anti-PD-1 therapy showed an exceptional response accompanied by the development of several irAEs, comprising vitiligo. TCR-sequencing of the primary tumor, as well as of different metastatic samples, identified identical T cell clones in the examined tissues (11). Certainly, future researchers would benefit from a deeper understanding of this immunological mechanism, also in order to determine the best application of vaccine-based or T cell-based therapies, currently under study in clinical trials for the treatment of cutaneous melanoma.

Similarities in immune molecular processes involved in autoimmunity and in anti-tumor responses have already been observed (12). Indeed, cancer-specific mortality was significantly lower in patients with an autoimmune background (12), and accordingly cancer patients showing clinically relevant anti-tumor immune responses accompany with a "beneficial autoimmunity", also important in the processes of cancer immunosurveillance (13). In this context, we have hypothesized that the immunological molecular pathways observed in vitiligo may also occur in melanoma patients who show positive response to immunotherapy. In a previous study, we demonstrated that soluble CD25 (sCD25) and CXCL9, two known circulating vitiligo-specific biomarkers, were also higher in sera of stable and responsive metastatic melanoma patients undergoing anti-PD-1 therapy compared to non-responders (14). Moreover, peripheral blood mononuclear cells (PBMCs) of responders showed a lower blood frequency of T regulatory lymphocytes (T-reg), a suppressive T cell immune population, compared to non-responder patients, either before or after three months of anti-PD-1 therapy (14). Altogether, these data underlined the presence of immune mechanisms in cutaneous melanoma, common to spontaneous vitiligo and potentially mediating both autoimmune responses accountable for vitiligo development and anti-tumor immune responses. As a further demonstration of this hypothesis, in the present study we extended the analysis to circulating- and tissue-related immune cells, comparing frequency and activation features in patients who developed or not vitiligo under anti-PD-1 therapy. Our results give insight into the immune mechanisms which mediate the onset of this irAE and that may predict the occurrence of an effective anti-tumor immune response.

2 Materials and methods

2.1 Patients

This study was conducted according to the Good Clinical Practice Guidelines and the Declaration of Helsinki. The study was approved by the Institutional Review Boards of Istituto Dermopatico dell'Immacolata (IDI)-IRCCS (510/3, April 2018). All patients enrolled in the study provided written informed consent. This study included patients with unresectable metastatic melanoma, stage IIIc or IV based on American Joint Committee on Cancer (AJCC, version 7) staging (15), enrolled for treatment with anti-PD-1 inhibitors at IDI-IRCCS. Peripheral blood samples were collected before therapy and at every therapy administration up to one-year, disease progression or vitiligo appearance. Nivolumab (Opdivo®) was given at the dose of 480 mg every 4 weeks, pembrolizumab (Keytruda®) at the dose of 200 mg every 3 weeks. Patients underwent physical examination and assessment of biochemical parameters monthly, whereas investigator-determined objective response was assessed radiologically with computed tomography scans approximately every 12 weeks after treatment initiation. Tumor response was classified as immune complete response (iCR), partial response (iPR), or stable disease (iSD), according to the immune response evaluation criteria in solid tumors (iRECIST 1.1) (16, 17). Therapy efficacy evaluation was based on best overall response (iOR) determined as best time point response according to iRECIST.

2.2 PBMC isolation and cytofluorimetric analysis

Whole blood samples were collected into vacutainer sodium citrate tubes (cat. no. 367704, BD Biosciences, Plymouth, UK) and PBMCs were isolated by Ficoll gradient centrifugation (GE Healthcare, Little Chalfont, UK). Cryopreserved PBMCs were stained with the following antibodies, as previously described (14): Panel 1- anti-human CD4 FITC (1:100) (cat. no. 130-114-531, Miltenyi Biotech, Auburn, CA, USA) (1:100), anti-human CRTh2-PE (1:150) (cat. no. 130-114-128, Miltenyi Biotech), anti-human CD161-PE/Dazzle594 (1:50) (cat. no. 339939, Biolegend, San Diego, CA, USA), anti-human CD3 PercP-Cy5.5 (1:300) (cat. no. 300327, Beckman Coulter, Brea, CA, USA), anti-human CXCR3-APC Alexa647 (1:40) (cat. no. 353711, Biolegend), anti-human CD8-APC Alexa700 (1:120) (cat. no. A66332, Beckman Coulter), anti-human CCR6-BV421 (1:30) (cat. no. 353407, Biolegend), anti-human PD1-BV650 (1:30) (cat. no. 564104, BD Biosciences), and LIVE/DEAD™ Fixable Aqua Dead Cell Stain Kit (1:200) (cat. no. l34957, Invitrogen, Waltham, MA, USA). Panel 2: anti-human CD4 FITC (1:100) (cat. no. 130-114-531, Miltenyi Biotech), anti-human CD3-ECD (1:100) (cat. no. IM2705U, Beckman Coulter), anti-human CD127-APC Alexa700 (1:200) (cat. no. 351343, Beckman Coulter), anti-human CD25-BV421 (1:60) (cat. no. 564033, BD Biosciences), anti-human PD1-BV650 (1:30) (cat. no. 564104, BD Biosciences), and LIVE/DEAD™ Fixable Aqua Dead Cell Stain Kit (1:200) (cat. no. l34957, Invitrogen). Samples were acquired using Cytoflex cytometer (Beckman Coulter) and analyzed using FlowJo-10 software version 10.3.0. Gating strategy for discrimination of different cell populations is described in Supplementary Figure 1. Briefly, CD3 ($CD3^+$); CD4 ($CD3^+$, $CD4^+$); CD8 ($CD3^+$, $CD8^+$); CD8-MAIT ($CD3^+$, $CD8^+$, $CD161^{high}$) as previously reported (18, 19); NK cells ($CD3^-$, $CD56^{dim}$); NK bright cells ($CD3^-$, $CD56^{high}$); TCR-γδ ($CD3^+$, TCR-$\gamma\delta^+$); B cells ($CD3^-$, $CD19^+$); naïve CD4 T cells ($CD3^+$, $CD4^+$, $CD45RA^{high}$), memory CD4 T cells ($CD3^+$, $CD4^+$, $CD45RA^-$). For CD4 T cells we performed analysis as previously reported (20, 21): Th1 ($CD3^+$, $CD4^+$, $CRTH2^-$, $CXCR3^+$, $CCR6^-$); Th17 ($CD3^+$, $CD4^+$, $CRTH2^-$, $CXCR3^-$, $CD161^+$, $CCR6^+$); Th1/17 ($CD3^+$, $CD4^+$, $CRTH2^-$, $CXCR3^+$, $CD161^+$, $CCR6^+$); Treg ($CD3^+$, $CD4^+$, $CD127^-$, $CD25^{high}$). All cell populations were analyzed within alive cells, excluding debris and doublets.

2.3 Immunohistochemistry and immunofluorescence

Formalin-fixed, paraffin-embedded (FFPE) sample blocks of normal skin (2 patients), primary melanomas (10 patients), metastases (5 samples from 3 patients), or vitiligo in patients without concomitant melanoma (10 patients), were collected from the archive of the IDI-IRCCS Histopathology Unit. Biopsies from melanoma patients who developed vitiligo during therapy (10 patients) were surgically taken at the lesion margin, fixed in 10% formalin, and embedded in paraffin. Four-µm sections were obtained from each sample, dewaxed, and rehydrated. After quenching endogenous peroxidase, achieving antigen retrieval, and blocking non-specific binding sites, sections were incubated with the following antibodies: mouse monoclonal antibody anti-CD25 (cod. LSBio-B7396-50; LS Bio, Seattle, WA; 1:5); mouse monoclonal antibody anti-interleukin (IL)-17A (cod. AF-317-NA, R&D Systems, Minneapolis, MSP; 1:30); monoclonal antibody anti-CD56 (cod. NCL-CD56, Novocastra Scytek, Wetzlar, Germany; 1:20), mouse monoclonal antibody anti-CD3 (cod. A0452, Dako, Santa Clara, CA; 1:100), mouse monoclonal antibody anti-CD8 (cod. CM154A, Biocare Medical, Concord, CA; 1:75) overnight at 4° C in a humid chamber. Secondary biotinylated polyclonal Abs and staining kits were obtained from Vector Laboratories (Burlingame, CA). Immunoreactivity was visualized with peroxidase reaction using 3-amino-9-ethylcarbazole (AEC) in H_2O_2 and specimen counterstained with hematoxylin. As a negative control, primary Abs was omitted. Stained sections were analyzed with the AxioCam digital camera coupled to the Axioplan 2 microscope (Carl Zeiss AG, Oberkochen, Germany). Staining intensity was evaluated by quantitative analysis (Image J color deconvolution) in five adjacent fields of each section by two independent observers, blinded to the status of the specimens. For immunofluorescence, 4-µm sections were dewaxed, rehydrated, and after quenching endogenous peroxidase with 3% bovine serum albumin in 1x phosphate buffer, achieving antigen retrieval and blocking non-specific binding sites, sections were incubated with the monoclonal antibody anti-TCR V alpha 7.2 FITC conjugated (cod.130-123-

929, Miltenyi Biotech; 1:50) and incubated for 1 hour at 37°C in a humid chamber. After a few washes, sections were closed using mounting medium with DAPI for stained nuclei (Antifade Mounting Medium, Vectashield, Vector Laboratories). Images were acquired with the ApoTome System (Zeiss) connected with an Axiovert200 inverted microscope (Zeiss); image analysis was performed with ZEN software (Zeiss). Fluorescence was evaluated by quantitative analysis (Image J color deconvolution) in three adjacent fields of each section by two independent observers, blinded to the status of the specimens.

2.4 TCR sequencing

Sample preparation. Five to 10 slices of 5 μm thickness from vitiligo or primary/metastatic melanoma biopsies from the same patient were obtained from FFPE samples and used for DNA extraction. For tissue samples, QIAamp DNA FFPE Tissue Kit (Qiagen, Valencia, CA) was used in conjunction with an incubation at 55°C for 4 hours to complete tissue lysis. Next, samples were incubated at 90°C for 1 hour to reverse formaldehyde modification of nucleic acids. For blood samples, DNA extraction from PBMCs was performed following the DNeasy Blood & Tissue Kit (Qiagen). Proteinase K was used for digestion and extraction of DNA following a blood/cell protocol with RNase treatment and using spin-column method. After isolation by QIAamp MinElute column (Qiagen), variable amounts of buffer were added to each column to elute the DNA. Samples were quantified using Dropsense96 and diluted for library preparation in DEPC water.

Library preparation. Extracted DNA was used for TCR Vβ analysis using the ImmunoSEQ hsTCRB Kit (Adaptive Biotechnologies, Seattle, WA), according to the manufacturer's instructions. For PBMCs and metastasis samples, 1 μg of total DNA was used for duplicate, whilst for primary melanoma samples, 200-1000 ng of total DNA was used for duplicates. For FFPE vitiligo samples, the staring gDNA was poor (50-325 ng) and, when possible, sequencing was repeated in order to increase the output. Due to the *post-hoc* nature of this study, we decided to perform the sequencing as well, at the best of our conditions using at least 50 ng of starting gDNA. The somatically rearranged human CDR3 was amplified from genomic DNA using a two-step, amplification bias-controlled multiplex PCR approach (22–24). The first PCR consists of forward and reverse amplification primers specific for every V and J gene segment and amplifies the hypervariable complementarity-determining region 3 (CDR3) of the immune receptor locus. The second PCR adds a proprietary barcode sequence and Illumina® adapter sequences (25, 26). Following purification with the Agencourt™ AMPure™ XP Reagent (Beckman Coulter, Inc.), 10 μl of each sample were pooled in equimolar concentration into three final libraries (46 libraries/pool). Final libraries were quantified using KAPA Library Quantification Kits (Roche, Switzerland, CH), diluted to 4 nM, and denatured using 0.2N NaOH.

Sequencing. CDR3 libraries were loaded at 20 pM on an Illumina NextSeq 550 system with 156 paired-end sequencing (Illumina, San Diego, CA). Sample data was generated using the immunoSEQ® Assay (Adaptive Biotechnologies, Seattle, WA). For the runs, ~146.92M reads where generated and ~128.58M passing filter. The coverage for each sample varied with the highest being 92x. The release of sequencing data and the QC control were performed by Adaptive Biotechnologies technical support.

The starting material (gDNA) was not always compliant to manufacturer's instructions. When possible, the sequencing was repeated using other specimens, to increase the output. As this was a small cohort, the threshold we established is considered exploratory.

Data Analysis. Raw sequence reads were demultiplexed according to Adaptive' s proprietary barcode sequences. Demultiplexed reads were then further processed to remove adapter and primer sequences; identify and correct for technical errors introduced through PCR and sequencing; and remove primer dimer, germline, and other contaminant sequences. Data were filtered and clustered using both the relative frequency ratio between similar clones and a modified nearest-neighbor algorithm, to merge closely related sequences. The resulting sequences were sufficient to allow annotation of the V(N)D(N)J genes constituting each unique CDR3 and the translation of the encoded CDR3 amino acid sequence. V, D and J gene definitions were based on annotation in accordance with the IMGT database (www.imgt.org). The set of observed biological human CDR3 sequences were normalized to correct for residual multiplex PCR amplification bias and quantified against a set of synthetic human CDR3 sequence analogues (26, 27). Data was analyzed using the immunoSEQ Analyzer toolset (ImmunoSEQ Analyzer 3.0 https://clients.adaptivebiotech.com/). Libraries were sequenced and organized providing productive and non-productive sequences (CDR3 regions explicitly encoding a premature stop, and those predicted to put the receptor gene out-of-frame downstream of the CDR3 rearrangement, were considered non-productive). Productive TCR-β CDR3 frequencies were used for generating scatterplots. Additional analyses were performed using GraphPad prism (GraphPad Software) and the R graphical library ggplot2. Alluvial flow diagrams (28) were used to describe common TCR sequences that can be viewed as multiple streams that flow smoothly throughout different samples of the same patient (primary melanoma, vitiligo and, if present, metastasis). To generate an alluvial map, common V(D)J rearrangements data from ImmunoSeq Analyzer were used in order to generate a series of networks for shared TCR sequence across different specimens, and these networks were loaded into the alluvial generator (gg alluvial library; https://cran.r-project.org/web/packages/ggalluvial/vignettes/ggalluvial.html).

Details on V(D)J usage for each productive sequence in the samples are reported as **VDJ usage** Supplementary File. For each patient, the nucleotide sequence of CDR3 unique region of shared TCR-β clonotypes and the productive frequency are listed in Supplementary Table II.

2.5 Statistical analysis

For TCR Vβ statistical analysis, a limited number of findings were evaluated for statistical significance. Groups were compared using the Producting Simpson Clonality Index (ImmunoSEQ™ software) and Kruskal-Wallis nonparametric test was used to

analyze the difference in TCR clonality between different sample types. Two-stage linear step-up procedure of Benjamini, Krieger and Yekutieli was used for *post-hoc* analysis.

For flow cytometry data, differences between pairs were analyzed by paired Student's t-test, and multiple comparisons by two-way ANOVA test.

For tissue analyses, before proceeding with the hypothesis tests, we analyzed the data of each group through a Shapiro-Wilk test which highlighted a non-normal distribution of our observations. Furthermore, given some values far from the mean for some groups and the limited data available, we decided to compare the experimental groups using a Kruskal-Wallis test which is a non-parametric test which highlights the differences between the medians. Statistical significance was set at $p<0.05$ and all statistical analyzes were conducted using GraphPad Prism software (La Jolla, CA, USA) and R.

3 Results

3.1 Patients who developed vitiligo during immunotherapy have a diverse frequency of circulating immune cells

To investigate whether the immune profile of melanoma patients undergoing anti-PD-1 immunotherapy was associated to the irAE vitiligo, we performed flow cytometry analyses on patients' PBMCs. Twelve patients who had a positive response to anti-PD-1 immunotherapy were examined: six developed vitiligo during therapy, while the other six did not. After stratification of patients into two groups matched for sex and age, we compared immune cell frequency considering as the unique variant the development of vitiligo (Table 1). Cells were isolated from blood samples taken before therapy initiation (T0), and on-treatment at each administration up to one year or at vitiligo development. For the comparison, two time points of collection were considered: before therapy (T0) and at the number of treatment when vitiligo onset was observed, for patients who developed vitiligo; before therapy (T0) and at treatment number 4 or 5, for patients who did not develop vitiligo. Control time points were chosen according to the onset of vitiligo, which did not occur earlier than the fourth therapeutic administration in the matching group. Our results showed a reduction of circulating CD8-mucosal associated invariant T (MAIT), T helper (Th)-17, and T-reg cells associated to vitiligo onset. Moreover, a reduction in natural killer (NK) $CD56^{bright}$ cell frequency was detected during treatment in both patient groups, suggesting its association with a positive clinical response (Figures 1A, B).

To analyze immune cell subtypes potentially responding to anti-PD-1 immunotherapy, we examined PD-1 expression in different immune cell subsets. A reduction in the frequency of PD-1 expressing $CD3^+$, $CD4^+$, $CD8^+$, Th1, Th1/17, and Th17 cells was seen in patients not experiencing vitiligo during therapy (Figure 2A). A trend of such a reduction was also observed in patients developing vitiligo but was significant only for Th1 cells. Conversely, as therapy cycles increase, increased PD-1 expression of NK $CD56^{bright}$ cells distinguished patients developing vitiligo (Figure 2A). In order to evaluate the activation status of different immune cell subtypes, we examined the expression of CD69, classical early marker of lymphocyte activation due to its rapid appearance on the surface of the plasma membrane after stimulation of different immune cell subsets (29). As shown in Figure 2B, there were neither significant changes in CD69 expression during therapy nor differences in CD69 expression before therapy in patients who developed vitiligo or not. Supplementary Figures 2, 3 report the frequency data obtained for each patient at every time-point of treatment.

TABLE 1 Characteristics and treatment outcome of melanoma patients who developed or not vitiligo during therapy.

	Patients who developed vitiligo									Patients who did not develop vitiligo							
	Stage[a]	Checkpoint inhibitor[b]	BRAF	Sex[c]	Age[d]	iOR	PBMCs			Stage[a]	Checkpoint inhibitor[b]	BRAF	Sex[c]	Age[d]	iOR	PBMCs	
							Before therapy	Vitiligo onset								Before therapy	Control time
IMM-1	M1b	Pembro	MUT	M	72	iCR	T0	T10	IMM-7	M1a	Pembro	WT	M	89	iPR	T0	T5
IMM-2	M1d	Pembro	WT	M	84	iSD	T0	T4	IMM-8	M1a	Pembro	WT	M	68	iPR	T0	T5
IMM-3	M1a	Pembro	WT	F	91	iPR	T0	T6	IMM-9	M1c	Nivo	WT	M	86	iCR	T0	T4
IMM-4	M1c	Nivo	NA	M	80	iPR	T0	T12	IMM-10	M1c	Nivo	MUT	M	71	iPR	T0	T4
IMM-5	IIIc	Nivo	WT	M	55	iCR	T0	T10	IMM-11	M1b	Nivo	WT	F	69	iCR	T0	T4
IMM-6	M1b	Pembro	WT	M	81	iPR	T0	T8	IMM-12	M1b	Nivo	WT	F	53	iPR	T0	T5

[a]Staging before starting therapy; [b]Pembro, pembrolizumab; Nivo, nivolumab; [c]M, male; F, female; [d]Age in years at the time of therapy initiation; iOR: Immune Objective Response; iCR, immune complete response, iSD, immune stable disease, iPR, immune partial response. BRAF: analysis for BRAF600E mutation. MUT= presence of the mutated gene; WT, wild type; NA, not available. PBMCs, peripheral blood mononuclear cells. Blood samples were taken before therapy initiation (T0). The number of therapeutic treatments (T) that patients underwent when the onset of vitiligo occurred, corresponds to the time in which PBMCs were isolated. For patients who did not develop vitiligo, a corresponding therapeutic treatment point (T) was chosen as a control.

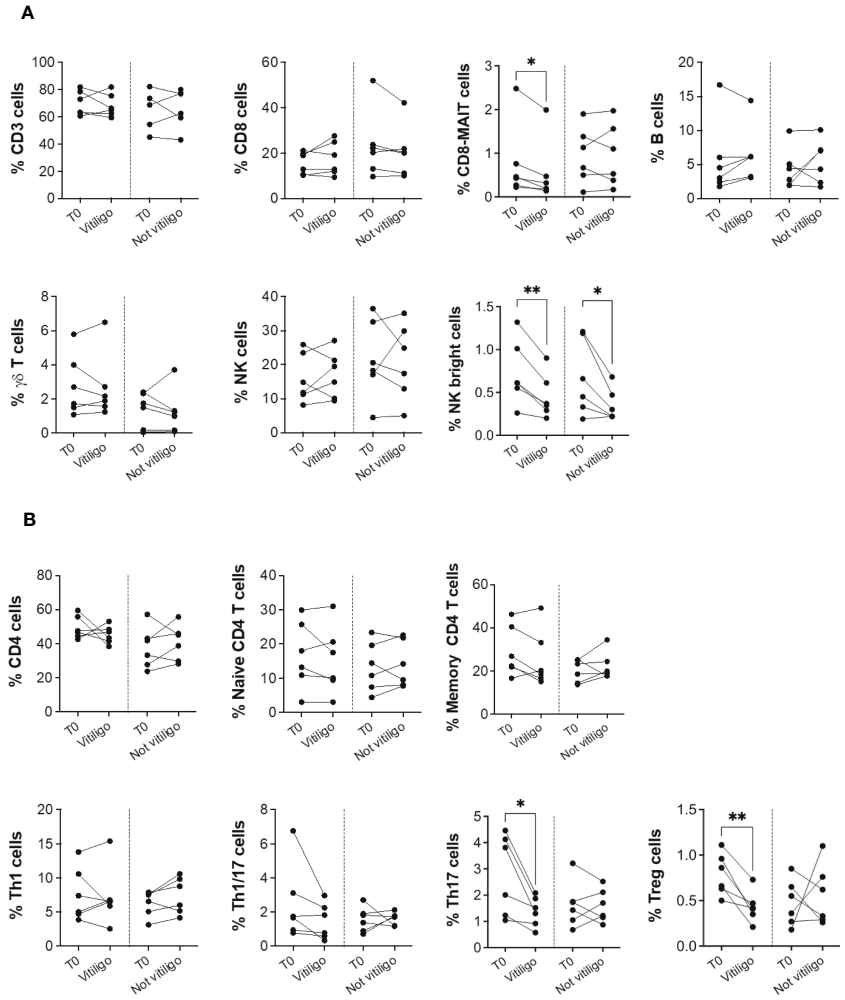

FIGURE 1
Vitiligo development due to anti-PD-1 immunotherapy alters the frequencies of subsets of circulating immune cells. **(A)** Blood frequencies of $CD3^+$, $CD8^+$, CD8-MAIT, B, γδ T, NK, NK bright cells and **(B)** several $CD4^+$ cell subsets were analyzed by flow cytometry in PBMCs from melanoma patients before therapy (T0), at the time of vitiligo onset during therapy (Vitiligo), or at a corresponding control time for patients who did not develop vitiligo (Not vitiligo). Frequencies of each cell subset are reported as percentage within parental gate, which is defined in bold above each dot plot of Supplementary Figure 1. Data are indicated as mean value ± standard error of the mean (SEM). *p<0.05, **p<0.005 as assessed by paired t-test or two-way ANOVA test.

3.2 Differential immune profile in immunotherapy-induced and spontaneous vitiligo

To analyze at the tissue level the role of immune cells differently modulated in melanoma patients developing vitiligo, we performed immunohistochemistry and immunofluorescence analyses on vitiligo specimens collected from ten melanoma patients treated with anti-PD-1 antibodies (Table 2). We compared them with the specimens from ten patients developing vitiligo in the absence of concomitant melanoma or immunotherapy. Two normal skin specimens were used as a control. As shown in Figures 3, 4, we observed a trend of increased number of cells positive to an anti-CD25 antibody, that could correspond to T-reg cells or other activated conventional T cells, and a significant increment of cells stained with an anti-IL-17A antibody in vitiligo lesions induced by immunotherapy compared to the other vitiligo samples. Interestingly, this high number of IL-17-positive cells detected in immunotherapy-induced vitiligo lesions may suggest the recruitment of Th17 cells *in situ*, according to the decrease of circulating Th17 cells observed over treatment in this patient population (Figure 1). Although not significant, we observed a lower amount of TCR V alpha 7.2 positive cells, possibly MAIT cells, in the immunotherapy-derived vitiligo patients compared to vitiligo samples without melanoma.

3.3 T-cells infiltrating immunotherapy-induced vitiligo share V(D)J rearrangements with T-cells infiltrating metastasis lesions and primary melanomas

To further characterize T cells in vitiligo lesions of melanoma patients, we performed sequencing of CDR3 variable region of the

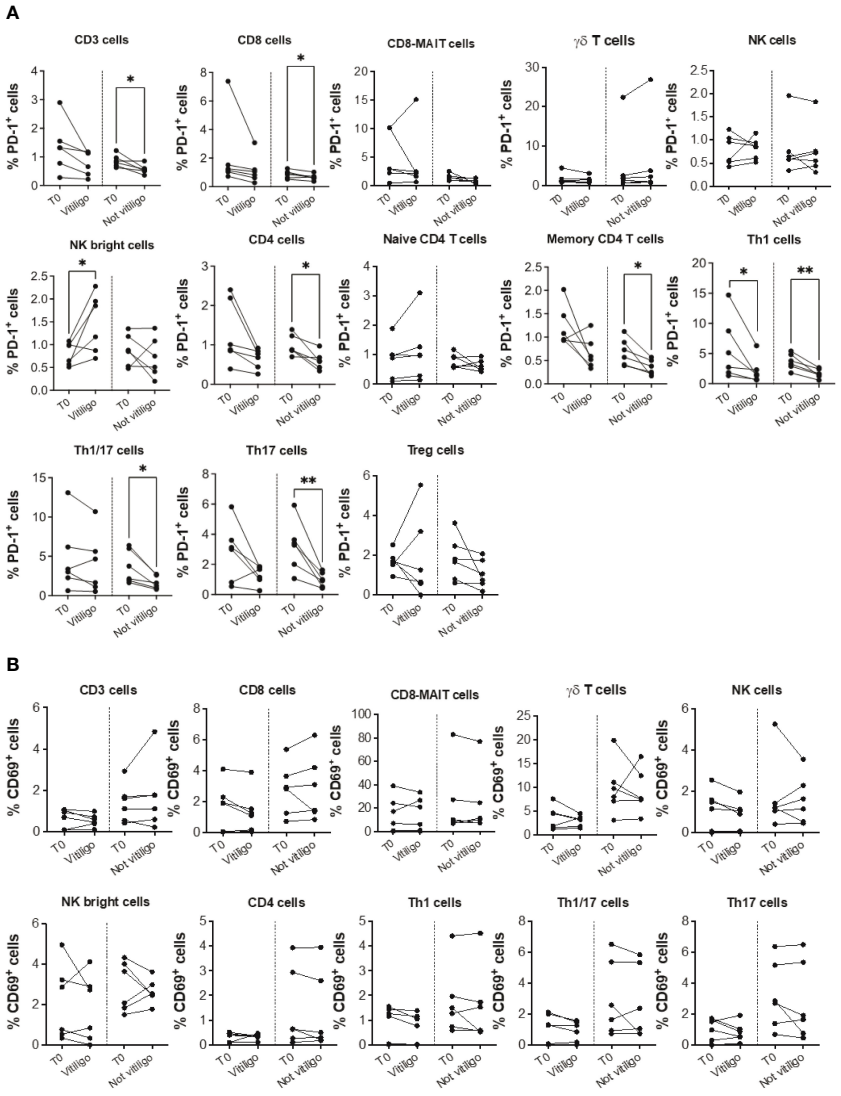

FIGURE 2
Vitiligo development during anti-PD-1 therapy alters PD-1 and CD69 expression in circulating immune cells. Percentage of PD-1 positive cells **(A)** and CD69 positive cells **(B)** gated within $CD3^+$, $CD8^+$, CD8-MAIT, γδ T, NK, NK bright cells and within several CD4+ cell subsets was analyzed by flow cytometry in PBMCs from melanoma patients before therapy (T0), at the time of vitiligo onset during therapy (Vitiligo), or at a corresponding control time for patients who did not develop vitiligo (Not vitiligo). Data are indicated as mean value ± standard error of the mean (SEM). *p<0.05, **p<0.005 as assessed by paired t-test or two-way ANOVA test.

β-chain of the T-cell receptor (TCR-seq) on gDNA extracted from samples of vitiligo biopsies. Moreover, from the same patient, we have also carried out a TCR sequencing of PBMCs at the time of vitiligo onset, and on retrospective samples from the same patient of primary melanoma and of metastasis sites, when occurred (n=4). Table 2 summarizes the melanoma patients included in the TCR-Seq, and their clinical features, whereas Supplementary Table I reports the most relevant metrics from the TCR-Seq for all the analyzed samples, including total and productive templates and rearrangements, as well as the productive and sample Simpson clonality of the TCR-seq.

The TCR sequence analysis revealed a differential productive TCR clonality among tissues (peripheral blood: range 0.0081-0.2048; n=10; primary melanoma: range 0.0035-0.2401; n=13; vitiligo tissues: range 0.0053-0.0609; n=10. metastasis: range 0.0078-0.199; n=5) and productive templates as shown in Figure 5B (p value=0.0139).

Notably, we observed common V(D)J TCR rearrangements between samples derived from the same patients at different time points (Table 2 and Figure 5A). Clonotypes shared by metastasis, surgically removed during the anti-PD-1 therapeutic period, and vitiligo samples are higher compared to the number of clonotypes shared by primary melanoma and vitiligo specimens. Interestingly, we observed the highest number of shared clonotypes between vitiligo and primary melanoma in the two patients achieving iCR (n=21 and n=15; Table 2 and Figure 5A). Furthermore, shared TCR clonotypes have been sequenced in primary melanoma and in metastasis of all the four patients, underlying the possibility that

10.3389/fimmu.2023.1197630

TABLE 2 Characteristics and TCR clonotype number of melanoma patients who developed vitiligo during therapy.

	Stage[a]	Checkpoint inhibitor[b]	BRAF	Sex[c]	Age[d]	iOR	TCR clones shared by primary melanoma and vitiligo (N)	TCR clones shared by primary melanoma and PBMCs (N)	TCR clones shared by vitiligo and PBMCs (N)	TCR clones shared by metastasis and vitiligo (N)	TCR clones shared by metastasis and PBMCs (N)	TCR clones shared by metastasis and vitiligo (N)
VIT-1	M1b	Pembro	MUT	M	69	iCR	22	9	11	–	–	–
VIT-2	M1a	Pembro	WT	F	48	iPR	1	317	9	5	241	5
VIT-3	M1a	Nivo	WT	F	72	iPR	1	5	6	–	–	–
VIT-4	M1c	Nivo	WT	F	54	iPR	2	3	0	12	6	12
VIT-5	M1d	Nivo	MUT	F	41	iPR	8	68	29	14	307	14
VIT-6	M1b	Pembro	WT	F	53	iPR	ND	1	3	–	–	–
VIT-7	M1a	Nivo	WT	M	56	iPR	4	19	23	–	–	–
VIT-8	M1a	Nivo	WT	M	66	iPR	2	6	12	9 (spleen) and 32 (lymph node)	28 (spleen) and 112 (lymph node)	9 (spleen) and 32 (lymph node)
VIT-9	M1b	Nivo	WT	F	73	iPR	ND	7	5	–	–	–
VIT-10	M1c	Pembro	WT	M	83	iCR	13	50	18	–	–	–

[a]Staging before starting therapy; [b]Pembro, pembrolizumab; Nivo, nivolumab. BRAF: analysis for BRAF600E mutation. MUT= presence of the mutated gene; WT,wild type; [c]M, male; F, female; [d]Age in years at the time of therapy initiation; iOR: Immune Objective Response; iCR, immune complete response, iPR, immune partial response; ND, not detected shared clones; PBMC samples were sequenced at the time of vitiligo onset.

tumor-infiltrating T cells sharing the same specificity, are present in both primary and metastatic sites.

The TCR sequences of PBMC samples has been performed at the time of vitiligo occurrence, and as expected PBMCs showed the lowest Simpson clonality respect to the other tissues. It was also noted that several TCRs sequenced in the PBMCs samples were already present in the primary melanoma or in the metastasis, as shown in Table 2 and in Figure 5.

3.4 Immune cell profile of primary melanomas in patients who developed or not vitiligo during immunotherapy and in matched metastases

Flow cytometry analysis showed that frequency of Th17, NK, and CD8-MAIT cells was differently modulated in the blood of patients developing vitiligo compared to those who did not develop

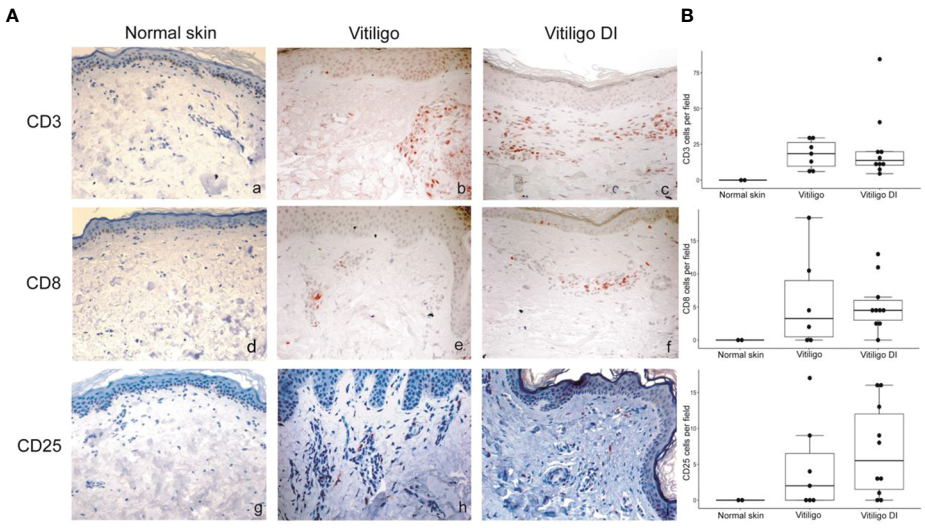

FIGURE 3
Vitiligo tissue expression of the immune cell subsets modulated differently in the circulation of melanoma patients developing vitiligo during anti-PD-1 therapy. **(A)** Representative images of immunohistochemistry analysis performed using antibodies directed against CD3 (panels a–c), CD8 (panels d–f), and CD25 (panels g–i), on normal skin biopsies and on biopsies from patients affected by vitiligo without melanoma (vitiligo) and who developed vitiligo during immunotherapy (vitiligo DI). Magnification 200x. **(B)** Quantitative analyses of immunohistochemical staining. Data are indicated as mean value + standard error of the mean (SEM), as assessed by Kruskal-Wallis test.

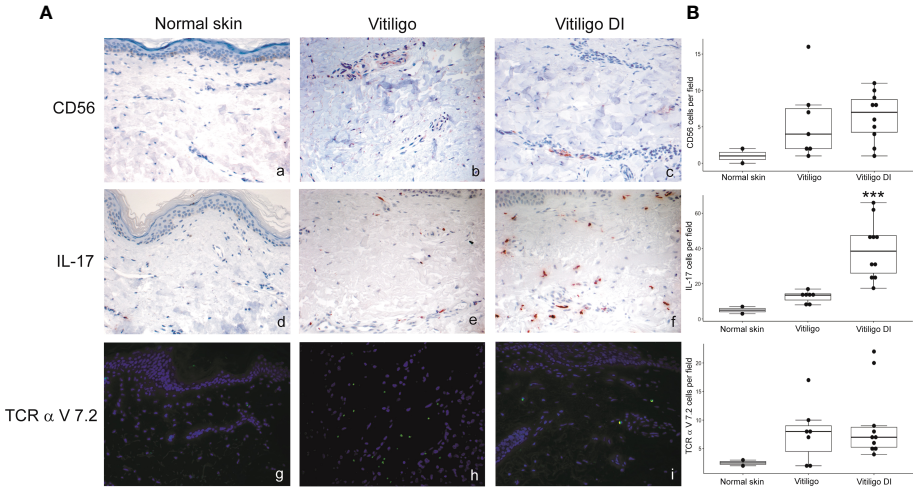

FIGURE 4
IL-17-expressing cells are differently modulated in the skin lesion and in the circulation of melanoma patients developing vitiligo during anti-PD-1 therapy. **(A)** Representative images of the immunohistochemistry (panels a to d) and immunofluorescence (panels e, f) analysis performed using antibodies directed against CD56 (panels a–c), IL-17 (panels d–f) and TCR alpha V 7.2 (panels g–i) on normal skin biopsies and on biopsies from patients affected by vitiligo without melanoma (vitiligo) and who developed vitiligo during immunotherapy (vitiligo DI). Magnification 200x. **(B)** Quantitative analyses of immunohistochemical staining. The mean value + standard error of the mean (SEM) of the cell count obtained for five different fields is shown, ***p<0.05 as assessed by Kruskal-Wallis test.

it. To investigate whether a correspondence could be seen between circulating immune cell profiles and those present in the tumor tissues, we analyzed by immunohistochemistry and immunofluorescence the primary melanomas of patients who developed vitiligo and primary melanoma of three patients who did not developed vitiligo during therapy, selected from patients listed in Table 1 (IMM-9, IMM-11, and IMM-12), as a tissue reference to T0 circulating samples. Lymph node metastases from patients VIT_02, VIT_04, and VIT_08 (Table 2), who developed vitiligo, were chosen as a reference for on-going therapy reference tissues, in addition to vitiligo skin samples examined in Figures 3, 4.

No significant differences were observed for cells stained with anti-CD56 and anti-TCR V alpha 7.2 antibodies. We detected a trend of lower CD25 positive cells in the lymph nodal metastases in respect to primary melanomas (Figure 6). Interestingly, a significative lower frequency of IL-17A positive cells was detected in primary melanomas of patients developing vitiligo during therapy in respect to patients not developing this irAE (Figure 6).

4 Discussion

Antibodies that block immunological checkpoints can result in long-lasting benefit for patients with many different malignancies. PD-1 is one of the first immunologic checkpoint to be clinically targeted and the anti-PD-1 antibodies Nivolumab and Pembrolizumab have been shown to improve overall survival in a subset of metastatic melanoma patients (30). Identifying patients who are most likely to benefit from PD-1 blockade and why they respond to such a therapy remains an active area of investigation. Since Nivolumab and Pembrolizumab exert their antitumor effects through T-cells, several studies have investigated T lymphocyte populations and correlates immunological changes with patient outcomes (31). Other investigations have focused on T-cell receptor (TCR) repertoire and have proved that PD-1 blockade induces diversification of TCR repertoire status 2 (32, 33) before and after immunotherapy and results in improved prognosis (34, 35).

In this study, we used available blood and tissue samples from melanoma patients who developed vitiligo, a known irAE emerging upon anti-PD-1 therapy, to further understand the immune mechanisms characterizing vitiligo onset and anti-tumoral responses. Vitiligo is an immune-mediated disease involving a complex relationship between immune system and melanocytes physiology (36). A causality of vitiligo is the melanocyte oxidative stress, an initial condition often present in the earliest stages of the disease. The consequence of the oxidative stress is an early activation of the innate immune cells by recognition of damage-associated molecules, which in turn stimulates an adaptive immune response accountable for the anti-melanocyte immunity. Specifically, the release of reactive oxygen species by stressed melanocytes leads to production of several damage-associated molecules recognized by dendritic cells that, as a result, trigger autoreactive T lymphocytes. Impairment of T-reg cell function, as well as reduction in T-reg cell number, further enhance $CD8^+$ T cell autoreactivity against melanocytes (36).

We found that vitiligo onset in anti-PD-1 treated patients was characterized by reduction of circulating Th17, CD8-MAIT, and T-reg cells. Th17 lymphocytes are a subset of $CD4^+$ T cells implicated in the pathogenesis of various autoimmune diseases. Th17 cells secrete several immune modulating molecules including IL-17 and IL-22 (37). Previous data reported a significant correlation between Th17 cells and IL-17 with spontaneous vitiligo and indicated an involvement of Th17 cells in vitiligo progression and severity (38). Th17 cells and IL-17 expression are higher at the leading edge of a

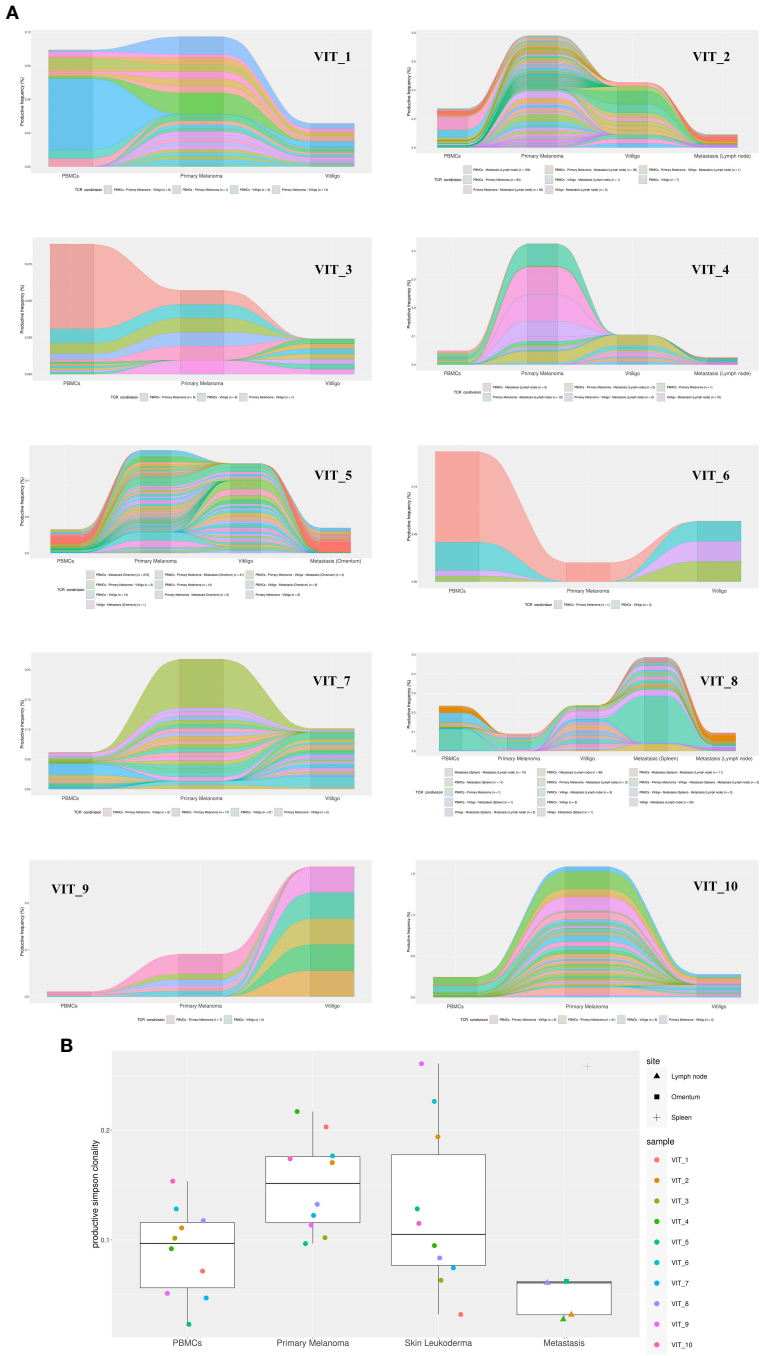

FIGURE 5
TCR-Seq analysis of T-cells infiltrating vitiligo, primary melanoma and metastasis lesions of patients treated with anti-PD1 immunotherapy. **(A)** Alluvial plots depicting common V(D)J TCR rearrangements between PBMCs, primary melanoma, vitiligo lesions and metastasis (when present) of the same patient. Alluvial flow diagrams are designed to describe common patterns in an evolving network. The division and merging of common TCR sequences can be viewed as multiple streams that flow smoothly throughout different samples of the same patient. **(B)** Productive Simpson clonality of TCR clonotypes sequenced in primary melanoma, vitiligo developed during therapy (blue), metastases, and PBMCs samples. Specimens from the same patient are color-matched. Metastasis samples were collected from different sites: lymph node, spleen and omentum. Simpson clonality score ranges from 0 to 1. Values near 1 represent samples with one or a few predominant rearrangements (monoclonal or oligoclonal samples) dominating the observed repertoire. Clonality values near 0 represent more polyclonal samples. Nonparametric Kruskal-Wallis test was used to analyze the difference in TCR clonality between different sample types (*p-value* = 0.01393). Two-stage linear step-up procedure of Benjamini, Krieger and Yekutieli was used for *post-hoc* analysis (*p value* vitiligo vs metastasis = 0.0139; primary melanoma vs metastasis= 0.0139).

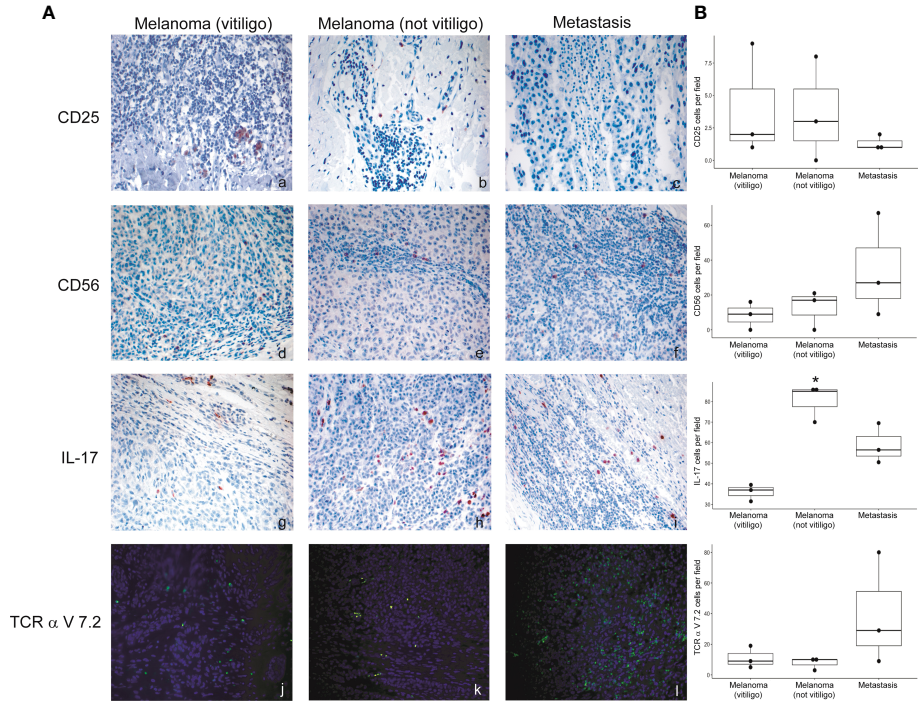

FIGURE 6
Expression of the immune cell subsets in the primary melanoma and metastases of patients developing or not vitiligo during anti-PD-1 therapy. **(A)** Representative images of immunohistochemistry (panels a to i) and immunofluorescence (l–n) obtained using anti-CD25 (a–c), anti-CD56 (d–f), anti-IL-17A (g–i), and anti-TCR alpha V 7.2 (j–l) in primary melanoma and metastasis from patients who developed (vitiligo) or not vitiligo (not vitiligo) during therapy. A–I 100x magnification, panel L-N 200X magnification. Magnification 200x. **(B)** Quantitative analyses of immunohistochemical staining. The mean value + standard error of the mean (SEM) of the cell count obtained for five different fields is shown, *p<0.05 as assessed by Kruskal-Wallis test.

vitiligo lesion compared to a non-lesional skin (39). Consistently, in melanoma patients under immunotherapy, we found that Th17 cells are reduced in the blood of subjects developing vitiligo compared to those not developing the irAE and that IL-17A-expressing cells are enriched in skin biopsy of immunotherapy-mediated vitiligo compared to the spontaneous disease. These results suggest that Th17 cells are involved in pathogenetic mechanisms of both immune therapy-induced and spontaneous vitiligo. Moreover, the higher amount of IL-17A positive cells in the anti-PD-1 therapy-dependent vitiligo may indicate that Th17 cells in the skin lesion could be a distinctive feature of vitiligo as an irAE. In addition, the reduction of Th17 cells in the blood of these patients could be related to cell migration into the skin lesion. The role of Th17 cells in vitiligo pathogenesis is still unclear. A mechanism could involve the cytokine IL-17A, which may act as a chemoattractant for cytotoxic $CD8^+$ T cells and recruit melanocyte-specific T lymphocytes to the skin (38). Additionally, IL-17A has been shown to antagonize melanogenesis and promote melanocyte apoptosis, two mechanisms causing depigmentation in vitiligo (38).

Interestingly, our analysis of primary melanomas from patients who developed or not vitiligo under anti-PD-1 therapy showed a higher number of IL-17A-expressing cells in the tumor samples of patients not developing vitiligo. Since all the patients examined were responding ones, expression of IL-17A does not have here any prognostic value. However, this data could indicate that vitiligo development mainly derived from the individual response to anti-PD-1 therapy and not from primary melanoma immune features.

Another cell population able to release IL-17 is represented by MAIT cells, whose physiological role is the defense of mucosa from bacterial and mycobacterial infections (40). In our study, we detected a lower frequency of CD8-MAIT cells in the blood of melanoma patients with the onset of vitiligo. Given their ability to produce IL-17, we hypothesize common mechanisms of action with Th17 cells. Moreover, other cell types could express IL-17A, such as NK cells (41) or γ/δ T cells (42) further sustaining a role for innate immunity in vitiligo pathogenesis. However, no significant differences were found in our cohort of patients regarding the amount of circulating NK and γ/δ T cells between patients developing or not vitiligo during anti-PD-1 therapy.

We previously observed that a lower number of T-reg cells before therapy initiation was present in the blood of patients, positive responders on anti-PD-1 therapy in respect to not responders (14). In that case, we did not observe a reduction of circulating T-reg throughout the treatment. Here, we found a frequency reduction of circulating T-reg cells in patients developing vitiligo during therapy. Therefore, since not all the responding patients develop vitiligo, our data indicate that the reduction of circulating T-reg cells is specifically related to vitiligo occurrence, as previously reported (36). Of note, the trend of lower

CD25 positive cells we observed in the metastatic tissues of the four patients who developed vitiligo, in respect to primary melanomas, could also be interpreted as a reduction of T-reg cells connected with vitiligo development.

Interestingly, a common mechanism shared among all patient groups was the reduction of circulating NK CD56^{bright} cells during treatment, a phenomenon possibly related to the positive response to therapy. Nevertheless, comparison of data from complete and partial responders with the ones of progressive disease patients did not highlight a significant difference in blood frequency of NK CD56^{bright} (our unpublished data). The cytotoxic activity of NK CD56^{bright} cells is lower than that of the NK CD56^{dim} cells, thus a reduction in the number of NK CD56^{bright} cells during treatment could represent their switch to a more effective cell type, potentially reflecting a positive response to immunotherapy (43). Moreover, we observed that PD-1 expression, reduced in most cell subset after anti-PD-1 treatment, is significantly increased on NK CD56^{brigh} cells from subjects developing vitiligo. This result indicates that NK CD56^{brigh} cells are not responsive to anti-PD-1 therapy and suggests that PD-1 expression on NK CD56^{brigh} cells could be upregulated by a compensatory mechanism triggered by therapy and could be related to response to therapy and/or vitiligo development. Consistently, it has been demonstrated a positive correlation between PD-1 expression on NK CD56^{brigh} cells and overall survival of patients with lung cancer undergoing immunotherapy (44). However, a higher number of patients should be considered to clarify this point.

In order to understand whether immunotherapy would induce reactivation of T cell clones already present in the primary melanoma and whether T cell clones were directed against antigens common to melanoma cells and normal melanocytes, we investigated, by TCR sequencing, the T cell clonality in patient's matched specimens from primary melanoma and vitiligo lesion developed after anti-PD-1 therapy. In fact, a previous study identified one common TCR clone in the primary tumor and in the concomitantly developed vitiligo lesion in a patient affected by cutaneous melanoma (10). We found that although in vitiligo lesions TCR sequences were generally different from those in the primary melanoma, shared clonotypes could be identified between the vitiligo tissue and primary or metastasis site, especially for those patients achieving a iCR upon anti-PD1 therapy. Moreover, in all evaluated patients, the number of shared TCR clonotypes between vitiligo and metastatic sites was superior compared to that observed in the primary tumor, underlying that the T cells immunoreacting against normal melanocytes are also able to selectively infiltrate the metastatic sites.

These data are also indicating that the immunotherapy-stimulated T cell response against normal melanocytes, which is involved in vitiligo onset, is not mediated by the reactivation of specific T cell clones infiltrating the primary melanoma but may be elicited *de novo* by T cell clones targeting metastatic tissues. In fact, all the patients we examined had primary melanoma surgically removed before immunotherapy initiation, whereas they still presented distal metastasis. Interestingly, the two patients achieving complete response under anti-PD-1 therapy were also the unique two patients showing high amount of T cell clones common to primary melanoma and vitiligo. We suppose that these T cell clones are directed against tumor-associated antigens, which are mainly found in tumor cells, but can also be expressed by normal melanocytes. In fact, melanoma tumor antigens could be grouped in two types: antigens that are specifically expressed by tumor cells, also known as neoantigens or tumor antigens, and tumor-associated antigens, shared among tumor cells and normal melanocytes (45). Although previous studies claimed that tumor-associated antigens do not induce an effective cytotoxic T cell response and tumor-specific CD4^{+} T lymphocytes (45), our present data suggest that tumor-associated antigens have a predominant role in advanced melanoma. In line with the concept of "beneficial autoimmunity" (13), the presence of shared TCRs able to recognize tumor-associated antigens in matched vitiligo and metastatic lesions of positive responders, strongly suggests the active role of these T cell clones in fighting advanced forms of tumor. In addition, the assessment of specific T cell clones against tumor-associated antigen in primary tumors of complete responders further supports this concept, highlighting the beneficial contribution that these specific cells may have in driving the complete resolution of the tumoral lesions.

Finally, we found that common TCR clones were present in the primary melanomas and in the metastasis of patients experiencing tumor relapse during immunotherapy, as well as in their PBMCs at the time of vitiligo onset. Similar data have been already reported for one patient affected by uveal melanoma (11). In this context, Riaz et al. previously demonstrated that tumor cell mutations, potentially recognized by T cells in the pre-therapy melanoma samples, were still detectable in on-therapy tumor tissues, and that a high proportion of mutations detectable during immunotherapy was associated with treatment resistance (46). Actually, mutation burden decreases with successful checkpoint blockade therapy in patients with melanoma, suggesting that immune cell selection against mutant neoepitopes may be a critical mechanism of response to therapy (46).

This study is limited by the sample size, in part due to the low frequency of vitiligo irAE (15%) in melanoma patients who were treated with checkpoint inhibitor therapy (9). In fact, we enrolled more than 40 patients to select those analyzed in this study. However, this pilot study gives indications for future validation with a larger sample size.

Even considering the bias of the small numbers, our results still represent consequent frames showing the dynamic development of tumor immune responses induced by the anti-PD-1 immunotherapy, also causing the irAE vitiligo in some patients. Considering the prognostic significance of vitiligo onset during immunotherapy, our analysis of the immune profile of blood and tumoral tissues of melanoma patients sheds light on immunological mechanisms in melanoma setting. The cell mechanisms demonstrated here will contribute to the identification of potential biomarkers of response, as well as novel therapeutic targets.

Data availability statement

The datasets presented in this study can be found in online repositories. The names of the repository/repositories and accession number(s) can be found below: GSE229557 (GEO).

Ethics statement

The studies involving humans were approved by Istituto Dermopatico dell'Immacolata (IDI)-IRCCS. The studies were conducted in accordance with the local legislation and institutional requirements. The participants provided their written informed consent to participate in this study. The study was conducted in accordance with the local legislation and institutional requirements.

Author contributions

Conceptualization, MC, CQ, EV, and CF; methodology, MC, AC, MG, SR, and DL; investigation, MC, AC, MG, SR, DS, DL, and CR; data curation, MC, AC, MG, DS, DL, and DP; writing original draft preparation, MC, MG, EV, CQ, and CF; writing review and editing, MC, AC, MG, DP, CQ, EV, and CF; supervision, CQ, EV, and CF; funding acquisition, EV, CQ, CF. All authors contributed to the article and approved the submitted version.

Funding

This work was supported by grants from Ricerca Corrente of Italian Ministry of Health IDI-3.4 to CF and RC-MoH to CQ, and from Fondazione AIRC per la ricerca sul cancro MFAG 21979 to CQ. MC was the recipient of a Fondazione Umberto Veronesi Fellowship.

Acknowledgments

Authors would like to thank the clinicians and nurses of the Department of Oncology and Dermatological Oncology and the technicians from the Histopathology Unit, IDI-IRCCS, for their continuous help and attention, and Fondazione Umberto Veronesi for the support of MLC research work

Conflict of interest

The authors declare that the research was conducted in the absence of any commercial or financial relationships that could be construed as a potential conflict of interest.

Publisher's note

Supplementary material

The Supplementary Material for this article can be found online at: https://www.frontiersin.org/articles/10.3389/fimmu.2023.1197630/full#supplementary-material

References

1. Jardim DL, Goodman A, de Melo Gagliato D, Kurzrock R. The challenges of tumor mutational burden as an immunotherapy biomarker. *Cancer Cell* (2021) 39:154–73. doi: 10.1016/j.ccell.2020.10.001

2. Lee PP, Yee C, Savage PA, Fong L, Brockstedt D, Weber JS, et al. Characterization of circulating T cells specific for tumor-associated antigens in melanoma patients. *Nat Med* (1999) 5:677–85. doi: 10.1038/9525

3. Herzberg B, Fisher DE. Metastatic melanoma and immunotherapy. *Clin Immunol* (2016) 172:105–10. doi: 10.1016/j.clim.2016.07.006

4. Larkin J, Chiarion-Sileni V, Gonzalez R, Grob JJ, Cowey CL, Lao CD, et al. Combined nivolumab and ipilimumab or monotherapy in untreated melanoma. *N Engl J Med* (2015) 373:23–34. doi: 10.1056/NEJMoa1504030

5. Failla CM, Carbone ML, Fortes C, Pagnanelli G, D'Atri S. Melanoma and vitiligo: in good company. *Int J Mol Sci* (2019) 20:5731. doi: 10.3390/ijms20225731

6. Hua C, Boussemart L, Mateus C, Routier E, Boutros C, Cazenave H, et al. Association of vitiligo with tumor response in patients with metastatic melanoma treated with pembrolizumab. *JAMA Dermatol* (2016) 152:45–51. doi: 10.1001/jamadermatol.2015.2707

7. Teulings HE, Limpens J, Jansen SN, Zwinderman AH, Reitsma JB, Spuls PI, et al. Vitiligo-like depigmentation in patients with stage III-IV melanoma receiving immunotherapy and its association with survival: a systematic review and meta-analysis. *J Clin Oncol* (2015) 33:773–81. doi: 10.1200/JCO.2014.57.4756

8. Nakamura Y, Tanaka R, Asami Y, Teramoto Y, Imamura T, Sato S, et al. Correlation between vitiligo occurrence and clinical benefit in advanced melanoma patients treated with nivolumab: A multi-institutional retrospective study. *J Dermatol* (2017) 44:117–22. doi: 10.1111/1346-8138.13520

9. Verkhovskaia S, Di Pietro FR, Mastroeni S, Carbone ML, Abeni D, Morese R, et al. Vitiligo-like leukoderma as an indicator of clinical response to immune checkpoint inhibitors in late-stage melanoma patients. *J Cancer Res Clin Oncol* (2021) 148:2529–38. doi: 10.21203/rs.3.rs-827134/v1

10. Becker JC, Guldberg P, Zeuthen J, Bröcker EB, Straten PT. Accumulation of identical T cells in melanoma and vitiligo-like leukoderma. *J Invest Dermatol* (1999) 113:1033–8. doi: 10.1046/j.1523-1747.1999.00805.x

11. Rapisuwon S, Izar B, Batenchuk C, Avila A, Mei S, Sorger P, et al. Exceptional response and multisystem autoimmune-like toxicities associated with the same T cell clone in a patient with uveal melanoma treated with immune checkpoint inhibitors. *J Immunother Cancer* (2019) 7:61. doi: 10.1186/s40425-019-0533-0

12. Elkoshi Z. Cancer and Autoimmune diseases: a tale of two immunological opposites? *Front Immunol* (2022) 13:821598. doi: 10.3389/fimmu.2022.821598

13. Zitvogel L, Perreault C, Finn OJ, Kroemer G. Beneficial autoimmunity improves cancer prognosis. *Nat Rev Clin Oncol* (2021) 18:591–602. doi: 10.1038/s41571-021-00508-x

14. Carbone ML, Madonna G, Capone A, Bove M, Mastroeni S, Levati L, et al. Vitiligo-specific soluble biomarkers as early indicators of response to immune

checkpoint inhibitors in metastatic melanoma patients. *Sci Rep* (2022) 12:5448. doi: 10.1038/s41598-022-09373-9

15. Gershenwald JE, Scolyer RA. Melanoma staging: american joint committee on cancer (AJCC) 8th edition and beyond. *Ann Surg Oncol* (2018) 25:2105–10. doi: 10.1245/s10434-018-6513-7

16. Seymour L, Bogaerts J, Perrone A, Ford R, Schwartz LH, Mandrekar S, et al. iRECIST: guidelines for response criteria for use in trials testing immunotherapeutics. *Lancet Oncol* (2017) 18:e143–e52. doi: 10.1016/S1470-2045(17)30074-8

17. Persigehl T, Lennartz S, Schwartz LH. iRECIST: how to do it. *Cancer Imaging* (2020) 20:2. doi: 10.1186/s40644-019-0281-x

18. Dias J, Boulouis C, Gorin JB, van den Biggelaar R, Lal KG, Gibbs A, et al. The CD4(-)CD8(-) MAIT cell subpopulation is a functionally distinct subset developmentally related to the main CD8(+) MAIT cell pool. *Proc Natl Acad Sci U.S.A.* (2018) 115:E11513–e22. doi: 10.1073/pnas.1812273115

19. Gargano F, Guerrera G, Piras E, Serafini B, Di Paola M, Rizzetto L, et al. Proinflammatory mucosal-associated invariant CD8+ T cells react to gut flora yeasts and infiltrate multiple sclerosis brain. *Front Immunol* (2022) 13:890298. doi: 10.3389/fimmu.2022.890298

20. Acosta-Rodriguez EV, Rivino L, Geginat J, Jarrossay D, Gattorno M, Lanzavecchia A, et al. Surface phenotype and antigenic specificity of human interleukin 17-producing T helper memory cells. *Nat Immunol* (2007) 8:639–46. doi: 10.1038/ni1467

21. Capone A, Volpe E. Identification and purification of human memory T helper cells from peripheral blood. *Methods Mol Biol* (2021) 2285:27–34. doi: 10.1007/978-1-0716-1311-5_2

22. Robins HS, Campregher PV, Srivastava SK, Wacher A, Turtle CJ, Kahsai O, et al. Comprehensive assessment of T-cell receptor beta-chain diversity in alphabeta T cells. *Blood* (2009) 114:4099–107. doi: 10.1182/blood-2009-04-217604

23. Carlson CS, Emerson RO, Sherwood AM, Desmarais C, Chung MW, Parsons JM, et al. Using synthetic templates to design an unbiased multiplex PCR assay. *Nat Commun* (2013) 4:2680. doi: 10.1038/ncomms3680

24. Robins H, Desmarais C, Matthis J, Livingston R, Andriesen J, Reijonen H, et al. Ultra-sensitive detection of rare T cell clones. *J Immunol Methods* (2012) 375:14–9. doi: 10.1016/j.jim.2011.09.001

25. Yousfi Monod M, Giudicelli V, Chaume D, Lefranc MP. IMGT/JunctionAnalysis: the first tool for the analysis of the immunoglobulin and T cell receptor complex V-J and V-D-J JUNCTIONs. *Bioinformatics* (2004) 20 Suppl 1:i379–85. doi: 10.1093/bioinformatics/bth945

26. Emerson RO, Sherwood AM, Rieder MJ, Guenthoer J, Williamson DW, Carlson CS, et al. High-throughput sequencing of T-cell receptors reveals a homogeneous repertoire of tumour-infiltrating lymphocytes in ovarian cancer. *J Pathol* (2013) 231:433–40. doi: 10.1002/path.4260

27. Wu D, Sherwood A, Fromm JR, Winter SS, Dunsmore KP, Loh ML, et al. High-throughput sequencing detects minimal residual disease in acute T lymphoblastic leukemia. *Sci Transl Med* (2012) 4:134ra63. doi: 10.1126/scitranslmed.3003656

28. Rosvall M, Bergstrom CT. Mapping change in large networks. *PloS One* (2010) 5:e8694. doi: 10.1371/journal.pone.0008694

29. Cibrián D, Sánchez-Madrid F. CD69: from activation marker to metabolic gatekeeper. *Eur J Immunol* (2017) 47:946–53. doi: 10.1002/eji.201646837

30. Tumeh PC, Harview CL, Yearley JH, Shintaku IP, Taylor EJ, Robert L, et al. PD-1 blockade induces responses by inhibiting adaptive immune resistance. *Nature* (2014) 515:568–71. doi: 10.1038/nature13954

31. Hogan SA, Levesque MP, Cheng PF. Melanoma immunotherapy: next-generation biomarkers. *Front Oncol* (2018) 8:178. doi: 10.3389/fonc.2018.00178

32. Inoue H, Park JH, Kiyotani K, Zewde M, Miyashita A, Jinnin M, et al. Intratumoral expression levels of PD-L1, GZMA, and HLA-A along with oligoclonal T cell expansion associate with response to nivolumab in metastatic melanoma. *Oncoimmunology* (2016) 5:e1204507. doi: 10.1080/2162402X.2016.1204507

33. Bajor DL, Xu X, Torigian DA, Mick R, Garcia LR, Richman LP, et al. Immune activation and a 9-year ongoing complete remission following CD40 antibody therapy and metastasectomy in a patient with metastatic melanoma. *Cancer Immunol Res* (2014) 2:1051–8. doi: 10.1158/2326-6066.CIR-14-0154

34. Roh W, Chen PL, Reuben A, Spencer CN, Prieto PA, Miller JP, et al. Integrated molecular analysis of tumor biopsies on sequential CTLA-4 and PD-1 blockade reveals markers of response and resistance. *Sci Transl Med* (2017) 9:eaah3560. doi: 10.1126/scitranslmed.aah3560

35. Poran A, Scherer J, Bushway ME, Besada R, Balogh KN, Wanamaker A, et al. Combined TCR repertoire profiles and blood cell phenotypes predict melanoma patient response to personalized neoantigen therapy plus anti-PD-1. *Cell Rep Med* (2020) 1:100141. doi: 10.1016/j.xcrm.2020.100141

36. Hlača N, Žagar T, Kaštelan M, Brajac I, Prpić-Massari L. Current concepts of vitiligo immunopathogenesis. *Biomedicines* (2022) 10:1639. doi: 10.3390/biomedicines10071639

37. Eyerich K, Dimartino V, Cavani A. IL-17 and IL-22 in immunity: driving protection and pathology. *Eur J Immunol* (2017) 47:607–14. doi: 10.1002/eji.201646723

38. Singh RK, Lee KM, Vujkovic-Cvijin I, Ucmak D, Farahnik B, Abrouk M, et al. The role of IL-17 in vitiligo: a review. *Autoimmun Rev* (2016) 15:397–404. doi: 10.1016/j.autrev.2016.01.004

39. Wang CQF, Cruz-Inigo AE, Fuentes-Duculan J, Moussai D, Gulati N, Sullivan-Whalen M, et al. Th17 cells and activated dendritic cells are increased in vitiligo lesions. *PloS One* (2011) 6:e18907. doi: 10.1371/journal.pone.0018907

40. Hinks TSC, Zhang XW. MAIT cell activation and functions. *Front Immunol* (2020) 11:1014. doi: 10.3389/fimmu.2020.01014

41. Liman N, Park JH. Markers and makers of NKT17 cells. *Exp Mol Med* (2023) 55:1090–8. doi: 10.1038/s12276-023-01015-y

42. Fiala GJ, Gomes AQ, Silva-Santos B. From thymus to periphery: Molecular basis of effector γδ-T cell differentiation. *Immunol Rev* (2020) 298:47–60. doi: 10.1111/imr.12918

43. Poli A, Michel T, Thérésine M, Andrès E, Hentges F, Zimmer J. CD56bright natural killer (NK) cells: an important NK cell subset. *Immunology* (2009) 126:458–65. doi: 10.1111/j.1365-2567.2008.03027.x

44. Gascón-Ruiz M, Ramírez-Labrada A, Lastra R, Martínez-Lostao L, Paño-Pardo JR, Sesma A, et al. A subset of PD-1-expressing CD56(bright) NK cells identifies patients with good response to immune checkpoint inhibitors in lung cancer. *Cancers (Basel)* (2023) 15:329. doi: 10.3390/cancers15020329

45. Antohe M, Nedelcu RI, Nichita L, Popp CG, Cioplea M, Brinzea A, et al. Tumor infiltrating lymphocytes: the regulator of melanoma evolution. *Oncol Lett* (2019) 17:4155–61. doi: 10.3892/ol.2019.9940

46. Riaz N, Havel JJ, Makarov V, Desrichard A, Urba WJ, Sims JS, et al. Tumor and microenvironment evolution during immunotherapy with nivolumab. *Cell* (2017) 171:934–49.e16. doi: 10.1016/j.cell.2017.09.028

frontiers | Frontiers in Immunology

TYPE Mini Review
PUBLISHED 31 October 2023
DOI 10.3389/fimmu.2023.1286696

OPEN ACCESS

EDITED BY
Silvia Monticelli,
Institute for Research in Biomedicine (IRB), Switzerland

REVIEWED BY
Marco Craveiro,
National Institutes of Health (NIH), United States

*CORRESPONDENCE
Mark S. Sundrud
mark.sundrud@dartmouth.edu

RECEIVED 31 August 2023
ACCEPTED 11 October 2023
PUBLISHED 31 October 2023

CITATION
Balasubramanian A and Sundrud MS (2023) ATP-dependent transporters: emerging players at the crossroads of immunity and metabolism. *Front. Immunol.* 14:1286696. doi: 10.3389/fimmu.2023.1286696

ATP-dependent transporters: emerging players at the crossroads of immunity and metabolism

Akshaya Balasubramanian[1] and Mark S. Sundrud[1,2,3,4]*

[1]Department of Microbiology and Immunology, Geisel School of Medicine at Dartmouth, Hanover, NH, United States, [2]Department of Medicine, Geisel School of Medicine at Dartmouth, Hanover, NH, United States, [3]Center for Digestive Health, Dartmouth Health, Lebanon, NH, United States, [4]Dartmouth Cancer Center, Lebanon, NH, United States

Nearly 50 ATP-binding cassette (ABC) transporters are encoded by mammalian genomes. These transporters are characterized by conserved nucleotide-binding and hydrolysis (i.e., ATPase) domains, and power directional transport of diverse substrate classes – ions, small molecule metabolites, xenobiotics, hydrophobic drugs, and even polypeptides – into or out of cells or subcellular organelles. Although immunological functions of ABC transporters are only beginning to be unraveled, emerging literature suggests these proteins have under-appreciated roles in the development and function of T lymphocytes, including many of the key effector, memory and regulatory subsets that arise during responses to infection, inflammation or cancers. One transporter in particular, MDR1 (Multidrug resistance-1; encoded by the *ABCB1* locus in humans), has taken center stage as a novel player in immune regulation. Although MDR1 remains widely viewed as a simple drug efflux pump in tumor cells, recent evidence suggests that this transporter fills key endogenous roles in enforcing metabolic fitness of activated CD4 and CD8 T cells. Here, we summarize current understanding of the physiological functions of ABC transporters in immune regulation, with a focus on the anti-oxidant functions of MDR1 that may shape both the magnitude and repertoires of antigen-specific effector and memory T cell compartments. While much remains to be learned about the functions of ABC transporters in immunobiology, it is already clear that they represent fertile new ground, both for the definition of novel immunometabolic pathways, and for the discovery of new drug targets that could be leveraged to optimize immune responses to vaccines and cancer immunotherapies.

KEYWORDS

ABC transporters, MDR1, P-glycoprotein, metabolism, reactive oxygen species, TCR signaling, oxidative stress, redox

1 Introduction

The field of immunometabolism has exploded over the past two decades. Among many notable discoveries, it is now understood that the activation and differentiation of immune cells – including T cells – involves rapid and profound metabolic reprogramming. On one hand, antigen- and TCR-mediated increases in aerobic glycolysis and mitochondrial respiration allows primed T cells to meet the bioenergetic and biosynthetic demands of cell growth and proliferation. On the other, differences in the magnitude and type of metabolic activities an antigen-primed T cell undertakes can play instructive roles in the commitment of emergent effector, memory and/or regulatory T cell subsets (1–5). CD8 effector T cells and CD4 Th17 and Th1 cells, for example, rely mainly on glycolysis to support rapid proliferation and potent effector functions, whereas CD8 memory cells and CD4 T regulatory (Treg) cells utilize mitochondrial respiration and fatty acid oxidation (FAO) to establish long-term persistence in nutrient-sparse tissues and execute immunosuppressive functions, respectively (3). It is thus not surprising that genetic or environmental perturbations to metabolic pathways have profound influence over the type and quality of T cell responses; further elucidation of the underlying mechanisms holds promises of revealing new preventative or treatment strategies for human infectious or malignant diseases.

Flux through growth-supporting metabolic pathways requires active transport of numerous organic and inorganic molecules across biological membranes. Adenosine triphosphate (ATP)-binding cassette (ABC) transporters constitute one of the largest super-families of transmembrane proteins encoded by the human genome. These transporters utilize ATP hydrolysis to power directional translocation of diverse substrates, against chemical gradients, and across lipid membranes, including the plasma membrane and membranes of intracellular organelles (6). ABC transporters are evolutionarily conserved and present throughout all kingdoms of life, from prokaryotes to humans (7), with major functions centering on either the direct promotion of cellular (e.g., lipid, heme) metabolism, or facilitating cellular detoxification via transport of potentially toxic metabolic byproducts or xenobiotic compounds (8–11). Indeed, loss of function polymorphisms in human ABC transporter loci are now linked to many human diseases, including anemia, obesity, atherosclerosis (AS), congenital cholestasis, peroxisome disorders, cystic fibrosis (CF) and Tangier disease (TD) (8, 9, 12).

More recent studies have begun to highlight direct, important and endogenous functions of ABC transporters in adaptive immune regulation generally, and development and function of T cells specifically (13–25). Here, we discuss the current state of understanding of the ABC transporters in regulating T cell differentiation and function, while also providing forward-looking perspectives as to how transport-dependent cellular metabolic pathways may intersect with antigen receptor signaling to shape T cell lineage commitment, and even the clonality of emergent effector and memory T cell pools.

2 Classification and structure of ABC transporters

48 human genes encode ABC transport proteins, most of which have direct orthologs in mice and lower vertebrates. In the early 2000's, ABC transporters were renamed and reclassified into seven sub-families (ABCA to ABCG), based on phylogenetic analysis and sequence/structural similarity (7, 26–28). Members of the ABCE and ABCF sub-families are notable in that they do not appear to function as transporters per se, but rather participate in translational regulation and mRNA surveillance (29–32).

X-ray crystallographic studies of several ABC transporters have provided atomic-level resolution of the canonical structure of ABC transporters, and specifically the organization of four main functional domains — two nucleotide binding domains (NBD1, NBD2) and two transmembrane domains (TMD1, TMD2). Most eukaryotic ABC transporters are expressed as either a single polypeptide containing all four functional domains, or as half-transporters capable of homo- or hetero-dimerization (33). The NBD contain several conserved functional motifs, whereas the TMDs are more variable and contain 6-11 membrane-spanning α-helices which form the transmembrane pore and mediate substrate binding (33). Diversity amongst TMDs allow the various ABC transporters to bind, and subsequently transport, diverse substrate classes (e.g., heme, lipids, xenobiotics, etc.), and also underlies the phylogenetic relationships between sub-family members. In all cases, ABC transport activity involves ATP-dependent NBD dimerization, which induces conformational changes in the TMDs that exposes the inner region of the pore to the outside and allows for unidirectional transport against chemical gradients (34).

3 ABC transporters in T cells

The first described and arguably most famous ABC transporters within the immune system are the transporters associated with antigen processing (TAP1/2), which transport cytosolic peptides into the endoplasmic reticulum (ER) for loading onto MHC Class I molecules (35). Another immunologically notable ABC transporter is ABCC7 [*a.k.a.*, cystic fibrosis transmembrane conductance regulator (CFTR)], which functions as an apical chloride channel on lung epithelium, and whose loss-of-function leads to chronic bacterial infections of the lung (36). However, numerous ABC transporters are now recognized for filling essential functions within the adaptive immune system generally, and immunometabolism specifically. The obligate mitochondrial transporters ABCB7 and ABCB10, for example, are considered heme transporters based on their roles in erythropoiesis, and are necessary for the development of B cells and CD4 memory T cells, respectively (23, 24). In addition, lipid and multi-drug transporters have recently emerged as key regulators of T cell metabolism and function (Table 1).

TABLE 1 ABC transporters and their associated function in T cells.

ABC Transporter (in humans)	Mouse ortholog	Transport Substrate	Function in T cells	References
ABCA1	*Abca1*	Phospholipid and cholesterol	Regulates TCR signaling by maintaining lipid raft composition in peripheral lymphocytes.	Armstrong et al., (13); Zhao et al., (25); Bazioti et al., (37)
ABCA7	*Abca7*	Phospholipid	Disrupts lipid rafts and CD1d expression in iNKT cells.	Nowyhed et al., (20)
ABCB1	*Abcb1a*	Broad-spectrum drug efflux pump	Suppresses oxidative stress and promotes survival of T cells found in mucosal sites and CD8 T cells responding to infection.	Boddupalli et al., (16); Cao et al., (18); Xie et al., (21); Chen et al., (22)
	Abcb1b			
ABCB10	*Abcb10*	Possible heme transporter	Necessary to maintain stable CD4 memory pool and aid in switching metabolic states during activation.	Sun et al., (24)
ABCC4	*Abcc4*	Endogenous metabolites and xenobiotics	Induced in response to hypoxic conditions in Th17 cells.	Xie et al., (21)
ABCG1	*Abcg1*	Phospholipid and cholesterol	Regulates TCR signaling by maintaining lipid raft composition in thymic and peripheral lymphocytes.	Bensinger et al., (38); Armstrong et al., (13); Cheng et al., (17); Bazioti et al., (37)
ABCG2	*Abcg2*	Broad-spectrum drug efflux pump	Characteristic features of Trm cells and is necessary for maintenance of Trm niche in the gut.	Boddupalli et al., (16)
	Abcg3			

3.1 Lipid transporters

As many as 20 human ABC transporters are thought to transport discrete lipids or lipid metabolites. Among these, ABCA1 and ABCG1 are perhaps the best characterized for the roles they play in cholesterol transport and homeostasis, and for regulating TCR signaling intensity (13, 17, 25, 37). These transporters maintain structural organization and integrity of lipid bilayers, at least in part by regulating the number and density of cholesterol-rich lipid rafts (13, 17, 25). Given the key and ubiquitous roles of lipid rafts in signal transduction generally, and in immune cell signaling specifically, it is not surprising that these cholesterol and lipid transporters exert powerful influences over the development and function of T cells (39).

Abcg1$^{-/-}$ mice display larger thymuses than wild-type controls due to thymocyte hyperproliferation and an increase in total thymic cellularity (13). ABCG1 also affects thymic and peripheral development of Foxp3^{+} Treg cells (17). An increase in thymic (i.e., 'natural') Treg cells is observed when *Abcg1* is conditionally ablated in T cells using *Lck-Cre* (17). In the periphery, preferential differentiation of naïve CD4 T cells into Tregs is evoked in the absence of ABCG1 by an increase in cellular cholesterol levels, which inhibits mammalian target of rapamycin (mTOR), triggers the phosphorylation and activation of signal transducer and activator of transcription (STAT)-5, and promotes the induction and stability of *Foxp3* expression (Figure 1) (17).

ABCA1 and ABCG1 are necessary for the maintenance of peripheral T cell homeostasis (13, 17, 25, 37). Expression of *Abca1* and *Abcg1* decreases following naïve T cell activation, which in turn promotes increased membrane cholesterol content to support cell growth and proliferation (38, 40). Intriguingly, ABCA1 and ABCG1 appear to work synergistically in T cells, as ablation of both *Abca1* and *Abcg1* in a T-cell specific manner enhances TCR signaling in CD4 and CD8 T cells (25, 37). This enhancement of TCR signaling has been attributed to an increase in lipid raft formation (13). On the other hand, upregulation of *Abcg1* expression in T cells by the nuclear receptor, liver X receptor (LXR), reduces T cell proliferation (38). The need for tightly regulated lipid transport to support TCR signaling is not limited to conventional T cells; ABCG1, as well as another lipid transporter, ABCA7, are both essential for thymic maturation of invariant natural killer T (iNKT) cells (14, 20). Hence, regulation of cholesterol efflux by ABCA1, ABCG1 and ABCA7 each appear to participate in the regulation of signal transduction, and in establishing a full complement of peripheral lymphocytes.

3.2 Multi-drug transporters

Another class of ABC transporters recently implicated in immune regulation are the so-called multi-drug transporters. This historical classification derives from a combination of functional studies in eukaryotic cells and examination of homologs in bacterial model systems, which together show that multi-drug transporters are capable of effluxing a variety of structurally-unrelated cytostatic drugs from tumor cells (18). However, considering the repeated and high-profile failures of drugs designed to block multi-drug transporters in clinical cancer studies (41), and the emerging endogenous functions of at least some of these transporters, this semantic classification may require updating. Indeed, 'multi-drug' transporters – including multidrug resistance protein 1 (MDR1/ABCB1), multidrug resistance protein 4 (MRP4/ABCC4) and breast cancer resistance protein (BCRP1/ABCG2) – each display considerable evolutionary conservation and thus may also be considered 'orphan' transporters, as endogenous transport substrates have not yet been described. An important and common theme among these multi-drug transporters is their

incredibly broad substrate specificity; MDR1, for example, has been proposed to efflux a variety of synthetic drugs, antiretroviral drugs, glucocorticoids, lipids, fluorescent dyes and even peptide hormones (in yeast) (42–45). Yet many of these same transporters display endogenous antioxidant functions in several cell types and tissues during normal physiology, including in T cells. Thus, it is worth considering that the core evolutionary function of 'multi-drug' transporters centers on the regulation of oxidation-reduction (redox) metabolism, which have become masked in recent decades by their proclivity to efflux 20th century medicines.

MDR1 is the most extensively characterized multi-drug transporter within the ABC family for its role as a regulator of oxidative stress. MDR1 is endogenously expressed in a variety of normal cell types and tissues, with highest levels seen in the liver, intestines, brain, kidney and adrenal glands (46–48). In the hematopoietic system, comprehensive profiling of a fluorescent *Abcb1a*-ametrine reporter allele in mice showed that MDR1 is expressed in a number of mature innate and adaptive lymphocytes, but is notably absent in most hematopoietic stem and progenitor cells, early thymocytes, and also mature granulocyte and B lymphocyte lineages (22). In CD4 T cells, MDR1 expression is absent in naïve cells, low in Foxp3$^+$ Treg cells, but increased markedly in pro-inflammatory effector subsets, namely IFNγ-secreting Th1 and IL-17-producing Th17 cells, in particular following infiltration of small intestine lamina propria (15). In contrast to this conditional expression in CD4 T cells, MDR1 expression is both constitutive and developmentally regulated in cytotoxic lymphocyte lineages (e.g., NK cells, iNKT cells, CD8 T cells) where the expression of MDR1 is at least partly controlled by Runx family transcription factors (22). Expression of MDR1 (and ABCG2) are also characteristic of tissue-resident memory (Trm) CD8 T cells, as well as of human mucosal associated invariant T (MAIT) cells (16, 19, 49). In line with constitutively high MDR1 expression, mouse CD8 T cells null for MDR1 transport activity (*Abcb1a/b*$^{-/-}$) are incapable of becoming productively activated, of accumulating efficiently in response to acute viral or bacterial infections, and of forming functional memory cells (22). By contrast, naïve CD8 T cells do not require MDR1 function for steady-state persistence (22), which suggests that MDR1 transport activity in CD8 T cells is primarily called upon after TCR-stimulation. Indeed, the inability of *Abcb1a/b*$^{-/-}$ CD8 T cells to accumulate following TCR-stimulation is due to increased cell death, not reduced proliferation, and coincides with a failure of these cells to suppress oxidative stress and maintain functional mitochondria (Figure 1) (22). Others have shown that Th17 cells require both MDR1 and ABCC4 to suppress oxidative stress during states of hypoxia (21). Further, high MDR1 expression in Th1 and Th17 cells in the distal small intestine (i.e., ileum) counters oxidative stress induced by naturally circulating bile acids, an abundant class of liver-derived lipid-emulsifying metabolites that are also potent oxidizing agents (18, 50). Even outside of the immune system, MDR1 has been shown to suppress oxidative stress and safeguard mitochondrial integrity in colonic epithelial cells (51). Collectively, these findings support a broader and more fundamental role for the MDR1 transporter in suppressing oxidative stress upon T cell exposure to intra- or extra-cellular oxidizing agents (e.g., toxic metabolic byproducts, bile acids, etc.). Such transport-dependent antioxidant functions of MDR1 raise intriguing new concepts in the convergence of TCR signaling, metabolic reprogramming, oxidative stress, and even clonal selection in T cells.

4 Determinants of peripheral T cell responses: TCR signaling and ROS

T cell proliferation, lineage commitment, and the execution of effector or regulatory functions are all markedly influenced by the strength and duration of TCR/peptide-MHC engagement (52–54). Upon infection, the size of the antigen-specific CD8 T cell compartment correlates directly with the duration of antigen exposure (55). Strength and duration of TCR signaling also shapes both CD4 and CD8 memory T cell compartments, as highlighted by the preferential skewing of the memory pool towards clones with higher-affinity TCRs (55–57). It is increasingly clear that TCR signaling thresholds also regulate functional outcomes of individual T cell clones (e.g., proliferative capacity, differentiation, etc.); pathways that regulate successful integration of TCR, co-stimulatory and cytokine signaling pathways thus determine the magnitude, type and antigen-specificities of T cell responses.

Proximal TCR signaling induces rapid Ca^{2+} release into the cytosol from reserves in the endoplasmic reticulum (ER), which upon being emptied, activate extracellular Ca^{2+} influx across the plasma membrane (58, 59). Besides serving as a potent signal to activate early transcription factors, such as the NFATs, cytosolic Ca^{2+} is also taken up in mass by mitochondria, which facilitates ATP synthesis and promotes corresponding increases in levels of reactive oxygen species (ROS) (60). This increase in intracellular ROS occurs within minutes of TCR activation, with the majority of ROS production in activated T cells owing to mitochondrial superoxide ($O_2^{\bullet -}$) that "leak" from complexes I and III of the mitochondrial electron transport chain (ETC) (61).

ROS function as key secondary messengers in T cells and are required, at moderate levels, to promote proliferation, differentiation and survival. The activation of extracellular signal-regulated kinase (ERK) 1/2, for example, is highly ROS-dependent, and promotes activation and translocation of several transcription factors, including AP-1 family members, that are necessary for T cell growth and proliferation (62, 63). ROS production has also been implicated in promoting IL-2 production in activated T cells through NF-κB activation (64). At the same time, inappropriately elevated ROS levels are highly cytotoxic, and can stimulate apoptosis by covalently modifying and damaging proteins, nucleic acids, and lipids (65). Oxidative stress also promotes increased expression of Fas ligand (FasL), which on binding to Fas initiates the recruitment and activation of caspases causing activation induced cell death (AICD) (Figure 1) (62, 66, 67).

Considering the dual nature of intracellular ROS – where ROS is both required for T cell activation, but also toxic at increased levels – activated T cells upregulate a host of anti-oxidant enzymes

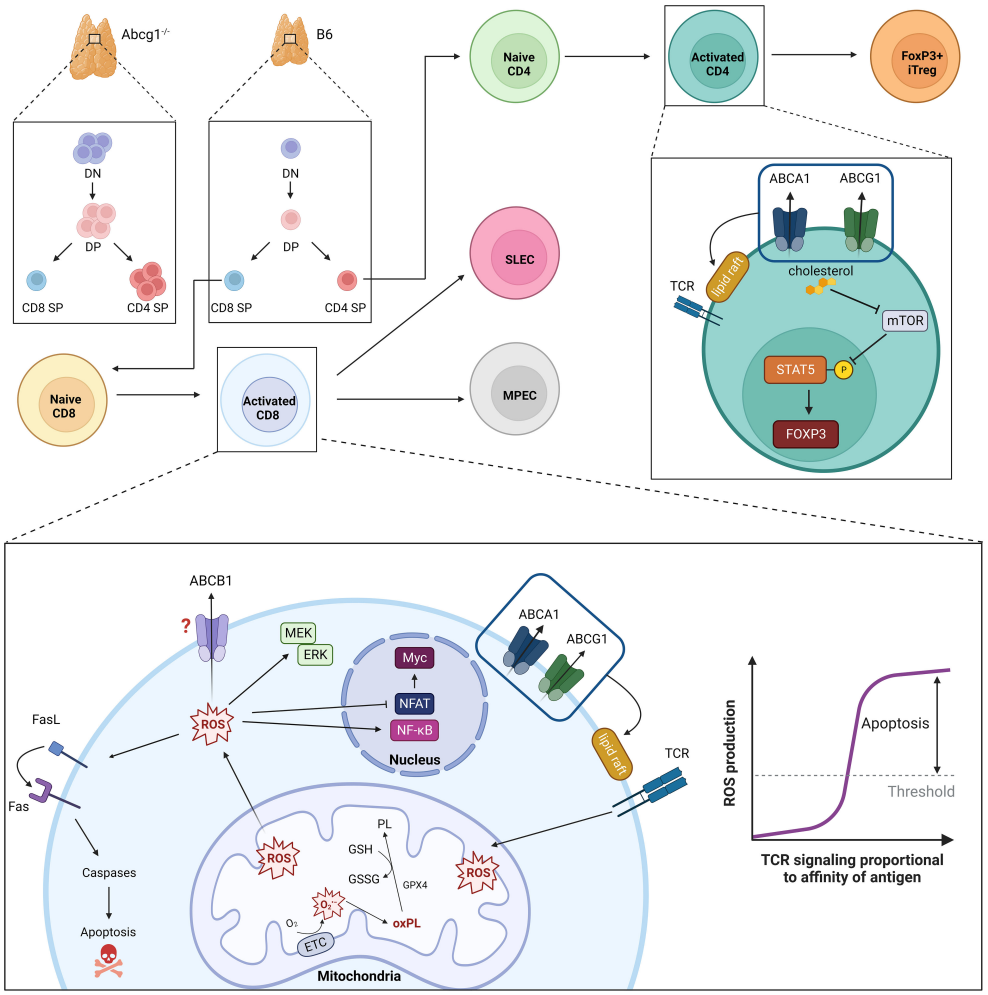

FIGURE 1
ABC transporters in regulation of T cell development, TCR intensity and oxidative stress. Loss of ABCG1 transport activity results in increased thymic cellularity and frequency of double negative (DN), double positive (DP) and CD4 single positive (SP) cells. Intensity of TCR signaling is modulated by ABCA1- and ABCG1-mediated phospholipid transport; loss of these transporters is associated with increased numbers and densities of cholesterol-rich lipid rafts. Parallel accumulation of intracellular cholesterol also promotes peripheral development of CD4+Foxp3+ induced (i)Treg cells. TCR signaling strength and duration is proportional to the amount of intracellular ROS produced. Moderate ROS levels (i.e., during T cell responses to low- or intermediate-affinity antigens) facilitate T cell proliferation, differentiation and survival through MEK-ERK1/2 and NF-κB activation. Conversely, elevated ROS levels (i.e., produced during T cell responses to high-affinity ligands) impair NFAT and Myc expression and promote activation-induced cell death (AICD) via Fas-Fas ligand (FasL). To maintain functional, but not toxic, ROS levels, activated T cells leverage endogenous anti-oxidant systems (e.g., glutathione peroxidase, GPX4) to reduce oxidized phospholipids (oxPL) within mitochondrial membranes using reduced glutathione (GSH) as a cofactor. MDR1 also suppresses oxidative stress in activated T cells, though underlying mechanisms remain ill-defined.

(superoxide dismutases (SODs), catalases, glutathione peroxidases (GPXs), glutathione reductases, etc.) to convert ROS into less reactive products, or to increase production of ROS scavenging molecules, such as glutathione, ascorbate, pyruvate, α-ketoglutarate, and oxaloacetate (65). Disruptions in these anti-oxidant systems result in elevated ROS production and affect metabolic reprogramming in developing T cells. Inhibition of glutathione production, which is important for ROS buffering, negatively affects TCR-induced Myc expression and NFAT activation, which are essential for activated CD8 T cells to switch to glycolytic metabolism (68). Similarly, loss of *Gpx4* impairs CD8 T cell responses to viral infections due to accumulation of lipid peroxides, leading to death by ferroptosis (69). Thus, productive immune responses demand that T cells tightly regulate both the production and scavenging of intracellular ROS. Discrete roles for ABC transporters in T cell redox regulation and metabolism remain unclear, but stand to provide exciting new molecular insights into the formation and regulation of effector and memory T cells.

5 Conclusions and future perspectives

Considering that both the developmental trajectories and functions of individual T cell clones involve unique TCR signaling dynamics, and thus discrete redox demands, it becomes increasingly important to decipher whether and how ABC transporters not only

regulate the magnitude of monoclonal (i.e., TCR transgenic) T cell responses, but also the selection of T cell clones specific for high- vs. low-affinity antigens. Given the preponderance of available evidence, it is reasonable to expect that MDR1, and perhaps other lipid and multidrug transporters, preferentially regulate T cell responses to abundant and high-affinity (i.e., immunodominant) antigens, in which the highest levels of intracellular ROS are generated. If true, these pathways (and ABC transporters) may prove vital for advancing the next generation of medicines that can improve T cell-mediated immunity to infectious diseases and cancers, where the survival of T cells specific for immunodominant antigens are paramount for efficacy.

Despite being one of the largest families of human transmembrane proteins, a comprehensive understanding of endogenous ABC transporter functions remains lacking. Historically, this has been due to the inherent difficulty of working with membrane proteins and transporters, as well as a dearth of contemporary research reagents (e.g., engineered mouse alleles, antibodies, etc.). While significant strides have been made in recent decades with regard to the structural organization of these transporters, meaningful insights into the physiological and immunological functions of these transporters have lagged. Mechanistic understanding of these transporters remains largely based on data from pharmacological and *in vitro* studies, but it is becoming increasingly apparent that these transporters have important and context-dependent functions that need to be evaluated *in vivo*, during both normal- and patho-physiology. This is especially true for transporters, like MDR1, which remain classified as 'multi-drug' efflux pumps, despite continued elaboration of new and potent endogenous functions in *in vivo* mouse and *ex vivo* human systems. For these, the key unanswered question is why would an ABC transporter be conserved throughout evolution unless it serves a core endogenous function? The continued pursuit of basic science, and the advancement of next-generation medicines, await answers.

Author contributions

MS: Conceptualization, Funding acquisition, Supervision, Writing – review & editing. AB: Conceptualization, Writing – original draft, Writing – review & editing.

Funding

The author(s) declare financial support was received for the research, authorship, and/or publication of this article. This work was supported by startup funds provided to the Sundrud Lab by the Dartmouth Cancer Center.

Acknowledgments

All figures were created using BioRender.com.

Conflict of interest

The authors declare that the research was conducted in the absence of any commercial or financial relationships that could be construed as a potential conflict of interest.

Publisher's note

References

1. van der Windt GJ, Everts B, Chang CH, Curtis JD, Freitas TC, Amiel E, et al. Mitochondrial respiratory capacity is a critical regulator of CD8+ T cell memory development. *Immunity* (2012) 36(1):68–78. doi: 10.1016/j.immuni.2011.12.007

2. Michalek RD, Gerriets VA, Jacobs SR, Macintyre AN, MacIver NJ, Mason EF, et al. Cutting edge: distinct glycolytic and lipid oxidative metabolic programs are essential for effector and regulatory CD4+ T cell subsets. *J Immunol* (2011) 186 (6):3299–303. doi: 10.4049/jimmunol.1003613

3. Geltink RIK, Kyle RL, Pearce EL. Unraveling the complex interplay between T cell metabolism and function. *Annu Rev Immunol* (2018) 36:461–88. doi: 10.1146/annurev-immunol-042617-053019

4. MacIver NJ, Michalek RD, Rathmell JC. Metabolic regulation of T lymphocytes. *Annu Rev Immunol* (2013) 31:259–83. doi: 10.1146/annurev-immunol-032712-095956

5. Ma EH, Verway MJ, Johnson RM, Roy DG, Steadman M, Hayes S, et al. Metabolic profiling using stable isotope tracing reveals distinct patterns of glucose utilization by physiologically activated CD8(+) T cells. *Immunity* (2019) 51(5):856–870 e5. doi: 10.1016/j.immuni.2019.09.003

6. Rees DC, Johnson E, Lewinson O. ABC transporters: the power to change. *Nat Rev Mol Cell Biol* (2009) 10(3):218–27. doi: 10.1038/nrm2646

7. Higgins CF. ABC transporters: from microorganisms to man. *Annu Rev Cell Biol* (1992) 8:67–113. doi: 10.1146/annurev.cb.08.110192.000435

8. Yamamoto M, Arimura H, Fukushige T, Minami K, Nishizawa Y, Tanimoto A, et al. Abcb10 role in heme biosynthesis in *vivo*: Abcb10 knockout in mice causes anemia with protoporphyrin IX and iron accumulation. *Mol Cell Biol* (2014) 34 (6):1077–84. doi: 10.1128/MCB.00865-13

9. Ichikawa Y, Bayeva M, Ghanefar M, Potini V, Sun L, Mutharasan RK, et al. Disruption of ATP-binding cassette B8 in mice leads to cardiomyopathy through a decrease in mitochondrial iron export. *Proc Natl Acad Sci USA* (2012) 109(11):4152–7. doi: 10.1073/pnas.1119338109

10. Schaedler TA, Thornton JD, Kruse I, Schwarzländer M, Meyer AJ, van Veen HW, et al. A conserved mitochondrial ATP-binding cassette transporter exports glutathione polysulfide for cytosolic metal cofactor assembly. *J Biol Chem* (2014) 289 (34):23264–74. doi: 10.1074/jbc.M114.553438

11. Wang X, Collins HL, Ranalletta M, Fuki IV, Billheimer JT, Rothblat GH, et al. Macrophage ABCA1 and ABCG1, but not SR-BI, promote macrophage reverse cholesterol transport. *vivo*. *J Clin Invest* (2007) 117(8):2216–24. doi: 10.1172/JCI32057

12. Fitzgerald ML, Mujawar Z, Tamehiro N. ABC transporters, atherosclerosis and inflammation. *Atherosclerosis* (2010) 211(2):361–70. doi: 10.1016/j.atherosclerosis.2010.01.011

13. Armstrong AJ, Gebre AK, Parks JS, Hedrick CC. ATP-binding cassette transporter G1 negatively regulates thymocyte and peripheral lymphocyte proliferation. *J Immunol* (2010) 184(1):173–83. doi: 10.4049/jimmunol.0902372

14. Sag D, Wingender G, Nowyhed H, Wu R, Gebre AK, Parks JS, et al. ATP-binding cassette transporter G1 intrinsically regulates invariant NKT cell development. *J Immunol* (2012) 189(11):5129–38. doi: 10.4049/jimmunol.1201570

15. Ramesh R, Kozhaya L, McKevitt K, Djuretic IM, Carlson TJ, Quintero MA, et al. Pro-inflammatory human Th17 cells selectively express P-glycoprotein and are refractory to glucocorticoids. *J Exp Med* (2014) 211(1):89–104. doi: 10.1084/jem.20130301

16. Boddupalli CS, Nair S, Gray SM, Nowyhed HN, Verma R, Gibson JA, et al. ABC transporters and NR4A1 identify a quiescent subset of tissue-resident memory T cells. *J Clin Invest* (2016) 126(10):3905–16. doi: 10.1172/JCI85329

17. Cheng HY, Gaddis DE, Wu R, McSkimming C, Haynes LD, Taylor AM, et al. Loss of ABCG1 influences regulatory T cell differentiation and atherosclerosis. *J Clin Invest* (2016) 126(9):3236–46. doi: 10.1172/JCI83136

18. Cao W, Kayama H, Chen ML, Delmas A, Sun A, Kim SY, et al. The xenobiotic transporter mdr1 enforces T cell homeostasis in the presence of intestinal bile acids. *Immunity* (2017) 47(6):1182–1196.e10. doi: 10.1016/j.immuni.2017.11.012

19. Fergusson JR, Ussher JE, Kurioka A, Klenerman P, Walker LJ. High MDR-1 expression by MAIT cells confers resistance to cytotoxic but not immunosuppressive MDR-1 substrates. *Clin Exp Immunol* (2018) 194(2):180–91. doi: 10.1111/cei.13165

20. Nowyhed HN, Chandra S, Kiosses W, Marcovecchio P, Andary F, Zhao M, et al. ATP binding cassette transporter ABCA7 regulates NKT cell development and function by controlling CD1d expression and lipid raft content. *Sci Rep* (2017) 7:40273. doi: 10.1038/srep40273

21. Xie A, Robles RJ, Mukherjee S, Zhang H, Feldbrügge L, Csizmadia E, et al. HIF-1α-induced xenobiotic transporters promote Th17 responses in Crohn's disease. *J Autoimmun* (2018) 94:122–33. doi: 10.1016/j.jaut.2018.07.022

22. Chen ML, Sun A, Cao W, Eliason A, Mendez KM, Getzler AJ, et al. Physiological expression and function of the MDR1 transporter in cytotoxic T lymphocytes. *J Exp Med* (2020) 217(5):e20191388. doi: 10.1084/jem.20191388

23. Lehrke MJ, Shapiro MJ, Rajcula MJ, Kennedy MM, McCue SA, Medina KL, et al. The mitochondrial iron transporter ABCB7 is required for B cell development, proliferation, and class switch recombination in mice. *Elife* (2021) 10:e69621. doi: 10.7554/eLife.69621

24. Sun W, Jia X, Liesa M, Tantin D, Ward DM. ABCB10 loss reduces CD4+ T cell activation and memory formation. *J Immunol* (2022) 208(2):328–37. doi: 10.4049/jimmunol.2100514

25. Zhao Y, Zhang L, Liu L, Zhou X, Ding F, Yang Y, et al. Specific loss of ABCA1 (ATP-binding cassette transporter A1) suppresses TCR (T-cell receptor) signaling and provides protection against atherosclerosis. *Arterioscler Thromb Vasc Biol* (2022) 42 (12):e311–26. doi: 10.1161/ATVBAHA.122.318226

26. Dean M, Rzhetsky A, Allikmets R. The human ATP-binding cassette (ABC) transporter superfamily. *Genome Res* (2001) 11(7):1156–66. doi: 10.1101/gr.184901

27. Borst P, Elferink RO. Mammalian ABC transporters in health and disease. *Annu Rev Biochem* (2002) 71:537–92. doi: 10.1146/annurev.biochem.71.102301.093055

28. Dean M, Annilo T. Evolution of the ATP-binding cassette (ABC) transporter superfamily in vertebrates. *Annu Rev Genomics Hum Genet* (2005) 6:123–42. doi: 10.1146/annurev.genom.6.080604.162122

29. Hassel BA, Zhou A, Sotomayor C, Maran A, Silverman RH. A dominant negative mutant of 2-5A-dependent RNase suppresses antiproliferative and antiviral effects of interferon. *EMBO J* (1993) 12(8):3297–304. doi: 10.1002/j.1460-2075.1993.tb05999.x

30. Bisbal C, Martinand C, Silhol M, Lebleu B, Salehzada T. Cloning and characterization of a RNAse L inhibitor. *A New component interferon-regulated 2-5A pathway. J Biol Chem* (1995) 270(22):13308–17. doi: 10.1074/jbc.270.22.13308

31. Tyzack JK, Wang X, Belsham GJ, Proud CG. ABC50 interacts with eukaryotic initiation factor 2 and associates with the ribosome in an ATP-dependent manner. *J Biol Chem* (2000) 275(44):34131–9. doi: 10.1074/jbc.M002868200

32. Zhao Z, Fang LL, Johnsen R, Baillie DL. ATP-binding cassette protein E is involved in gene transcription and translation in Caenorhabditis elegans. *Biochem Biophys Res Commun* (2004) 323(1):104–11. doi: 10.1016/j.bbrc.2004.08.068

33. Thomas C, Tampé R. Multifaceted structures and mechanisms of ABC transport systems in health and disease. *Curr Opin Struct Biol* (2018) 51:116–28. doi: 10.1016/j.sbi.2018.03.016

34. Alam A, Locher KP. Structure and mechanism of human ABC transporters. *Annu Rev Biophys* (2023) 52:275–300. doi: 10.1146/annurev-biophys-111622-091232

35. Ritz U, Seliger B. The transporter associated with antigen processing (TAP): structural integrity, expression, function, and its clinical relevance. *Mol Med* (2001) 7 (3):149–58. doi: 10.1007/BF03401948

36. Corradi V, Vergani P, Tieleman DP. Cystic fibrosis transmembrane conductance regulator (CFTR): CLOSED AND OPEN STATE CHANNEL MODELS. *J Biol Chem* (2015) 290(38):22891–906. doi: 10.1074/jbc.M115.665125

37. Bazioti V, La Rose AM, Maassen S, Bianchi F, de Boer R, Halmos B, et al. T cell cholesterol efflux suppresses apoptosis and senescence and increases atherosclerosis in middle aged mice. *Nat Commun* (2022) 13(1):3799. doi: 10.1038/s41467-022-31135-4

38. Bensinger SJ, Bradley MN, Joseph SB, Zelcer N, Janssen EM, Hausner MA, et al. LXR signaling couples sterol metabolism to proliferation in the acquired immune response. *Cell* (2008) 134(1):97–111. doi: 10.1016/j.cell.2008.04.052

39. Jury EC, Flores-Borja F, Kabouridis PS. Lipid rafts in T cell signalling and disease. *Semin Cell Dev Biol* (2007) 18(5):608–15. doi: 10.1016/j.semcdb.2007.08.002

40. Yang W, Bai Y, Xiong Y, Zhang J, Chen S, Zheng X, et al. Potentiating the antitumour response of CD8(+) T cells by modulating cholesterol metabolism. *Nature* (2016) 531(7596):651–5. doi: 10.1038/nature17412

41. Waghray D, Zhang Q. Inhibit or evade multidrug resistance P-glycoprotein in cancer treatment. *J Med Chem* (2018) 61(12):5108–21. doi: 10.1021/acs.jmedchem.7b01457

42. Young L, Leonhard K, Tatsuta T, Trowsdale J, Langer T. Role of the ABC transporter Mdl1 in peptide export from mitochondria. *Science* (2001) 291 (5511):2135–8. doi: 10.1126/science.1056957

43. Sakaeda T, Nakamura T, Okumura K. MDR1 genotype-related pharmacokinetics and pharmacodynamics. *Biol Pharm Bull* (2002) 25(11):1391–400. doi: 10.1248/bpb.25.1391

44. Minuesa G, Arimany-Nardi C, Erkizia I, Cedeño S, Moltó J, Clotet B, et al. P-glycoprotein (ABCB1) activity decreases raltegravir disposition in primary CD4+P-gphigh cells and correlates with HIV-1 viral load. *J Antimicrob Chemother* (2016) 71 (10):2782–92. doi: 10.1093/jac/dkw215

45. Whyte-Allman SK, Kaul R, Bendayan R. Regulation of ABC drug efflux transporters in human T-cells exposed to an HIV pseudotype. *Front Pharmacol* (2021) 12:711999. doi: 10.3389/fphar.2021.711999

46. Sugawara I, Kataoka I, Morishita Y, Hamada H, Tsuruo T, Itoyama S, et al. Tissue distribution of P-glycoprotein encoded by a multidrug-resistant gene as revealed by a monoclonal antibody, MRK 16. *Cancer Res* (1988) 48(7):1926–9.

47. Thiebaut F, Tsuruo T, Hamada H, Gottesman MM, Pastan I, Willingham MC. Cellular localization of the multidrug-resistance gene product P-glycoprotein in normal human tissues. *Proc Natl Acad Sci USA* (1987) 84(21):7735–8. doi: 10.1073/pnas.84.21.7735

48. Thiebaut F, Tsuruo T, Hamada H, Gottesman MM, Pastan I, Willingham MC. Immunohistochemical localization in normal tissues of different epitopes in the multidrug transport protein P170: evidence for localization in brain capillaries and crossreactivity of one antibody with a muscle protein. *J Histochem Cytochem: Off J Histochem Soc* (1989) 37(2):159–64. doi: 10.1177/37.2.2463300

49. Dusseaux M, Martin E, Serriari N, Péguillet I, Premel V, Louis D, et al. Human MAIT cells are xenobiotic-resistant, tissue-targeted, CD161hi IL-17-secreting T cells. *Blood* (2011) 117(4):1250–9. doi: 10.1182/blood-2010-08-303339

50. Bernstein H, Bernstein C, Payne CM, Dvorak K. Bile acids as endogenous etiologic agents in gastrointestinal cancer. *World J Gastroenterol: WJG* (2009) 15 (27):3329–40. doi: 10.3748/wjg.15.3329

51. Ho GT, Aird RE, Liu B, Boyapati RK, Kennedy NA, Dorward DA, et al. MDR1 deficiency impairs mitochondrial homeostasis and promotes intestinal inflammation. *Mucosal Immunol* (2018) 11(1):120–30. doi: 10.1038/mi.2017.31

52. Constant S, Pfeiffer C, Woodard A, Pasqualini T, Bottomly K. Extent of T cell receptor ligation can determine the functional differentiation of naive CD4+ T cells. *J Exp Med* (1995) 182(5):1591–6. doi: 10.1084/jem.182.5.1591

53. Fazilleau N, McHeyzer-Williams LJ, Rosen H, McHeyzer-Williams MG. The function of follicular helper T cells is regulated by the strength of T cell antigen receptor binding. *Nat Immunol* (2009) 10(4):375–84. doi: 10.1038/ni.1704

54. Marchingo JM, Kan A, Sutherland RM, Duffy KR, Wellard CJ, Belz GT, et al. T cell signaling. Antigen affinity, costimulation, and cytokine inputs sum linearly to amplify T cell expansion. *Science* (2014) 346(6213):1123–7. doi: 10.1126/science.1260044

55. Kretschmer L, Flossdorf M, Mir J, Cho YL, Plambeck M, Treise I, et al. Differential expansion of T central memory precursor and effector subsets is regulated by division speed. *Nat Commun* (2020) 11(1):113. doi: 10.1038/s41467-019-13788-w

56. Daniels MA, Teixeiro E. TCR signaling in T cell memory. *Front Immunol* (2015) 6:617. doi: 10.3389/fimmu.2015.00617

57. Akondy RS, Johnson PLF, Nakaya HI, Edupuganti S, Mulligan MJ, Lawson B, et al. Initial viral load determines the magnitude of the human CD8 T cell response to yellow fever vaccination. *Proc Natl Acad Sci USA* (2015) 112(10):3050–5. doi: 10.1073/pnas.1500475112

58. Weiss A, Imboden J, Shoback D, Stobo J. Role of T3 surface molecules in human T-cell activation: T3-dependent activation results in an increase in cytoplasmic free calcium. *Proc Natl Acad Sci USA* (1984) 81(13):4169–73. doi: 10.1073/pnas.81.13.4169

59. Trebak M, Kinet JP. Calcium signalling in T cells. *Nat Rev Immunol* (2019) 19 (3):154–69. doi: 10.1038/s41577-018-0110-7

60. Görlach A, Bertram K, Hudecova S, Krizanova O. Calcium and ROS: A mutual interplay. *Redox Biol* (2015) 6:260–71. doi: 10.1016/j.redox.2015.08.010

61. Kowaltowski AJ, de Souza-Pinto NC, Castilho RF, Vercesi AE. Mitochondria and reactive oxygen species. *Free Radical Biol Med* (2009) 47(4):333–43. doi: 10.1016/j.freeradbiomed.2009.05.004

62. Devadas S, Zaritskaya L, Rhee SG, Oberley L, Williams MS. Discrete generation of superoxide and hydrogen peroxide by T cell receptor stimulation: selective regulation of mitogen-activated protein kinase activation and fas ligand expression. *J Exp Med* (2002) 195(1):59–70. doi: 10.1084/jem.20010659

63. Jackson SH, Devadas S, Kwon J, Pinto LA, Williams MS. T cells express a phagocyte-type NADPH oxidase that is activated after T cell receptor stimulation. *Nat Immunol* (2004) 5(8):818–27. doi: 10.1038/ni1096

64. Kamiński MM, Sauer SW, Kamiński M, Opp S, Ruppert T, Grigaravičius P, et al. T cell activation is driven by an ADP-dependent glucokinase linking enhanced glycolysis with mitochondrial reactive oxygen species generation. *Cell Rep* (2012) 2 (5):1300–15. doi: 10.1016/j.celrep.2012.10.009

65. Belikov AV, Schraven B, Simeoni L. T cells and reactive oxygen species. *J Biomed Sci* (2015) 22:85. doi: 10.1186/s12929-015-0194-3

66. Kamiński MM, Röth D, Sass S, Sauer SW, Krammer PH, Gülow K. Manganese superoxide dismutase: a regulator of T cell activation-induced oxidative signaling and cell death. *Biochim Biophys Acta* (2012) 1823(5):1041–52. doi: 10.1016/j.bbamcr.2012.03.003

67. Hildeman DA, Mitchell T, Kappler J, Marrack P. T cell apoptosis and reactive oxygen species. *J Clin Invest* (2003) 111(5):575–81. doi: 10.1172/JCI200318007

68. Mak TW, Grusdat M, Duncan GS, Dostert C, Nonnenmacher Y, Cox M, et al. Glutathione primes T cell metabolism for inflammation. *Immunity* (2017) 46(4):675–89. doi: 10.1016/j.immuni.2017.03.019

69. Matsushita M, Freigang S, Schneider C, Conrad M, Bornkamm GW, Kopf M. T cell lipid peroxidation induces ferroptosis and prevents immunity to infection. *J Exp Med* (2015) 212(4):555–68. doi: 10.1084/jem.20140857

frontiers | Frontiers in Immunology

TYPE Review
PUBLISHED 03 November 2023
DOI 10.3389/fimmu.2023.1304281

OPEN ACCESS

EDITED BY
Daniela Latorre,
ETH Zürich, Switzerland

REVIEWED BY
Christian Muenz,
University of Zurich, Switzerland
Jens Geginat,
University of Milan, Italy

*CORRESPONDENCE
Olivia G. Thomas
olivia.thomas@ki.se

RECEIVED 29 September 2023
ACCEPTED 23 October 2023
PUBLISHED 03 November 2023

CITATION
Thomas OG and Olsson T (2023) Mimicking the brain: Epstein-Barr virus and foreign agents as drivers of neuroimmune attack in multiple sclerosis. *Front. Immunol.* 14:1304281. doi: 10.3389/fimmu.2023.1304281

Mimicking the brain: Epstein-Barr virus and foreign agents as drivers of neuroimmune attack in multiple sclerosis

Olivia G. Thomas[1,2]* and Tomas Olsson[1]

[1]Therapeutic Immune Design, Centre for Molecular Medicine, Department of Clinical Neuroscience, Karolinska Institute, Stockholm, Sweden, [2]Neuroimmunology Unit, Department of Clinical Neuroscience, Centre for Molecular Medicine, Karolinska Institute, Stockholm, Sweden

T cells have an essential role in adaptive immunity against pathogens and cancer, but failure of thymic tolerance mechanisms can instead lead to escape of T cells with the ability to attack host tissues. Multiple sclerosis (MS) occurs when structures such as myelin and neurons in the central nervous system (CNS) are the target of autoreactive immune responses, resulting in lesions in the brain and spinal cord which cause varied and episodic neurological deficits. A role for autoreactive T cell and antibody responses in MS is likely, and mounting evidence implicates Epstein-Barr virus (EBV) in disease mechanisms. In this review we discuss antigen specificity of T cells involved in development and progression of MS. We examine the current evidence that these T cells can target multiple antigens such as those from pathogens including EBV and briefly describe other mechanisms through which viruses could affect disease. Unravelling the complexity of the autoantigen T cell repertoire is essential for understanding key events in the development and progression of MS, with wider implications for development of future therapies.

KEYWORDS

autoimmunity, Epstein-Barr virus, T cell, multiple sclerosis, cross-reactivity, antibody, central nervous system, autoreactive B and T cells

Introduction

MS is the second most common cause of neurological disability amongst young adults after trauma affecting approximately 2.8million people globally (1). MS is more common in females with onset generally between 20 to 40 years of age, and occurs due to the formation of focal inflammatory demyelinating lesions in the CNS. Initial disease has a predominantly inflammatory component and approximately 85% of cases present with a relapsing-remitting phenotype, but over time accumulated damage and neurodegenerative mechanisms can lead to permanent disability. Genetic aetiology is estimated to be around 20-30% for MS with the remaining risk lying with stochastic events and environmental factors such as obesity, smoking, low serum vitamin D and EBV (2).

The brain and spinal cord, once thought to be an immune privileged compartment (3), are surveyed by patrolling T cells which guard against infection and also have roles in brain development and behaviour (4–8). However, the CNS is sensitive to inflammation-mediated damage and therefore, under healthy conditions, a carefully controlled balance is maintained between protection from infections and prevention of injurious inflammation. Loss or impairment of such CNS T cell immunosurveillance leads to an increased risk of CNS infections or malignancies (9).

Focal CNS lesions in early MS disease show widespread inflammatory infiltrates which contain a variety of immune cells including $CD4^+$ T cells, $CD8^+$ T cells B cells and monocytes. Genome-wide association studies (GWAS), as well as clinical therapeutic observations, indicate that T cells and B cells alongside innate immune cells have a key roles in MS neuroinflammatory mechanisms (10–15). The majority of MS-associated genes have functions in antigen presentation, cytokine production, proliferation, T helper (T_H) cell differentiation, co-stimulation, signal transduction and function. Associated polymorphisms have been identified in the human leukocyte antigen (HLA) locus as well as in *IL-2Rα*, *IL-7Rα*, *CXCR5*, *CD40*, *CD86*, *STAT3* and many other genes (15–17). However, the strongest known genetic risk factor associated with MS is the *HLA-DRB1*15:01* allele with an odds ratio (OR) of approximately 3 (15–18), and has also been shown to interact with multiple other environmental risk factors to increase risk further (19–24). The HLA locus also contains several other class II alleles which confer risk for developing MS and several identified HLA class I alleles which protect from disease such as *HLA-A*02:01* (17, 25). $CD4^+$ T cells recognise peptides presented in the context of HLA class II molecules, whereas $CD8^+$ T cells recognise class I-presented peptides. Given that the function of HLA is to present peptides to T cells for recognition via T cell receptors (TCR), the association of *HLA-DRB1*15:01* with MS development suggests a role for class II-presented peptides and autoreactive $CD4^+$ T cell responses and has led to substantial investigation of the autoantigens responsible for priming of pathogenic responses.

Early research established in particular the role of $CD4^+$ T cells which target these antigens due to several observations, such as the presence of CNS-infiltrating $CD4^+$ T cells in MS brain lesions, genetic risk conferred by *HLA-DR* and *HLA-DQ* alleles, increased experimental autoimmune encephalomyelitis (EAE) susceptibility of transgenic mice expressing MS-associated HLA class II molecules, and it is likely that $CD4^+$ T cells also contribute to MS pathogenesis via their influence on both adaptive and innate immune processes such as antibody production by B cells and $CD8^+$ T cell maturation.

To prevent production of T cells which can target self-tissues and trigger autoimmunity, T cells undergo central tolerance mechanisms in the thymus during their maturation, where cells expressing T cell receptors (TCRs) that bind strongly to peptide: HLA complexes on thymic epithelial cells and dendritic cells are negatively selected, and those that do not bind at all die by neglect (26). Additional mechanisms in the periphery also act to remove self-reactive T cells which escape central tolerance (27). Due to these mechanisms, TCRs which pass thymic tolerance quality control and bind foreign antigens generally have high affinity for their cognate antigen, however some responses may also have the ability to bind other peptides presented on HLA at different affinity which could include those from self-antigens. The classical view of T cells is that a single TCR expressed at the cell surface allows them to bind one peptide:HLA complex but the reality is that a single TCR can likely bind multiple peptides, and possibly also different HLA molecules (28). This existence of cross-reactivity might be an evolutionary advantage of a limited genome-encoded TCR repertoire against the myriad of possible peptide combinations which can occur in nature, estimated to be around 10^{15} possible peptides (29, 30). This T cell degeneracy indicates a potential for TCRs which were originally selected during exposure to prior foreign antigens to also bind self-peptides presented by HLA, and therefore the pathogens which we encounter throughout life shape both the memory T cell repertoire as a whole and also its autoreactive potential.

As well as T cells, there is strong evidence supporting a role for B cells in MS development, in particular due to the dramatic therapeutic effect of anti-CD20 therapies (11, 12). The reasons for which include B cell antigen presentation to T cells, production of pro-inflammatory cytokines, elimination of Epstein-Barr virus (EBV), and finally production of pathogenic autoantibodies – not in prime focus for this review. This review will discuss the current knowledge surrounding T cell specificity in MS, evaluating the existing evidence that CNS autoreactive responses may originally have been generated in response to non-self antigens and briefly describing other mechanisms through which viruses could affect disease.

Selected evidence for the role of T cells in MS

For many years $CD4^+$ T cells have been considered an important cell type involved in MS pathogenesis due to early observations in experimental autoimmune encephalomyelitis (EAE) – the animal model for MS – that CNS demyelinating disease can be transferred by adoptive transfer of myelin-reactive $CD4^+$ T cells (31, 32), and further evidenced by the observation that EAE cannot be transferred by antibodies alone. The role of $CD4^+$ T cells in MS has been further demonstrated by the strongest genetic susceptibility conferred by HLA class II alleles (15), susceptibility of HLA class II-carrying mice to demyelinating disease (33–36), presence of $CD4^+$ T cells in inflammatory brain lesions (37), and the involvement of $CD4^+$ T cells in several other arms of adaptive immunity such as antibody production and $CD8^+$ T cell maturation.

T_H1 and T_H17 $CD4^+$ T cells have been linked to MS disease with identification of these specific subsets in MS brain lesions and correlation of T_H1 cytokine-producing cells in peripheral blood with MS relapses (38–41). Further studies have also demonstrated a role for a unique intermediate population of T_H1-like T_H17 $CD4^+$ T cells in MS which are associated with relapse, predominant in the

CSF of early disease pwMS and can be isolated from MS brain lesions (42, 43). High avidity $CD4^+$ T cells with specificity for selected myelin antigens have also been shown to produce interferon-γ (IFNγ) and have a T_H1 phenotype in persons with MS (pwMS) (44–47). A clinical trial of a myelin basic protein (MBP) altered peptide ligand (APL) showed exacerbations in some MS patients, and further investigation showed cross-recognition between the APL and MBP driven by $CD4^+$ T cells which were skewed towards a T_H1 phenotype (45). In addition to T_H1, $CD4^+$ T cells with a T_H17 phenotype have also been detected in MS brain lesions and have been shown to be necessary for the development of EAE (48, 49). Follicular helper $CD4^+$ T cells (T_{FH}) cells provide help to B cells for their maturation, affinity maturation and antibody production, and germinal centre formation, and this essential link between humoral and cellular immunity makes them of key interest in MS pathology due to the involvement of B cells in disease. Activated T_{FH} cells have been shown to be increased in peripheral blood, their frequency correlated with disability and are detectable in brain lesions in MS (50–52).

The role of $CD8^+$ T cells is less clear though several observations suggest their involvement in MS such as high abundance in MS lesions, low or transient expression of HLA class I molecules on the surface of microglia, oligodendrocytes and neurons (53, 54), and observations that EAE does not develop in B2-microglobulin knockout mice (55). Several HLA class I associations with MS have also been identified, such as the strongest known protective alleles *HLA-A*02:01* and *HLA-B*38:01* (25) mentioned above, although untangling HLA associations with disease is notoriously difficult due to linkage disequilibrium and also other factors such as killer-immunoglobulin receptor (KIR) type, which can have a significant effect on immune activation in natural killer (NK) cell subsets (56). In addition, *HLA-A*02:01* protection against MS may be related to actions in the type I interferon system rather than peptide binding and activation of $CD8^+$ T cells (57). Myelin-reactive CD8+ T cells have also been characterised – although to a lesser extent than $CD4^+$ T cells – and have been isolated from both pwMS and healthy individuals. Studies of brain-infiltrating $CD8^+$ T cells in MS have shown their TCR repertoire to be oligoclonal, suggesting antigen-specific migration or expansion within the CNS (58, 59), and other studies have directly enumerated autoantigen-specific $CD8^+$ T cells from peripheral blood of pwMS (60, 61).

Mechanisms of pathogenic cross-reactivity

A long array of infectious agents have been associated with MS however the strongest evidence lies with EBV and – to some extent – human herpesvirus 6A (HHV-6A) (2, 62–65). In addition to this, the long-list of MS-associated autoantigens has grown in recent years which has broadened the focus of research in this area and led to some debate on which antigens and pathogens are pathologically relevant in neuroimmunological demyelinating disease (66–72). The association of these viruses and other pathogens in the context of the molecular mimicry with CNS autoantigens in MS will be discussed in this review.

MS has long been associated with previous EBV infection (73) and, while the exact mechanism remains to be fully characterised, the different theories have been summarised previously (65) (Figure 1). Despite uncertainty surrounding the sequence of events which eventually lead to MS, it has been established that EBV infection almost always precedes disease development. There is in fact a delay between infection and onset of neurological symptoms and also a lack of neurological symptoms in individuals with acute symptomatic EBV infection, also known as infectious mononucleosis (IM) (73–76). This interval between infection and neurological disease onset could potentially reflect a time delay between initial priming of pathogenic immune responses and epitope spreading within antigens or to new ones, which over time leads to inflammatory demyelinating disease. In support of this view, altered adaptive immune responses to EBV antigens have been identified in MS (77–80) and some have been found to cross-react with human proteins, leading researchers to conclude that molecular mimicry may have a key role in MS development.

Despite many links between viruses and MS, direct evidence that viruses can trigger molecular mimicry leading to initial CNS autoimmune demyelinating disease is lacking in humans. However, proof of concept was shown in an EAE model using recombinant Theiler's murine encephalomyelitis virus (TMEV) expressing a naturally occurring proteolipid protein (PLP) molecular mimic from *H. influenzae*. Early onset EAE could be induced in SJL/J mice by TMEV infection, but disease was not triggered when the same peptide was used to vaccinate in complete Freud's adjuvant, suggesting that virus activation of antigen presenting cells (APC) is necessary for disease development in this model (81). An additional study by Ji et al. used a recombinant Vaccinia virus expressing myelin basic protein (MBP) to trigger autoimmunity in $Rag2^{-/-}$ mice expressing an MBP-specific $CD8^+$ TCR (82). Disease was also triggered in mice after infection with the wild type Vaccinia vector which did not contain MBP but immunisation with peptide plus adjuvant only did not trigger disease, indicating that viral infection was necessary to break tolerance to CNS antigens in these models. A further study investigating the role of $CD8^+$ T cells used a mouse model where oligodendrocytes expressed ovalbumin (OVA) and showed that even high numbers of high avidity OVA-specific $CD8^+$ T cells could not induce EAE, and that these cells were in fact deleted from the immune repertoire to prevent autoimmunity under normal non-infected CNS conditions or during peripheral infection with OVA-expressing Listeria bacteria. In contrast, when mice were intracerebrally infected, OVA-specific $CD8^+$ T cells destroyed oligodendrocytes and induced demyelination (83).

These examples from EAE indicate that autoreactive T cell responses to myelin antigens are not solely sufficient to initiate CNS autoimmunity and that additional triggers are required to break tolerance, such as virus-mediated activation of APC or a blood-brain barrier permeabilisation event. In support of this view is the observation that myelin-specific T cells can be detected in healthy individuals (84, 85), however it could be that activation of these autoreactive T cells in the periphery through molecular mimicry to

foreign antigens skews them towards a pathogenic phenotype capable of migrating to and targeting CNS tissue (Figure 1).

Particular examples of cross-reactivity between CNS and foreign antigens in MS

A general problem with most descriptions of molecular mimicry T cell specificities is to know if these indeed have pathogenic roles or whether they represent innocuous epiphenomena, which is difficult to prove in humans. However, for some, there is epidemiological evidence for an association to disease and in the following paragraphs we discuss a set of autoantigen mimicry suspects. A full list of the foreign antigen cross-reactivity with CNS proteins discussed in this article is summarised in Table 1.

EBNA1 as a source of mimicry epitopes to Anoctamin-2, α-crystallin B and Glial cell adhesion molecule

Several studies have shown that elevated antibody responses to certain antigens from EBV are elevated in MS, in particular immunoglobulin G (IgG) responses to the EBNA1$_{380\text{-}440}$ region

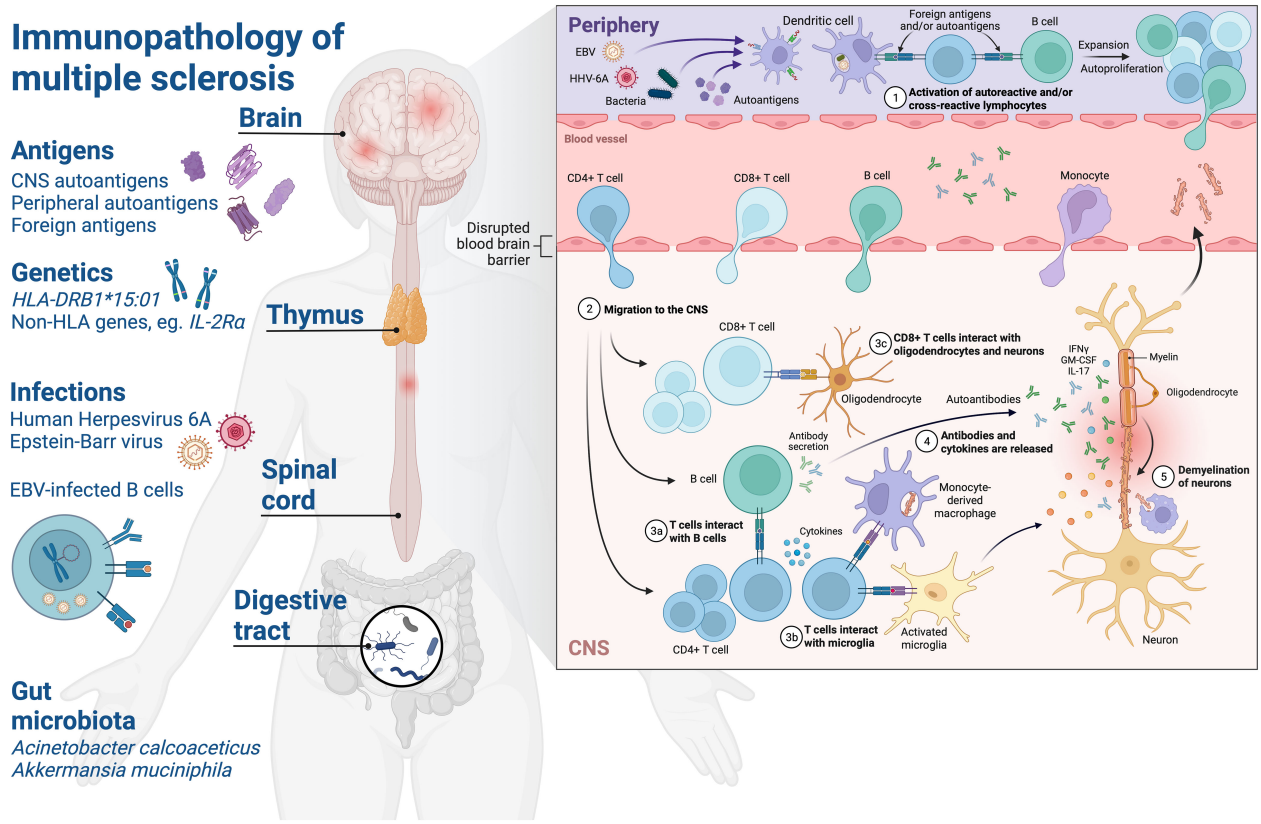

FIGURE 1
Schematic of the immunopathology of multiple sclerosis. Environmental and genetic factors affect development of neuroinflammatory mechanisms in MS. Exposure to foreign antigens primes humoral and cellular immune responses with cross-reactivity to self-antigens in the CNS. Human leukocyte antigen (HLA) – HLA-DRB1*15:01 – on the surface of APC present foreign or autoantigen peptides and shape the CD4$^+$ T cell repertoire via central tolerance mechanisms in the thymus. Infections such as EBV and HHV-6A are associated with increased MS risk and drive elevated antibody responses to viral proteins which have been observed in pwMS, such as increased EBNA1-specific antibodies. The role of the EBV-infected memory B cell compartment in MS is not fully understood, but may be attributed to several factors which could predispose to autoimmunity such as: providing a source of molecular mimicry epitopes throughout life which can prime pathogenic and cross-reactive CD4$^+$ T cell and antibody responses, processing and presentation of antigens to prime T cells, production of proinflammatory cytokines, rescuing of autoreactive B cells from apoptosis and/or modulation of innate and adaptive immune mechanisms via expression of viral immune evasion proteins. Gut microbiota associated with MS such as Acinetobacter calcoaceticus and Akkermansia muciniphila may influence CNS autoimmunity by providing molecular mimicry epitopes or driving a proinflammatory milieu which could lead to breakdown of immune tolerance via bystander activation of autoreactive T and B cells. (1) Priming of T cells and B cells with reactivity to foreign antigens and/or autoantigens in the periphery, autoproliferation is driven via interactions between T cells and B cells in pwMS and leads to clonal expansion. Elevation of antibodies with reactivity to viral and/or autoantigen in the periphery. (2) Blood-brain barrier alterations lead to migration of lymphocytes to the CNS where they mediate inflammation. (3) CD4$^+$ T cells interact with B cells and activated microglia in the CNS, CD8$^+$ T cells interact with neurons and oligodendrocytes via HLA class I molecules. (3) Antibodies and cytokines are released driving inflammation and lesion formation. (4) Breakdown of myelin sheaths leads to neuronal axonal damage and demyelination over time. CNS, central nervous system; HLA, human leucocyte antigen; EBV, Epstein-Barr virus; HHV-6A, Human herpesvirus 6A; IFNγ, interferon-γ; IL-2Rα, interleukin-2 receptor α; IL-17, interleukin-17; GM-CSF, granulocyte macrophage stimulating factor. Created with BioRender.com.

TABLE 1 Selected molecular mimicry between foreign and host CNS antigens in MS.

Autoantigen	Human T cell response	Human B cell/anti-body response	EAE	T cell molecular mimicry	B cell/anti-body molecular mimicry
Myelin oligodendrocyte glycoprotein (MOG)	(45, 85–92)	(87, 93–97)	(98–103)	Human NFM (104)	Butyrophilin (105, 106), HERV-W (*in vitro* only) (107), Influenza-A virus haemagglutinin (108), *Acinetobacter* sp. 3-oxo-adipate-CoA-transferase subunit A (EAE) (93)
Proteolipid protein (PLP)	(45, 47, 109–113)	(94, 113–116)	(117, 118)	Human coronavirus 229E (119), Human coronavirus OC43 (119), *A. castellanii* (EAE model) (120), *H. influenzae* (EAE model) (81, 121), *S.cerevisae* (CD8+) (122)	-
Myelin Basic protein (MBP)	(45, 46, 123–129)	(93, 94, 97, 116, 128, 130, 131)	(36, 102, 103, 132–134), HBV polymerase molecular mimicry (135)	EBV BALF5 (136–138), Herpes simplex UL15 (136), Herpes simplex DNA polymerase (136), Adenovirus type 12 ORF (136), *Pseudomonas* sp. phosphomannomutase (136), HPV type 7 L2 (136), Influenza type A HA (136), Reovirus type 3 sigma 2 protein (136), EBV EBNA1 (EAE) (139), EBV LMP1 (EAE) (140), HHV-6 U24 (141), Human coronavirus 229E (119, 142), Human coronavirus OC43 (119), human and bacterial GDPLFS (70), Vaccina virus (EAE) (82), large T antigen JC virus (EAE) (143), Herpesvirus saimiri (EAE) (144), Cpn0483 *C. pneumoniae* (EAE, rat MBP) (145).	EBV EBNA1 (139, 146), EBV LMP1 (140, 147), *Acinetobacter* sp. 4-CMLD (EAE) (93), *P. aeruginosa* γ-CMLD (93)
α-crystallin B (CRYAB)	(69, 148)	(69, 94, 97, 149, 150)	Priming in EAE (69) (103, 151),	–	EBV EBNA1 (69, 152)
Glial cell adhesion molecule (GlialCAM)	(153)	(153)	(153)	–	EBV EBNA1 (153)
Anoctamin-2 (ANO2)	–	(67, 68)	-	–	EBV EBNA1 (68)
RAS guanyl releasing protein 2 (RASGRP2)	(71, 72)	-	-	HLA-DR (71), EBV BPLF1 (71), EBV BHRF1 (71), *A. muciniphila* (71), HLA-DR-derived self-peptides (71)	-
GDP-L-fucose synthase (GDPLFS)	(70, 92)	-	-	Bacterial GDPLFS (70), MBP (70)	-
HLA-DR-derived self-peptides	(71)	–	–	RASGRP2 (71), EBV BHRF1 (71), EBV BPLF1 (71), *A. muciniphila* (71)	–
Myelin-associated glycoprotein (MAG)	-	(94, 97, 154)	(102)	–	Bovine casein (154)

have a MS odds ratio of approximately 8 and have also been shown to interact with *HLA-DRB1*15:01* to increase disease risk further (19, 24, 64). In addition, elevated serum neurofilament levels have been shown to positively correlate with EBNA1 IgG in MS, indicating that there is a relationship between CNS injury and humoral responses to EBNA1 which occurs before disease onset (73). However it is not fully understood what is causing elevated EBNA1 antibody responses in MS and, as this elevation is specific to MS and interacts with *HLA-DRB1*15:01*, may suggest that molecular mimicry with CNS antigens are driving the EBNA1 antibody response. In support of this view, several epitopes within the MS-associated EBNA1 region have been identified with similar amino acid sequences to CNS autoantigens (68, 69, 139, 153). On the other hand, increased EBNA1 antibody responses in MS may be due to a frustrated EBV-specific immune response, where *HLA-DRB1*15:01* is a poor class II allele in the context of EBV immune control. In one study humanised mice that were immune reconstituted from *HLA-DRB1*15:01*$^+$ donors had increased steady state activation of CD4$^+$ and CD8$^+$ T cells and poor virus control evidenced by high EBV viral loads, compared to mice which were reconstituted with an allele not associated with increased MS risk (155). These findings suggests a synergistic interaction between EBV infection and *HLA-DRB1*15:01* which primes a hyperactive adaptive immune compartment, leading to poor viral control and

facilitating the generation of cross-reactive pathogenic T cell responses.

A-crystallin B (CRYAB) is a small heat shock protein which is expressed in oligodendrocytes and has been shown to have paradoxical roles in MS: both in protection from harmful inflammatory innate immune mechanisms via chaperone activity and also conversely as the target of adaptive T cell responses in a proinflammatory environment (148–150, 156). This multifaceted role somewhat confounded the MS field and cast doubt on CRYAB's role as an autoantigen in MS, however antibody responses to CRYAB were recently revisited in a large Swedish cohort and showed 27.6% of pwMS and 16.9% of controls to have IgG responses to CRYAB peptides with homology to EBNA1, and were associated with MS (OR=1.98) (69). Risk was further increased with an OR of 8.99 when combined with high EBNA1 IgG responses in individuals. Reciprocal blocking experiments showed that CRYAB IgG responses were blocked when the homologous EBNA1 epitope was spiked into sera, and the core homologous epitope between these antigens was mapped to a RRPFF motif at $CRYAB_{11\text{-}15}$ and $EBNA1_{402\text{-}406}$. Similarly, another group identified cross-reactive antibodies targeting the RRPFF motif in oligoclonal bands of pwMS (152), and interestingly the CRYAB sequence contains a PxxP motif similar to that found in MBP and several antigens from herpesviruses discussed later in this review. In addition, the high frequencies of EBNA1- and CRYAB-specific T cells observed in natalizumab-treated pwMS produced IFNγ and immunisation of mice with CRYAB or EBNA1 protein elicited T cell responses to the reciprocal antigen, also indicating cross-reactivity on the T cell level (69). The role of CRYAB as an autoantigen is complex and autoantibodies such as those that target intracellular antigens may not be directly pathogenic, however generation of high affinity antibodies depends on T cell help, and therefore they could be markers of a T cell response which is able to target intracellular antigens in autoimmune disease. In support of this view, B cells have been shown process and present epitopes from the antigen that they have Ig specificity with greater efficiency to T cells which have TCRs that respond to the same antigen (157). In addition, LMP1 expression has been shown to enhance antigen presentation and co-stimulation in EBV-transformed B cells via CD70, OX40 ligand and 4-1BB, which may have a role in priming of pathogenic autoreactive T cell responses (158).

The presence of CRYAB IgG in only a subset of pwMS suggests involvement of other autoantigens in the non-responders, and a recent study by Lanz et al. identified clonally expanded plasmablasts in the CNS of pwMS and identified their target epitope as a sequence shared between EBNA1 and glial cell adhesion molecule (GlialCAM) (153). These antibodies bound a core epitope within the MS-associated region of EBNA1 at residues 394-399 which is directly next to the CRYAB homologous epitope and cross-reacted with $GlialCAM_{377\text{-}383}$, again both sequences contain PxxP motifs. In addition to this, the authors noted that affinity for the GlialCAM epitope was increased with the phosphorylation of the serine residue at position 376, and increased antibody reactivity to these core epitopes was also demonstrated in the plasma of pwMS compared to controls. SJL/J mice which were initially immunised with $EBNA1_{386\text{-}405}$ peptide had a worse EAE disease course compared to a scrambled peptide control and the mice developed antibody responses to GlialCAM indicating generation of cross-reactive responses. Also similar to CRYAB, GlialCAM is expressed by oligodendrocytes and astrocytes in the CNS and is also present in chronic active lesions of MS (159, 160). Whilst no study so far has investigated both GlialCAM and CRYAB responses in individuals, it would be interesting to understand whether pwMS have responses to both antigens or whether these are restricted by different HLA. It is possible that the close proximity of these epitopes could lead them to be differentially processed and presented on surface HLA, or it could lead to their restriction by the same HLA.

Anoctamin-2 (ANO2) is a calcium-activated chloride channel with 8 membrane-spanning domains which is predominantly expressed in neurons and glial cells in the CNS, and also has high expression in the retina and in MS lesions (67). ANO2 was identified as a target of autoantibodies in MS in a large screening study and responses were found to be positively associated with *HLA-DRB1*15:01*, with an adjusted OR of 17.3 (67). Furthermore, combination of several risk factors including ANO2 IgG positivity, high EBNA1 IgG, presence of *HLA-DRB1*15:01* and absence of *HLA-A*02:01*, produced a combined OR of over 26 (68). A later study went on to confirm the association of ANO2 IgG with MS in a larger cohort of almost 16,000 individuals, and identified cross-reactivity of $ANO2_{140\text{-}149}$ antibody responses with $EBNA1_{431\text{-}440}$ which is also in the MS-associated region (68). In addition to *HLA-DRB1*15:01*, 14 other HLA alleles were found to be associated with ANO2 IgG levels, indicating that epitopes from ANO2 can be presented by multiple different HLA and providing indirect evidence that there may also be ANO2 T cells in MS. Interestingly the strongest HLA effect on ANO2 IgG levels was a protective effect for *HLA-DRB1*04:01*, which the authors speculate could be due to increased elimination of high affinity ANO2-specific T cells in the thymus; the same effect was also observed for EBNA1 IgG levels, again indicating potential cross-reactivity on the T cell level.

Given that EBNA1-specific antibodies have now been reported in several studies to cross-react with multiple human proteins including MBP (discussed later in this review), CRYAB, GlialCAM and ANO2 (68, 69, 139, 146, 153), all of which were found to be elevated in pwMS and were associated with disease, what evidence is that EBV infection may have triggered these responses? Tengvall et al. showed that ANO2 IgG responses could be detected in a pre-MS cohort (68), indicating that responses appear before clinical onset of disease, an observation that has also been published for EBNA1 IgG (73). Additionally, it is very rare to detect antibody responses to ANO2, GlialCAM and CRYAB in individuals without evidence for a prior EBV infection, particularly EBNA1 IgG, indicating that EBV infection may be a prerequisite for the development of these autoantibodies and implying that molecular mimicry may be driving development of these responses. Presence of a CRYAB IgG response was also shown to be negatively correlated with ANO2 IgG in individuals, suggesting that these autoantibodies likely do not develop in the same individuals which could be due to factors such as HLA type (69) and that different autoantigens lead to MS disease in individuals.

However, the autoantibodies with cross-reactivity to EBNA1 described above were each only detected in a relatively small subset of pwMS, suggesting that these cross-reactive antibodies are not

necessary for disease in all patients. It is likely that further undiscovered autoantigen cross-reactivity exists or it could be that the cross-reactive antibodies are not themselves pathogenic in the majority of MS cases, but are instead biomarkers for a T cell response which is responsible for mediating autoimmune damage, as has been observed for other autoimmune diseases such as Addison's disease and diabetes mellitus (161, 162). Additionally, GlialCAM and ANO2 epitopes are both within intracellular domains and CRYAB is expressed intracellularly and are therefore not exposed, making it difficult to assume direct autoantibody-mediated damage to the CNS; although this cannot necessarily be excluded as several examples exist of pathogenic autoantibodies which bind intracellular targets such as GAD65, proinsulin and IA-2 in diabetes (163). Plasmapheresis is only therapeutically effective in a subset of MS patients (164) which suggests that it is not the antibodies themselves that are responsible for MS disease but the pathogenic T cell responses that they mark. Although positive responses to plasmapheresis in patients with histological lesion patterns type I and II, and particularly in individuals who showed signs of a humoral response, could indicate that autoantibodies drive disease in some individuals (165). In addition to this, evidence for T cell responses to EBNA1 mimics has been shown both in EAE immunisation models and in humans (69, 139, 153) and, although no direct evidence for cross-reactivity on the single T cell level has been so far shown, this is likely to be present, although the potential relevance of these responses to MS development and progression remains to be determined.

Other scant reports of further antibody cross-reactivity between EBV proteins and autoantigens have been described such as that of EBNA1 IgG with heterogeneousnuclear ribonucleoprotein L (HNRNPL) (166), although these were not found to be increased in the plasma of pwMS compared to controls. Antibody cross-reactivity has also been reported for BFRF3 with septin-9 and BRRF2 with the mitochondrial protein dihydrolipoyllysine-residue succinyltransferase (DLST), although again these responses were only in a subset of patients and need to be confirmed in larger cohorts (167). As with most of these reports, validation in large cohorts are required to identify the frequency of these responses in patients and their relevance to neuroinflammatory disease, however the mounting reports of cross-reactivity between EBV and self-antigens suggest that there are multiple disease relevant autoantigens in MS and that each individual may have specific profiles of reactivity.

Another potential consideration is the promotion of tolerance breakdown and molecular mimicry by EBV-mediated immune dysregulation. EBV encodes several viral mimics of human proteins with essential roles in immunity and have evolved over thousands of years to facilitate viral escape from the immune system, and one such example is the viral CD40 mimic latent membrane protein 1 (LMP1). CD40 is a co-stimulatory molecule expressed on APC and is particularly essential for B cell activation via its function as a co-receptor for the B cell receptor (BCR), interaction with CD40 ligand (CD40L) on T cells and amplification of innate mechanisms such as TLR signalling (168–172). LMP1 has been demonstrated to self-aggregate and facilitate downstream signalling in B cells with promote activation, germinal centre formation and production of cytokines and antibodies (173). One study of a transgenic mouse model which constitutively expressed the cytoplasmic tail of LMP1 showed that animals were prone to autoantibody production and immune dysregulation but had no signs of clinical disease (174). However, when these animals were immunised with EBNA1, they showed markedly increased inflammatory cellular and humoral responses compared to animals without LMP1 with T cells producing IFNγ and IL-17 cytokines. Additionally, expression of LMP1 was shown to drive molecular mimicry between EBNA1 and the systemic lupus erythematosus-associated autoantigen Sm (174). Incidentally, the Sm-homologous epitope is at $EBNA1_{398\text{-}404}$ and overlaps almost identically with the region reported to contain homology to GlialCAM and CRYAB in MS (69, 153). Whilst the authors do not report increased neurological symptoms in these animals, it would be pertinent to also investigate whether transgenic expression of LMP1 also facilitates molecular mimicry with CNS autoantigens.

Other EBV-encoded mimics of host antigens include BCRF1 which contains homology to interleukin-10 (IL-10) and BHRF1 which is a mimic of Bcl-2, proteins which limit host immune responses to pathogens and promote survival of infected B cells respectively (175, 176). In addition to this, multiple EBV proteins have been shown to modulate antigen processing and presentation in infected B cells, suggesting even further ways in which the virus may shape adaptive immune responses to mimicry epitopes (176–179), and this is an avenue in which there has been very little research in the context of autoimmunity. Given these observations, one can easily imagine how high expression of EBV-encoded immune mimics and modulators such as LMP1 during acute infection or IM may facilitate the breakdown of tolerance, and indeed history of IM has been demonstrated to increase MS risk (19, 22, 23). Of further relevance to MS immunopathology is how EBV-mediated modulation of immunity differs throughout life from childhood to adolescence given the increased risk of developing MS with delayed EBV primary infection (62). For example, studies in mice have shown that a specific population of early-differentiated natural killer (NK) cells expand prior to CD8+ T cells and is involved in virus control during early infection (180, 181). Further study of the analogous population in humans showed that early differentiated NK cells diminished with age and may be involved in protection of children from EBV infection and IM (182). Furthermore, proliferative and cytokine production of $CD56^{BRIGHT}$ NK cell have been demonstrated to be diminished in pwMS (183) indicating that this population may also be impaired in its response against EBV, but further study of NK cell function in pwMS are needed to establish their relevance.

It is evident that cross-reactivity occurs between CNS and viral antigens, however the time and space of exposure to virus antigens may be one of the key determinants for developing MS. Indeed, does EBV's unique life cycle and persistence in the B cell compartment throughout life mean that this virus is uniquely positioned to trigger CNS autoimmunity? Evidence for this could be derived from observations that the T cell and antibody response

to EBNA1 only emerge 3-6 months post primary infection (184) and the delay also exists between seroconversion and development of MS in individuals (74).

Myelin basic protein

Proof of concept that virus peptides could induce CNS autoimmunity to was shown by Fujinami and Oldstone in 1985, where rabbits immunised with either MBP or a homologous peptide from Hepatitis B virus (HBV) polymerase developed EAE (135). Since then, multiple studies in both human and animal models have demonstrated the ability of T cells generated against MBP to target other antigens.

T cell molecular mimicry between myelin and EBV antigens in humans was first reported by Wucherpfenning and Strominger who isolated T cell clones which responded to $MBP_{85\text{-}99}$ (136). Amongst the epitopes which activated the $MBP_{85\text{-}99}$-specific T cell clones was a peptide from EBV DNA polymerase ($BALF5_{627\text{-}641}$) in the context of MS-associated alleles *HLA-DRB1*15:01* and *HLA-DRB5*01:01* respectively, and these clones were subsequently tracked to the cerebrospinal fluid (CSF) of patients and the TCR:peptide-HLA structure solved (137, 138). This cross-recognition of BALF5 and MBP peptides in the context of different HLA molecules demonstrated that TCRs can even recognise different complexes as long as there is similar overall structure and charge of residues. Interestingly, the same study showed that $MBP_{85\text{-}99}$-specific T cell clones were also activated by multiple other viral and bacterial epitopes – some of them with no clear amino acid homology to the original MBP peptide – including peptides from human papilloma virus (HPV), herpes simplex virus and influenza A virus amongst others (136).

The long-established association of elevated EBNA1 IgG with MS suggests that this response may have a role in disease pathology. Early research by Bray et al. discovered two homologous epitopes in EBNA1 and MBP and isolated antibodies with specificity for the MBP-homologous EBNA1 epitope from oligoclonal bands in the cerebrospinal fluid (CSF) of 85% pwMS in their cohort (146). This provided early evidence that, rather than simply biomarkers, elevated EBNA1-specific IgG responses may target myelin and have a role in MS disease mechanisms. A later study identified antibody responses to $EBNA1_{411\text{-}426}$ which were specific to untreated MS-patients and were also able to bind $MBP_{205\text{-}224}$ (139). Whilst the study cohort was small, IgG responses to $EBNA1_{411\text{-}426}$ were higher in untreated pwMS but low/no responses could be detected in individuals undergoing interferon-β therapy. Furthermore, mice immunised with $EBNA1_{411\text{-}426}$ amounted both T cell and antibody responses to MBP, despite low amino acid sequence homology between these two regions (139). Whilst this data from a mouse model is intriguing and suggests T cell cross-reactivity, there are currently no examples of dual-reactive human EBNA1-specific T cells which have been investigated on the single cell level. It is also important to note that oligoclonal bands in MS have been shown to contain specificities for multiple viruses in addition to EBV EBNA1, and therefore there is some debate around their role in CNS autoimmunity (185), however EBNA1 remains a top candidate for molecular mimicry.

Sequence similarity between MBP and the EBV latent antigen LMP1 was also identified by a small study which used phage display to recreate clones from B cells in peripheral blood of pwMS (147). Reverse engineering of sequences from MBP-specific antibody variable domains showed similarity to previously identified LMP1-specific antibody sequences, and were subsequently found to bind recombinant LMP1 by Western blot. Further *in vivo* analysis showed that MBP- or LMP1-immunised mice produced antibody responses to the reciprocal antigen, and comparison of responding B cell repertoire clonality was suggestive of greater epitope spreading in the LMP1-immunised animals (140). $CD4^+$ T cells from LMP1-immunised mice also showed proliferation following *in vitro* MBP re-stimulation suggesting cross-priming of T cell responses *in vivo* (140). Despite these findings, no obvious amino acid homology exists between MBP and LMP1 antigens, however this does not necessarily exclude the presence of structurally similar epitope/s as has been previously shown (186). However, as for EBNA1 T cell responses, comprehensive analysis of LMP1-specific adaptive responses in MS cohorts is needed to determine the relevance of this cross-reactivity for disease pathogenesis.

Epidemiological evidence has also linked HHV-6A to increased risk for developing MS, and antibody responses to immediate early protein 1 (IE1) from HHV-6A in a pre-MS cohort showed an increased MS risk with an OR of 2.22 (63). Interestingly, this effect was only observed for IE1 IgG responses to HHV-6A and not for the HHV-6B strain which was instead negatively associated with disease (OR=0.74) (63). As the study used sequence variation in IE1 to distinguish between infection with HHV-6A and 6B, it is so far not known whether the risk associated with HHV-6A IE1 IgG responses is due to the IE1 response itself or the virus that it marks. However, a previous study by Tejada-Simon et al. identified dual-specific T cell responses with reactivity to $MBP_{96\text{-}102}$ epitope and HHV-6 $U24_{4\text{-}10}$ which share 6 out of 6 identical amino acids across a PxxP motif (141). Approximately 50% of T cells which responded to MBP also responded to this HHV-6 U24 epitope and produced predominantly T_H1 cytokines and patients with dual-specific responses also had increased antibody titres to both peptides, indicating a direct link between dual-specific cellular and humoral responses to the same epitopes (141). HHV-6A and B strains share over 90% sequence identity and the U24 PxxP amino acid motif which is relevant for cross-recognition with MBP is conserved between both A and B strains. However, different phosphorylation patterns in the MBP-homologous U24 region may affect immune recognition of this epitope or interaction with cellular proteins (187). Alternatively, the difference in MS risk between these strains could be due to increased susceptibility to HHV-6A infection of KIR2DL2-carrying MS patients or to U24-mediated disruption of MBP-Fyn interactions which stabilise myelin (188, 189), and further research is needed to elucidate the exact mechanisms of HHV-6A in MS.

Proof that a virus peptide with homology to a myelin antigen with a core of only 5 amino acids could induce disease in EAE was first demonstrated in by Gautam et al. in 1998, where a PxxP motif

peptide from Herpesvirus Saimiri with amino acid homology to MBP_{1-11} was able to induce disease in EAE (144). PxxP amino acid motifs can be found in MBP and multiple other proteins from herpesviruses such as HHV-6 U24, Human Herpesvirus 7 (HHV-7) U24, human Cytomegalovirus (HCMV) UL25 and UL42, Varicella Zoster Virus (VZV) ORF0, Herpes Simplex Virus-1 (HSV-1) UL56 and EBV LMP2A – the latter of which contains four PxxP motifs (189). These viruses are all in the Herpesviridae family and persist in the human host throughout life, although they have vastly different cell tropisms and immune evasion mechanisms which may affect the availability of antigens to prime responses. As previously mentioned, several of these viruses are associated with MS risk – with EBV and HHV-6A showing increased odds ratios (62, 63, 190) whilst CMV is associated with protection (191, 192). So far, T cell molecular mimicry has only been identified between HHV-6 U24 and MBP in humans, and it is possible that sequence of infection with these viruses throughout childhood and early adulthood shapes the T cell repertoire, predisposing some individuals to CNS autoimmunity through cross-reactivity. Further research is needed to establish the relevance of cross-reactive MBP PxxP motifs with viral antigens, and in particular how this might develop throughout challenge with multiple homologous epitopes from viruses.

It seems evident that multiple virus infections have the potential to induce immune responses which cross-recognise MBP, however this may be in part due to pre-existing T cells in the periphery with low to moderate avidity for MBP which escape thymic tolerance mechanisms, despite some expression of MBP in the thymus (193, 194). The escape of MBP-specific T cells from negative selection during central tolerance may be due to the generally lower avidity with which MBP peptides bind to *HLA-DRB1*15:01* rendering them unstable, and peptides from MBP have also been reported as promiscuous binders to multiple HLA class II alleles (123, 195, 196). One study demonstrated the ability of an MBP-specific TCR to bind peptide:HLA with a wide range of orientation angles which is possibly due to the scarcity of hydrogen bonds between at the TCR:peptide interface, and this low affinity interaction may explain TCR degeneracy and escape from thymic negative selection (197). MBP-specific T cells can also be detected in healthy individuals which suggests that they occur naturally but are less frequent, have a less pathogenic phenotype, do not gain access to the CNS or are prevented from causing disease by regulatory or other mechanisms under normal conditions (46, 124, 198–202). Differences in MBP peptide immunodominance have also been identified between pwMS and controls (40, 124) although other studies have found no changes in peptides targeted (109, 203, 204). However, it is plausible that environmental exposure to pathogens which contain molecular mimics to MBP – such as to Herpesviruses – could prime or skew responses to different epitopes with higher potential to cause CNS inflammation leading to MS development; so far there is only sero-epidemiological evidence supporting for a role for EBV in MS and to some extent HHV-6A.

More recently, microbiome studies in MS cohorts have led researchers to investigate elevated antibody responses to some bacterial species – such as *Acinetobacter calcoaceticus*, *Akkermansia muciniphila* and *Pseudomonas aeruginosa* – for potential molecular mimicry (205, 206). These studies showed that antibodies from pwMS with reactivity to MBP_{43-57} could bind to epitopes from both *A. calcoaceticus* and *P. aeruginosa* 4- and γ-carboxymuconolactone decarboxylase (CMLD) respectively (93). A similar homology between myelin oligodendrocyte glycoprotein (MOG) and 3-oxo-adipate-CoA-transferase subunit A from *Acinetobacter* species was identified (93), however only the MOG_{43-57}-immunised animals showed any sign of disease activity in ABH mice and disease could not be induced by immunisation with the homologous bacterial peptides. On the other hand, molecular mimicry is not the only mechanism through which these bacteria have been suggested to play a role in MS, and studies have shown that *A. calcoaceticus* and *A.muciniphila* species are increased in the gut microbiota of pwMS. Mice which are mono-colonised with these bacterial species have a more severe EAE disease course and produce more proinflammatory adaptive immune responses with fewer IL-10-producing regulatory T cells (T_{REG}) (207). In theory, induction of a proinflammatory environment by these bacteria in the MS host could help to skew pre-existing molecular mimicry responses to a pathogenic phenotype which could lead to or influence progression of CNS autoimmunity.

Proteolipid protein

PLP is the most abundant protein in myelin and has two main isoforms: the full-length version which is almost exclusively expressed in the CNS, and the slightly shorter DM20 variant which is missing a loop of 35 amino acids and is only expressed in the periphery, thymus and lymph nodes (208, 209). The sequence excluded from the thymus-expressed DM20 variant contains the immunodominant $PLP_{139-151}$ epitope which is a strong encephalitogen in some EAE models such as SJL/J (117, 210). SJL/J is a mouse model which is strongly predisposed to develop EAE with epitope spreading during subsequent relapses to other PLP epitopes and to MBP (117, 210). $PLP_{139-151}$ is a frequent target of high avidity T cells in MS (45) – most likely due to its exclusion from thymic tolerance mechanisms – but several other encephalitogenic PLP peptides have been identified in humans such as $PLP_{104–117}$, $PLP_{142–153}$, $PLP_{184–199}$, and $PLP_{190–209}$, all of which can be presented by the MS risk allele *HLA-DRB1*15:01* (47, 109). PLP is also the target of antibody responses, with up to 58% of pwMS in some studies showing antibody responses which are sensitive to protein conformation (114, 115).

Although fewer examples of CNS cross-reactivity between PLP and non-self antigens have been reported than for MBP, homology between human coronaviruses (HCoV) and PLP led to the isolation of several T cell clones from pwMS with dual-specificity for PLP and HCoV 229E and OC43 strains. Clonality and TCRVβ chain usage off cross-reactive T cell clones was confirmed, although the study did not enumerate frequency of these cells in peripheral blood of pwMS (119). The relevance of HCoV T cell molecular mimicry with CNS antigens is not certain and so far no further studies have replicated these findings with no large-scale sero-epidemiological studies have been presented. However, several reports globally of new MS cases and disease exacerbations following severe acute respiratory syndrome coronavirus 2 (SARS-CoV-2) infection or

vaccination could suggest that exposure to SARS-CoV-2 antigens may trigger autoimmune attack on the CNS in some individuals (211), although there is currently no published functional evidence to support this. However, a recent *in silico* study showed that the nucleocapsid protein from SARS-CoV-2 shares significant overlap with several MS-associated myelin proteins including PLP (212), although this has not yet been investigated *in vitro*. On the other hand, increased numbers of MS cases following SARS-CoV-2 exposure could be attributed to bystander activation of pre-existing myelin-reactive T cells, or simply chance occurrences due to the immense number of people who were infected or vaccinated during the global Covid-19 pandemic. Further investigation is warranted to determine if cross-reactivity between coronavirus and neuronal antigens occurs *in vivo*.

As for MBP, sequence similarity between PLP and bacterial antigens have been reported, and one study demonstrated that EAE could be induced by both immunisation with $PLP_{139-151}$ peptide or with homologous epitopes from *Haemophilus influenzae* and *Acanthamoeba castellanii* (81, 120, 121). The homologous peptide from *A. castellanii* was able to induce EAE in SJL/J mice and interestingly adoptive transfer of *A. castellanii*-specific T cells from female mice could also induce disease, however the same T cells derived from males could not (120). Further investigation of the PLP-homologous epitope from *H. influenzae* showed that induction of EAE required delivery of the pathogenic epitope in a recombinant Theiler's encephalomyelitis virus (TMEV) vector, suggesting that CNS autoimmunity requires virus-specific activation of innate immune mechanisms in APCs such as Toll-like receptors (TLR) to fully break immune tolerance and lead to disease (81). In addition, further study of this model showed that mice infected with the recombinant *H. influenzae* TMEV had a T_H1 $CD4^+$ response to the homologous $PLP_{139-151}$ peptide but no epitope spreading to $PLP_{178-191}$. This was in contrast to the $PLP_{139-151}$ TMEV, where epitope spreading to $PLP_{178-191}$ could be detected and marked initial disease relapse in the SJL/J model (213). Amino acid substitution in the primary contact residue of $PLP_{139-151}$ removed the ability of the virus to induce early EAE and therefore indicated that this residue was necessary for induction of pathogenic $CD4^+$ T cell responses which drive early disease (121). Together these data indicate the strong adjuvant effect of viruses on autoreactive responses which are able to induce pathogenic T_H1 $CD4^+$ responses with rapid onset disease when combined with molecular mimics to myelin antigens. However, in this model epitope spreading readily occurred between PLP epitopes and mediated disease relapse and/or progression but this was not achieved between the foreign peptide and PLP. This suggests that further factors may be needed to sustain chronic CNS autoinflammation and long-term disease in this setting.

Although current evidence suggests a more important role for $CD4^+$ T cells in MS pathogenesis, the high abundance of $CD8^+$ T cells in MS lesions and oligoclonal TCR repertoires suggest that these expand and may be antigen-specific (58, 59). However, other studies have also shown myelin-specific $CD8^+$ T cells to be present in peripheral blood at the same frequency in pwMS as in healthy individuals (214). The generally higher avidity of $CD8^+$ TCR interactions with peptide:HLA and lower degeneracy of $CD8^+$ T cells make cross-reactivity in this compartment less likely (215), features which perhaps emerged via evolution in order to limit cross-reactive responses with the ability to bind peptide:HLA class I complexes that are expressed almost ubiquitously on nucleated cells. However, examples of $CD8^+$ T cell cross-reactivity do occur and Honma et al. described a *HLA-A*03:01*-restricted $CD8^+$ T cell clone with specificity for PLP_{45-53} that could cross-recognise a peptide from *Saccharomyces cerevisae* in the context of *HLA-A*02:01* (122). Although infrequent reports of myelin-reactive $CD8^+$ T cell degeneracy may be in part due to the focus on $CD4^+$ T cells in the MS research field. However, evidence from TCR sequencing of blood, CSF and MS lesions all suggest a clonal expansion of the $CD8^+$ compartment in MS which may indicate migration of antigen-specific $CD8^+$ T cells to the CNS during disease (58, 59), although the targets remain to be characterised and these could equally have a regulatory or suppressive phenotype. Interestingly, acute EBV infection – also known as infectious mononucleosis (IM) – is also characterised by enormously expanded oligoclonal $CD8^+$ T cell repertoires directed against EBV antigens which subside over several weeks to months (216–218), however how these compare to the $CD8^+$ compartment of MS patients remains to be determined.

Even though few examples exist of direct mimicry between PLP and foreign antigens, PLP remains one of the strongest encephalitogens, and *in vivo* inter- and intramolecular epitope spreading from initial PLP epitope responses is well-characterised in some EAE models as is described above (117, 210, 219). Further studies have shown EAE to be dependent on B cell presentation of PLP and MOG antigens to $CD4^+$ T cells (220, 221), and efficacy of B cell depletion therapy in MS is thought to be partially due to removal of the antigen-presenting function of B cells. In contrast, fewer examples of epitope spreading from an initial PLP response have been reported for MS, however there are reports of spreading from MBP epitopes to PLP, and it is likely that each patient has a unique sequence of responses which develop through disease depending on their HLA type and other factors (222). However, this does not discount the possibility that an immunodominant T cell response to $PLP_{139-151}$ in humans could, under the right circumstances, lead to an inflammatory event causing breakdown of the blood-brain barrier and lesion formation, after which epitope spreading to other CNS autoantigens may occur. These events are extremely difficult to investigate in humans due to the long prodromal phase of MS and also the difficulty and ethical barriers to sampling the affected tissue, ie. the brain and spinal cord.

Myelin oligodendrocyte glycoprotein

MOG is a minor myelin component and is a transmembrane protein of the Ig superfamily. Overall, it constitutes less than 0.05% of myelin and is located in the outer membrane, and this location contributes to its relevance as an autoantigenic target as it is readily accessible by autoantibodies targeting its extracellular domain (223, 224). MOG was identified as a candidate autoantigen following observations that immunisation induces EAE and also the presence of MOG-specific autoantibodies and T cell responses in MS (45, 85–

87, 94, 95, 98). In the EAE model, MOG-specific autoantibodies work synergistically with T cells to induce an inflammatory demyelinating disease which replicates observations from MS pathology (99, 225). An additional factor is MOG's almost undetectable expression in the thymus (208), leading to escape of MOG-specific T cells from central tolerance mechanisms and which also partly accounts for the detection of MOG-specific T cells in some healthy controls as well as pwMS (85). MOG-reactive T cells retained in the immune repertoire may then become activated by environmental antigens with homology, which could lead to CNS inflammation and disease.

Mode and situation of cross-reactivity has been demonstrated to be important for priming of pathogenic cross-reactive responses, such as that demonstrated for cross-reactivity between MOG and the milk protein butyrophilin (BTN). BTN is a protein expressed in mammary tissue and is a major component of milk fat globules and has homology to MOG_{76-87} in its extracellular IgV-like domain. Immunisation of rats with MOG_{76-87} caused disseminated CNS inflammation characterised by infiltration of macrophages and $CD4^+$ T cells, but interestingly this could be ameliorated by administration of the homologous BTN peptide either intravenously or intranasally with animals showing markedly decreased clinical scores (105). This amelioration is potentially due to induction of T_{REG} cells by the homologous BTN peptide, and this protective effect could in theory also occur in humans who consume bovine milk products into adulthood. However, further studies have shown that mechanisms of oral tolerance are poorly developed in babies, and tolerance may only be maintained when oral exposure is continued past a certain age – as has been demonstrated for oral tolerance to MBP in EAE (226). On the other hand, consumption of dairy products has also been linked to MS (227) and, although this finding remains controversial, cross-reactivity of antibodies which could bind homologous epitopes from both BTN and MOG were detected in the blood and CSF of pwMS (106). In addition to BTN, animals immunised with bovine casein were demonstrated to develop severe spinal cord pathology and demyelination which was attributed to induction of antibodies which bind to casein and cross-react with myelin associated glycoprotein (MAG) (154). The authors also noted increased antibody responses in pwMS compared to other neurological disease controls, suggesting that loss of tolerance to casein and molecular mimicry with MAG could contribute to disease in a subset of patients. However, the contribution of dietary milk proteins to MS pathogenesis remains to be fully elucidated in large cohort studies.

In addition to dietary antigens, sequence similarity has been identified between MOG and the human endogenous retrovirus W (HERV-W) envelope protein. This led to the finding that MOG autoantibodies could bind HERV-W protein (107) and one study used a nanotechnology approach to show a proof of principle that antibodies raised against MOG could cross-react with HERV-W (107). HERV are remnant genetic material left in the human genome following infection with retroviruses and constitute around 7% of the human genome (228). Initial investigation of HERV-W in MS brains was driven by isolation of HERV-W protein from sera, CSF and brain samples of affected individuals (229). It has also been demonstrated that HERV can also lead to activation of innate immune mechanisms through activation of Toll-like receptor 4 (TLR4) in APC and contributing to a proinflammatory milieu by driving T_H1 responses. However, under these conditions, it is also possible that autoreactive cells could become activated via bystander mechanisms, and therefore the biological relevance of this MOG cross-reactivity with HERV-W remains to be verified in an MS cohort. Further studies by Sutkowski et al. demonstrated that the env protein of HERV-K18 – a superantigen capable of activating T cells expressing TCRVB13 – can become transcriptionally activated by EBV (230, 231). This activation of TCRBV13+ T cells was HLA-dependent but not restricted and may be involved in autoproliferative mechanisms in MS.

Although several factors likely contribute to epitope spreading as was discussed above for EAE, T cells isolated in response to the encephalitogenic epitope MOG_{35-55} have also been characterised as polyreactive to a similar sequence in neurofilament medium protein (NFM_{15-35}) in mice (104). Both epitopes share the same TCR contact residues and could therefore potentially contribute to epitope spreading in disease. However, observations from EAE showed that NFM peptide did not expand MOG-specific T cells to a sufficient threshold to induce disease and NFM knockout mice had identical EAE disease to wild type animals indicating that, although NFM is immunogenic at the polyclonal level, it fails to expand high affinity MOG-specific T cells necessary for EAE induction (104).

Guanosine diphosphate-L-fucose synthase, RAS guanyl releasing protein 2 and HLA-DR

Reactivity to guanosine diphosphate (GDP)-L-fucose synthase (GDPLFS) was first identified by systematically screening brain-infiltrating $CD4^+$ T cell clones from MS patients for reactivity to a peptide library (70). T cell clones which responded to this antigen secreted T_H2 cytokines and were identified in the CSF and brain of *HLA-DRB3*02:02* positive individuals. Interestingly, GDPLFS clones were found to cross-recognise a number of bacterially-derived antigens as well as epitopes from other autoantigens such as MBP, PLP and MOG (70). T cell clones which reacted to GDPLFS could also respond to the dominant MBP_{83-99} epitope, with other clones showing reactivity to $PLP_{139-154}$. Given the dual reactivity with bacterial epitopes, secretion of T_H2 cytokines by the cross-reactive GDPLFS T cell clone is interesting as T_H2 cells have a role in chronic inflammation and tissue repair (232). Given that the T cell clones respond to bacterial epitopes it is possible that they were initially primed in the gut. Also intriguing is that they were isolated from an individual with pattern II lesion pathology which is characterised by autoantibodies and complement deposition (233, 234), and an interesting avenue of future investigation would be to characterise whether the organ in which they were primed affects pathogenic T cell phenotype or subsequent lesion pathology in MS.

Auto-proliferation is defined as a spontaneous *in vitro* T cell proliferation without stimulus and is an observed feature of MS

patient peripheral blood mononuclear cells (PBMC) in several studies (72, 235). Thorough examination of this phenomenon in pwMS was performed by Jelcic et al. who identified that there was a significant overlap of TCRVβ sequences from brain-infiltrating T cells in lesions and the auto-proliferating $CD4^+$ T cell compartment in peripheral blood (72). T cell clones were isolated from the auto-proliferating blood compartment and their TCRVβ sequence was compared to those recovered from active lesions of the same *HLA-DRB1*15:01* homozygous MS patient. The authors were then able to investigate specific clones which had infiltrated the brain and map their the antigen specificity using combinatorial peptide libraries. The cognate peptide from one T cell clone was mapped to a sequence from RAS guanyl-releasing protein 2 (RASGRP2), a previously unidentified MS autoantigen which is expressed in B cells, striatal neurons and cortical grey matter in the brain but is not a constituent of myelin, indicating that autoantigenic targets in MS do not necessarily need to be myelin proteins (72).

Identification of this situation in MS pathogenesis identifies a crucial link between peripheral activation of autoreactive $CD4^+$ T cells by B cells and their subsequent infiltration into the CNS. In this scenario, B cells expressing high levels of HLA-DR present self-peptides from autoantigens such as RASGRP2 and stimulate auto-proliferative and auto-aggressive $CD4^+$ T cells which subsequently enter the brain. After their infiltration into the CNS, these cells recognise RASGRP2 peptides presented in neuronal tissue and mediate inflammation. However, in this case the activating autoantigen in the periphery is the same as the target in the CNS, indicating that there should in theory be removal of autoreactive T cells via central tolerance mechanisms if the specified autoantigen is expressed in the thymus. RASGRP2's expression in the thymus is not completely certain and it was not detected in thymic epithelial cells (71, 236). However, RASGRP2 expression was detected in some APCs in the thymus, indicating that RASGRP2-reactive T cells may be negatively selected from the repertoire via interaction with B cells and plasmacytoid dendritic cells (pDC) in the thymus (236).

Evidence that RASGRP2 autoreactivity could be stimulated by foreign antigens was demonstrated by Wang et al. who showed that peptides from MS associated pathogens EBV and *A. muciniphila* could also stimulate RASGRP2-specific $CD4^+$ T cell clones *in vitro* (71). Interestingly, the cross-reactive EBV peptide sequences were derived from two lytic cycle antigens BHRF1 and BPLF1 which are expressed at high levels during acute infection where their functions are as a viral Bcl-2 homologue and a tegument deubiquitinase respectively (175, 237). No responses were observed to peptides from human HCMV or the bacterium *Prevotella histicola*, two pathogens have been negatively associated with MS (191, 206, 238). RASGRP2-specific T cell clones could also recognise HLA-derived self-peptides (HLA-SP) from HLA-DRB1 albeit with lower avidity, indicating that self-derived peptides are also partial agonists for $CD4^+$ T cells targeting RASGRP2 and may help to maintain these T cells in the peripheral tissues via molecular mimicry (71). Some RASGRP2-specific T cell clones were shown to have an $IFN\gamma^+$ T_H1 phenotype, although the clone which was stimulated by EBV and *A. muciniphila* peptides had a T_H2 phenotype and was isolated from a MS patient with type II lesion pathology (71, 72). *Ex vivo* analysis of T cell responses to peptides from RASGRP2, EBV and *A. muciniphila* showed these to be targets of responses in natalizumab-treated MS patients, indicating responses that had been primed *in vivo* and supporting their pathological relevance in this setting (71).

These data together suggest that *HLA-DRB1*15:01*-restricted RASGRP2-specific T cells can become activated in the periphery via both self-antigens and foreign peptides derived from EBV and *A. muciniphila*, and also that these $CD4^+$ T cells specifically infiltrate the brain where they can be found in active lesions. This supports the hypothesis in MS that CNS autoimmunity is either initiated or maintained by pathogenic $CD4^+$ T cell responses which are initially primed by exogenous antigens but can respond to autoantigens, leading to their recruitment to the brain where they mediate inflammatory tissue damage. These data are striking, and further investigation of RASGRP2 in large MS cohorts to establish the frequency of responses to this autoantigen are warranted.

Conclusion

It is clear that cross reactivity between a variety of microbial agents and host CNS autoantigens has been demonstrated, though in most cases of unclear relevance for MS pathogenesis due to experiments with low numbers of T cell clones or in artificial experimental animal models. However, in large sero-epidemiological studies, EBV – and to some extent HHV-6A – stand out. Especially for EBV, clear evidence for molecular mimicry epitopes has been demonstrated and antibody responses directed against these epitopes strikingly associate to an increased risk for MS. This strongly supports their role in MS pathogenesis, perhaps as markers for a concomitant T cell autoimmunity.

These observations make a case for therapeutic intervention, in particular if EBV drives the chronicity of the disease, perhaps with EBV-specific low molecular antiviral agents, or vaccination of individuals at risk for MS or at onset of disease. However, due to the multiple CNS autoantigen mimics now identified in $EBNA1_{390-440}$, development of future EBV vaccines or adoptive T cell therapies which include this antigen should either be designed with extreme caution or avoided altogether lest MS disease be triggered or exacerbated. The MS research field has reached an exciting stage, however further extensive research is needed to fully elucidate the role of foreign antigens which mimic autoantigens in the development and progression of CNS demyelinating disease.

Author contributions

OT: Conceptualization, Writing – original draft, Writing – review & editing. TO: Funding acquisition, Supervision, Writing – review & editing.

Funding

The author(s) declare financial support was received for the research, authorship, and/or publication of this article. This study has received grant support from the Swedish Research Council, the Swedish Brain Foundation, Knut and Alice Wallenbergs Foundation and Margaretha af Ugglas Foundation.

Conflict of interest

TO has received unrestricted MS research grants from Biogen, Merck, Novartis and Sanofi, as well as lecture and/or advisory board honoraria from the same companies. None of which have had any relation to the content of this review.

The remaining author declares that the research was conducted in the absence of any commercial or financial relationships that could be construed as a potential conflict of interest.

Publisher's note

References

1. Walton C, King R, Rechtman L, Kaye W, Leray E, Marrie RA, et al. Rising prevalence of multiple sclerosis worldwide: Insights from the Atlas of MS, third edition. *Mult Scler Houndmills Basingstoke Engl* (2020) 26(14):1816–21. doi: 10.1177/1352458520970841

2. Olsson T, Barcellos LF, Alfredsson L. Interactions between genetic, lifestyle and environmental risk factors for multiple sclerosis. *Nat Rev Neurol* (2017) 13(1):25–36. doi: 10.1038/nrneurol.2016.187

3. Medawar PB. Immunity to homologous grafted skin; the fate of skin homografts transplanted to the brain, to subcutaneous tissue, and to the anterior chamber of the eye. *Br J Exp Pathol* (1948) 29(1):58–69.

4. Ziv Y, Ron N, Butovsky O, Landa G, Sudai E, Greenberg N, et al. Immune cells contribute to the maintenance of neurogenesis and spatial learning abilities in adulthood. *Nat Neurosci* (2006) 9(2):268–75. doi: 10.1038/nn1629

5. Wolf SA, Steiner B, Akpinarli A, Kammertoens T, Nassenstein C, Braun A, et al. CD4-positive T lymphocytes provide a neuroimmunological link in the control of adult hippocampal neurogenesis. *J Immunol Baltim Md* (1950) 182(7):3979–84. doi: 10.4049/jimmunol.0801218

6. Kipnis J, Cohen H, Cardon M, Ziv Y, Schwartz M. T cell deficiency leads to cognitive dysfunction: implications for therapeutic vaccination for schizophrenia and other psychiatric conditions. *Proc Natl Acad Sci U S A* (2004) 101(21):8180–5. doi: 10.1073/pnas.0402268101

7. Louveau A, Smirnov I, Keyes TJ, Eccles JD, Rouhani SJ, Peske JD, et al. Structural and functional features of central nervous system lymphatic vessels. *Nature.* (2015) 523 (7560):337–41. doi: 10.1038/nature14432

8. Absinta M, Ha SK, Nair G, Sati P, Luciano NJ, Palisoc M, et al. Human and nonhuman primate meninges harbor lymphatic vessels that can be visualized noninvasively by MRI. *eLife* (2017) 6:e29738. doi: 10.7554/eLife.29738

9. Schmidt-Hieber M, Zweigner J, Uharek L, Blau IW, Thiel E. Central nervous system infections in immunocompromised patients: update on diagnostics and therapy. *Leuk Lymphoma* (2009) 50(1):24–36. doi: 10.1080/10428190802517740

10. Farh KKH, Marson A, Zhu J, Kleinewietfeld M, Housley WJ, Beik S, et al. Genetic and epigenetic fine mapping of causal autoimmune disease variants. *Nature.* (2015) 518(7539):337–43. doi: 10.1038/nature13835

11. Hauser SL, Waubant E, Arnold DL, Vollmer T, Antel J, Fox RJ, et al. B-cell depletion with rituximab in relapsing-remitting multiple sclerosis. *N Engl J Med* (2008) 358(7):676–88. doi: 10.1056/NEJMoa0706383

12. Salzer J, Svenningsson R, Alping P, Novakova L, Björck A, Fink K, et al. Rituximab in multiple sclerosis: A retrospective observational study on safety and efficacy. *Neurology.* (2016) 87(20):2074–81. doi: 10.1212/WNL.0000000000003331

13. Fox RJ, Cree BAC, De Sèze J, Gold R, Hartung HP, Jeffery D, et al. MS disease activity in RESTORE: a randomized 24-week natalizumab treatment interruption study. *Neurology.* (2014) 82(17):1491–8. doi: 10.1212/WNL.0000000000000355

14. Polman CH, O'Connor PW, Havrdova E, Hutchinson M, Kappos L, Miller DH, et al. A randomized, placebo-controlled trial of natalizumab for relapsing multiple sclerosis. *N Engl J Med* (2006) 354(9):899–910. doi: 10.1056/NEJMoa044397

15. Sawcer S, Hellenthal G, Pirinen M, Spencer CCA, Patsopoulos NA, Moutsianas L, et al. Genetic risk and a primary role for cell-mediated immune mechanisms in multiple sclerosis. *Nature.* (2011) 476(7359):214–9. doi: 10.1038/nature10251

16. Beecham AH, Patsopoulos NA, Xifara DK, Davis MF, Kemppinen A, Cotsapas C, et al. Analysis of immune-related loci identifies 48 new susceptibility variants for multiple sclerosis. *Nat Genet* (2013) 45(11):1353–60. doi: 10.1038/ng.2770

17. Moutsianas L, Jostins L, Beecham AH, Dilthey AT, Xifara DK, Ban M, et al. Class II HLA interactions modulate genetic risk for multiple sclerosis. *Nat Genet* (2015) 47 (10):1107–13. doi: 10.1038/ng.3395

18. Brynedal B, Duvefelt K, Jonasdottir G, Roos IM, Akesson E, Palmgren J, et al. HLA-A confers an HLA-DRB1 independent influence on the risk of multiple sclerosis. *PloS One* (2007) 2(7):e664. doi: 10.1371/journal.pone.0000664

19. Hedström AK, Huang J, Michel A, Butt J, Brenner N, Hillert J, et al. High levels of epstein-barr virus nuclear antigen-1-specific antibodies and infectious mononucleosis act both independently and synergistically to increase multiple sclerosis risk. *Front Neurol* (2019) 10:1368. doi: 10.3389/fneur.2019.01368

20. De Jager PL, Simon KC, Munger KL, Rioux JD, Hafler DA, Ascherio A. Integrating risk factors: HLA-DRB1*1501 and Epstein-Barr virus in multiple sclerosis. *Neurology.* (2008) 70(13 Pt 2):1113–8. doi: 10.1212/01.wnl.0000294325.63006.f8

21. Hedström AK, Lima Bomfim I, Barcellos L, GianFrancesco M, Schaefer C, Kockum I, et al. Interaction between adolescent obesity and HLA risk genes in the etiology of multiple sclerosis. *Neurology.* (2014) 82(10):865–72. doi: 10.1212/WNL.0000000000000203

22. Disanto G, Hall C, Lucas R, Ponsonby AL, Berlanga-Taylor AJ, Giovannoni G, et al. Assessing interactions between HLA-DRB1*15 and infectious mononucleosis on the risk of multiple sclerosis. *Mult Scler Houndmills Basingstoke Engl* (2013) 19 (10):1355–8. doi: 10.1177/1352458513477231

23. Nielsen TR, Rostgaard K, Askling J, Steffensen R, Oturai A, Jersild C, et al. Effects of infectious mononucleosis and HLA-DRB1*15 in multiple sclerosis. *Mult Scler Houndmills Basingstoke Engl* (2009) 15(4):431–6. doi: 10.1177/1352458508100037

24. Sundström P, Nyström M, Ruuth K, Lundgren E. Antibodies to specific EBNA-1 domains and HLA DRB1*1501 interact as risk factors for multiple sclerosis. *J Neuroimmunol* (2009) 215(1–2):102–7. doi: 10.1016/j.jneuroim.2009.08.004

25. International Multiple Sclerosis Genetics Consortium. Multiple sclerosis genomic map implicates peripheral immune cells and microglia in susceptibility.. *Science* (2019) 365(6460):eaav7188. doi: 10.1126/science.aav7188

26. Klein L, Hinterberger M, Wirnsberger G, Kyewski B. Antigen presentation in the thymus for positive selection and central tolerance induction. *Nat Rev Immunol* (2009) 9(12):833–44. doi: 10.1038/nri2669

27. Walker LSK, Abbas AK. The enemy within: keeping self-reactive T cells at bay in the periphery. *Nat Rev Immunol* (2002) 2(1):11–9. doi: 10.1038/nri701

28. Wooldridge L, Ekeruche-Makinde J, van den Berg HA, Skowera A, Miles JJ, Tan MP, et al. A single autoimmune T cell receptor recognizes more than a million different peptides. *J Biol Chem* (2012) 287(2):1168–77. doi: 10.1074/jbc.M111.289488

29. Sewell AK. Why must T cells be cross-reactive? *Nat Rev Immunol* (2012) 12 (9):669–77. doi: 10.1038/nri3279

30. Mason D. A very high level of crossreactivity is an essential feature of the T-cell receptor. *Immunol Today* (1998) 19(9):395–404. doi: 10.1016/S0167-5699(98)01299-7

31. Pettinelli CB, McFarlin DE. Adoptive transfer of experimental allergic encephalomyelitis in SJL/J mice after in *vitro* activation of lymph node cells by myelin basic protein: requirement for Lyt 1+ 2- T lymphocytes. *J Immunol Baltim Md 1950* (1981) 127(4):1420–3. doi: 10.4049/jimmunol.127.4.1420

32. Zamvil SS, Steinman L. The T lymphocyte in experimental allergic encephalomyelitis. *Annu Rev Immunol* (1990) 8:579–621. doi: 10.1146/annurev.iy.08.040190.003051

33. Das P, Drescher KM, Geluk A, Bradley DS, Rodriguez M, David CS. Complementation between specific HLA-DR and HLA-DQ genes in transgenic mice determines susceptibility to experimental autoimmune encephalomyelitis. *Hum Immunol* (2000) 61(3):279–89. doi: 10.1016/S0198-8859(99)00135-4

34. Kawamura K, Yamamura T, Yokoyama K, Chui DH, Fukui Y, Sasazuki T, et al. Hla-DR2-restricted responses to proteolipid protein 95-116 peptide cause autoimmune encephalitis in transgenic mice. *J Clin Invest* (2000) 105(7):977–84. doi: 10.1172/JCI8407

35. Forsthuber TG, Shive CL, Wienhold W, de Graaf K, Spack EG, Sublett R, et al. T cell epitopes of human myelin oligodendrocyte glycoprotein identified in HLA-DR4 (DRB1*0401) transgenic mice are encephalitogenic and are presented by human B cells. *J Immunol Baltim Md 1950* (2001) 167(12):7119–25. doi: 10.4049/jimmunol.167.12.7119

36. Madsen LS, Andersson EC, Jansson L, Krogsgaard M, Andersen CB, Engberg J, et al. A humanized model for multiple sclerosis using HLA-DR2 and a human T-cell receptor. *Nat Genet* (1999) 23(3):343–7. doi: 10.1038/15525

37. Traugott U, Reinherz EL, Raine CS. Multiple sclerosis: distribution of T cell subsets within active chronic lesions. *Science.* (1983) 219(4582):308–10. doi: 10.1126/science.6217550

38. Nakajima H, Fukuda K, Doi Y, Sugino M, Kimura F, Hanafusa T, et al. Expression of TH1/TH2-related chemokine receptors on peripheral T cells and correlation with clinical disease activity in patients with multiple sclerosis. *Eur Neurol* (2004) 52(3):162–8. doi: 10.1159/000081856

39. Shimizu Y, Ota K, Kubo S, Kabasawa C, Kobayashi M, Ohashi T, et al. Association of Th1/Th2-related chemokine receptors in peripheral T cells with disease activity in patients with multiple sclerosis and neuromyelitis optica. *Eur Neurol* (2011) 66(2):91–7. doi: 10.1159/000329576

40. Tejada-Simon MV, Zang YC, Yang D, Hong J, Li S, Singh RA, et al. Aberrant T cell responses to myelin antigens during clinical exacerbation in patients with multiple sclerosis. *Int Immunol* (2000) 12(12):1641–50. doi: 10.1093/intimm/12.12.1641

41. Calabresi PA, Fields NS, Farnon EC, Frank JA, Bash CN, Kawanashi T, et al. ELI-spot of Th-1 cytokine secreting PBMC's in multiple sclerosis: correlation with MRI lesions. *J Neuroimmunol* (1998) 85(2):212–9. doi: 10.1016/S0165-5728(98)00008-3

42. van Langelaar J, van der Vuurst de Vries RM, Janssen M, Wierenga-Wolf AF, Spilt IM, Siepman TA, et al. T helper 17.1 cells associate with multiple sclerosis disease activity: perspectives for early intervention. *Brain.* (2018) 141(5):1334–49. doi: 10.1093/brain/awy069

43. Kebir H, Ifergan I, Alvarez JI, Bernard M, Poirier J, Arbour N, et al. Preferential recruitment of interferon-γ–expressing TH17 cells in multiple sclerosis. *Ann Neurol* (2009) 66(3):390–402. doi: 10.1002/ana.21748

44. Olsson T, Zhi WW, Höjeberg B, Kostulas V, Jiang YP, Anderson G, et al. Autoreactive T lymphocytes in multiple sclerosis determined by antigen-induced secretion of interferon-gamma. *J Clin Invest* (1990) 86(3):981–5. doi: 10.1172/JCI114800

45. Bielekova B, Sung MH, Kadom N, Simon R, McFarland H, Martin R. Expansion and functional relevance of high-avidity myelin-specific CD4+ T cells in multiple sclerosis. *J Immunol Baltim Md 1950* (2004) 172(6):3893–904. doi: 10.4049/jimmunol.172.6.3893

46. Olsson T, Sun J, Hillert J, Höjeberg B, Ekre HP, Andersson G, et al. Increased numbers of T cells recognizing multiple myelin basic protein epitopes in multiple sclerosis. *Eur J Immunol* (1992) 22(4):1083–7. doi: 10.1002/eji.1830220431

47. Correale J, McMillan M, McCarthy K, Le T, Weiner LP. Isolation and characterization of autoreactive proteolipid protein-peptide specific T-cell clones from multiple sclerosis patients. *Neurology.* (1995) 45(7):1370–8. doi: 10.1212/WNL.45.7.1370

48. Langrish CL, Chen Y, Blumenschein WM, Mattson J, Basham B, Sedgwick JD, et al. IL-23 drives a pathogenic T cell population that induces autoimmune inflammation. *J Exp Med* (2005) 201(2):233–40. doi: 10.1084/jem.20041257

49. Kebir H, Kreymborg K, Ifergan I, Dodelet-Devillers A, Cayrol R, Bernard M, et al. Human TH17 lymphocytes promote blood-brain barrier disruption and central nervous system inflammation. *Nat Med* (2007) 13(10):1173–5. doi: 10.1038/nm1651

50. Romme Christensen J, Börnsen L, Ratzer R, Piehl F, Khademi M, Olsson T, et al. Systemic inflammation in progressive multiple sclerosis involves follicular T-helper, Th17- and activated B-cells and correlates with progression. *PloS One* (2013) 8(3):e57820. doi: 10.1371/journal.pone.0057820

51. Kaufmann M, Evans H, Schaupp AL, Engler JB, Kaur G, Willing A, et al. Identifying CNS-colonizing T cells as potential therapeutic targets to prevent progression of multiple sclerosis. *Med.* (2021) 2(3):296–312.e8. doi: 10.1016/j.medj.2021.01.006

52. Morille J, Mandon M, Rodriguez S, Roulois D, Leonard S, Garcia A, et al. Multiple sclerosis CSF is enriched with follicular T cells displaying a th1/eomes signature. *Neurol Neuroimmunol Neuroinflammation* (2022) 9(6):e200033. doi: 10.1212/NXI.0000000000200033

53. Höftberger R, Aboul-Enein F, Brueck W, Lucchinetti C, Rodriguez M, Schmidbauer M, et al. Expression of Major Histocompatibility Complex class l Molecules on the Different Cell Types in Multiple Sclerosis Lesions. *Brain Pathol* (2004) 14(1):43–50. doi: 10.1111/j.1750-3639.2004.tb00496.x

54. Jurewicz A, Biddison WE, Antel JP. MHC class I-restricted lysis of human oligodendrocytes by myelin basic protein peptide-specific CD8 T lymphocytes. *J Immunol Baltim Md 1950* (1998) 160(6):3056–9. doi: 10.4049/jimmunol.160.6.3056

55. Sun D, Whitaker JN, Huang Z, Liu D, Coleclough C, Wekerle H, et al. Myelin antigen-specific CD8+ T cells are encephalitogenic and produce severe disease in C57BL/6 mice1. *J Immunol* (2001) 166(12):7579–87. doi: 10.4049/jimmunol.166.12.7579

56. Hollenbach JA, Oksenberg JR. The immunogenetics of multiple sclerosis: A comprehensive review. *J Autoimmun* (2015) 64:13–25. doi: 10.1016/j.jaut.2015.06.010

57. Lundtoft C, Pucholt P, Imgenberg-Kreuz J, Carlsson-Almlöf J, Eloranta ML, Syvänen AC, et al. Function of multiple sclerosis-protective HLA class I alleles revealed by genome-wide protein-quantitative trait loci mapping of interferon signalling. *PloS Genet* (2020) 16(10):e1009199. doi: 10.1371/journal.pgen.1009199

58. Babbe H, Roers A, Waisman A, Lassmann H, Goebels N, Hohlfeld R, et al. Clonal expansions of cd8+ T cells dominate the T cell infiltrate in active multiple sclerosis lesions as shown by micromanipulation and single cell polymerase chain reaction. *J Exp Med* (2000) 192(3):393–404. doi: 10.1084/jem.192.3.393

59. Salou M, Garcia A, Michel L, Gainche-Salmon A, Loussouarn D, Nicol B, et al. Expanded CD8 T-cell sharing between periphery and CNS in multiple sclerosis. *Ann Clin Transl Neurol* (2015) 2(6):609–22. doi: 10.1002/acn3.199

60. Sabatino JJ Jr, Wilson MR, Calabresi PA, Hauser SL, Schneck JP, Zamvil SS. Anti-CD20 therapy depletes activated myelin-specific CD8+ T cells in multiple sclerosis. *Proc Natl Acad Sci U S A* (2019) 116(51):25800–7. doi: 10.1073/pnas.1915309116

61. Liu PJ, Yang TT, Fan ZX, Yuan GB, Ma L, Wang ZY, et al. Characterization of antigen-specific CD8+ memory T cell subsets in peripheral blood of patients with multiple sclerosis. *Front Immunol* (2023) 14:1110672. doi: 10.3389/fimmu.2023.1110672

62. Biström M, Jons D, Engdahl E, Gustafsson R, Huang J, Brenner N, et al. Epstein-Barr virus infection after adolescence and human herpesvirus 6A as risk factors for multiple sclerosis. *Eur J Neurol* (2021) 28(2):579–86. doi: 10.1111/ene.14597

63. Engdahl E, Gustafsson R, Huang J, Biström M, Lima Bomfim I, Stridh P, et al. Increased serological response against human herpesvirus 6A is associated with risk for multiple sclerosis. *Front Immunol* (2019) 10:2715. doi: 10.3389/fimmu.2019.02715

64. Sundqvist E, Sundström P, Lindén M, Hedström AK, Aloisi F, Hillert J, et al. Epstein-Barr virus and multiple sclerosis: interaction with HLA. *Genes Immun* (2012) 13(1):14–20. doi: 10.1038/gene.2011.42

65. Thomas OG, Rickinson A, Palendira U. Epstein-Barr virus and multiple sclerosis: moving from questions of association to questions of mechanism. *Clin Transl Immunol* (2023) 12(5):e1451. doi: 10.1002/cti2.1451

66. Bronge M, Högelin KA, Thomas OG, Ruhrmann S, Carvalho-Queiroz C, Nilsson OB, et al. Identification of four novel T cell autoantigens and personal autoreactive profiles in multiple sclerosis. *Sci Adv* (2022) 8(17):eabn1823. doi: 10.1126/sciadv.abn1823

67. Ayoglu B, Mitsios N, Kockum I, Khademi M, Zandian A, Sjöberg R, et al. Anoctamin 2 identified as an autoimmune target in multiple sclerosis. *Proc Natl Acad Sci U S A* (2016) 113(8):2188–93. doi: 10.1073/pnas.1518553113

68. Tengvall K, Huang J, Hellström C, Kammer P, Biström M, Ayoglu B, et al. Molecular mimicry between Anoctamin 2 and Epstein-Barr virus nuclear antigen 1 associates with multiple sclerosis risk. *Proc Natl Acad Sci U S A* (2019) 116(34):16955–60. doi: 10.1073/pnas.1902623116

69. Thomas OG, Bronge M, Tengvall K, Akpinar B, Nilsson OB, Holmgren E, et al. Cross-reactive EBNA1 immunity targets alpha-crystallin B and is associated with multiple sclerosis. *Sci Adv* (2023) 9(20):eadg3032. doi: 10.1126/sciadv.adg3032

70. Planas R, Santos R, Tomas-Ojer P, Cruciani C, Lutterotti A, Faigle W, et al. GDP-l-fucose synthase is a CD4(+) T cell-specific autoantigen in DRB3*02:02 patients with multiple sclerosis. *Sci Transl Med* (2018) 10(462):eaat4301. doi: 10.1126/scitranslmed.aat4301

71. Wang J, Jelcic I, Mühlenbruch L, Haunerdinger V, Toussaint NC, Zhao Y, et al. HLA-DR15 molecules jointly shape an autoreactive T cell repertoire in multiple sclerosis. *Cell.* (2020) 183(5):1264–1281.e20. doi: 10.1016/j.cell.2020.09.054

72. Jelcic I, Al Nimer F, Wang J, Lentsch V, Planas R, Jelcic I, et al. Memory B cells activate brain-homing, autoreactive CD4(+) T cells in multiple sclerosis. *Cell.* (2018) 175(1):85–100. doi: 10.1016/j.cell.2018.08.011

73. Bjornevik K, Cortese M, Healy BC, Kuhle J, Mina MJ, Leng Y, et al. Longitudinal analysis reveals high prevalence of Epstein-Barr virus associated with multiple sclerosis. *Science.* (2022) 375(6578):296–301. doi: 10.1126/science.abj8222

74. Levin LI, Munger KL, O'Reilly EJ, Falk KI, Ascherio A. Primary infection with the Epstein-Barr virus and risk of multiple sclerosis. *Ann Neurol* (2010) 67(6):824–30. doi: 10.1002/ana.21978

75. Yea C, Tellier R, Chong P, Westmacott G, Marrie RA, Bar-Or A, et al. Epstein-Barr virus in oral shedding of children with multiple sclerosis. *Neurology.* (2013) 81(16):1392–9. doi: 10.1212/WNL.0b013e3182a841e4

76. Dunmire SK, Grimm JM, Schmeling DO, Balfour HHJ, Hogquist KA. The incubation period of primary epstein-barr virus infection: viral dynamics and immunologic events. *PloS Pathog* (2015) 11(12):e1005286. doi: 10.1371/journal.ppat.1005286

77. Cepok S, Zhou D, Srivastava R, Nessler S, Stei S, Büssow K, et al. Identification of Epstein-Barr virus proteins as putative targets of the immune response in multiple sclerosis. *J Clin Invest* (2005) 115(5):1352–60. doi: 10.1172/JCI200523661

78. Jilek S, Schluep M, Meylan P, Vingerhoets F, Guignard L, Monney A, et al. Strong EBV-specific CD8+ T-cell response in patients with early multiple sclerosis. *Brain J Neurol* (2008) 131(Pt 7):1712–21. doi: 10.1093/brain/awn108

79. Höllsberg P, Hansen HJ, Haahr S. Altered CD8+ T cell responses to selected Epstein-Barr virus immunodominant epitopes in patients with multiple sclerosis. *Clin Exp Immunol* (2003) 132(1):137–43. doi: 10.1046/j.1365-2249.2003.02114.x

80. Pender MP, Csurhes PA, Burrows JM, Burrows SR. Defective T-cell control of Epstein-Barr virus infection in multiple sclerosis. *Clin Transl Immunol* (2017) 6(1): e126.

81. Croxford JL, Olson JK, Anger HA, Miller SD. Initiation and exacerbation of autoimmune demyelination of the central nervous system *via* virus-induced molecular mimicry: Implications for the pathogenesis of multiple sclerosis. *J Virol* (2005) 79 (13):8581–90. doi: 10.1128/JVI.79.13.8581-8590.2005

82. Ji Q, Perchellet A, Goverman JM. Viral infection triggers central nervous system autoimmunity *via* activation of CD8+ T cells expressing dual TCRs. *Nat Immunol* (2010) 11(7):628–34. doi: 10.1038/ni.1888

83. Na SY, Hermann A, Sanchez-Ruiz M, Storch A, Deckert M, Hünig T. Oligodendrocytes enforce immune tolerance of the uninfected brain by purging the peripheral repertoire of autoreactive CD8+ T cells. *Immunity*. (2012) 37(1):134–46. doi: 10.1016/j.immuni.2012.04.009

84. Burns J, Rosenzweig A, Zweiman B, Lisak RP. Isolation of myelin basic protein-reactive T-cell lines from normal human blood. *Cell Immunol* (1983) 81(2):435–40. doi: 10.1016/0008-8749(83)90250-2

85. Bronge M, Ruhrmann S, Carvalho-Queiroz C, Nilsson OB, Kaiser A, Holmgren E, et al. Myelin oligodendrocyte glycoprotein revisited-sensitive detection of MOG-specific T-cells in multiple sclerosis. *J Autoimmun* (2019) 102:38–49. doi: 10.1016/j.jaut.2019.04.013

86. Wallström E, Khademi M, Andersson M, Weissert R, Linington C, Olsson T. Increased reactivity to myelin oligodendrocyte glycoprotein peptides and epitope mapping in HLA DR2(15)+ multiple sclerosis. *Eur J Immunol* (1998) 28(10):3329–35. doi: 10.1002/(SICI)1521-4141(199810)28:10<3329::AID-IMMU3329>3.0.CO;2-B

87. Sun J, Link H, Olsson T, Xiao BG, Andersson G, Ekre HP, et al. T and B cell responses to myelin-oligodendrocyte glycoprotein in multiple sclerosis. *J Immunol Baltim Md 1950* (1991) 146(5):1490–5. doi: 10.4049/jimmunol.146.5.1490

88. Koehler NKU, Genain CP, Giesser B, Hauser SL. The human T cell response to myelin oligodendrocyte glycoprotein: a multiple sclerosis family-based study. *J Immunol Baltim Md 1950* (2002) 168(11):5920–7. doi: 10.4049/jimmunol.168.11.5920

89. Kerlero de Rosbo N, Hoffman M, Mendel I, Yust I, Kaye J, Bakimer R, et al. Predominance of the autoimmune response to myelin oligodendrocyte glycoprotein (MOG) in multiple sclerosis: reactivity to the extracellular domain of MOG is directed against three main regions. *Eur J Immunol* (1997) 27(11):3059–69. doi: 10.1002/eji.1830271144

90. Weissert R, Kuhle J, de Graaf KL, Wienhold W, Herrmann MM, Müller C, et al. High immunogenicity of intracellular myelin oligodendrocyte glycoprotein epitopes. *J Immunol Baltim Md 1950* (2002) 169(1):548–56. doi: 10.4049/jimmunol.169.1.548

91. Lindert RB, Haase CG, Brehm U, Linington C, Wekerle H, Hohlfeld R. Multiple sclerosis: B- and T-cell responses to the extracellular domain of the myelin oligodendrocyte glycoprotein. *Brain J Neurol* (1999) 122(Pt 11):2089–100. doi: 10.1093/brain/122.11.2089

92. Cruciani C, Puthenparampil M, Tomas-Ojer P, Jelcic I, Docampo MJ, Planas R, et al. T-cell specificity influences disease heterogeneity in multiple sclerosis. *Neurol Neuroimmunol Neuroinflamm* (2021) 8(6):e1075. doi: 10.1212/NXI.0000000000001075

93. Hughes LE, Smith PA, Bonell S, Natt RS, Wilson C, Rashid T, et al. Cross-reactivity between related sequences found in Acinetobacter sp., Pseudomonas aeruginosa, myelin basic protein and myelin oligodendrocyte glycoprotein in multiple sclerosis. *J Neuroimmunol* (2003) 144(1–2):105–15. doi: 10.1016/s0165-5728(03)00274-1

94. Kuerten S, Lanz TV, Lingampalli N, Lahey LJ, Kleinschnitz C, Mäurer M, et al. Autoantibodies against central nervous system antigens in a subset of B cell-dominant multiple sclerosis patients. *Proc Natl Acad Sci U S A* (2020) 117(35):21512–8. doi: 10.1073/pnas.2011249117

95. Wang H, Munger KL, Reindl M, O'Reilly EJ, Levin LI, Berger T, et al. Myelin oligodendrocyte glycoprotein antibodies and multiple sclerosis in healthy young adults. *Neurology*. (2008) 71(15):1142–6. doi: 10.1212/01.wnl.0000316195.52001.e1

96. Pröbstel AK, Dornmair K, Bittner R, Sperl P, Jenne D, Magalhaes S, et al. Antibodies to MOG are transient in childhood acute disseminated encephalomyelitis. *Neurology*. (2011) 77(6):580–8. doi: 10.1212/WNL.0b013e318228c0b1

97. Hecker M, Fitzner B, Wendt M, Lorenz P, Flechtner K, Steinbeck F, et al. High-density peptide microarray analysis of igG autoantibody reactivities in serum and cerebrospinal fluid of multiple sclerosis patients. *Mol Cell Proteomics MCP* (2016) 15 (4):1360–80. doi: 10.1074/mcp.M115.051664

98. Abdul-Majid KB, Jirholt J, Stadelmann C, Stefferl A, Kjellén P, Wallström E, et al. Screening of several H-2 congenic mouse strains identified H-2(q) mice as highly susceptible to MOG-induced EAE with minimal adjuvant requirement. *J Neuroimmunol* (2000) 111(1–2):23–33. doi: 10.1016/S0165-5728(00)00360-X

99. Weissert R, Wallström E, Storch MK, Stefferl A, Lorentzen J, Lassmann H, et al. MHC haplotype-dependent regulation of MOG-induced EAE in rats. *J Clin Invest* (1998) 102(6):1265–73. doi: 10.1172/JCI3022

100. Mendel I, Kerlero de Rosbo N, Ben-Nun A. A myelin oligodendrocyte glycoprotein peptide induces typical chronic experimental autoimmune encephalomyelitis in H-2b mice: fine specificity and T cell receptor V beta expression of encephalitogenic T cells. *Eur J Immunol* (1995) 25(7):1951–9. doi: 10.1002/eji.1830250723

101. Bettelli E, Pagany M, Weiner HL, Linington C, Sobel RA, Kuchroo VK. Myelin oligodendrocyte glycoprotein-specific T cell receptor transgenic mice develop spontaneous autoimmune optic neuritis. *J Exp Med* (2003) 197(9):1073–81. doi: 10.1084/jem.20021603

102. Berger T, Weerth S, Kojima K, Linington C, Wekerle H, Lassmann H. Experimental autoimmune encephalomyelitis: the antigen specificity of T lymphocytes determines the topography of lesions in the central and peripheral nervous system. *Lab Investig J Tech Methods Pathol* (1997) 76(3):355–64.

103. Ellmerich S, Mycko M, Takacs K, Waldner H, Wahid FN, Boyton RJ, et al. High incidence of spontaneous disease in an HLA-DR15 and TCR transgenic multiple sclerosis model. *J Immunol Baltim Md 1950* (2005) 174(4):1938–46. doi: 10.4049/jimmunol.174.4.1938

104. Blanchfield L, Sabatino JJJ, Lawrence L, Evavold BD. NFM cross-reactivity to MOG does not expand a critical threshold level of high-affinity T cells necessary for onset of demyelinating disease. *J Immunol Baltim Md 1950* (2017) 199(8):2680–91. doi: 10.4049/jimmunol.1700792

105. Stefferl A, Schubart A, Storch M, Amini A, Mather I, Lassmann H, et al. Butyrophilin, a milk protein, modulates the encephalitogenic T cell response to myelin oligodendrocyte glycoprotein in experimental autoimmune encephalomyelitis. *J Immunol* (2000) 165(5):2859–65. doi: 10.4049/jimmunol.165.5.2859

106. Guggenmos J, Schubart AS, Ogg S, Andersson M, Olsson T, Mather IH, et al. Antibody cross-reactivity between myelin oligodendrocyte glycoprotein and the milk protein butyrophilin in multiple sclerosis. *J Immunol Baltim Md 1950* (2004) 172 (1):661–8. doi: 10.4049/jimmunol.172.1.661

107. de Luca V, Martins Higa A, Malta Romano C, Pimenta Mambrini G, Peroni LA, Trivinho-Strixino F, et al. Cross-reactivity between myelin oligodendrocyte glycoprotein and human endogenous retrovirus W protein: nanotechnological evidence for the potential trigger of multiple sclerosis. *Micron Oxf Engl 1993* (2019) 120:66–73. doi: 10.1016/j.micron.2019.02.005

108. Markovic-Plese S, Hemmer B, Zhao Y, Simon R, Pinilla C, Martin R. High level of cross-reactivity in influenza virus hemagglutinin-specific CD4+ T-cell response: implications for the initiation of autoimmune response in multiple sclerosis. *J Neuroimmunol* (2005) 169(1–2):31–8. doi: 10.1016/j.jneuroim.2005.07.014

109. Greer JM, Csurhes PA, Cameron KD, McCombe PA, Good MF, Pender MP. Increased immunoreactivity to two overlapping peptides of myelin proteolipid protein in multiple sclerosis. *Brain J Neurol* (1997) 120(Pt 8):1447–60. doi: 10.1093/brain/120.8.1447

110. Pelfrey CM, Trotter JL, Tranquill LR, McFarland HF. Identification of a novel T cell epitope of human proteolipid protein (residues 40-60) recognized by proliferative and cytolytic CD4+ T cells from multiple sclerosis patients. *J Neuroimmunol* (1993) 46 (1–2):33–42. doi: 10.1016/0165-5728(93)90231-M

111. Pelfrey CM, Trotter JL, Tranquill LR, McFarland HF. Identification of a second T cell epitope of human proteolipid protein (residues 89-106) recognized by proliferative and cytolytic CD4+ T cells from multiple sclerosis patients. *J Neuroimmunol* (1994) 53(2):153–61. doi: 10.1016/0165-5728(94)90025-6

112. Kondo T, Yamamura T, Inobe J, Ohashi T, Takahashi K, Tabira T. TCR repertoire to proteolipid protein (PLP) in multiple sclerosis (MS): homologies between PLP-specific T cells and MS-associated T cells in TCR junctional sequences. *Int Immunol* (1996) 8(1):123–30. doi: 10.1093/intimm/8.1.123

113. Greer JM, Csurhes PA, Muller DM, Pender MP. Correlation of blood T cell and antibody reactivity to myelin proteins with HLA type and lesion localization in multiple sclerosis. *J Immunol Baltim Md 1950* (2008) 180(9):6402–10. doi: 10.4049/jimmunol.180.9.6402

114. Owens GP, Fellin TJ, Matschulat A, Salas V, Schaller KL, Given KS, et al. Pathogenic myelin specific antibodies in multiple sclerosis target conformational proteolipid protein 1 anchored membrane domains. *J Clin Invest* (2023) 10:e162731. doi: 10.1172/JCI162731

115. Greer JM, Trifilieff E, Pender MP. Correlation between anti-myelin proteolipid protein (PLP) antibodies and disease severity in multiple sclerosis patients with PLP response-permissive HLA types. *Front Immunol* (2020) 11:1891. doi: 10.3389/fimmu.2020.01891

116. Quintana FJ, Farez MF, Izquierdo G, Lucas M, Cohen IR, Weiner HL. Antigen microarrays identify CNS-produced autoantibodies in RRMS. *Neurology*. (2012) 78 (8):532–9. doi: 10.1212/WNL.0b013e318247f9f3

117. Kennedy MK, Tan LJ, Dal Canto MC, Tuohy VK, Lu ZJ, Trotter JL, et al. Inhibition of murine relapsing experimental autoimmune encephalomyelitis by immune tolerance to proteolipid protein and its encephalitogenic peptides. *J Immunol Baltim Md 1950* (1990) 144(3):909–15. doi: 10.4049/jimmunol.144.3.909

118. Waldner H, Whitters MJ, Sobel RA, Collins M, Kuchroo VK. Fulminant spontaneous autoimmunity of the central nervous system in mice transgenic for the myelin proteolipid protein-specific T cell receptor. *Proc Natl Acad Sci U S A* (2000) 97 (7):3412–7. doi: 10.1073/pnas.97.7.3412

119. Boucher A, Desforges M, Duquette P, Talbot PJ. Long-term human coronavirus-myelin cross-reactive T-cell clones derived from multiple sclerosis patients. *Clin Immunol Orlando Fla* (2007) 123(3):258–67. doi: 10.1016/j.clim.2007.02.002

120. Massilamany C, Thulasingam S, Steffen D, Reddy J. Gender differences in CNS autoimmunity induced by mimicry epitope for PLP 139-151 in SJL mice. *J Neuroimmunol* (2011) 230(1–2):95–104. doi: 10.1016/j.jneuroim.2010.09.011

121. Olson JK, Croxford JL, Calenoff MA, Dal Canto MC, Miller SD. A virus-induced molecular mimicry model of multiple sclerosis. *J Clin Invest* (2001) 108 (2):311–8. doi: 10.1172/JCI200113032

122. Honma K, Parker KC, Becker KG, McFarland HF, Coligan JE, Biddison WE. Identification of an epitope derived from human proteolipid protein that can induce autoreactive CD8+ cytotoxic T lymphocytes restricted by HLA-A3: evidence for cross-reactivity with an environmental microorganism. *J Neuroimmunol* (1997) 73(1–2):7–14. doi: 10.1016/S0165-5728(96)00161-0

123. Valli A, Sette A, Kappos L, Oseroff C, Sidney J, Miescher G, et al. Binding of myelin basic protein peptides to human histocompatibility leukocyte antigen class II molecules and their recognition by T cells from multiple sclerosis patients. *J Clin Invest* (1993) 91(2):616–28. doi: 10.1172/JCI116242

124. Ota K, Matsui M, Milford EL, Mackin GA, Weiner HL, Hafler DA. T-cell recognition of an immunodominant myelin basic protein epitope in multiple sclerosis. *Nature.* (1990) 346(6280):183–7. doi: 10.1038/346183a0

125. Martino G, Olsson T, Fredrikson S, Hojeberg B, Kostulas V, Grimaldi LM, et al. Cells producing antibodies specific for myelin basic protein region 70-89 are predominant in cerebrospinal fluid from patients with multiple sclerosis. *Eur J Immunol* (1991) 21(12):2971–6. doi: 10.1002/eji.1830211211

126. Chou YK, Vainiene M, Whitham R, Bourdette D, Chou CH, Hashim G, et al. Response of human T lymphocyte lines to myelin basic protein: association of dominant epitopes with HLA class II restriction molecules. *J Neurosci Res* (1989) 23 (2):207–16. doi: 10.1002/jnr.490230211

127. Schmidt S, Linington C, Zipp F, Sotgiu S, de Waal Malefyt R, Wekerle H, et al. Multiple sclerosis: comparison of the human T-cell response to S100 beta and myelin basic protein reveals parallels to rat experimental autoimmune panencephalitis. *Brain J Neurol* (1997) 120(Pt 8):1437–45. doi: 10.1093/brain/120.8.1437

128. Wucherpfennig KW, Catz I, Hausmann S, Strominger JL, Steinman L, Warren KG. Recognition of the immunodominant myelin basic protein peptide by autoantibodies and HLA-DR2-restricted T cell clones from multiple sclerosis patients. Identity of key contact residues in the B-cell and T-cell epitopes. *J Clin Invest* (1997) 100(5):1114–22. doi: 10.1172/JCI119622

129. Vergelli M, Kalbus M, Rojo SC, Hemmer B, Kalbacher H, Tranquill L, et al. T cell response to myelin basic protein in the context of the multiple sclerosis-associated HLA-DR15 haplotype: peptide binding, immunodominance and effector functions of T cells. *J Neuroimmunol* (1997) 77(2):195–203. doi: 10.1016/S0165-5728(97)00075-1

130. García-Merino A, Persson MA, Ernerudh J, Díaz-Gil JJ, Olsson T. Serum and cerebrospinal fluid antibodies against myelin basic protein and their IgG subclass distribution in multiple sclerosis. *J Neurol Neurosurg Psychiatry* (1986) 49(9):1066–70. doi: 10.1136/jnnp.49.9.1066

131. Olsson T, Baig S, Höjeberg B, Link H. Antimyelin basic protein and antimyelin antibody-producing cells in multiple sclerosis. *Ann Neurol* (1990) 27(2):132–6. doi: 10.1002/ana.410270207

132. Jansson L, Olsson T, Höjeberg B, Holmdahl R. Chronic experimental autoimmune encephalomyelitis induced by the 89-101 myelin basic protein peptide in B10RIII (H-2r) mice. *Eur J Immunol* (1991) 21(3):693–9. doi: 10.1002/eji.1830210323

133. Goverman J, Woods A, Larson L, Weiner LP, Hood L, Zaller DM. Transgenic mice that express a myelin basic protein-specific T cell receptor develop spontaneous autoimmunity. *Cell.* (1993) 72(4):551–60. doi: 10.1016/0092-8674(93)90074-Z

134. Lafaille JJ, Nagashima K, Katsuki M, Tonegawa S. High incidence of spontaneous autoimmune encephalomyelitis in immunodeficient anti-myelin basic protein T cell receptor transgenic mice. *Cell.* (1994) 78(3):399–408. doi: 10.1016/0092-8674(94)90419-7

135. Fujinami RS, Oldstone MB. Amino acid homology between the encephalitogenic site of myelin basic protein and virus: mechanism for autoimmunity. *Science.* (1985) 230(4729):1043–5. doi: 10.1126/science.2414848

136. Wucherpfennig KW, Strominger JL. Molecular mimicry in T cell-mediated autoimmunity: viral peptides activate human T cell clones specific for myelin basic protein. *Cell.* (1995) 80(5):695–705. doi: 10.1016/0092-8674(95)90348-8

137. Lang HLE, Jacobsen H, Ikemizu S, Andersson C, Harlos K, Madsen L, et al. A functional and structural basis for TCR cross-reactivity in multiple sclerosis. *Nat Immunol* (2002) 3(10):940–3. doi: 10.1038/ni835

138. Holmøy T, Kvale EØ, Vartdal F. Cerebrospinal fluid CD4+ T cells from a multiple sclerosis patient cross-recognize Epstein-Barr virus and myelin basic protein. *J Neurovirol* (2004) 10(5):278–83. doi: 10.1080/13550280490499524

139. Jog NR, McClain MT, Heinlen LD, Gross T, Towner R, Guthridge JM, et al. Epstein Barr virus nuclear antigen 1 (EBNA-1) peptides recognized by adult multiple sclerosis patient sera induce neurologic symptoms in a murine model. *J Autoimmun* (2020) 106:102332. doi: 10.1016/j.jaut.2019.102332

140. Lomakin Y, Arapidi GP, Chernov A, Ziganshin R, Tcyganov E, Lyadova I, et al. Exposure to the epstein–barr viral antigen latent membrane protein 1 induces myelin-reactive antibodies in vivo. *Front Immunol* (2017) 8:777. doi: 10.3389/fimmu.2017.00777

141. Tejada-Simon MV, Zang YCQ, Hong J, Rivera VM, Zhang JZ. Cross-reactivity with myelin basic protein and human herpesvirus-6 in multiple sclerosis. *Ann Neurol* (2003) 53(2):189–97. doi: 10.1002/ana.10425

142. Talbot PJ, Paquette JS, Ciurli C, Antel JP, Ouellet F. Myelin basic protein and human coronavirus 229E cross-reactive T cells in multiple sclerosis. *Ann Neurol* (1996) 39(2):233–40. doi: 10.1002/ana.410390213

143. Mao YS, Lu CZ, Wang X, Xiao BG. Induction of experimental autoimmune encephalomyelitis in Lewis rats by a viral peptide with limited homology to myelin basic protein. *Exp Neurol* (2007) 206(2):231–9. doi: 10.1016/j.expneurol.2007.04.015

144. Gautam AM, Liblau R, Chelvanayagam G, Steinman L, Boston T. A viral peptide with limited homology to a self peptide can induce clinical signs of experimental autoimmune encephalomyelitis. *J Immunol Baltim Md 1950* (1998) 161 (1):60–4. doi: 10.4049/jimmunol.161.1.60

145. Lenz DC, Lu L, Conant SB, Wolf NA, Gérard HC, Whittum-Hudson JA, et al. A chlamydia pneumoniae-specific peptide induces experimental autoimmune encephalomyelitis in rats1. *J Immunol* (2001) 167(3):1803–8. doi: 10.4049/jimmunol.167.3.1803

146. Bray PF, Luka J, Bray PF, Culp KW, Schlight JP. Antibodies against Epstein-Barr nuclear antigen (EBNA) in multiple sclerosis CSF, and two pentapeptide sequence identities between EBNA and myelin basic protein. *Neurology.* (1992) 42(9):1798–804. doi: 10.1212/WNL.42.9.1798

147. Gabibov AG, Belogurov AAJ, Lomakin YA, Zakharova MY, Avakyan ME, Dubrovskaya VV, et al. Combinatorial antibody library from multiple sclerosis patients reveals antibodies that cross-react with myelin basic protein and EBV antigen. *FASEB J Off Publ Fed Am Soc Exp Biol* (2011) 25(12):4211–21. doi: 10.1096/fj.11-190769

148. van Noort JM, van Sechel AC, Bajramovic JJ, Ouagmiri M, Polman CH, Lassmann H, et al. The small heat-shock protein alpha B-crystallin as candidate autoantigen in multiple sclerosis. *Nature.* (1995) 375(6534):798–801. doi: 10.1038/375798a0

149. Ousman SS, Tomooka BH, van Noort JM, Wawrousek EF, O'Connor KC, Hafler DA, et al. Protective and therapeutic role for alphaB-crystallin in autoimmune demyelination. *Nature.* (2007) 448(7152):474–9. doi: 10.1038/nature05935

150. van Noort JM, Bsibsi M, Gerritsen WH, van der Valk P, Bajramovic JJ, Steinman L, et al. Alphab-crystallin is a target for adaptive immune responses and a trigger of innate responses in preactive multiple sclerosis lesions. *J Neuropathol Exp Neurol* (2010) 69(7):694–703. doi: 10.1097/NEN.0b013e3181e4939c

151. Thoua NM, van Noort JM, Baker D, Bose A, van Sechel AC, van Stipdonk MJ, et al. Encephalitogenic and immunogenic potential of the stress protein alphaB-crystallin in Biozzi ABH (H-2A(g7)) mice. *J Neuroimmunol* (2000) 104(1):47–57. doi: 10.1016/S0165-5728(99)00246-5

152. Rand KH, Houck H, Denslow ND, Heilman KM. Molecular approach to find target(s) for oligoclonal bands in multiple sclerosis. *J Neurol Neurosurg Psychiatry* (1998) 65(1):48–55. doi: 10.1136/jnnp.65.1.48

153. Lanz TV, Brewer RC, Ho PP, Moon JS, Jude KM, Fernandez D, et al. Clonally expanded B cells in multiple sclerosis bind EBV EBNA1 and GlialCAM. *Nature.* (2022) 603(7900):321–7. doi: 10.1038/s41586-022-04432-7

154. Chunder R, Weier A, Mäurer H, Luber N, Enders M, Luber G, et al. Antibody cross-reactivity between casein and myelin-associated glycoprotein results in central nervous system demyelination. *Proc Natl Acad Sci U S A* (2022) 119(10):e2117034119. doi: 10.1073/pnas.2117034119

155. Zdimerova H, Murer A, Engelmann C, Raykova A, Deng Y, Gujer C, et al. Attenuated immune control of Epstein-Barr virus in humanized mice is associated with the multiple sclerosis risk factor HLA-DR15. *Eur J Immunol* (2021) 51(1):64–75. doi: 10.1002/eji.202048655

156. Bsibsi M, Peferoen LAN, Holtman IR, Nacken PJ, Gerritsen WH, Witte ME, et al. Demyelination during multiple sclerosis is associated with combined activation of microglia/macrophages by IFN-γ and alpha B-crystallin. *Acta Neuropathol (Berl)* (2014) 128(2):215–29. doi: 10.1007/s00401-014-1317-8

157. Lanzavecchia A. Antigen-specific interaction between T and B cells. *Nature* (1985) 314(6011):537–9. doi: 10.1038/314537a0

158. Choi IK, Wang Z, Ke Q, Hong M, Qian Y, Zhao X, et al. Signaling by the Epstein-Barr virus LMP1 protein induces potent cytotoxic CD4(+) and CD8(+) T cell responses. *Proc Natl Acad Sci U S A* (2018) 115(4):E686–95. doi: 10.1073/pnas.1713607115

159. Uhlén M, Fagerberg L, Hallström BM, Lindskog C, Oksvold P, Mardinoglu A, et al. Tissue-based map of the human proteome. *Science.* (2015) 347(6220):1260419. doi: 10.1126/science.1260419

160. Han MH, Hwang SI, Roy DB, Lundgren DH, Price JV, Ousman SS, et al. Proteomic analysis of active multiple sclerosis lesions reveals therapeutic targets. *Nature.* (2008) 451(7182):1076—1081. doi: 10.1038/nature06559

161. Pugliese A. Autoreactive T cells in type 1 diabetes. *J Clin Invest* (2017) 127 (8):2881–91. doi: 10.1172/JCI94549

162. Dawoodji A, Chen JL, Shepherd D, Dalin F, Tarlton A, Alimohammadi M, et al. High frequency of cytolytic 21-hydroxylase-specific CD8+ T cells in autoimmune Addison's disease patients. *J Immunol Baltim Md 1950* (2014) 193(5):2118–26. doi: 10.4049/jimmunol.1400056

163. Pihoker C, Gilliam LK, Hampe CS, Lernmark A. Autoantibodies in diabetes. *Diabetes.* (2005) 54 Suppl 2:S52–61. doi: 10.2337/diabetes.54.suppl_2.S52

164. Lipphardt M, Wallbach M, Koziolek MJ. Plasma exchange or immunoadsorption in demyelinating diseases: A meta-analysis. *J Clin Med* (2020) 9 (5):1597. doi: 10.3390/jcm9051597

165. Stork L, Ellenberger D, Beißbarth T, Friede T, Lucchinetti CF, Brück W, et al. Differences in the reponses to apheresis therapy of patients with 3 histopathologically classified immunopathological patterns of multiple sclerosis. *JAMA Neurol* (2018) 75 (4):428–35. doi: 10.1001/jamaneurol.2017.4842

166. Lindsey JW, deGannes SL, Pate KA, Zhao X. Antibodies specific for Epstein-Barr virus nuclear antigen-1 cross-react with human heterogeneous nuclear ribonucleoprotein L. *Mol Immunol* (2016) 69:7–12. doi: 10.1016/j.molimm.2015.11.007

167. Lindsey JW. Antibodies to the Epstein-Barr virus proteins BFRF3 and BRRF2 cross-react with human proteins. *J Neuroimmunol* (2017) 310:131–4. doi: 10.1016/j.jneuroim.2017.07.013

168. Peters AL, Stunz LL, Bishop GA. CD40 and autoimmunity: the dark side of a great activator. *Semin Immunol* (2009) 21(5):293–300. doi: 10.1016/j.smim.2009.05.012

169. Haxhinasto SA, Bishop GA. Synergistic B cell activation by CD40 and the B cell antigen receptor: role of B lymphocyte antigen receptor-mediated kinase activation and tumor necrosis factor receptor-associated factor regulation. *J Biol Chem* (2004) 279 (4):2575–82. doi: 10.1074/jbc.M310628200

170. Haxhinasto SA, Hostager BS, Bishop GA. Cutting edge: molecular mechanisms of synergy between CD40 and the B cell antigen receptor: role for TNF receptor-associated factor 2 in receptor interaction. *J Immunol Baltim Md 1950* (2002) 169 (3):1145–9. doi: 10.4049/jimmunol.169.3.1145

171. Buchta CM, Bishop GA. Toll-like receptors and B cells: functions and mechanisms. *Immunol Res* (2014) 59(1–3):12–22. doi: 10.1007/s12026-014-8523-2

172. Vanden Bush TJ, Bishop GA. TLR7 and CD40 cooperate in IL-6 production *via* enhanced JNK and AP-1 activation. *Eur J Immunol* (2008) 38(2):400–9. doi: 10.1002/eji.200737602

173. Stunz LL, Busch LK, Munroe ME, Sigmund CD, Tygrett LT, Waldschmidt TJ, et al. Expression of the cytoplasmic tail of LMP1 in mice induces hyperactivation of B lymphocytes and disordered lymphoid architecture. *Immunity.* (2004) 21(2):255–66. doi: 10.1016/j.immuni.2004.07.008

174. Munroe ME, Anderson JR, Gross TF, Stunz LL, Bishop GA, James JA. Epstein-barr functional mimicry: pathogenicity of oncogenic latent membrane protein-1 in systemic lupus erythematosus and autoimmunity. *Front Immunol* (2021) 11:606936. doi: 10.3389/fimmu.2020.606936

175. Fitzsimmons L, Cartlidge R, Chang C, Sejic N, Galbraith LCA, Suraweera CD, et al. EBV BCL-2 homologue BHRF1 drives chemoresistance and lymphomagenesis by inhibiting multiple cellular pro-apoptotic proteins. *Cell Death Differ* (2020) 27(5):1554–68. doi: 10.1038/s41418-019-0435-1

176. Jochum S, Moosmann A, Lang S, Hammerschmidt W, Zeidler R. The EBV immunoevasins vIL-10 and BNLF2a protect newly infected B cells from immune recognition and elimination. *PloS Pathog* (2012) 8(5):1–11. doi: 10.1371/journal.ppat.1002704

177. Quinn LL, Zuo J, Abbott RJM, Shannon-Lowe C, Tierney RJ, Hislop AD, et al. Cooperation between Epstein-Barr virus immune evasion proteins spreads protection from CD8+ T cell recognition across all three phases of the lytic cycle. *PloS Pathog* (2014) 10(8):e1004322. doi: 10.1371/journal.ppat.1004322

178. Quinn LL, Williams LR, White C, Forrest C, Zuo J, Rowe M. The missing link in epstein-barr virus immune evasion: the BDLF3 gene induces ubiquitination and downregulation of major histocompatibility complex class I (MHC-I) and MHC-II. *J Virol* (2016) 90(1):356–67. doi: 10.1128/JVI.02183-15

179. Zuo J, Quinn LL, Tamblyn J, Thomas WA, Feederle R, Delecluse HJ, et al. The Epstein-Barr virus-encoded BILF1 protein modulates immune recognition of endogenously processed antigen by targeting major histocompatibility complex class I molecules trafficking on both the exocytic and endocytic pathways. *J Virol* (2011) 85 (4):1604–14. doi: 10.1128/JVI.01608-10

180. Chijioke O, Müller A, Feederle R, Barros MHM, Krieg C, Emmel V, et al. Human natural killer cells prevent infectious mononucleosis features by targeting lytic Epstein-Barr virus infection. *Cell Rep* (2013) 5(6):1489–98. doi: 10.1016/j.celrep.2013.11.041

181. Chijioke O, Landtwing V, Münz C. NK cell influence on the outcome of primary epstein-barr virus infection. *Front Immunol* (2016) 7:323. doi: 10.3389/fimmu.2016.00323

182. Azzi T, Lünemann A, Murer A, Ueda S, Béziat V, Malmberg KJ, et al. Role for early-differentiated natural killer cells in infectious mononucleosis. *Blood.* (2014) 124 (16):2533–43. doi: 10.1182/blood-2014-01-553024

183. Lünemann A, Tackenberg B, DeAngelis T, da Silva RB, Messmer B, Vanoaica LD, et al. Impaired IFN-γ production and proliferation of NK cells in multiple sclerosis. *Int Immunol* (2011) 23(2):139–48. doi: 10.1093/intimm/dxq463

184. Long HM, Chagoury OL, Leese AM, Ryan GB, James E, Morton LT, et al. MHC II tetramers visualize human CD4+ T cell responses to Epstein-Barr virus infection and demonstrate atypical kinetics of the nuclear antigen EBNA1 response. *J Exp Med* (2013) 210(5):933–49. doi: 10.1084/jem.20121437

185. Sindic CJM, Monteyne PH, Laterre EC. The intrathecal synthesis of virus-specific oligoclonal IgG in multiple sclerosis. *J Neuroimmunol* (1994) 54(1):75–80. doi: 10.1016/0165-5728(94)90233-X

186. Birnbaum ME, Mendoza JL, Sethi DK, Dong S, Glanville J, Dobbins J, et al. Deconstructing the peptide-MHC specificity of T cell recognition. *Cell.* (2014) 157 (5):1073–87. doi: 10.1016/j.cell.2014.03.047

187. Pi KS, Bortolotti D, Sang Y, Schiuma G, Beltrami S, Rizzo S, et al. Studying the interactions of U24 from HHV-6 in order to further elucidate its potential role in MS. *Viruses* (2022) 14(11):2384. doi: 10.3390/v14112384

188. Rizzo R, Gentili V, Casetta I, Caselli E, De Gennaro R, Granieri E, et al. Altered natural killer cells' response to herpes virus infection in multiple sclerosis involves KIR2DL2 expression. *J Neuroimmunol* (2012) 251(1–2):55–64. doi: 10.1016/j.jneuroim.2012.07.004

189. Pi KS, Sang Y, Straus SK. Viral proteins with pxxP and PY motifs may play a role in multiple sclerosis. *Viruses* (2022) 14(2):281. doi: 10.3390/v14020281

190. Ascherio A, Munch M. Epstein-Barr virus and multiple sclerosis. *Epidemiol Camb Mass* (2000) 11(2):220–4. doi: 10.1097/00001648-200003000-00023

191. Sundqvist E, Bergström T, Daialhosein H, Nyström M, Sundström P, Hillert J, et al. Cytomegalovirus seropositivity is negatively associated with multiple sclerosis. *Mult Scler Houndmills Basingstoke Engl* (2014) 20(2):165–73. doi: 10.1177/1352458513494489

192. Grut V, Biström M, Salzer J, Stridh P, Jons D, Gustafsson R, et al. Cytomegalovirus seropositivity is associated with reduced risk of multiple sclerosis—a presymptomatic case–control study. *Eur J Neurol* (2021) 28(9):3072–9. doi: 10.1111/ene.14961

193. Gotter J, Brors B, Hergenhahn M, Kyewski B. Medullary epithelial cells of the human thymus express a highly diverse selection of tissue-specific genes colocalized in chromosomal clusters. *J Exp Med* (2004) 199(2):155–66. doi: 10.1084/jem.20031677

194. Pribyl TM, Campagnoni C, Kampf K, Handley VW, Campagnoni AT. The major myelin protein genes are expressed in the human thymus. *J Neurosci Res* (1996) 45(6):812–9. doi: 10.1002/(SICI)1097-4547(19960915)45:6<812::AID-JNR18>3.0.CO;2-X

195. Wucherpfennig KW, Sette A, Southwood S, Oseroff C, Matsui M, Strominger JL, et al. Structural requirements for binding of an immunodominant myelin basic protein peptide to DR2 isotypes and for its recognition by human T cell clones. *J Exp Med* (1994) 179(1):279–90. doi: 10.1084/jem.179.1.279

196. Vogt AB, Kropshofer H, Kalbacher H, Kalbus M, Rammensee HG, Coligan JE, et al. Ligand motifs of HLA-DRB5*0101 and DRB1*1501 molecules delineated from self-peptides. *J Immunol Baltim Md 1950* (1994) 153(4):1665–73. doi: 10.4049/jimmunol.153.4.1665

197. Li Y, Huang Y, Lue J, Quandt JA, Martin R, Mariuzza RA. Structure of a human autoimmune TCR bound to a myelin basic protein self-peptide and a multiple sclerosis-associated MHC class II molecule. *EMBO J* (2005) 24(17):2968–79. doi: 10.1038/sj.emboj.7600771

198. Martin R, Jaraquemada D, Flerlage M, Richert J, Whitaker J, Long EO, et al. Fine specificity and HLA restriction of myelin basic protein-specific cytotoxic T cell lines from multiple sclerosis patients and healthy individuals. *J Immunol Baltim Md 1950* (1990) 145(2):540–8. doi: 10.4049/jimmunol.145.2.540

199. Tejada-Simon MV, Hong J, Rivera VM, Zhang JZ. Reactivity pattern and cytokine profile of T cells primed by myelin peptides in multiple sclerosis and healthy individuals. *Eur J Immunol* (2001) 31(3):907–17. doi: 10.1002/1521-4141(200103)31:3<907::AID-IMMU907>3.0.CO;2-1

200. Moldovan IR, Rudick RA, Cotleur AC, Born SE, Lee JC, Karafa MT, et al. Interferon gamma responses to myelin peptides in multiple sclerosis correlate with a new clinical measure of disease progression. *J Neuroimmunol* (2003) 141(1):132–40. doi: 10.1016/S0165-5728(03)00221-2

201. Hedegaard CJ, Krakauer M, Bendtzen K, Lund H, Sellebjerg F, Nielsen CH. T helper cell type 1 (Th1), Th2 and Th17 responses to myelin basic protein and disease activity in multiple sclerosis. *Immunology.* (2008) 125(2):161–9. doi: 10.1111/j.1365-2567.2008.02837.x

202. Zhang J, Markovic-Plese S, Lacet B, Raus J, Weiner HL, Hafler DA. Increased frequency of interleukin 2-responsive T cells specific for myelin basic protein and proteolipid protein in peripheral blood and cerebrospinal fluid of patients with multiple sclerosis. *J Exp Med* (1994) 179(3):973–84. doi: 10.1084/jem.179.3.973

203. Greer JM, Csurhes PA, Pender MP, McCombe PA. Effect of gender on T-cell proliferative responses to myelin proteolipid protein antigens in patients with multiple sclerosis and controls. *J Autoimmun* (2004) 22(4):345–52. doi: 10.1016/j.jaut.2004.03.004

204. Pender MP, Csurhes PA, Greer JM, Mowat PD, Henderson RD, Cameron KD, et al. Surges of increased T cell reactivity to an encephalitogenic region of myelin proteolipid protein occur more often in patients with multiple sclerosis than in healthy subjects1. *J Immunol* (2000) 165(9):5322–31. doi: 10.4049/jimmunol.165.9.5322

205. Hughes LE, Bonell S, Natt RS, Wilson C, Tiwana H, Ebringer A, et al. Antibody responses to Acinetobacter spp. and Pseudomonas aeruginosa in multiple sclerosis: prospects for diagnosis using the myelin-acinetobacter-neurofilament antibody index. *Clin Diagn Lab Immunol* (2001) 8(6):1181–8. doi: 10.1128/CDLI.8.6.1181-1188.2001

206. Jangi S, Gandhi R, Cox LM, Li N, von Glehn F, Yan R, et al. Alterations of the human gut microbiome in multiple sclerosis. *Nat Commun* (2016) 7(1):12015. doi: 10.1038/ncomms12015

207. Cekanaviciute E, Yoo BB, Runia TF, Debelius JW, Singh S, Nelson CA, et al. Gut bacteria from multiple sclerosis patients modulate human T cells and exacerbate symptoms in mouse models. *Proc Natl Acad Sci U S A* (2017) 114(40):10713–8. doi: 10.1073/pnas.1711235114

208. Bruno R, Sabater L, Sospedra M, Ferrer-Francesch X, Escudero D, Martínez-Cáceres E, et al. Multiple sclerosis candidate autoantigens except myelin oligodendrocyte glycoprotein are transcribed in human thymus. *Eur J Immunol* (2002) 32(10):2737–47. doi: 10.1002/1521-4141(2002010)32:10<2737::AID-IMMU2737>3.0.CO;2-0

209. Tsuchida T, Parker KC, Turner RV, McFarland HF, Coligan JE, Biddison WE. Autoreactive CD8+ T-cell responses to human myelin protein-derived peptides. *Proc Natl Acad Sci U S A* (1994) 91(23):10859–63. doi: 10.1073/pnas.91.23.10859

210. Vanderlugt CL, Miller SD. Epitope spreading in immune-mediated diseases: implications for immunotherapy. *Nat Rev Immunol* (2002) 2(2):85–95. doi: 10.1038/nri724

211. Tavazzi E, Pichiecchio A, Colombo E, Rigoni E, Asteggiano C, Vegezzi E, et al. The potential role of SARS-coV-2 infection and vaccines in multiple sclerosis onset and reactivation: A case series and literature review. *Viruses* (2023) 15(7):1569. doi: 10.3390/v15071569

212. Lake CM, Breen JJ. Sequence similarity between SARS-CoV-2 nucleocapsid and multiple sclerosis-associated proteins provides insight into viral neuropathogenesis following infection. *Sci Rep* (2023) 13(1):389. doi: 10.1038/s41598-022-27348-8

213. Miller SD, Vanderlugt CL, Begolka WS, Pao W, Yauch RL, Neville KL, et al. Persistent infection with Theiler's virus leads to CNS autoimmunity *via* epitope spreading. *Nat Med* (1997) 3(10):1133–6. doi: 10.1038/nm1097-1133

214. Berthelot L, Laplaud DA, Pettré S, Ballet C, Michel L, Hillion S, et al. Blood CD8 + T cell responses against myelin determinants in multiple sclerosis and healthy individuals. *Eur J Immunol* (2008) 38(7):1889–99. doi: 10.1002/eji.200838023

215. Wilson DB, Wilson DH, Schroder K, Pinilla C, Blondelle S, Houghten RA, et al. Specificity and degeneracy of T cells. *Mol Immunol* (2004) 40(14–15):1047–55. doi: 10.1016/j.molimm.2003.11.022

216. Callan MF, Tan L, Annels N, Ogg GS, Wilson JD, O'Callaghan CA, et al. Direct visualization of antigen-specific CD8+ T cells during the primary immune response to Epstein-Barr virus In vivo. *J Exp Med* (1998) 187(9):1395–402. doi: 10.1084/jem.187.9.1395

217. Callan MF, Steven N, Krausa P, Wilson JD, Moss PA, Gillespie GM, et al. Large clonal expansions of CD8+ T cells in acute infectious mononucleosis. *Nat Med* (1996) 2 (8):906–11. doi: 10.1038/nm0896-906

218. Taylor GS, Long HM, Brooks JM, Rickinson AB, Hislop AD. The immunology of Epstein-Barr virus-induced disease. *Annu Rev Immunol* (2015) 33:787–821. doi: 10.1146/annurev-immunol-032414-112326

219. McMahon EJ, Bailey SL, Castenada CV, Waldner H, Miller SD. Epitope spreading initiates in the CNS in two mouse models of multiple sclerosis. *Nat Med* (2005) 11(3):335–9. doi: 10.1038/nm1202

220. Wilhelm CR, Upadhye MA, Eschbacher KL, Karandikar NJ, Boyden AW. Proteolipid protein-induced mouse model of multiple sclerosis requires B cell-mediated antigen presentation. *J Immunol Baltim Md 1950* (2023) 7:ji2200721. doi: 10.4049/jimmunol.2200721

221. Molnarfi N, Schulze-Topphoff U, Weber MS, Patarroyo JC, Prod'homme T, Varrin-Doyer M, et al. MHC class II-dependent B cell APC function is required for induction of CNS autoimmunity independent of myelin-specific antibodies. *J Exp Med* (2013) 210(13):2921–37. doi: 10.1084/jem.20130699

222. Muraro PA, Wandinger K, Bielekova B, Gran B, Marques A, Utz U, et al. Molecular tracking of antigen-specific T cell clones in neurological immune-mediated disorders. *Brain.* (2002) 126(1):20–31. doi: 10.1093/brain/awg021

223. Macrini C, Gerhards R, Winklmeier S, Bergmann L, Mader S, Spadaro M, et al. Features of MOG required for recognition by patients with MOG antibody-associated disorders. *Brain J Neurol* (2021) 144(8):2375–89. doi: 10.1093/brain/awab105

224. Tea F, Lopez JA, Ramanathan S, Merheb V, Lee FXZ, Zou A, et al. Characterization of the human myelin oligodendrocyte glycoprotein antibody response in demyelination. *Acta Neuropathol Commun* (2019) 7(1):145. doi: 10.1186/s40478-019-0786-3

225. Storch MK, Stefferl A, Brehm U, Weissert R, Wallström E, Kerschensteiner M, et al. Autoimmunity to myelin oligodendrocyte glycoprotein in rats mimics the spectrum of multiple sclerosis pathology. *Brain Pathol Zurich Switz* (1998) 8(4):681–94. doi: 10.1111/j.1750-3639.1998.tb00194.x

226. Miller A, Lider O, Abramsky O, Weiner HL. Orally administered myelin basic protein in neonates primes for immune responses and enhances experimental autoimmune encephalomyelitis in adult animals. *Eur J Immunol* (1994) 24(5):1026–32. doi: 10.1002/eji.1830240503

227. Malosse D, Perron H, Sasco A, Seigneurin JM. Correlation between milk and dairy product consumption and multiple sclerosis prevalence: a worldwide study. *Neuroepidemiology.* (1992) 11(4–6):304–12. doi: 10.1159/000110946

228. Smit AF. Interspersed repeats and other mementos of transposable elements in mammalian genomes. *Curr Opin Genet Dev* (1999) 9(6):657–63. doi: 10.1016/S0959-437X(99)00031-3

229. Ryan FP. Human endogenous retroviruses in multiple sclerosis: potential for novel neuro-pharmacological research. *Curr Neuropharmacol* (2011) 9(2):360–9. doi: 10.2174/157015911795596568

230. Sutkowski N, Conrad B, Thorley-Lawson DA, Huber BT. Epstein-barr virus transactivates the human endogenous retrovirus HERV-K18 that encodes a superantigen. *Immunity.* (2001) 15(4):579–89. doi: 10.1016/S1074-7613(01)00210-2

231. Sutkowski N, Palkama T, Ciurli C, Sekaly RP, Thorley-Lawson DA, Huber BT. An Epstein-Barr virus-associated superantigen. *J Exp Med* (1996) 184(3):971–80. doi: 10.1084/jem.184.3.971

232. Walker JA, McKenzie ANJ. T(H)2 cell development and function. *Nat Rev Immunol* (2018) 18(2):121–33. doi: 10.1038/nri.2017.118

233. Lucchinetti C, Brück W, Parisi J, Scheithauer B, Rodriguez M, Lassmann H. Heterogeneity of multiple sclerosis lesions: implications for the pathogenesis of demyelination. *Ann Neurol* (2000) 47(6):707–17. doi: 10.1002/1531-8249(200006)47:6<707::AID-ANA3>3.0.CO;2-Q

234. Planas R, Metz I, Ortiz Y, Vilarrasa N, Jelčić I, Salinas-Riester G, et al. Central role of Th2/Tc2 lymphocytes in pattern II multiple sclerosis lesions. *Ann Clin Transl Neurol* (2015) 2(9):875–93. doi: 10.1002/acn3.218

235. Mohme M, Hotz C, Stevanovic S, Binder T, Lee JH, Okoniewski M, et al. HLA-DR15-derived self-peptides are involved in increased autologous T cell proliferation in multiple sclerosis. *Brain J Neurol* (2013) 136(Pt 6):1783–98. doi: 10.1093/brain/awt108

236. Gabrielsen ISM, Helgeland H, Akselsen H, D. Aass HC, Sundaram AYM, Snowhite IV, et al. Transcriptomes of antigen presenting cells in human thymus. *PloS One* (2019) 14(7):1–18. doi: 10.1371/journal.pone.0218858

237. Lui WY, Bharti A, Wong NHM, Jangra S, Botelho MG, Yuen KS, et al. Suppression of cGAS- and RIG-I-mediated innate immune signaling by Epstein-Barr virus deubiquitinase BPLF1. *PloS Pathog* (2023) 19(2):1–33. doi: 10.1371/journal.ppat.1011186

238. Chen J, Chia N, Kalari KR, Yao JZ, Novotna M, Paz Soldan MM, et al. Multiple sclerosis patients have a distinct gut microbiota compared to healthy controls. *Sci Rep* (2016) 6:28484. doi: 10.1038/srep28484

frontiers | Frontiers in Immunology

TYPE Original Research
PUBLISHED 05 January 2024
DOI 10.3389/fimmu.2023.1304798

OPEN ACCESS

EDITED BY
Dominik Aschenbrenner,
Novartis, Switzerland

REVIEWED BY
Liye Chen,
University of Oxford, United Kingdom
Arundhoti Das,
National Institutes of Health (NIH),
United States

*CORRESPONDENCE
Scheherazade Sadegh-Nasseri
ssadegh@jhmi.edu

†PRESENT ADDRESS
Chan-Su Park,
Department of Pharmaceutics, College of Pharmacy, Chungbuk National University, Cheongju, Republic of Korea

RECEIVED 30 September 2023
ACCEPTED 11 December 2023
PUBLISHED 05 January 2024

CITATION
Welsh RA, Song N, Park C, Peske JD and Sadegh-Nasseri S (2024) H2-O deficiency promotes regulatory T cell differentiation and CD4 T cell hyperactivity.
Front. Immunol. 14:1304798.
doi: 10.3389/fimmu.2023.1304798

H2-O deficiency promotes regulatory T cell differentiation and CD4 T cell hyperactivity

Robin A. Welsh, Nianbin Song, Chan-Su Park†, J. David Peske and Scheherazade Sadegh-Nasseri*

Department of Pathology, Johns Hopkins School of Medicine, Baltimore, MD, United States

Regulatory T cells (Treg) are crucial immune modulators, yet the exact mechanism of thymic Treg development remains controversial. Here, we present the first direct evidence for H2-O, an MHC class II peptide editing molecular chaperon, on selection of thymic Tregs. We identified that lack of H2-O in the thymic medulla promotes thymic Treg development and leads to an increased peripheral Treg frequency. Single-cell RNA-sequencing (scRNA-seq) analysis of splenic CD4 T cells revealed not only an enrichment of effector-like Tregs, but also activated CD4 T cells in the absence of H2-O. Our data support two concepts; a) lack of H2-O expression in the thymic medulla creates an environment permissive to Treg development and, b) that loss of H2-O drives increased basal auto-stimulation of CD4 T cells. These findings can help in better understanding of predispositions to autoimmunity and design of therapeutics for treatment of autoimmune diseases.

KEYWORDS

immunology, class II antigen presentation, regulatory T cells, thymic selection, CD4 T cells

Introduction

T cells are key players in humoral immune responses. Upon infection with a pathogen, CD4 T cells utilize their T cell receptor (TCR) to survey for peptides bound to MHC class II molecules (pMHCII) presented by professional antigen presenting cells (APCs). Identification of cognate pMHCII complexes by the TCR leads to CD4 T cell activation and ultimately clearance of the foreign pathogen. Faulty activation, however, can lead to deleterious inflammation causing possible autoimmune diseases and cancer development. Hence, multiple regulatory processes exist to ensure T cell activation remains in check.

Regulation of T cell activation begins during thymic development where immature thymocytes are screened for self-reactivity. Broadly divided into positive and negative

selection, this process ensures that CD4 T cells expressing high avidity self-reactive TCRs are either eliminated (1), or become CD4 regulatory T cells (Tregs) (2). MHC Class II antigen processing machinery expressed by medullary thymic epithelium cells (mTECs) and thymic antigen presenting cells (APCs) are critical for screening for auto-reactive T cells. Two chaperone proteins, H2-M (murine; human, HLA-DM), and H2-O (murine; human, HLA-DO) are major components of the MHC II processing pathway. While H2-M is expressed in all APCs, H2-O is expressed in the thymic medulla, B cells and various dendritic cell subpopulations (3, 4). H2-M plays a critical role in MHC class II antigen processing by dissociating the Class II Invariant Chain peptide (CLIP) from the newly synthesized MHC II. Dissociation of CLIP promotes a peptide-receptive MHC II conformation to which denatured protein antigens can be screened for the best MHC II groove fitting epitopes. However, a peptide-receptive MHC II conformation is highly transient and in the absence of suitable peptides readily reverts to a closed conformation (5–8). We have proposed that H2-O binds to MHC II in receptive conformation (9) and works cooperatively with H2-M to stabilize the peptide-receptive MHC II conformation for an optimized epitope selection process (10). Together, H2-M and H2-O molecules can ensure that the best MHC II groove fitting epitopes are selected for presentation to cognate CD4 T cells.

While the exact mechanism of Treg selection remains to be fully understood (11), two critical requirements have been recognized as necessary for a successful thymic Treg development. First, thymic Treg development requires relatively strong TCR signaling in the thymic medulla (12), and second, Treg development relies on signaling by the common γ chain (γC) cytokines, mainly IL-2, for driving Foxp3 expression (13). While a strong TCR signaling during negative selection normally leads to CD4 T cell deletion (1), a somewhat weaker TCR signaling has been suggested to promote Treg selection (11, 14, 15). TCR signaling is affected by both the nature and density of the presented self-peptides (16, 17). If epitopes are in high abundance and more ubiquitously expressed in the medulla, then cognate CD4 T cells will undergo clonal deletion. However, if epitopes are in lower abundance and have a sparser expression, leading to discontinuous TCR stimulation, then cognate CD4 T cells might undergo Treg selection. This model of Treg selection relies on the level of TCR signaling that medulla localized CD4 single-positive (SP) T cells receive. As loss of H2-O in naïve peripheral B cells has been shown to alter both the repertoire and density of presented peptides (18, 19) we questioned if loss of H2-O in the thymus could affect whether CD4 T cells are signaled for deletion, or survival during thymic deletion. Should a lower density of self pMHCII be presented in the thymic medulla, an increased number of self-reactive CD4 T cells might escape deletion leading to an increased frequency of auto-reactive T cell clones in the periphery. Or, alternatively, presentation of a lower density of self pMHCII could promote selection of regulatory T cells. Here, we demonstrate that loss of H2-O generates a more stimulatory *in vivo* environment impacting both the thymic development and peripheral activation of regulatory T cells.

Results

Loss of H2-O increases the activation state of auditing medulla CD4 T cells

Previously, we demonstrated that loss of H2-O expression correlated with both an increased B cell presentation of low-affinity MHC II peptides, and an increased frequency of a MOG_{35-55} specific, self-reactive CD4 T cell (18). Because of H2-O expression in the medullary thymus we speculated that H2-O deficiency might lead to presentation of lower densities of high-affinity self-peptides in the medulla, thereby causing altered clonal deletion. Based upon findings by Breed et al. positively selected (TCR-β+ CD5+) medulla CD4 T cells can be subdivided into two main populations, "Auditing" (CCR7 + Caspase-3_{neg}) and "Clonally Deleted" (CCR7+ Caspase-3_{pos}) T cells (20). Using this strategy, we examined the levels of positively selected (TCR-β+CD5+) CD4 T cells undergoing auditing (CCR7+ CD4 +Caspase-3_{neg}) or clonal deletion (CCR7+ CD4+Caspase-3_{pos}) in 6 week old male and female H2-O WT and H2-O mice (Figure 1; Supplementary Figure 1). Loss of H2-O was found to significantly increase the expression of the activation marker CD69 on CD4 T cells undergoing active self-auditing (Figure 1A), but not those selected for clonal deletion (Figure 1B).

CD69 in combination with MHC-I defines 3 medullary maturation stages: semi-mature (CD69+ MHC-I -), mature 1 (CD69+ MHC-I +), and mature 2 (CD69- MHC-I -) (20). Subdivision of auditing H2-O-KO CD4 T cells identified a significant increase in CD4 T cells with a Mature 1 phenotype (Figure 1C middle). Conversely, both the semi-mature and mature 2 stages were decreased in H2-O KO mice (Figure 1C left/right). No differences in any maturation stage were found in the clonally deleted CD4 T cell population (Supplementary Figure 2). Furthermore, H2-O deficiency, did not appear to alter the rate of CD4 T cells undergoing clonal deletion (Figure 1C). Importantly, no differences were observed in thymocytes undergoing positive selection (Supplementary Figure 3). These data suggest that loss of H2-O drives a more stimulatory thymic medulla environment, but with similar levels of clonal deletion. It is therefore likely that the increased peripheral frequencies of MOG-specific CD4 T cells previously identified is due to increased peripheral expansion of the MOG-reactive clone, not a general alteration in clonal deletion.

H2-O KO thymi have increased regulatory T cell development

With increased levels of peripheral Tregs previously identified in H2-O KO mice (18), we also questioned if H2-O deficiency was affecting Treg selection. In fact, one model of thymic Treg selection centers around the concept of antigen density (14, 21). Within this "mosaic" model, sporadic MHC-TCR interactions with sparsely presented self-epitopes leads to Treg development. Since it has been shown that peripheral loss of H2-O leads to alterations in peptide presentation (18, 19, 22), we postulated that altering the level of self-

10.3389/fimmu.2023.1304798

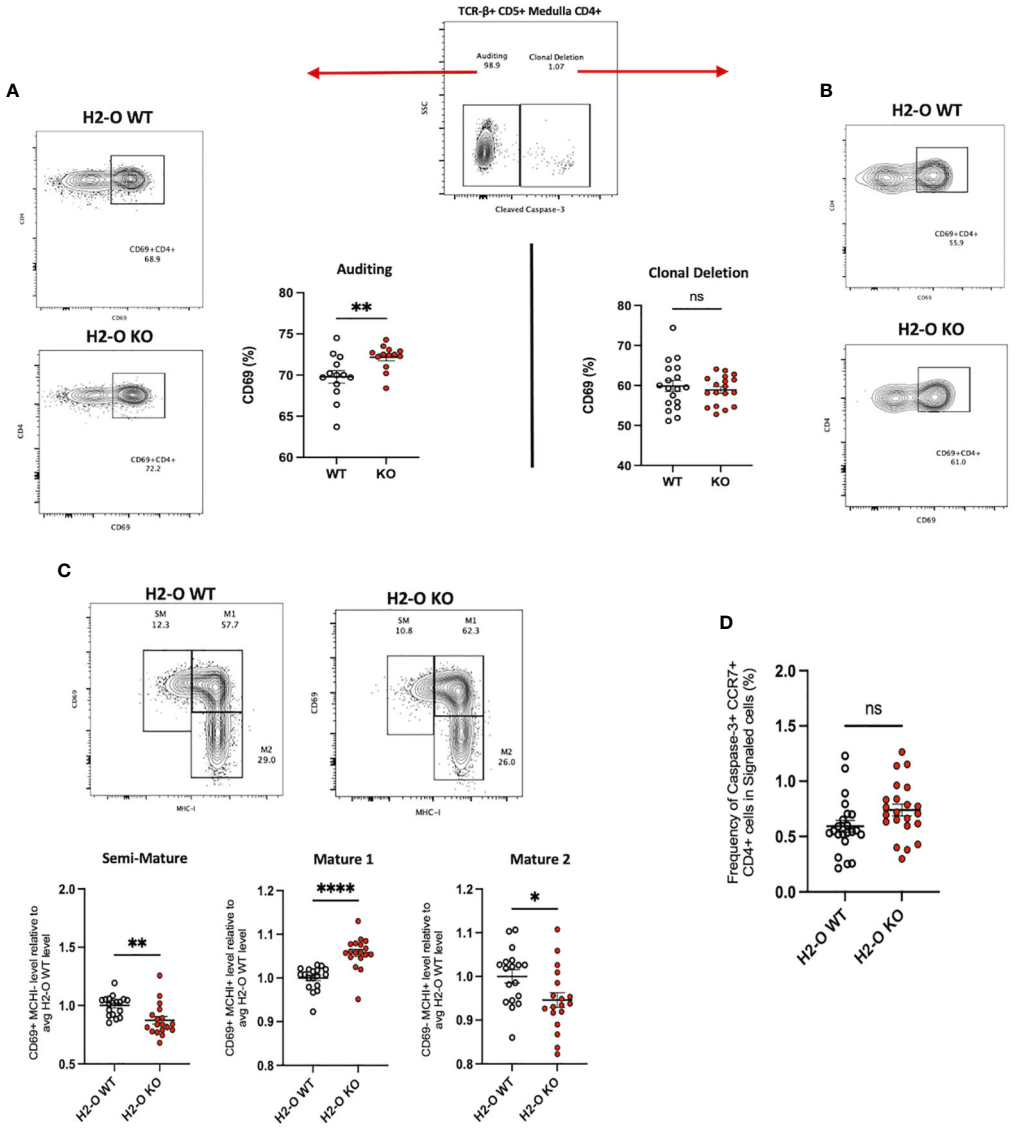

FIGURE 1
Loss of thymic H2-O increases the activation state of auditing CD4 T cells **(A)** Left: representative contour plots showing total CD69 expression in auditing (Caspase-3 negative) signaled (TCR-B+CD5+) CCR7+CD4+ T cells from 6-week-old H2-O WT (Top) and H2-O KO (Bottom) thymi. Right: Combined CD69 expression data from 5 repeat experiments. N= 18 mice per genotype **(B)** Right: representative contour plots showing total CD69 expression in Clonally deleted (Caspase-3 positive) signaled (TCR-B+CD5+) CCR7+CD4+ T cells from 6-week-old H2-O WT (Top) and H2-O KO (Bottom) thymi. Left: Combined CD69 expression data from 5 repeat experiments. N= 18 mice per genotype **(C)** Top: representative contour plots showing the subdivision of auditing (Caspase-3 negative) signaled (TCR-B+CD5+) CCR7+CD4+ T cells from 6-week-old H2-O WT (Left) and H2-O KO (Right) thymi into three maturation stages: Semi-Mature (SM), Mature 1 (M1), and Mature 2 (M2). Bottom: Cumulative maturation state data from 5 repeat experiments, N = 18 mice per genotype. Expression has been normalized to the average H2-O WT levels within each experiment to allow for comparison across experiments. Raw percentage data can be found in Supplementary Figure 3. **(D)** Frequency of medulla specific (CCR7+) CD4 T cells selected for clonal deleted (Caspase-3+) ns, not significant,*<0.05, **<0.001, ***<0.0001, ****<0.00001 Statistics: unpaired student T-test.

epitopes present in the medulla could alter Treg selection. Analysis of CD4 single-positive T cells identified an increased frequency of CD25+Foxp3+ T cells in H2-O KO mice (Figure 2A). Furthermore, H2-O KO thymic Tregs (tTregs) expressed higher levels of the high affinity IL-2 receptor (CD25) (Figure 2B/left), and the orphan nuclear receptor Nur77 (Figure 2B/right). As Nur77 has been associated with the level of TCR engagement (23), increased Nur77 expression strongly indicates that absence of H2-O leads to increased TCR engagement suggesting an increased self-reactivity. Finally, maturation state analysis found that H2-O KO tTregs were enriched in the M1 stage (Figure 2C).

Since peripheral Tregs are known to recirculate back to the thymus (24) we investigated what percentage of the identified tTreg pool in H2-O WT and H2-O KO thymi came from the periphery. As show in Figure 2D, similar levels of recirculating (CCR6+ CD73+) Tregs were identified in both H2-O WT and H2-O KO thymi. Supporting the identification of increased M1 stage Tregs, CCR6- CD73+ (mature) Tregs were statistically increased in H2-O KO mice.

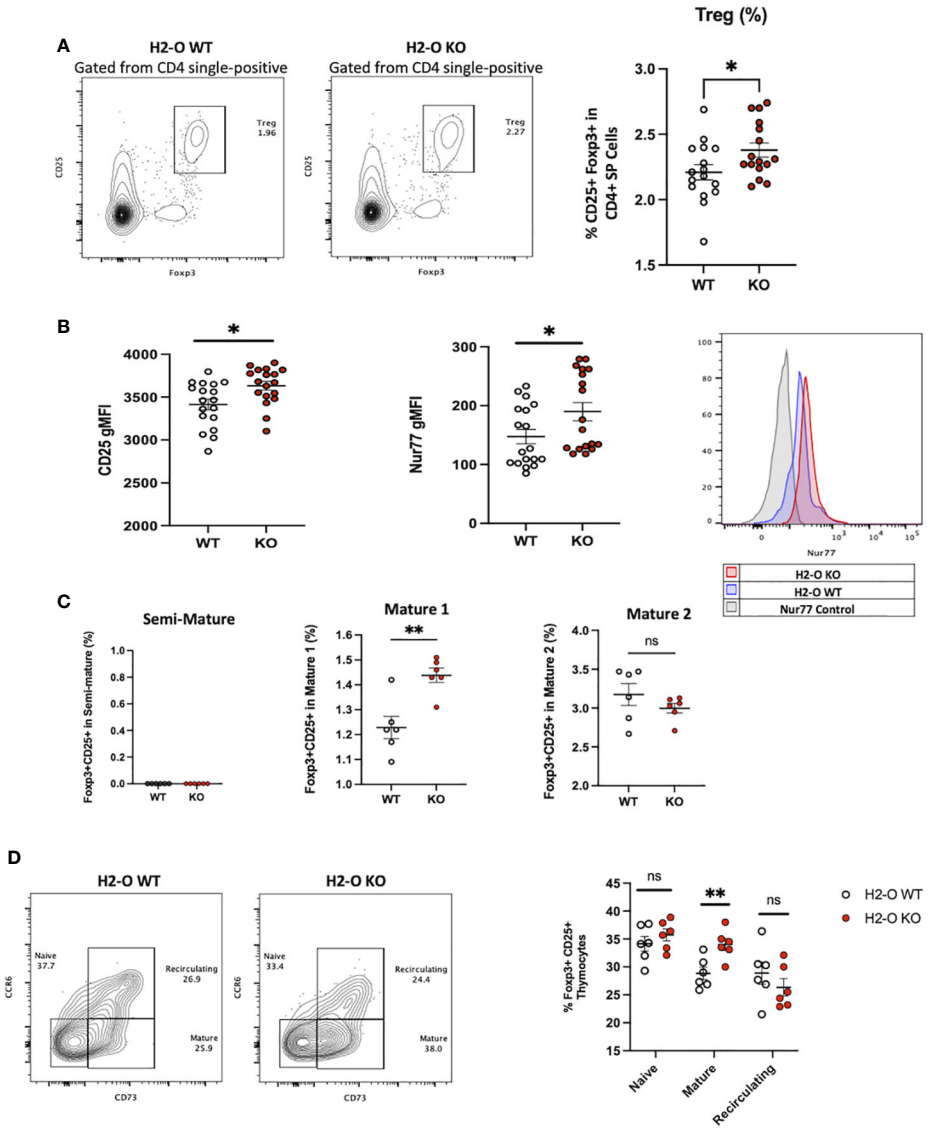

FIGURE 2
H2-O KO thymi have increased regulatory T cell levels. **(A)** Left: representative contour plots showing the frequency of Tregs (CD25+ Foxp3+) cells in the CD4 single-positive thymus population. Right: cumulative percentage of Foxp3+ CD25+ cells within the CD4 single-positive thymus population in H2-O WT (white) or H2-O KO (red) cells. Data from 3 replicate experiments, N= 16 mice per genotype. **(B)** Geometric mean fluorescence intensity (gMFI) of CD25 (left), Nur77 (right) expressed by Foxp3+ CD4+ T cells in the thymus of H2-O WT (white) or H2-O KO (red) mice. **(C)** Subdivision of Treg cells into three maturation stages: Semi-Mature (Left), Mature 1 (Middle), and Mature 2 (Right). Data from 2 replicate experiments. **(D)** Left: representative contour plots showing the frequency of Naive (CCR6- CD73-), Mature (CCR6- CD73+), and Recirculating (CCR6+ CD73+) Foxp3+ CD25+ Tregs in 6-week-old H2-O WT and H2-O KO thymi. Right: Summary plots showing the frequency of Naive (CCR6- CD73-), Mature (CCR6- CD73+), and Recirculating (CCR6+ CD73+) Foxp3+ CD25+ Tregs from 2 independent repeat experiments, N= 6 mice per group. ns = not significant, * = <0.05, ** = <0.001. Statistics: unpaired student T-test.

No major differences were found in the level of naïve (CCR6- CD73-) Tregs. These findings suggest that the increased Treg levels observed in H2-O KO thymi are likely due to an increased *de novo* Treg selection not an increased recirculation of peripheral Treg.

Loss of H2-O correlates with increased peripheral CD4 T cell activation

Considering the observation that lack of H2-O did not appear to alter clonal deletion frequencies but did affect the level of thymic CD4 T cell activation, we next evaluated whether peripheral loss of H2-O also increased CD4 T cells activation. Unimmunized H2-O KO spleens had an increased frequency of CD4 T cells co-expressing the key activation markers CD44+ and CD69+ (Figure 3A) and the tissue homing marker CCR7 (Figure 3B). We further assessed the levels of "non-activated" (CCR7+ CD62L+) versus "activated" (CCR7- CD62L-) CD4 T cells (25), and found lower frequencies of non-activated CD4 T cells in H2-O KO mice (Figure 3C, left). Importantly, this correlated with an increase in percentage of activated CD4 T cells (Figure 3C, right). Collectively, these phenotypic analyses support the idea that loss of H2-O leads

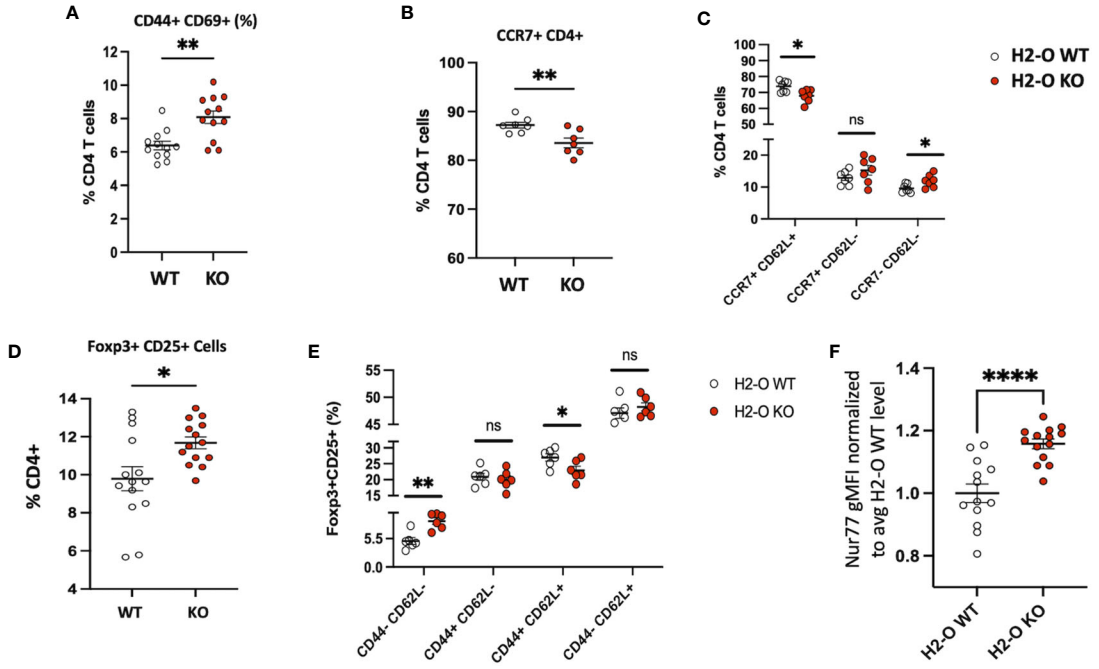

FIGURE 3
H2-O KO mice have an increased activated peripheral CD4 T cell population **(A)** Basal levels of CD44 and CD69 expressed by H2-O WT (white) and H2-O KO (red) splenic CD4 T cells. Increased CD69 expression, a marker of recent activation showed increased levels on H2-O KO CD4 T cells **(B)** Percentage of CD4+ T cells expressing the lymphoid tissue homing receptor CCR7 **(C)** CCR7 and CD62L expression levels in unimmunized splenic CD4 T cells **(D)** Frequency of Foxp3+CD25+ cells in splenic CD4+ T cell population of unimmunized mice **(E)** H2-O KO peripheral Tregs express decreased levels of naïve (CD44+ CD62L+) expressing cells **(F)** Normalized Nur77 gMFI levels in Foxp3+CD25+ Treg cells in H2-O WT (white) and H2-O KO (red) cells. To account for experimental variation the average Nur77 gMFI level in H2-O WT samples was calculated. gMFI levels in both H2-O WT and H2-O KO samples were then divided by the calculated H2-O WT average. An increased Nur77 ratio indicates increased Nur77 gMFI levels. Summary of 3 repeat experiments. *<0.05, **<0.001, ***<0.0001,****<0.00001.

to increased basal levels of activated CD4 T cells in unimmunized H2-O KO mice.

As discussed above, H2-O KO thymi promoted Tregs selection. Consistent with these observations and our previously published data (18, 26), H2-O KO spleens had an increased frequency of CD25+ Foxp3+ Tregs (Figure 3D). Furthermore, H2-O KO Tregs showed decreased levels of CD62L (Figure 3E) and increased levels of Nur77 (Figure 3F) indicating a larger proportion of Tregs cells are likely more activated and circulating through the periphery of H2-O KO mice.

Single cell RNA-sequencing of H2-O KO splenic CD4 T cells confirms increased activation

Based upon the strong FACS data above exhibiting increased numbers of Tregs, and more activated CD4 T cells, we attempted single-cell RNA-sequencing (scRNA-seq) to gain a more holistic unbiased characterization. CD3+ CD4+ NK1.1- CD19- cells were sorted from spleens of 3 unimmunized H2-O WT and 3 unimmunized H2-O KO mice and subjected to 10x Genomics scRNA-seq analyses. In total, 11 distinct CD4 T cell clusters were identified (Figure 4A; Supplementary Figure 4). Separation of the clusters based upon H2-O expression identified a dramatic increase in cluster 0, cluster 2 and cluster 3 in the H2-O KO samples. Conversely, clusters 1 and 4 were significantly increased in H2-O WT samples. Further refinement based upon expression of CD44 and CD62L (Sell) showed that most of clusters 0, 5 and 1 were naïve (CD44- CD62L+) CD4 T cells and CD44+CD62L- effector CD4 T cells were mainly located in clusters 2, 3, and 4. Supplementary Figure 5 shows key genes significantly upregulated in Clusters 0, 1, 2, 3, and 4. No detectable difference was observed in cells expressing central memory markers (CD44+ CD62L+) within Cluster 0 (Figure 4B).

Comparing the genes from Clusters 0, 1 and 5 to the published CD4 T cell datasets using the "My Geneset" function on the Immunological Genome Project (www.immgen.org) suggested that upregulated genes (Log_2Avg Fold-change (FC) 0.5) were present in both "naïve" and "activated" CD4 T cell datasets (Figure 4C). Based upon the high expression of CCR7 however, these clusters were labeled as "non-activated". Clusters 3, 6, 7, and 11 aligned with mainly an "activated" CD4 T phenotype. Cluster 3 was found to have increased expression of the activation marker CD44, while Cluster 11 expressed high Ki67. Clusters 2 and 4 contained the known Treg genes Foxp3 and Il2ra (CD25) (Supplementary Table 1). Clusters 8, 9, and 10 were small populations of Macrophages and NKT cell (Supplementary Table 1). Condensing the cluster analysis further supported our initial FACS data that unimmunized

10.3389/fimmu.2023.1304798

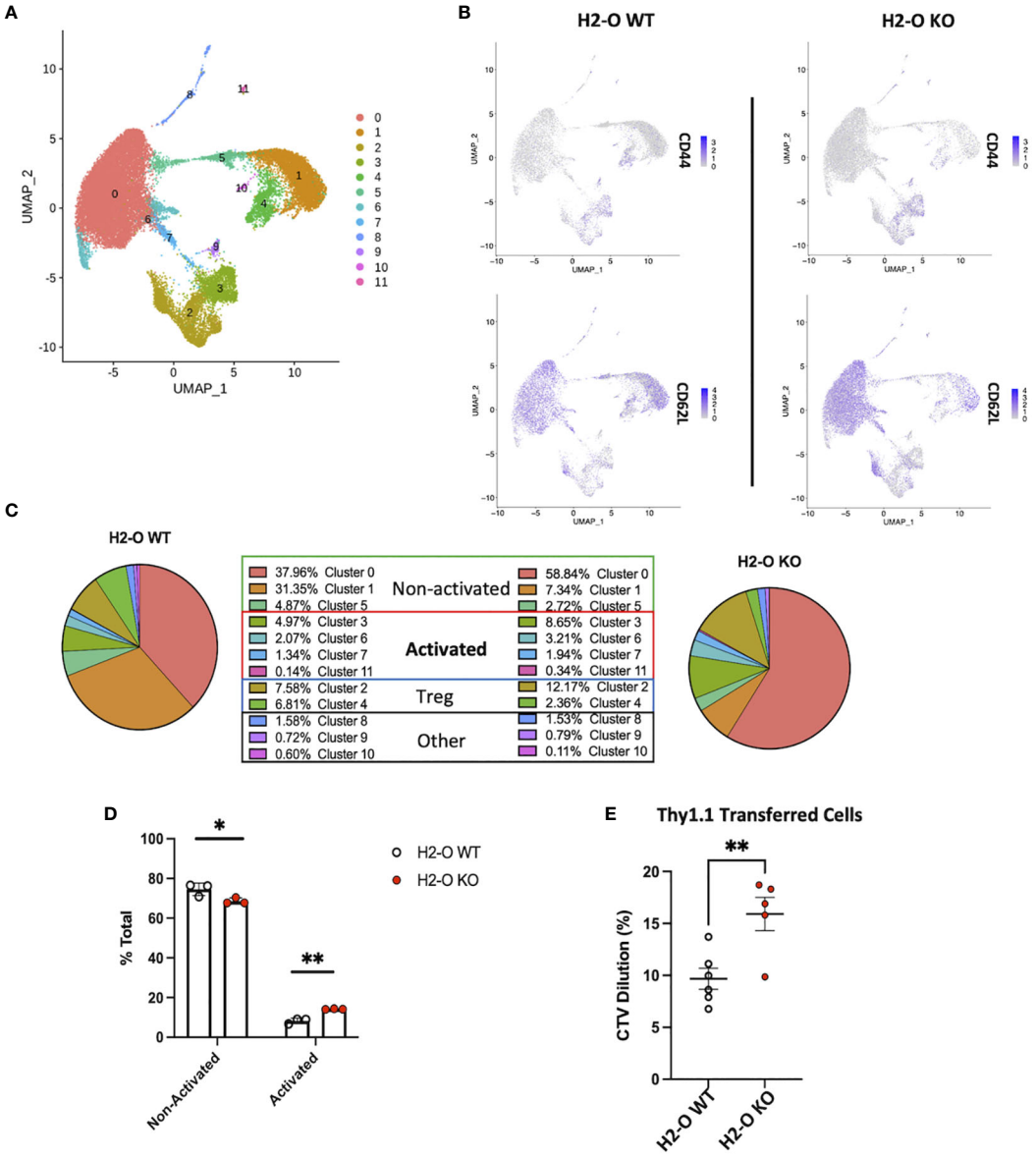

FIGURE 4
Loss of H2-O function causes increased basal CD4 cell activation. **(A)** scRNA-seq clustering of CD4 T cells after Seurat analysis. Data represents the average of of 3 biological replicates per genotype. **(B)** Co-expression of CD44 (top) and CD62L (bottom) within either H2-O WT (left) or H2-O KO (right) clusters. **(C)** Breakdown of clusters in H2-O WT (Left) or H2-O KO (Right) samples. Clusters are grouped based upon, (1) known CD4 T cell subset markers and (2) gene comparison to published CD4 T cell data sets available on the Immunological Genome Project (www.immgen.org). Identified CD4 Cell phenotypes were: Non-activated, Activated, and Regulatory T cells. "Other" refers to a minor macrophage and NKT cell contamination from the sorting process. **(D)** Distribution of the for the Non-activated and Activated phenotypes across the H2-O WT and H2-O KO biological replicates (N = 3 mice per genotype). **(E)** *In vivo* proliferation of adoptively transferred naïve Thy1.1+ CD4 T cells (Thy1.1+ CD3+ CD4+ CD44- CD25-) after 7 days in either Thy1.2 H2-O WT (white) or Thy1.2 H2-O KO (red) hosts. Pooled data from 2 independent experiments (N= 6 H2-O WT, 5 H2-O KO). ns = not significant, * = <0.05, ** = <0.001, ***= <0.0001, **** = <0.00001. Statistics: unpaired student T-test.

H2-O-KO mice have a decreased frequency of "Non-activated" CD4 T cells (68.90% avg H2-O KO vs 74.17% avg H2-O WT with a coinciding increase in "Activated" (14.14% avg H2-O KO vs 8.53% avg H2-O WT) CD4 T cells (Figure 4D).

To test whether the higher activated state in H2-O KO T cells were possibly induced by the *in vivo* environment, we performed an adoptive transfer experiment of Treg depleted naïve Thy1.1+ CD4+ T cells from H2-O WT mice into either unimmunized Thy1.2+ H2-O WT, or Thy1.2+ H2-O KO hosts. Seven days post-transfer we observed that H2-O KO hosts induced significantly more *in vivo* proliferation of the Thy1.1+ WT donor cells as compared to the H2-O WT hosts (Figure 4E). These data further support our working model that loss of H2-O promotes increased T cell activation by APCs presenting a wider range of self-epitopes (18).

10.3389/fimmu.2023.1304798

H2-O KO Tregs have a more activated phenotype

Initial analyses of the two Treg clusters revealed that the frequency of Clusters 2 and 4 were roughly equal in H2-O WT samples, whereas H2-O KO samples had an overrepresentation of Cluster 2 (Figure 5A). Further analysis showed that both clusters 2 and 4 expressed the classic Treg genes, Foxp3 (Figure 5B), IL2ra [CD25] (Figure 5C), Pdcd1 [PD-1] (Figure 5D), and CTLA-4 (Supplementary Table 1). However, we noted that the Foxp3+ cells in cluster 2 segregated into two populations based upon CD25 expression, Foxp3+ CD25^{Low} and Foxp3+ CD25+, with a distinct enrichment of the Foxp3+ CD25^{Low} populations in H2-O KO samples. This was noteworthy as it has been shown that CD25-low FOXP3+ Treg are associated with a more inflammatory state (27). Cluster 2 analysis also identified a small number of cells that expressed the Th17 transcription factor Rorc (RORγ), but only in cells from H2-O KO mice (Supplementary Figures 5, 6). These findings support the association of H2-O with a less inflammatory environment.

Also identified with the Treg clusters was the transcription factor Ikzf2 [Helios], a marker of stable Treg lineage commitment in inflammatory conditions (28), and a controversial marker of thymic Tregs (29–32). FACS analysis of Helios protein expression not only

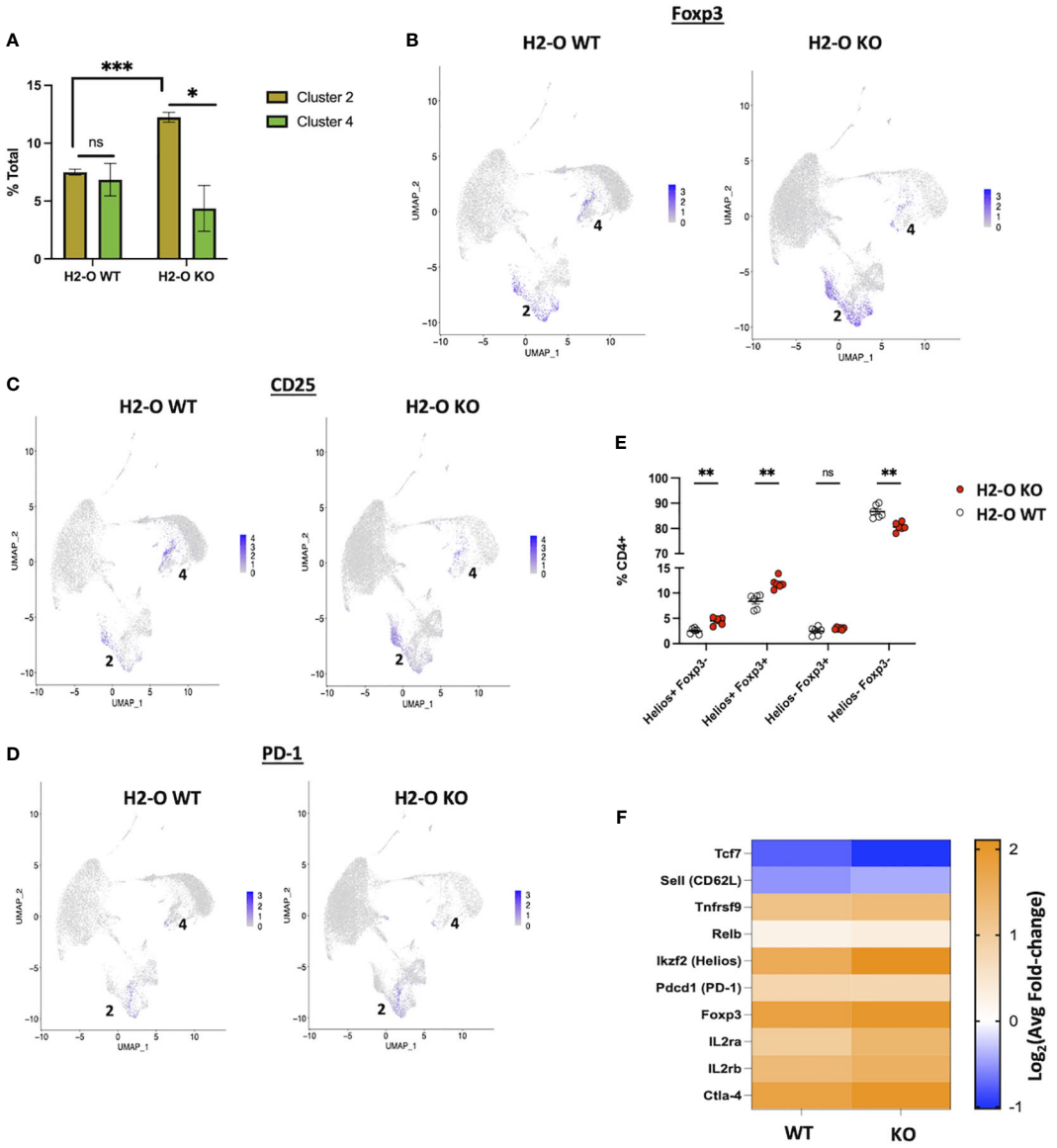

FIGURE 5
The H2-O KO Treg population has a more effector like phenotype. **(A)** (Left) distribution of the two scRNA-seq Treg clusters in either H2-O WT (left) or H2-O KO (right) samples. (Right) Expression of key Treg phenotypic markers: Foxp3 (Top) and CD25 [Il2ra] (Bottom). **(B)** Expression of Foxp3 in H2-O WT (Left) or H2-O KO (Right) clusters. **(C)** Expression of CD25 (IL2ra) in H2-O WT (Left) or H2-O KO (Right) clusters. **(D)** Expression of PD-1 (Pdcd1) in H2-O WT (Left) or H2-O KO (Right) clusters. **(E)** Subdivision of the splenic CD4+ T cell population by Foxp3 and Helios expression. **(F)** Comparison of cluster 2 upregulated genes (Log2Avg FC >0.5) in H2-O WT and H2-KO samples to a published (Miragaia et al.) splenic effector Treg genetic profile. ns = not significant, * = <0.05, ** = <0.001, ***= <0.0001. Statistics: unpaired student T-test.

supported the scRNA-Seq data that both H2-O WT and H2-O KO CD4 Tregs express Helios but also revealed that H2-O KO mice have an increased frequency of Helios+Foxp3+ Tregs (Figure 5E). Since UMAPs preserve information about the distance between clusters (33) we hypothesized that Tregs from Cluster 2 were transcriptional distinct from those in Cluster 4. Comparison of the Cluster 2 genetic signature with a published Treg data set (34) indicated that these cells are likely effector-like Tregs. Furthermore, breaking down Cluster 2 showed that H2-O KO Tregs had a larger fold change in expression of the core effector gene signature (Figure 5F). We propose that this activated Treg state is likely driven by the increased basal CD4 T cell activation. Expansion of this Treg population could certainly be a mechanism controlling spontaneous autoimmunity in H2-O KO mice.

In summary, both scRNA-seq and FACs analyses showed that H2-O KO mice have an increased frequency of both conventional and regulatory CD4 T cells in the spleens of unimmunized mice. Loss of thymic H2-O expression correlated with an increased tTreg population that was not from peripheral recirculation and have received increased TCR stimulation which suggests increased autoreactivity. Furthermore, increased activation of conventional splenic CD4 T cells is likely a driving factor for the increased effector-like Treg status that was identified by scRNA-seq analyses of H2-O-KO CD4 cells.

Discussion

In this study, we have refined our understanding of how loss of H2-O alters CD4 T cell activity *in vivo*. Thymic analysis of medulla localized CD4 T cells pointed to a novel role for H2-O on CD4 T cells undergoing self-auditing. Importantly, lack of H2-O expression led to an increased frequency of both thymic and peripheral Tregs.

Tregs play a fundamental role in maintenance of homeostasis, hence a better understanding of the mechanism of their development is highly desirable and the subject of numerous studies (14, 21). Our studies here are the first attempt in demonstrating that H2-O is a critical player in Treg development. While the exact mechanism by which thymic Treg cells are selected remains somewhat uncertain, recent studies support the idea that intermittent TCR signaling along with cytokine signaling drive Treg development (15). These findings and others (35–39) support a more avidity based model of Treg selection, in which alterations to the density of self-ligands present in the medulla will have differential effects on CD4 T cell selection. Intermittent TCR signaling as the driving force in Treg selection is very relevant to our understanding of how HLA-DO contributes to epitope selection during antigen processing. HLA-DO in complex with HLA-DM leads to better refinement of the epitopes from denatured antigens, promoting selection of the best fitting epitopes in the groove of MHC II molecules (10, 40). While this idea conflicts with the original model of how DO functions (41), recent studies using multiple human HLA-DO variants showed that certain variants enhanced DM activity (42). As such, when DO is present, higher affinity peptides are more likely to be presented. Conversely, in the absence of DO a larger percent of lower affinity epitopes are selected. Indeed, we have recently reported that peptides eluted from H2-O KO mice expressing either murine I-A^b (18) or human HLA-DR1 (Welsh et al, unpublished data) were of a lower general affinity. Accordingly, presentation of a larger portion of lower affinity peptides in the thymic medulla of H2-O KO mice is possible. Intermittent TCR signaling is typically generated by either pMHCII that are less stable (16, 43–45), or TCR/pMHC of lower affinity (46). Our findings here support the former. We associate increased Treg development as a consequence of the presentation of lower affinity peptides to self-auditing CD4 T cells.

Due to the continuous egress of mature CD4 T cells from the thymus, we also analyzed splenic CD4 T cells from unimmunized H2-O WT and H2-O KO mice. H2-O KO splenic CD4 T cells in unimmunized mice revealed an increased frequency of CD44hiCD69+ antigen experienced CD4 T cells, which suggests an increased level of antigen-specific TCR signaling in H2-O KO mice. As previously implied (47), a simple explanation for this activated state is incomplete thymic deletion in H2-O KO mice. While we were able to show that H2-O KO mice failed to delete specific CD4 clonal populations (18), detection of differences at the global levels did not show significant changes between the two genotypes. Nonetheless, we suggest that presentations of different arrays of self-antigens as well as their lower densities on thymic medulla leads to a less than optimal thymic deletion of self-reactive CD4 T cells and their routing to the periphery. Similar to activated CD4 T cells in the periphery, H2-O KO Treg cells also had a more effector-like phenotype, indicating enhanced Treg activation in unimmunized mice (34, 48).

In conclusion, our studies add a new dimension to our understanding of the role of H2-O in both CD4 T cell selection and activation. For the first time, we report on thymic negative selection in H2-O KO mice and demonstrate that loss of H2-O enhances thymic selection of regulatory T cells. Once in the periphery, an increased proportion of H2-O KO Tregs appear to be activated in a TCR dependent manner. These effector-like Tregs will likely help control increased basal CD4 T cell activation. However, the exact mechanism by which increased Treg cells are selected in the H2-O KO thymus remains to be determined. While we propose that alterations in medulla pMHCII-TCR avidity interactions could lead to enhanced Treg selection, increased presentation of self-antigens in a more tissue restricted antigenic (TRA) manner could also be possible (14).

Methods

Mice

Male and female C57BL/6J (H2-O WT, stock no: 000664), Female B6.PL-Thy1a/CyJ (stock no: 000406) were purchased from Jackson Laboratories and bred in house. Generation of the H2-O knock-out mice has been previously described (49) and mice bred in house. Unless otherwise stated analyzed mice were 6-8 weeks. All mouse procedures were approved by the Johns Hopkins

University Animal Care and Use Committee and were following relevant ethical regulations.

Antibodies/reagents

Flow Cytometry: anti-CD3e (17A2), anti-CD4 (RM4-5), anti-CD5 (53-7.3), anti-CD8α (53-6.7), CD11c (N418), anti-CD19 (ID3), anti-CD25 (PC61), anti-CD44 (IM7), anti-CD45R/B220 (RA3-6B2), anti-CD62L (MEL-14), anti-CD69 (H1.2F3), anti-CD197/CCR7 (4B12), anti-NK1.1 (PK136), anti-TCRβ (H57-597), anti-TCRγδ (GL3), anti-Cleaved Caspase 3 (D3E9) Cell signaling (Danvers, MA); Foxp3 (150D), anti-Helios (22F6), anti-Nur77 (12.14), Fixable viability dye eFluor 780 (eBioscience).

FACs Sorting: anti-CD3e, anti-CD4, anti-CD19, anti-NK1.1, Propidium iodide. Briefly, 30,000 live CD4 T cells [Gating: CD3+, CD4, CD19-, NK1.1-, PI-] were FACs sorted from the spleens of 3 unimmunized 10 week-old H2-O WT and 3 unimmunized 10 week-old unimmunized H2-O KO female mice.

Cell staining

For cleaved caspase 3 staining (20) homogenized mice thymocyte cells were stained with anti-CCR7/CD197 at a final dilution of 1:50 for 30 min at 37°C prior to additional surface stains. Following surface staining, cells were fixed with Cytofix/Cytoperm (BD Biosciences) for 20 min at 4°C. Cells were then washed with Perm/Wash buffer (BD Biosciences) twice. Cells were stained with anti–cleaved caspase 3 at a 1:50 dilution at 23°C for 30 min.

For transcription factor staining, cells were incubated with surface antibody at 4°C for 20 min, permeabilized at 4°C for 30 min using a Foxp3/Transcription factor buffer set (Invitrogen, ThermoFisher Scientific), and then stained with anti–Foxp3 and/or anti-Helios at 23°C for 30 min.

Adoptive cell transfer

Naïve CD4 T cells were isolated from the pooled spleens and LNs of 4 week old Thy1.1 expressing C57BL/6J mice using the EasySep Mouse Naive CD4 T cell Isolation Kit (StemCell Technologies). Isolated cells were stained with eFluor 450 viability dye (eBiosciences) according to manufactures directions. $3x10^6$ dye labeled Thy1.1 cells were IV injected into 10 week old H2-O WT or H2-O KO hosts. Transferred cells were recovered 7 days post-transfer.

scRNA-sequencing

Library & sequencing

The samples were prepared using the 10x Genomics Chromium Next GEM Single Cell 5' Library and Gel Bead Kit v1.1, Chromium Next GEM Chip and Dual Index Kit TN Set A. They were run on the Illumina NovaSeq6000 with a run configuration of 28bp x 10bp x 10bp x 91bp.

Analysis

Analyses of T-cell scRNA-seq were performed with the package Seurat (50), as follows. Data was filtered to remove cells with low gene count (<200), large number of UMIs (>12,000) and high (>5%) fraction of mitochondrial reads. Expression levels of genes were log-normalized, and the most variable 2000 genes were selected for linear dimensionality reduction with Principal Component Analysis (PCA). The first 15 principal components were then used to performed unsupervised clustering using the Seurat SNN clustering package, with a resolution of 0.2. To identify cell types, potential markers for each cluster were calculated as the set of genes significantly differentially expressed in each cluster compared to all others, using the function FindAllMarkers, and by searching existing literature and marker databases. Lastly, differentially expressed genes for each cell type between conditions were determined using the function FindMarkers with the default function (bimod).

Defining clusters – Genes with an average fold-change (avgFC) >0.5 and an adjusted p-value <0.05 were run against CD4 T cell data sets available on the Immunological Genome Project (https://www.immgen.org/) using the "My Geneset" data browser function.

Statistical testing

GraphPad Prism was used for all statistical analyses. A standard Student T-test was used for estimation of statistical significance. Data is shown as mean ± SEM. *p<0.05, **p<0.01, ***p<0.001, ****p<0.0001.

Data availability statement

The scRNA-Seq data presented in the study are deposited in the NCBI GEO repository, accessionnumber: GSE246253.

Ethics statement

The animal study was approved by Johns Hopkins Animal Care and Use Committee. The study was conducted in accordance with the local legislation and institutional requirements.

Author contributions

RW: Conceptualization, Data curation, Formal analysis, Investigation, Methodology, Project administration, Resources, Validation, Visualization, Writing – original draft, Writing – review & editing. NS: Investigation, Methodology, Resources, Validation, Visualization, Writing – review & editing. C-SP: Conceptualization, Methodology, Visualization, Writing – review & editing. JP: Conceptualization, Investigation, Writing – review & editing. SS-N: Conceptualization, Data curation, Funding acquisition, Methodology, Project administration, Resources, Supervision, Visualization, Writing – original draft, Writing – review & editing.

Funding

The author(s) declare financial support was received for the research, authorship, and/or publication of this article. Supported by grants from NIAID, R01AI063764, R21AI101987, and R01AI120634, to SS-N, and R01AI130210, R01AI149341 to Nilabh Shastri and transferred to SS-N.

Acknowledgments

We thank Dr. Ellen Robey at UC Berkeley for productive discussions, Corina Antonescu and Liliana Floera from the Computational Biology Computing Core at Johns Hopkins School of Medicine for scRNA-Seq analysis, and Drs. Lars Karlsson and Peter Jensen for H-2O KO mice. FACs analysis was performed in the BD Immunology and Flow Cytometry Laboratory at the Johns Hopkins School of Public Health.

Conflict of interest

The authors declare that the research was conducted in the absence of any commercial or financial relationships that could be construed as a potential conflict of interest.

The author(s) declared that they were an editorial board member of Frontiers, at the time of submission. This had no impact on the peer review process and the final decision.

Publisher's note

Supplementary material

The Supplementary Material for this article can be found online at: https://www.frontiersin.org/articles/10.3389/fimmu.2023.1304798/full#supplementary-material

SUPPLEMENTARY FIGURE 1
Gating strategy used for detection of Auditing *vs* Clonally Deleted Medulla CD4 T cells Red arrows indicate how Auditing *vs* Clonal Deletion was identified in 6-week-old H2-O WT and H2-O KO thymi. Blue arrows indicate additional gating corresponding to . Black Arrows indicate additional gating corresponding to (Figure 1B).

SUPPLEMENTARY FIGURE 2
The frequency of auditing Mature 1 CD4 T cells was increased in H2-O KO thyme **(A)**. Percentage of auditing (Caspase-3 negative) CD4 T cells in the Semi-mature (CD69+ MHC-I neg), Mature 1 (CD69+ MHC-1+), and Mature 2 (CD69- MHC-I+) in H2-O WT (white) and H2-O KO (red) mice N= 18 mice per group **(B)**. Percentage of clonally deleted (Caspase-3+) CD4 T cells in the Semi-mature (CD69+ MHC-I neg), Mature 1 (CD69+ MHC-1+), and Mature 2 (CD69- MHC-I+) in H2-O WT (white) and H2-O KO (red) mice. N= 18 mice per group Statistical Testing: unpaired student T-test.

SUPPLEMENTARY FIGURE 3
Positive Selection is not affected by loss of H2-O **(A)**. Representative plots showing CD4, CD8 and Double Positive (DP) percentages in H2-O WT (Top) and H2-O KO (Bottom) **(B)**. Summary plots of the single-positive CD4 (Top) and CD8 (Bottom) percentages from 5 repeat experiments. **(C)**. (Left) representative flow plots showing the "Signaled" *vs* "Non-signaled" thymocytes in H2-O WT (Top) or H2-O KO (Bottom). (Right) Summary plots of >5 repeat experiments. **(D)**. Frequency of signaled CCR7+ medulla CD4 T cells in H2-O WT (white) and H2-O KO (red) mice.

SUPPLEMENTARY FIGURE 4
Top: breakdown of H2-O KO (right) and H2-O WT (Left) Seurat clustering Bottom: Seurat clustering for each individual biological replicate.

SUPPLEMENTARY FIGURE 5
Key genes in Clusters 0-4. (Top) Top genes (Avg(log_2)FC >1, p-value<0.05) for clusters 0-4 in concatenated data. (Bottom) Key gene expression broken into H2-O WT (left) or H2-O KO (right).

SUPPLEMENTARY FIGURE 6
Rorc expression is found within H2-O KO Tregs. Red outline indicates that minor RORγ expression was found in H2-O KO cluster 2.

References

1. Murphy K, Weaver C. Janeway's immunobiology. *New York London: Garland Science;* (2016). doi: 10.1201/9781315533247

2. Nishizuka Y, Sakakura T. Thymus and reproduction: sex-linked dysgenesia of the gonad after neonatal thymectomy in mice. *Science* (1969) 166(3906):753–5. doi: 10.1126/science.166.3906.753

3. Karlsson L, Surh CD, Sprent J, Peterson PA. A novel class II MHC molecule with unusual tissue distribution. *Nature* (1991) 351(6326):485–8. doi: 10.1038/351485a0

4. Fallas JL, Yi W, Draghi NA, O'Rourke HM, Denzin LK. Expression patterns of H2-O in mouse B cells and dendritic cells correlate with cell function. *J Immunol* (2007) 178(3):1488–97. doi: 10.4049/jimmunol.178.3.1488

5. Narayan K, Su KW, Chou CL, Khoruzhenko S, Sadegh-Nasseri S. HLA-DM mediates peptide exchange by interacting transiently and repeatedly with HLA-DR1. *Mol Immunol* (2009) 46(15):3157–62. doi: 10.1016/j.molimm.2009.07.001

6. Chou CL, Mirshahidi S, Su KW, Kim A, Narayan K, Khoruzhenko S, et al. Short peptide sequences mimic HLA-DM functions. *Mol Immunol* (2008) 45(7):1935–43. doi: 10.1016/j.molimm.2007.10.033

7. Natarajan SK, Assadi M, Sadegh-Nasseri S. Stable peptide binding to MHC class II molecule is rapid and is determined by a receptive conformation shaped by prior association with low affinity peptides. *J Immunol* (1999) 162(7):4030–6. doi: 10.4049/jimmunol.162.7.4030

8. Sadegh-Nasseri S. A step-by-step overview of the dynamic process of epitope selection by major histocompatibility complex class II for presentation to helper T cells. *F1000Res* (2016) 5. doi: 10.12688/f1000research.7664.1

9. Alfonso C, Williams GS, Han JO, Westberg JA, Winqvist O, Karlsson L. Analysis of H2-O influence on antigen presentation by B cells. *J Immunol* (2003) 171(5):2331–7. doi: 10.4049/jimmunol.171.5.2331

10. Poluektov YO, Kim A, Hartman IZ, Sadegh-Nasseri S. HLA-DO as the optimizer of epitope selection for MHC class II antigen presentation. *PloS One* (2013) 8(8): e71228. doi: 10.1371/journal.pone.0071228

11. Savage PA, Klawon DEJ, Miller CH. Regulatory T cell development. *Annu Rev Immunol* (2020) 38:421–53. doi: 10.1146/annurev-immunol-100219-020937

12. Hsieh CS, Lee HM, Lio CW. Selection of regulatory T cells in the thymus. *Nat Rev Immunol* (2012) 12(3):157–67. doi: 10.1038/nri3155

13. Tai X, Erman B, Alag A, Mu J, Kimura M, Katz G, et al. Foxp3 transcription factor is proapoptotic and lethal to developing regulatory T cells unless counterbalanced by cytokine survival signals. *Immunity* (2013) 38(6):1116–28. doi: 10.1016/j.immuni.2013.02.022

14. Klein L, Robey EA, Hsieh CS. Central CD4(+) T cell tolerance: deletion versus regulatory T cell differentiation. *Nat Rev Immunol* (2019) 19(1):7–18. doi: 10.1038/s41577-018-0083-6

15. Tai X, Indart A, Rojano M, Guo J, Apenes N, Kadakia T, et al. How autoreactive thymocytes differentiate into regulatory versus effector CD4(+) T cells after avoiding clonal deletion. *Nat Immunol* (2023) 24(4):637–51. doi: 10.1038/s41590-023-01469-2

16. Mirshahidi S, Ferris LC, Sadegh-Nasseri S. The magnitude of TCR engagement is a critical predictor of T cell anergy or activation. *J Immunol* (2004) 172(9):5346–55. doi: 10.4049/jimmunol.172.9.5346

17. Dalai SK, Khoruzhenko S, Drake CG, Jie CC, Sadegh-Nasseri S. Resolution of infection promotes a state of dormancy and long survival of CD4 memory T cells. *Immunol Cell Biol* (2011). doi: 10.1038/icb.2011.2

18. Welsh RA, Song N, Foss CA, Boronina T, Cole RN, Sadegh-Nasseri S. Lack of the MHC class II chaperone H2-O causes susceptibility to autoimmune diseases. *PloS Biol* (2020) 18(2):e3000590. doi: 10.1371/journal.pbio.3000590

19. Nanaware PP, Jurewicz MM, Leszyk J, Shaffer SA, Stern LJ. HLA-DO modulates the diversity of the MHC-II self-peptidome. *Mol Cell Proteomics* (2018). doi: 10.1074/mcp.RA118.000956

20. Breed ER, Watanabe M, Hogquist KA. Measuring thymic clonal deletion at the population level. *J Immunol* (2019) 202(11):3226–33. doi: 10.4049/jimmunol.1900191

21. Li MO, Rudensky AY. T cell receptor signalling in the control of regulatory T cell differentiation and function. *Nat Rev Immunol* (2016) 16(4):220–33. doi: 10.1038/nri.2016.26

22. Yi W, Seth NP, Martillotti T, Wucherpfennig KW, Sant'Angelo DB, Denzin LK. Targeted regulation of self-peptide presentation prevents type I diabetes in mice without disrupting general immunocompetence. *J Clin Invest.* (2010) 120(4):1324–36. doi: 10.1172/JCI40220

23. Moran AE, Holzapfel KL, Xing Y, Cunningham NR, Maltzman JS, Punt J, et al. T cell receptor signal strength in Treg and iNKT cell development demonstrated by a novel fluorescent reporter mouse. *J Exp Med* (2011) 208(6):1279–89. doi: 10.1084/jem.20110308

24. Santamaria JC, Borelli A, Irla M. Regulatory T cell heterogeneity in the thymus: impact on their functional activities. *Front Immunol* (2021) 12:643153. doi: 10.3389/fimmu.2021.643153

25. Golubovskaya V, Wu L. Different subsets of T cells, memory, effector functions, and CAR-T immunotherapy. *Cancers (Basel).* (2016) 8(3). doi: 10.3390/cancers8030036

26. Welsh R, Sadegh-nasseri S. The love and hate relationship of HLA-DM/DO in the selection of immunodominant epitopes. *Curr Opin Immunol* (2020) 64:117–23.

27. Ferreira RC, Simons HZ, Thompson WS, Rainbow DB, Yang X, Cutler AJ, et al. Cells with Treg-specific FOXP3 demethylation but low CD25 are prevalent in autoimmunity. *J Autoimmun* (2017) 84:75–86.

28. Lam AJ, Uday P, Gillies JK, Levings MK. Helios is a marker, not a driver, of human Treg stability. *Eur J Immunol* (2022) 52(1):75–84.

29. Thornton AM, Korty PE, Tran DQ, Wohlfert EA, Murray PE, Belkaid Y, et al. Expression of Helios, an Ikaros transcription factor family member, differentiates thymic-derived from peripherally induced Foxp3+ T regulatory cells. *J Immunol* (2010) 184(7):3433–41.

30. Thornton AM, Lu J, Korty PE, Kim YC, Martens C, Sun PD, et al. Helios(+) and Helios(-) Treg subpopulations are phenotypically and functionally distinct and express dissimilar TCR repertoires. *Eur J Immunol* (2019) 49(3):398–412.

31. Serre K, Benezech C, Desanti G, Bobat S, Toellner KM, Bird R, et al. Helios is associated with CD4 T cells differentiating to T helper 2 and follicular helper T cells in *vivo* independently of Foxp3 expression. *PloS One* (2011) 6(6):e20731. doi: 10.1371/journal.pone.0020731

32. Akimova T, Beier UH, Wang L, Levine MH, Hancock WW. Helios expression is a marker of T cell activation and proliferation. *PloS One* (2011) 6(8):e24226. doi: 10.1371/journal.pone.0024226

33. Armstrong G, Martino C, Rahman G, Gonzalez A, Vazquez-Baeza Y, Mishne G, et al. Uniform manifold approximation and projection (UMAP) reveals composite patterns and resolves visualization artifacts in microbiome data. *mSystems* (2021) 6(5):e0069121. doi: 10.1128/mSystems.00691-21

34. Miragaia RJ, Gomes T, Chomka A, Jardine L, Riedel A, Hegazy AN, et al. Single-cell transcriptomics of regulatory T cells reveals trajectories of tissue adaptation. *Immunity* (2019) 50(2):493–504 e7. doi: 10.1016/j.immuni.2019.01.001

35. Simons DM, Picca CC, Oh S, Perng OA, Aitken M, Erikson J, et al. How specificity for self-peptides shapes the development and function of regulatory T cells. *J Leukoc Biol* (2010) 88(6):1099–107. doi: 10.1189/jlb.0310183

36. Relland LM, Mishra MK, Haribhai D, Edwards B, Ziegelbauer J, Williams CB. Affinity-based selection of regulatory T cells occurs independent of agonist-mediated induction of Foxp3 expression. *J Immunol* (2009) 182(3):1341–50. doi: 10.4049/jimmunol.182.3.1341

37. Picca CC, Oh S, Panarey L, Aitken M, Basehoar A, Caton AJ. Thymocyte deletion can bias Treg formation toward low-abundance self-peptide. *Eur J Immunol* (2009) 39(12):3301–6. doi: 10.1002/eji.200939709

38. Feuerer M, Jiang W, Holler PD, Satpathy A, Campbell C, Bogue M, et al. Enhanced thymic selection of FoxP3+ regulatory T cells in the NOD mouse model of autoimmune diabetes. *Proc Natl Acad Sci U S A.* (2007) 104(46):18181–6. doi: 10.1073/pnas.0708899104

39. Atibalentja DF, Murphy KM, Unanue ER. Functional redundancy between thymic CD8{alpha}+ and sirp{alpha}+ Conventional dendritic cells in presentation of blood-derived lysozyme by MHC class II proteins. *J Immunol* (2011) 186(3):1421–31. doi: 10.4049/jimmunol.1002587

40. Poluektov YO, Kim A, Sadegh-Nasseri S. HLA-DO and its role in MHC class II antigen presentation. *Front Immunol* (2013) 4:260. doi: 10.3389/fimmu.2013.00260

41. Denzin LK. Inhibition of HLA-DM mediated MHC class II peptide loading by HLA-DO promotes self tolerance. *Front Immunol* (2013) 4:465.

42. Denzin LK, Khan AA, Virdis F, Wilks J, Kane M, Beilinson HA, et al. Neutralizing antibody responses to viral infections are linked to the non-classical MHC class II gene H2-ob. *Immunity* (2017) 47(2):310–22 e7.

43. Sadegh-Nasseri S, Dalai SK, Korb Ferris LC, Mirshahidi S. Suboptimal engagement of the T-cell receptor by a variety of peptide-MHC ligands triggers T-cell anergy. *Immunology* (2010) 129(1):1–7.

44. Baumgartner CK, Ferrante A, Nagaoka M, Gorski J, Malherbe LP. Peptide-MHC class II complex stability governs CD4 T cell clonal selection. *J Immunol* (2010) 184(2):573–81.

45. Smyth LA, Williams O, Huby RDJ, Norton T, Acuto O, Ley SC, et al. Altered peptide ligands induce quantitatively but not qualitatively different intracellular signals in primary thymocytes. *PNAS* (1998) 95(14):8193–8.

46. Lucas B, Stefanova I, Yasutomo K, Dautigny N, Germain RN. Divergent changes in the sensitivity of maturing T cells to structurally related ligands underlies formation of a useful T cell repertoire. *Immunity* (1999) 10(3):367–76. doi: 10.1016/S1074-7613(00)80036-9

47. Gu Y, Jensen PE, Chen X. Immunodeficiency and autoimmunity in H2-O-deficient mice. *J Immunol* (2013) 190(1):126–37. doi: 10.4049/jimmunol.1200993

48. Shevyrev D, Tereshchenko V. Treg heterogeneity, function, and homeostasis. *Front Immunol* (2019) 10:3100. doi: 10.3389/fimmu.2019.03100

49. Liljedahl M, Winqvist O, Surh CD, Wong P, Ngo K, Teyton L, et al. Altered antigen presentation in mice lacking H2-O. *Immunity* (1998) 8(2):233–43. doi: 10.1016/S1074-7613(00)80475-6

50. Stuart T, Butler A, Hoffman P, Hafemeister C, Papalexi E, Mauck WM 3rd, et al. Compr Integration Single-Cell Data. Cell (2019) 177(7):1888–902.e21.

frontiers | Frontiers in Immunology

TYPE Review
PUBLISHED 13 February 2024
DOI 10.3389/fimmu.2024.1343575

OPEN ACCESS

EDITED BY
Silvia Monticelli,
Institute for Research in Biomedicine (IRB), Switzerland

REVIEWED BY
Balbino Alarcón,
Spanish National Research Council (CSIC), Spain
Johannes Bernhard Huppa,
Medical University of Vienna, Austria

*CORRESPONDENCE
Oreste Acuto
oreste.acuto@path.ox.ac.uk

RECEIVED 23 November 2023
ACCEPTED 17 January 2024
PUBLISHED 13 February 2024

CITATION
Acuto O (2024) T-cell virtuosity in "knowing thyself".
Front. Immunol. 15:1343575.
doi: 10.3389/fimmu.2024.1343575

T-cell virtuosity in "knowing thyself"

Oreste Acuto*

Sir William Dunn School of Pathology, University of Oxford, Oxford, United Kingdom

Major Histocompatibility Complex (MHC) I and II and the αβ T-cell antigen receptor (TCRαβ) govern fundamental traits of adaptive immunity. They form a membrane-borne ligand-receptor system weighing host proteome integrity to detect contamination by nonself proteins. MHC-I and -II exhibit the "MHC-fold", which is able to bind a large assortment of short peptides as proxies for self and nonself proteins. The ensuing varying surfaces are mandatory ligands for Ig-like TCRαβ highly mutable binding sites. Conserved molecular signatures guide TCRαβ ligand binding sites to focus on the MHC-fold (MHC-restriction) while leaving many opportunities for its most hypervariable determinants to contact the peptide. This riveting molecular strategy affords many options for binding energy compatible with specific recognition and signalling aimed to eradicated microbial pathogens and cancer cells. While the molecular foundations of αβ T-cell adaptive immunity are largely understood, uncertainty persists on how peptide-MHC binding induces the TCRαβ signals that instruct cell-fate decisions. Solving this mystery is another milestone for understanding αβ T-cells' self/nonself discrimination. Recent developments revealing the innermost links between TCRαβ structural dynamics and signalling modality should help dissipate this long-sought-after enigma.

KEYWORDS

T cell, T cell antigen receptor (TCR), antigen recognition, TCR signalling, allosteric activation

Building T-cell adaptive immunity

"Immunology: The Science of Self/Nonself Discrimination", a book by Jan Klein published in 1982 (1), condenses what an immune system normally does, quizzing the biochemical make-up of the host for potential alterations by exogenous or endogenous sources, which reduce fitness and prompt actions to eradicate the causing agent. This central tenet is materialised through biomolecular interactions trained on evolutionary timescales to make binary decisions such as abstaining from reacting to (tolerating) the host's biomolecules or reacting to unfamiliar ones. Immunity is traditionally divided into innate (or inborn) and adaptive (acquired or combinatorial), which in its most sophisticated form, as discussed here, operates only in jawed vertebrates. Innate immunity is a first line of protection discriminating between the molecular differences in

microbial and host nucleic acids, carbohydrates, or proteins that are maintained during the evolutionary time scale (2). Adaptive immunity is a powerful fail-safe system generally set in motion by warnings originating from innate immunity responses (2). Its distinctive character is a vast repertoire of clonally-unique (clonotypic) surface receptors, each with a different ligand-binding site, borne only by lymphocytes. Their characteristic immunoglobulin (Ig)-superfamily fold offers opportunities for molecular recognition of organic polymers, preferentially folded proteins, or small fragments thereof, achieving specificity at single-residue resolution. Quadrillions of diverse binding sites can be theoretically generated by DNA recombination mechanisms involving the juxtaposition of diverse genetically-encoded variable (V), diversity (D), and joining (J) segments and random mutations occurring at the splice sites (3). Such an immense diversity is *de novo* generated during most of the host life span in a ligand-independent fashion and beyond actual needs, like a pro-active plan anticipating an uncertain future. Optimisation and safety processes operate thorough positive selection for clonotypic receptors trained over self-biomolecular structures and deemed apt to bind and signal, and discard those that are highly auto-reactive. The resulting receptor stock is competent for facing nonself entities, predominantly pathogenic micro-organisms. The prodigious chemical and physical diversity afforded by proteins is appropriate for such an undertaking as it provides protein-protein interfaces with a breath of combinatorial of enthalpy-entropy solutions for favourable binding free energy (4) and specific recognition. Contrary to the classical "one receptor one (or few) ligand(s)" paradigm, pairing of clonotypic receptors with ligands requires a process of trial and error to hit an affinity range compatible with a signal delivered to the cell. Depending on their strength, signals can drive lymphocyte homeostasis/survival, death or change of functional fate change for coordinating the removal of a micro-organism or oncoprotein-transformed cell. Binding with adequate affinity and occupancy to nonself ligands (antigens) elicits signals for lymphocyte clonal expansion, a key trait of adapting immunity, ensuring that only receptors that specifically recognise an invading nonself (*e.g.*, a microorganism) are selectively amplified. One fraction of the clonally expanded cell pool is not used for immediate needs but stored as a resting, long-term memory of the specific event, another unique feature of adaptive immunity. Memory cells are selectively expanded upon re-exposure to the same antigen providing faster and more effective protection. These biological marks are shared by B-cells and T-cells that together form the complementary arms of adaptive immunity.

The appearance of primordial components of this extraordinary system about 450 million years ago, manifestly offered considerable survival advantage to jawed vertebrates, as witnessed by the rapid expansion of genes governing adaptive immunity by duplication and diversification into composite families (5). Evolutionary geneticists trace the dawn of adaptive immunity to three founding events: the appearance of Major Histocompatibility Complex (MHC) genes encoding classical class-I and -II proteins (5) (for simplicity, hereafter referred to as MHC-I and-II), genes encoding T-cell antigen receptor (TCR) αβ and γδ dimers and Immunoglobulin (Ig) heavy and light chains that form the B-cell antigen receptor (BCR) and ensuing antibodies (Abs), and, coincidentally, of site-specific recombination-activation genes (RAG1/2) (6). TCR and BCR defined two major lineages of vertebrate lymphocytes that act in concert to protect the host by recognising nonself and organise its neutralisation. Excellent and comprehensive reviews on the origin of adaptive immunity can be found in (5–9).

TCR and MHC-I and -II are membrane proteins presumably originated from a rudimentary receptor-ligand pair involved in cell-cell recognition. Despite being encoded on different chromosomes MHC and TCR co-evolved, witnessing the importance of their interaction for jaw vertebrate fitness (5). TCR α and β together form a variable membrane-distal Ig-like binding site with a definitive preference for targeting the so-called "MHC-fold" (5), the membrane-distal domain of MHC-I and -II. The MHC-fold exhibits highly promiscuous binding with 1:1 stoichiometry of diverse short peptides derived from the degradation of proteins of self or nonself origin. The peptide binding site tolerates single and multiple mutations without compromising protein stability, a property exploited to diversify further the already large repertoire of peptides accommodated by each MHC-I or II allomorph, ranking MHC-I and II among the most polymorphic genes in Chordata (10). Another key founding event in adaptive immunity was the appearance in early jawed vertebrates of mandatory companions of TCRαβ, namely four genes whose products form three smaller dimers (εγ, εδ, ζζ, called CD3). CD3 serves to communicate to the cell interior ligand engagement by TCRαβ, via immunoreceptor tyrosine-based activation motifs (ITAMs). The TCRαβεγεδζζ complex forms an octamer made of four non-covalently bound dimers (11), significantly distinct from hundreds of membrane receptors prototypes successfully tested in evolution for intercellular communication, a singularity that continues to question T-cell biologists.

TCRαβ ligands: staging self-identity and its modifications

In jawed vertebrates, nucleated cells parade on their surface a significant sample of their individual proteome, such as a "QR-code" granting proof of self-identity. Using intact proteins would be physically and biologically unfeasible. A nifty energy-saving alternative is to employ instead protein surrogates naturally available in great abundance and variety in every cell: peptides issued from the physiological degradation of proteins of every cellular compartment or seized from the extra-cellular milieu (12). A providential gift of evolutionary adaptation for this job was the MHC-fold, born by MHC-I and -II proteins (the latter being the presumed MHC-I ancestor (5). The MHC-fold is the membrane-distal domain of MHC-I α1 chain, stabilised by the β_2-microglobulin (β_2m) subunit (13, 14). An analogous MHC-fold in MHC-II arises from the complementation of two "half-MHC-folds" of the α1 and α2 subunits forming a very stable dimer (15). The MHC-fold is made of eight β-strands fashioning a relatively rigid platform (the floor) delimited by two anti-parallel α-helices (the walls), called α_1 and α_2 for MHC-I (13, 14) and α_1 and β_1 for MHC-

II (15). This fold forms a narrow and deep groove (or cleft) of dimensions and chemistry suitable for housing many diverse short peptides. MHC I and II possess molecular signatures for being dispatched near or at protein-grinding machines/compartments (proteosome or endosomal vesicles) where a vast cellular peptidome is generated (12). Generic and dedicated peptidases produce candidate peptides of 8-10 and 10-15 amino acid-long for preferential binding to MHC-I (in the endoplasmic reticulum) (16) and MHC-II (in late endosomal or lysosomal compartments) (17), respectively. MHC-I and -II are assisted by bestowed peptide-loading complexes performing trial and error casting to select peptides that bind with medium-high affinity (K_D of 100 to 5 nM (12). Only MHC-I and -II molecules filled with tightly bound peptides are granted access to the PM, thus guaranteeing stable surface presentation of a highly diverse immunopeptidome. Host and microbial proteomes are subject to the same rules of degradation and peptide loading, thus creating a considerable assortment of cellular self-proteome with occasional contamination with peptides derived from non-self proteins (12, 18). A unique feature of MHC-I and -II is their ability to bind large numbers of diverse peptides. A single HLA allomorph can bind 2,000 to 10,000 unique peptides (19), a huge promiscuity apparently incongruous with medium-low nM peptide binding affinities. Crystallographic, mutagenesis and thermodynamic studies explain this apparent paradox (14, 15, 20). Short peptides behave as random coils, yet the entropic cost for accommodating them in the MHC groove in an extended conformation is largely compensated by a dense array of hydrogen-bonding with the peptide main-chain. MHC-I groove is closed at both hands by conserved residues that hook the N- and C-termini of 8-10 amino acid-long peptides via hydrogen bonds. The MHC-II groove has open ends and can bind longer peptides, whose termini extend outside the groove. This generic peptide binding mode alone would make specificity vanishingly small, resulting in loose binding of a good peptide portion and an exceedingly large peptide repertoire, ultimately limiting the ability of TCRαβ to accomplish its task. Imposing some degree of specificity, hence a more frugal choice of peptide diversity is crucial. Indeed, the MHC floor features a few pockets with varying selectivity for certain peptide side chains. Some pockets (generally one per molecular type) are deep and narrow, hence selective for side chains of particular character at some peptide positions that contribute substantially to the binding energy. Other pockets, roomy and shallow accommodate diverse side chains at other positions, adding further contribution for peptide affinity and selectivity. Moreover, the side chains of number of residues in the groove can assume diverse tortional angles for optimal interaction with the peptide, while deep pockets burying peptide side chains afford high hydrophobic and hydrogen bonding energy (20). These few pockets of individual physicochemical character achieve a fair compromise between peptide promiscuity, specificity, and affinity. MHC-I (A, B and C) and MHC-II (DP, DQ, and DR) exhibit the entire human immunopeptidome, which is considerably higher than in a single individual, considering that just for HLA-A and B > 12,000 alleles exist (21). Such huge polymorphism concerns mostly MHC floor and wall residues and much less resides at the top of the α-helices. Peptide residues that cannot bond with floor and walls residues, either interact weakly with the rims of the groove or afford high conformational freedom, both targeted by TCRαβ. 10^5-10^6 MHC molecules/cell offer a large mosaic of the individual cellular immunopeptidomes, which, considering all tissues, it represents a spatiotemporal steady-state snapshot of virtually every cellular activity in the organism. This self-panorama is perturbed when MHC-I and/or -II are occasionally loaded with microbially-derived (or mutated oncogene-derived) peptides eventually unmasking the presence of microbial (or mutated host) proteins. While nucleated cells exhibit their own immunopeptidome, specialised innate immunity cells, such as Dendritic cells (DC) residing in critical tissue whereabouts (*e.g.*, in lymph nodes (LNs) display also extracellular peptidomes as they constitutively express MHC-II. DCs possess highly specialised peptide-loading systems for efficient presentation of microbial pathogen-derived or mutated onco-protein immunopeptidome released in the extracellular space. In LNs, DCs select αβ-T cells for the ability to distinguish self and nonself immunopeptidomes. The latter are usually very scarcely represented before host acute morbidity manifests, making hard at this stage for αβ-T cells to perceive them among a vast sample of self-peptides and to engage in rapid and potent countermeasures to prevent chronic morbidity or death.

TCR αβ diagonal binding to p-MHC

When undertaking a cursory glimpse, TCRαβ and Ig binding sites look alike. Both V domains feature similar β-strands sandwich scaffolds with bulging loops forming analogous complementarity-determining regions (CDRs) 1, 2, and 3 making up the ligand binding site, with the CDR3s centrally located. TCRαβ and BCR ligand binding sites can attain a comparable huge magnitude of diversity (> 10^{15}) by similar DNA recombination rules assembling analogous V, D, and J gene segments (22). As for BCR, TCRαβ CDR1, and CDR2 are encoded by germline V segments organised into families (in human ≈ 70 Vα divided into 41 families and ≈ 47 Vβ divided into 23 families) and the CDR3s arise from the somatic juxtaposition of V-J (67 Jα) or V-D-J (13 Jβ and 2 Dβ) segments that substantially augment binding site diversity by imperfect joining and template-independent nucleotides additions. However, similarities stop here as MHC-restricted recognition of peptides implies that Vα and/or Vβ should possess structural signatures virtually absent in V_HV_L binding sites. Indeed, genetic manipulation in mice indicates that MHC restriction is encoded by TCRαβ genes (23, 24). Unlike Abs, TCRαβ diversity in CDR3s is much higher than in CDR1 and CDR2, which feature conserved residues involved in MHC binding (25), incidentally making affinity maturation by somatic hypermutation afforded by Abs prohibitive for TCRαβ. Unlike the BCR, TCRTCRαβ does not have a soluble form. The structural principles of p-MHC recognition by TCRαβ have been largely clarified by crystal structures (15, 26, 27) and reviewed in (28–30). Thus, Ab binding sites exhibit considerable shape variability, typified by geomorphic grouping as cave, crater, canyon, valley, and plain (31), and high binding complementarity often achieved by affinity maturation (32, 33). Catalytic Abs that

detect chemical reaction transition states are another illuminating example of Ab binding site structural malleability. The TCRαβ binding site is instead relatively flat with mild undulations and slightly protruding CDR3s (28, 29). Wiley and co-workers vividly portrayed TCRαβ positioning over ligand as suspended over the edges of the MHC groove delimited by two high peaks of α-helices, with bulging CDR3s trying to catch peptide side chains arising from the bottom (27). Most notably, TCRαβ is invariably orientated diagonally with respect to the peptide long axis, an emplacement that maximises the chances for the hypervariable CDR3s to contact the peptide, the most variable portion of the ligand surface. CDR3s focus on the peptide centre but at times on more C- or N-terminally positioned residues. The relatively exiguous peptide surface makes Vα and/or Vβ CDR3s often contacting also MHC residues (26, 27, 30), though alone are unlikely to be the major drivers for the diagonal orientation. Rather, Vα and Vβ CDR2s, which are symmetrically distal from the CDR3s, often contact exclusively conserved residues of MHC-I α2 and α1 (or with MHC-II β1 and α1), respectively. CDR1 loops of Vα and Vβ second systematically a hybrid role by contacting peptide eccentric, N- and C-terminally, residues, as well as MHC-I α2 and α1 (or MHC-II β1 and α1), respectively. A few Vα and Vβ framework residues and, so-called CDR4 loops, occasionally contribute to ligand contacts. The angle of diagonal orientation (or crossing angle) varies considerably in different complexes, though hardly exceeding certain limits (27°≤ θ ≤70°) (34), such that Vα invariably sits on the taller and broken α-helix, whereas Vβ prefers the lower, shorter and smoother α-helix. The different elevation of the MHC α-helices over the groove results in a characteristic tilting (or incident) angle between TCRαβ and ligand that can vary in different complexes (0°≤ θ ≤ 25°) (34). Rare complexes showing limited TCRαβ contacts with peptide or unconventional orientations have been reported (26, 30, 35–37). Variation of diagonal and tilting angles, and of register and extent of peptide contacts suggests that, while systematically zeroing in on MHC, TCRαβ binding site exploits many opportunities for subtle or overt adjustments aimed to augment specificity for the peptide and ligand affinity. Binding promiscuity favoured by roomy shape complementarity and electrostatic interactions between pairs of conserved residues in MHC α-helices and Vα and/or Vβ families may promote an initial docking phase that imposes limits to the orientation of TCRαβ over p-MHC. However, such docking leaves scope for additional energy contributions offered to CDR3s by the physicochemical nature of the peptide and by subtle re-adjustments of all CDRs bonding with MHC (30, 38, 39). Diagonal orientation and binding tuning negotiate MHC restriction and peptide specificity compatible with affinities that elicit receptor signalling of biological relevance, the latter being the definitive arbitration of ligand effectiveness (EC_{50}). p-MHC-TCRαβ binding geometry may help explain the TCRαβ-CD3 signalling mechanism (discussed below). Consistent with some earlier suggestions on self-recognition, a few structures of TCRαβ in complex with self p-MHC show limited peptide contacts, yet conserve diagonal orientation (26, 35). In agreement with gradual binding adjustments, thermodynamics, and structural data have suggested considerable conformational changes occurring at the p-MHC-TCRαβ binding interface, indicative of an enthalpically-driven reaction with considerable entropic penalty, reflected by agonist weak/medium solution K_D (200 - 0.05 μM), as estimated by surface plasmon resonance using monomers of TCRαβ and p-MHC extracellular domains (40–47). However, evidence for both enthalpy and entropy-driven binding have also been documented (48, 49). 2D affinity measurements in intact T cells using artificial membrane-tethered p-MHC show 100 times higher on-rates and no or some off-rates increase (50, 51), resulting in considerable K_D reduction, a realistic estimate of ligand potency compounding the membrane tethered nature of ligand-receptor pairs and stochastic noise. However, KD or the combination of KD and $t_{1/2}$ alone does not satisfactorily explain ligand potency in general and especially for high K_{on} and K_{off} (discussed in 43), leading to the proposal of an "aggregate occupancy dwell-time" by fast rebinding of TCRαβ to the same p-MHC (43, 52). Diffusion-influenced reaction, co-receptors, signal decay slower than ligand unbinding (43), but also enhanced membrane tethering by "short" receptor-ligand pairs, as well as the potential for very fast ligand-mediated TCR-CD3 activation and tight clustering of signalling TCR-CD3 (the latter two discussed below) may be invoked to explain how signals emanating from TCR-CD3 lead to T-cell activation.

Building on previous discussion of MHC-restriction, we will now briefly consider the process that moulds TCR αβ clonotypic repertoires restricted to MHC. Only αβ T-cell precursors reacting sufficiently with p-MHC presented in the thymus environment of the host will generate signals sufficient to survive (positive selection) and further pruned of TCRαβ reacting too strongly to tissue-specific host self p-MHC (negative selection). This mechanism forges immunologically competent αβ T cells that exhibit TCRαβ clonotypes with recognition patterns for self p-MHC at low affinity that will compete with each other for cell survival. Teleologically, the thymic learning process allows to "memorise" the molecular thyself of Socratic wisdom a process that inevitably results in awareness of nonself. In LNs αβ T cells are continuously reminded of such precept by self-pMHC that induce weak signals above background ("tonic" signals). Tonic signal is vital for phenotypic stability and survival of αβ T cells (53, 54), incidentally demonstrating that the peripheral T cells pool is inherently self-reactive. 2D binding data of self-reactive TCRs in intact cells show amazingly short dwell times of ≈100 ms or less (55), yet sufficient to elicit signals that positively select thymocytes and αβ-TCR cell survival. This αβ T cell pool should be cross-reactive to the host immunopeptidome, as weak signalling elicited by a single self-molecular species of the huge immunopeptidome repertoire might be insufficient to ensure αβ T cell survival. Diffused TCRαβ cross-reactivity should be essential for responding to a much larger universe of potential nonself peptides (56), using parsimoniously a TCRαβ clonotypic repertoires estimated in humans to be ≅ 10^{11} out of total number of 10^{12} αβ T cells (57). Such vast cross-reactivity arises from the considerable molecular plasticity of p-MHC -TCRαβ binding (58). Various mechanisms are in place to ensure that self-reactivity never exceeds accidentally a threshold that might result in auto-immunity. This is a particularly delicate exercise as negative feedback of TCR-proximal signalling responsible for signal

thresholding are closely connected to positive feedback, whose activation allows to surmount signal threshold (59). Coupling of these devices likely constitutes prototypical steps of a proof-reading signalling regime thought to implement ligand discrimination (60) and determine the sigmoidal trend of αβ T-cell responses to ligand dose.

p-MHC-induced TCR-CD3 activation

Spatiotemporal organisation

As for many other membrane receptors, TCR-CD3 signal amplitude and duration depend on ligand affinity and concentration, which together provide non-linear signal inputs (59). Signals of varying intensity (or strength) can generate different scales of cellular responses that may result in cell fate changes (61, 62). Weak agonists (*i.e.*, self p-MHC) support survival of αβ-T-cell precursors during thymic development (63, 64) and of peripheral αβ-T cells (53, 54). αβ-T-cell proliferation, differentiation, and exhaustion, or thymocyte negative selection are induced by strong p-MHC agonists.

TCR-CD3 activation strictly refers to the molecular process by which p-MHC binding converts inactive TCR-CD3 into an active isoform able to deliver a signal to the cell interior (signal transduction). TCR-CD3 "signalling" is often used as a shortcut to mean not only TCR-CD3 "activation" but also signal amplification - *i.e.*, TCR-CD3 special property of multiplying the number of CD3 phosphorylated ITAMs -, signal stabilisation and intracellular propagation or even T-cell activation (Figure 1). This semantic lapsus overlooks the necessary spatiotemporal sequence of events (or cascade, Figure 1) and the specific physicochemical condition associated with membrane signalling, both being relevant for understanding the idiosyncratic molecular structure and functional behaviour of TCR-CD3. Thus, in a natural setting, where a p-MHC agonist is typically very scarce, TCR-CD3 activation and consequent signal firing likely is started by individual p-MHC-TCR-CD3 pairs (discussed below) at minuscule portions of the plasma membrane (< 60 nm^2, as calculated from TCR-CD3 structure (11). However, signal firing by distant individual receptors may not add up effectively for achieving functionally relevant outcomes, due to the limited supply of enzymes and substrates and to stochastic noise (mechanical disturbance, protein crowdedness) that may inevitably slow down reaction rates. Clustering of individually activated receptors, a feature of virtually every membrane receptor (65, 66), provides great benefits to signalling: local increase of concentration of dedicated enzymes and substrates; the chance for weak non-Michaelis-Menten interactions favouring enzyme-substrate binding and rebinding; membrane lipid-dependent regulation; ligand rebinding (52) and protraction of allosterically-activated state of the receptor (65, 66). Early claims that TCR-CD3 forms abundant clusters at steady state (67) have been challenged by more perfected super-resolution imaging approaches (51, 68–70), including data analysis that limits particle over-counting (71). These investigations suggest that

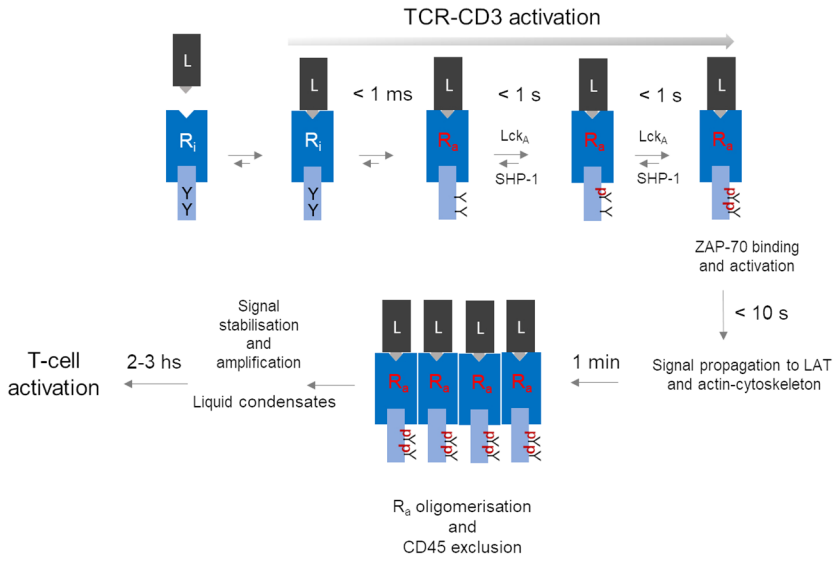

FIGURE 1
A hypothetical unifying model for TCR-CD3 activation leading to T-cell activation. The series of events depicted here is a summary of the process described in the paper, omitting for simplicity molecular details. The model contemplates a temporal cascade that initiates with an allosterically regulated-activation of the inactive TCR-CD3 (inactive Receptor (R_i) induced simply by peptide-MHC (L) binding, leading to very fast (< 1 ms) tyrosine (Y) exposure in R_a to active-Lck (Lck_A). Lck_A and SHP-1 negotiate ITAM phosphorylation (pY-ITAMs), eventually leading to 2pY-ITAMs if receptor occupancy is adequate and R_a can now bind and activate ZAP-70 to connect to the LAT protein scaffold for signal diversification (59). Data discussed in the text suggest that all sequelae of events take 10 s or so after ligand binding. The proposed model considers that only R_a can form tight clusters, while ZAP-70 (not shown) remains dynamically bound to R_a. For simplicity, co-receptors have been omitted but if they are required for weak ligands, at a certain point they might depart from clustered R_{as}. Other events should further stabilise the signal perhaps by condensation of signalling effectors near clustered R_{as}. It is in the next few hours that key cell decisions will be made that involve nuclear events necessary for cell cycle entry and differentiation.

ligand-unbound TCR-CD3 is largely organised not into clusters (72). Thus, clustering could be a critical tipping point to increase and stabilise ITAMs phosphorylation rate and signal propagation (Figure 1).

TCR-CD3 emanates signals using molecular rules shared by other immune receptors (*e.g.*, BCR, FcRs, NKRs) but apparently not by classical membrane receptors activated by soluble ligands (*e.g.*, EGR receptor (EGFR), G protein-coupled receptor (GPCR), cytokine receptors). Thus, shortly after p-MHC binding, the tyrosine kinase Lck phosphorylates the ITAMs (each one containing two tyrosines (Y) in the cytoplasmic tails of the CD3 subunits ζ, ε, γ and δ (schematised in Figure 1). ITAM of different subunits are semi-conserved, with ζ harbouring three ITAMs and ε, γ and δ only one each, making a total of twenty tyrosines that could potentially be phosphorylated in a single TCR-CD3 molecule. ITAMs phosphorylated at a single tyrosine (pY-ITAM) cannot support productive cell activation because only phosphorylation of both tyrosines (2pY-ITAM) allows stable association and activation of ZAP-70 (73), a tyrosine kinase essential for TCR-CD3 signal propagation (73). ZAP-70 affinity for 2pY-ITAM is about 10 nM, much greater than the usual affinity range of p-MHC agonists suggesting signal stabilisation already at this early signalling stage. The degree of ITAM phosphorylation correlates with p-MHC binding duration (or dwell-time). ZAP-70 is mandatory for the positive selection of αβ T cells (74, 75), indicating that even weak p-MHC agonists induce sizable rates of 2pY-ITAM and of activated-ZAP-70 generation. Genetic data have shown that ITAMs multiplicity plays a quantitative role (76), strongly suggesting that the ITAMs are an expandable source of 2pY-ITAM and activated ZAP-70 generated at a rate dependent on ligand affinity and abundance. This rate is likely to be the most important parameter arbitrating whether a p-MHC agonist will make an αβ T cell either survive or clonally expand and differentiate or immolate. Estimates in individual cells and bulk populations suggest that it should take less than one second after TCRαβ binding to a medium/strong p-MHC agonist to induce pY-ITAMs elevation that shortly after activates major signalling pathways (*i.e.*, raise of IP_3 and calcium) (59, 77) (Figure 1). Typical p-MHC agonists show dwell times of 5 to 60 seconds or longer, compatible with the timing of p-ITAMs detection. Weak ligands - *i.e.*, self-p-MHC inducing T-cell or thymocytes survival exhibit dwell-times as low as 100 ms or less (55). Thus, any molecular model of TCR-CD3 activation must be coherent with such a fast time scale. It has been suggested that very weak p-MHC agonists take longer times for pY-ITAM, leading to an approximate signal-storage phenomenon (78). However, the stochastic nature of signals just above the threshold may require time to attain sufficient synchrony of individual TCR-CD3 signal firing, eventually leading to pY-ITAM detection. Single-digit p-MHC agonists may suffice to elevate calcium concentration and activate Ras (79) and also induce the expression of genes activated by these pathways (80). However, priming a T cell for clonal expansion and full differentiation (or thymocyte death for negative selection) requires sustained engagement by p-MHC, forming persistent TCR-CD3 clustering and relatively stable signalling complexes beneath them (Figure 1) (59). Positive cooperativity between TCR-CD3 engaged with p-MHC monomers may be initiated by long-range effects, not necessarily mediated by lipid phase-like "rafts", but rather by the TCR-CD3 "lipid fingerprint" (81, 82), followed by the multivalent assembly by lateral receptor clustering cemented more stably by direct protein-protein interactions and interactions with intracellular multi-protein signalling complexes (59). Such large molecular gathering forms 3D "signalling territories" at the cell-cell junctions or immunological synapses (IS) (83) between αβ T cells and APC (or target cells for cytotoxic αβ T cells). They are though to generate quasi-phases called "liquid condensates" (70, 84) ensuring sufficiently insulated environments for stabilisation and amplification of incoming signals.

Coreceptors

Textbooks and review articles describing αβ T-cell activation often portray TCR-CD3 intracellular tails as rigid sticks freely floating in the cytosol, happily waiting to be phosphorylated by Lck brought by coreceptors CD8 or CD4 bound to MHC coincidentally with TCRαβ. Such representation implies that TCR-CD3 is a rigid protein complex barely capable, if not unable of MHC-restricted recognition and doing nothing to promote ITAMs phosphorylation, begging therefore a companion receptor to do it on its behalf. Such misrepresentation reduces to nil many valued publications of the past three decades that indicate a different setting, first and foremost that coreceptors play only a quantitative role in TCR-CD3 activation, hence they can be dispensable. Co-receptors come on stage to compensate for poor TCR-CD3 activation to achieve adequate αβ T-cell activation. Early genetic evidence in mice showed that CD8- or CD4-deficiency does not stop the development of mature MHC-I-restricted (cytotoxic) (85) and II-restricted (helper) αβ T cells (86), but reduces their number (85, 86), presumably compensating for co-receptor absence by selecting TCRαβ of higher affinity. Moreover, CD4-deficient mice restore normal numbers of MHC-II-restricted helper αβ T cells upon over-expression of a CD4 mutant unable to associate with Lck (87). Consistently, CD8 decreases the k_{off} of p-MHC binding to TCRαβ (88) and CD8 is fully dispensable for p-MHC agonists of $K_D \leq 5$ μM (89). Feeble activation of CD8-deficient αβ T-cell by weak agonists can be largely compensated by increasing p-MHC concentration (*i.e.*, higher EC_{50} is observed) (89). These conclusions are backed by more recent data (90, 91). Coreceptor-bound Lck may act as an intracellular adaptor guiding preferential association to p-MHC-bound and activated TCR-CD3 (92, 93). This mechanism is supported by clever experiments showing that TCR binding to a weak p-MHC agonist experiences a sequential two-step increase in strength (94). The first binding component is sensed immediately after p-MHC ligation and it is coreceptor-independent, followed shortly after by a coreceptor-dependent binding increase. This second component disappears upon pharmacological inactivation of Lck (94), indicating that it is mediated by conformationally-open/active-Lck bound to the co-receptor. Moreover, super-resolution imaging suggests that co-receptor-unbound (or free) Lck augments in the proximity of

TCR-CD3 soon after p-MHC binding, followed shortly after by the coreceptor-associated Lck (95). These data and the inherent bias for MHC-restriction of preselection TCRαβ repertoire indicate that CD4 and CD8 are a resource not for initiating but rather for invigorating, if needed, TCR-CD3 activation, incidentally making coreceptor-based TCR-CD3 activation models unlikely.

Active-Lck, membrane-hung ITAMs, and ITAM phosphorylation

Akin to other Src-family kinases in other cell types, a fraction of constitutive enzymatically active-Lck is permanently present in T cells and thymocytes (96). The active-Lck pool is 40-60% of plasma membrane-resident-Lck (96, 97). Active-Lck is the net product of a highly dynamic equilibrium between Lck active and non-active (closed or auto-inhibited Lck) isoforms, the formation of the former being triggered and controlled by the membrane protein tyrosine phosphatase (PTP) CD45, which is also constitutively active (82, 96). Molecular details of this surprising mechanism have been recently documented (82). Such a condition was dubbed "stand-by" (96) to designate a state of cellular preparedness for TCR-CD3 activation, perhaps responsible for αβ T-cell sensitivity to low affinity ligands. It was suggested that ligand occupancy could initiate allosterically-regulated changes in TCRαβ that propagate to CD3 so that the ITAMs become accessible to active-Lck to initiate intracellular signal propagation (96). This idea prompts the question of whether ITAM tyrosines are somewhat concealed from constitutively active-Lck and become exposed only after TCRαβ engagement. An affirmative answer to this question is likely. More than twenty years ago, it was shown that the cytosolic tail of ζ (ζ_{cyt}) behaves in solution like a random-coil (*i.e.*, devoid of secondary structure) that can be readily phosphorylated by Lck (98). ζ_{cyt} bound avidly to liposomes containing negatively-charged lipids, accompanied by bound-ζ_{cyt} showing some α-helix content and highly reduced phosphorylation by Lck (98). These observations are reminiscent of a paradigm-changing discovery in membrane biology made in the 1980s (99) revealing that some cytoplasmic membrane proteins contain unstructured clusters of basic and aromatic residues capable of mediating interaction with the inner leaflet of the lipid bilayer that are enriched with negatively-charged lipids (phosphatidyl-serine (PS) and phosphoinositide lipids (PIPs). Basic and aromatic residues strongly interact with PIPs (called also structural lipids) and with the bilayer hydrophobic core, respectively. Consistent with these notions, NMR studies showed that the CD3 ε-ITAM interacts with lipid micelles containing negatively-charged lipids, with the tyrosines partitioning dynamically into the lipid hydrophobic core (100), presumably reducing Lck access. FRET data in live cells showed that ε-ITAM interacts with the lipid bilayer inner leaflet of the plasma membrane (100). A cryo-EM structure of detergent-extracted TCR-CD3 complex is a major advancement towards understanding the mechanism of TCR-CD3 activation (11) that has revealed unsuspected features of the octameric complex. VαVβ is not standing vertically but leaning forward by an acute angle with respect to CαCβ. The CD3 dimers are asymmetrical arranged around CαCβ, with the upper loops of ε, γ and δ CD3 ectodomains making contacts with the distal loops of Cα and/or Cβ. The ζζ dimer is loosely bound to the rest of the complex via the transmembrane domain (TMD), making contacts primarily with αβ TMDs but surprisingly also with the TMDs of virtually all the other CD3 subunits (11, 101). These features indicate that TCRαβ and CD3 subunits form a highly interlaced quaternary structure with mutualistic contributions to TCR-CD3 topology that seamlessly connect αβ ligand binding site to the TMDs. This quaternary structure arrangement evokes opportunities for allosteric connections to promote ITAM exposure and phosphorylation upon ligand binding. However, the highly flexible CD3 tails cannot be seen in cryo-EM structures. To try and overcome this limitation, a computational tour-de-force by molecular dynamics simulations (MDS) of the entire cryo-EM structure with intracellular tails modelled as random-coils was carried out (101). This investigation has revealed that the cytosolic tails of all CD3 subunits interact with each other primarily by virtue of their random-coil nature, forming dynamic "skeins of tails" that are abutted against the plasma membrane (Figure 2A). CD3 ζ and ε (101) make the strongest contribution to membrane binding and show dynamic partitioning of some tyrosines in the hydrophobic core of the bilayer, in good agreement with the NMR data (100). The absence of PIPs in the modelled bilayer drastically reduces the formation of CD3 tail-skeins and interactions with the membrane (101). This study consolidated and extended observations suggesting that basic-rich stretches (BRS) preceding CD3 ζ and ε ITAMs interact with negatively charged PIPs (102, 103). Consistently, PIPs depletion in live T cells by the inositol polyphosphates Inp54p delivered to TCR-CD3 proximity leads to ITAMs phosphorylation by constitutive active-Lck without TCRαβ ligation (104), supporting the idea that ITAM unbinding from the membrane initiates TCR-CD3 signalling. The MDS study revealed also an unexpected movement of VαVβ bending down, with Vβ making dynamic contacts via charged residues with CD3γ, reaching a configuration of TCR-CD3 that makes it look "closed" (Figure 2B), suggesting perhaps a potential mode of ligand-induced allosteric activation. This MDS prediction is comforted by the latest available cryo-EM structure of TCR-CD3 embedded in a nanodisk that mimicks a membrane bilayer composed of a variety of lipids (105) and shows a "resting" configuration very similar to the "closed" configuration observed by Prakaash et al. (101). Also, the tail configuration may depend on changes in the relative positioning of the TMDs (Figure 2A) (101), in turn affecting the lipid composition in and around TCR-CD3 TMDs (or "lipid fingerprint" (81), including cholesterol (106) and ultimately PIPs (104), with the potential for altering CD3 tails interaction with the membrane and favour ITAM phosphorylation.

Ligand discrimination, a trait that αβ T cells are so gifted for, is key for preventing auto-immunity (107, 108) and effectively facing non-self (56). It requires a precise choice of a signal bandwidth, that should compromise between noise rejection (negative feedback) and reward (positive feedback) only for signals persistently levitating above the threshold (59). At steady-state, ITAMs

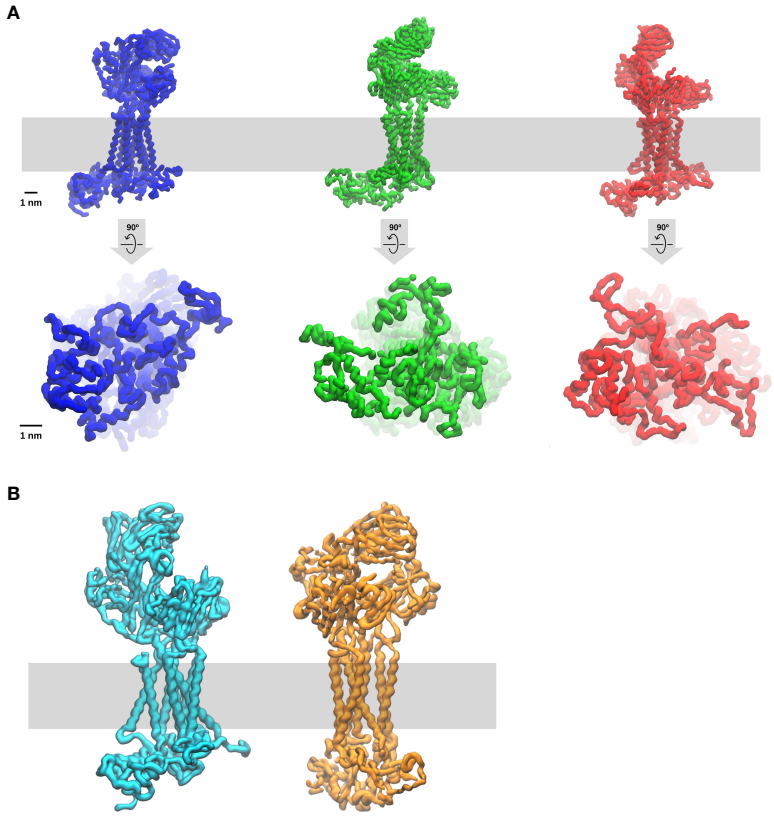

FIGURE 2
Molecular dynamic simulation of the entire TCR-CD3 complex (Courtesy of Dr Dheeraj Prakaash). The simulation of the full TCR-CD3 complex, including the CD3 intracellular tails, was for a total of five times for five μs and carried out according to the conditions described in (101). The lipid bilayer was composed of seven different lipids (including cholesterol and PIPs) and it is depicted as a grey band. Three snapshots are shown. **(A)** upper and lower panels are TCR-CD3 side and bottom (cytosol) views, respectively. Note the changes in the configurations of ectodomains, TMDs, and intracellular tails, indicate that TCR-CD3 is a relatively flexible complex with great potential for allosterically-regulated activation. Of interest is also the potential for correlated movements of these three TCR-CD3 domains perhaps exploited for the propagation of allosterically-driven changes in the three isoforms shown ("closed", semi-open, fully-open). **(B)** TCR-CD3 side of two snapshots emphasising two extreme configurations one "open" (left) and the other "closed" (right). In the simulations, the transition from open to closed takes two-three hundred ns.

partially accessible by Lck (98, 100, 101) experience low-grade/stochastic phosphorylation with pY-ITAM largely over-represented (Figure 1). The two net negative charges of pYs forbid interaction with the membrane hydrophobic core and may disturb BRS contacts as well, with some pY-ITAMs converted to 2Y-ITAMs that stably bind ZAP-70. If unopposed by a cytoplasmic PTP, such noise might become unstoppable. It has been suggested that the PTP SHP-1 controls ITAMs phosphorylation by Lck (109, 110) (Figure 1). Moreover, recent genetic evidence in mice agrees with this idea in that very weak agonists induce rapid SHP-1 association with pY-ζ-ITAMs and that mutation of all ζ tyrosines increases TCR-CD3 signalling and functional responses (111). This mechanism perhaps explains why pY-ITAMs are poorly, or not at all detectable at the steady state and how a signalling threshold is set by a dynamical antagonism between active-Lck and SHP-1 for ITAMs phosphorylation (discussed in Paster et al. (110), as part of the ligand discrimination mechanism (111). Presumably, 2pY-ITAMs increase above threshold drives ZAP-70 binding that decisively out-competes SHP-1 binding (a double-negative feedback) and protects 2pY-ITAMs from dephosphorylation, resulting in ZAP-70 enzymatic activation by Lck (a positive feedback) and rapid active-ZAP-70 accumulation (108). Such a mechanism could be the very first in a series of kinase-PTP control devises alongside the entire signal trajectory, initiating a proof-reading mechanism believed to implement αβ T-cell ligand discrimination (60).

A critical appraisal of TCR-CD3 activation models

Structural and functional complexity is undoubtedly the main reason for contentious models on the TCR-CD3 activation mechanism. Some models privilege certain molecular or functional properties, yet neglect others, borrow in part paradigms of classical membrane receptors, or invoke entirely new paradigms. Unfortunately, little has been done to conceive discriminatory experiments and cooperation to nail down a unifying model. Currently, TCR-CD3 activation mechanisms (excluding coreceptor-dependent activation, as discussed above) can be segregated according to two major discordant structural notions: stiffness or flexibility, the former excluding allosterically-driven processes.

Oligomerisation

TCR-CD3 oligomerisation (or clustering) causes a local increase of ITAMs concentration, raising by mass action the kinetics of their phosphorylation by Lck over the background (112). The simplest version suggested that TCR-CD3 activation is induced by binding to constitutively pre-clustered p-MHC (112). This and other oligomerisation models do not require TCR-CD3 structural flexibility (the receptor can be a "rigid body"). A major obstacle to activation by pre-clustered p-MHC is that αβ T cells comfortably respond to just a few p-MHC agonists dispersed among a huge excess of self p-MHC (79, 80, 113) and the probability of finding two or more rare p-MHC agonists associated at random in the same oligomer is vanishingly small. Also, crystal structures of p-MHC alone or complexed with TCRαβ are monomeric and accurate super-resolution imaging found no evidence for MHC-II clusters on agonist-loaded APC that otherwise stimulate T cells (114). Alternatively, p-MHC-TCR-CD3 pairs may laterally segregate and be drawn closer if receptor-ligand pairs of much longer size (*e.g.*, ICAM-LAF-1) form nearby (115). These effects can be driven by nanometre-scale membrane curvature resulting from tension for uneven membrane tethering (115). This model requires high agonist density, again antithetical to αβ T-cell high sensitivity and speed of TCR-CD3 activation (59, 77, 79, 80, 113). Moreover, genetic ablation of both major LFA-1 ligands, ICAM1 and 2 only attenuates TCR-CD3 signalling (116). The existence of steady-state pre-clustered TCR-CD3 is not supported by more recent super-resolution imaging investigations (51, 69, 70). Rather, single-molecule tracking coincident with early p-MHC binding suggests that monomerically-engaged TCR-CD3 can carry ZAP-70 (hence, it is already activated as a monomer) and experiences decreased lateral diffusion as compared to free-TCR-CD3, not due to clustering but presumably because already of this activated stage it is found bound to the actin cytoskeleton (51). Consistently, evidence suggests that clustering may be the consequence rather than the cause of TCR-CD3 activation (117). Moreover, soluble mono-dispersed p-MHC monomer alone suffices to induce early TCR-CD3 signalling, such as Erk activation (117). TCR-CD3 oligomerisation commonly observed at T cell-APC interfaces does not explain TCR-CD3 activation but is most likely a step following receptor activation (Figure 2) that is capital for triggering αβ T-cell activation.

CD45 kinetics segregation (KS): can 6.6 nm stature difference decide whether TCR-CD3 is activated?

KS is an unconventional model based on mechanical force acting on a "rigid-body" membrane protein. KS is an elegant and intuitive model in cartoon representation. Moreover, its eccentricity in membrane receptor biology that addition does not require allosteric activation, proscribed by early crystallographic data (118), explains perhaps a relatively favourable reception by the immunologists' community. However, at a closer look, the KS mechanism is non-trivial and rather convoluted. It requires some assumptions difficult to demonstrate, which together with existing data raise a number of disquieting questions. For KS to work, multiple TCR-CD3 bonding to p-MHC with adequate affinity must occur to enable the formation of relatively tight, nanometre-scale membrane junctions between T cell and APC membranes (119). KS implicitly assumes that TCR-CD3 and p-MHC are mono-dispersed at the steady-state but p-MHC-TCR-CD3 pairs rapidly oligomerise to achieve both tighter binding (by avidity) for relatively stable and laterally tight membrane tethering. Sufficient TCR-CD3 occupancy at small zipped-up areas should enable exclusion in a reasonable time of membrane proteins possessing long, encumbering, and rigid ectodomains (119, 120). The membrane PTP CD45 is a potential candidate for such lateral exclusion. KS relies on the basic notion that membrane receptor signalling requires a highly dynamical equilibrium of the contrasting action of protein tyrosine kinases (PTKs) and PTPs. Alteration of this equilibrium can tip the balance toward fast accumulation of ligand-bound receptor phosphorylation. While initial versions of KS suggested that CD45 controlled activation of Lck, a change of this paradigm (96, 121) made KS supporters propose instead that CD45 directly opposes ITAM phosphorylation by constitutively active-Lck (122). At steady-state, Lck-CD45 antagonism on Y-ITAMs would maintain pY-ITAMs ≅ zero. Reducing CD45 access to engaged-TCR-CD3 should lead to rapid pY-ITAMs increase, hence receptor activation. In simple terms, the higher and longer ligand receptor occupancy, the higher and longer CD45 is excluded, with consequent pY-ITAM increase. Earlier *in vitro* data suggested that CD45 dephosphorylates pY-ITAM (123). However, either CD45 genetic ablation or decreased gene dose or pharmacological inhibition of CD45 cannot be used to support KS. This is because, in agreement with the CD45 primary function discussed above (82), these manipulations strongly increase the pool of constitutively active-Lck (82, 121), hence TCR-independent pY-ITAM accumulation. Also, genetic evidence showed that CD45 ectodomain contributes to control constitutive levels of active-Lck (124), presumably by CD45 carbohydrates binding to membrane galectins (125, 126), a study that discouraged the use of chimeric CD45 with short ectodomains borrowed by other proteins to support KS. Evidence that the cytoplasmic PTP SHP-1 regulates pY-ITAM has also been gathered (109, 110) and strongly supported by recent data in mutant mice carrying CD3-ζ with all-tyrosine mutated to phenylalanine that show increased responses to weak p-MHC ligands (111). The authors show that SHP-1 is recruited pY-ζ soon after TCR-CD3 ligation, suggesting a direct control of pY-ITAMs by SHP-1, questioning the central assumption of the KS model. Super-resolution imaging has captured CD45 exclusion tens nm away from tight membrane junctions between the T-cell membrane and a surface densely coated with TCR-CD3 Abs, tens of seconds after cell spreading (127). However, this evidence is obtained under exceptional supra-physiological TCR-CD3 engagement in artificial conditions and similar evidence for CD45 exclusion is missing for physiological stimulatory conditions when the presentation of just a few agonists induces TCR-CD3 activation and very fast (77, 79, 80, 113). Idem for single p-MHC-TCR-CD3 pairs (51, 70). KS cannot easily explain how TCR-CD3 is activated by extremely weak ligands sufficient to guarantee thymic positive

selection and mature αβ T-cell survival. The ectodomain of a major isoform of CD45 is ≈ 22 nm long (128), exceeding by 6.6 nm the sum of p-MHC and TCRαβ ectodomain. Since CD45 does not have a ligand on the APC, exclusion should be the result of mechanical compression exerted on CD45 ectodomain by the APC membrane bilayer (a relatively elastic surface). However, in the cartoon representation of KS the membrane and CD45 ectodomain are represented as rigid (*i.e.*, surprisingly, the APC membrane is not at all deformed by CD45, so depicted as rigid, a rather unlikely condition). Thus, the 6.6 nm gap should determine the mechanical work required for CD45 ectodomain bending and exclusion, and the total energy of TCRαβ-pMHC bonding must exceed by a good margin the energy required for extruding CD45. According to KS, CD45 isoforms with ectodomains of considerably different length should differently affect T-cell activation. However, transgenic mice expressing only the longest or shortest CD45 isoform in comparable amounts show no functional effect on thymocytes development or activation of naïve and memory αβ-T cells (129). CD45 exclusion from c-SMACs can be observed hundreds of seconds after TCR-CD3 activation, generally in response to abundant agonist p-MHC amounts. However, cytotoxic αβ T-cells killing of target cells, which notoriously require very few agonist p-MHC, do not form c-SMACs and there are other instances in which αβ T-cell activation does not require c-SMACs. KS proponents have recently added a new twist to the model (128, 130), namely that ligand-engaged "small receptors" - *e.g.*, CD2 forms "close-contact zones" or a membrane zipper excluding CD45, a kind of signalling "heaven" where TCR-CD3 diffuses and gets activated. Besides the obvious inconvenience for TCR-CD3 competing for space in areas already densely occupied by CD2, such an idea is unsupported by evidence that thymocyte development and T-cell activation occur *in vivo* and *in vitro* in CD2 KO mice (131), corroborated by recent data in additional mouse mutants (132). Moreover, TCR-CD3 signals in artificial planar lipid membranes offer just cognate p-MHC. The KS (and oligomerisation) model does not explain how CD3 ITAMs detach from the plasma membrane to become accessible to active-Lck and how soluble p-MHC-tetramers or soluble mono-dispersed p-MHC induces ligand dose-dependent Ras activation (117). Most recent data suggests that CD45 exclusion serves the purpose of ligand discrimination (133), hence not TCR-CD3 activation *per se*. In conclusion, it stands to reason that KS is unlikely to explain TCR-CD3 activation.

Mechano-transduction

It has been proposed that TCR-CD3 activation is triggered by forces pulling and/or pushing p-MHC-engaged TCR-CD3. The sources of force are T-cell motility and/or actin-myosin cytoskeleton dynamics acting directly on TCR-CD3 (134–139). The first proposition clashes in part with the notion that T-cell motility vis-à-vis the APC slows considerably and rapidly upon agonist-mediated TCR-CD3 activation (140), so force might not sustain signalling. Moreover, p-MHC presented on planar artificial bilayers can activate a T-cell that is kept essentially immobile for imaging purposes. With one notable exception (141, 142), crystal structures of many p-MHC-TCR αβ complexes do not show noticeable conformational changes occurring past the TCRαβ binding site (see below). However, the initial idealisation of TCR-CD3 quaternary structure has prompted some authors to propose that, if subject to force, TCR-CD3 could undergo conformation changes, otherwise invisible in crystal structures (135). Indeed, using experimental devices that generate ramping of traction force on p-MHC, TCR-CD3-dependent calcium rise is observed with force reaching tens of nanonewtons (138, 143). While attractive and intuitively simple, a serious caveat of mechano-transduction models is the lack of evidence that a uniform force (in time, space and ramp) of sufficient magnitude develops at the T-cell-APC contact sites after TCR-CD3 engagement. Only such ideal conditions should guarantee stereotypic conformational changes for TCR-CD3 activation. It is also unclear whether calcium rise depends on the ligation of single TCR-CD3 or multiples (already clustered) TCR-CD3, as in one experimental setting it was observed only after rapid serial TCR-CD3 pulling (143) and calcium rise was recorded considerably later after cell-cell contact (138). Recent data have suggested that the force developed at the T cell-APC interface upon TCR-CD3 ligation by p-MHC is considerably lower than the pulling force experienced by TCR-CD3 using artificial devices (144). Thus, although in a natural setting αβ T cell recognition of p-MHC undoubtedly occurs under some tensile force, its magnitude may not be as high as suggested (137). Actin-myosin cytoskeletal dynamics has been suggested to be the force provider (137). However, while pharmacological inhibition of actin-myosin dynamics in primary T cells does affect cytokine production, it does not affect very early TCR-CD3 signalling events such as ITAM phosphorylation (145) and actin appears to associate with TCR-CD3 already activated (51). Surprisingly, no test asking whether specific inhibition of Lck abolishes or decreases mechanical forces experienced by TCR-CD3 at the IS has been done. Mechano-transduction models cannot explain why soluble p-MHC small oligomers (tetramers, trimers, and dimers) or monomers (*i.e.*, conditions where no force is involved) activate TCR-CD3 (117, 146). Moreover, TCR-CD3 activation by just a few p-MHC agonists, as is often the case, may be perturbed rather than encouraged by force of certain intensity and reduce ligand discrimination (147). Force strength and direction of any origin (including long-range and slow lipid bilayer thermal fluctuation) at opposing cell membranes are likely to change randomly, and instead of inducing canonical conformational changes as suggested (135), it may rather perturb receptor-ligand engagement (147). However, under precise circumstances, the force could produce catch-bonding that reduces ligand off-rate, thus influencing ligand discrimination (138, 139), but catch-bonds do not occur with weak agonists (*e.i.*, self p-MHC) (55), making catch bonds not required for TCR-CD3 activation.

Oligomerisation-induced allostery

Alarcon and co-workers provided the first experimental evidence that binding TCR-CD3 by soluble anti-CD3 Abs or p-

MHC tetramers exposes in the CD3ε cytosolic tail a determinant situated in close proximity of the membrane (148). Such long-distance structural change upon receptor ligation is evidence for allosteric communication, prompting the authors to propose that TCR-CD3 signalling is allosterically regulated by conformational changes. The field was instantly divided into a few believers and many opponents and "wait-and-see". Opponents thought that crystal structures are the ultimate revelation of protein mechanism of action (a pernicious misconception discussed in (149). Because conformational changes were not seen past the TCRαβ binding site in crystal structures, allosteric activation was unworkable. Certainly, opponents and sceptics were unaware that allostery must be first demonstrated empirically (by genetics and biochemistry approaches) and then studied by various means to understand which allosteric mechanism is at play (150). Indeed, NMR approaches can reveal distantly correlated dynamical changes that explain allosteric regulation without obvious structural changes, impossible to observe by conventional crystallography or cryo-EM. Advanced MDS approaches can also be useful to uncover distant correlated movements of the protein main chain induced by ligand binding to suggest the existence of allosteric trajectories (151, 152). Schamel and co-workers have suggested that ligand-induced TCR-CD3 oligomerisation with the precise lateral arrangement ("permissive geometry") is promoted by pre-clustered p-MHC dimers on APCs and that this condition is responsible for inducing TCR-CD3 allosteric activation (153). In this model, p-MHC binding to TCRαβ alone does not trigger allosteric activation but ligand-induced TCR-CD3 oligomerisation does. "Permissive geometry" excludes therefore that monomeric p-MHC binding activates TCR-CD3. In essence, "permissive geometry" suggests that conformation changes are promoted by lateral interaction of the CD3 subunits triggered by pre-clustered agonists and propagate to the ε ζ intracellular tails. This idea is partly reminiscent of elegant models proposed by Bray and co-workers suggesting that oligomerisation increases ligand sensitivity by laterally spreading receptor activation (65). Although having some value for a more elaborated allosteric mechanism (see below), permissive geometry is crippled by the proposition that pre-clustered p-MHC agonists is mandatory for allosteric activation, a highly unlikely condition since the likelihood of finding at least p-MHC two agonist in the same hypothetical dimer of p-MHC should be extremely low, as discussed above.

Evidence for allosteric sites in TCRαβ

Almost all crystal structures have shown that conformational changes are not found to significantly propagate beyond the binding interface (118). However, two NMR studies of mouse and human TCRαβ ectodomain unbound or bound to p-MHC independently showed compelling evidence for allosteric sites in Cβ (154, 155). Specifically, p-MHC binding produced dynamical changes in Vβ CDR3 residues that temporally correlated with dynamical changes in Cβ. Similar observations were made for MHC-I- and MHC-II-restricted TCRs and for different ligand affinities. These data constitute solid evidence for ligand-induced structural changes at long distances from the TCRαβ binding site β (155) without force or clustering. It is suspected that the relatively large interface connecting Vβ to Cβ (via the FG loop) contains the determinants that vehiculate such dynamic changes from Vβ to Cβ. Importantly, the Cβ residues that change dynamics upon ligand binding are exactly at sites that make contacts with residues of the CD3 ectodomains (155). Evidence for p-MHC-induced allosteric changes at Cα loops making contact with CD3 ectodomains has also been reported (141, 142). Comprehensively, these data suggest the tantalising hypothesis that the ectodomain of CD3 ε, γ and δ could be the intermediate receiver site sensing p-MHC binding to αβ for changes in the octamer TMDs and finally to the CD3 tails (see discussion in (117). Crystallography and other cryo-techniques that exploit ultra-low temperatures (- 190°C) can hardly capture ligand-induced dynamics gains characteristic of higher-energy (activated) states. They are therefore inadequate to reveal dynamically-driven (entropic) allostery, mediated by changes in protein flexibility as predicted theoretically in the 80s and now recognised to be much more diffused than originally thought, as demonstrated experimentally by NMR studies (156). It should therefore not come as a surprise that crystal structures of some liganded GPCRs that are certified allosteric receptors have at times failed to reveal expected structural changes, leaving room for entropic allostery. NMR can reveal allosteric connection by temporally correlating fast local conformational changes (at ps or ns timescales) occurring at sites tens of nm apart and inform on the remarkable speed at which allosteric changes travel along individual proteins or protein complexes – *e.g.*, one nm/μs (154, 157). Given the discrepancy between crystallographic data (and a recent cryo-EM structure (158) and NMR data, it is legitimate to suspect that TCR-CD3 activation relies on entropic allostery.

Allosteric activation by monodispersed p-MHC monomers

Prompted by highly divergent models, a multi-pronged unbiased approach was set up using genetic perturbation of TCR-CD3 quaternary structure to probe for signalling alteration and integrated by biochemical approaches and MDS (117). The hope was to contribute to a unifying model. It was anticipated that small structural perturbations at particular sites, namely the TMDs of TCRαβ or CD3 subunits, could provide discrimination between "rigid-body" and allosteric models (for details of the rational, see (117). If allostery was found a plausible option, then other experimental criteria could be envisaged to include or exclude mechano-transduction and/or permissive geometry models. Surprisingly, mutations in TMDs of TCRβ or CD3ζ that minimally perturbed the stability of native TCR-CD3 quaternary structure, produced weak constitutive TCR-CD3 activation (*i.e.*, ζ phosphorylation without receptor stimulation) (117). These gain-of-function mutations did not promote receptor clustering *per se*, nor did they increase TCRαβ binding affinity or avidity for p-MHC. However, they did augment the proof-reading constant (k_p), an indication of increased signalling efficiency (117), as if the mutations had pushed inactive TCR-CD3 (R_i) towards an active

(R_a) isoform (Figure 1), somewhat reducing the activation energy required for this transition. Remarkably, mutation-induced basal activation of TCR-CD3, resulted in a perceptible increase in size distribution and frequency of TCR-CD3 clustering that was zeroed by pharmacological inhibition of Lck activity, suggesting that clustering was caused by TCR-CD3 activation and not vice versa (117). Importantly, all gain-of-function mutations reduced TCRαβ cohesion to ζ (and ε), as shown by a biochemical assay conceived to test changes (DDM-stability assay, DSA) (117). A similar behaviour of the gain-of-function mutations was observed for three TCRs of different specifcity. Such phenotype was corroborated by MDS studies of the mutants using the TCR-CD3 cryo-EM structure (117). This evidence made rigid-body models less likely. To exclude or include force and clustering, signalling recording (*e.g.*, Ras activation) and DSA were performed using p-MHC tetramers or rigorously controlled mono-dispersed p-MHC monomers and TCRs at the higher spectrum of affinity (*e.g.*, K_D of 0.05 μM) (117). Both p-MHC monomers and tetramers induced Ras activation in a dose-response fashion in the absence of co-receptors, though tetramers elicited higher pErk amplitude and duration. Most importantly, both p-MHC tetramers and monomers loosened TCR-CD3 quaternary structure similar to the gain-of-function mutations, and such an effect was observed also if Lck was inhibited and at 4°C in intact cells or after TCR-CD3 solubilisation. Remarkably, activating anti-CD3 Ab binding to TCR-CD3 showed very similar allosteric changes (117). Ligand-dependent quaternary structure relaxation implies that p-MHC binding must necessarily affect contacts between TCRαβ and CD3 ectodomains, as suggested by the NMR studies (155), and ultimately perturb contacts in the TMD of the octamer complex that mediate ζζ (and possibly the other CD3 subunits) interactions with the other subunits (discussed in Lanz et al., 2021) (117). Comprehensively, the data gathered by this unbiased approach suggest that TCR-CD3 activation is controlled by an allosteric mechanism requiring only p-MHC monomer binding; thus independently of either force or oligomerisation or CD45 exclusion. Since pioneering studies rewarded with three Nobel prizes in 2013 (149), MDS has considerably advanced through vast improvements in software and access to powerful super-computers so that it is possible to obtain hundreds of ns-scale to single-digit μs-scale simulations in reasonable time frames to observe the dynamical behaviour of protein complexes embedded in a lipid bilayer, with constantly improving corroborative and precise predictive value (159). Recent MDS work using simulation times relatively long for all-atoms MDS (1 μs) has revealed p-MHC binding by different affinities to different TCRαβ consistently induce coordinated changes in dynamics in the main chain of Vβ and Cβ (152), in agreement with the NMR data. Similar effects were reproduced in the simulation of the entire TCR-CD3 ectodomain anchored to a lipid bilayer (151). Significantly, allosteric changes propagate at distances of several nm in just 1-2 ms (Kern and Zuiderweg, 2003; Natarajan et al., 2017), much faster than the shortest pMHC-TCRαβ 2D half-lives recorded thus far (*e.g.*, 50 – 100 ms). This key notion makes allosteric activation a valid mechanism to explain TCR-CD3 activation by very weak p-MHC ligands, and signal persistence by rebinding occurring faster than the disassembling of TCR signalling complexes (43). How ligand-induced changes at some contact sites of TCR-CD3 ectodomains (perhaps increasing CD3 conformational dynamics) lead to changes in TMDs to allow ITAMs phosphorylation remains to be deciphered. Slight modifications in TMD configuration may allow exchanges between lipids bound to TMD helices and bulk lipids, with potential for altering PIPs disposition and possible Y-ITAMs exposure. The signalling mechanism proposed for the EGFR also contemplates ligand-induced modifications in the configuration of the TMDs in the EGFR dimer (160). EGFR determinants in the cytosol side close to the plasma membrane carry stretches of basic resides that mutational analysis and MDS suggest to interact with PIPs (160, 161), a condition that may change upon ligand binding and cause a reorientation of the tween kinase domains (160). Consistent with the implication of membrane lipids in TCR-CD3 allosteric activation, mutations affecting cholesterol interaction with TCRβ TMD produce gain-of-function (106, 162). MDS indicate that changes in TMD inter-helical configuration may correlate with changes in the ectodomains and the CD3 tails (101) (Figure 2A), suggesting further mutational mapping strategies for augmenting or decreasing signalling. Models for allosterically regulated receptor tyrosine kinases (RTKs) and GPCRs able to bind different ligands of wide affinity differences, now integrate binding kinetics elements to better explain the ensuing biased agonism (163–165). The scenario suggested by Lanz et al., supported by NMR and MDS studies, implies that ligand efficacy for TCR-CD3 activation may be dependent on both allosteric changes and ligand affinity. There is indeed room for testing this idea using p-MHC that binds to TCRαβ with unorthodox orientations (166). In models of allosterically-regulated activation of TCR-CD3 by monomer p-MHC binding, ligand occupancy will determine the time of ITAMs accessibility to Lck and amplitude and duration of ITAMs phosphorylation. The "allosteric factor" could then be seen as an unsuspected manifestation of MHC restriction, in that some particular orientations of p-MHC over TCRαβ may elicit poor or invalid allosteric activation of the entire complex.

Reconciling controversy?

Allosteric activation of TCR-CD3 dubbed some years ago as high unlikely (118, 167), has taken two-decades to mature into a plausible mechanism (101, 117, 148, 151, 152, 155, 162, 168). This is perhaps a sign that cartoon simplifications are often preferred to facts and interdisciplinary knowledge and that TCR-CD3 is a "smart receptor" (63), whose "reasoning" still holds secrets. The difficulty of easily accommodating oligomerisation, KS, and mechano-transduction as mechanisms that activate TCR-CD3 should be an occasion for conceiving a sensible unifying model, such as the one illustrated in Figure 1. This model orders in chronological order molecular events that begin with ligand-induced allosteric activation, the most hard-wired, fastest and finely tuneable mechanism for connecting the extra-cellular environment with the cell interior. Indeed, allosteric activation mediated just by ligand binding alone as the initiator of membrane receptor molecular activation has proved extremely valid in evolution as witnessed by thousands of different membrane receptors working

according to its principles. Singly and sparsely firing signals by activated receptors (R_a) cannot go very far in eliciting full cell responses and mandatorily require clustering, perhaps favoured by the actin cytoskeleton. R_a clustering is a sure fact in membrane biology and TCR-CD3 is no exception. Force cannot be completely excluded and together with CD45 segregation may create occasions for "positive effects" of biological impact, such as ligand discrimination. Considering the difficult conditions in which TCR-CD3 operates to activate a T cell, clustering must be of great value for extruding negative regulators and reducing physical and chemical noise from the membrane areas where and when action is going on for implementing signal propagation and diversification (59) and gene-wide activation required for αβ T-cell clonal expansion and differentiation. Such "signalling territories" is another welcome surprise for TCR-CD3 to face the best it can the uncertainty inherent with adaptive immunity.

Author contributions

OA: Conceptualization, Funding acquisition, Investigation, Methodology, Supervision, Writing – original draft, Writing – review & editing.

Funding

The author(s) declare financial support was received for the research, authorship, and/or publication of this article. This review was possible thanks to the generous support of The Wellcome Trust (grant number: WT200844/Z/16/Z and GR076558MA to OA) and the Edward, P. Abraham Trust, University of Oxford.

Acknowledgments

I would like to thank my former collaborators, Giulia Masi, Anna-Lisa Lanz, André Cohnen, Nicla Porciello, Deborah Cipria, Konstintina Nika, Dheeraj Prakaash, Antreas Kalli, Mark Sansom, Josephine Alba, Marco D'Abramo, Omer Dushek, Michael Dustin, Marco Lepore, and David Cole for their continuous contributions to the work discussed in this review. I thank Brian Baker, Brian Pierce, Roy Mariuzza, Balbino Alarcon, Wolfgang Schamel, Gennaro De Libero, Johannes Huppa, Gerhard Schütz Hai-Tao He, and Jim Kaufman for discussing unpublished data filling gaps in my knowledge on the topics reviewed here. Special thanks to Dheeraj Prakaash for providing MDS snapshots for Figure 2. I apologise to colleagues whose papers are not cited because of space limitations.

Conflict of interest

The author declares that the research was conducted in the absence of any commercial or financial relationships that could be construed as a potential conflict of interest.

Publisher's note

References

1. Klein J. *Immunology: The science of Self/Non-self discrimination*. New York: John Wiley & Sons, Inc (1982). 687 p.

2. Janeway CA Jr., Medzhitov R. Innate immune recognition. *Annu Rev Immunol* (2002) 20:197–216. doi: 10.1146/annurev.immunol.20.083001.084359

3. Schatz DG, Swanson PC. V(D)J recombination: mechanisms of initiation. *Annu Rev Genet* (2011) 45:167–202. doi: 10.1146/annurev-genet-110410-132552

4. Chodera JD, Mobley DL. Entropy-enthalpy compensation: role and ramifications in biomolecular ligand recognition and design. *Annu Rev Biophys* (2013) 42:121–42. doi: 10.1146/annurev-biophys-083012-130318

5. Kaufman J. Unfinished business: evolution of the MHC and the adaptive immune system of jawed vertebrates. *Annu Rev Immunol* (2018) 36:383–409. doi: 10.1146/annurev-immunol-051116-052450

6. Liu C, Zhang Y, Liu CC, Schatz DG. Structural insights into the evolution of the RAG recombinase. *Nat Rev Immunol* (2022) 22(6):353–70. doi: 10.1038/s41577-021-00628-6

7. Boehm T, Hirano M, Holland SJ, Das S, Schorpp M, Cooper MD. Evolution of alternative adaptive immune systems in vertebrates. *Annu Rev Immunol* (2018) 36:19–42. doi: 10.1146/annurev-immunol-042617-053028

8. Feschotte C, Pritham EJ. DNA transposons and the evolution of eukaryotic genomes. *Annu Rev Genet* (2007) 41:331–68. doi: 10.1146/annurev.genet.40.110405.090448

9. Flajnik MF. Re-evaluation of the immunological big bang. *Curr Biol* (2014) 24 (21):R1060–5. doi: 10.1016/j.cub.2014.09.070

10. Radwan J, Babik W, Kaufman J, Lenz TL, Winternitz J. Advances in the evolutionary understanding of MHC polymorphism. *Trends Genet* (2020) 36(4):298–311. doi: 10.1016/j.tig.2020.01.008

11. Dong D, Zheng L, Lin J, Zhang B, Zhu Y, Li N, et al. Structural basis of assembly of the human T cell receptor-CD3 complex. *Nature* (2019) 573(7775):546–52. doi: 10.1038/s41586-019-1537-0

12. Pishesha N, Harmand TJ, Ploegh HL. A guide to antigen processing and presentation. *Nat Rev Immunol* (2022) 22(12):751–64. doi: 10.1038/s41577-022-00707-2

13. Bjorkman PJ, Saper MA, Samraoui B, Bennett WS, Strominger JL, Wiley DC. Structure of the human class I histocompatibility antigen, HLA-A2. *Nature* (1987) 329 (6139):506–12. doi: 10.1038/329506a0

14. Fremont DH, Matsumura M, Stura EA, Peterson PA, Wilson IA. Crystal structures of two viral peptides in complex with murine MHC class I H-2Kb. *Science* (1992) 257(5072):919–27. doi: 10.1126/science.1323877

15. Stern LJ, Brown JH, Jardetzky TS, Gorga JC, Urban RG, Strominger JL, et al. Crystal structure of the human class II MHC protein HLA-DR1 complexed with an influenza virus peptide. *Nature* (1994) 368(6468):215–21. doi: 10.1038/368215a0

16. Cresswell P, Ackerman AL, Giodini A, Peaper DR, Wearsch PA. Mechanisms of MHC class I-restricted antigen processing and cross-presentation. *Immunol Rev* (2005) 207:145–57. doi: 10.1111/j.0105-2896.2005.00316.x

17. Blum JS, Wearsch PA, Cresswell P. Pathways of antigen processing. *Annu Rev Immunol* (2013) 31:443–73. doi: 10.1146/annurev-immunol-032712-095910

18. Yewdell JW. MHC class I immunopeptidome: past, present, and future. *Mol Cell Proteomics* (2022) 21(7):100230. doi: 10.1016/j.mcpro.2022.100230

19. Abelin JG, Keskin DB, Sarkizova S, Hartigan CR, Zhang W, Sidney J, et al. Mass spectrometry profiling of HLA-associated peptidomes in mono-allelic cells enables more accurate epitope prediction. *Immunity* (2017) 46(2):315–26. doi: 10.1016/j.immuni.2017.02.007

20. Matsumura M, Fremont DH, Peterson PA, Wilson IA. Emerging principles for the recognition of peptide antigens by MHC class I molecules. *Science* (1992) 257 (5072):927–34. doi: 10.1126/science.1323878

21. Robinson J, Baker DJ, Georgiu X, Cooper MM, Flicek P, Marsh SGE. IPD-IMGT/HLA database. *Nucleic Acid Res* (2020) 48(D1):D948–D-55. doi: 10.1093/nar/gkz950

22. Davis MM, Bjorkman PJ. T-cell antigen receptor genes and T-cell recognition. *Nature.* (1988) 334(6181):395–402. doi: 10.1038/334395a0

23. Zerrahn J, Held W, Raulet DH. The MHC reactivity of the T cell repertoire prior to positive and negative selection. *Cell.* (1997) 88(5):627–36. doi: 10.1016/S0092-8674(00)81905-4

24. Krovi SH, Kappler JW, Marrack P, Gapin L. Inherent reactivity of unselected TCR repertoires to peptide-MHC molecules. *Proc Natl Acad Sci U S A* (2019) 116 (44):22252–61. doi: 10.1073/pnas.1909504116

25. Marrack P, Scott-Browne JP, Dai S, Gapin L, Kappler JW. Evolutionarily conserved amino acids that control TCR-MHC interaction. *Annu Rev Immunol* (2008) 26:171–203. doi: 10.1146/annurev.immunol.26.021607.090421

26. Garcia KC, Degano M, Stanfield RL, Brunmark A, Jackson MR, Peterson PA, et al. An alphabeta T cell receptor structure at 2.5 A and its orientation in the TCR-MHC complex. *Science* (1996) 274(5285):209–19. doi: 10.1126/science.274.5285.209

27. Garboczi DN, Ghosh P, Utz U, Fan QR, Biddison WE, Wiley DC. Structure of the complex between human T-cell receptor, viral peptide and HLA-A2. *Nature.* (1996) 384(6605):134–41. doi: 10.1038/384134a0

28. Rudolph MG, Stanfield RL, Wilson IA. How TCRs bind MHCs, peptides, and coreceptors. *Annu Rev Immunol* (2006) 24:419–66. doi: 10.1146/annurev.immunol.23.021704.115658

29. Hennecke J, Wiley DC. T cell receptor-MHC interactions up close. *Cell* (2001) 104(1):1–4. doi: 10.1016/S0092-8674(01)00185-4

30. Gras S, Burrows SR, Turner SJ, Sewell AK, McCluskey J, Rossjohn J. A structural voyage toward an understanding of the MHC-I-restricted immune response: lessons learned and much to be learned. *Immunol Rev* (2012) 250(1):61–81. doi: 10.1111/j.1600-065X.2012.01159.x

31. Lee M, Lloyd P, Zhang X, Schallhorn JM, Sugimoto K, Leach AG, et al. Shapes of antibody binding sites: qualitative and quantitative analyses based on a geomorphic classification scheme. *J Org Chem* (2006) 71(14):5082–92. doi: 10.1021/jo052659z

32. Li Y, Li H, Yang F, Smith-Gill SJ, Mariuzza RA. X-ray snapshots of the maturation of an antibody response to a protein antigen. *Nat Struct Biol* (2003) 10 (6):482–8. doi: 10.1038/nsb930

33. Kuroda D, Gray JJ. Shape complementarity and hydrogen bond preferences in protein-protein interfaces: implications for antibody modeling and protein-protein docking. *Bioinformatics* (2016) 32(16):2451–6. doi: 10.1093/bioinformatics/btw197

34. Singh NK, Abualrous ET, Ayres CM, Noe F, Gowthaman R, Pierce BG, et al. Geometrical characterization of T cell receptor binding modes reveals class-specific binding to maximize access to antigen. *Proteins* (2020) 88(3):503–13. doi: 10.1002/prot.25829

35. Hahn M, Nicholson MJ, Pyrdol J, Wucherpfennig KW. Unconventional topology of self peptide-major histocompatibility complex binding by a human autoimmune T cell receptor. *Nat Immunol* (2005) 6(5):490–6. doi: 10.1038/ni1187

36. Gras S, Chadderton J, Del Campo CM, Farenc C, Wiede F, Josephs TM, et al. Reversed T cell receptor docking on a major histocompatibility class I complex limits involvement in the immune response. *Immunity* (2016) 45(4):749–60. doi: 10.1016/j.immuni.2016.09.007

37. Singh NK, Alonso JA, Devlin JR, Keller GLJ, Gray GI, Chiranjivi AK, et al. A class-mismatched TCR bypasses MHC restriction via an unorthodox but fully functional binding geometry. *Nat Commun* (2022) 13(1):7189. doi: 10.1038/s41467-022-34896-0

38. Adams JJ, Narayanan S, Birnbaum ME, Sidhu SS, Blevins SJ, Gee MH, et al. Structural interplay between germline interactions and adaptive recognition determines the bandwidth of TCR-peptide-MHC cross-reactivity. *Nat Immunol* (2016) 17(1):87–94. doi: 10.1038/ni.3310

39. Blevins SJ, Pierce BG, Singh NK, Riley TP, Wang Y, Spear TT, et al. How structural adaptability exists alongside HLA-A2 bias in the human alphabeta TCR repertoire. *Proc Natl Acad Sci U S A* (2016) 113(9):E1276–85. doi: 10.1073/pnas.1522069113

40. Boniface JJ, Reich Z, Lyons DS, Davis MM. Thermodynamics of T cell receptor binding to peptide-MHC: evidence for a general mechanism of molecular scanning. *Proc Natl Acad Sci U S A* (1999) 96(20):11446–51. doi: 10.1073/pnas.96.20.11446

41. Willcox BE, Gao GF, Wyer JR, Ladbury JE, Bell JI, Jakobsen BK, et al. TCR binding to peptide-MHC stabilizes a flexible recognition interface. *Immunity.* (1999) 10 (3):357–65. doi: 10.1016/S1074-7613(00)80035-7

42. Stone JD, Chervin AS, Kranz DM. T-cell receptor binding affinities and kinetics: impact on T-cell activity and specificity. *Immunology* (2009) 126(2):165–76. doi: 10.1111/j.1365-2567.2008.03015.x

43. Govern CC, Paczosa MK, Chakraborty AK, Huseby ES. Fast on-rates allow short dwell time ligands to activate T cells. *Proc Natl Acad Sci U S A* (2010) 107(19):8724–9. doi: 10.1073/pnas.1000966107

44. Hawse WF, Champion MM, Joyce MV, Hellman LM, Hossain M, Ryan V, et al. Cutting edge: Evidence for a dynamically driven T cell signaling mechanism. *J Immunol* (2012) 188(12):5819–23. doi: 10.4049/jimmunol.1200952

45. Baker BM, Scott DR, Blevins SJ, Hawse WF. Structural and dynamic control of T-cell receptor specificity, cross-reactivity, and binding mechanism. *Immunol Rev* (2012) 250(1):10–31. doi: 10.1111/j.1600-065X.2012.01165.x

46. Bridgeman JS, Sewell AK, Miles JJ, Price DA, Cole DK. Structural and biophysical determinants of alphabeta T-cell antigen recognition. *Immunology.* (2012) 135(1):9–18. doi: 10.1111/j.1365-2567.2011.03515.x

47. Cole DK, Fuller A, Dolton G, Zervoudi E, Legut M, Miles K, et al. Dual molecular mechanisms govern escape at immunodominant HLA A2-restricted HIV epitope. *Front Immunol* (2017) 8:1503. doi: 10.3389/fimmu.2017.01503

48. Ely LK, Beddoe T, Clements CS, Matthews JM, Purcell AW, Kjer-Nielsen L, et al. Disparate thermodynamics governing T cell receptor-MHC-I interactions implicate extrinsic factors in guiding MHC restriction. *Proc Natl Acad Sci U S A* (2006) 103 (17):6641–6. doi: 10.1073/pnas.0600743103

49. Armstrong KM, Insaidoo FK, Baker BM. Thermodynamics of T-cell receptor-peptide/MHC interactions: progress and opportunities. *J Mol Recognit* (2008) 21 (4):275–87. doi: 10.1002/jmr.896

50. Huppa JB, Axmann M, Mortelmaier MA, Lillemeier BF, Newell EW, Brameshuber M, et al. TCR-peptide-MHC interactions *in situ* show accelerated kinetics and increased affinity. *Nature.* (2010) 463(7283):963–7. doi: 10.1038/nature08746

51. O'Donoghue GP, Pielak RM, Smoligovets AA, Lin JJ, Groves JT. Direct single molecule measurement of TCR triggering by agonist pMHC in living primary T cells. *Elife.* (2013) 2:e00778. doi: 10.7554/eLife.00778.017

52. Dushek O, Das R, Coombs D. A role for rebinding in rapid and reliable T cell responses to antigen. *PLoS Comput Biol* (2009) 5(11):e1000578. doi: 10.1371/journal.pcbi.1000578

53. Tanchot C, Lemonnier FA, Perarnau B, Freitas AA, Rocha B. Differential requirements for survival and proliferation of CD8 naive or memory T cells. *Science* (1997) 276(5321):2057–62. doi: 10.1126/science.276.5321.2057

54. Witherden D, van Oers N, Waltzinger C, Weiss A, Benoist C, Mathis D. Tetracycline-controllable selection of CD4(+) T cells: half-life and survival signals in the absence of major histocompatibility complex class II molecules. *J Exp Med* (2000) 191(2):355–64. doi: 10.1084/jem.191.2.355

55. Hong J, Ge C, Jothikumar P, Yuan Z, Liu B, Bai K, et al. A TCR mechanotransduction signaling loop induces negative selection in the thymus. *Nat Immunol* (2018) 19(12):1379–90. doi: 10.1038/s41590-018-0259-z

56. Mason D. A very high level of crossreactivity is an essential feature of the T-cell receptor. *Immunol Today* (1998) 19(9):395–404. doi: 10.1016/S0167-5699(98)01299-7

57. Lythe G, Callard RE, Hoare RL, Molina-Paris C. How many TCR clonotypes does a body maintain? *J Theor Biol* (2016) 389:214–24. doi: 10.1016/j.jtbi.2015.10.016

58. Riley TP, Hellman LM, Gee MH, Mendoza JL, Alonso JA, Foley KC, et al. T cell receptor cross-reactivity expanded by dramatic peptide-MHC adaptability. *Nat Chem Biol* (2018) 14(10):934–42. doi: 10.1038/s41589-018-0130-4

59. Acuto O, Di Bartolo V, Michel F. Tailoring T-cell receptor signals by proximal negative feedback mechanisms. *Nat Rev Immunol* (2008) 8(9):699–712. doi: 10.1038/nri2397

60. McKeithan TW. Kinetic proofreading in T-cell receptor signal transduction. *Proc Natl Acad Sci U S A* (1995) 92(11):5042–6. doi: 10.1073/pnas.92.11.5042

61. Gottschalk RA, Hathorn MM, Beuneu H, Corse E, Dustin ML, Altan-Bonnet G, et al. Distinct influences of peptide-MHC quality and quantity on *in vivo* T-cell responses. *Proc Natl Acad Sci U S A* (2012) 109(3):881–6. doi: 10.1073/pnas.1119763109

62. Gottschalk RA, Corse E, Allison JP. Expression of Helios in peripherally induced Foxp3+ regulatory T cells. *J Immunol* (2012) 188(3):976–80. doi: 10.4049/jimmunol.1102964

63. Jameson SC, Hogquist KA, Bevan MJ. Positive selection of thymocytes. *Annu Rev Immunol* (1995) 13:93–126. doi: 10.1146/annurev.iy.13.040195.000521

64. Stritesky GL, Jameson SC, Hogquist KA. Selection of self-reactive T cells in the thymus. *Annu Rev Immunol* (2012) 30:95–114. doi: 10.1146/annurev-immunol-020711-075035

65. Bray D, Levin MD, Morton-Firth CJ. Receptor clustering as a cellular mechanism to control sensitivity. *Nature.* (1998) 393(6680):85–8. doi: 10.1038/30018

66. Duke T, Graham I. Equilibrium mechanisms of receptor clustering. *Prog Biophys Mol Biol* (2009) 100(1-3):18–24. doi: 10.1016/j.pbiomolbio.2009.08.003

67. Schamel WW, Alarcon B. Organization of the resting TCR in nanoscale oligomers. *Immunol Rev* (2013) 251(1):13–20. doi: 10.1111/imr.12019

68. Brameshuber M, Kellner F, Rossboth BK, Ta H, Alge K, Sevcsik E, et al. Monomeric TCRs drive T cell antigen recognition. *Nat Immunol* (2018) 19(5):487–96. doi: 10.1038/s41590-018-0092-4

69. Rossboth B, Arnold AM, Ta H, Platzer R, Kellner F, Huppa JB, et al. TCRs are randomly distributed on the plasma membrane of resting antigen-experienced T cells. *Nat Immunol* (2018) 19(8):821–7. doi: 10.1038/s41590-018-0162-7

70. McAffee DB, O'Dair MK, Lin JJ, Low-Nam ST, Wilhelm KB, Kim S, et al. Discrete LAT condensates encode antigen information from single pMHC:TCR binding events. *Nat Commun* (2022) 13(1):7446. doi: 10.1038/s41467-022-35093-9

71. Veatch SL, Machta BB, Shelby SA, Chiang EN, Holowka DA, Baird BA. Correlation functions quantify super-resolution images and estimate apparent clustering due to over-counting. *PloS One* (2012) 7(2):e31457. doi: 10.1371/journal.pone.0031457

72. Rochussen AM, Lippert AH, Griffiths GM. Imaging the T-cell receptor: new approaches, new insights. *Curr Opin Immunol* (2023) 82:102309. doi: 10.1016/j.coi.2023.102309

73. Au-Yeung BB, Shah NH, Shen L, Weiss A. ZAP-70 in signaling, biology, and disease. *Annu Rev Immunol* (2018) 36:127–56. doi: 10.1146/annurev-immunol-042617-053335

74. Negishi I, Motoyama N, Nakayama K, Nakayama K, Senju S, Hatakeyama S, et al. Essential role for ZAP-70 in both positive and negative selection of thymocytes. *Nature* (1995) 376(6539):435–8. doi: 10.1038/376435a0

75. Au-Yeung BB, Melichar HJ, Ross JO, Cheng DA, Zikherman J, Shokat KM, et al. Quantitative and temporal requirements revealed for Zap70 catalytic activity during T cell development. *Nat Immunol* (2014) 15(7):687–94. doi: 10.1038/ni.2918

76. Hwang S, Palin AC, Li L, Song KD, Lee J, Herz J, et al. TCR ITAM multiplicity is required for the generation of follicular helper T-cells. *Nat Commun* (2015) 6:6982. doi: 10.1038/ncomms7982

77. Huse M, Klein LO, Girvin AT, Faraj JM, Li QJ, Kuhns MS, et al. Spatial and temporal dynamics of T cell receptor signaling with a photoactivatable agonist. *Immunity* (2007) 27(1):76–88. doi: 10.1016/j.immuni.2007.05.017

78. Shao H, Wilkinson B, Lee B, Han PC, Kaye J. Slow accumulation of active mitogen-activated protein kinase during thymocyte differentiation regulates the temporal pattern of transcription factor gene expression. *J Immunol* (1999) 163 (2):603–10. doi: 10.4049/jimmunol.163.2.603

79. Irvine DJ, Purbhoo MA, Krogsgaard M, Davis MM. Direct observation of ligand recognition by T cells. *Nature.* (2002) 419(6909):845–9. doi: 10.1038/nature01076

80. Huang J, Brameshuber M, Zeng X, Xie J, Li QJ, Chien YH, et al. A single peptide-major histocompatibility complex ligand triggers digital cytokine secretion in CD4(+) T cells. *Immunity.* (2013) 39(5):846–57. doi: 10.1016/j.immuni.2013.08.036

81. Corradi V, Mendez-Villuendas E, Ingolfsson HI, Gu RX, Siuda I, Melo MN, et al. Lipid-protein interactions are unique fingerprints for membrane proteins. *ACS Cent Sci* (2018) 4(6):709–17. doi: 10.1021/acscentsci.8b00143

82. Porciello N, Cipria D, Masi G, Lanz AL, Milanetti E, Grottesi A, et al. Role of the membrane anchor in the regulation of Lck activity. *J Biol Chem* (2022) 298(12):102663. doi: 10.1016/j.jbc.2022.102663

83. Grakoui A, Bromley SK, Sumen C, Davis MM, Shaw AS, Allen PM, et al. The immunological synapse: a molecular machine controlling T cell activation. *Science* (1999) 285(5425):221–7. doi: 10.1126/science.285.5425.221

84. Xiao Q, McAtee CK, Su X. Phase separation in immune signalling. *Nat Rev Immunol* (2022) 22(3):188–99. doi: 10.1038/s41577-021-00572-5

85. Goldrath AW, Hogquist KA, Bevan MJ. CD8 lineage commitment in the absence of CD8. *Immunity* (1997) 6(5):633–42. doi: 10.1016/S1074-7613(00)80351-9

86. Rahemtulla A, Fung-Leung WP, Schilham MW, Kundig TM, Sambhara SR, Narendran A, et al. Normal development and function of CD8+ cells but markedly decreased helper cell activity in mice lacking CD4. *Nature* (1991) 353(6340):180–4. doi: 10.1038/353180a0

87. Killeen N, Littman DR. Helper T-cell development in the absence of CD4-p56lck association. *Nature* (1993) 364(6439):729–32. doi: 10.1038/364729a0

88. Luescher IF, Vivier E, Layer A, Mahiou J, Godeau F, Malissen B, et al. CD8 modulation of T-cell antigen receptor-ligand interactions on living cytotoxic T lymphocytes. *Nature* (1995) 373(6512):353–6. doi: 10.1038/373353a0

89. Holler PD, Kranz DM. Quantitative analysis of the contribution of TCR/pepMHC affinity and CD8 to T cell activation. *Immunity* (2003) 18(2):255–64. doi: 10.1016/S1074-7613(03)00019-0

90. Laugel B, van den Berg HA, Gostick E, Cole DK, Wooldridge L, Boulter J, et al. Different T cell receptor affinity thresholds and CD8 coreceptor dependence govern cytotoxic T lymphocyte activation and tetramer binding properties. *J Biol Chem* (2007) 282(33):23799–810. doi: 10.1074/jbc.M700976200

91. Cole DK, Laugel B, Clement M, Price DA, Wooldridge L, Sewell AK. The molecular determinants of CD8 co-receptor function. *Immunology.* (2012) 137(2):139–48. doi: 10.1111/j.1365-2567.2012.03625.x

92. Xu H, Littman DR. A kinase-independent function of Lck in potentiating antigen-specific T cell activation. *Cell.* (1993) 74(4):633–43. doi: 10.1016/0092-8674(93)90511-N

93. Duplay P, Thome M, Herve F, Acuto O. p56lck interacts via its src homology 2 domain with the ZAP-70 kinase. *J Exp Med* (1994) 179(4):1163–72. doi: 10.1084/jem.179.4.1163

94. Jiang N, Huang J, Edwards LJ, Liu B, Zhang Y, Beal CD, et al. Two-stage cooperative T cell receptor-peptide major histocompatibility complex-CD8 trimolecular interactions amplify antigen discrimination. *Immunity.* (2011) 34(1):13–23. doi: 10.1016/j.immuni.2010.12.017

95. Casas J, Brzostek J, Zarnitsyna VI, Hong JS, Wei Q, Hoerter JA, et al. Ligand-engaged TCR is triggered by Lck not associated with CD8 coreceptor. *Nat Commun* (2014) 5:5624. doi: 10.1038/ncomms6624

96. Nika K, Soldani C, Salek M, Paster W, Gray A, Etzensperger R, et al. Constitutively active Lck kinase in T cells drives antigen receptor signal transduction. *Immunity* (2010) 32(6):766–77. doi: 10.1016/j.immuni.2010.05.011

97. Wan R, Wu J, Ouyang M, Lei L, Wei J, Peng Q, et al. Biophysical basis underlying dynamic Lck activation visualized by ZapLck FRET biosensor. *Sci Adv* (2019) 5(6): eaau2001. doi: 10.1126/sciadv.aau2001

98. Aivazian D, Stern LJ. Phosphorylation of T cell receptor zeta is regulated by a lipid dependent folding transition. *Nat Struct Biol* (2000) 7(11):1023–6. doi: 10.1038/80930

99. McLaughlin S, Wang J, Gambhir A, Murray D. PIP(2) and proteins: interactions, organization, and information flow. *Annu Rev Biophys Biomol Struct* (2002) 31:151–75. doi: 10.1146/annurev.biophys.31.082901.134259

100. Xu C, Gagnon E, Call ME, Schnell JR, Schwieters CD, Carman CV, et al. Regulation of T cell receptor activation by dynamic membrane binding of the CD3epsilon cytoplasmic tyrosine-based motif. *Cell* (2008) 135(4):702–13. doi: 10.1016/j.cell.2008.09.044

101. Prakaash D, Cook GP, Acuto O, Kalli AC. Multi-scale simulations of the T cell receptor reveal its lipid interactions, dynamics and the arrangement of its cytoplasmic region. *PLoS Comput Biol* (2021) 17(7):e1009232. doi: 10.1371/journal.pcbi.1009232

102. Deford-Watts LM, Tassin TC, Becker AM, Medeiros JJ, Albanesi JP, Love PE, et al. The cytoplasmic tail of the T cell receptor CD3 epsilon subunit contains a phospholipid-binding motif that regulates T cell functions. *J Immunol* (2009) 183 (2):1055–64. doi: 10.4049/jimmunol.0900404

103. DeFord-Watts LM, Dougall DS, Belkaya S, Johnson BA, Eitson JL, Roybal KT, et al. The CD3 zeta subunit contains a phosphoinositide-binding motif that is required for the stable accumulation of TCR-CD3 complex at the immunological synapse. *J Immunol* (2011) 186(12):6839–47. doi: 10.4049/jimmunol.1002721

104. Chouaki Benmansour N, Ruminski K, Sartre AM, Phelipot MC, Salles A, Bergot E, et al. Phosphoinositides regulate the TCR/CD3 complex membrane dynamics and activation. *Sci Rep* (2018) 8(1):4966. doi: 10.1038/s41598-018-23109-8

105. Notti RQ, Yi F, Heissel S, Molina H, Klebanoff CA, Walz T. The resting state of the human T-cell receptor. *bioRxiv.* (2023). doi: 10.1101/2023.08.22.554360

106. Pathan-Chhatbar S, Drechsler C, Richter K, Morath A, Wu W, OuYang B, et al. Direct regulation of the T cell antigen receptor's activity by cholesterol. *Front Cell Dev Biol* (2020) 8:615996. doi: 10.3389/fcell.2020.615996

107. Daniels MA, Teixeiro E, Gill J, Hausmann B, Roubaty D, Holmberg K, et al. Thymic selection threshold defined by compartmentalization of Ras/MAPK signalling. *Nature* (2006) 444(7120):724–9. doi: 10.1038/nature05269

108. Gascoigne NR, Acuto O. THEMIS: a critical TCR signal regulator for ligand discrimination. *Curr Opin Immunol* (2015) 33:86–92. doi: 10.1016/j.coi.2015.01.020

109. Lorenz U. SHP-1 and SHP-2 in T cells: two phosphatases functioning at many levels. *Immunol Rev* (2009) 228(1):342–59. doi: 10.1111/j.1600-065X.2008.00760.x

110. Paster W, Bruger AM, Katsch K, Gregoire C, Roncagalli R, Fu G, et al. A THEMIS:SHP1 complex promotes T-cell survival. *EMBO J* (2015) 34(3):393–409. doi: 10.15252/embj.201387725

111. Gaud G, Achar S, Bourassa FXP, Davies J, Hatzihristidis T, Choi S, et al. CD3zeta ITAMs enable ligand discrimination and antagonism by inhibiting TCR signaling in response to low-affinity peptides. *Nat Immunol* (2023) 24:2121–34. doi: 10.1038/s41590-023-01725-5

112. Cochran JR, Aivazian D, Cameron TO, Stern LJ. Receptor clustering and transmembrane signaling in T cells. *Trends Biochem Sci* (2001) 26(5):304–10. doi: 10.1016/S0968-0004(01)01815-1

113. Sykulev Y, Joo M, Vturina I, Tsomides TJ, Eisen HN. Evidence that a single peptide-MHC complex on a target cell can elicit a cytolytic T cell response. *Immunity* (1996) 4(6):565–71. doi: 10.1016/S1074-7613(00)80483-5

114. Platzer R, Hellmeier J, Gohring J, Perez ID, Schatzlmaier P, Bodner C, et al. Monomeric agonist peptide/MHCII complexes activate T-cells in an autonomous fashion. *EMBO Rep* (2023) 24:e57842. doi: 10.15252/embr.202357842

115. Weikl TR. Membrane-mediated cooperativity of proteins. *Annu Rev Phys Chem* (2018) 69:521–39. doi: 10.1146/annurev-physchem-052516-050637

116. Feigelson SW, Solomon A, Biram A, Hatzav M, Lichtenstein M, Regev O, et al. ICAMs are not obligatory for functional immune synapses between naive CD4 T cells and lymph node DCs. *Cell Rep* (2018) 22(4):849–59. doi: 10.1016/j.celrep.2017.12.103

117. Lanz AL, Masi G, Porciello N, Cohnen A, Cipria D, Prakaash D, et al. Allosteric activation of T cell antigen receptor signaling by quaternary structure relaxation. *Cell Rep* (2021) 36(2):109375. doi: 10.1016/j.celrep.2021.109375

118. Housset D, Malissen B. What do TCR-pMHC crystal structures teach us about MHC restriction and alloreactivity? *Trends Immunol* (2003) 24(8):429–37. doi: 10.1016/S1471-4906(03)00180-7

119. Anton van der Merwe P, Davis SJ, Shaw AS, Dustin ML. Cytoskeletal polarization and redistribution of cell-surface molecules during T cell antigen recognition. *Semin Immunol* (2000) 12(1):5–21. doi: 10.1006/smim.2000.0203

120. Carbone CB, Kern N, Fernandes RA, Hui E, Su X, Garcia KC, et al. *In vitro* reconstitution of T cell receptor-mediated segregation of the CD45 phosphatase. *Proc Natl Acad Sci U S A* (2017) 114(44):E9338–E45. doi: 10.1073/pnas.1710358114

121. McNeill L, Salmond RJ, Cooper JC, Carret CK, Cassady-Cain RL, Roche-Molina M, et al. The differential regulation of Lck kinase phosphorylation sites by CD45 is critical for T cell receptor signaling responses. *Immunity* (2007) 27(3):425–37. doi: 10.1016/j.immuni.2007.07.015

122. Davis SJ, van der Merwe PA. Lck and the nature of the T cell receptor trigger. *Trends Immunol* (2011) 32(1):1–5. doi: 10.1016/j.it.2010.11.003

123. Furukawa T, Itoh M, Krueger NX, Streuli M, Saito H. Specific interaction of the CD45 protein-tyrosine phosphatase with tyrosine-phosphorylated CD3 zeta chain. *Proc Natl Acad Sci U S A* (1994) 91(23):10928–32. doi: 10.1073/pnas.91.23.10928

124. Irles C, Symons A, Michel F, Bakker TR, van der Merwe PA, Acuto O. CD45 ectodomain controls interaction with GEMs and Lck activity for optimal TCR signaling. *Nat Immunol* (2003) 4(2):189–97. doi: 10.1038/ni877

125. Earl LA, Bi S, Baum L.G. N- and O-glycans modulate galectin-1 binding, CD45 signaling, and T cell death. *J Biol Chem* (2010) 285(4):2232–44. doi: 10.1074/jbc.M109.066191

126. Chen IJ, Chen HL, Demetriou M. Lateral compartmentalization of T cell receptor versus CD45 by galectin-N-glycan binding and microfilaments coordinate basal and activation signaling. *J Biol Chem* (2007) 282(48):35361–72. doi: 10.1074/jbc.M706923200

127. Razvag Y, Neve-Oz Y, Sajman J, Reches M, Sherman E. Nanoscale kinetic segregation of TCR and CD45 in engaged microvilli facilitates early T cell activation. *Nat Commun* (2018) 9(1):732. doi: 10.1038/s41467-018-03127-w

128. Chang VT, Fernandes RA, Ganzinger KA, Lee SF, Siebold C, McColl J, et al. Initiation of T cell signaling by CD45 segregation at 'close contacts'. *Nat Immunol* (2016) 17(5):574–82. doi: 10.1038/ni.3392

129. Wu Z, Yates AL, Hoyne GF, Goodnow CC. Consequences of increased CD45RA and RC isoforms for TCR signaling and peripheral T cell deficiency resulting from heterogeneous nuclear ribonucleoprotein L-like mutation. *J Immunol* (2010) 185(1):231–8. doi: 10.4049/jimmunol.0903625

130. Fernandes RA, Ganzinger KA, Tzou JC, Jonsson P, Lee SF, Palayret M, et al. A cell topography-based mechanism for ligand discrimination by the T cell receptor. *Proc Natl Acad Sci U S A* (2019) 116(28):14002–10. doi: 10.1073/pnas.1817255116

131. Killeen N, Stuart SG, Littman DR. Development and function of T cells in mice with a disrupted CD2 gene. *EMBO J* (1992) 11(12):4329–36. doi: 10.1002/j.1460-2075.1992.tb05532.x

132. Li B, Lu Y, Zhong MC, Qian J, Li R, Davidson D, et al. Cis interactions between CD2 and its ligands on T cells are required for T cell activation. *Sci Immunol* (2022) 7 (74):eabn6373. doi: 10.1126/sciimmunol.abn6373

133. Jenkins E, Korbel M, O'Brien-Ball C, McColl J, Chen KY, Kotowski M, et al. Antigen discrimination by T cells relies on size-constrained microvillar contact. *Nat Commun* (2023) 14(1):1611. doi: 10.1038/s41467-023-36855-9

134. Lanzavecchia A, Iezzi G, Viola A. From TCR engagement to T cell activation: a kinetic view of T cell behavior. *Cell* (1999) 96(1):1–4. doi: 10.1016/s0092-8674(00)80952-6

135. Kim ST, Shin Y, Brazin K, Mallis RJ, Sun ZY, Wagner G, et al. TCR mechanobiology: torques and tunable structures linked to early T cell signaling. *Front Immunol* (2012) 3:76. doi: 10.3389/fimmu.2012.00076

136. Lee MS, Glassman CR, Deshpande NR, Badgandi HB, Parrish HL, Uttamapinant C, et al. A mechanical switch couples T cell receptor triggering to the cytoplasmic juxtamembrane regions of CD3zetazeta. *Immunity* (2015) 43(2):227–39. doi: 10.1016/j.immuni.2015.06.018

137. Feng Y, Reinherz EL, Lang MJ. alphabeta T cell receptor mechanosensing forces out serial engagement. *Trends Immunol* (2018) 39(8):596–609. doi: 10.1016/j.it.2018.05.005

138. Kim ST, Takeuchi K, Sun ZY, Touma M, Castro CE, Fahmy A, et al. The alphabeta T cell receptor is an anisotropic mechanosensor. *J Biol Chem* (2009) 284 (45):31028–37. doi: 10.1074/jbc.M109.052712

139. Zhu C, Chen W, Lou J, Rittase W, Li K. Mechanosensing through immunoreceptors. *Nat Immunol* (2019) 20(10):1269–78. doi: 10.1038/s41590-019-0491-1

140. Dustin ML, Bromley SK, Kan Z, Peterson DA, Unanue ER. Antigen receptor engagement delivers a stop signal to migrating T lymphocytes. *Proc Natl Acad Sci U S A* (1997) 94(8):3909–13. doi: 10.1073/pnas.94.8.3909

141. Kjer-Nielsen L, Clements CS, Purcell AW, Brooks AG, Whisstock JC, Burrows SR, et al. A structural basis for the selection of dominant alphabeta T cell receptors in antiviral immunity. *Immunity* (2003) 18(1):53–64. doi: 10.1016/S1074-7613(02)00513-7

142. Beddoe T, Chen Z, Clements CS, Ely LK, Bushell SR, Vivian JP, et al. Antigen ligation triggers a conformational change within the constant domain of the alphabeta T cell receptor. *Immunity* (2009) 30(6):777–88. doi: 10.1016/j.immuni.2009.03.018

143. Liu B, Chen W, Evavold BD, Zhu C. Accumulation of dynamic catch bonds between TCR and agonist peptide-MHC triggers T cell signaling. *Cell.* (2014) 157 (2):357–68. doi: 10.1016/j.cell.2014.02.053

144. Gohring J, Kellner F, Schrangl L, Platzer R, Klotzsch E, Stockinger H, et al. Temporal analysis of T-cell receptor-imposed forces via quantitative single molecule FRET measurements. *Nat Commun* (2021) 12(1):2502. doi: 10.1038/s41467-021-22775-z

145. Purtic B, Pitcher LA, van Oers NS, Wulfing C. T cell receptor (TCR) clustering in the immunological synapse integrates TCR and costimulatory signaling in selected T cells. *Proc Natl Acad Sci U S A* (2005) 102(8):2904–9. doi: 10.1073/pnas.0406867102

146. Delon J, Gregoire C, Malissen B, Darche S, Lemaitre F, Kourilsky P, et al. CD8 expression allows T cell signaling by monomeric peptide-MHC complexes. *Immunity* (1998) 9(4):467–73. doi: 10.1016/S1074-7613(00)80630-5

147. Pettmann J, Awada L, Rozycki B, Huhn A, Faour S, Kutuzov M, et al. Mechanical forces impair antigen discrimination by reducing differences in T-cell receptor/peptide-MHC off-rates. *EMBO J* (2023) 42(7):e111841. doi: 10.15252/embj.2022111841

148. Gil D, Schamel WW, Montoya M, Sanchez-Madrid F, Alarcon B. Recruitment of Nck by CD3 epsilon reveals a ligand-induced conformational change essential for T cell receptor signaling and synapse formation. *Cell* (2002) 109(7):901–12. doi: 10.1016/S0092-8674(02)00799-7

149. Smith JC, Roux B. Eppur si muove! The 2013 Nobel Prize in Chemistry. *Structure.* (2013) 21(12):2102–5. doi: 10.1016/j.str.2013.11.005

150. Hilser VJ, Wrabl JO, Motlagh HN. Structural and energetic basis of allostery. *Annu Rev Biophys* (2012) 41:585–609. doi: 10.1146/annurev-biophys-050511-102319

151. Alba J, D'Abramo M. The full model of the pMHC-TCR-CD3 complex: A structural and dynamical characterization of bound and unbound states. *Cells* (2022) 11 (4):668. doi: 10.3390/cells11040668

152. Alba J, Rienzo LD, Milanetti E, Acuto O, D'Abramo M. Molecular dynamics simulations reveal canonical conformations in different pMHC/TCR interactions. *Cells* (2020) 9(4):942. doi: 10.3390/cells9040942

153. Minguet S, Schamel WW. A permissive geometry model for TCR-CD3 activation. *Trends Biochem Sci* (2008) 33(2):51–7. doi: 10.1016/j.tibs.2007.10.008

154. Natarajan K, McShan AC, Jiang J, Kumirov VK, Wang R, Zhao H, et al. An allosteric site in the T-cell receptor Cbeta domain plays a critical signalling role. *Nat Commun* (2017) 8:15260. doi: 10.1038/ncomms15260

155. Mariuzza RA, Agnihotri P, Orban J. The structural basis of T-cell receptor (TCR) activation: An enduring enigma. *J Biol Chem* (2020) 295(4):914–25. doi: 10.1016/S0021-9258(17)49904-2

156. Wodak SJ, Paci E, Dokholyan NV, Berezovsky IN, Horovitz A, Li J, et al. Allostery in its many disguises: from theory to applications. *Structure* (2019) 27(4):566–78. doi: 10.1016/j.str.2019.01.003

157. Kern D, Zuiderweg ER. The role of dynamics in allosteric regulation. *Curr Opin Struct Biol* (2003) 13(6):748–57. doi: 10.1016/j.sbi.2003.10.008

158. Sušac L, Vuong MT, Thomas C, von Bülow S, O'Brien-Ball C, Santos AM, et al. Structure of a fully assembled tumor-specific T cell receptor ligated by pMHC. *Cell* (2022) 185(August 18):3201–13. doi: 10.1016/j.cell.2022.07.010

159. Marrink SJ, Corradi V, Souza PCT, Ingolfsson HI, Tieleman DP, Sansom MSP. Computational modeling of realistic cell membranes. *Chem Rev* (2019) 119(9):6184–226. doi: 10.1021/acs.chemrev.8b00460

160. Endres NF, Das R, Smith AW, Arkhipov A, Kovacs E, Huang Y, et al. Conformational coupling across the plasma membrane in activation of the EGF receptor. *Cell* (2013) 152(3):543–56. doi: 10.1016/j.cell.2012.12.032

161. Lelimousin M, Limongelli V, Sansom MSP. Conformational changes in the epidermal growth factor receptor: role of the transmembrane domain investigated by coarse-grained metaDynamics free energy calculations. *J Am Chem Soc* (2016) 138:10611–22. doi: 10.1021/jacs.6b05602

162. Chen Y, Zhu Y, Li X, Gao W, Zhen Z, Dong D, et al. Cholesterol inhibits TCR signaling by directly restricting TCR-CD3 core tunnel motility. *Mol Cell* (2022) 82 (7):1278–87.e5. doi: 10.1016/j.molcel.2022.02.017

163. Freed DM, Bessman NJ, Kiyatkin A, Salazar-Cavazos E, Byrne PO, Moore JO, et al. EGFR ligands differentially stabilize receptor dimers to specify signaling kinetics. *Cell* (2017) 171(3):683–95.e18. doi: 10.1016/j.cell.2017.09.017

164. Lane JR, May LT, Parton RG, Sexton PM, Christopoulos A. A kinetic view of GPCR allostery and biased agonism. *Nat Chem Biol* (2017) 13(9):929–37. doi: 10.1038/nchembio.2431

165. Furness SGB, Liang YL, Nowell CJ, Halls ML, Wookey PJ, Dal Maso E, et al. Ligand-dependent modulation of G protein conformation alters drug efficacy. *Cell* (2016) 167(3):739–49.e11. doi: 10.1016/j.cell.2016.09.021

166. Zareie P, Szeto C, Farenc C, Gunasinghe SD, Kolawole EM, Nguyen A, et al. Canonical T cell receptor docking on peptide-MHC is essential for T cell signaling. *Science* (2021) 372(6546):eabe9124. doi: 10.1126/science.abe9124

167. Davis SJ, van der Merwe PA. The kinetic-segregation model: TCR triggering and beyond. *Nat Immunol* (2006) 7(8):803–9. doi: 10.1038/ni1369

168. Swamy M, Beck-Garcia K, Beck-Garcia E, Hartl FA, Morath A, Yousefi OS, et al. A cholesterol-based allostery model of T cell receptor phosphorylation. *Immunity* (2016) 44(5):1091–101. doi: 10.1016/j.immuni.2016.04.011

Frontiers in Immunology

Explores novel approaches and diagnoses to treat immune disorders.

The official journal of the International Union of Immunological Societies (IUIS) and the most cited in its field, leading the way for research across basic, translational and clinical immunology.

Discover the latest Research Topics

See more →

Frontiers

Avenue du Tribunal-Fédéral 34
1005 Lausanne, Switzerland
frontiersin.org

Contact us

+41 (0)21 510 17 00
frontiersin.org/about/contact